

**STUDY ON THE ENERGY PERFORMANCE OF
BLENDED CONCRETE AS CLADDING MATERIAL
IN A BUILDING SYSTEM**

THESIS SUBMITTED BY

AVIJIT GHOSH

DOCTOR OF PHILOSOPHY (ENGINEERING)

**SCHOOL OF ENERGY STUDIES
FACULTY COUNCIL OF ENGINEERING AND TECHNOLOGY
JADAVPUR UNIVERSITY
KOLKATA, INDIA
2019**

1. Title of the thesis:

“STUDY ON THE ENERGY PERFORMANCE OF BLENDED CONCRETE AS CLADDING MATERIAL IN A BUILDING SYSTEM”.

2. Name, Designation & Institution of Supervisors:

a) **Prof. Subhasis Neogi**, Former Professor, School of Energy Studies, Jadavpur University & Present Professor, Department of Mechanical Engineering. Aliah University, West Bengal, INDIA.

b) **Dr.Arup Ghosh**, Former Chief Scientist, CSIR-Central Glass & Ceramic Research Institute, Kolkata, West Bengal, INDIA.

3. List of Publication :

- i) **“Evaluation of physical and thermal properties of coal combustion residue blended concrete for energy efficient building application in India”**, Advances in Building Energy Research, Published Online : 20 December 2018, <https://doi.org/10.1080/17512549.2018.1557076>
- ii) **“Reuse of fly ash and bottom ash in mortars with improved thermal conductivity performance for buildings”**, Heliyon doi://10.1016/j.heliyon.2018.e00934
- iii) **“Preservation of sand and building energy conservation”**, Energy Procedia 90 (2016) 432-440.

4. List of Patents : Nil

5. List of Presentations in National / International Conferences / Workshops

- i) **Key Note Abstract accepted titled : “Coal Combustion Residues as Sand Substitute for Energy Efficient Building Envelop Construction”**, International Conference on Innovative Applied Energy, 14-15 March, 2019, St. Cross College, University of Oxford, United Kingdom.
- ii) **Abstract accepted titled : “Coal ash as Cool Material for Energy Efficient Building Envelop Construction”**, 5th International Conference on Countermeasures to Urban Heat Islands (IC2UHI), 02-04 December, 2019, IIT, Hyderabad, India.

CERTIFICATE FROM THE SUPERVISORS

This is to certify that the thesis entitled “**STUDY ON THE ENERGY PERFORMANCE OF BLENDED CONCRETE AS CLADDING MATERIAL IN A BUILDING SYSTEM**”, submitted by Shri Avijit Ghosh, who got his name registered on 22.4.2013 for the award of Ph.D.(Engineering) degree of Jadavpur University is absolutely based upon his own work under the supervision of Dr. Subhasis Neogi, Former Professor, School of Energy Studies, Jadavpur University, Presently Professor, Mechanical Engineering Department, Aliah University and Dr.Arup Ghosh, Former Chief Scientist, CSIR-Central Glass & Ceramic research Institute, Kolkata and that neither his thesis nor any part of the thesis has been submitted for any degree / diploma or any other academic award anywhere before.

1. _____ .

(Dr. Subhasis Neogi)

Signature of the Supervisor
and date with Office Seal

2. _____ .

(Dr. Arup Ghosh)

Signature of the Supervisor
and date with Office Seal

ACKNOWLEDGEMENT

I would like to put on record my sincerest gratitude to Prof. Indranil Manna, former Director, CSIR-CGCRI and present Professor, IIT, Kharagpur, who permitted me to pursue the research work in the chosen field.

I remain grateful to the present Director, Dr. K.Muraleedharan, who had encouraged me to complete the work.

I express my heartfelt gratitude to my Scientific and Technical colleagues, who not only helped me with various characterization tests, but also explained the intricate details with extreme patience. Mr. Subrata Mistry needs special mentioning, since he helped me tirelessly for preparing all the samples.

I like to mention about the help and support received from my alma mater fellow Researcher Mr. D.Choudhury. Dr.T.Jash, Professor and Head, School of Energy Studies, J.U. always encouraged me with positive note.

The mentioning of the names, without whose touch and support, neither the work could be started, nor completed are Prof. Subhasis Neogi and Dr. Arup Ghosh. I remain immensely indebted to both of the Supervisors, under whose guidance and tracking, I traversed through this research journey.

Lastly, I would like to mention that this research work was undertaken as per the earnest desire of my parents. My family members also silently co-operated, for which I remain grateful. I remain immensely fortunate to get an inspirational figure like Prof. Arabinda Ghosh in my life, and Prof. Sarajit Basu, as a true teacher and Academician, both of whose touches I have received with reverence.

Kolkata, January , 2019

Avijit Ghosh

This Research work is dedicated to
Smt. Reba Ghosh, My Mother

CONTENTS

<u>DESCRIPTION</u>	<u>Page No.</u>
Abstract	A-B
Chapter 1 (Energy Scenario and Building, Coal and Sand utilization)	1
1.1 General Introduction, Research Background	1
1.1.1 Energy Scenario & Green House Gas Emission	2
1.1.2 Growth in Population & Building Requirement	4
1.1.3 Building Energy	5
1.1.4 Thermal Power Plant Ash Production & Utilization Scenario	11
1.1.5 Sand Scenario	15
1.1.6(a) Role of Concrete as Cladding in Building	17
1.1.6(b) Role of Mortar as Cladding in Building	18
1.1.7 Research Objective	21
1.1.8 Scope of Research Work	22
Chapter 2 (Review of Earlier Works)	23
2.1 Introduction	23
2.2 Flyash generation and utilization scenario	23
2.3 Characterization of Coal ash from thermal power plants	25
2.4 Sand exploitation scenario	27
2.5 Sand alternative and application in Concrete and Mortar	28
2.6 Embodied energy, Insulation and Cool Roof	47
2.7 Environmental impact of materials and Energy Conservation in Building	50

Chapter 3 (Materials and its Characterization)	53
3.1 General view	53
3.2 Details of the materials used	54
3.2.1 Cement	54
3.2.2 Sand	56
3.2.3 Flyash and Bottomash	58
3.2.3(a) Flyash	58
3.2.3(b) Bottomash	58
3.2.4 Stone Aggregate	59
3.2.5 Water	59
3.2.6 Lime dust	60
3.2.7 Marble dust	60
3.2.8 Common Burnt Clay Building Bricks	60
3.2.9 Concrete and Mortar mix	60
3.3 Material Characterization	61
3.3.1 Cement	61
3.3.1(a) Quantitative Chemical Analysis	63
3.3.1(b) Phase Composition : XRD	64
3.3.1(c) Surface Morphology : FESEM	66
3.3.1(d) Physical test - Density	67
3.3.2 Flyash and Bottomash	68
3.3.2(a) Quantitative Chemical Analysis	68
3.3.2(b) Phase composition : XRD	68
3.3.2(c) Particle size analysis : Flyash	73
3.3.2(d) Physical test – Surface area : Flyash	75
3.3.2(e) Physical test – Sieve analysis : Bottomash	75
3.3.2(f) Surface morphology – FESEM : Flyash and Bottomash	77

3.3.2(g) Physical test – Density : Flyash	79
3.3.2(h) Physical test – Surface area : Bottomash	79
3.3.3 Sand	80
3.3.3(a) Sieve analysis	80
3.3.3(b) Phase analysis : XRD	83
3.3.3(c) Surface morphology – FESEM(Sand)	84
3.3.3(d) Physical Test – Density(Sand)	86
3.3.3(e) Physical Test – Surface Area (Sand)	86
3.3.4 Stone aggregate	86
3.3.4(a) Sieve analysis	86
3.3.5 Lime dust and Marble dust	89
3.3.5(a) Quantitative Chemical analysis	89
3.3.6 Burnt Clay Bricks	90
3.3.6(a) Physical test – Dimension	90
3.3.6(b) Physical test – Class designation	90
3.3.6(c) Physical test – Water absorption	91
3.3.6(d) Physical test – Efflorescence	91
Chapter 4 (Experimental Investigations)	93
4.1 Overview	93
4.2 Experimentation	93
4.2.1 Basic parameter of materials	94
4.2.2 Concrete mix design calculations	94
4.2.2.1 Concrete overview	94
4.2.2.2 Steps involved in designing the concrete mix	95
4.2.2.3 Calculations for mix proportioning	98
4.2.2.3.1 Design mix for M 15 Grade of Concrete	98
4.2.2.3.1(a) Sand replaced by Bottomash in the above Concrete	100
4.2.2.3.2 Alternate design mix for M 15 Grade of Concrete	101
4.2.2.3.2(a) Sand replaced by Bottomash in the above Concrete	103

4.2.2.3.3 Nominal mix for M 15 Grade of Concrete	104
4.2.2.3.3(a) Sand replaced by Bottomash in the above Concrete	104
4.2.2.3.4 Design mix for M 20 Grade of Concrete	105
4.2.2.3.4(a) Sand replaced by Bottomash in the above Concrete	107
4.2.2.3.5 Alternate design mix I for M 20 Grade of Concrete	108
4.2.2.3.5(a) Sand replaced by Bottomash in the above Concrete	111
4.2.2.3.5(b) Sand replaced by Flyash in the above Concrete	111
4.2.2.3.5(c) Sand replaced by Lime –Bottom/Flyash in the above Concrete	112
4.2.2.3.6 Alternate design mix II for M 20 Grade of Concrete	113
4.2.2.3.6(a) Sand replaced by Bottomash in the above Concrete	115
4.2.2.3.7 Nominal mix for M 20 Grade of Concrete	116
4.2.2.3.7(a) Sand replaced by Bottomash in the above Concrete	116
4.2.2.3.8 Nominal mix for M 25 Grade of Concrete	117
4.2.2.3.8(a) Sand replaced by Bottomash in the above Concrete	118
4.2.2.4 Mortar mix	119
4.2.2.4.1 General overview	119
4.2.2.4.2 Mix composition for MM3 Grade with Bottomash	120
4.2.2.4.3 Mix composition for MM3 Grade with Flyash	121
4.2.2.4.4 Mix composition for MM5 Grade with Bottomash	121
4.2.2.4.5 Mix composition for MM5 Grade with Flyash	122
4.2.2.4.6 Mix composition for MM3 & MM5 Grade without Sand	123
4.3 Concrete and Mortar sample preparation and curing	123
4.3.1 Introduction	123
4.3.2 Test Sample size	123
4.3.2.1 Destructive testing – overview(incl. Testing Machine)	123
4.3.2.2 Non-destructive testing – overview	125
4.4(a) XRD Analysis of Concrete Samples	129
4.4(b) XRD Analysis of Mortar Samples	137
4.4(c) XRD Analysis of Sand less Mortar Samples	139
4.5 Evaluation of Apparent Porosity and Bulk Density test of Samples	143

4.5.1 Introduction	143
4.5.2 Test method	143
4.6 Thermal conductivity test of samples	144
4.6.1 Introduction	144
4.6.2 Various test protocol	144
4.6.3 Samples tested to determine thermal conductivity parameter	154
4.7 Burnt Clay Brick	154
4.7.1 Introduction	154
4.7.2 Burnt clay brick with mortar on both faces	155
4.8 Overall heat transfer co-efficient test	157
4.8.1 Introduction	157
4.8.2 Heat flow mechanism	157
4.8.2.1 Conduction	157
4.8.2.2 Convection	158
4.8.2.3 Radiation	160
4.8.2.4 Combined heat transfer	161
4.8.3 Heat flow measurement methods	162
4.8.3.1 Guarded Hot Box method	162
4.8.3.1(a) Metering box	163
4.8.3.1(b) Guard box	163
4.8.3.1(c) Cold box	164
4.8.3.1(d) Test procedure	164
4.8.4 Guarded Hot Box test set-up(incl. Metering Box, Guard Box, Cold Box, Surround Panel, Temp. control...)	165
4.8.4.1 Sample preparation	169
4.8.4.2 125mm brick wall testing	170
Chapter 5 (Experimental Data Results)	171
5.1 Introduction	171
5.2 Tests undertaken	171
5.3 Design concrete mix	172
5.3.1 Design mix with Flyash (Set 1 Group A)	172

5.3.2	Design mix with Flyash-Lime (Set 2 Group A)	177
5.3.3	Design mix with Flyash-Lime & Bottomash-Lime (Set 3 Group A)	180
5.3.4	Design mix with Bottomash (Set 4 Group A)	185
5.3.5	Design mix with Bottomash & Flyash (Set 5 Group A)	190
5.3.6	Design mix with Bottomash (Set A Group B)	198
5.3.7	Design mix with Bottomash (Set B Group B)	203
5.3.8	Design mix with Bottomash (Set C Group B)	208
5.3.9	Design mix with Bottomash (Set D Group B)	213
5.4	Nominal mix concrete	218
5.4.1	Nominal mix with Bottomash (Set A Group C)	218
5.4.2	Nominal mix with Bottomash (Set B Group C)	223
5.4.3	Nominal mix with Bottomash (Set C Group C)	228
5.5	Masonry Mortar	233
5.5.1	Introduction	233
5.5.2	Masonry Mortar Grade MM3 with Flyash & Bottomash	233
5.5.3	Masonry Mortar Grade MM5 with Flyash & Bottomash	240
5.5.4	Masonry Mortar Grade MM3 Sandless with Flyash & Bottomash	247
5.5.5	Masonry Mortar Grade MM5 Sandless with Flyash & Bottomash	252
5.6	Thermal transmittance or U-value	258
5.6.1	Introduction	258
5.6.2	Test Samples and Other parameters	259
5.6.3	Test conditions	266
5.6.4	U-value Calculations & Test Result	267
Chapter 6 (Discussions, Conclusions & Recommendations)		271
6.1	Introduction	271
6.2	Summary Analysis and Results	272
6.3	Conclusive Remarks	275
6.4	Future Scope of Work	276
References		277 – 291
Published Papers & Accepted Abstract		

LIST OF TABLES

Chapter 1		Page
Table 1.1	All India Coal consumption	11
Table 1.2	Per capita consumption of electricity by Indian population	12
Table 1.3	Flyash generation and utilization in India	13
 Chapter 3		
Table 3.1	Comparison of different parameters of PPC	61
Table 3.2	Comparison of different parameters of OPC-43, OPC-53, PSC and PPC	61
Table 3.3	Quantitative Chemical Analysis of PPC used	63
Table 3.4	Peak list of PPC	64
Table 3.5	Bulk Density of Cement	67
Table 3.6	Quantitative Chemical Analysis Result of Flyash and Bottomash	68
Table 3.7	Peak list of Fly ash	69
Table 3.8	Peak list of Bottom ash	70
Table 3.9	Particle size analysis data of Fly ash	73
Table 3.10	Bulk Density of Flyash	79
Table 3.11	Grading Zones Classification of Sand	80
Table 3.12	Density value of Sand	86
Table 3.13	Chemical composition of Lime dust and Marble dust	89
Table 3.14	Classes of Common Burnt Clay Bricks	90

Chapter 4

Table 4.1	M-15 Design Mix Composition with Sand replacement by Bottom Ash	100
Table 4.2	M-15 Alt. Design Mix composition with Sand replacement by Bottom ash	103
Table 4.3	M-15 Nominal Mix composition with Sand replacement by Bottom ash	104
Table 4.4	M-20 Design Mix composition with Sand replacement by Bottom ash	107
Table 4.5	M-20 Alt. Design Mix composition with Sand replacement by Bottom ash	110
Table 4.6	M-20 Alt. Design Mix composition with Sand replacement by Fly ash	111
Table 4.7	M-20 Design Mix composition with Lime-Bottom ash/Lime- Fly ash	111
Table 4.8	M-20Alt.Design MixII composition with Sand replacement by Bottom ash	114
Table 4.9	M-20 Nominal Mix composition with Sand replacement by Bottom ash	115
Table 4.10	M-25 Nominal Mix composition with Sand replacement by Bottom ash	117
Table 4.11	MM3 Grade Mortar mix with Sand substitution by Bottom ash	119
Table 4.12	MM3 Grade Mortar mix with Sand substitution by Fly ash	120
Table 4.13	MM5 Grade Mortar mix with Sand substitution by Bottom ash	120
Table 4.14	MM5 Grade Mortar mix with Sand substitution by Fly ash	121
Table 4.15	Mortar Mix composition (Conventional & Non-conventional)	122
Table 4.16	Different Sensors used in Hot Disk Analyzer	148

Chapter 5

Table 5.1	Compressive Strength test result for (Set-1, Group-A) 1:1.6:2.4 Concrete Mix with Flyash	172
Table 5.2	Thermal Conductivity test result for (Set-1, Group-A) 1:1.6:2.4 Concrete Mix with Flyash	173
Table 5.3	Apparent Porosity and Bulk Density Test Results for (Set-1, Group-A) 1:1.6:2.4 Concrete Mix with Flyash	174

Table 5.4	Compressive Strength test result for (Set-2, Group-A) 1:1.6:2.4 Concrete mix with Flyash & Lime	177
Table 5.5	Thermal Conductivity test results for (Set-2, Group-A) Concrete Mix with Flyash & Lime	178
Table 5.6	Apparent Porosity and Bulk Density Test Results for (Set-2, Group-A) 1:1.6:2.4 Concrete Mix with Flyash and Lime	179
Table 5.7	Compressive Strength values of (Set-3, Group-A) 1:1.6:2.4 Concrete mix	180
Table 5.8	Thermal Conductivity values of (Set-3, Group-A) 1:1.6:2.4 Concrete mix	181
Table 5.9	Apparent Porosity and Bulk Density Test Results of (Set-3, Group-A) 1:1.6:2.4 Concrete mix	182
Table 5.10	Compressive Strength test result for (Set- 4, Group-A) 1:1.6:2.4 Concrete Mix with Bottomash	185
Table 5.11	Thermal Conductivity test results for (Set-4, Group-A) 1:1.6:2.4 Concrete mix with Bottomash	186
Table 5.12	Apparent Porosity and Bulk Density test results for (Set-4, Group-A) 1:1.6:2.4 Concrete mix with Bottomash	187
Table 5.13	Concrete mix identity and composition with Sand/ Flyash/Bottomash (Set-5, Group-A)	190
Table 5.13(a)	Compressive Strength test results for (Set-5, Group-A) Concrete mix with Sand / Bottomash / Flyash	191
Table 5.14	Thermal Conductivity test results for (Set-5, Group-A) Concrete mix with Sand / Bottomash / Flyash	192
Table 5.15	Apparent Porosity and Bulk Density Test Results of (Set-5, Group-A) 1:1.6:2.4 Concrete mix	193
Table 5.16	Compressive Strength test results for (Set-A, Group-B) 1:1.5:2.5 Concrete mix with Bottomash	198
Table 5.17	Thermal Conductivity test results for (Set-A, Group-B) 1:1.5:2.5 Concrete mix with Bottomash	199

Table 5.18	Apparent Porosity and Bulk Density Test Results for (Set-A, Group-B) 1:1.5:2.5 Concrete mix	200
Table 5.19	Compressive Strength test results of (Set-B, Group-B) 1:1.62:2.78 Concrete mix with Bottomash	203
Table 5.20	Thermal Conductivity test results for (Set-B, Group-B) 1:1.62:2.78 Concrete mix with Bottomash	204
Table 5.21	Apparent Porosity and Bulk Density test results for (Set-B, Group-B) 1:1.62:2.78 Concrete mix with Bottomash	205
Table 5.22	Compressive Strength test results for (Set-C, Group-B) 1:2.4:3.6 Concrete mix with Bottomash	208
Table 5.23	Thermal Conductivity test results for (Set-C, Group-B) Concrete mix with Bottomash	209
Table 5.24	Apparent Porosity and Bulk Density test results for (Set-C, Group-B) 1:2.4:3.6 Concrete mix with Bottomash	210
Table 5.25	Compressive Strength test results for (Set-D, Group-B) Concrete mix with Bottomash	213
Table 5.26	Thermal Conductivity test results for (Set-D, Group-B) 1:2:3 Concrete mix with Bottomash	214
Table 5.27	Apparent Porosity and Bulk Density test results for (Set-D, Group-B) 1:2:3 Concrete mix with Bottomash	215
Table 5.28	Compressive Strength test results for (Set-A, Group-C) 1:1:2 Concrete mix with Bottomash	218
Table 5.29	Thermal Conductivity test results for (Set-A, Group-C) 1:1:2 Concrete mix with Bottomash	219
Table 5.30	Apparent Porosity and Bulk Density test results for (Set-A, Group-C) 1:1:2 Concrete mix with Bottomash	220
Table 5.31	Compressive Strength test results for (Set-B, Group-C) 1:1.5:3 Concrete mix with Bottomash	223
Table 5.32	Thermal Conductivity test results for (Set-B, Group-C) 1:1.5:3 Concrete mix with Bottomash	224

Table 5.33	Apparent Porosity and Bulk Density test results for (Set-B, Group-C) 1:1.5:3 Concrete mix with Bottomash	225
Table 5.34	Compressive Strength test results for (Set-C, Group-C) 1:2:4 Concrete mix with Bottomash	228
Table 5.35	Thermal Conductivity test results for (Set-C, Group-C) 1:2:4 Concrete mix with Bottomash	229
Table 5.36	Apparent Porosity and Bulk Density test results for (Set-C, Group-C) 1:2:4 Concrete mix with Bottomash	230
Table 5.37	Gradual replacement of Sand by Fly ash and Bottom ash in MM3 Grade Mortar	233
Table 5.37(a)	Test results of physical and thermal parameters of MM3 Grade Mortar (Gradual replacement of Sand by Flyash and Bottomash)	234
Table 5.38	Gradual replacement of Sand by Flyash & Bottomash in MM5 Grade Mortar	240
Table 5.38(a)	Test results of physical and thermal parameters of MM5 Grade Mortar	240
Table 5.39	Total replacement of Sand by Flyash and Bottomash in MM3 Grade Mortar	247
Table 5.39(a)	Test results of physical and thermal parameters of MM3 Grade Mortar (Total replacement of Sand by Fly ash and Bottom ash)	247
Table 5.40	Total replacement of Sand by Flyash and Bottomash in MM5 Grade Mortar	252
Table 5.40(a)	Test results of physical and thermal parameters of MM5 Grade Mortar (Total replacement of Sand by Flyash and Bottomash)	252
Table 5.41	Actual test parameters	266
Table 5.42	Summary Result of U-value test performed on two brick panels	270

LIST OF FIGURES

Chapter 1	Page
Fig. 1 Fuel-wise share of World Primary Energy Consumption	2
Fig. 2 Fuel-wise share of India Primary Energy Consumption	2
Fig. 3 Global GHG Emission by various Sectors in 2015	4
Fig. 4 Global final energy sharing by various sectors during 2015	6
Fig. 5 Electricity consumption in India during 2016-17	6
Fig. 6 Global CO ₂ Emission by various sectors in 2015	7
Fig. 7 Electricity consumption by various sections of a typical Residential Building	8
Fig. 8 Electricity consumption by various sections of a typical Commercial Building	8
Fig. 9 Utilization of coal ash from thermal power plants in India	14
Chapter 3	
Fig.3.1 Cement Production by different variety (Million MT) year wise	55
Fig.3.2 X-Ray Diffractogram of PPC Sample, showing constituent phases	65
Fig.3.2(a) PPC at 60X	66
Fig.3.2(b) PPC at 100X	66
Fig.3.2(c) PPC at 500X	67
Fig. 3.2(d) PPC at 1000X	67
Fig. 3.2(e) PPC at 2000X	67

Fig. 3.3 X-Ray Diffractogram of Fly ash sample showing constituent phases	70
Fig. 3.4 X-Ray Diffractogram pattern of Bottom ash sample showing constituent phases	72
Fig.3.5 Particle size distribution for fly ash, used in the experiment	75
Fig.3.6(a) Grading curve for Bottom ash	76
Fig.3.6(b) Grading curve for Bottom ash	76
Fig. 3.6(c) Grading curve for Bottom ash	77
Fig. 3.7(a) SEM of Fly ash 2000X	78
Fig.3.7(b) SEM of Fly ash 6000X	78
Fig. 3.7(c) SEM of Fly ash 9000X	78
Fig. 3.7(d) SEM of Fly ash10000X	78
Fig. 3.8(a) SEM of Bottom ash 200X	78
Fig. 3.8(b) SEM of Bottom ash 500X	78
Fig. 3.8(c) SEM of Bottom ash 1500X	79
Fig. 3.8(d) SEM of Bottom ash 20000X	79
Fig. 3.9(a) Grading curve of Sand type – 1	81
Fig. 3.9(b) Grading curve of Sand type – 2	81
Fig. 3.9(c) Grading curve of sand type – 3	82
Fig. 3.9(d) Grading curve of Sand type – 4	82
Fig. 3.10 X-Ray Diffractogram pattern of Sand sample showing constituent phases	84

Fig.3.11(a) SEM of Sand at 60X	85
Fig.3.11(b) SEM of Sand at 200X	85
Fig. 3.11(c) SEM of Sand at 500X Magnification	85
Fig.3.11(a) Grading curve of Stone aggregate type – 1	87
Fig.3.11(b) Grading curve of Stone aggregate type – 2	87
Fig.3.11(c) Grading curve of Stone aggregate type – 3	88
Fig. 3.11(d) Grading curve of Stone aggregate type – 4	88
Fig. 3.12 Plastered-puttied-coloured Wall Sample after U-value testing	92

Chapter 4

Fig.4.1 Typical Sand-Cement Plaster work on masonry surface	118
Fig.4.2 Compressive strength testing of cube samples	124
Fig.4.3 Vibrating table set up	125
Fig.4.4 Curing of Samples	125
Fig.4.5 Flow diagram of various test protocol for samples	126
Fig.4.6 Display of cast samples	127
Fig.4.7 300mmX300mmX25mm Flyash Tiles (1:1.6:2.4 Concrete mix)	127

Fig.4.8 Phase Diagram of Concrete with 100% Sand (1:1.5:2.5) at 7 days [Sample id 11(7)]	128
Fig.4.9 Phase Diagram of Concrete with 100% Sand (1:1.5:2.5) at 28 days [Sample id 11(28)].	129
Fig.4.10 Phase Diagram of Concrete with 50% Sand and 50% Bottomash (1:0.75:0.75:2.5) at 7 days [Sample id. 16(7)].	129
Fig.4.11 Phase Diagram of Concrete with 50% Sand and 50% Bottomash (1:0.75:0.75:2.5) at 28 days [Sample id.28(7)].	130
Fig.4.12 Phase Diagram of Concrete with 100% Bottomash (1:1.5:2.5) at 7 days [Sample id.21(7)].	131
Fig.4.13 Phase Diagram of Concrete with 100% Bottomash (1:1.5:2.5) at 28 days [Sample id.21(28)].	131
Fig.4.14 Phase Diagram of Concrete with 100% Sand (1:1.6:2.4) at 7 days [Sample id..CC(7)].	132
Fig.4.15 Phase Diagram of Concrete with 100% Sand (1:1.6:2.4) at 28 days [Sample id. CC(28)].	133
Fig. 4.16 Phase Diagram of Concrete with 50% Sand and 50% Flyash (1:1.6:2.4) at 7 days [Sample id. D 5(7)].	133
Fig.4.17 Phase Diagram of Concrete with 50% Sand and 50% Flyash (1:1.6:2.4) at 28 days [Sample id. D 5(28)].	134
Fig.4.18 Phase Diagram of Concrete with 100% Flyash (1:1.6:2.4) at 7 days [Sample id. D10(7)].	135
Fig. 4.19 Phase Diagram of Concrete with 100% Flyash (1:1.6:2.4) at 28 days [Sample id. D10(28)].	135
Fig.4.20 Phase Diagram of Mortar MM5 Grade with 100% sand (1:4) at 28 days [Sample id. A(28)].	136
Fig.4.21 Phase Diagram of Mortar MM3 Grade with 100% Sand (1:6) at 28 days [Sample id. B(28)].	137
Fig.4.22 Phase Diagram of Mortar MM3 Grade with 100% Bottomash (1:6) at 28 days [Sample id. C(28)].	138

Fig.4.23 Phase Diagram of Mortar MM5 Grade with 100% Bottomash (1:4) at 28 days [Sample id. D(28)].	139
Fig.4.24 Phase Diagram of Mortar MM3 Grade with 50% Lime and 50% Bottomash (1:6) at 28 days [Sample id. F(28)].	140
Fig.4.25 Phase Diagram of Mortar MM5 Grade with 50% Lime and 50% Bottomash (1:4) at 28 days [Sample id. E(28)].	141
Fig.4.26 Guarded Hot Plate Test Apparatus	144
Fig. 4.27 Probe with bifilar spiral as sensing element	147
Fig.4.28 Hot Disk TPS 2500S Set up	148
Fig.4.29 Typical test result vis Screenshot	152
Fig.4.30 Burnt Clay Brick sample under thermal conductivity test	154
Fig. 4.31 Flow diagram of various test protocol for samples	155
Fig.4.32. Conductive heat transfer through a sample	157
Fig.4.33. Convective heat transfer between a wall and fluid flow	158
Fig.4.34. Velocity and thermal boundary layer	159
Fig.4.35 Schematic arrangement of Guarded Hot Box Test Set up	161
Fig.4.36. Guarded Hot Box test setup with data logging and recording.	164
Fig.4.37. Wall sample placed in position with Sensors	167
Fig.4.38. Construction of the brick wall sample under progress	168

Chapter 5

Fig.5.1 Variation in Compressive Strength for (Set-1, Group-A) Concrete Mix with Flyash	172
Fig. 5.2 Variation in Thermal Conductivity values for (Set-1, Group-A) Concrete Mix.	173
Fig.5.3 Variation in Apparent Porosity and Bulk Density for (Set-1, Group-A) Concrete Mix with Flyash	174
Fig. 5.4 Relationship between Apparent Porosity and Thermal Conductivity for the Concrete mix sample(Set 1, Group-A)	175
Fig. 5.5 Relationship between Bulk Density and Thermal Conductivity for the Concrete mix sample (Set 1, Group-A)	176
Fig. 5.6 Variation in Compressive Strength test results for (Set-2, Group-A) Concrete Mix with Flyash & Lime	177
Fig. 5.7 Variation in Thermal Conductivity test results for (Set-2, Group-A) Concrete Mix with Flyash & Lime	178
Fig. 5.8 Variation in Apparent Porosity and Bulk Density Test Results for (Set-2, Group-A) Concrete Mix with Flyash and Lime	179
Fig.5.9 Variations in Compressive Strength values of (Set-3, Group-A) Concrete mix	180
Fig.5.10 Variations in Thermal Conductivity values of (Set-3, Group-A) Concrete mix	181
Fig. 5.11 Variations in Apparent Porosity and Bulk Density values of (Set-3, Group-A) Concrete mix	182
Fig. 5.12 Relationship between Apparent Porosity and Thermal Conductivity for the Concrete mix sample	183
Fig. 5.13 Relationship between Bulk Density and Thermal Conductivity for the Concrete mix sample	184
Fig. 5.14 Variations in Compressive Strength Test values of (Set-4, Group-A) Concrete mix	185

Fig. 5.15 Variation in Thermal Conductivity values for (Set-4, Group-A) Concrete mix with Bottomash	186
Fig. 5.16 Variations in Apparent Porosity and Bulk Density test results for (Set-4, Group-A) Concrete mix with Bottomash	187
Fig. 5.17 Relationship between Apparent Porosity and Thermal Conductivity for the Concrete mix sample	188
Fig. 5.18 Relationship between Bulk Density and Thermal Conductivity for the Concrete mix sample	189
Fig. 5.19 Variations in Compressive Strength of (Set-5, Group-A) Concrete mix	191
Fig. 5.20 Variations in Thermal Conductivity values for (Set-5, Group-A) Concrete mix with Bottomash and Flyash	192
Fig. 5.21 Variations in Apparent Porosity and Bulk Density values of (Set-5, Group-A) Concrete mix	193
Fig. 5.22 Relationship between Apparent Porosity and Thermal Conductivity for the Concrete mix sample with BA	194
Fig. 5.23 Relationship between Bulk Density and Thermal Conductivity for the Concrete mix sample with BA	195
Fig. 5.24 Relationship between Apparent Porosity and Thermal Conductivity for the Concrete mix sample with FA	196
Fig. 5.25 Relationship between Bulk Density and Thermal Conductivity for the Concrete mix sample with FA	197
Fig. 5.26 Variation in Compressive Strength for (Set-A, Group-B) Concrete mix with Bottomash	198
Fig. 5.27 Variation in Thermal Conductivity values for (Set-A, Group-B) Concrete mix with Bottomash	199
Fig. 5.28 Variations in Apparent Porosity and Bulk Density values of (Set-A, Group-B) Concrete mix	200
Fig. 5.29 Relationship between Apparent Porosity and Thermal Conductivity for the Concrete mix sample	201

Fig. 5.30 Relationship between Bulk Density and Thermal Conductivity for the Concrete mix sample	202
Fig.5.31 Variations in Compressive Strength values for (Set-B, Group-B) Concrete mix with Bottomash	203
Fig. 5.32 Variations in Thermal Conductivity values for (Set-B, Group-B) Concrete mix with Bottomash	204
Fig. 5.33 Variations in Apparent Porosity and Bulk Density values for (Set-B, Group-B) Concrete mix with Bottomash	205
Fig. 5.34 Relationship between Apparent Porosity and Thermal Conductivity for the Concrete mix sample	206
Fig. 5.35 Relationship between Bulk Density and Thermal Conductivity for the Concrete mix sample	207
Fig. 5.36 Variations in Compressive Strength values (Set-C, Group-B)) Concrete mix with Bottomash	208
Fig. 5.37 Variations in Thermal Conductivity values for (Set-C, Group-B) Concrete mix with Bottomash	209
Fig. 5.38 Variations in Apparent Porosity and Bulk Density values for (Set-C, Group-B) Concrete mix with Bottomash	210
Fig. 5.39 Relationship between Apparent Porosity and Thermal Conductivity for the Concrete mix sample	211
Fig. 5.40 Relationship between Bulk Density and Thermal Conductivity for the Concrete mix sample	212
Fig. 5.41 Variations in Compressive Strength values for (Set-D, Group-B) Concrete mix with Bottomash	213
Fig. 5.42 Variations in Thermal Conductivity values for (Set-D, Group-B) Concrete mix with Bottomash	214
Fig. 5.43 Variations in Apparent Porosity and Bulk Density values for (Set-D, Group-B) Concrete mix with Bottomash	215
Fig. 5.44 Relationship between Apparent Porosity and Thermal Conductivity for the Concrete mix sample	216

Fig. 5.45 Relationship between Bulk Density and Thermal Conductivity for the Concrete mix sample	217
Fig. 5.46 Variations in Compressive Strength values for (Set-A, Group-C) Concrete mix with Bottomash	218
Fig. 5.47 Variations in Thermal Conductivity values for (Set-A, Group-C) Concrete mix with Bottomash	219
Fig. 5.48 Variations in Apparent Porosity and Bulk Density values for (Set-A, Group-C) Concrete mix with Bottomash	220
Fig. 5.49 Relationship between Apparent Porosity and Thermal Conductivity for the Concrete mix sample (Set A, Group-C)	221
Fig. 5.50 Relationship between Bulk Density and Thermal Conductivity for the Concrete mix sample (Set A, Group-C)	222
Fig. 5.51 Variations in Compressive Strength values for (Set-B, Group-C) Concrete mix with Bottomash	223
Fig. 5.52 Variations in Thermal Conductivity values for (Set-B, Group-C) Concrete mix with Bottomash	224
Fig. 5.53 Variations in Apparent Porosity and Bulk Density values for (Set-B, Group-C) Concrete mix with Bottomash	225
Fig. 5.54 Relationship between Apparent Porosity and Thermal Conductivity for the Concrete mix sample (Set B, Gr. C)	226
Fig. 5.55 Relationship between Bulk Density and Thermal Conductivity for the Concrete mix sample (Set B, Group-C)	227
Fig. 5.56 Variations in Compressive Strength values for (Set-C, Group-C) Concrete mix with Bottomash	228
Fig. 5.57 Variations in Thermal Conductivity values for (Set-C, Group-C) Concrete mix with Bottomash	229
Fig. 5.58 Variations in Apparent Porosity and Bulk Density values for (Set-C, Group-C-) Concrete mix with Bottomash	230
Fig. 5.59 Relationship between Apparent Porosity and Thermal Conductivity for the Concrete mix sample (Set C, Group-C)	231

Fig. 5.60 Relationship between Bulk Density and Thermal Conductivity for the concrete mix sample (Set C, Group-C)	232
Fig. 5.61 Compressive Strength test values of MM3 Grade Mortar (Gradual replacement of Sand by Flyash in Series A and that by Bottomash in Series B)	234
Fig. 5.62 Thermal Conductivity test values of MM3 Grade Mortar (Gradual replacement of Sand by Flyash in Series A and that by Bottomash in Series B)	235
Fig. 5.63 Apparent Porosity and Bulk Density test values of MM3 Grade Mortar (Gradual replacement of Sand by Flyash in Series A and that by Bottomash in Series B)	236
Fig. 5.64 Relationship between Apparent Porosity and Thermal Conductivity for the MM3 Grade Flyash Mortar mix sample	237
Fig. 5.65 Relationship between Bulk Density and Thermal Conductivity for the MM3 Grade Flyash Mortar mix sample	237
Fig. 5.66 Relationship between Apparent Porosity and Thermal Conductivity for the MM3 Grade Bottomash Mortar mix sample	238
Fig. 5.67 Relationship between Bulk Density and Thermal Conductivity for the MM3 Grade Bottomash Mortar mix sample	239
Fig. 5.68 Compressive Strength test values of MM5 Grade Mortar (Gradual replacement of Sand by Flyash in Series C and by Bottomash in Series D)	241
Fig. 5.69 Thermal Conductivity test values of MM5 Grade Mortar (Gradual replacement of Sand by Flyash in Series C and by Bottomash in Series D)	242
Fig. 5.70 Apparent Porosity and Bulk Density test values of MM5 Grade Mortar (Gradual replacement of Sand by Flyash in Series C and by Bottomash in Series D)	243
Fig. 5.71 Relationship between Apparent Porosity and Thermal Conductivity for the MM5 Grade Flyash Mortar mix sample	244
Fig. 5.72 Relationship between Bulk Density and Thermal Conductivity for the MM5 Grade Flyash Mortar mix sample	245

Fig. 5.73 Relationship between Apparent Porosity and Thermal Conductivity for the MM5 Grade Bottomash Mortar mix sample	245
Fig. 5.74 Relationship between Bulk Density and Thermal Conductivity for the MM5 Grade Bottomash Mortar mix sample	246
Fig. 5.75 Compressive Strength test values of MM3 Grade Mortar (Total replacement of Sand by Flyash and Bottomash)	248
Fig. 5.76 Thermal Conductivity test values of MM3 Grade Mortar (Total replacement of Sand)	248
Fig. 5.77 Apparent Porosity and Bulk Density test values of MM3 Grade Mortar (Total replacement of Sand by Flyash and Bottomash)	249
Fig. 5.78 Relationship between Apparent Porosity and Thermal Conductivity for the MM3 Grade Sand free Mortar mix sample	250
Fig. 5.79 Relationship between Bulk Density and Thermal Conductivity for the MM3 Grade Sand free Mortar mix sample	251
Fig. 5.80 Compressive Strength test values of MM5 Grade Mortar (Total replacement of Sand by Flyash and Bottomash)	253
Fig. 5.81 Thermal Conductivity test values of MM5 Grade Mortar (Total replacement of Sand by Flyash and Bottomash)	254
Fig. 5.82 Apparent Porosity and Bulk Density test values of MM5 Grade Mortar (Total replacement of Sand by Flyash and Bottomash)	255
Fig. 5.83 Relationship between Apparent Porosity and Thermal Conductivity for the MM5 Grade Sand-free Mortar mix sample	256
Fig. 5.84 Relationship between Bulk Density and Thermal Conductivity for the MM5 Grade Sand-free Mortar mix sample	257
Fig. 5.85 Air temperature profile inside Metering Box for Consecutive 3 days (U-value Test)	260
Fig. 5.86 Air temperature profile inside Guard Box for Consecutive 3 days (U-value Test)	260
Fig. 5.87 Hot side sample surface temperature profile for consecutive 3 days (U-value Test)	261

Fig. 5.88 Air temperature profile inside Cold Box for Consecutive 3 days (U-value Test)	261
Fig. 5.89 Cold side sample surface temperature profile for consecutive 3 days (U-value Test)	262
Fig. 5.90 Hot side sample surface temperature profile for consecutive 3 days (U-value Test)	263
Fig. 5.91 Air temperature profile inside Guard Box for consecutive 3 days(U-value Test)	263
Fig. 5.92 Air temperature profile inside Cold Box for consecutive 3 days (U-value Test)	264
Fig. 5.93 Cold side sample surface temperature profile for consecutive 3 days (U-value Test)	264
Fig. 5.94 Air temperature profile inside Metering Box for consecutive 3 days(U-value Test)	265

NOMENCLATURE

f_t	Target mean strength (N mm ⁻²)
f_{ck}	Characteristic Compressive Strength (N mm ⁻²)
k	A constant in Concrete strength calculation
S	Standard Deviation (N mm ⁻²)
V	Absolute volume of fresh concrete (m ³)
W	Mass of water (Kg)
C	Mass of cement (Kg)
S_c	Specific gravity of cement
C_a	Total mass of coarse aggregate (Kg)
f_a	Total mass of fine aggregate (Kg)
S_{ca}	Specific gravity of coarse aggregate
f_{ca}	Specific gravity of coarse aggregate
p	Ratio of fine aggregate to total aggregate by absolute volume
K	Kelvin
C_p	Specific heat capacity ($\frac{\lambda}{\alpha}$) (J m ⁻³ K ⁻¹)
t	Measuring time of the experiment (sec)
T_h	Temperature in hot side (°K)
T_c	Temperature in cold side (°K)
Q_x	Total heat flow in x-direction (W)
q_x	Heat flux (W m ⁻²)
A	Surface area (m ²)
k	Proportionality constant (in the case of one dimensional heat conduction)

dT / dx	Temperature gradient
h	Convective heat transfer co-efficient ($W m^{-2} K^{-1}$)
T_w	Wall temperature ($^{\circ}K$)
T_f	Fluid temperature ($^{\circ}K$)
P_r	Prandtl Number
T	Absolute temperature of the surface ($^{\circ}K$)
$h_{conductive}$	Conductive heat transfer co-efficient
$h_{convective}$	Convective heat transfer co-efficient
$h_{radiative}$	Radiative heat transfer co-efficient
L	Length or thickness of the material, through which heat will pass
$q_{emitted}$	Surface emissive power ($W m^{-2}$)
U	Overall heat transfer co-efficient ($W m^{-2}K^{-1}$)
Q	Total heat transfer through any component (Watt)
C_3S	Tri-calcium Silicate
C_2S	Di-calcium Silicate
C_3A	Tri-calcium Aluminate
C_4AF	Tetra-calcium Alumino-Ferrite
C	CaO – Calcium oxide (calcia)
S	SiO_2 - Silicon dioxide (silica)
A	Al_2O_3 – Aluminium oxide (alumina)
F	Fe_2O_3 – Iron oxide (ferric oxide)
CO_2	Carbon-di-oxide
SO_2	Sulphur-di-oxide

NO	Nitrous oxide
SO ₃	Sulphur-tri-oxide
MgO	Magnesium oxide
TiO ₂	Tin oxide
MnO	Manganese oxide
P ₂ O ₅	Phosphorus Pentoxide
Na ₂ O	Sodium oxide
K ₂ O	Potassium oxide
K ₂ SiF ₆	Potassium Silico-fluoride
H ₂ SO ₄	Sulphuric acid
HF	Hydrofluoric acid
SiO ₂	Quartz
FeO ₃ Si	Iron Silicate
CaCO ₃	Calcite
(Ca ₃ SiO ₄)O	Hartrurite
CaAlO	Calcium Aluminium oxide
Mg	Magnesium
TiFeO	Titanium Iron oxide
Ca ₃ Ti ₂ (Fe ₂ +3Si)O ₁₂	Schorlomite
3Al ₂ O ₃ 2SiO ₂	Mullite
Al ₂ TiO ₅	Aluminium Titanate
Fe ₂ O ₃	Hematite
(Ca _{0.96} Mg _{0.57} Fe _{0.22} Al _{0.16} Ti _{0.059})(Si _{1.73} Al _{0.27})O ₆	Pseudobrookite

Greek

μ	Dynamic viscosity (poise)
δ_t	Thermal boundary layer (cm)
δ	Velocity boundary layer (cm)
u_∞	Free stream velocity at large axial distance (m sec^{-1})
Δ_p	Probing depth (mm)
λ	Thermal conductivity ($\text{W m}^{-1} \text{K}^{-1}$)
α	Thermal diffusivity ($\text{m}^2 \text{s}^{-1}$)
ΔT	Temperature differential ($^\circ\text{K}$)
ϵ	Emissivity
σ	Stefan Boltzmann Constant = $5.67 \times 10^{-8} \text{ (Wm}^{-2}\text{K}^{-4}\text{)}$

Abbreviations

AC	Alinite Cement
ADP	Adiabatic Depletion Potential
AP	Apparent Porosity (%)
AR 5	Annual Report 5
ASTM	American Society for Testing and Materials
BA	Bottom Ash
BAU	Business As Usual
BBTPS	Budge Budge Thermal Power Station
BCS	Best Case Scenario
BD	Bulk Density (gm/cm ³)
BEE	Bureau of Energy Efficiency
BET	Brunauer-Emmett-Teller
BIS	Bureau of Indian Standard
CAGR	Compounded Annual Growth Rate
CEA	Central Electricity Authority
CEU	Central European Union
COP	Conference of Parties
EC	Expansive Cement
ECBC	Energy Conservation Building Code
EDTA	Ethylene Diamine Tetra acetic Acid
EJ	Exa-Joules
EMIS	Euromoney Institutionsl Investor Company
ESP	Electro Static Precipitator
FA	Fly Ash
FESEM	Field Emission Scanning Electron Microscopy
GBPN	Global Building Performance Network
GDP	Gross Domestic Product
GEF	Global Environment Facility

GHG	Green House Gas
Gt	Giga-tonnes
GW	Gigawatt
GWh	Giga-watt hour
GWP	Global Warming Potential
IBEF	India Brand Equity Foundation
ICP-AES	Inductively coupled plasma atomic emission spectroscopy
IEA	International Energy Agency
IESS	Indian Energy Security Scenario
INDC	Intended Nationally Determined Contributions
IS	Indian Standard
ISO	International Standards Organization
Kg	Kilogram
KWh	Kilo-watt hour
LOI	Loss on Ignition
M	Mix
M15	Mix with characteristic compressive strength of 15 N/mm ² at 28 days maturity
M20	Mix with characteristic compressive strength of 20 N/mm ² at 28 days maturity
M25	Mix with characteristic compressive strength of 25 N/mm ² at 28 days maturity
MC	Masonry Cement
MHPC	Moderate Heat Portland Cement
MM	Masonry Mortar
MM	Masonry Mortar
MM3	Grade of masonry mortar with Compressive Strength 3 N mm ⁻² .
MM5	Grade of masonry mortar with Compressive strength 5 N mm ⁻² .
MMT	Million Metric Tonne
MoEF&CC	Ministry of Environment, Forest & Climate Change
MT	Million Tonnes
MTPA	Million Tonnes per Annum
MW	Megawatt
OPC	Ordinary Portland Cement

OWC	Oil Well Cement
PBFSC	Portland Blast Furnace Slag Cement
POCP	Photochemical Ozone Creation Potential
PPC	Portland Pozzolana Cement
RHC	Rapid Hardening Cement
SC	Speciality Cement
SHSC	Super High Strength Cement
SRC	Sulphate Resistant Cement
TERI	The Energy and Resources Institute
TPS	Thermal Power Station
TWh	Tera-watt hour
UN	United Nations
UNDP	United Nations Development Programme
UNEP	United Nations Environment Programme
USAID	United States Agency for International Development
VOC	Volatile Organic Compound
W/c	Water-Cement ratio
WC	White Cement
XRD	X-Ray Diffractogram

ABSTRACT

Considering the rapid pace of urbanization, economic growth, and increasing population, energy demand along with demand for habitat are touching a new scale. Globally, building sector is one of the major stakeholder and consumer of energy. To meet the challenges of Climate Change issue and sustainable development of the society, energy efficient building design and construction are of utmost importance. Coal combustion residues from thermal power plants are partially utilized for cement making, building block manufacturing, embankment / road sub-base construction etc. The unutilized portion of the same are dumped in ash ponds/dykes, leading to environmental degradation through ground water contaminations. On the other hand, the unplanned sand mining all around the globe is also threatening the ecological balances. Flyash is utilized as one of the substitute ingredients in cement making, and upto 35% of flyash in blended cements are permitted as per Indian Standard Code IS-1489 (Part-1):1991 provision. In this work, flyash and bottomash had been studied for chemical, mineralogical and physical parameters and compared with that of sand. Later, it had been tried as a replacement / substitute of sand, one of the non-reacting conventional filler component in concrete. Building envelop is the main barrier for external heat ingress and egress inside of building core of which the roof and wall components play the key role for energy efficient building design. Nominal and design mixes for various grades of concrete and mortars were prepared (altogether 12 Sets of Concrete mixes and 8 Sets of Mortar mixes), and the physical parameters of the samples with gradual reduction in sand component were analysed as per Bureau of Indian Standard Code provisions to verify their suitability from strength and durability points of views. Furthermore, the thermal properties of those samples were evaluated by Transient Plane Source method and the results were found to be encouraging within energy efficiency domain. Depending upon the grade of concrete, thermal conductivity reduction percentage varied, but a general declining trend in all the cases were observed with the value as high as 56% to lowest 30%. Similar reduction trend observed for mortar samples also, which was to the tune of around 60% for an equivalent MM3 Grade of Mortar. Brick wall samples with both side plaster of conventional composition and modified blended compositions were prepared for Overall Heat Transfer Co-efficient (U-value) test by Guarded Hot Box Method as per BS EN ISO

8990 : 1996. Around 15.58% reduction in U-value were noticed after the test. Now such modified concrete in rooftop, and mortar composition for brick wall construction would offer insulating effect and as a consequence, less heat would be transmitted through the building shell.

Eventually by this medium technology application, without additional energy input, four important issues are addressed, as below :-

- ❖ *Reduction in heating/cooling Energy requirement by Buildings,*
- ❖ *Maximum Coal ash utilization and*
- ❖ *Saving of Sand from rapid depletion rate.*
- ❖ *Reduction in Green House Gas Emission due to Energy Conservation in Buildings.*

.....

Chapter 1
Energy Scenario and Building,
Coal ash & Sand utilization

Chapter1: Energy Scenario and Building, Coal Ash and Sand utilization

1.1 General Introduction

Globally building sector consumes around 40% of total energy produced. With the rapid pace of development and linked urbanization, the energy consumption scenario is going to be matter of concern to the planners. Apart from reducing fossil fuel consumption, and switching over to renewable based energy, energy conservation is considered as another effective alternative fuel to restrict Global warming and Climate Change phenomena. The cumulative accumulation of Coal ash without 100% utilization, also creating enormous pressure on landmass and environment due to air and soil contamination. On the other hand, sand, the natural soft mineral is being extracted at the rate more than the replenishment rate. Apart from law and order issues related to scarcity of this fine aggregate component in concrete and mortar making, mindless sand mining from river bed also impacting the adjoining agricultural productions due to lowering of water-table, changing of course of the river, soil erosion and submergence of land etc.

Research Background

- ❖ *Energy Scenario and Green House Gas Emission.*
- ❖ *Cumulative accumulation of coal ash from Thermal Power plants and Rapid Sand depletion due to mindless sand mining.*
- ❖ *Huge Energy requirement by Building Sector.*

The Sub-sections on the following pages shall elaborate the issues linked to the above background.

1.1.1 Energy Scenario and Green House Gas Emission (Global & Indian perspective)

In view of developmental requirement by any country, particularly developing and under-developed countries all around the globe, energy is absolutely essential. Fossil fuel based energy production is the culprit for Greenhouse Gas (GHG) Emission linked Global warming phenomena. A look in to the global fuel use and distributions furnished below-

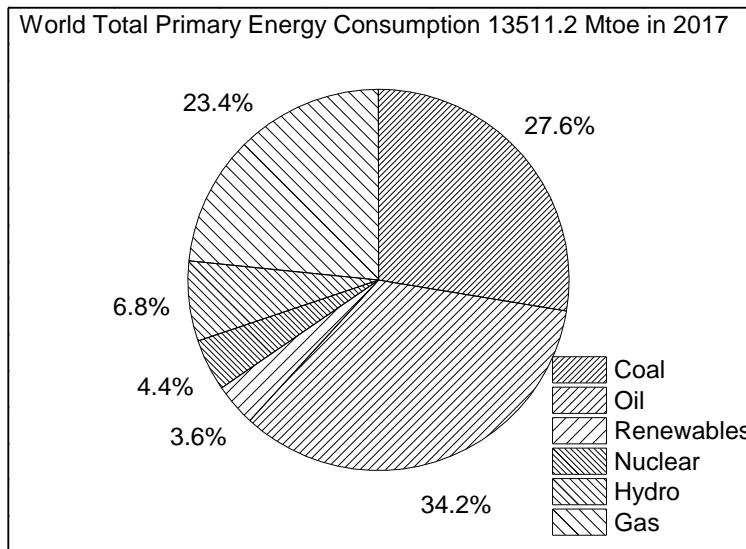


Fig.1 Fuel-wise share of World Primary Energy Consumption (BEE, 2018)

India’s primary energy consumption during the year 2017 was 5.6% of world’s consumption and was third highest after China and US. The distribution in primary energy mix is shown in the following pie-chart.

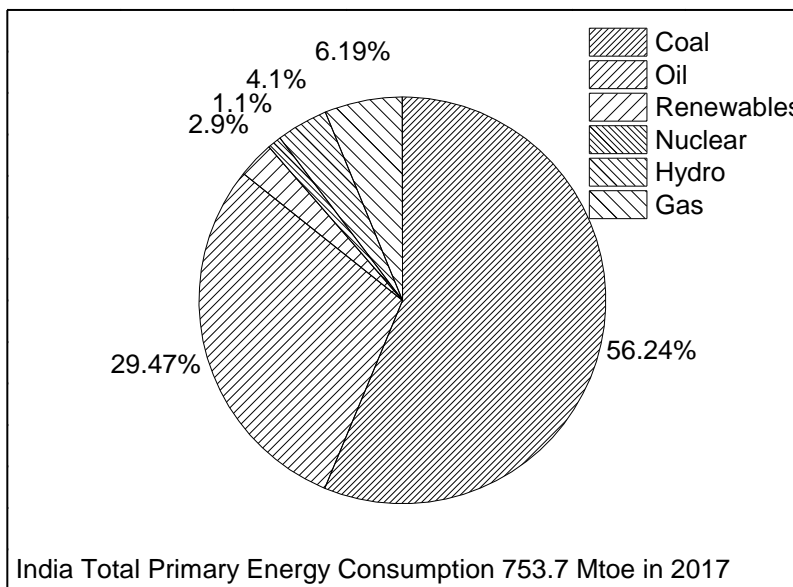


Fig.2 Fuel-wise share of India Primary Energy Consumption (BEE, 2018)

Considering the projection of energy requirement and energy mix, as envisaged by the Planners of India, coal based energy generation shall be in major existence during 2047, exactly 100 years after India attained independence. India, as a signatory in COP 21, Paris Agreement, has been working towards Intended Nationally Determined Contributions (INDC) mapping. This is done in sync with the country's growth projection. It is also mentioned that Climate Change negotiations in global level are largely focussed on the year 2050, and the Niti Aayog Document titled Indian Energy Security Scenario (IESS) is prepared with a projection up to the year 2047 (100 years since country's independence), which is closer to above timeline. From the Niti Aayog document, Level 2 scenario (determined) has been considered in the following data projection levels. GDP for the country is assumed to grow at a CAGR of 7.4% from the base year of 2012 until 2047. Electricity demand within different sectors put together stands at a staggering count of 18635 TWh in the year 2047 from the figure of 4929 TWh during 2012. Among different sectors, building sector demand stands at 2287 TWh in 2047 from 238 TWh in 2012. From a 4.83% share during 2012, it reaches up to 12.27% share of total electricity demand in 2047 under determined effort scenario. Other Sectors like Industry, Agriculture and Telecom / Transport / Cooking etc. also poised for incremental growth rate at varying intensity. Coal being the major fuel in Indian electricity generation scenario, shall be up from 47% during 2011-12 to 52% in 2047. The overall power installed capacity (including Hydro, RE and Biomass, and fossil fuel based) increases from 193 GW in 2011-12 to 1112 GW in 2047, among which coal based power capacity is projected from 106 GW during 2012 to 482 GW during 2047. The Coal based power generation is projected at 3153.6 TWh in 2047. Regarding Green House Gas emission rate w.r.t electricity generation from various sources as above, the same is projected to 5.8 t/capita in 2047 from a level of 1.7 t/capita in 2012 (Niti Aayog, 2015). The increase in GHG emission rate is attributable to the large demand of energy requirement by the economic growth rate and available huge coal reserves in the country, resulting largest power mix through coal route only. According to an estimate by Mittal et al.(2012), the emissions per unit of electricity are to be in the range of 0.91 to 0.95 kg/kWh for CO₂, 6.94 to 7.20 g/kWh for SO₂ and 4.22 to 4.38 g/kWh for NO during the period 2001-02 to 2009-10. The future emission scenario, based on the projected coal consumption in Indian thermal power plants by Planning Commission of India under

‘Business-as Usual (BAU)’ and ‘Best Case Scenario (BCS)’ show the emission in the range of 714976 to 914680 Gg CO₂, 4734 to 6051 Gg SO₂ and 366 to 469 Gg NO in the year 2020-21. Coal remains a major component of global fuel supplies, but concerns about air pollution and greenhouse gas emissions cloud the future of coal (IEA, 2018). According to IPCC, AR5 Report, the total global emission is divided among the sectors as below –

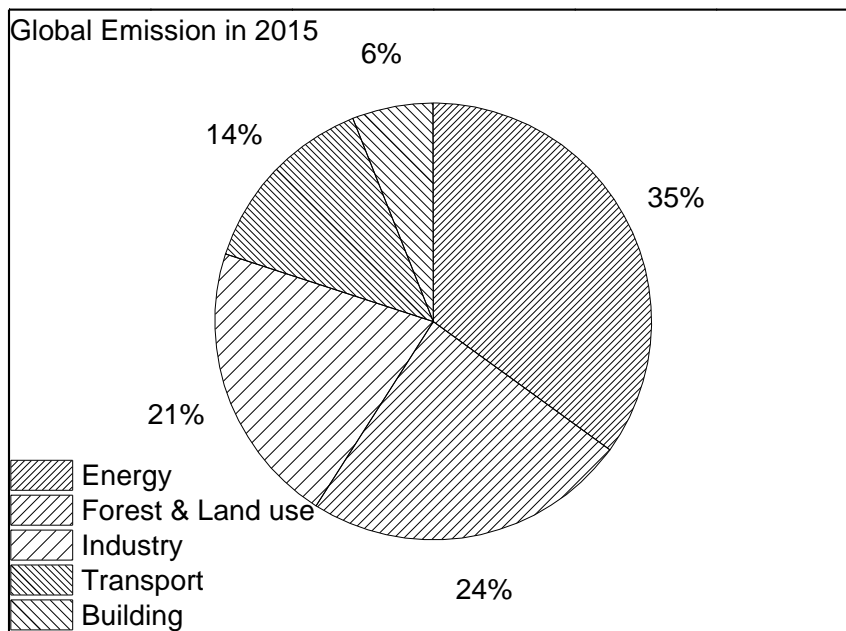


Fig. 3 Global GHG Emission by various Sectors in 2015

The total Green House Gas emission by India is around 2.34 billion tonnes equivalent of CO₂ per year, which is around 7% of global emission. India’s per capita emission is 1.84 tonnes in 2016 (BEE, 2018). In the COP 21, Paris Agreement, India had committed as INDC commitment to reduce its GHG emissions by 33-35% by 2030, in comparison with 2005 level. This target is planned to fulfil by enhanced energy efficiency, energy conservation, switching to renewable based energy from fossil fuel based energy, increasing carbon sink by 2.5 – 3.0 billion tonnes of CO₂ equivalent through additional forest and tree cover etc.

1.1.2 Growth in Population and Building Requirement:

According to the Census of India Report (2006), India’s total population will touch around 1.4 billion mark by 2026, and the urbanization rate is projected to rise from 28.6 percent in 2006 to 33.4 percent in 2026. In 2001, India had the second largest urban

population in the world with about 286 Million were living in urban areas across India (Vaidya, 2009). As per the Indian Census, 2011, the urban population increased to 377 Million, thereby registering a growth of around 24%. As per recent estimates, nearly 590 Million people will live in Indian cities by 2030. Moreover, as per Government of India policy Housing for All by 2022 is another factor for increase in building construction activities, and India is experiencing an unprecedented construction boom. The country had doubled its floor space between 2001 and 2005 and is expected to add 35 billion m² of new buildings by 2050 (GBPN, 2013).

An increase of 400% in the aggregate floor area of buildings and 20 billion m² of new building floor area is expected by 2030 (Kumar, 2011). By 2030, India is expected to have 6 mega-cities with populations above 10 million. Currently 17% of India's urban population lives in slums.

1.1.3 Building Energy

The world-wide building sector consumed around 125 Exa-Joules (EJ) or in other term 30% of total final energy use during 2016. Building construction including manufacturing of constituent materials such as Cement and Steel accounted for an additional 26 EJ or around 6% of global final energy use. The share in total global final energy use by building and building construction sector along with other sectors are shown in the below pie-diagram. 82% of final energy consumption by buildings was supplied by fossil fuels. Corresponding CO₂ emission by all the sectors are shown in subsequent pie-diagram.

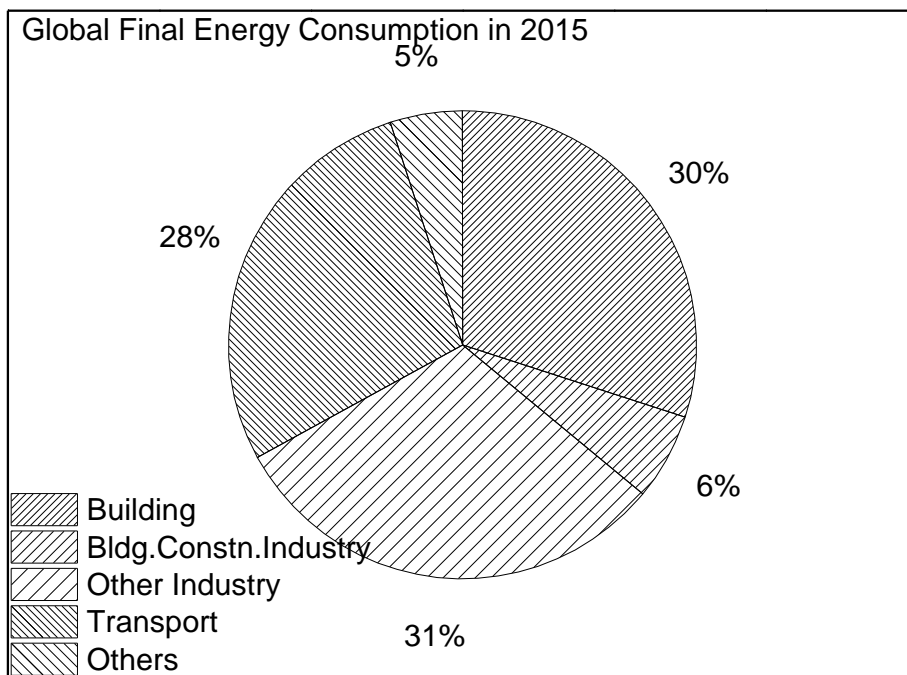


Fig. 4 Global final energy sharing by various sectors during 2015 (UN Env & IEA, 2017)

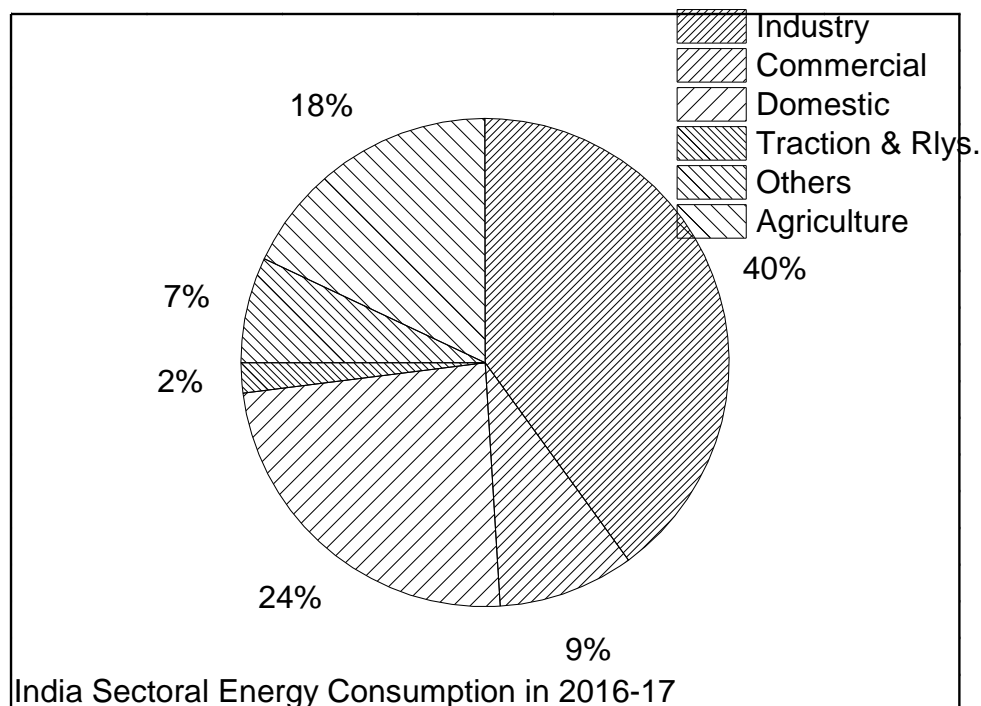


Fig. 5 Electricity consumption in India during 2016-17 (Source :Energy Statistics 2018)

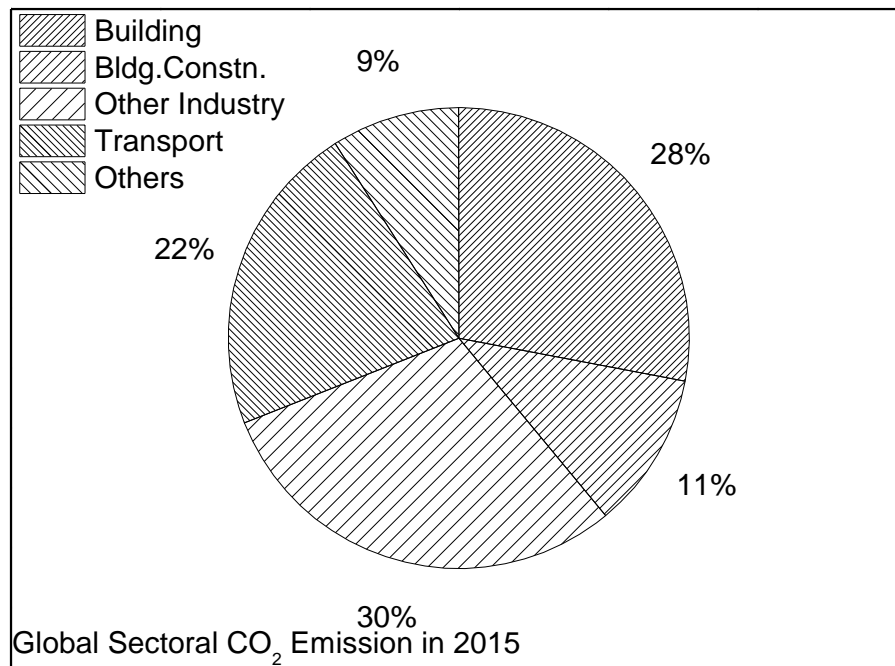


Fig.6 Global CO₂ Emission by various sectors in 2015 (UN Env & IEA, 2017)

CO₂ emission from building sector rose by 1% p.a. during 2010 – 2016, and the cumulative emission during that period from building sector was 76 Gt CO₂ (UN Environment and IEA, 2017). India’s domestic energy consumption has increased from 80 TWh in 2000 to 186 TWh in 2012, and constitutes 22% of total current electrical consumption (CEA, 2013). Furthermore, due to the constant increase of Indian GDP, consumer purchasing power is predicted to grow leading to greater use of domestic appliances. Consequently, household electrical demand is expected to rise sharply in the coming decade. This growth of residential floor space, combined with expectations of improved domestic comfort, will require an increase in electricity production, leading to a significant escalation in damaging emissions. Energy consumption from residential buildings is predicted to rise by more than eight times by 2050 under the business as usual scenario. [IESS, 2015]

India’s aggregated primary energy demand is expected to grow by 2.3 times in the next two decades due to sustained economic growth in the building, transportation and industrial sectors, reaching energy consumption of 40 EJ (GBPN, 2014). Currently, the residential and commercial sectors account for 30% (22% residential and 8% commercial) of total electricity use and consumption in these sectors is rising at 8%

annually (Kumar, 2011). The distribution of typical energy consumption by various heads in residential and commercial buildings are shown in the following pie diagrams (TERI, 2015).

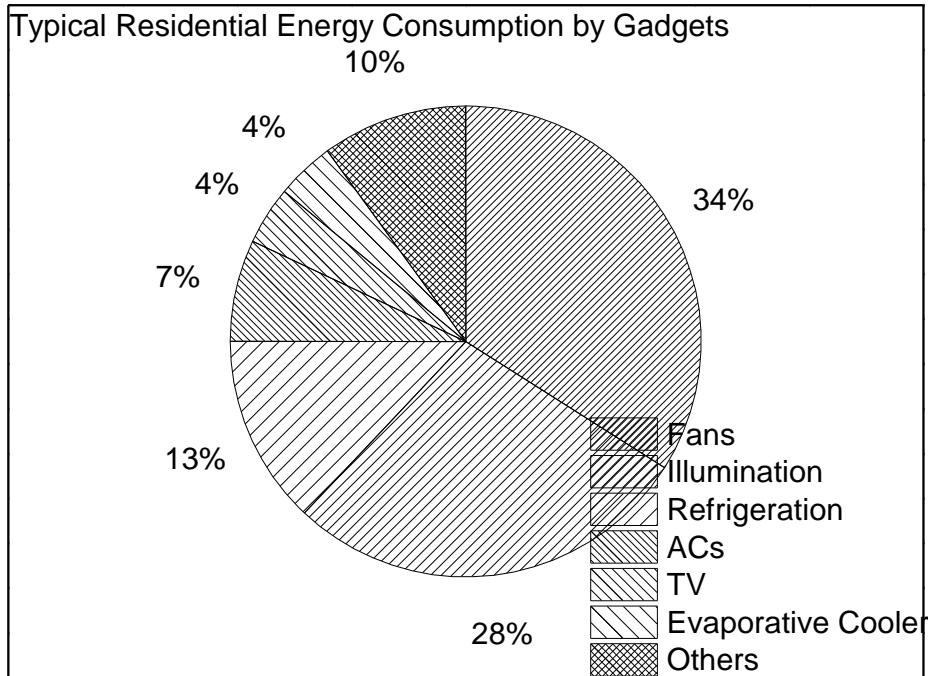


Fig.7 Electricity consumption by various sections of a typical Residential Building

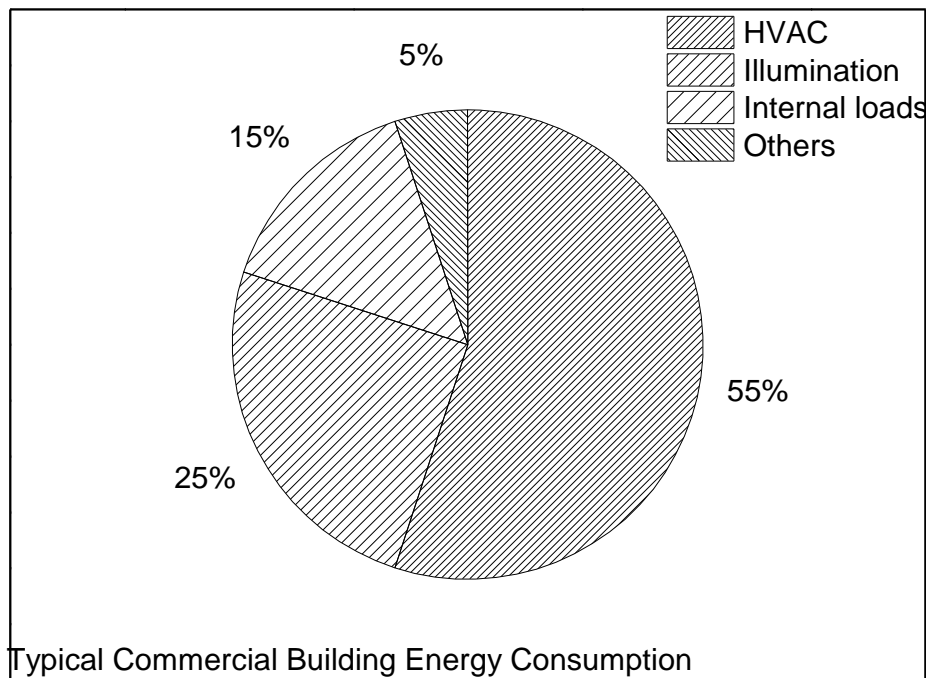


Fig. 8 Electricity consumption by various sections of a typical Commercial Building

Due to growing demand for floor space, and to accommodate emerging service industries and urban migration, India is under apprehension about 2X of existing floor space by 2030 (GBPN, 2014). The increase in energy intensity per unit area of floor, combined with an increase in floor area, have put heightened pressure on energy demand for buildings. The Bureau of Energy Efficiency, a Government of India agency already predicted that India's constructed floor area will increase by around 5X from 2005 level to 2030 (Kumar, 2011). This parallels other projections, such as the CEU study, which estimated an increase of around 400% by 2040, and the McKinsey study, which estimated an increase of more than 400% by 2030. All these studies predict that India's total residential floor area will be much larger than its total commercial floor area in 2030. CEU data suggests that, by 2050, 85% of floor space will be in residential use, while 15% will be used for commercial purposes. Single family and multi-family households are projected to showcase the highest growth rates between 2005 and 2050. Furthermore, CEU projections showed that major share of the growth in energy consumption will occur in residential buildings. The residential sector must therefore be monitored effectively to secure a low energy future. Ensuring efficiency and conservation in this sector can produce a large number of additional advantages, as well as a reduction in energy use (GBPN, 2014). Buildings account for approximately 35% of total final energy consumption in India today, and building energy use is growing at 8% annually (Rawal et al., 2012). Chaturvedi et al. (2014) predicted that, if there are no specific sectoral policies to curb building energy use, final energy demand of the Indian building sector will grow over five times by the end of this century, driven by rapid income and population growth. Technologically it is possible to restrict energy consumption through energy efficient design of new buildings and with the adoption of effective retrofitting solutions in existing buildings. The need for lighting, heating, ventilation and air conditioning are to be reduced with optimum design considerations. Most commercial buildings in India have an Energy Performance Index of 200-400 kWh/sq.mtr./year as compared to lesser EPI in similar buildings in North America and Europe. Energy conscious building design possess the potentiality to reduce EPI to 100-150 kWh/sqm/year. (UNDP and GEF, 2011)

By the rapid increase in building stock during next 20 years or so, there lies the scope for increase in building energy efficiency, and reduce the energy demand through adoption of Energy Conservation Building Code (ECBC), Star labelled equipment etc. in India.

During the period 2011-12, the electricity use in residential and commercial buildings was 170 and 70 TWh respectively (CEA, 2013). It was further estimated that around 31% and 7% of total electricity utilized by Commercial and Residential buildings were for air-conditioners alone during that period (USAID and BEE, 2014). In 2005, the residential and commercial floor spaces were estimated at 1.6 and 0.5 billion m² respectively (USAID & BEE, 2014), which doubled to 3.5 and 1 billion m² in 2012. It is estimated that residential and commercial floor space will grow to 7.0 and 1.5 billion m² by 2030 (USAID & BEE, 2014). Energy consumption could increase by the same proportion. However, an opportunity exists to raise the standard for energy efficiency and reduce the demand for air-conditioning per m² of built space. With the adoption of ECBC in all new commercial buildings, changes in the set-point of air-conditioners, modified lighting design, fenestration design and appropriate shading and insulations on building roof and walls to comply with the Code provisions may result additional savings of 7500GWh, 5900 GWh and 450 GWh in a year respectively (Mathur, 2018).

The building envelope is that component of a building which creates the primary thermal barrier between interior and exterior. It performs a key role in determining levels of comfort, and lighting and ventilation requirements, depending upon the functionality of entire building or part thereof, which ultimately transforms to energy demand for the building. Building envelope consists of the walls, roof, windows and fenestration. According to the National Building Code (2016) and Handbook on Functional Requirement for Buildings, SP 41 (1987), a direct correlation has been established between the design of building envelop and the heat gains from the building envelope. Heat gains in turn determine the indoor temperatures, thermal comfort and sensible cooling demand. The building envelope incorporates significant amount of construction materials and is a key determinant for the embodied energy and creates substantial environmental impacts by CO₂ emission. The design of the building envelop influences heat conduction through roof, opaque wall, and glazed windows and determine the quantum of sensible cooling/heating load. It also determines the amount of natural ventilation and day lighting. Due to rising frequency of hot and extreme weather events throughout the globe, the demand for space cooling is expected to triple between 2010 and 2050 (IEA, 2013). Thermal insulation and thermal mass have been used by building envelop designers for minimizing energy requirement. Since the commercially available insulations are manufactured from petroleum by-products, the cost and embodied energy content of those are very high. Choice of materials for energy efficient envelop

construction should address issues of durability, ability of material to assist in passive design, local sourcing of materials to reduce transportation etc. For a conventional building, excluding fenestration area, balance opaque wall area is made up of brick-mortar-plaster combinations, and roof area is mostly made up of reinforced concrete slab construction. To restrict the heat flow through the roof, cool roof technology, over-deck and under-deck insulations, radiant heat barrier, green roof etc. are adopted with fairly good results as far as arresting the heat flow inside the room is concerned. But such arrangements come with an extra cost, specialized manpower, and added embedded energy, all combined.

1.1.4 Thermal Power Plant Ash Production and Utilization scenario

Coal contributes over 50% of India's primary commercial energy and it is likely to remain so for the next 3 decades. Coal production from 600 MTPA during 2012 shall stand at 1157 MTPA during 2047 under business as usual scenario (Level 2) [as per Niti Aayog document.] All India Coal consumption for Power Generation since 2004 is shown below, followed by per capita electricity consumption trend (CEA, 2018)

Table 1.1 All India Coal consumption (April 2004 - March 2018)

Year	Coal Consumption (Million Tonnes)
2004-05	278.00
2005-06	281.00
2006-07	302.00
2007-08	330.00
2008-09	355.00
2009-10	367.00
2010-11	387.00
2011-12	417.56
2012-13	454.60
2013-14	489.40
2014-15	530.40
2015-16	545.90
2016-17	574.30
2017-18	608.00

Source : Executive Summary on Power Sector Oct-18, Central Electricity Authority

Table 1.2 Per capita consumption of electricity by Indian population

Year	Per Capita Consumption (kWh)
2005-06	631.4
2006-07	671.9
2007-08	717.1
2008-09	733.5
2009-10	778.6
2010-11	818.8
2011-12	883.6
2012-13	914.4
2013-14	957.0
2014-15	1010.0
2015-16	1075.0
2016-17	1122.0
2017-18	1149.0

Indian coal is of low grade with ash content of the order of 30-45 % and that for imported coal is of the order of 10-15%. Large quantity of ash is, thus being generated at coal/lignite based Thermal Power Stations in the country, which not only requires large area of precious land for its disposal but is also one of the sources of pollution and contamination for both air, water and land mass.

Central Electricity Authority (CEA) on behalf of Ministry of Power has been monitoring the fly ash generation and setting the target for its utilization in the country since 1996. The Notification of 3rd November, 2009 prescribed targets of Flyash utilization in a phased manner for all Coal/Lignite based Thermal Power Stations in the country so as to achieve 100% utilization of fly ash. The Thermal Power Stations in operation before the date of the Notification (i.e. 3rd November, 2009) were to achieve the target of fly ash utilization in successive 5 years like 50% in first year; 60% in second year; 75% in third year; 90% in fourth year and 100% in fifth year. The new Thermal Power Stations coming into operation after the MoEF&CC’s notification (i.e. 3rd November 2009) were to achieve the target of fly ash utilization as 50% in the first year, 70% during two years, 90% during three years and 100% during four years depending upon their date of commissioning.

The report on Flyash generation and its utilization at coal/lignite based thermal power stations provides the status of fly ash generation as well as utilization in the country. The report also contains the information regarding the level of fly ash utilization achieved by various power stations in relation to targets prescribed in MoEF&CC’s notification of 3rd November, 2009 and to take corrective measures in the cases of Thermal Power Stations

(TPS) lagging behind in achieving the prescribed targets of fly ash utilization. As per Flyash generation and utilization report for the year 2017-18, the %age utilization was only 67.13 (overall) from 167 TPSs, though the Government directive stands for 100% effective utilization across the country. Out of 167 TPSs, 69 TPSs could utilize 100% ash, generated by those. The Flyash generation and utilization scenario in the country for the period from 1998-99 till 2017-18 is produced in the below furnished table.

Table 1.3 Flyash generation and utilization in India during April 1996- March 2018

Year	Flyash Generation (MMT)	Flyash Utilization (MMT)	Flyash Utilization (%)	FlyashUn-utilization (%)
1996-97	68.88	6.64	9.63	90.37
1997-98	78.06	8.43	10.80	89.20
1998-99	78.99	9.22	11.68	88.32
1999-2000	74.03	8.91	12.03	87.97
2000-2001	86.29	13.54	15.70	84.30
2001-2002	82.81	15.57	18.80	81.20
2002-2003	91.65	20.79	22.68	77.32
2003-2004	96.28	28.29	29.39	70.61
2004-2005	98.57	37.49	38.04	61.96
2005-2006	98.97	45.22	45.69	54.31
2006-2007	108.15	55.01	50.86	49.14
2007-2008	116.94	61.98	53.00	47.00
2008-2009	116.69	66.64	57.11	42.89
2009-2010	123.15	77.33	62.60	37.4
2010-2011	131.09	73.13	55.79	44.21
2011-2012	145.41	85.05	58.48	41.52
2012-2013	163.56	100.37	61.37	38.63
2013-2014	172.87	99.62	57.63	42.37
2014-2015	184.14	102.54	55.69	44.31
2015-2016	176.74	107.77	60.97	39.03
2016-2017	169.25	107.10	63.28	36.72
2017-2018	196.44	131.87	67.13	32.87

The following diagram is showing mode of utilization of Flyash in India in different sectors during 2017-18.

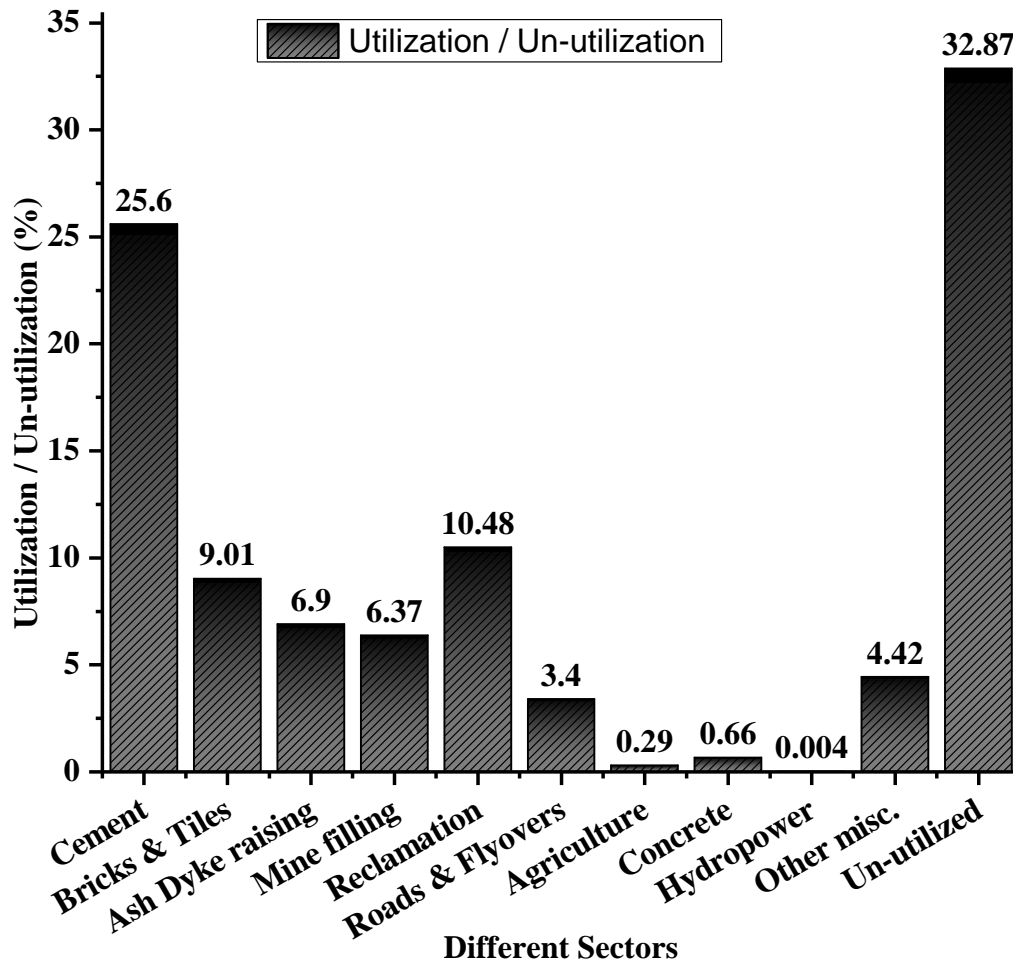


Fig. 9 Utilization of coal ash from thermal power plants in India (CEA, 2018)

From the above data, it is clear that Flyash utilization is far behind the target of 100% utilization, as set by Govt. of India. The total un-utilized coal ash accumulated in ash dykes has reached an alarming figure of 1045.27 MMT for last 17 years period. In the areas of mine filling, reclamation of low lying areas, road and embankment construction, building materials production etc. the utilization need to be increased, and awareness campaign should be initiated among the user group about the efficacy of such utilization.

1.1.5 Sand Scenario

Worldwide metropolitan cities are growing bigger and reaching to touch the sky to accommodate more and more habitants. As an obvious fall out, Globe's natural resources are pushed to the limiting boundaries. That strain is creating sand less scenario with every passing day. Sand, apparently an inert soft natural mineral, and a certain identity for building and infrastructural development, which are linked to economic progress by any country. Sand mining to meet increasing demand over the years has become a thriving multi-billion dollar industry worldwide.

Sand and gravel represent the highest volume of natural mineral consumed globally after water. This information is not very familiar to common masses. Every particle of sand originates from rock on a mountain. The sand grains, which are formed by such geological transformations over thousands of years, route its way through the course of springs, streams and rivers to the ocean. Tides and waves with the Sun-Moon influences, distribute those across the ocean floors, and also carry those up to the sea beaches. During the journey, due to many environmental factors and obstructions, some of the eroded particles find their way in to the riverbed itself. The dammed obstructions in the rivers drastically obstruct this century old processes. According to a very rough estimate, almost half of the sand and gravels extracted every year for use in the various industries and purposes viz. construction industry, glass manufacturing industry, land reclamation, mine filling, oil exploration etc. are never replenished. In India, the main sources of sand are from river flood plain, coastal, paleo channel, and from agricultural fields. River sand mining is the most common practice in India. River sand mining can damage private and public properties as well as aquatic habitats. Excessive removal of sand may significantly distort the natural equilibrium of a stream channel.

Removing sediment from the active channel bed in river create obstructions in the continuity of sediment transport through the river system. The magnitude of the impact basically depends on the rate of the extraction relative to bed load sediment supply and transport through the route channel.

Effect of Sand and Gravel mining on the environment may be summarized as –

- a) Extraction of bed material in excess of replenishment by transport from upstream causes the bed to degrade heavily upstream and downstream of the site of removal.
- b) In-stream habitat is impacted enormously by increase in river gradient, suspended load, and sediment transport rate. Excessive sediment extraction increases turbidity,

causing less penetration of light required for photosynthesis and reduces food availability of aquatic fauna, including reduction of dissolved O₂ level.

c) Riparian habitat including vegetative cover on and adjacent to the river banks control erosion, and also act as filter against pollutants in the stream through runoff. Bank erosion and change in meandering of the river can severely disturb the riparian vegetative cover.

d) Bed degradation are responsible for channel shifting, causing loss of properties and, it can also unstable structurally the bridge supports, pipe lines or other structures.

e) Lowering of riverbed due to sand and gravel extraction also results in lowering of the ground water table in the flood plain. If a floodplain aquifer drains to the stream, groundwater levels can be lowered as a result of bed degradation.

f) Excessive pumping of ground water in the process of mining in abandoned channels depletes ground water causing scarcity of irrigation and drinking water.

g) An un-scientific and unregulated sand and gravel mining cause large degree of meandering of rivers and sometimes it could be in kms. and cause village after village inundation.

Globally, between 47 and 59 billion tonnes of material is estimated to be mined every year, of which sand and gravel, hereafter known as aggregates, account for both the largest share (from 68 per cent to 85 per cent) (UNEP, 2014). The demand for these aggregates come from variety of sectors like Glass, Electronics and Aeronautics, besides the biggest sector of Construction Industry including Buildings (both Commercial and Residential). Sand is an integral part of concrete and masonry mortar, and gravel as aggregate in the concrete. The trend for aggregate extraction can be worked out from Cement consumption as a proxy measure. Due to rapid economic growth in Asia region, this consumption has increased three-fold in last 20 years period. Another massive level use is in land reclamation. Singapore is the highest importer of sand from Indonesia and Malaysia for land reclamation. Singapore has increased its land area by 20% during last 40 years, by importing 517 MMT of Sand, and got the rank of highest sand importer world-wide, and the world's per capita highest sand consumer at 5.4 MT per resident (UNEP, 2014). India has also joined the rank of importer of sand recently to satiate the growing demand of its construction industry. On October 14, 2017 sand containing ship arrived at Tuticorin Port with more than 55000 MT load from Malaysia's Sungai Pahang riverbed (Down to Earth, 2018). With the growing demand-supply deficit in Punjab, Rajasthan, Maharashtra, Gujarat, Karnataka, Tamilnadu, Andhra Pradesh, Telengana,

States of India, this golden granules are becoming a commodity with law and order issues, as well as damaging the environmental balances beyond repair.

1.1.6(a) Role of Concrete as Cladding in Building

Concrete refers to a mixture of aggregates, usually sand, and either gravel or crushed stone, held together by a binder of cementitious paste. The paste is typically made up of Cement (either ordinary portland cement or blended cement) and water and may also contain supplementary cementing additive materials to impart some additional properties like delay in setting, high early strength, improved workability for ease of placement among congested reinforcement etc. Concrete including mortar are inseparable component of modern buildings, and offers the following ten best qualities as under –

1. Long Service Life : Reinforced concretes' durability property confirms that the structure will retain its structural and aesthetic capabilities intended for . The Carbon footprint is reduced considerably, when the necessity for replacement does not arise.
2. Safety : Reinforced concrete structures can withstand vagaries of nature including Earthquake and High Wind induced damages, provided adequately designed. This quality also reduces the chances of replacement or major repair.
3. Shape design : Any shape is possible to adopt by proper design.
4. Lower Maintenance : Reinforced concrete offers long term durability and therefore reduces the requirements for extensive maintenance ,while compared with other materials of construction. Cast-in-situ reinforced concrete gives a monolithic approach to design.
5. Waste minimization : Concrete components typically are cast as specified, with little excess produced. Waste accrued through vutouts, change orders etc. can be recycled.
6. Minimized harvesting impact : Concrete producers can replace significant amounts of cement in their mixtures with industrial by-products such as silica fume, blast furnace slag, coal ash. Their use in concrete removes the disposal headache to a considerable extent.
7. Transportation cost minimization : Concrete can be produced in-situ by blending the required ingredients like cement, aggregate and water. For big projects or site space limitations or rigid quality assurance parameters, Ready-mix concrete is produced at the manufacturing place, and transported through insulated agitator transit mixers. In such cases, though transportation energy is added, but due to optimized selection of all ingredients, considerable economy is attained.

8. Design flexibility : Reinforced concrete offers highest flexibility to the Architect designers. Concrete is used in a wide spectrum of applications, starting from housing to infrastructures.

9. Improved Indoor Air Quality - Concrete contains no VOC and thus adds improved indoor air quality. It does not support mold growth due to its inorganicity.

10. Ease of workmanship: In-situ concrete production and placement does not require special skill, and therefore advantageous.

Role of concrete in a building generally comes in the main skeletal form, which is termed as framed structure consisting column, beam and slab. Besides the above stated qualities of concrete, the flat reinforced concrete roof slab of a building plays very important role in absorbing solar radiation, acts as thermal mass, and transmit it inwards, after emitting certain portion of the heat. In other words, a roof is the uppermost part of a building whose main function is to enclose the space and to protect the same from the effects of weather elements such as rain, wind, sun, heat and snow. A good roof is just as essential as a safe foundation. As a well-designed foundation secures the building against destruction starting at the bottom, similarly a good roof affords protection for the building itself like a sound head of a human being.

1.1.6 (b) Role of Mortar as Cladding in Building

Mortar is a homogenous mixture, produced by thoroughly mixing cementitious material, water and inert material to the desired consistency for use in building mainly. The need for mortar arises in bonding bricks or stones layer by layer, and requires a minimum strength, as prescribed in various Codes. The grades of a masonry mortar is defined by its compressive strength, attained at 28 days of maturity after casting and spread over a range from MM0.5 to MM7.5, wherein MM stands for masonry mortar. The physical and chemical changes occurred in a mortar mix due to the hydration of hydraulic part of the mortar. This mixture composition is also used as external and internal plaster on the surface of masonry work. The selection of mortar for various uses depend on i) type of masonry namely brickwork, stonework, concrete block, concrete wall etc., ii) place of use of masonry like foundation, super-structure etc. iii) load which the masonry will withstand during intended period of service, iv) condition of exposure to weather or soil condition, v) type and grading of fine aggregate or filler inert material, to be used in mortar mix etc. The criteria for selection of particular grade of masonry mortar from

durability consideration should satisfy both the loading and exposure conditions, against which it would be subjected to, during the service period. In the case of masonry, exposed to frequent rains and where there is further protection by way of plastering or rendering the internal and external surfaces, the grade of mortar shall not be less than MM0.7, but shall preferably be of grade MM2 (IS 2250, 1981). Where no protection is provided, the grade of mortar for external wall would be not less than MM2. In the case of load bearing internal walls, the grade of mortar shall preferably be MM0.7 or more for higher durability aspect, but never be lesser than MM0.5. In the case of masonry in foundation, the grade may vary between minimum MM0.7 to MM3, depending upon soil dry / moist / inundated condition etc. For masonry in buildings, subjected to vibration effect, grade should not be less than MM3, for Parapet, where the height is three times more than width shall be not less than MM3, and for low parapet, the wall criteria above may be followed. Grade of mortar for bedding joints in case of large concrete blocks shall not be lower than MM3.

The type of mortar and plaster that should be used depend particularly on the method of construction and quality of construction. In general, except in the case of highly exposed walls in areas of heavy rain, a plaster should protect against wind, rain, knocks and abrasion, and should improve the thermal insulation and appearance of a wall. At the same time it has to be easy to apply without requiring expensive and elaborate tools, and must be affordable. All types of mud plasters, but especially those on external surfaces, need to offer erosion resistance, impermeability to moisture, and impact resistance, and be well bonded to the wall. The widely used mortar and plaster compositions in the Indian building industry are of the proportion 1:6 (MM3 Grade) and 1:4 (MM4 Grade) respectively. Other richer or leaner mix compositions also used on very specific case basis.

Roof and Wall elements in a building form the envelope, which actually protects the interior from vagaries of nature, and plays crucial role from energy conservation point of view. Constituent design of concrete and mortar mixes affect the heat transmission from outdoor to indoor and vice-versa. Depending upon the climatic conditions of a place either heat conducting or heat insulating concrete and mortar are thought to be designed for reducing heating / cooling energy load. It was found that Ordinary Portland Cement (OPC) contain the highest Green House Gas (GHG) emission potential, Global warming Potential (GWP), Photochemical Ozone Creation Potential (POCP), and Adiabatic

Depletion Potential (ADP). To exhibit higher thermal resistance in building envelop, different insulation materials and cool roof paints are randomly considered by the energy efficient building designers, but the embodied energy content and GWP of common insulations like expanded polystyrene slabs, extruded polystyrene slab, mineral wool, fibre glass etc. are quite high. Therefore, the choice of sustainable materials, which might be blended with the conventional materials, and cause least damage to the environment are to be promoted seriously. Such blended concrete and mortar as cladding material in a building system is highly recommended. In selecting such materials, attention should be given to waste utilization (if possible), and restrict depletion of natural materials, which are being depleted at a faster rate than its replenishment rate. In this research work, coal ash has been explored as a substitute material to sand, and the physical and thermal properties have been evaluated to establish the suitability within the Indian Standard Code stipulations related to strength and durability both for actual application. It has also been given due importance that no additional energy is involved for production of such blended concrete (including mortar) and during application, finishing etc. thus maintaining the embodied energy content to be minimum.

1.1.7 Research Objective

The research objective can be described in a single word as “Sustainability”. Thermal Power Plant waste in the form of coal ash has been tried to be utilized as a substitute for sand in building construction. By indiscriminate sand mining from river bed and other sources, serious ecological imbalances are set in, since the replenishment rate is outnumbered by the extraction rate. On the other hand, huge coal ash is generated continuously from thermal power plants, the safe disposal and utilization of which is another serious issue. To keep pace with developmental target of the country, more and more power is required to be generated, most of which are from thermal route for heavy dependence on huge coal reserves of the country. Rapid urbanization with growing population demand more habitat which in turn require more and more building materials. Buildings consume nearer to 40% of the total power generated, and 65% of which goes to satiate the cooling demand in the country like ours. If building can be made cooler even by 10-15%, the same can save huge amount of energy. The objective of this research work is to explore the possibility of utilizing coal ash as partial sand replacement without sacrificing strength and other physical parameters of the blended concrete, and to study the energy performance of such concrete as cladding material in a building system to reduce heat transmittance. The coal ash could be used for both roof concrete and wall construction (in mortar and plaster composition, where sand replacement is possible) in building. Flyash and Bottomash both were used as sand replacement material in different proportions right from 0% to 100% replacement of sand in this work. Heat transfer mechanism gets resistance with increasing percentage of coal ash addition, as observed with diminishing rate of thermal conductivity with increasing rate of coal ash substitution. By modifying the concrete and masonry mortar mixes with insulating characteristics to some extent, without the addition of any energy intensive material or technique, huge energy conservation in building sector is possible. With lesser cooling / heating energy requirement by a building, Green House Gas emission from thermal power generation plants shall eventually be reduced.

1.1.8 Broad Methodology of the Research work

The present work envisages the scope of huge energy conservation without going into costly and complicated methodologies. The methodology followed in this work are as below-

1. To study the physical, chemical, mineralogical and radiological properties of constituent materials of concrete and mortar/plaster, which are used as internal - external cladding material of building envelop.
2. To study the physical parameters of matured concrete and mortar mix samples.
3. To study the thermal properties of matured concrete and mortar samples.
4. To compare the thermal transmittance rate change between the wall panels, built with conventional materials and modified material combinations.
5. To compare the obtained results out of Steps 1 – 4 above, and conclude about suitability of proposed waste material with the targeted advantages.

Chapter 2
Review of Earlier Works

Chapter 2: Review of Earlier Works

2.1 Introduction

This Chapter presents a brief overview on earlier works, carried out by other researchers in the field of Coal ash utilization proposal, Ordinary Portland Cement replacement by Flyash in concrete and mortar making, Sand replacement by coal ash (both Flyash and Bottomash) in concrete and mortar making, and studying its effects on physical and chemical parameters etc. The thermal parameter change, if any was studied under very limited extent by few researchers, that too in the context of cement replacement. Under an established code provision, satisfying the strength requirement, how best the replacement be fruitful from actual application / usage angle was found limited.

2.2 Flyash generation & utilization scenario :

Kandpal et al.(2002) had presented a framework for the estimation of Flyash utilization in India. The analysis considered major areas like cement production, brick manufacturing and construction of road embankments by utilizing Flyash, since the volume requirement was found more in those area. The mathematical models were developed to estimate the projected Flyash utilization in the above stated area, and also estimation of resource saving like land, water, limestone, soil and coal were made. Considering all the factors under other areas for increasing utilization percentage was recommended by the authors.

Haque et al.(2013) discussed about Flyash production and its utilization scenario in India. From CEA Report, it was presented that the percentage utilization of Flyash rose from a meagre 9.63 during 1996-97 to 55.79 during 2010-11. An encouraging picture of utilizing the same in cement industry in larger volume during coming decades were projected, and suggested some areas for further studies like, economic value analysis, development of cement less ash-slag concrete, and utilization of Flyash in the polymer industries without any further elaboration.

Loya et al.(2014) had tried to develop one forecasting tool for the key application areas of Flyash in coming days. Since 100% utilization of Flyash is the target by Government of India since long, which could not be achieved, this analysis was undertaken. Central Electricity Authority described seven key application areas were chosen, and a consequential chart was prepared using annual time series data with the help of Statistical software SPSS version 20.0, and regression model was developed to identify the growth pattern of Flyash utilization under all the seven sectors. Considering the existing trend (1998-2012), further forecast was made in the model for the period from 2013 to 2020, and the application areas were ranked 1 to 7. Cement and Concrete sector utilization was ranked 1 with 65 MT utilization, the second rank holder was the group consisting road, embankment construction and raising of ash-dykes together with 22 MT, and the group consisting reclamation of low lying areas, land filling stood third with 18 MT consumption during 2020.

Asokan et al.(2005) attempted to assess the world wide generation of coal combustion residues (CCR), present utilization and acceptability under Indian context, and future potentials to tackle environmental management well. It was reported by the authors that globally around 33% and in India around 27% CCRs were being utilized in various sectors like road, cement, extraction of metal and cenospheric ash, paints etc. and further utilization in reclamation of old coalmines. For the long term management of CCR in connection with environmental safe-keeping, some more areas were need to be explored.

Disposal of huge quantity Flyash is a serious concern both globally as well as in India, as explored by **Surabhi et al.(2017)**, and various utilization avenues were described in the paper. From the paper, the findings were summarized as the overall utilization of total Flyash generated was much behind 100% utilization target in India, some area needed to be found to increase utilization percentage, technological intervention was required for dry collection in lieu of wet Flyash collection and disposal in ash ponds, and thermal power plant adjoining areas need to utilize for all possible construction and developmental activities.

Utilizing various wastes and industrial by-products, green concrete production prospect was explored by **Liew et al.(2017)**. It was thought to limit greenhouse gas emission, land-filling scarcity and natural resources conservation aspects. The green concrete was described under

various forms like high-strength concrete, ultra-high strength concrete, self-consolidated concrete, high performance concrete, lightweight concrete, high volume flyash concrete and geopolymer concrete. Flyash, bottomash, ground granulated blast furnace slag, silica fume, rice husk ash etc. with other chemical additives helped production of all the above stated concrete.

Pramila Kumari et al.(2008) discussed about some environmental issues associated with Flyash disposal and Government directives towards the disposal of the same. In the review, Flyash was proposed to be used as a resource material for alumina, magnetite, carbon, cenosphere, mineral fillers, enhanced pozzolana and other minor and trace items in future technology area.

2.3 Characterization of Coal ash from thermal power plants :

Singh et al.(2017) attempted through a research work to improve the quality of Bottomash for use as pozzolanic material. The samples were made fine by grinding and physico-chemical, mineralogical and leaching characteristics of original and made samples were studied and compared. On studying the results, it was revealed that porosity, water holding capacity and loss of ignition decreased after grounding. Pozzolanic properties found to be improved after grounding of the samples.

A comparative study was undertaken by **Rattanasak et al.(2009)** regarding the characterization of Flyash and Bottomash geo-polymers. Sodium hydroxide and sodium silicate solutions acted as activators under a mass ratio of 1.5 and under 5,10 and 15M concentrations at 65⁰C for 448 hours. Scanning electron microscope (SEM), Differential scanning calorimeter (DSC), and Fourier transform infrared spectrometer (FT-IR) were used on the prepared geopolymer pastes, and mortar samples were also prepared to test the compressive strength of the samples. The results showed that both Flyash and Bottomash are suitable as geopolymer source material, only the properties of Flyash and Bottomash and the concentration of NaOH are responsible to alter the properties of geopolymerisation. 10M concentration of NaOH was found to be ideal for Flyash and Bottomash gopolymers with compressive strength of 35 and 18 MPa respectively.

Das et al. (2011) had explored the effect of Flyash particle size on mullite content enhancement and glass formation. It was found that the quantity and crystallinity of mullite phase in the Flyash determined the strength increment and stability of Flyash mixed composites. Nanocrystallinity and effect of temperature were investigated on Flyash particles mullite content. Quantitative estimation of mullite content and residual quartz content were done through FESEM, XRD and FT-IR tests. Results showed that finer Flyash (sieved through mesh size 250 holes/cm²) contain more mullite content and glassy phase formation was faster and maximum under 1600⁰C than coarse Flyash.

Saxena et al.(2012) characterised the coal ash for potential end use. Physical characteristics of coal ash sample in the form of bulk density, specific gravity, water holding capacity and PH were determined on as received basis. Mineralogical analysis was carried out through XRD test, particle size analysis was done by Laser diffraction analysis, morphological properties of coal ash sample were determined by FT-IR and SEM. Bottomash samples were found to have larger fused masses of irregular shape, and floatation experiment revealed that +212 µm fraction among the particle sizes had higher carbon content, which was found fit for use as domestic fuel, and the fraction with lesser carbon content fit for brick making, road stabilization etc.

Kumar et al.(2015) had characterized Indian Bottomash from its potential utilization aspect. Comprehensive characterization of Bottomash samples collected from four different thermal power plants were undertaken for bulk density, particle size distribution, settling characteristics, specific gravity, porosity, water holding capacity, permeability etc. parameters. To detect trace metal elements, leaching test was also performed on the samples. Among the most abundant elements, Mn, Mg, Cr, Zn, Ni and Cu were available and Pb, Mo, Fe and Co were the least abundant. Silica and Alumina were found in all primary phases, and quartz, hematite and mullite were found in mineral phases. These constituents of Bottomash made it a solid civil engineering construction material, as concluded from the study.

An assessment of physical properties of coal combustion residues (CCRs) with respect to their utilization aspect was undertaken by **Mishra et al.(2012)**. Various physical parameters of CCRs like water holding capacity, specific gravity, moisture content, permeability, bulk density, Atterberg limits, Proctor test, texture analysis, particle size analysis, proximate

analysis and loss on ignition tests were carried out for all four types of samples collected from four different locations. From the test data, it was observed that on account of higher water holding capacity and lower permeability, those can be mixed with poor soils for ease of plant nutrients movement, low specific gravity could be advantageous for stowing in mines, and due to lower weight, it could serve as ideal backfilling material for road embankments, which would exert low pressure. Road construction was found to be another area of application with tested properties, and it could be used as additive with clayey soil for brick making.

Patel et al.(2013) had undertaken an assessment study on sand and pond ash under Indian context. Physical parameters like sieve analysis, specific gravity, fineness modulus, water absorption and bulk density values for both sand and pond ash were evaluated, and chemical composition was also evaluated. On comparison, it was concluded that properties of pond ash were comparable with that of sand and within the limit specified by respective IS Codes, and hence suitable for use.

2.4 Sand exploitation scenario :

Gavriletea et al.(2017) had studied about the environmental impact of sand exploitation in connection with the sand market. With respect to the limited sand resources, illegal sand mining and resultant environmental effect had been explored with recommendation of sustainable methods and ways of mining under the ambit of law and its enforcement.

Bruce Edwards et al.(2015) had tried to focus upon the true picture on sand availability and failure to cope up with rising demand globally in a report. With an exponential increase in sand extraction without any regulation to monitor and restrict, the damage to the environment is certain.

Pitchaiah et al.(2017) had reviewed the impact of sand mining on environment. The illegal and mindless sand mining across the globe had been observed to be a potential threat to the environment. River course distraction, food web change through agricultural disturbances due to water table lowering, flood occurrence chances, destruction in marine habitats etc. happened due to such sand extraction without replenishment scope.

UNEP (2014)ad presented one grim picture about the fast depletion rate of sand and its rarity beyond considerations. The impact of high volume extraction on river delta and coastal area and also marine eco-system was discussed in the article. The over dependence on this natural mineral once again be cited in the paper, and an alternative route as well as proper legislation to stop such extraction were also highlighted.

Hemalatha et al.(2005) had presented the grim picture out of sand mining in the state of Karnataka. She had described about the extraction up to the bottom level resulted failure in irrigation wells in riparian areas. It was suggested to impose a penalty tax to compensate the farmers against their loss incurred due to failure in irrigation well out of sand extraction consequences.

2.5 Sand alternatives and application in Concrete and Mortar :

Gardner et al.(2016) had investigated the performance of manufactured sand or stone crusher dust on 100% fine aggregate replaced concrete. The manufactured sand was characterized for its physical and mineralogical properties, and their influences on the workability and strength of concrete was modelled by using artificial neural network (ANN). It was revealed from the experiment that manufactured sand concrete required higher water-cement ratio to maintain the same degree of workability like that by sand mixed concrete. That shortcoming could be addressed by adding water-reducing admixtures, and the strength also found to be increased. ANN predicted model was found to be useful for determining strength and workability of manufactured sand mixed concrete. It was also concluded that use of such models could eliminate length laboratory trials to select an appropriate mix design and to establish the properties of fresh and hardened concrete.

Futane et al.(2016) had investigated with Flyash, m-sand and rubber crumb as partial sand replacement in M-20 grade concrete, due to the scarcity of fine aggregate. Different percentage replacement of sand by the above mentioned alternative materials were done and observed that mixture of Flyash and m-sand up to 30% replacement of sand produced good strength concrete. Other combinations produced mixed result with loss in workability etc.

Effect of fine aggregate replacement by Flyash in concrete was investigated by **Siddique (2003)**. The mechanical properties of the concrete was evaluated as an effect of such

replacement. Class F Flyash was utilized as sand replacement material in five percentages viz. 10, 20, 30, 40 and 50% by weight. Splitting tensile strength, flexural strength, compressive strength and modulus of elasticity parameters were tested at 7,14,28,56,91 and 365 days of maturities respectively. The maximum values of splitting tensile, modulus of elasticity, flexural and compressive strength were obtained at 50% replacement and at all ages, though after 28 day's of maturity, the strengths increased significantly. It was concluded out of the experimental results that Flyash could be used conveniently for structural concrete.

Deo et al.(2010) had carried out one long term comparative study on concrete mix design with replacement of fine aggregate by Flyash. Minimum voids method and maximum density method were used for the study. It was observed that increase in compressive strength to the tune of 20% and increase in flexural strength in the order of 15% were obtained in the Flyash blended mix than the controlled concrete. The addition of super-plasticizer @ 0.5% by weight of cement could enhance the above stated strength parameters by 30% and 20% respectively with respect to the controlled concrete. Minimum voids method of mix design could give higher result than that by maximum density method. On the basis of experimental results obtained, correlations were developed to predict compressive strength, flexural strength, cost per N/mm², slump and dry density for sand percentage replaced by Flyash. From the experimental results, finally it was concluded that by following minimum voids method, Flyash could be conveniently used as partial replacement of sand in structural concrete.

Rajamane et al.(2007) had developed a predictive formula to determine the compressive strength of concrete with Flyash as sand replacement material. The 28 day compressive strength of Flyash concrete could be estimated by the suggested equation, which was based on cementing factor "k" of Flyash. Different replacement percentage of sand was also considered in the equation. The suggested prediction formula could be used to modify any cement concrete mix so that the concretes with and without sand replacement by Flyash had similar strength.

Rajamane et al. (2013) observed that sand can be substituted by fly ash in cement concrete mix. This type of concrete has lower density and other advantages. Further analysis suggested that such concrete possess more strength efficiency and energy efficiency than

ordinary concrete. It was revealed through tests that up to 60% sand replacement is possible without compromising workability and strength requirements of concrete.

ArunaKanthi et al.(2014) studied the effect of partial replacement of sand by Flyash in concrete. The design mix concrete with proportion 1:1.58:3.2 and w/c ratio of 0.48 was developed, within which sand was replaced by Flyash in increasing order of 20, 40, 60, 80 and 100% respectively. The workability was constant at all stages of replacement. Compressive strength, split tensile strength and modulus of elasticity were evaluated at 7,14 and 28 days. From the experimental results, it was found that the workability level was compromised in comparison with mix with sand. Both the strength parameters were found increasing up to 40% replacement of sand by Flyash, and decreasing beyond that. The modulus of elasticity increased up to 60% replacement level.

Demirboga (2003) had studied the effect of cement replacement by Class C Flyash and blast furnace slag on thermal conductivity of mortar and cement paste. Influence of these mineral admixtures on density, water absorption and compressive strengths at different maturity period were also recorded. Reduction in thermal conductivity on account of Flyash and slag were found to be 54 and 21% for mortar and 60 and 31% for cement paste. Sand increased thermal conductivity in cement paste by 83%. Flyash and slag addition decreased compressive strength and increased water absorption values respectively.

Ramesh et al.(2013) had explored with furnace slag and welding slag as waste raw material for replacement of sand in concrete in different percentages of 5%, 10% and 15%. Physical and chemical analysis for both type of slag was done. Mix design for M 25 grade of plain concrete was prepared according to Indian standard code of practice. The compressive strengths at 28 days with 5% and 10% sand replacement by slag was found to be 41 N/mm² and 39.7 N/mm² respectively. These replacement ratios with welding slag and furnace slag was recommended for attaining such higher strength value.

Copper slag as partial sand replacement material in concrete was tested by **Madheswaran et al.(2014)**. Copper slag was initially tried as mortar in brickwork, and found to be good to use up to 50% sand replacement ratio for plaster in flooring and horizontal surfaces, and up to 25% replacement for vertical surfaces, except on ceiling surfaces. Corresponding to the control concrete strength of 35 MPa, 50% replaced sand by copper slag concrete produced

concrete of same mix with 43 MPa. Based on the results obtained, it was concluded that up to 50% replacement of sand by copper slag for conventional concrete was possible, whereas for higher strength concrete, this replacement was found possible up to 75%.

Sangoju et al.(2017) evaluated the durability aspect of concrete made up of river sand and manufactured sand. To evaluate the comparative parameters of such prepared concrete, rapid chloride permeability test, rapid chloride migration test and accelerated carbonation tests were done after 90 days of curing. These tests were selected from chloride attack and carbonation points of views. Analyzing the test results, it was concluded that concrete prepared with manufactured sand was found more durable than concrete with river sand.

Bhadoriya et al.(2015) explored about the effect in mechanical properties of concrete mix by partial replacement of cement with Flyash and sand by marble dust and stone dust. Cement was replaced by Flyash in two percentages viz. 25% and 35%. Sand was replaced by marble dust and stone dust by 30 and 40%. By recording the properties of fresh concrete and hardened concrete, it was found that the concrete mix with 25% Flyash (as equivalent percentage of cement in the control concrete) and 30% marble dust and stone dust as replacement of sand produced concrete of comparable value, and the compressive strength values were only lower by 3-4% than the control concrete.

Use of Flyash and marble powder in self-compacting concrete was done by **Pala et al.(2015)**. By using these two waste products, flowability of concrete was explored for application in congested reinforcement area. Target mean strength was achieved by 10% marble powder and 25% Flyash substituted concrete mix. It was also observed that increase of marble powder increased the slump value.

Dinakar et al.(2017) had explored the performance of Flyash waste lightweight aggregate in the lightweight concrete mix design. From the experimental investigation, it was found that sintered lightweight aggregate concrete was produced with 28 and 70 MPa strength and air dry densities of all concrete samples were maintained below 2000 kg/m³ mark. A new water-cement ratio correlation was established for the development of sintered Flyash lightweight aggregate concrete. The tensile strength values indicated that those were suitable for structural applications.

Sankh et al.(2015) had reviewed the various alternative to sand in the concrete mix. Copper slag replacement resulted improvement in compressive strength, flexural strength and tensile strength. Up to 40% replacement, strength improvement occurred and beyond that, segregation and bleeding resulted. Increase in compressive strength of mortar occurred with inclusion of ground granulated blast-furnace slag as alternative to sand up to a level of 75%. Optimum replacement percentage by washed bottom ash was observed to be 30% for adequate strength improvement in concrete. In case of quarry dust alternative, it was reported that replacement percentage for enhanced compressive strength was 55-75%. 100% replacement of sand was made possible by mix of stone dust and Flyash. Improvement in compressive strength and flexural strength in concrete was observed, while foundry sand is partially replaced by normal river sand. Crushed waste sandcrete block (CWSB) was used as partial replacement of sand, and up to 50% replacement of normal fine aggregate was adequate for concrete strength up to 30 N/mm². Crushed spent fire brick (CSFB) was used as sand replacement, and found that up to 25% level, strength was adequate, beyond which, there was no improvement. Another industrial waste like sheet glass powder was observed to add strength gain (compressive) and tensile strength reduced for all percentages of addition. The optimum level found was 10%.

Bahoria et al. (2013) had reviewed various by-products and recyclable materials as sand replacement in concrete. Various by-products like screenings, sheet glass powder, crushed granite fine, spent fire brick, crushed rock flour, coal combustion by-products, municipal solid waste bottom ash, bottom ash, olive oil waste (husk) and burnt husk (ash), and incinerated sewage sludge ash were used as alternative to sand in concrete. It was concluded that screening could be used, where durability was not the main criteria. Sheet glass powder blended concrete showed improved tensile strength. Crushed fine granite could be used up to 20% replacement of sand in concrete, used for rigid pavement construction. Spent fire brick crushing could be equivalent to Zone-II Sand, and maximum strength achieved at 25% replacement of sand. Sand was replaced with favourable result up to 40% replacement of sand by crushed rock flour. Flyash as partial replacement material in cement, brick making, and road construction works already proved. Ground waste glass also found to be a favourable material as sand alternate. Incinerated sewage sludge ash was proposed to be used in automated aerated concrete block. Calcium silicate brick was manufactured with crushed building demolition waste in place of sand with favourable result. Bottom ash replacement also produced favourable result.

Parvati et al. (2013) had carried out a feasibility study for sand replacement by Flyash in concrete, and performance under elevated temperatures. The replacement was done in 10% stages, starting from 0 – 80%, and at elevated temperatures of 200, 400, 600 and 800°C. Compressive, tensile, Flexural and Shear strengths were evaluated. All the strength parameters were observed to improve up to 40% replacement and at 200°C. Strength parameters were found maximum at that replacement percentage and for 400, 600 and 800°C elevated temperatures. Slump values though reduced with increasing percentage replacement of sand by Flyash, the same could be improved by super-plasticizer addition.

Sukesh et al. (2013) had attempted to use quarry dust to replace sand partially in concrete. Up to 20% replacement level, compressive strength of such quarry dust blended concrete was found to be increased, but the workability level was compromised.

Demirboga et al. (2007) investigated about the influence of mineral admixtures as replacement of cement on various properties of concrete. Class C flyash, blast furnace slag and their combinations were utilized for replacing certain percentage of cement and the density, water absorption, strength and thermal conductivity of concrete were tested. It was observed that with the replacement of cement by those mineral admixtures, thermal conductivity of concrete decreases, but compressive strength also declines. It was also observed that reduction in thermal conductivity value in case of blast furnace slag replacement was highest than other two combinations.

Dan Ravina et al. (1997) had studied the role of Class F Flyash in properties of concrete as partial replacement of fine sand. It was observed that the workability was reduced with reference to the normal mix (without Flyash in lieu of sand). The water requirement by Flyash blended concrete was observed to be either the same or higher by approximately 9% than the normal mix with sand, and the bleeding rate was also found to be lower in the Flyash mix.

Karim et al. (2011) discussed in this review paper about role of Flyash in concrete and mortar, considering its chemical, mineralogical and physical parameters. It was concluded that in spite of slow rate of strength gain, the Flyash blended concrete and mortar had edge on durability criteria and cost effectiveness.

Deo et al. (2015) studied the effect of partial replacement of sand by Flyash through an extensive mix design procedure. They found that besides maintaining desired strength parameters, the modified concrete was economical too. Based on experimental results, correlation was also developed to predict compressive strength, flexural strength and corresponding cost per N/mm² for percentage sand substituted by Flyash.

Suresh et al. (2013) had studied the feasibility of marble sludge dust usage as sand replacement in concrete. 2.5, 5, 7.5 and 10% substitution of sand was made by marble sludge dust. Compressive strength at 7 and 28 days for all the substitutions showed enhanced strength and SEM image analysis also revealed uniform pore space and hydration, resulting development in adequate strength.

Brito et al. (2018) had reviewed all earlier works done by the other researchers on the environmental impact and toxicity characteristics of recycled concrete aggregates (rca), fly ash (fa), cement production as well as their substitution aspect. The analysis with respect to abiotic depletion potential, ozone depletion potential, photochemical ozone creation, acidification potential, eutrophication potential, toxicity, leachability etc. were considered. It was revealed that environmental impact and cost of concrete reduced considerably with such incorporations, and also requirement of landfill space reduced drastically. While incorporated in concrete, the leaching metals which were otherwise present in fly ash were also found diminished.

Rafieizonooz et al. (2017) had studied the toxicity parameters and durability aspects of concrete blended with coal ash as replacement of cement and sand were studied. Concrete mixes with various replacement percentages of sand by bottom ash and ordinary Portland cement by fly ash with fixed percentage were prepared and tested for toxicity characteristics leaching procedure, sulfate and acid attack and elevated temperature effects. All the tests revealed satisfactory results without any adverse effect, and recommended to be useful as replacement of clean construction materials.

Rafieizonooz et al. (2016) had investigated about usage of bottom ash and fly ash as replacement of sand and cement respectively in concrete mix. Concrete mixes were made with 0, 20, 50, 75 and 100% bottom ash by replacing sand, and 20% flyash as partial

replacement of ordinary Portland cement. After analysing fresh and hardened conditions of blended and control concrete specimens, it was found that till 28 day's of age, no considerable change in strength parameters took place, except reduction in workability with enhance addition of bottomash. After curing till 91 and 180 days, strengths were found higher for both control and blended concrete samples. Drying shrinkage in samples with 50, 75 and 100% bottomash were found lesser than control mix. The usage of both the varieties of coal ash were recommended satisfactorily.

More et al.(2015) observed that the bottom residue in thermal power plant's ash collection system was having coarser particles. The replacement of sand in concrete by this pond ash was tried in 0, 5, 10, 15, 20, 25 and 30%, and the workability and other strength parameters like compressive strength, tensile strength, and flexural strength were evaluated. The results were found advantageous and it was concluded that the replacement could be made without any negative impact.

Ganesh et al. (2011) was exploring about alternative to sand , and observed that pond ash, could be utilized in mortar and concrete. With that objective, its various properties like shape, gradation, grain diameter, texture, physical, morphological and chemical properties were studied to find out the similarity with that of sand. Observing the favourable parametric values, it was recommended as a suitable alternative to sand for use in concrete and mortar.

Arumugam et al. (2011) explored about the possibilities of utilization of pond ash in cement concrete mixture. The percentages of replacement fixed at 0, 20, 40 and 60%. It was observed that density reduced with increased percentage of pond ash, and compressive strength values increased with increased period of curing. Split tensile strength and flexural strengths were found increased up to 20% replacement, and with increasing percentages of pond ash replacement, workability found reduced.

Rafat Siddique (2014) had studied various waste by-products, their physical and chemical properties and final performance of their blending in concrete as fine aggregate alternative. Waste foundry sand (wfs), coal bottom ash (cba), cement kiln dust (ckd) and wood ash (wa) were selected for study. After carrying out the experimental tests, it was concluded that cba was the most suitable material, followed by wfs and ckd, though the workability criteria were not favourable.

Akbari et al. (2015) studied about geo-polymerization of coal fly ash to utilize the same as binder in lieu of cement in concrete and mortar. Coal fly ash sample was used in a chemical process to develop geo-polymer binder. Mortar and concrete samples were prepared cement free with the help of adding this newly developed geo-polymer. On 60th days of maturity, mortar and concrete strengths were found to be 46 MPa and 40 MPa respectively. It was concluded that with the help of such geo-polymer binder, cement linked greenhouse gas emission burden could be reduced drastically.

Usability of brown coal fly ash was explored by **Gamage et al.(2013)**. Brown coal fly ash samples mixed with cement, lime and aggregate to produce mortar and concrete. On testing its compressive strength, it was observed that those might be suitable for use as mortar. With 30% cement and fly ash content up to 70% (maximum), the minimum desired compressive strength value of 5 MPa at 14 days maturity could be achieved. With increased cement content, the strength also found to be increased, but at carbon footprint cost. It was recommended to further test the durability aspect and thermal properties of such mix.

Sorption and sorptivity characteristics of air-entrained concrete was investigated from durability point of view by **Ramamurthy et al.(2007)**. The moisture movement through such concrete depend upon the filler type, material and composition. Flyash in different percentage replacement of sand was tried in the mix and sorptivity was studied. It was concluded that sorption depended upon filler type, density, pore structure and permeation mechanism. Water absorption and sorptivity of foam concrete were found lesser than the base mixes without ash. They found decreased with increasing foam content.

Konstantin Kovler (2012) had tried to explore about the toxicity characteristics of coal fly ash in concrete construction. Analyzing the experimental results. It was observed that radon exhalation rate of concrete containing flyash were higher in some occasions than the reference concrete, but the radon emanation co-efficient was found lower. Since standards which control radioactivity in building materials did not mention about radon emanation co-efficient value, the same might create confusion in free use of flyash in concrete, which required to be addressed properly.

Yu et al.(2017) explored the mechanical properties of green structural concrete with ultra-high volume flyash (uhvf). From the earlier works, it was observed that such concrete with uhvf could achieve compressive strength of 40 MPa at 28 days under normal curing condition and without chemical activation. The materials used in this study was Ordinary Portland Cement, Class C / Class F flyash, Silica-fume, Sand, Granite gravel, water and Polycarboxylate based super plasticizer. The cement was replaced by flyash in 20, 40, 60 and 98% respectively. At 80% cement replacement point with water-binder ratio of 0.2, and addition of super plasticizer dosage, the concrete could reach strength of 40 MPa at 7 days and 60 MPa at 28 days respectively. Through this study, it was also established that a small addition of silica fume could enhance mechanical properties and also sorptivity performance. Such concrete could reduce carbon footprint considerably.

Chousidis et al. (2016) presented the results from an experimental study to show the influence exhibited by the chemical properties of flyash on physico-mechanical and chloride penetration aspects of concrete. Two types of flyash were used with 5% and 10% cement replacement. Half-cell potential and corrosion current tests were performed to see the reinforcement mass loss and other strength tests like compressive strength, tensile strength, porosity and modulus of elasticity were undertaken. XRD patterns and SEM images coupled with EDX analysis were also recorded. The performance of hardened concrete revealed that CaO, SiO₂ content of flyash and its fineness, free lime and sulphate ions played vital role. Durability property of concrete found improved with higher SO₃ and CaO contents in flyash, but flyash with clay content showed lesser chloride penetration resistance and strength.

Chousidis et al. (2015) presented the effect of Greek flyash as partial replacement material of cement on durability and mechanical properties of reinforced concrete. The flyash was added at 5% and 10% w/w ratio of cement, and such samples were partially immersed in 3.5% w.w NaCl solution. The anti-corrosive effect on account of flyash addition was measured with the help of calculations to determine open porosity, sorptivity, chloride concentration and mass loss in steel reinforcement embedded in samples. The experimental results revealed that compressive strength and elastic modulus of concrete improved for all ages of curing. The porosity and sorptivity parameters decreased in comparison with control concrete sample, and loss of steel on account of corrosion was found to be equal to that in control concrete after 13 months of exposure under NaCl environment.

Chahal et al.(2012) had investigated through experiments the effect of bacteria on the physical strength, water absorption and chloride permeability of Flyash blended concrete. Cement was substituted by Flyash at 10, 20 and 30%, and *Sporosarcina pasteurii* bacterias were added in three cell concentrations viz. 10^3 , 10^5 , 10^7 cells/ml respectively. Test results at 28 days indicated that compressive strength was enhanced up to 22% (maximum), porosity and permeability got reduced by the inclusion of *S. pasteruii* by four times than the conventional concrete mix without Flyash and bacterium addition. Reduction in chloride permeability was almost eight times. Hence addition of *S.pasteruii* in Flyash blended concrete was found advantageous.

Hwang et al.(2004) had developed one predictive model for compressive strength of Flyash concrete. The predictive equation was developed by the researchers on the basis of experimental results obtained. In the form of a developed co-efficient to express Flyash as binder as a function of age of curing, flyash percentage and Blaine's specific surface area. The equation could explain the early strength while sand substituted by Flyash, and reduction in early strength when cement was substituted by Flyash, the increase in strength during extended time period on account of pozzolanic reaction and the relationship between flyash replacement ratio and the ratio of strength increase / decrease respectively.

Sata et al. (2015) had explored the effect of Flyash as geo-polymer binder and Bottomash as coarse aggregate to produce pervious concrete. With pozzolanic property in Flyash, the same was used as geo-polymer binder with partial replacement of cement, NaOH addition and enhanced curing temperature (90^0C) etc. were all investigated. Results showed that compressive strength of pervious geo-polymer concrete was increased on account of combined effect of NaOH addition, elevated temperature, and Ordinary Portland Cement substitution. Due to perviousness, thermal conductivity value was found as 0.30-0.33 W/m.K, density in the range of 1466 – 1502 kg/m^3 , and compressive strength to the order of 5.7 – 8.6 MPa.

Aggarwal et al. (2014) studied the effect of waste foundry sand and Bottomash in equal quantities for partial replacement (0-60%) of fine aggregate in concrete mix. Mechanical strength parameters and durability aspects of such blended concrete samples were tested. It was observed that water content was required to increase gradually up to 60% replacement, and the mechanical strength for all the mixes up to 50% replacement were found comparable

with control concrete values, including the maximum value obtained at 30% replacement level. The morphology of such mixes due to above stated blending did not alter the inner structure considerably.

Properties of special concrete manufactured with washed Bottomash (wba) as partial sand replacement was explored by **Sani et al. (2010)**. The Bottomash was kept submerged fully for 3 days before utilizing the same in concrete to reduce the effect of carbon. At constant water-cement ratio of 0.55, the wba was used in different ratios with respect to sand replacement. The mechanical strength was observed to be maximum at 30% fine aggregate replacement level.

Kadam et al.(2014) had studied the effect of sieved coal Bottomash as sand substitute in concrete with cement percentage variation. M-35 grade concrete was prepared with fixed water-cement ratio of 0.45 and 70% sieved Bottomash+30% sand as fixed fine aggregate and with additional cement content at 5, 10, 15, 20, 25 and 30%. Various mechanical strengths like compressive strength, flexural strength, split tensile strength, density, and water permeability were tested, and maximum strength values were obtained at 20% additional cement mix level.

Shahidan et al.(2016)had experimented with power plant waste coal Bottomash to find out physical and chemical characteristics and compare the same with that of natural river sand. Specific gravity, density, particle size distribution, SEM and XRF analysis were carried out. The porous structure, angular and rough texture of Bottomash resulted lower specific gravity and density values in comparison with sand. It was recommended to use Bottomash as alternative to sand, to be used in concrete.

Abubakar et al. (2013) investigated about the physical parameters of concrete with bottomash as partial replacement of fine aggregate and Flyash as partial replacement of cement. Workability was found to be compromised with high volume of fine aggregate replacement, and the compressive strength values found increased with high volume of Bottomash substitution, but the density values decreased.

Abubakar et al. (2012) experimented with coal Bottomash and Flyash as partial replacement of sand and cement in concrete mix. The replacement percentage fixed at 5, 10,

15 and 20% for both Bottomash and Flyash. The age of compressive strength tests were fixed at 7, 28, 56 and 90 days at fixed water-cement ratio of 0.48. It was observed from the test results that at 56 days age all the mixes achieved the targeted strength.

Rocha et al. (2009) had investigated about the effect of coal Bottomash as a substitute for natural fine aggregate on the fresh properties of concrete. Different tests like setting time, water loss through bleeding and plastic shrinkage were carried out. The porosity effect on water loss was noted. The test results revealed that during initial stage of casting, the mix was susceptible to water loss through bleeding, and with the increase in Bottomash content, the plastic shrinkage ratio decreased. Delay in setting time was also observed.

Lee et al. (2011) had undertaken experimental investigation to find out the suitability of coal Bottomash as coarse and fine aggregate in high strength concrete (60-80 Compressive strength range) preparation. The physical and chemical properties of Bottomash were evaluated. The fine and coarse Bottomash were utilized as replacement of sand and gravel by 25, 50, 75 and 100%. Flow characteristics and density of fresh mixes were noted and compressive strength, flexural strength and modulus of elasticity were evaluated. There was some changes in flow characteristics with increasing percentages of Bottomash and the influence on flexural strength values were more than on compressive strength values.

Strength properties of concrete with coal Bottomash as manufactured sand (m-sand) replacement materials were investigated by **Soman et al.(2014)**. The target grade of concrete was M-30 at fixed water-cement ratio of 0.45, and the m-sand replacement by Bottomash was fixed at 10, 20, 30 and 50% respectively. To obtain a fixed workability, superplasticizer was used at 0.40 for control mix (without Bottomash), and 0.45, 0.50, 0.60 and 0.70 for Bottomash substituted mixes at the above mentioned percentages respectively. From the compressive strength test results at 3 days, 7 days and 28 days, the values found lower than the corresponding control mix values, but the target mean strength for M-30 grade was achieved at 30% replacement level. Hence, it was concluded that utilization of Bottomash in place of m-sand could be made.

Singh et al. (2016) had explored about the effect of Bottomash as sand replacement material on workability and strength properties of concrete. Two designed mix of 38 MPa and 34 MPa strength varieties were prepared under “A” and “B” nomenclatures respectively. In

both grades, sand was replaced by Bottomash in 20, 30, 40, 50, 75 and 100% stages. On observing freshly produced concretes with such proportions, it was noted that workability and bleeding resided with increasing percentages of replacement. Further, it was noted that while Bottomash replaced sand with fineness modulus of 1.97 in “A” category mix, compressive and splitting tensile strength did not change significantly in comparison with control concrete. In category “B”, sand with fineness modulus value of 2.58 while replaced by Bottomash by above percentages, the strength parameters found reduced at early curing age, but at 90 days, it was found comparable with control concrete. Bottomash mixed concrete showed lower modulus of elasticity and at enhanced age, abrasion resistance value improved. Overall, Bottomash blended concrete was recommended for utilization.

Singh et al. (2015) had tried to evaluate properties of concrete made with high volume of Bottomash as fine aggregate. Laboratory tests were undertaken to find out the suitability of coal Bottomash as substitute of river sand in concrete at the percentages of 0, 30, 50, 75 and 100. From the obtained test results, it was observed that the compressive strength and pulse velocity values were not affected. Water absorption varied between 4.68 and 5.56% at 28 days age, and with increased age, it showed reduction in permeable pore spaces and water absorption. Bottomash blended concrete samples showed lesser abrasion resistance than controlled one, which decreased with age.

Singh et al. (2014) had carried out experimental tests to find out the suitability of coal Bottomash as partial replacement of fine aggregate in concrete. The properties evaluated include unit weight, compressive strength, split tensile strength, modulus of elasticity and micro-structure of concrete with coal Bottomash and compared with conventional concrete with sand. Workability and loss of water decreased with increasing percentages of Bottomash. Compressive strength at 28 days were not affected but at 90 days age, the strength surpassed that of conventional concrete with sand. Split tensile strength values were found increased at all ages and modulus of elasticity decreased with addition of Bottomash at all the curing ages. SEM and XRD analysis revealed C-S-H gel structure was less monolithic than that of controlled concrete and total intensity of ettringite remained constant, even with the addition of Bottomash in all stages.

Siddique, Rafat (2003) had carried out one experimental program to study the properties of Self Compacting Concrete (SCC) made with Bottomash as replacement of sand in three

percentages viz. 10, 20 and 30% respectively. The properties of SCC evaluated include slump, j-ring, v-funnel, u-box and l-box, compressive strength, abrasion resistance, chloride permeability up to 365 days and absorption and sorptivity tests were done at 28 days. On analysing the test results, it was found that the SCC mixes exhibited compressive strength between 25.8 – 35.2 MPa, and very low chloride permeability resistances at 90 and 365 days. Abrasion resistance and sorptivity characteristics were found increased with increase in Bottomash content at a particular age, but got decreased with increase in age.

Maliki et al. (2017) had tried to ascertain the compressive and tensile strength of coal Bottomash (CBA) concrete. Due to declining sand reserve, and increasing demand from construction industry, CBA was thought of as suitable alternative material, but the usability linked to the strength of concrete. By appearance and from other physical properties, CBA possess similarities and dissimilarities also with that of sand. The percentage replacement of sand by CBA was fixed at 10% intervals, starting from 0 to 100%. Maximum compressive strength attained at 60% replacement and maximum tensile strength attained at 70% replacement ratio.

Kasemchaisiri et al. (2008) had presented the test results of fresh and hardened Self Compacting Concrete (SCC) by incorporating coal Bottomash in the concrete mix as sand substitution by 0, 10, 20 and 30% respectively. It was observed that the addition of Bottomash resulted reduction in compressive strength and increase in porosity in the hardened concrete. Chloride penetration, carbonation depth, drying shrinkage, sulphate resistance etc. were also increased with enhanced percentages of Bottomash in SCC. Overall, the 10% replacement was suggested for Bottomash blended SCC.

Kannan et al. (2017) had studied the effect of coal bottom ash on mechanical properties of concrete. The coal Bottomash was substituted in place of sand by 0-50% at regular interval of 10%. The compressive and flexural strength values showed declining trend with each percentage addition of Bottomash, but split tensile value was found improved in comparison with controlled concrete value.

Dinesh Kumar et al. (2016) had experimented with coal Bottomash in concrete mix, as sand replacement material and to compare the physical strengths. The sand component in M-25 grade concrete mix was substituted by Bottomash in 0, 10, 20, 30, 40 and 50%

respectively. Compressive strength and split tensile strengths were observed to be highest in 20% replacement ratios, beyond which the values started falling.

Dilip Kumar et al. (2014) tried to study the properties of blended concrete of grade M-30, prepared with Ordinary Portland Cement of 43 grade, Bottomash from NTPC, Anpara plant, local sand and aggregate. The sand was substituted in the mix at 10, 20, 30, 40 and 50% by Bottomash and strengths were measured at 7, 14, 28 and 56 days of maturity. On comparing the test results, it was revealed that at all substitutions and all ages of maturities, compressive and flexural strength values were more than that of controlled one.

Use of unprocessed coal Bottomash as sand alternative in structural concrete was investigated by **Cadersa et al. (2014)**. Experiments were undertaken for sand replacement at 20, 30, 40, 60 and 80% by unprocessed Bottomash. Results indicated workability and plastic density decreased with increase in Bottomash. It was also observed that beyond 40% replacement level, compressive strength, flexural strength and modulus of elasticity decreased sharply. Increase in Bottomash percentage improved drying shrinkage performance of the concrete. The optimum percentage for replacement of sand was observed to be 20%.

Balasubramaniam et al. (2015) investigated about the mechanical properties of Bottomash blended concrete. Manufactured sand (m-sand) was used as total replacement of natural sand, cement was substituted by silica fume at 10%, and coal bottom ash was utilized at 10, 20, 30, 40 and 50% replacement of m-sand in the concrete mix. Mechanical properties like compressive strength, flexural strength and modulus of elasticity were analyzed and it was concluded that strength properties improved at later ages.

Ertug Aydin (2016) had explored about the potential use of coal Bottomash waste composites through literature survey. As reported in the literature, the physical, mechanical and sulphate test results indicated that final products were suitable for the use of manufacturing of construction materials. Incorporation of 70% coal Bottomash in a pure cement matrix found suitable for alternate cement materials with higher performance.

Aggarwal et al. (2007) presented the experimental investigation on Bottomash for replacing fine aggregate. Compressive strength, flexural strength, splitting tensile strength etc. all were

studied. The various percentages for replacement were in the range of 0 – 50%. Workability and density values decreased with increased percentage of Bottomash. All the strength parameters found decreasing during 28 days age of maturity, and beyond that period, strengths were following increasing trend.

Hardjito et al. (2010) presented the results of parametric study on mechanical properties of Flyash based geo-polymer mortar with Bottomash as replacement of sand. The mortar samples were prepared without cement, but with Flyash added with K_2SiO_3 and KOH solutions, which were basically some alkaline activator and Bottomash in replacement of sand. From the various proportions, it was observed that maximum strength could be produced with 10% Bottomash in place of sand, and also at the elevated temperatures of $1000^{\circ}C$.

Ramadoss et al.(2014) investigated about the suitability of Bottomash as replacement of fine aggregate in masonry mortar. Among the various percentages tried, 20% replacement was found optimum from the point of view of mechanical parameters. Durability test also corroborated earlier findings by other researchers.

Baboo Rai et al.(2014) carried out experimental investigations on mortars, modified with quarry dust and Flyash in different ratios as substitute of sand and cement respectively. The compressive and transverse strength results revealed better order due to micro-filling and pozzolanic activities by the two substitutes.

Mustafa et al.(2006) assessed the self-compacting properties of mortars with various mineral additives and chemical admixtures. Four mineral additives like Flyash, brick powder, limestone powder and kaolinite were used to produce Self Compacting Mortar (SCM). Besides, three superplasticizers and two viscosity modifiers were also used. Workability, setting time and hardened properties of mortars were evaluated. It was observed that Flyash and limestone powder mixing increased workability and setting time was increased by Flyash influence alone, which could be adjusted by the ternary mix of Flyash and limestone powder. Brick powder and kaolinite adversely affected workability criteria. When part of cement was replaced by mineral additives, reduction in strength was resulted.

Herrera Duran A et al.(2016) had studied the thermal conductivity effect by introducing a novel co-polymer on ordinary Portland cement - Class F Flyash combination mortar with water reducing super-plasticizer. Mortars were made with three different water-binder ratios to arrive at an optimized ratio to reach a target 3.4 MPa compressive strength as per Mexican Standard for non-structural masonry constructions. The reduction in thermal conductivity to the tune of 33% exhibited identical result by commercially available cellular concrete. Beneficial contribution by fly ash in the mixture was established and also confirmed consistent thermal conductivity versus density correlation.

Thaarrini et al.(2015) proposed to utilize ground bottom ash in geo-polymer mortar. Influence of alkaline activator Molar ratio and curing mode on compressive strength of such mortars were studied. With different molar ratio with different activator, improvement in compressive strength was observed under both ambient curing and steam curing atmospheres respectively.

Kwon et al.(2013) had studied the engineering properties of two varieties of pond ash or Bottomash. Cement mortars with three different w/c ratios and three replacement ratios of sand were prepared for study. Flow-ability, setting time and compressive strength tests were performed. Some more durability tests like carbonation, chloride penetration etc. were also studied. Without high water reducing agent, both the pond ash varieties showed decrease in compressive strength. Sample saturation was observed to be necessary for better hydration and improved physical strength and durability aspects.

Kim et al.(2015) had experimented with sieved and ground coal Bottomash in high strength cement mortar. The Bottomash powder was observed to increase the workability than the equivalent mortar made of cement and fly ash. Hydration of mortar also increased and compressive strength at 3 days and 28 days improved in comparison with Flyash blended mortar.

Brake et al.(2017) had explored the re-usability of coal Bottomash as cement replacement in mortar. The Bottomash was made pulverized and the effect on workability and setting time were studied. Improvement in micro-structure of cement mortar could effectively increase the strength parameter of such product with lower Ca/Si ratio, as observed.

Gencel et al.(2015) had investigated Flyash as constituent fine aggregate material for mortar. Various physical and mechanical parameters like flow-ability, unit weight ultrasound pulse velocity, compressive and flexural strength, modulus of elasticity, stress-strain relationship etc. tests were performed on mortars. Up to 70% ratio of Flyash, mortar was found acceptable without considerable property change.

Aydin et al. (2017) investigated about the effects of high volume of Flyash in cement mix for low strength applications. Wide ranges of slump values were recorded in this study. Predictive correlations between pore volume and physical parameters showed higher R^2 value. Supplementary cementitious material in the mix was optimized and physical and mechanical properties were evaluated. The model can be followed for low strength application of cement paste by incorporating supplementary cementitious materials in the mix.

A review of available literatures on the application aspect of Coal Bottomash (CBA) in building industry had been done by **Sadon et al.(2017)**. The properties of Bottomash were analysed and use of the same in different proportions in concrete were tried by various researchers. The summary of the review works on CBA by the authors was based on physical and chemical properties and application of CBA in building construction. It was observed to be a well graded material with sp. gravity range between 1.39 – 2.98, and thermally stable with loss on ignition 2% - 8%. Slump loss in increasing percentage of CBA in the mix was observed due to extra fineness of particles and the related demand for water to maintain constant workability. Though the early strength gain was slower than normal concrete with sand, CBA mixed concrete was found to gain higher strength at the age beyond 28 days, due to pozzolanic action by CBA particles.

Ramamurthy et al. (2010) had presented the work on utilization of coal Bottomash as coarse aggregate through pelletization. The raw Bottomash was not found suitable for direct pelletization due to its inherent coarseness. To increase the pelletization efficiency and strength of the pellets, different clay binders and cementitious binders were trialled. Addition of Ca(OH)_2 improved the pelletization efficiency, reduced the duration of operation, and reduced the binder dosage. For aggregate with clay binders, cementitious binders, Ca(OH)_2 dosage, the pelletization was ideal.

Brito et al. (2017) had presented an overview on the mixed influence of re-cycled concrete aggregate (RCA) and Flyash (FA) with higher quantities on concrete. The concentration was given on fresh and hardened properties of concrete, where fine and coarse particles of RCA had been utilized as full or partial replacement of fine aggregate and the FA acted the role of binder. In the majority of earlier studies, it was revealed that FA up to 40%, the compressive strength of FA-concrete at 90 days maturity was either higher or at least equivalent to normal concrete in 28 days. For higher incorporation of FA percentages, reverse trend was observed. In EN 1992-1-1, the strength criteria of normal concrete was found based on 28 days age, but for FA concrete, the period was not adequate. This study recommended that strength of FA concrete should be decided on 90 days of maturity. It was observed in the study that incorporation of RCA increased shrinkage effect in concrete, and the reverse effect was observed in case of FA incorporation. It was revealed that both FA and RCA incorporation increased the carbonation depth of concrete. In general, it was observed that up to 30% RCA addition, significant concrete property alteration was not affected, but addition of FA around 20-25% increased the mechanical strength of concrete. Observing the properties like mechanical strength, carbonation depth, durability characteristic and drying shrinkage of concrete, RCA incorporation up to the percentages 0-35% were more or less steady.

2.6 Embodied energy, Insulation and Cool Roof :

Bribain et al. (2011) had undertaken life cycle assessment of building materials. The assessment of building materials included energy requirement at production stage as also during utilization stage, based on which selection of appropriate material could be made for obtaining true energy efficiency.

Monahan et al.(2011) had undertaken embodied and carbon analysis for modern construction methods, adopted in housing. It was found that concrete was having 51% more embodied carbon than offsite panelised timber framed house. Some suggestions were made to save embodied carbon like selection of sustainable materials by cement substitute, thermal storage consideration, waste minimization at on-site location etc.

Thormark et al. (2002) investigated about the total energy use in low energy building including embodied energy of materials, operational energy during effective usage period and recycling at the end of life. It was found in one of the most energy efficient building that embodied energy content was 40% of total energy and recycling potential was 15% of total energy, so it was advisable to address such potentialities adequately.

Lacouture et al. (2009) explored about the selection methodology for appropriate building materials on the basis of LEED based Green building rating system in Columbia. The system in Columbia is highly dependent on use of material with low VOC content, and a high content of recycling potential, influenced by cost aspect.

Pajchrowski et al.(2014) had compared four types of constructions with different material compositions from Life Cycle Analysis point of view and concluded that the building with lesser electrical energy demand was more environmentally beneficial, even though the building may not be passively oriented or designed.

Lawrence et al.(2015) had made a study with renewable bio based materials to reduce embodied and operational energy in the buildings. Straw-bale/ straw-clay/ hemp-lime constructions, sheep wool as insulation material etc. were explored as materials with above two advantages.

Asdrubali et al.(2015) had tried to find out an alternative insulation material other than petroleum based polystyrene or glass / rock wool which were actually high process energy based materials. It was explored that organic plant based by-products and residues and recycled materials could be the viable alternative against the conventional commercially available highly energy intensive EPS/XPS insulation materials.

Yukseket al.(2015) explored the selection of energy efficient materials in designing energy efficient buildings. The embodied energy content and embodied CO₂ equivalent of commercial insulating materials also analysed before selection. Natural materials like wood, gypsum mud bricks, pumice, perlite, cellular concrete etc. were assessed on parameters like local availability, recycle content, renewable source, consuming low energy at site, low thermal conductivity etc. and found to be more advantageous from energy efficiency as also from environmental sustainability point of views.

Pennacchio et al. (2017) experimented with hemp and sheep-wool semi-rigid panel, which were tested as thermal insulation as well as acoustic purposes respectively. The test results for both the parameters were found more than satisfactory and fit to use.

More et al. (2014) had tried to analyse embodied energy of various building materials, and concrete mixes from other research works. It was observed that cement had the highest amount of embodied energy content in a building construction, followed by bricks, aggregates etc. It was concluded through the study to increase use of flyash in building construction by way of using flyash brick etc. to check the overall embodied energy of building under control.

Dixit et al. (2017) had worked with 21 common building materials and found an improved Input-Output (IO) based hybrid model for accurate result. To calculate embodied energy of building materials, IO analysis with the help of economic data is useful. Analyzing the relationship of the cost and embodied energy of a building, a strong and positive correlation could be established. However, it was observed that when analysis was done at the material level, the correlation weakened.

Mani et al. (2017) had examined the embodied energy, operational energy and life-cycle energy of 27 dwelling units, spread across four different Climatic zones of India. With the accessibility of modern transportations, energy intensive construction materials are available in rural areas also, and the life-cycle energy values remain within the range of 0.77-4.05 GJ/m².

Arumugam et al. (2014) had studied the effect of cool roof for an un-conditioned institutional building under Composite Climatic condition in India. Monitoring the effect of cool roof condition on a concrete surface for six months, it was observed that seasonal average air temperature was reduced by 1.07° C, and average heat flux reduction was around 14.4 W/m². Around 8% increase in adaptive comfort hours effected in comparison with dark roof.

Role of cool material in arresting heat transmission through roof was explored by **Costanzo et al. (2013)** in an existing office building at Southern Italy. Simulation study was carried

out to see the effect of cool paint on roof area from energy saving and thermal comfort points of views.

Akbari et al. (2013) had studied the effect of increasing the albedo of roofs of Greater Montreal area on air and skin temperature distribution patterns. Performing simulation study during Summer period, considerable reduction in air and skin temperature were predicted in comparison with cool roof effect.

2.7 Environmental impact of materials and Energy Conservation in Building

Butera et al.(2010) had observed that to mitigate the global warming impact, a balancing pathway with low-carbon energy solutions must be in place, applicable equally for poor and rich cities with variations in standards of living. The analysis found the availability of technological solutions to reach the target of such convergence to mitigate global warming phenomena.

Mathur et al.(2018) had described the scope exist under Energy Conservation of Buildings through building design optimization in conformity with Energy Conservation Building Code leading to reduction in air-conditioning load in building. Since the majority of building stock yet to come up, the scope seemed to be bright in keeping India's commitment towards energy conservation and related greenhouse gas emission. Designing of building envelop with optimum energy usage, depending upon the functional requirement(s) had been one of the key area in Energy Conservation Building Code.

According to **Higgins (2006)**, 17% less CO₂ emission to the atmosphere, 14% less primary energy requirement and 4% less mineral extraction effected for production of 1 tonne of concrete by PPC with 30% Flyash in comparison with OPC.

To exhibit higher thermal resistance in building envelop, different insulation materials and cool roof paints are randomly considered by the energy efficient building designers, but the embodied energy content and global warming potential of popularly used insulation materials made of polystyrene, polyurethane, mineral wool, fibre glass etc. are quite high as was found by **Harvey, (2007)**.

Vijayalakshmi et al. (2006) investigated the thermo-physical behaviour of opaque wall materials under the influence of solar radiation. Finite difference mathematical model was

developed and the result was compared with actual test results of different combination wall elements on U-value, Temperature Time Delay and Decrement Factor parameters respectively.

Buddhi et al. (2012), had made comparison between fire-clay brick made construction and ash brick made construction for calculating energy and environment indices. Ash block was found to be better option for heat load reduction and saving of natural resources and environment.

Tae et al. (2016) had investigated the environmental impact of cement manufacturing, aggregate extraction, and transportation of the same for concrete making. Concrete production involve Global Warming potential (GWP), Acidification potential (AP), Eutrophication potential (EP), Ozone Depletion potential (ODP), Photo-chemical Ozone Creation potential (POCP), and Abiotic Depletion Potential (ADP). It was observed that higher the strength of concrete, higher were the GWP, POCP and ADP, but AP and EP were slightly lower. Summarily, Ordinary Portland Cement was observed to have highest GWP, POCP and ADP impact, while aggregate had the most influence on AP, EP and ODP.

Shah et al. (2017) had reviewed the environmental impact role of cement in concrete industry, and remedial measures thereof. It was observed that for production of one tonne cement, required energy content was 4 MJ with CO₂ emission in the tune of 0.89 – 1.1 tonnes. Supplementary cementing materials like pulverized fuel ash (PFA), ground granulated blast furnace slag (GGBS), silica fume (SF), rice husk ash (RHA) etc. are utilized as partial replacement of Portland Cement (PC). According to report by Concrete Centre, UK, Climate Change Agreement performance had been enhanced by cement sector by 44.8% between 1990 – 2010 against the set target of 30%. GGBS replacement could be up to 50% and the curing temperature of 20° C found ideal for best result. PFA concrete also found to be advantageous from structural strength point of view, in spite of slower pace of strength gain at early stage. PFA improves sulphate resistance, reduce chloride diffusion, prevent alkali-silica reaction, and produce less heat of hydration. Each tonne of PFA re-utilized in cement production, avoids 0.9 tonne of CO₂ emission. RHA up to 10% replacement was found beneficial.

Rashad et al. (2015) had observed through a review work that disposal of flyash from thermal power plants was a major incremental challenge from environmental perspective, due to increasing level of ash produce and corresponding decreasing rate of land availability for land-fill. Re-use of high volume of fly ash (HVFA) as cement substitution in building materials was explored. An overview was drawn with respect to utilization of Class F flyash as partial replacement of ordinary Portland cement in conventional paste/ mortar / concrete mixtures etc. Fresh mix properties, mechanical properties, abrasion resistance, porosity, water absorption, chemical resistance, carbonation resistance of mixes with greater than 45% flyash substitution was reviewed. Inclusion of HVFA as cement replacement decreased bleeding, segregation, density, heat of hydration etc. in the mixes. Addition of HVFA decreased the mechanical strength almost immediately, but the abrasion resistance only during the early ages. The gap between the strength and abrasion resistance was narrowed down with increasing period of curing. Freeze / thaw resistance did not change much, but the drying shrinkage and PH values were reduced with increasing rate of HVFA, and the porosity and water absorption rate increased with increasing HVFA. Addition of HVFA in the matrix increased sulphate resistance, acid resistance, but decreased the carbonation resistance and electrical conductivity. The properties could be modified favourably in case of poor shows, by inclusion of additives and chemical enhancers at various dosages.

2.7 Concluding Remarks :

In this Section, altogether 118 research papers have been mentioned by carefully exploring the relevance of the works by earlier researchers to the present work. Utilization of flyash have been made as partial replacement of cement mostly, and in some cases for sand replacement also. Bottomash have been used by few researchers to explore the possibility of utilizing the same as alternate to conventional sand in concrete. Thermal conductivity tests of concrete were also reported by some researchers, where flyash used as partial replacement of Ordinary Portland Cement. But no work has been reported with Portland Pozzolana Cement (flyash based) as binder, and sand replacement by flyash and bottomash separately up to the extent of 100%, and to study the physical strength parameter as well as thermal parameter of such blended concrete and mortar of different grades, complying relevant Indian Standard Specifications, so that the suitability of such industrial waste could be established with definite environmental and economic advantages.

Chapter 3
Materials and its Characterizations

Chapter 3 : Materials and its Characterization

3.1 General view

This Chapter focusses on the constituent materials required for Concrete and Masonry Mortar preparation in connection with building construction activity, which also contribute to overall energy consumption by buildings. Generally, the concrete and mortar constituent materials are chosen from durability and physical strength point of views respectively. Big quantities of wastes and industrial by-products could be used as secondary resource material, and thus provide actual savings in primary raw materials, energy, labour and capital investment. Use of coal-ash in cement production, road construction, land filling, brick manufacturing etc. are some examples of sustainable use. Sustainable materials broadly possess the following benefits:-

1. Those have lower cost than conventional material.
2. Those do not exhaust non-renewable materials.
3. Those save energy and reduce emission in environment.

This chapter focusses on different raw materials used in the research work, and their characterization. Among the materials, cement, fly ash, bottom ash, sand, stone aggregate, lime, marble dust (as cutting / polishing waste), water and burnt clay bricks were taken in to consideration. Except fly ash, bottom ash, and marble dust (all of which are industrial waste / by-product), all other materials were collected from the local market. The coal combustion residues, i.e. fly ash and bottom ash samples were collected from neighbourhood South West Kolkata based Budge Budge Thermal Power Station (BBTPS) of 3X250 MW capacity (situated within a distance of around 40 kilometres from the research centre), which produces around 1.33 MMT of total ash annually. Out of the total coal ash produced in the BBTPS, approximately 14% are of bottom ash variety, and balance 86% are of finer range of fly ash variety. Cement used for this work was Portland Pozzolana Cement variety, and for all the sample preparation one brand was used, while other brands of same grade and other varieties (Ordinary Portland Cement and Portland Slag Cement) were also compared for physical and other parameters. Sand is generally dredged from the river bed and transported to the local market at Kolkata for use in infra-structural works. Stone aggregates are quarried from Rajmahal, Pakur area, and transported to the local market. Burnt clay bricks are manufactured by using top soil and sometimes from river sediments, and bulk of the brick production follow the top soil extraction route. Water used for mixing different

constituents of concrete and mortar were taken from municipal supply source, which was of potable quality.

3.2 Details of the materials used

3.2.1 Cement

India is the world's second-largest cement manufacturer after China, accounting for about 7% of the global production. With nearly 455 million tonnes (MT) of cement production capacity during 2017-18, the cement production capacity is estimated to touch 550 MT by 2020. Cement production in India increased from 230.49 million tonnes in 2011-12 to 297.56 million tonnes in 2017-18. [IBEF, 2018].

Portland cement is the most common type of cement in general usage, as it is a basic ingredient of concrete and mortar. A mixture of limestone and clay is ground and burnt at a very high temperature (around 1450°C) to form clinker. The clinker is ground to a fine powder with the addition of gypsum (up to 5 per cent) to form Portland cement. The essential ingredients of Portland cement are lime, silica, alumina and iron oxide.

There are different types of Portland cement, based on their chemical compositions and resultant properties. However, the manufacturing process remains the same. Portland cement consists of tri-calcium silicate or C_3S , di-calcium silicate or C_2S , tri-calcium aluminate or C_3A , and tetra-calcium alumina-ferrite or C_4AF [C = CaO - calcium oxide (calcia), S = SiO_2 - silicon dioxide (silica), A = Al_2O_3 - aluminium oxide (alumina), F = Fe_2O_3 - iron oxide (ferric oxide)]. The varying proportion of these constituents imparts diverse properties to the different types of Portland cement namely Ordinary Portland Cement (OPC), Moderate Heat Portland Cement (MHPC), Rapid Hardening Cement (RHC), Sulphate Resistant Cement (SRC), Oil Well Cement (OWC), White Cement (WC), Portland Blast Furnace Slag Cement (PBFSC), Portland Pozzolana Cement (PPC), Masonry Cement (MC), Speciality Cement (SC), Expansive Cement (EC), Super High Strength Cement (SHSC) & Alinite Cement (AC).

The Cement industry has seen some major changes as far as production of various varieties i.e. OPC, PPC and PBFSC are concerned. The changes in cement production in India from 2007-08 to 2011-12 are visible in the following Column chart.

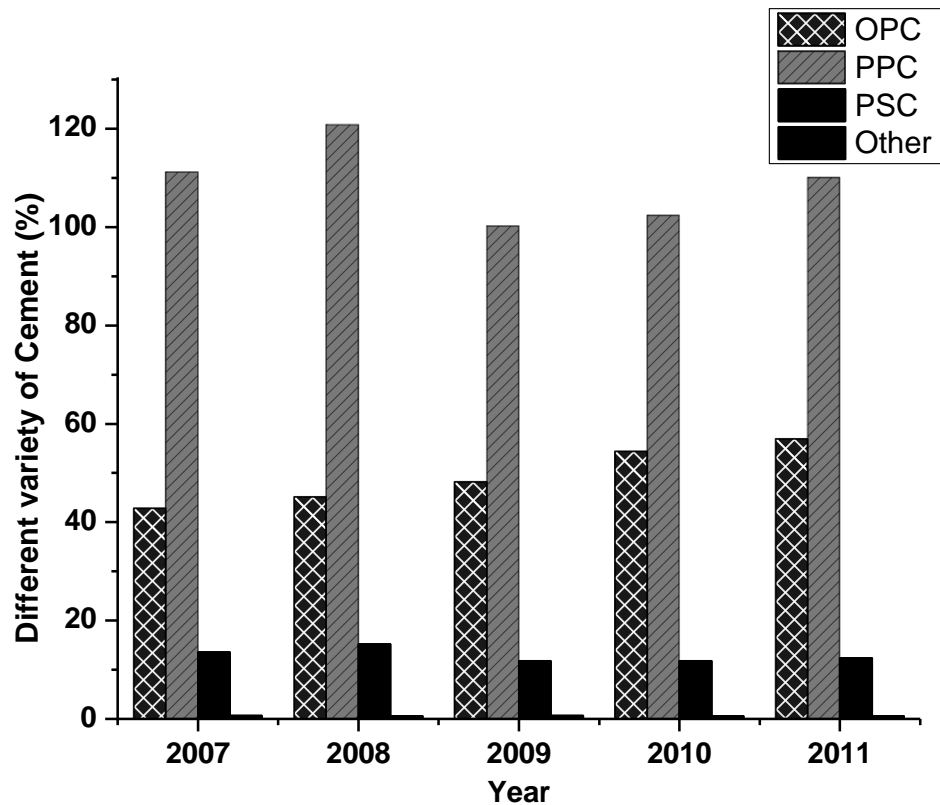


Fig.1 Cement Production by different variety (Million MT) year wise

[Source : Cement Production India, Feb.2014 by EMIS]

It is clearly visible from the above graph that types of cement production trend actually shifted from manufacturing OPC to increasing production of blended cement in the last 5-6 years. The proportion of blended cement has occupied the major share in cement production in India, primarily due to better margins offered in PPC, growing acceptability in the market and less pressure on the natural reserves of limestone.

The percentage of PPC in total cement production in the country has reached a plateau, and expected to be within the range of 65% - 70% in coming years. In future, the utilization of fly ash in PPC or in other words in cement industry can be increased with increase in demand from infrastructure sector. Since 2009 – 2010 up to end of 2015-16, percentage utilization of fly ash by Cement industry remains within 25% range overall. According to CEA Report for 2016-17, fly ash utilization in cement production was pegged at 23.98% of total ash produced during the period.

Due to maximum and easy availability of PPC(fly ash based) in the local market, the same has been used throughout, in connection with preparation of Concrete and Mortar samples

for the Research work. This type of Cement is also having least amount of embedded energy for flyash addition, replacing limestone percentage.

Portland Pozzolana Cement (PPC) conforming IS 1489 (Part-1) 1991 (reaffirmed 2005) is defined as “ an intimately inter-ground mixture of Portland clinker and pozzolana with the possible addition of gypsum (natural or chemical) or an intimate and uniform blending of Portland cement and fine pozzolana”. The fly ash constituent shall not be less than 15% and not more than 35% by mass of Portland pozzolana cement as per IS 1489, whereas blast furnace slag constituent is having a permitted IS range of 25-65% of the cement mass.

A mixture of limestone and clay is ground and burnt at a very high temperature of around 1450 °C to form clinker. The clinker is ground to a fine powder with the addition of gypsum (up to 5 per cent) to form Ordinary Portland cement or OPC. The essential major components in Portland cement are lime, silica, alumina and iron oxide. The manufacturing process of

Portland cement releases large amounts of CO₂ to the total emissions from construction industry, by the high energy demands during clinker formation and limestone calcination, aggregating 5% of the world’s GHG emissions (Worrell et al. 2001). With the strategy of replacing clinker with either blast furnace slag or coal ash, Portland Slag Cement (PSC) or Portland Pozzolana Cement (PPC) have been emerged as sustainable alternative to the huge energy consuming OPC. In this work, PPC had been used throughout, conforming to IS 1489 Pt.1 (Reaffirmed 2005). Though one single branded PPC was used for all sample preparation purpose, but some other branded PPCs were also collected to compare the properties.

3.2.2 Sand

Sand is the most used raw material for production of goods of our planet. It is found in concrete, glass, computers, detergents and even toothpaste. But sand is a finite resource, which took millions of years to become into present form through erosion and sedimentation. Sand is being extracted from rivers and ocean coasts in a so-far unknown

speed. In a matter of a few decades, sand will not be a resource anymore for our construction activities. The construction industry requires particular kinds of sand that can be found in aquatic environments. Massive mindless mining of natural coastal, alluvial and marine sand has devastating consequences for the environment as well as for the inhabitants. We need to look into alternative sources to reduce our dependency from this almost finite resource, particularly in the construction sector. The demand for sand can be reduced through recycling, substitution and synthesis. The rapid pace of urbanization in Asia, Africa and South America and the related urban design trends question the sustainability of current building materials and methods of construction from sustainability point of view. The areas mentioned above face gigantic building construction tasks. China alone consumed more cement in three years than the US over the whole 20th century. Developing countries use almost 90% of the global cement production (and twice as much sand as aggregate in concrete) and 70% of the global steel. This is due to the fact that the future urbanization will happen in developing territories.

We need sands with different characteristics. For fracking in oil extraction, we need sands with nicely rounded grains. For construction we need sands with angular grains. Salty sands collected from the bottom of the sea are no good for the production of concrete due to deleterious impurities. For glass manufacturing, we need high purity silica sands. For quality concrete, we need a proper grain size distribution. Different types of sands are formed during the continuous natural geological processes of erosion and transport by water and wind. During transport the grains are sorted out in different groups naturally, and deposited at different localities.

The composition of sand varies widely, depending on the rock sources and conditions, but the most common constituent of sand is silica (silicon dioxide, or SiO_2), usually in the form of quartz which because of its chemical inertness and considerable hardness, is the most common mineral resistant to weathering. ISO 14688 grades sands as fine, medium and coarse with ranges 0.063 mm to 0.2 mm, 0.25 mm to 0.50 mm and 0.63 mm to 2.0 mm respectively. Bureau of Indian Standards (BIS) Code 383 – 1970, explains two types of aggregates viz. Fine aggregate and coarse aggregate. Fine aggregate is defined as the aggregate which mostly passes through 4.75 mm IS sieve and divided in to different grading zones I, II, III & IV, depending upon the percentage fraction of coarser materials. The fine aggregate is further subdivided in to natural sand, crushed stone sand and crushed gravel sand. Our study is confined to natural sand, obtained by natural disintegration of rock and deposited by streams or glacial agencies.

River sand was used in this research work, conforming to IS 383 (1970, Reaffirmed 2002). The specific gravity of sand was tested. The fineness of the sand particles was determined from the grading curve generated by Sieve Analysis. All concrete and mortar mixes were prepared using two types of sand of coarser and finer varieties with different fineness modulus (FM) values. Several trials were carried out with different Sand-Fly ash and Sand-Bottom ash ratios to see the variations in physical strength and thermal parameters respectively. No chemical admixtures were used to maintain embodied energy content of both concrete and mortar samples minimum.

3.2.3 Fly ash and Bottom ash

3.2.3 (a) Fly ash

Coal/Lignite based Thermal Power Generation has been the backbone of power capacity addition in the country. Indian coal is of low grade with ash content of the order of 30-45 % in comparison to imported coals, which have low ash content of the order of 10-15%. Fly-ash is the best known pozzolan in the world. As per ASTM, definition of pozzolan is “a siliceous or siliceous and aluminous material, which in itself possess little or no cementitious value, but will in finely divided form and in the presence of moisture, chemically react with calcium hydroxide at ordinary temperature to form compounds possessing cementitious properties”. Two types of fly ash are produced namely Class C and Class F, out of coal burning in large thermal power plants. Class C fly ash is produced from coal with higher lime content, generally more than 15% and as high as 30%. Elevated CaO may exhibit self-hardening properties in presence of moisture in Class C. Class F is generally low in calcium content, lower than 15%, and having a greater combination of silica, alumina and iron (more than 70%) than Class C fly ash.

Mostly fly ash produced from Indian Thermal Power Plants are of Class F category, due to coal variety ranges in between anthracite and bituminous except those from lignite based Thermal Power Plants.

3.2.3 (b) Bottom ash

In the burning process of coal, minerals undergo thermal decomposition, fusion, dissolution, and agglomeration. Many elements present in a volatile form may vaporize and non-combustible material present in it results in production of coal ash. The finer and lighter particles of coal ash escape with the flue gases and are extracted in the Electro Static

Precipitators (ESP) before reaching the atmosphere. The coal ash collected from the ESP is named as fly ash (FA). Some melted ash accumulates on the boiler walls and against steam tubes and solidifies to form masses called clinkers. The clinkers build up and fall to the bottom of boiler/furnace and are cooled in the water sump before passing through clinker grinder. The coal ash collected at bottom of furnace is called bottom ash (BA). When pulverized coal is burned in a dry bottom boiler, major amount of the unburned material or ash is entrained in the flue gas and is captured and recovered as FA. The remaining of the ash is dry BA, a dark grey, granular, porous, mostly sand size material that is collected in water-filled hoppers at the bottom of the furnace. In general, coal ash in a power plant consists of up to 20 % BA and 80 % FA. But the thermal power plant, from where the ashes are collected for this work, produce around 14% BA and balance FA. The FA and BA used were conforming to IS 3812, and divided in to two grades Grade I and II from general use perspective.

The level of Coal ash utilization of about 62.6% was achieved in the year 2009-10, about 58.48 % in the year 2011-12, about 61.37 % in the year 2012-13, 57.63 % in the year 2013-14, 55.69 % in 2014-15, 60.97% in the year 2015-16, 63.28% in the year 2016-17, and 67.13% during 2017-18 respectively (*CEA reports*) . This utilization percentage include both flyash and bottom ash. The usage of bottom ash is mainly in the form of landfill and in ash dykes. Going by the composition of bottom ash, it can be recommended to be used as excellent sand replacement material in construction sector. It can be used in Concrete, Masonry Mortar, light weight aggregate material etc.

3.2.4 Stone Aggregate

As per IS 383, aggregates most of which is retained on 4.75 mm IS Sieve, and containing only so much of finer material, as permitted for various types, such as uncrushed gravel or stone which results from disintegration of rock, or crushed gravel or stone which results from crushing of hard rock or gravel or combination of both crushed and uncrushed ones. Those must be hard, strong, durable, clear and free from deleterious materials. We have used crushed stone from hard rock (granite), obtained from Pakur, Rajmahal. The grading and other physical parameters were tested.

3.2.5 Water

As per IS 456 and IS 2250, water to be used for concrete and mortar mixing and curing should be clean and free from acids, alkalis, salts, sugar, organic materials or other

substances, detrimental to concrete or steel. Potable water is generally considered as acceptable for concrete and mortar mixing / curing purpose. For this work, municipal supply water has been used.

3.2.6 Lime dust

As per IS 2541 (Preparation and use of Lime Concrete), commercially available manufactured lime was used in some trial mixes for full replacement of sand, in conjunction with fly ash and or bottom ash. The trial mixes were tested for concrete and masonry both the purposes respectively.

3.2.7 Marble dust

Marble dust used for this work was obtained as waste residue from marble stone cutting / polishing industries. It is mainly considered to be used as lime substitute or calcium to bind with alumina-silicate compound of fly ash or bottom ash.

3.2.8 Common Burnt Clay Building Bricks

Common burnt clay bricks are the oldest and most extensively used construction material. It is used in constructing a variety of structural members like masonry walls, foundation, columns etc. A common clay brick manufacturing, dimensions and physical requirements shall conform to IS 1077 and the bricks used for U-value of masonry wall assembly testing purpose was of 7.5 Class Designation.

3.2.9 Concrete and Mortar Mix

The experiments for this research work were carried out on concrete and mortar samples of different sizes and of various proportions. The concrete and mortar cubes were prepared for testing of its compressive strength (destructive testing) at 7 days and 28 days maturity and for 28 days maturity conditions respectively as per relevant IS Code provisions. Similarly for testing of apparent porosity, bulk density and thermal conductivity parameters (non-destructive testing), sample sizes were 50 mm by 50 mm by 25 mm and 50 mm by 50 mm by 12 mm respectively. The various mix proportions were arrived at by following IS 456, IS

10262, SP-41 (S&T), and IS 2250 respectively. All the cube and other samples were cured under immersed water at temperature $27 \pm 2^{\circ}\text{C}$.

3.3 Material Characterization

3.3.1 Cement

The cement used for this research work was PPC (fly ash based), conforming to IS 1489. The physical and other parameters were considered as per Manufacturer's Test Certificate, as shown under Table 3.1 below. To compare with OPC and PSC, those results are shown under Table 3.2. In this work, Rashmi branded PPC was used for all sample making.

Table 3.1 Comparison of different parameters of PPC

Parameters with Limits and Unit	As per IS 1489 Pt.1	As per Rashmi Cement Test Certificate	As per Ambuja Test Certificate
Loss on ignition, Max (%)	5.0	2.2	1.4
Insoluble residue, Max (%)	$X + \{4(100-X)\} / 100$, where X is %age of flyash	32.8	34.72
SO ₃ , Max (%)	3.5	1.88	2.49
MgO, Max (%)	6.0	2.76	2.83
Chloride, Max (%)	0.1	0.018	0.02
Specific Surface, Min. (m ² /kg)	300	440	300
Initial Setting Time, Min.(Minutes)	30	150	76
Final setting Time, Max (Minutes)	600	600	240
3 Day's Compressive Strength, Min.(MPa)	16	24.5	31.1
7 Day's Compressive Strength, Min.(MPa)	22	33.5	37.2
28 Day's Compressive Strength, Min.(MPa)	33	39.5	56.9
La Chatelier Test, Max.(mm)	10	1.0	5.0
Autoclave Expansion, Min.(%)	0.8	0.06	0.5
Drying Shrinkage, Max.(%)	0.15	0.006	0.04
Fly ash, Range (%), X	15 - 35	30	32

From the above parameter data, it may be seen that both the branded PPC had complied with IS Code provisions satisfactorily. Rashmi branded cement had a blending of fly ash to the tune of 30%, while that by Gujrat Ambuja branded cement had 32%. 28 Day's compressive strength, expansion, drying shrinkage values of Gujrat Ambuja branded cement were found to be more in comparison with that of Rashmi branded cement.

Table 3.2 Comparison of different parameters of OPC-43, OPC-53, PSC and PPC

Parameters with Limits and Unit	As per IS 1489 Pt.1	Rashmi Slag Cement Test Certificate	Rashmi OPC 43 Grade Cement	As per Rashmi OPC 53 Grade Cement
Loss on ignition, Max(%)	5.0	1.2<5	1.7 < 4	1.5 < 5
Insoluble residue, Max (%)	$X + \{4(100 - X)\} / 100$,	1.4<5	1.3 < 5	1.0 < 5
SO ₃ , Max (%)	3.5	1.52<3.5	2.15<3.5	2.15<3.0
MgO, Max (%)	6.0	4.54<6	2.76 < 6	2.41 < 6
Chloride, Max (%)	0.1	0.02<0.1	0.018 < 0.05	0.02 < 0.05
Specific Surface, Min. (m ² /kg)	300	365.3	365.3 > 225	378
Initial Setting Time, Min.(Minutes)	30	165	165	130
Final setting Time, Max (Minutes)	600	260	260	220
3Day's Compressive Strength, Min.(MPa)	16	22.5	33.5	37 > 27
7Day's Compressive Strength, Min.(MPa)	22	32.0	33.0	45 > 37
28Days Compressive Strength, Min.(MPa)	33	51.0	52.5	59.5 > 53
La Chatelier Test, Max.(mm)	10	1.0	1.0	1.0
Autoclave Expansion, Min.(%)	0.8	0.05	0.06	0.04

From the above test data, it may be concluded that PPC is very much identical from durability and strength point of view with PSC and OPCs, except the initial strength gain is slower due to pozzolanic property of fly ash.

3.3.1 (a) Quantitative Chemical Analysis

Materials falling into the group of alumina-silicate and non-hydrous alumina are mainly clays, feldspars, micas, ignited bauxites, corundum etc. which contain silica (SiO_2) and Alumina (Al_2O_3) as major and Fe_2O_3 , TiO_2 , MnO , P_2O_5 , CaO , MgO , Na_2O , K_2O as minor or trace constituents. SiO_2 may be analysed by Titrimetric method or by Gravimetric method or by Spectrophotometry method, Al_2O_3 by Complexometry method, Fe_2O_3 by Spectrophotometry and Polarography methods, TiO_2 by Spectrophotometry and Polarography methods, MnO by Spectrophotometry method, P_2O_5 by Spectrophotometry method, CaO , MgO both by Complexometry (EDTA) method, and Na_2O and K_2O both by Flame photometry method respectively.

Alternatively, silica may be determined by the titrimetric K_2SiF_6 (Potassium silico-fluoride) method from a separate sample. From another portion of the sample, Al_2O_3 , TiO_2 , Fe_2O_3 , P_2O_5 , MnO , CaO , MgO may be determined after decomposing the sample with $\text{H}_2\text{SO}_4 + \text{HF}$ and fusing the HF residue with potassium bisulphate. Alkali may be determined as described earlier. To determine loss on ignition, accurately 1g of the ground sample (200 mesh) is dried at 110°C into a platinum crucible. Place the crucible in to a muffle furnace and slowly raise the temperature to $1000 \pm 25^\circ\text{C}$. Ignite to constant weight at this temperature. Thirty minutes' ignition is usually sufficient. This is called Gravimetry method. (Dasgupta and Roy, 1985).

Chemical composition of PPC used for this work was tested at Central Glass & Ceramic Research Institute's Analytical Chemistry Test Laboratory and the result is shown under Table 3.3. Quantitative chemical analysis of cement was done by Wet Chemical method (for SiO_2 , Al_2O_3 , and LOI) and by ICP-AES and by Gravimetry method (for balance parameters) respectively.

Table 3.3 Quantitative Chemical Analysis of PPC used

Chemical parameters	Test value (%)
SiO_2	32.38
Al_2O_3	10.21
Fe_2O_3	3.97
CaO	41.67
MgO	1.49

Na ₂ O	0.32
K ₂ O	1.25
TiO ₂	0.71
SO ₃	3.73
LOI	3.21
Free Moisture	0.96

3.3.1 (b) Phase composition : XRD

To have some idea on phase composition of cement material, the samples of cement was prepared for XRD analysis (Mineralogical analysis) using a back loading preparation method. Those were analyzed with a PANalytical X’Pert’s Pro powder diffractometer with X’Celerator detector and variable divergence- and receiving slits with Fe filtered CuK α radiation in a diffraction angle (2θ) range of 20⁰- 69⁰. The phases were identified using X’Pert Highscore plus software. The relative phase amounts (weights %) were estimated using the Rietveld method (Autoquan Program). X-Ray Diffraction analysis, showing the constituent phases of cement, is shown under figure 3.1, as below –

Table 3.4 : Peak list of PPC

Pos.[$^{\circ}2\theta$.]	d-spacing[Å]	Rel.Int.[%]
20.9682	4.23679	14.56
23.0598	3.85701	8.98
24.4495	3.64084	4.51
25.5973	3.48012	21.47
26.7686	3.33045	69.25
28.0893	3.17680	5.39
29.5736	3.02064	85.36
30.2358	2.95597	20.12
31.5135	2.83899	13.22
32.3384	2.76843	96.37
32.7684	2.73307	100.00
33.3945	2.68325	27.43
34.5253	2.59791	76.55
35.8304	2.50622	7.21
36.8428	2.43965	13.63
37.4772	2.39980	8.31
38.9409	2.31290	21.04
39.5783	2.27711	10.10
41.4651	2.17775	53.03

43.0880	2.09941	15.35
44.3451	2.04277	5.86
45.9635	1.97455	12.14
47.1032	1.92939	13.95
47.5384	1.91274	11.08
50.2318	1.81632	11.50
51.0635	1.78867	1.87
51.9348	1.76069	45.10
54.2817	1.68999	5.17
56.7104	1.62324	20.62
58.7282	1.57219	3.05
60.1051	1.53943	18.03
60.8657	1.52200	5.52
62.4387	1.48739	32.70
63.8693	1.45748	5.75
67.5327	1.38706	4.09
68.4102	1.37026	5.24

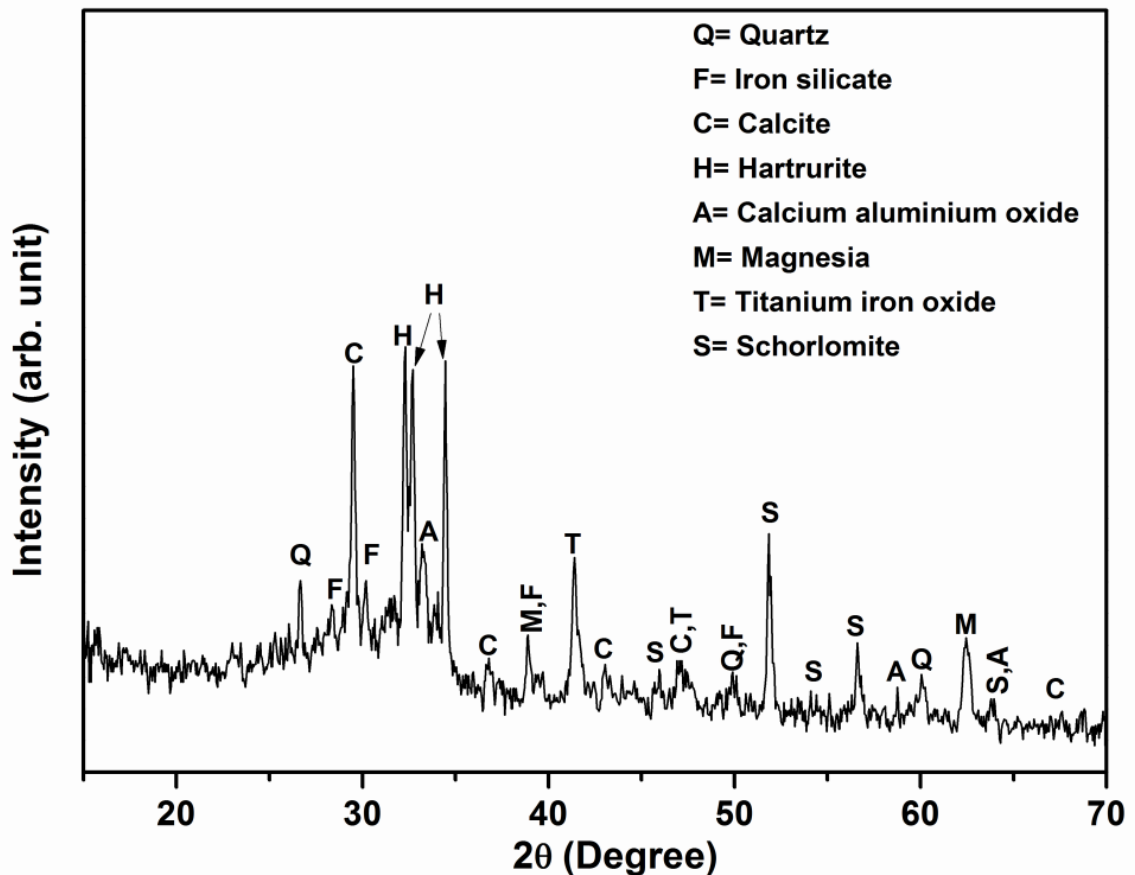


Fig.3.1 X-Ray Diffractogram of PPC Sample, showing constituent phases.

The X-Ray Diffraction pattern of the sample marked as PPC was recorded in X'Pert Pro MPD Diffractometer (PANalytical) operating at 40 KV and 30 ma, using Ni-filtered CuK α Radiation with the X'celerator with step size 0.05 $^{\circ}$ (2 θ) step time 50 sec from 20 $^{\circ}$ to 70 $^{\circ}$. It is revealed from the diffraction pattern that the sample contains following phases –

1. Quartz : SiO $_2$,
2. Iron silicate : FeO $_3$ Si,
3. Calcite : CaCO $_3$,
4. Hartrurite : (Ca $_3$ SiO $_4$)O,
5. Calcium Aluminium Oxide ; CaAlO,
6. Magnesia : Mg,
7. Titanium Iron oxide : TiFeO,
8. Schorlomite : Ca $_3$ Ti $_2$ (Fe $_2$ +3Si)O $_{12}$

3.3.1 (c) Surface morphology : FESEM

Field Emission Scanning Electron Microscopy is a complimentary technique for the investigation of the surface morphology. High Resolution Micro structural analysis or morphological analysis by Field Emission Scanning Electron Microscopy (FESEM ZEISS SUPRA 35VP) was carried out for cement sample under different magnification ranges. A pinch of the powdered sample was dispersed in organic solvent (acetone) by an ultrasonic vibrator. Using a micro pipette, a droplet of thus prepared solution was poured on a glass slide and dried under a IR lamp. The sample coated glass slide ware the mounted on FESEM Instrument stub. Keeping the desired surface upward, the sample was mounted on the sample-stub using a conducting tape. A thin layer of gold was applied on the sample surface to make it electrically conducting for analysis.

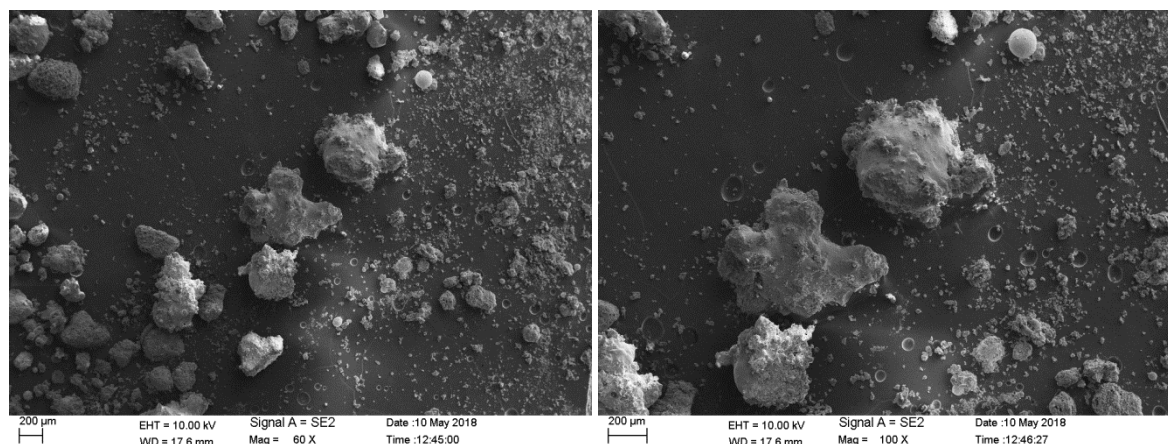


Fig.3.2(a) PPC at 60X

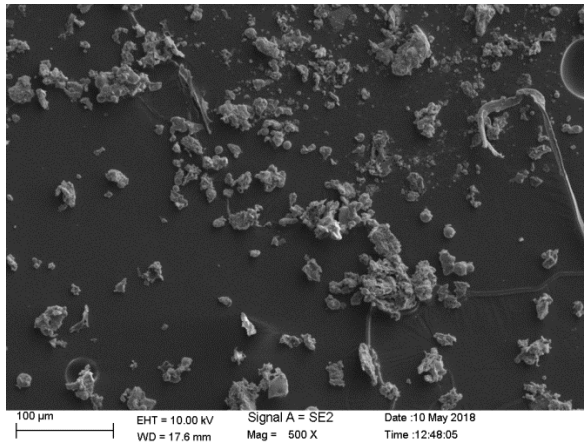


Fig.3.2(b) PPC at 100X

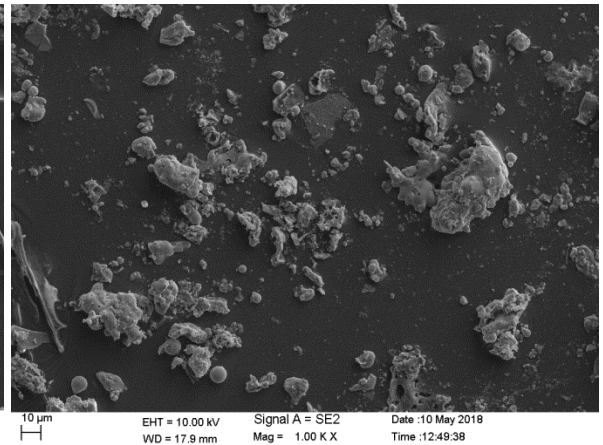


Fig.3.2(c) PPC at 500X

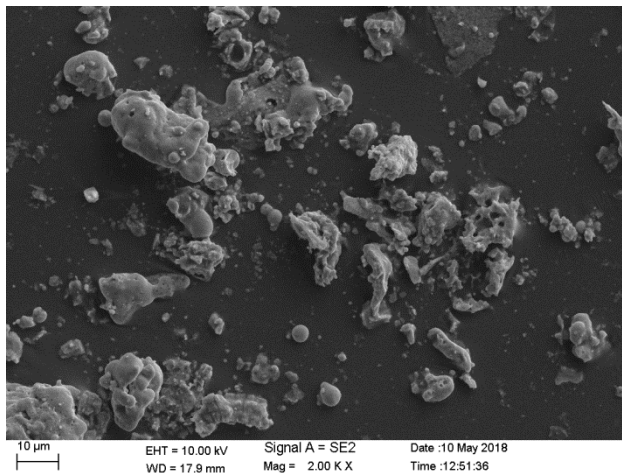


Fig. 3.2(d) PPC at 1000X

Fig. 3.2(e) PPC at 2000X

The surface of the sample was scanned in SE (in lens) modes of FESEM. The morphology and size of the powder particles were investigated. The recorded micrographs were taken at different magnifications (60X, 100X, 200X, 500X,1.0KX, 2.0KX) from various locations at the sample surfaces.

3.3.1 (d) Physical Test : Density

Density of powder samples were measured by Gas Pycnometry with the help of Micromeritics AccuPyc II 1340 V 1.05 instrument. Analysis Gas used was Helium, Test temperature was 22.48⁰ C and number of purges = 10

Table 3.5 Bulk Density of Cement

Identification of Sample	Volume (cm ³)	Bulk Density value (g/cm ³)
Ultratech PPC	2.4187	2.8773
Rashmi PPC	1.9016	3.0380

3.3.2 Flyash and Bottomash

3.3.2 (a) Quantitative Chemical Analysis

The quantitative chemical analysis of Flyash and Bottomash were done at Analytical Chemistry laboratory of Central Glass & Ceramic Research Institute under Wet Chemical method to determine various parameters, as listed under Table 3.4. The IS Code provision and the actual test results are shown side by side.

Table 3.6 Quantitative Chemical Analysis Result of Flyash and Bottomash

Parameters tested	Requirement as per IS 3812	Test data of Flyash used	Test data of Bottom ash used
Silicon-di-oxide (SiO ₂) + Aluminium oxide (Al ₂ O ₃) + Iron oxide (Fe ₂ O ₃) (%) by mass	70.0	51.38+33.12 +6.87=91.37	60.71+ 25.86 +6.81=93.38
Silicon di-oxide (SiO ₂)(%) by mass, Min.	35.0	51.38	60.71
Magnesium oxide (MgO)(%) by mass, Max.	5.0	0.47	0.63
Total Sulphur as Sulphur tri-oxide (SiO ₃) (%) by mass, Max.	2.75	0.09	0.15
Available Alkalis as Sodium oxide (Na ₂ O) % by mass, Max.	1.5	0.72	0.38
Loss on ignition, % by mass, Max.	12.0	1.80	0.92

3.3.2 (b) Phase Composition : XRD

The constituent phase analysis of fly ash and bottom ash was carried out with a PANalytical X'Pert's Pro powder diffractometer with X'Celerator detector and variable divergence- and receiving slits with Fe filtered Cu-K α radiation in a diffraction angle (2θ) range of 15⁰- 70⁰. Minimum Step size 2 Theta : 0.05, Scan step time (s) : 50.0737, Measurement temperature (⁰C) : 25, Anode material : Cu, Generator setting : 30 milli-Ampere, 40 KV, Goniometer radius (mm) : 240, Dist. Focus-Diverg Slit (mm) : 100. The phases were identified using

X'Pert Highscore plus software. The relative phase amounts (weights %) were estimated using the Rietveld method (Autoquan Program). X-Ray Diffraction analysis, showing the constituent phases of fly ash and bottom ash samples are shown under figure 3.2 and 3.3 respectively.

Table 3.7 : Peak list of Fly ash

Pos.[°2Th.]	d-spacing[Å]	Rel.Int.[%]
16.6595	5.32157	54.16
21.0624	4.21805	31.38
23.7683	3.74362	9.43
24.3923	3.64926	6.28
26.4411	3.37096	100.00
30.4148	2.93899	5.98
31.1837	2.86826	24.02
33.4465	2.67920	49.06
35.4698	2.53087	61.99
36.7448	2.44593	10.09
37.2379	2.41467	14.66
39.4796	2.28257	22.10
41.0603	2.19828	67.59
42.7830	2.11367	23.58
46.0180	1.97233	3.78
48.4065	1.88045	6.95
49.6316	1.83687	11.56
50.3500	1.81233	13.17
54.1777	1.69298	13.86
57.7491	1.59649	17.19
60.0918	1.53974	7.00
60.8373	1.52264	41.00
63.7649	1.45961	10.13
64.6804	1.44115	19.16
65.7305	1.42065	3.52
66.6411	1.40343	5.88
68.4248	1.37000	6.05

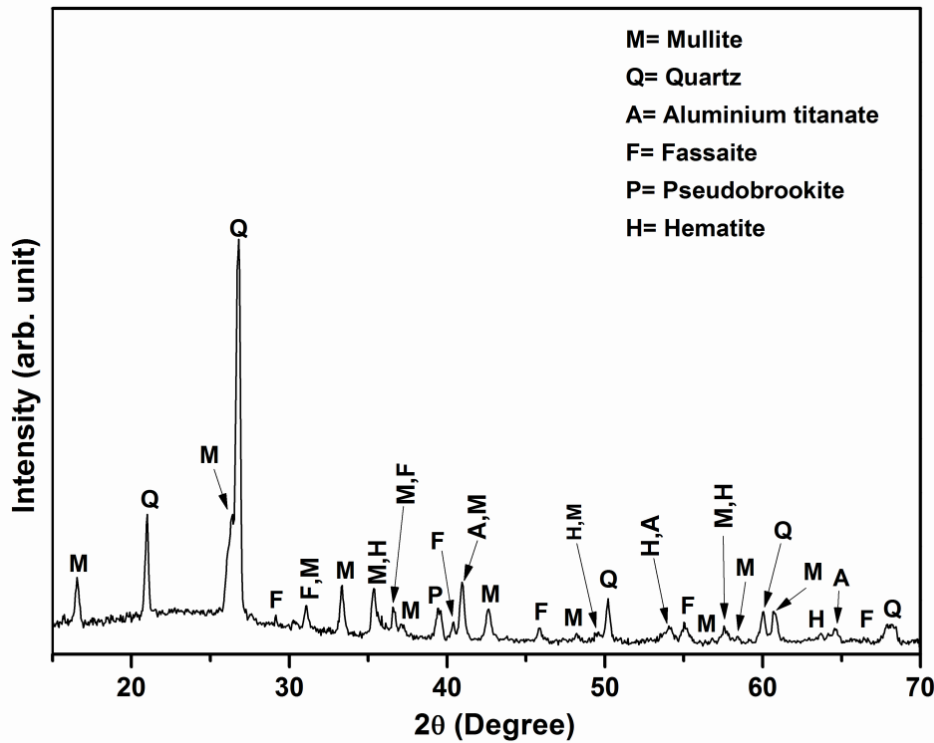


Fig. 3.3 X-Ray Diffractogram of Fly ash sample showing constituent phases.

The X-Ray Diffraction pattern of the sample marked as Fly ash and Bottom ash were recorded in X'Pert Pro MPD Diffractometer (PANalytical) operating at 40 KV and 30 ma, using Ni-filtered $\text{CuK}\alpha$ Radiation with the X'celerator with step size 0.05° (2θ) step time 50 sec from 15° to 70° . It is revealed from the diffraction pattern that the fly ash sample contains following phases –

1. Mullite : $3\text{Al}_2\text{O}_3 \cdot 2\text{SiO}_2$;
2. Quartz : SiO_2 ;
3. Aluminium titanate : Al_2TiO_5 ;
4. Fassite : $(\text{Ca}_{0.96}\text{Mg}_{0.57}\text{Fe}_{0.22}\text{Al}_{0.16}\text{Ti}_{0.059})(\text{Si}_{1.73}\text{Al}_{0.27})\text{O}_6$;
5. Pseudobrookite : $(\text{Fe}_2\text{O}_3 \cdot \text{TiO}_2)$;
6. Hematite : Fe_2O_3 .

Table 3.8 : Peak list of Bottom ash

Pos.[$^\circ 2\theta$.]	d-spacing[\AA]	Rel.Int.[%]
16.9056	5.24465	16.9056
21.2820	4.17501	16.28
22.1738	4.00909	4.84
25.1311	3.54362	4.70
26.3918	3.37713	19.36

27.1078	3.28954	100.00
27.8938	3.19861	3.69
31.3894	2.84992	6.38
33.6911	2.66031	12.82
35.7003	2.51506	15.74
37.0422	2.42698	5.04
37.4501	2.40147	3.70
39.9338	2.25765	10.72
41.2857	2.18680	18.45
42.9685	2.10497	7.68
46.2236	1.96404	4.09
48.6766	1.87065	1.67
49.8818	1.82824	2.65
50.5478	1.80570	9.51
53.9398	1.69989	2.30
54.5373	1.68267	4.25
55.1941	1.66419	2.87
57.9351	1.59181	5.19
58.7977	1.57050	2.00
60.4003	1.53261	14.56
61.0410	1.51805	11.41
64.0079	1.45466	2.14
64.9301	1.43621	5.40
66.8533	1.39949	1.21
68.8017	1.36341	13.91

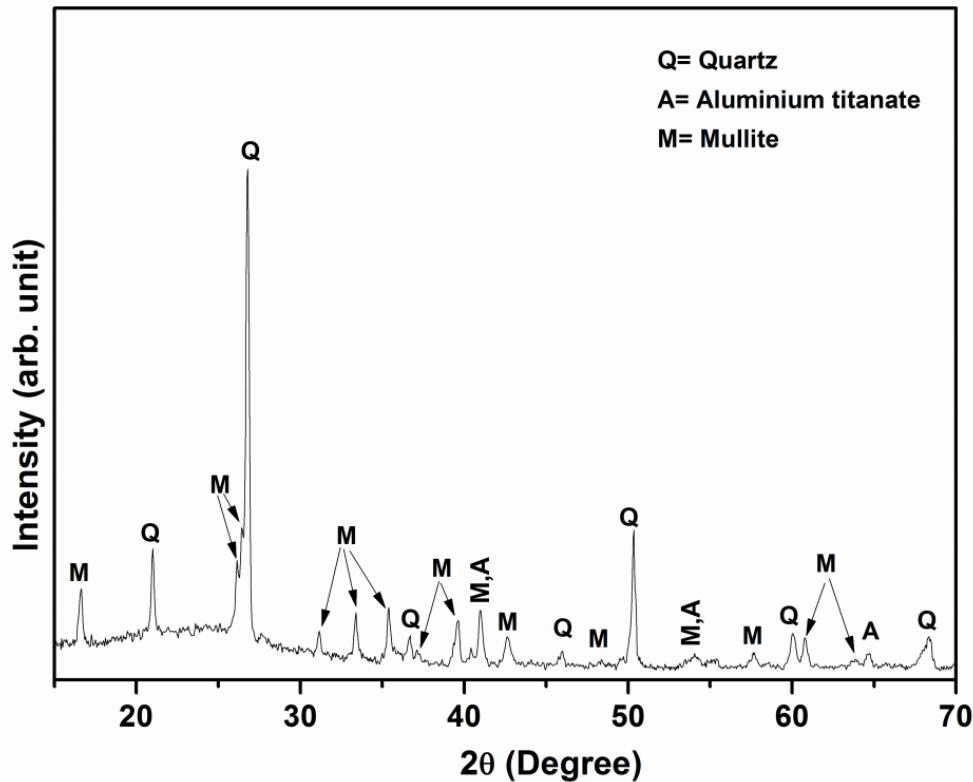


Fig. 3.4 X-Ray Diffractogram pattern of Bottom ash sample showing constituent phases.

It is revealed from the diffraction pattern that the fly ash sample contains following phases –

1. Quartz : SiO_2 ;
2. Aluminium Titanate : Al_2TiO_5
3. Mullite : $3\text{Al}_2\text{O}_3 \cdot 2\text{SiO}_2$;

From the XRD pattern of fly ash and bottom ash particles, it may be observed that both contain mullite, which is basically alumina-silicate compound. Mullite is an important and widely studied ceramic material. It is used in a diverse number of applications, including structural and refractory ceramics, microelectronic packaging, high-temperature protective coatings, microwave dielectrics and infrared-transmitting materials. Fly ash under enhanced temperature grow more mullite as well as glass formation also takes place (Das et al.2011). Mullite is an attractive ceramic for high temperature structural application as it has high creep resistance, low thermal expansion coefficients and good chemical and oxidation resistance (Ohira *et al* 1991; Schneider *et al* 1994).

3.3.2(c) Particle size Analysis : Flyash

The particle size analysis for fly ash was carried out by Microtrac 3500S (micron range) LASER Diffraction System, which are shown under Table 3.8 and Fig. 3.5 respectively. The sieve analysis result of bottom ash sample (being coarser variety) is plotted as per the limit prescribed in IS 383 for fine aggregate materials, which is shown under fig. 3.6.

Table 3.9: Particle size analysis data of Fly ash

Size(um)	%Chan	% Pass
1408	0.00	100.00
1184	0.00	100.00
995.6	0.00	100.00
837.2	0.00	100.00
704.0	0.00	100.00
592.0	0.00	100.00
497.8	0.00	100.00
418.6	0.34	100.00
352.0	0.68	99.66
296.0	1.48	98.98
248.9	3.04	97.50
209.3	5.31	94.46
176.0	7.46	89.15
148.0	8.34	81.69
124.5	8.34	73.35
104.7	7.60	65.01
88.00	6.88	57.41
74.00	6.31	50.53
62.23	5.73	44.22
52.33	4.99	38.49
44.00	4.18	33.50
37.00	3.46	29.32
31.11	2.95	25.86
26.16	2.64	22.91
22.00	2.44	20.27
18.50	2.32	17.83
15.56	2.21	15.51
13.08	2.10	13.30
11.00	1.97	11.20
9.25	1.80	9.23
7.78	1.59	7.43
6.54	1.34	5.84
5.50	1.10	4.50
4.62	0.89	3.40

3.89	0.72	2.51
3.27	0.59	1.79
2.750	0.48	1.20
2.312	0.40	0.72
1.945	0.32	0.32
1.635	0.00	0.00
1.375	0.00	0.00
1.156	0.00	0.00
0.972	0.00	0.00
0.818	0.00	0.00
0.688	0.00	0.00
0.578	0.00	0.00
0.486	0.00	0.00
0.409	0.00	0.00
0.344	0.00	0.00
0.2890	0.00	0.00
0.2430	0.00	0.00
0.2040	0.00	0.00
0.1720	0.00	0.00
0.1450	0.00	0.00
0.1220	0.00	0.00
0.1020	0.00	0.00

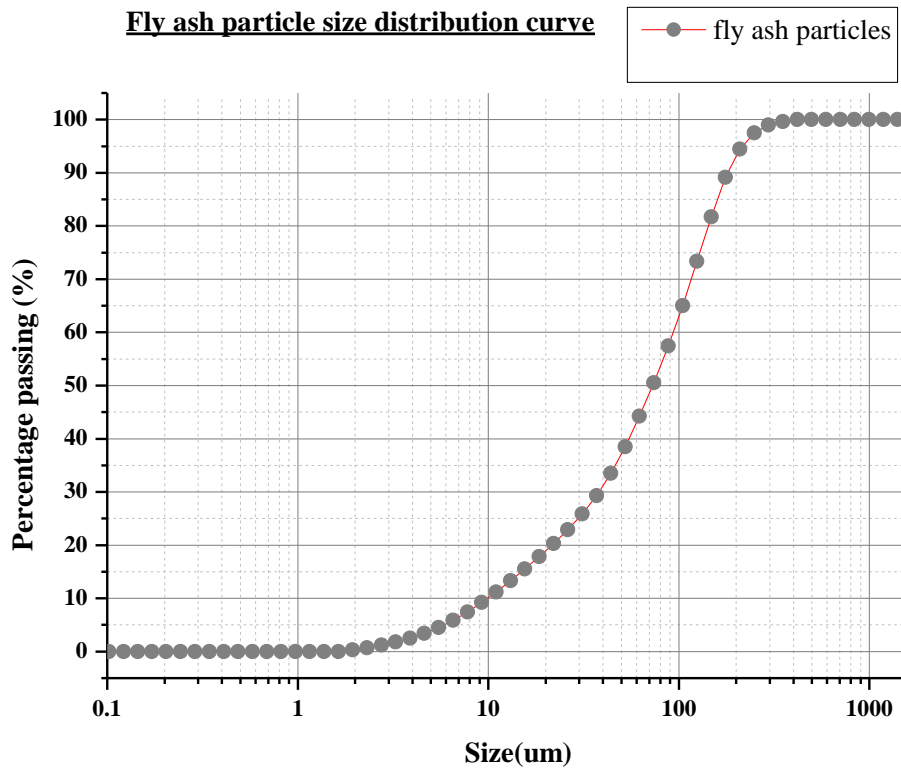


Fig.3.5 Particle size distribution for fly ash, used in the experiment.

3.3.2 (d) Physical Test – Surface Area : Flyash

Surface area measurement by BET method [ASTM B 922-10] with the help of Quantachrome Nova Station A , Novawin version 10.01 at CGCRI Material Characterization Division. Analysis gas used was Nitrogen.

Surface area = 0.552 m²/g.

3.3.2(e) Physical Test – Sieve Analysis : Bottomash

The IS Sieve analyzed Grading curves of Bottom ash samples are shown below -

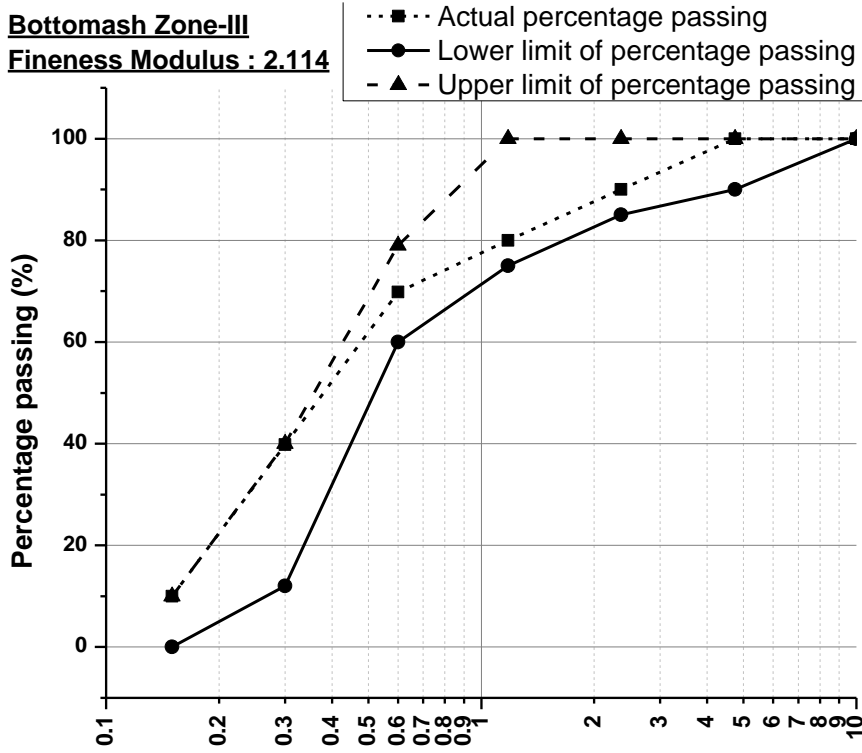


Fig.3.6 (a) Grading curve for Bottom ash

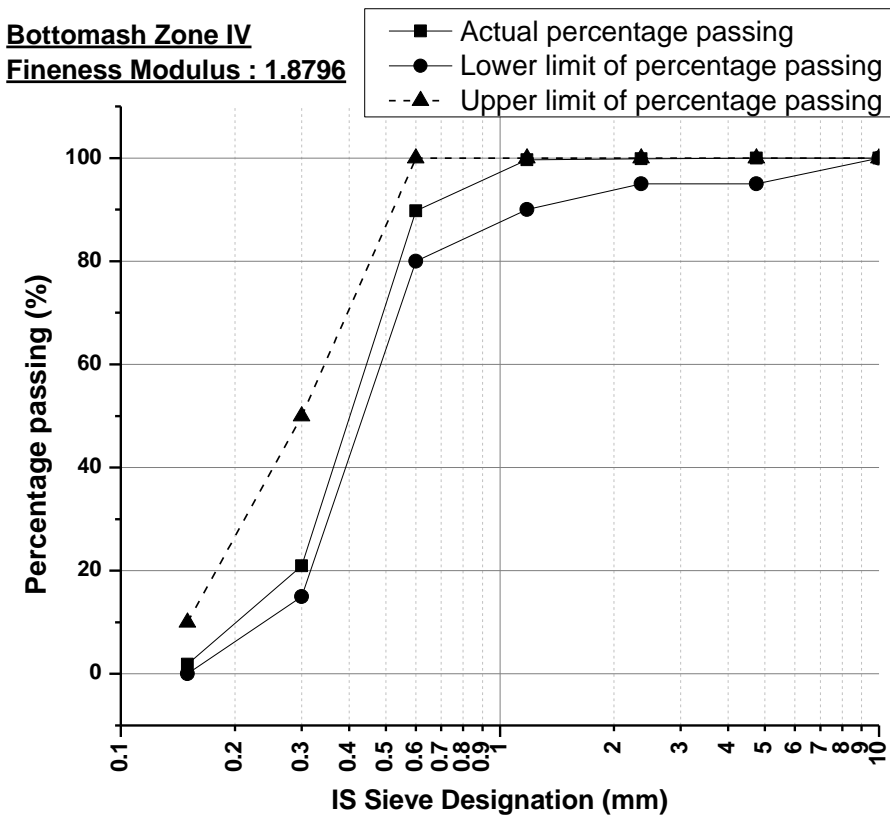


Fig.3.6 (b) Grading curve for Bottom ash

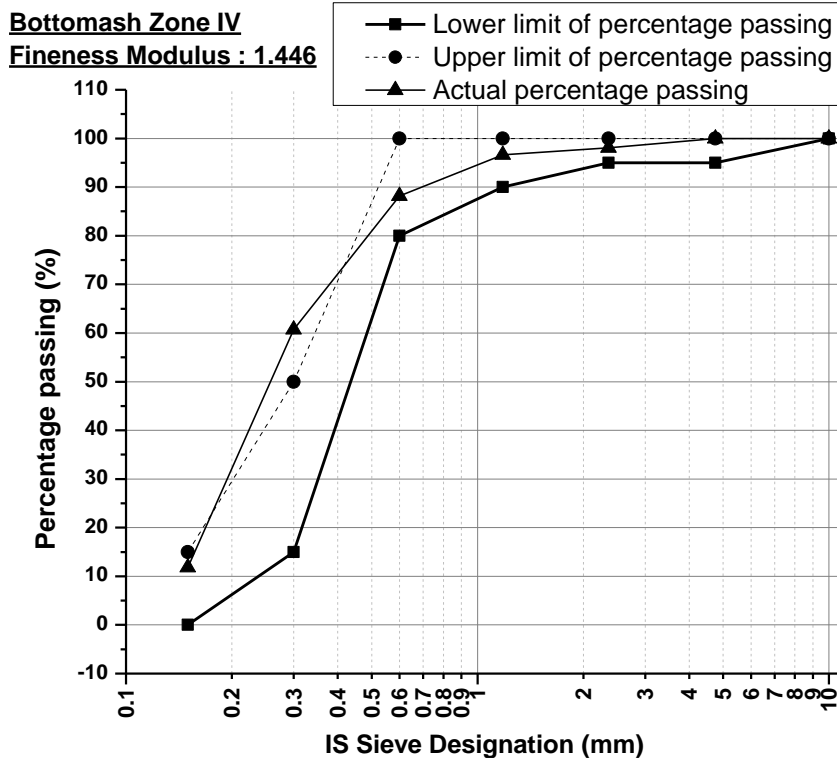


Fig. 3.6 (c) Grading curve for Bottom ash

From the above grading curves of bottom ash, it may be seen that the samples fall within finer to finest varieties of fine aggregate, as per limit specified by IS 383. However, both Zone-III and Zone IV varieties of fine aggregate are suitable for construction purposes, and as such may be considered as natural sand alternative.

3.3.2(f) Surface Morphology – FESEM : Flyash and Bottomash

Field Emission Scanning Electron Microscopy of fly ash and bottom ash samples were done with the help of high resolution Carl ZEISS SUPRA 35 VP instrument at CGCRI Laboratory under different magnifications as shown below.

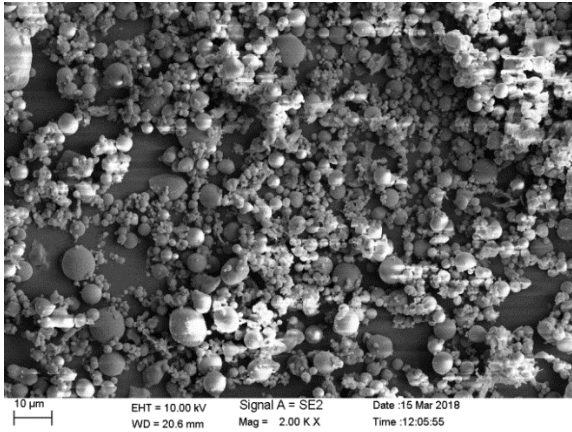


Fig. 3.7 (a) SEM of Fly ash 2000X

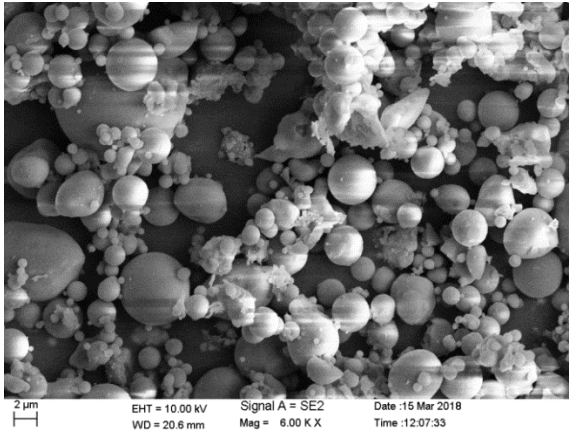


Fig.3.7 (b) SEM of Fly ash 6000X

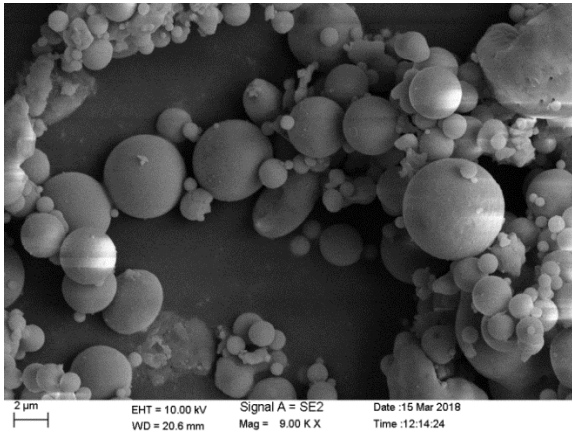


Fig. 3.7 (c) SEM of Fly ash 9000X

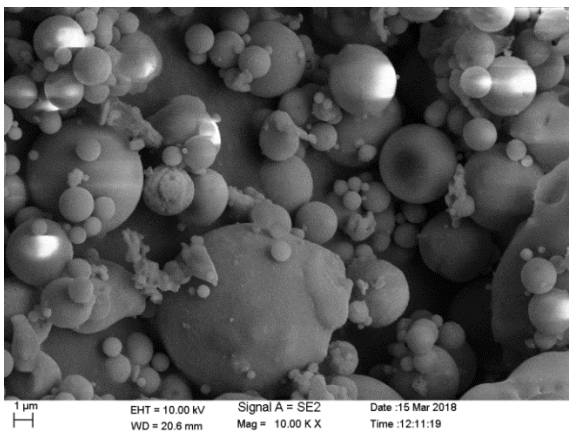


Fig. 3.7(d) SEM of Fly ash10000X

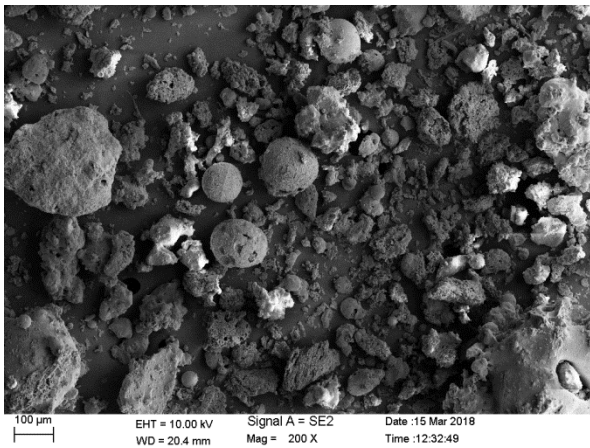


Fig. 3.8(a) SEM of Bottom ash 200X

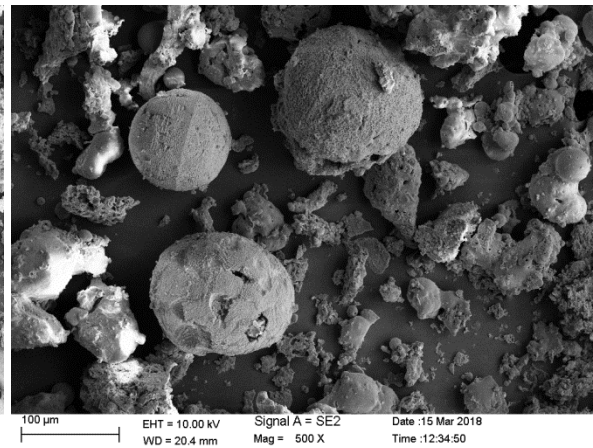


Fig. 3.8(b) SEM of Bottom ash 500X

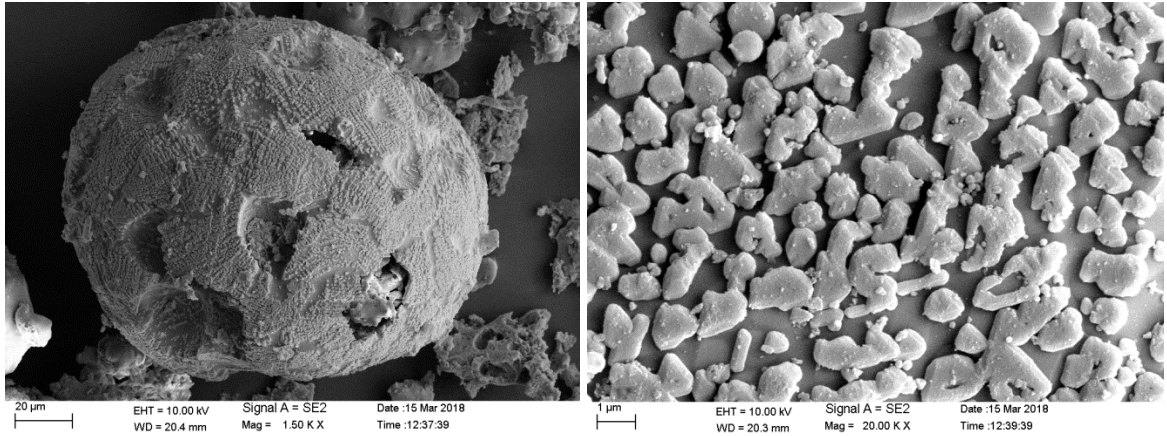


Fig. 3.8(c) SEM of Bottom ash 1500X

Fig. 3.8(d) SEM of Bottom ash 20000X

The surface of the sample was scanned in SE (in lens) modes of FESEM. The morphology and size of the powder particles were investigated. The recorded micrographs were taken at different magnifications (200X, 500X, 1.5KX, 20.0KX) from various locations at the sample surfaces. The hollowness and irregular shape are evident from the above magnifications.

3.3.2(g) Physical Test - Density : Flyash

Density of powder samples were measured by Gas Pycnometry with the help of Micromeritics AccuPyc II 1340 V 1.05 instrument. Analysis Gas used was Helium, Test temperature was 23.29⁰ C for fly ash and 22.55⁰C for fly ash and bottom ash samples respectively. Number of purges = 10

Table 3.10 Bulk Density of Flyash

Identification of Sample	Volume (cm ³)	Bulk Density value (g/cm ³)
Flyash	2.4795	2.4166

3.3.2(h) Physical Test – Surface Area : Bottomash

Surface area measurement by BET method [ASTM B 922-10] with the help of Quantachrome Nova Station A, Novawin version 10.01 at CGCRI Material Characterization Division. Analysis gas used was Nitrogen.

Surface area = 0.162 m²/g.

3.3.3 Sand

3.3.3(a) Sieve analysis

The fine aggregate most of which passes 4.75 mm IS Sieve size, and contains only so much of coarser material, which results in fitting within either of the four zones, as specified. Natural Sand falls within fine aggregate category and it is mainly sourced from rivers within the State. As specified in IS 383, Grading Zones I to IV have been earmarked, depending upon the coarsest variety to progressively down to finest variety respectively. In this work, different types of sands were collected from the local market, sieve analysis done and coarser variety was selected for concrete sample preparation work and relatively finer variety for Mortar and plaster work. All the grading curves are drawn to show the zoning classification under Fig.3.8.

Table 3.11 Grading Zones Classification of Sand as per IS 383

IS Sieve Designation	Percentage passing for			
	Grading Zone-I	Grading Zone-II	Grading Zone-III	Grading Zone-IV
10 mm	100	100	100	100
4.75 mm	90-100	90-100	90-100	95-100
2.36 mm	60-95	75-100	85-100	95-100
1.18 mm	30-70	55-90	75-100	90-100
600 micron	15-34	35-59	60-79	80-100
300 micron	5-20	8-30	12-40	15-50
150 micron	0-10	0-10	0-10	0-10

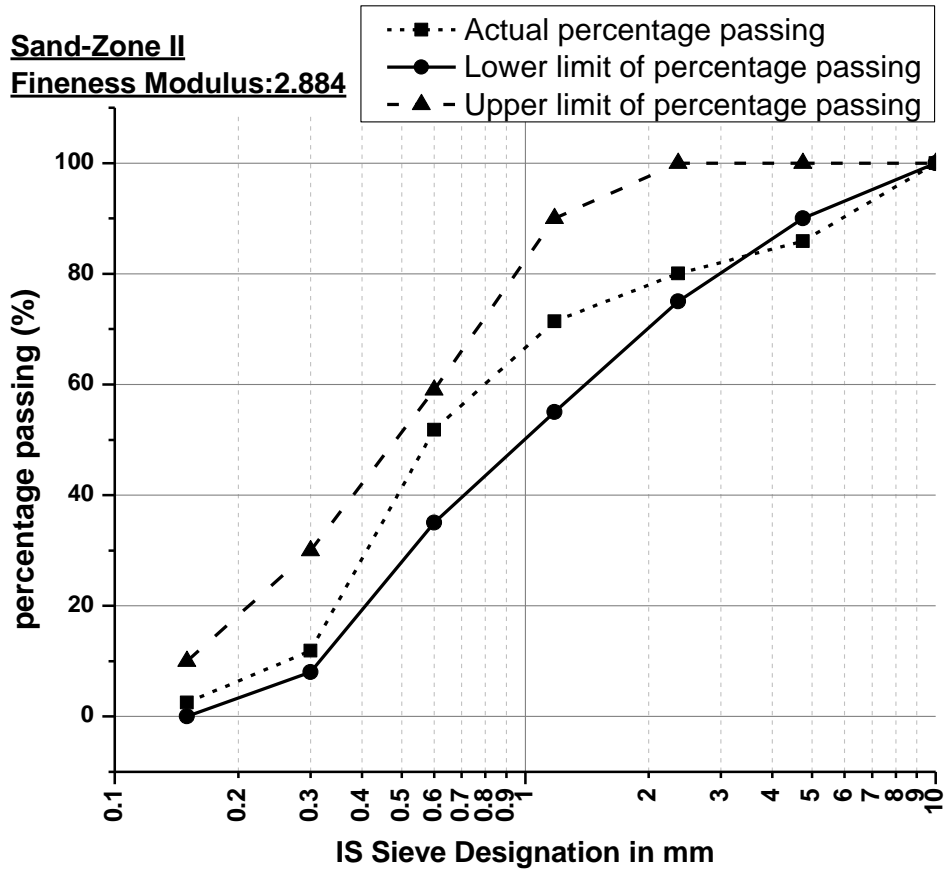


Fig. 3.9 (a) Grading curve of Sand type - 1

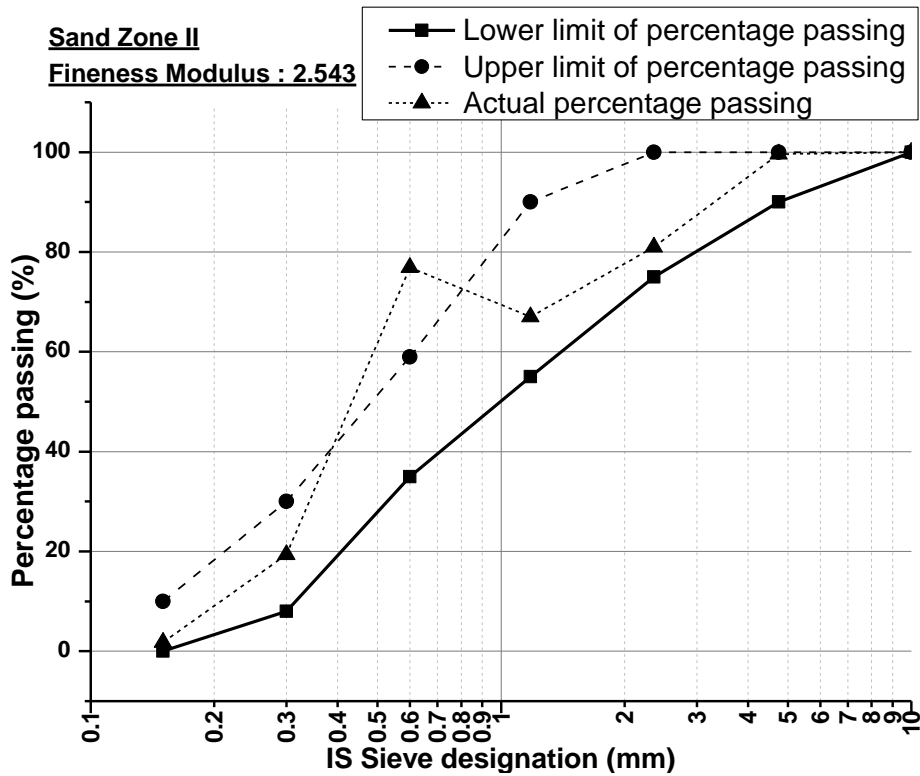


Fig. 3.9(b) Grading curve of Sand type - 2

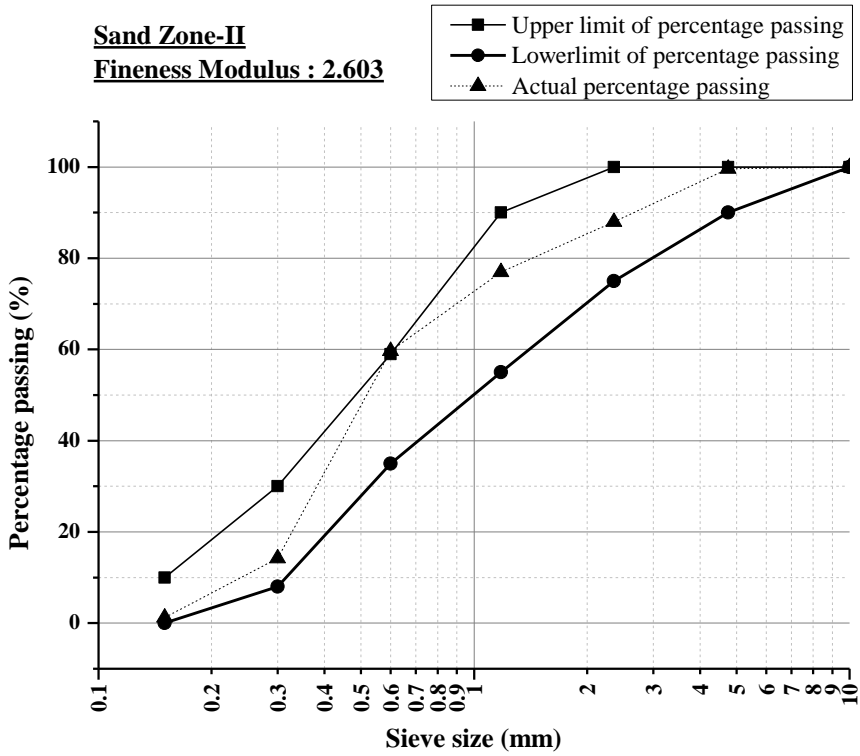


Fig. 3.9 (c) Grading curve of Sand type - 3

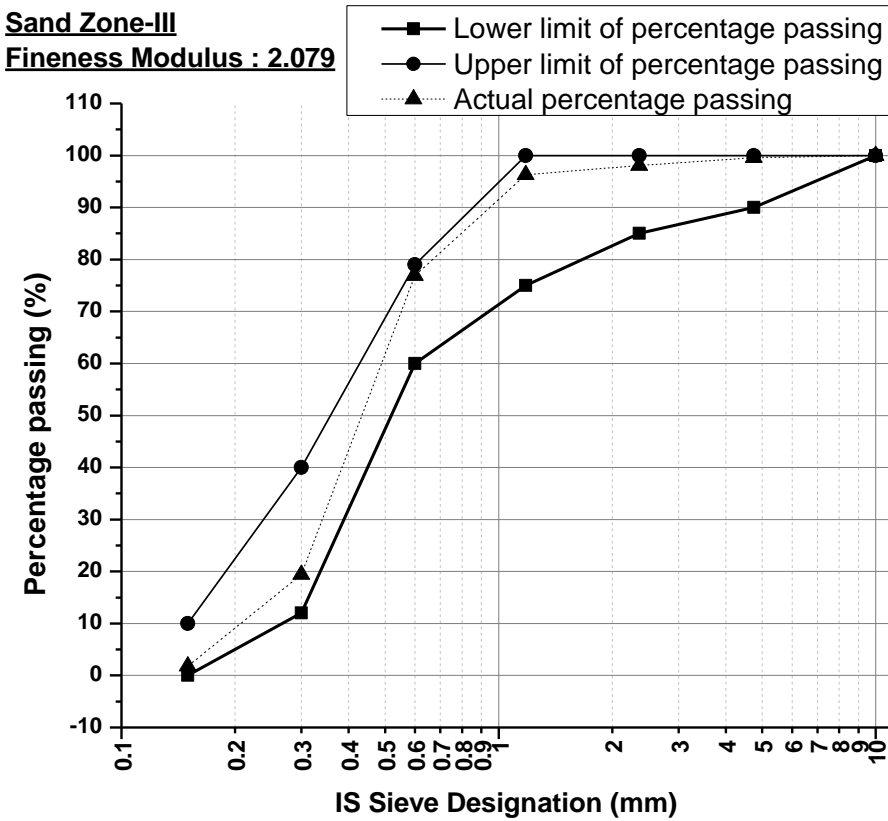


Fig. 3.9(d) Grading curve of Sand type - 4.

From the above 4 Nos. Grading curves, it may be concluded that sand samples are of coarse to medium coarse varieties, complying with respective zone, as mentioned in IS 383.

3.3.3(b) Phase analysis - XRD

The constituent phase analysis of sand was carried out with a PANalytical X'Pert's Pro powder diffractometer with X'Celerator detector and variable divergence- and receiving slits with Fe filtered Cu-K α radiation in a diffraction angle (2θ) range of 15° - 70° . The phases were identified using X'Pert Highscore plus software. The relative phase amounts (weights %) were estimated using the Rietveld method (Autoquan Program). X-Ray Diffraction analysis, showing the constituent phases of sample as shown under figure 3.9.

Table 3.12 : Peak list of Sand

Pos.[$^{\circ}2\theta$.]	d-spacing[\AA]	Rel.Int.[%]
21.3778	4.15652	3.14
22.4349	3.96302	2.14
24.2871	3.66481	18.64
25.2831	3.52266	1.48
27.0572	3.29557	100.00
27.6120	3.23061	16.31
32.6617	2.74176	1.61
34.9099	2.57017	7.99
36.9868	2.43048	15.50
38.2473	2.35323	0.93
39.9667	2.25587	44.70
41.2250	2.18988	3.47
42.3610	2.13374	0.95
42.9814	2.10437	3.81
46.2846	1.96159	11.58
47.6810	1.90735	0.75
48.9680	1.86019	2.84
50.5723	1.80488	5.45
51.2589	1.78231	1.80
52.9296	1.72993	1.26
54.5433	1.68250	0.47
55.3272	1.66050	2.85
58.0348	1.58931	1.02
60.4452	1.53158	3.24
66.2697	1.41039	0.56
68.6781	1.36556	5.31

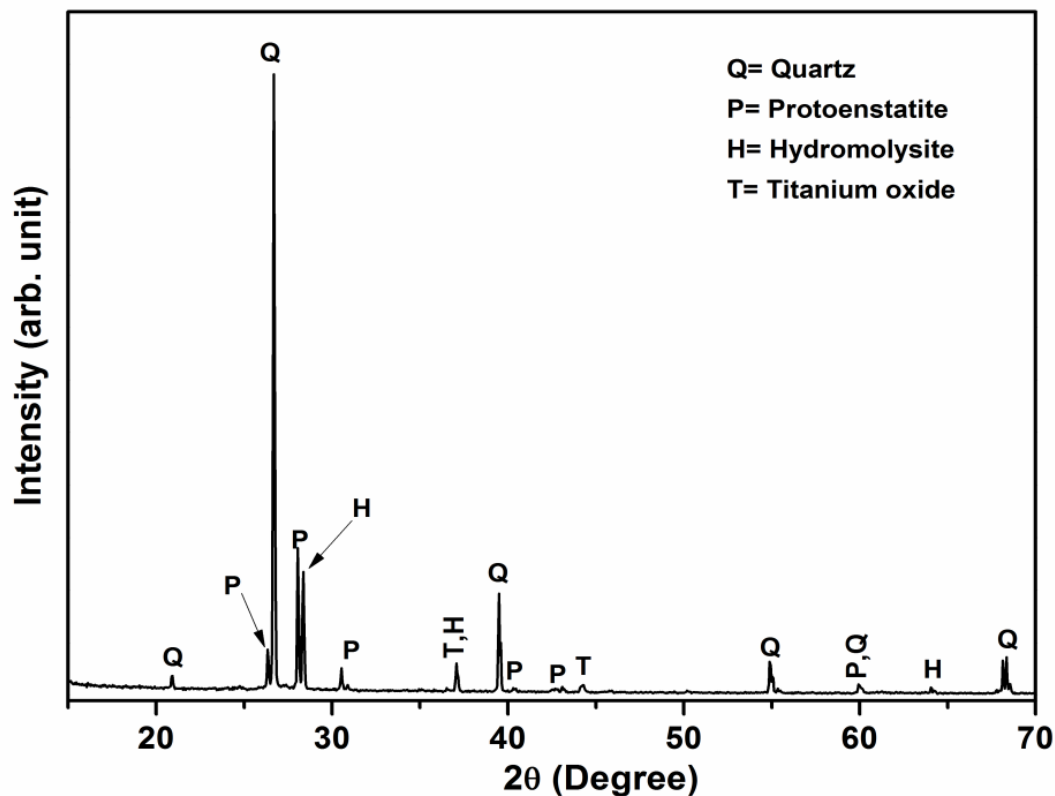


Fig. 3.10 X-Ray Diffractogram pattern of sand sample showing constituent phases.

It is revealed from the diffraction pattern that the fly ash sample contains following phases –

1. Quartz : SiO_2 ,
2. Protoenstatite (MgSiO_3),
3. Hydromolysite ($\text{FeCl}_3 \cdot 6\text{H}_2\text{O}$) ,
4. Titanium Oxide (TiO)

3.3.3(c) Surface Morphology – FESEM(Sand)

Field Emission Scanning Electron Microscopy of fly ash and bottom ash samples were done with the help of high resolution Carl ZEISS SUPRA 35 VP instrument at CGCRI Laboratory under different magnifications as shown below.

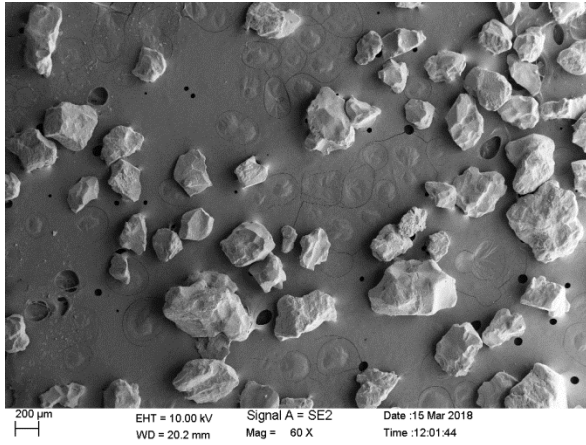


Fig.3.11(a) SEM of Sand at 60X

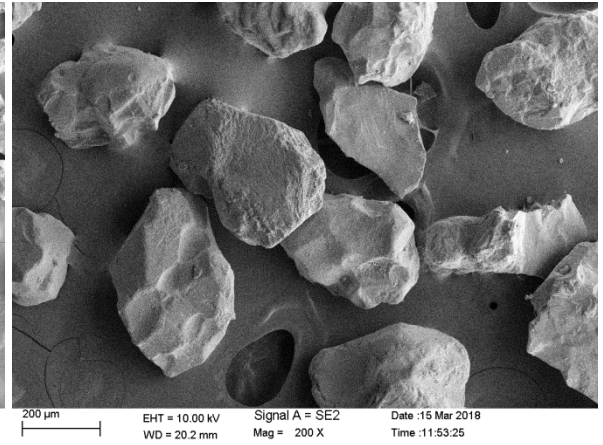


Fig.3.11(b) SEM of Sand at 200X

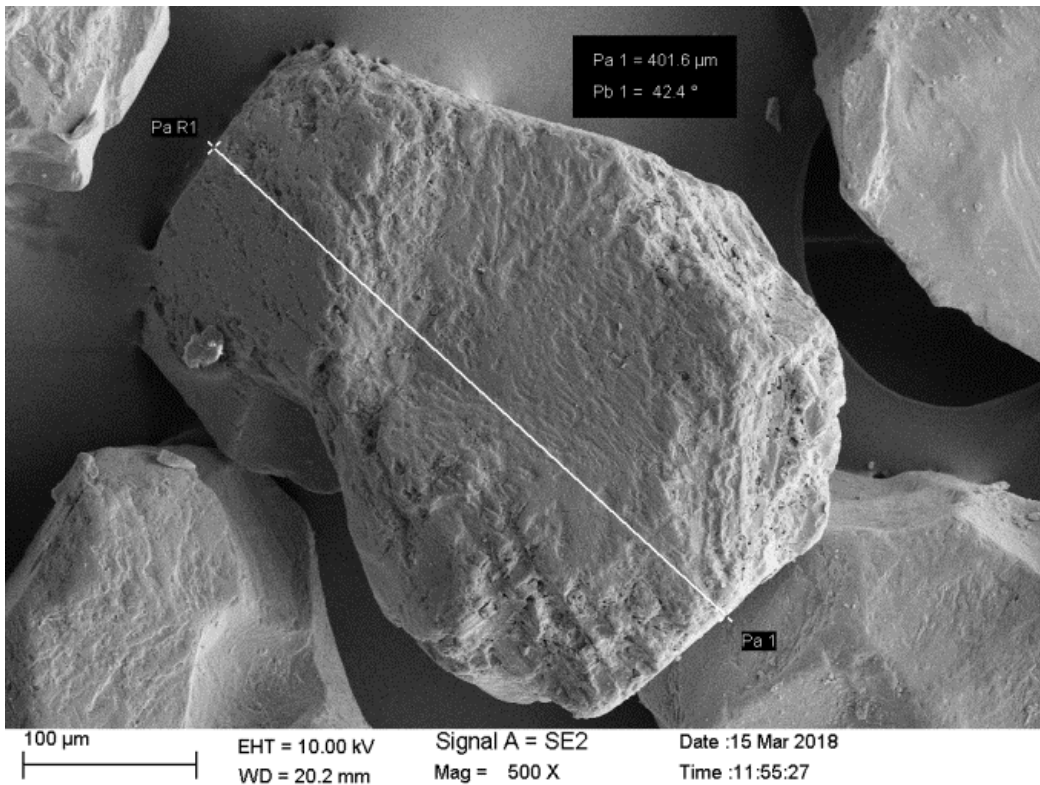


Fig. 3.11 (c) SEM of Sand at 500X Magnification

The surface of the sample was scanned in SE (in lens) modes of FESEM. The morphology and size of the powder particles were investigated. The recorded micrographs were taken at different magnifications (60X, 200X, 500X) from various locations at the sample surfaces.

3.3.3(d) Physical Test - Density of Sand

Density of powder samples were measured by Gas Pycnometry with the help of Micromeritics AccuPyc II 1340 V 1.05 instrument. Analysis Gas used was Helium, Test temperature was 22.31⁰ C. Number of purges = 10

Table 3.12 Density value of Sand

Identification of Sample	Volume (cm ³)	Bulk Density value (g/cm ³)
Sand	4.3283	2.6609

3.3.3(e) Physical Test – Surface Area (Sand)

Surface area measurement by BET method [ASTM B 922-10] with the help of Quantachrome Nova Station A, Novawin version 10.01 at CGCRI Material Characterization Division. Analysis gas used was Nitrogen.

Surface area = 0.198 m²/g.

3.3.4 Stone Aggregate

Coarse aggregate, most of which is retained on 4.75 mm IS Sieve and contains only so much finer material, as per code provision. It may also be defined as uncrushed gravel or stone from natural disintegration of rock Or crushed gravel / stone, results from crushing artificially the natural rock Or blending of both.

3.3.4(a) Sieve analysis

Following IS 383 Stipulations, the sieve analysis was carried out for below mentioned varieties of stone aggregates.

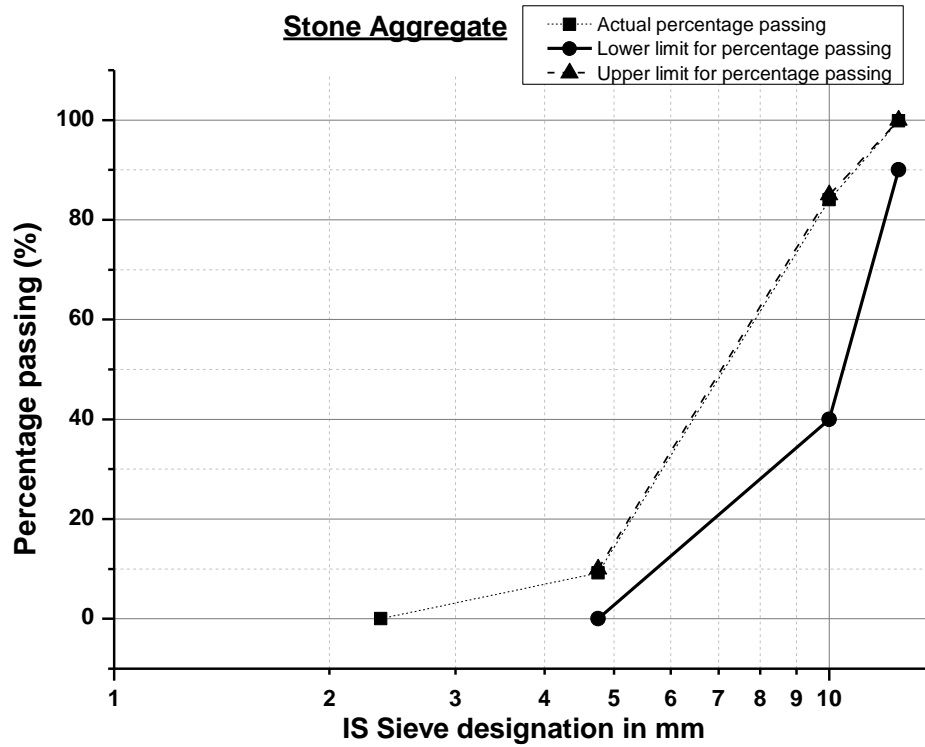


Fig.3.11(a) Grading curve of Stone aggregate type - 1

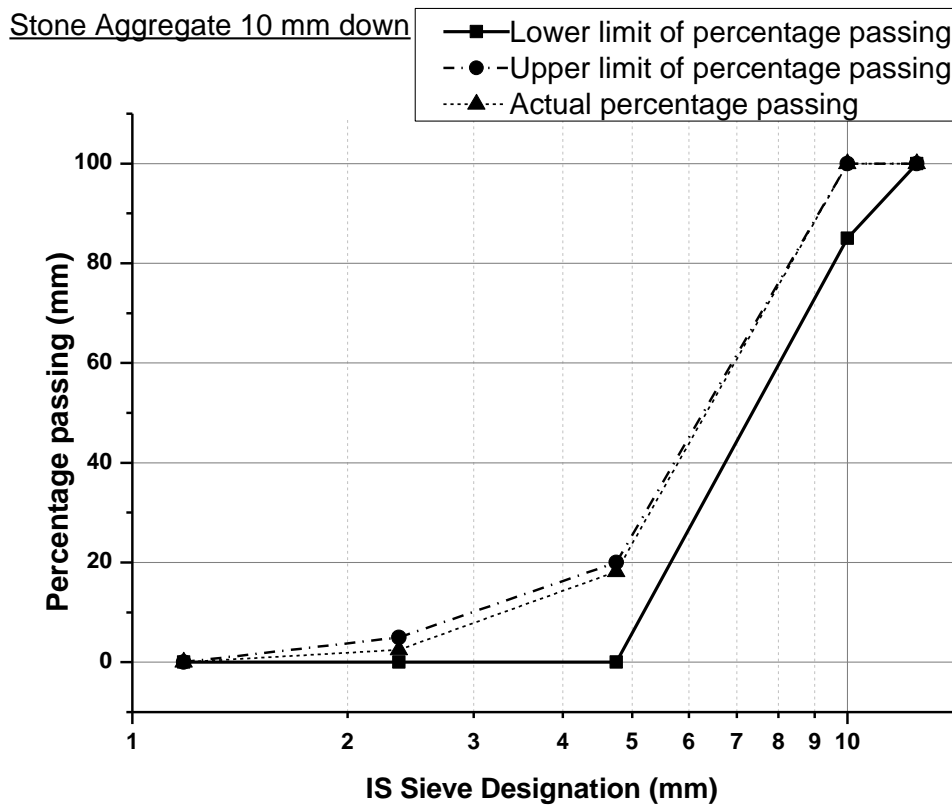


Fig.3.11(b) Grading curve of Stone aggregate type - 2

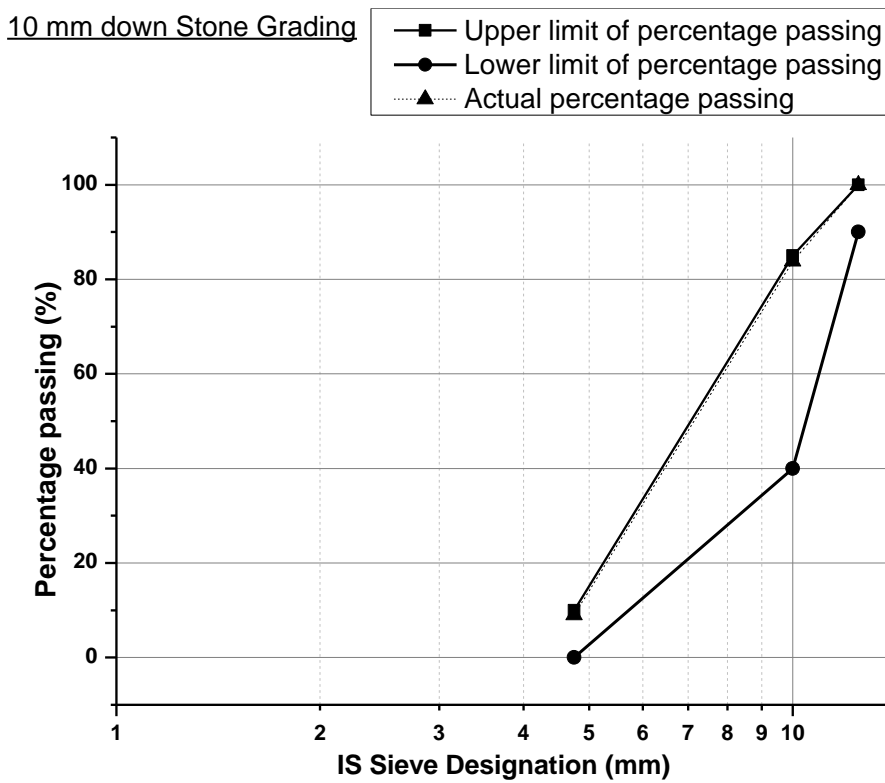


Fig.3.11 (c) Grading curve of Stone aggregate type - 3

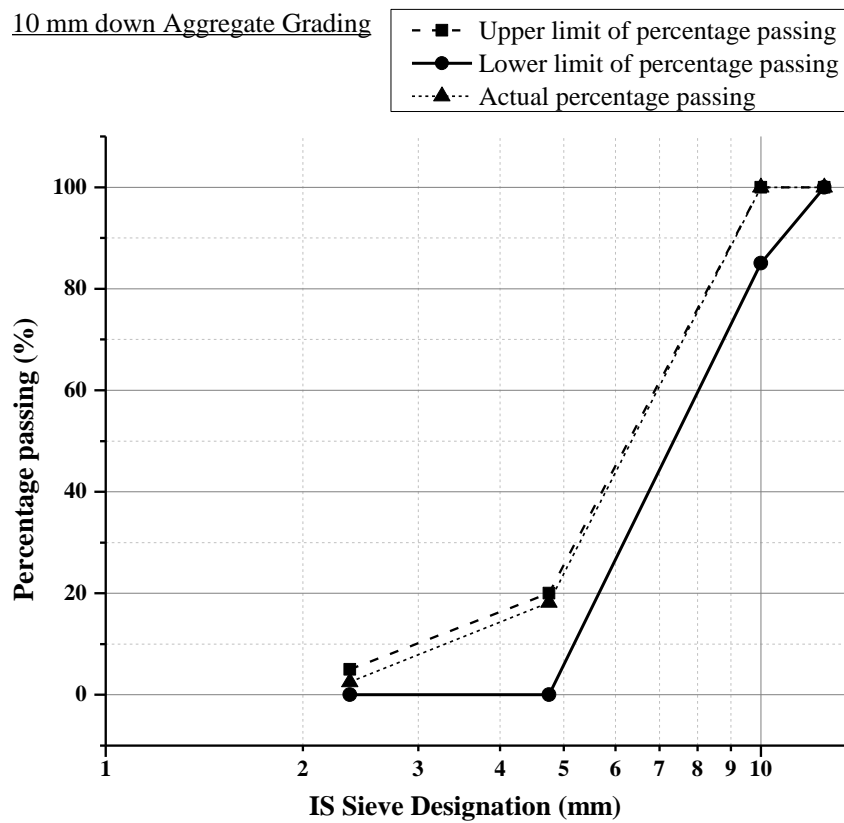


Fig. 3.11(d) Grading curve of Stone aggregate type – 4

3.3.5 Lime dust and Marble dust

3.3.5(a) Quantitative Chemical analysis

The samples were collected from local market and marble cutting/polishing industries respectively. Those were tested at Analytical Chemistry laboratory of CGCRI by WET Chemical method to find out the chemical constituents of the same.

Table 3.13 Chemical composition of Lime dust and Marble dust

Chemical constituent	Lime Powder (LM)	Marble Dust (MD)	Method used
SiO ₂	12.92	14.28	Volumetry
Al ₂ O ₃	0.94	1.20	ICP – AES
Fe ₂ O ₃	0.12	0.78	ICP - AES
CaO	61.65	27.25	Complexometry
MgO	0.97	17.76	ICP - AES
Na ₂ O	0.46	0.65	ICP - AES
K ₂ O	0.09	0.42	ICP - AES
TiO ₂	0.11	0.82	ICP - AES
LOI	22.53	36.66	Gravimetry

3.3.6 Burnt Clay Bricks

Bricks should be hand or machine molded and made of admixture of suitable soils. Bricks should be uniformly burnt, free from cracks and flaws such as nodules of stone, black coring and organic matter. Frog dimensions should same for both modular and non-modular size bricks. Burnt clay fly ash bricks are classified on the basis of average compressive strength as per IS 1077, as shown under Table 3.11. The brick used for this work was 3.5 Class Brick.

3.3.6(a) Physical Test – Dimension :

Around 20 Bricks were taken on random sampling and the dimensions were measured. The values observed to be matching with that of Non-modular ones and also within the tolerance limit prescribed by IS 1077-1992 Cl.6.2.

Average dimension of RUPSA brand bricks were : $230 \times 110 \times 70$

3.3.6(b) Physical Test –Class Designation :

As per laid down procedure in IS 3495 (Part-1)-1992, the average compressive strength of the brick used for this work was 3.5 MPa.

Hence, the Class Designation is 3.5, and the Class is shown in the following table –

Table 3.14 Classes of Common Burnt Clay Bricks

Class Designation	Average Compressive Strength (not less than)	
	N/mm ²	Kgf/cm ² (approx.)
35	35.0	350
30	30.0	300
25	25.0	250
20	20.0	200
17.5	17.5	175
15	15.0	150
12.5	12.5	125
10	10.0	100
7.5	7.5	75
5	5.0	50
3.5	3.5	35

3.3.6(c) Physical Test – Water Absorption :

As per IS 3495 (Pt.2) 1992, laid down procedure, the average water absorption values found to be around 18%.

3.3.6(d) Physical Test – Efflorescence :

As per IS 3495 (Pt.3) 1992, laid down procedure, the average efflorescence found to be moderate for 4 specimens, and slight for 2 specimens.

The bricks from Class designation 3.5 had been used for construction of pair of Masonry Wall Panel of size 480 mm by 480 mm by 110 mm, plastered on both sides of 12 mm thickness and finally putty and colour finish for making an even surface. These panels were tested to compare the U-factors. The mortar and plaster grade used was MM5. One part of Cement and four parts of fine aggregate were used for this grade of mortar and plaster. In one test panel mortar and plaster used were of conventional type (1 Cement : 4 Sand), and another panel, Fly ash and lime was used in 50 : 50, and no sand was used (1 Cement : 2 Fly ash : 2 Lime). The tested panel is shown in the following page.



Fig. 3.12 Plastered-puttied-coloured Wall Sample after U-value testing

Chapter 4
Experimental Investigations

Chapter 4: Experimental Investigations

4.1 Overview:

The main objective of the experimental investigation is to ascertain the physical strength of the Concrete and Mortar mixes and finding out the thermal conductivity value of such mixes. The different mixes were designed with replacement of natural mineral by Coal ash and the changes thereof with respect to the physical and thermal properties. Each of the ingredients of Concrete and Mortar mixes were tested for the individual parameters, beforehand for their suitability for the intended purpose.

4.2 Experimentation:

Total Experimental investigations have been divided in to following steps:

1. Basic parameter testing (chemical and physical) of main ingredients of concrete and mortar.
2. Concrete mix design on the basis of basic ingredient material properties and fixing of Proportions as per IS 456: 2000, IS 10262: 2009 and SP 23 : 1982 Code provisions. Mortar Mix selection as per relevant IS 2250: 1981 Code provisions.
3. Casting of concrete and mortar cubes (50 mm X 50 mm X 50 mm) for compressive strength test. Casting of concrete and mortar samples (50 mm X 50 mm X 25 mm) and (50 mm X 50 mm X 12.5 mm) for thermal conductivity, apparent porosity and bulk density tests. Curing of samples.
4. Compressive strength test of concrete and mortar cubes, and test results.
5. X-Ray Diffraction analysis of Concrete and Mortar mixes.
6. Evaluation of Apparent Porosity and Bulk Density of cast samples.
7. Evaluation of thermal property by Thermal Conductivity test of Concrete and Mortar samples.
8. Casting of Brick Wall samples with Mortar and plaster on both faces, curing and testing of wall assembly.
9. U-value test set up and test procedure.
10. U-value test results.

4.2.1 Basic parameter of materials had been tested and the details of instruments, methodologies and results are described in Chapter 3.

4.2.2 Concrete Mix Design calculations:

4.2.2.1 Concrete overview:

Concrete is a versatile heterogeneous man-made mix of different natural and/or artificial ingredients. Though use of Pozzolana was started by Greeks and Romans long back (600 BC), William Aspdin invented the modern Portland cement in 1840 (Steiger, 1995), and the reinforced cement concrete was first used by Joseph Monier in 1849 (Inventors and Inventions, Vol. 4). The main advantages of concrete is that it can be tailored to meet the specific requirements either strength or ingredient choice or shape issue etc. The advances in concrete technology has helped to make the best use of locally available material by proper mix. Considering various parameters from functionality and durability points of views by any structure made of Concrete and Mortar, appropriate factors can be incorporated while designing the mix. While the concrete acts as a single material, the role of action and interaction of the constituent materials are of significant importance, and sometimes create conflict in arriving at the desired result. For ease of placing concrete inside congested reinforcement grids, and spreading uniformly, the concrete requires to maintain certain degree of workability. The easiest way to maintain the desired degree of workability is to add water. Addition of more water than the limit, seriously affect the strength of concrete. Actually water is mixed to complete the hydration reaction of cement at the first instance and secondly to lubricate all the ingredients (sand particles and stone aggregates). Since Abram observed the phenomena of diminishing strength with addition of more water or increasing the water-cement ratio, and formulated the following empirical equation in 1918 :

$$S = \frac{A}{B^x} \quad (4.1)$$

where S is the concrete strength, A and B are constants for 28 days and x is the water-cement ratio by volume. It states that assuming full compaction and at a given age and normal temperature, strength of concrete can be considered to be inversely proportional to the water-cement ratio. Another important consideration is gel-space

ratio, which actually fills the voids between aggregates. Higher gel-space ratio increases strength, and decreases porosity and vice-versa. Again higher water-cement ratio decreases the gel-space ratio and increases the porosity. This reduces the strength as a final consequence. The total percentage of water, air (entrapped), cement, fine aggregate, coarse aggregate and or additives determine the final volume of concrete, and each of these parameters are calculated judiciously to maintain desired strength criteria, durability aspect and ease of workability combined.

4.2.2.2 Steps involved in Designing the Concrete Mix :

Step 1 – Grade of Concrete:

Depending upon the design of Concrete structure and its calculated strength, grade of concrete is chosen. M 10, M 15 and M 20 Grades of concrete fall under Ordinary Concrete category, and from M 25 to M 55 fall under Standard Concrete category and beyond that, those are termed as High strength Concrete (Table 2, Is 456). The letter “M” stands for mix and the numerical refers to the 28 day’s characteristic compressive strength in N/mm^2 or MPa.

Step 2 – Other parameters selection:

Those are to be selected viz.

- i) Maximum size of aggregate with shape
- ii) Degree of workability required
- iii) Degree of quality control
- iv) Type of exposure
- v) Cement used: type and grade
- vi) Specific gravity of cement to be used
- vii) Specific gravity of coarse (stone) aggregate
- viii) Specific gravity of fine (sand) aggregate
- ix) Water absorption by coarse aggregate
- x) Water absorption by fine aggregate
- xi) Free (surface) moisture of coarse aggregate
- xii) Free (surface) moisture of fine aggregate
- xiii) Sieve analysis result of fine aggregate and determination of zone
- xiv) Sieve analysis result of coarse aggregate

xv) Entrapped Air content against nominal maximum size of the Aggregate

Step 3 – Target mean strength :Considering the induced variability of concrete strength during production, it has been felt necessary to design the mix to have a target mean strength which is greater than the characteristic strength by a suitable margin. It is expressed as :

$$f_t = f_{ck} + k \times S \quad (4.2)$$

where f_t is the target mean strength , f_{ck} is the characteristic compressive strength of the grade of concrete, considered, k is a constant, derived from the mathematics of Normal distribution and S = standard deviation. The value of K is considered to be equal to 1.65, where not more than 5% of the test results are expected to fall below the characteristic strength.

Step 4 – Selection of Water-Cement Ratio :

Since different varieties of cements and aggregates of different size / shape, grading, surface texture are available, concrete of different compressive strength for the same free water-cement ratio may be produced. In case of availability of all the information beforehand, the preliminary free water-cement ratio corresponding to the target strength at 28 days may be selected from the given curve in IS 10262. Alternately, the preliminary free water-cement ratio corresponding to the target mean strength may be selected from the set of curves corresponding to the 28 days cement strength to be used for the purpose. The free water-cement ratio selected by following either of the process, and should be checked finally against the limiting water-cement ratio from durability point of view, as specified in Table 5 of IS 456 Code and the lower of the two values should be adopted.

Step 5 – Selection of Sand and Water content :

Approximate sand and water content have been prescribed in the IS 10262: 1982 against nominal maximum size of aggregate, subject to certain conditions against aggregate quality (both coarse and fine), water-cement ratio by mass and workability value. The given values are for reference, to start the calculation with, and subsequently the same need to be adjusted as per deviations to follow than the set conditions.

Step 6 – Determination of Cement content :

From the water content calculated in step 5 and water-cement ratio in step 4, the cement content shall be worked out.

Step 7 – Determination of coarse and fine aggregate content :

Considering the entrapped air percentage for nominal maximum size of aggregate to be used for the purpose, the following equations are required to be solved to determine the coarse and fine aggregate content –

$$V = \left\{ W + \frac{C}{S_c} + \frac{1}{p} \times \frac{f_a}{S_{f_a}} \right\} \times \frac{1}{1000} \quad (4.3)$$

And

$$V = \left\{ W + \frac{C}{S_c} + \frac{1}{(1-p)} \times \frac{C_a}{S_{c_a}} \right\} \times \frac{1}{1000} \quad (4.4)$$

Where, V = absolute volume of fresh concrete = gross volume (1 m³) minus the volume of entrapped air,

S_c = specific gravity of Cement,

S_{fa}, S_{ca} = specific gravity of fine aggregate and coarse aggregate respectively,

C = mass of Cement (kg) per m³ of concrete,

C_a, f_a = total masses of coarse and fine aggregates (kg) per m³ of concrete respectively,

W = mass of water (kg) per m³ of concrete,

p = ratio of fine aggregate to total aggregate by absolute volume.

Step 8 – Proportioning of Mix :

With Cement content from step 6 , and fine and coarse aggregate contents from step 7, the mix proportion can be arrived at.

Step 9 –Adjustments :

After allowing absorption by surface dry condition coarse aggregate and deduction for surface moisture in fine aggregate, final water content shall be calculated, and final coarse aggregate and fine aggregate content shall also be re-calculated after accommodating excess / less water respectively.

Step 10 – Final Mix proportion :

With the values obtained from step 9 above and from that of Step 6, final mix proportion is arrived, on the basis of which casting of cubes and samples shall be prepared to evaluate compressive strength, apparent porosity, bulk density and thermal conductivity.

4.2.2.3 Calculations for Mix proportioning :

4.2.2.3.1 Design Mix for M-15 Grade of Concrete

Step 1 : The characteristic compressive strength , $f_{ck} = 15 \text{ N/mm}^2$. (as explained under 4.2.2.2 Step 1).

Step 2 :Parameters of materials used –

- i) 10 mm down size stone aggregate, angular and to some extent flaky in nature.
- ii) Degree of Workability = Low , Slump 25-75 mm
- iii) Degree of Quality Control = Very Good
- iv) Type of exposure = Moderate
- v) Cement used - type and grade = Portland Pozzolana Cement (PPC)
- vi) Specific gravity of cement to be used = 3.04
- vii) Specific gravity of coarse (stone) aggregate = 2.949
- viii) Specific gravity of fine (sand) aggregate = 2.667
- ix) Water absorption by coarse aggregate = 2%
- x) Water absorption by fine aggregate = 1%
- xi) Free (surface) moisture of coarse aggregate = Nil
- xii) Free (surface) moisture of fine aggregate = 2%
- xiii) Sieve analysis result of fine aggregate and determination of zone = As indicated against Cl.3.2.3, Zone II
- xiv) Sieve analysis result of coarse aggregate = As indicated against Cl.3.2.4
- xv) Entrapped air content corresponding to nominal maximum size of Aggregate = 3% [Table 3, IS 10262].

Step 3 : Target Mean strength, $f_t = f_{ck} + 1.65 \times S$ (Eqn. 4.2)

$$\begin{aligned} &= 15 + 1.65 \times 2.5 \text{ [S=2.5, Table 1, IS 10262]} \\ &= 19.125 \text{ N/mm}^2 . \end{aligned}$$

Step 4 :As suggested under Cl.4.2.2.2 Step 4, the free water-cement ratio (w/c) against the target compressive strength of concrete (f_t) is found to be 0.58. With the alternate suggestion under the same clause, the w/c is found to be 0.61. From durability aspect, IS 456 provision under Table 5 states that maximum free w/c permitted is 0.60.

Choosing lowest of all the above, the w/c may be considered 0.58. However, for experimental purpose, the effort shall be made to restrict the same within 0.50 after adjusting free moisture etc.

Step 5 : As suggested under Cl. 4.2.2.2 Step 5, the approximate Sand content as percent of total aggregate by absolute volume is 40.0 , and Water content per cubic meter of concrete is 208 kg. These values are considered against nominal maximum size of aggregate, which is 10 mm for this case. To begin with, we assume Sand content as 42%, and therefore the Stone Aggregate content stands at 58%

Step 6 : Considering w/c = 0.50, and free water content as 165 kg < 208 kg,

$$\text{Cement content} = 165/0.50 = 330 \text{ kg/m}^3.$$

Step 7 : To determine fine aggregate and coarse aggregate contents, the various values related to the equation in Step 7 are taken from Step 2 above.

Therefore, for fine aggregate quantity determination, the Equation (4.3) followed as

$$(1 - 0.03) = \left\{ 165 + \frac{330}{3.04} + \left(\frac{1}{0.42} \right) \times \left(\frac{f_a}{2.667} \right) \right\} \times \frac{1}{1000}$$

Solving this, $f_a = 780.12 \text{ kg/m}^3$. Say 780 kg/m³

Again, for coarse aggregate quantity determination, the Equation (4.4) followed as

$$(1 - 0.03) = \left\{ 165 + \frac{330}{3.04} + \left(\frac{1}{1 - 0.42} \right) \times \left(\frac{C_a}{2.949} \right) \right\} \times \frac{1}{1000}$$

Solving this, $C_a = 1191.22 \text{ kg/m}^3$ Say 1190 kg/m^3 .

The final quantity stands as follows : -

Cement = 330 kg/m^3

Water = 165 kg/m^3

Fine Aggregate = 780 kg/m^3

Coarse Aggregate = 1190 kg/m^3

Water-Cement Ratio = 0.50

Workability = 25 mm

The Mix proportion for M-15 Grade Design Mix :1: 2. 4: 3. 6

4.2.2.3.1(a) Sand replacement by Bottomash in the above Mix proportion :

With Bottomash as gradual replacement of Sand, the proportions arrived at are tabulated below. As per the written down proportions, cubes had been cast and samples were made for various physical and thermal parameter testing.

Table 4.1 M-15 Design Mix Composition with Sand replacement by Bottom Ash

Mix proportion	Cement	Sand	Bottomash	Flyash	Coarse Aggregate
1:2.4:3.6 with 100% Sand	1	2.40	0.00	-	3.60
1:2.4:3.6 with 90% Sand & 10% Bottomash	1	2.16	0.24	-	3.60
1:2.4:3.6 with 80% Sand & 20% Bottomash	1	1.92	0.48	-	3.60
1:2.4:3.6 with 70% Sand & 30% Bottomash	1	1.68	0.72	-	3.60
1:2.4:3.6 with 60% Sand & 40% Bottomash	1	1.44	0.96	-	3.60
1:2.4:3.6 with 50% Sand & 50% Bottomash	1	1.20	1.20	-	3.60
1:2.4:3.6 with 40% Sand & 60% Bottomash	1	0.96	1.44	-	3.60
1:2.4:3.6 with 30% Sand & 70% Bottomash	1	0.72	1.68	-	3.60
1:2.4:3.6 with 20% Sand & 80% Bottomash	1	0.48	1.92	-	3.60
1:2.4:3.6 with 10% Sand & 90% Bottomash	1	0.24	2.16	-	3.60
1:2.4:3.6 with 0% Sand & 100% Bottomash	1	0.00	2.40	-	3.60

4.2.2.3.2 Alternate Design Mix for M-15 Grade of Concrete

Step 1 :

The characteristic compressive strength , $f_{ck} = 15 \text{ N/mm}^2$. (as explained under 4.2.2.2 Step 1).

Step 2 :

Parameters of materials used –

- i) 10 mm down size stone aggregate, angular and to some extent flaky in nature.
- ii) Degree of Workability = Low , Slump 25-75 mm
- iii) Degree of Quality Control = Very Good
- iv) Type of exposure = Moderate
- v) Cement used - type and grade = Portland Pozzolana Cement (PPC)
- vi) Specific gravity of cement to be used = 3.04
- vii) Specific gravity of coarse (stone) aggregate = 2.949
- viii) Specific gravity of fine (sand) aggregate = 2.667
- ix) Water absorption by coarse aggregate = 3%
- x) Water absorption by fine aggregate = 2%
- xi) Free (surface) moisture of coarse aggregate = Nil
- xii) Free (surface) moisture of fine aggregate = 2%
- xiii) Sieve analysis result of fine aggregate and determination of zone = As indicated against Cl.3.2.3, Zone II
- xiv) Sieve analysis result of coarse aggregate = As indicated against Cl.3.2.4
- xv) Entrapped air content corresponding to nominal maximum size of Aggregate = 3% [Table 3, IS 10262].

Step 3 :

Target Mean strength, $f_t = f_{ck} + 1.65 \times S$

$$= 15 + 1.65 \times 2.5 \text{ [S=2.5 Table 1, IS 10262]}$$

$$= 19.125 \text{ N/mm}^2.$$

Step 4 : As suggested under Cl.4.2.2.2 Step 4, the free water-cement ratio (w/c) against the target compressive strength of concrete (f_c) is found to be 0.58. With the alternate suggestion under the same clause, the w/c is found to be 0.61. From durability aspect, BIS 456 provision under Table 5 states that maximum free w/c permitted is 0.60.

Choosing lowest of all the above, the w/c may be considered 0.50.

Step 5 : As suggested under Cl. 4.2.2.2 Step 5, the approximate Sand content as percent of total aggregate by absolute volume is 40.0 , and Water content per cubic meter of concrete is 208 kg. These values are considered against nominal maximum size of aggregate, which is 10 mm for this case. Considering more Sand content, the value is fixed at 41.5%, and the coarse aggregate content stands at 58.5%.

Step 6 : Considering w/c = 0.50, and free water content as 183 kg < 208 kg,

$$\text{Cement content} = \frac{183}{0.50} = 366 \text{ kg/m}^3$$

Step 7 : To determine fine aggregate and coarse aggregate contents, the various values related to the equation in Step 7 are taken from Step 2 above.

Therefore, for fine aggregate quantity determination, from Equation 4.3

$$(1 - 0.03) = \left\{ 183 + \frac{366}{3.04} + \left(\frac{1}{0.415} \right) \times \left(\frac{f_a}{2.667} \right) \right\} \times \frac{1}{1000}$$

Solving this, = 737.802 kg/m³.

Again, for coarse aggregate quantity determination, from Equation 4.4

$$(1 - 0.03) = \left\{ 183 + \frac{366}{3.04} + \left(\frac{1}{1 - 0.415} \right) \times \left(\frac{C_a}{2.949} \right) \right\} \times \frac{1}{1000}$$

Solving this, = 1150.004 kg/m³ .

The final quantity stands after adjusting free moisture present in the aggregates, as follows :

Cement = 366 kg/m³

Water = 183 kg/m³

Fine Aggregate = 735 kg/m³

Coarse Aggregate = 1130 kg/m³

Water-Cement Ratio = 0.50

Workability = 25 mm

The Mix proportion for Alternate M-15 Grade Design Mix :1: 2. 0: 3. 0

4.2.2.3.2(a) Sand replacement by Bottomash in the Mix proportion :

With Bottomash as gradual replacement of Sand, the proportions arrived at are tabulated below. As per the written down proportions, cubes had been cast and samples were made for various physical and thermal parameter testing.

Table 4.2 M-15 Alt. Design Mix composition with Sand replacement by Bottom ash

Mix proportion	Cement	Sand	Bottomash	Flyash	Coarse Aggregate
1:2.0:3.0 with 100% Sand	1	2.00	0.00	-	3.00
1:2.0:3.0 with 90% Sand & 10% Bottomash	1	1.80	0.20	-	3.00
1:2.0:3.0 with 80% Sand & 20% Bottomash	1	1.60	0.40	-	3.00
1:2.0:3.0 with 70% Sand & 30% Bottomash	1	1.40	0.60	-	3.00
1:2.0:3.0 with 60% Sand & 40% Bottomash	1	1.20	0.80	-	3.00
1:2.0:3.0 with 50% Sand & 50% Bottomash	1	1.00	1.00	-	3.00
1:2.0:3.0 with 40% Sand & 60% Bottomash	1	0.80	1.20	-	3.00
1:2.0:3.0 with 30% Sand & 70% Bottomash	1	0.60	1.40	-	3.00
1:2.0:3.0 with 20% Sand & 80% Bottomash	1	0.40	1.60	-	3.00
1:2.0:3.0 with 10% Sand & 90% Bottomash	1	0.20	1.80	-	3.00
1:2.0:3.0 with 0% Sand & 100% Bottomash	1	0.00	2.00	-	3.00

4.2.2.3.3 *Nominal Mix for M-15 Grade of Concrete*

Generally the Nominal Mix concept is practised since long, and till the introduction of BIS 456 – 2000, it was mostly followed for all general construction purpose, particularly in Building industry. Guidelines are provided in IS 456 : 2000 Cl. 9.3 & 9.3.1 and summarized in Table 9 of the Code, which are as below :-

1. Against per 50 kg (by mass) of Cement, total quantity of Dry aggregate (sum of individual masses of fine and coarse aggregates) shall be 330 kg (max.).
2. Proportion of Fine aggregate to Coarse aggregate (by mass) generally considered as 1:2, subject to an upper limit of 1:1.5 and a lower limit of 1:2.5.
3. Quantity of Water per 50 kg of Cement (max.) is 32 kg.

As per the Guideline, Fine Aggregate is considered as 100 kg, Coarse aggregate is considered as 200 kg, Water as 25 kg. per 50 kg Cement.

Total quantity of Aggregate = (100+200) kg = 300 kg < 330 kg

Fine Aggregate : Coarse Aggregate :: 1:2

Water content = 25 kg < 32 kg

Therefore ,the **Nominal Mix proportion for M 15 Grade stands at 1: 2: 4 with $w/c = 0.50$**

4.2.2.3.3(a) *Sand replacement by Bottomash for the Nominal Mix proportion :*

With Bottomash as gradual replacement of Sand, the proportions arrived at are tabulated below. As per the written down proportions, cubes had been cast and samples were made for various physical and thermal parameter testing.

Table 4.3 M-15 Nominal Mix composition with Sand replacement by Bottom ash

Mix proportion	Cement	Sand	Bottomash	Flyash	Coarse Aggregate
1:2.0:4.0 with 100% Sand	1	2.00	0.00	-	4.00
1:2.0:4.0 with 90% Sand & 10% Bottomash	1	1.80	0.20	-	4.00
1:2.0:4.0 with 80% Sand & 20% Bottomash	1	1.60	0.40	-	4.00
1:2.0:4.0 with 70% Sand & 30% Bottomash	1	1.40	0.60	-	4.00
1:2.0:4.0 with 60% Sand & 40% Bottomash	1	1.20	0.80	-	4.00
1:2.0:4.0 with 50% Sand & 50% Bottomash	1	1.00	1.00	-	4.00
1:2.0:4.0 with 40% Sand & 60% Bottomash	1	0.80	1.20	-	4.00
1:2.0:4.0 with 30% Sand & 70% Bottomash	1	0.60	1.40	-	4.00
1:2.0:4.0 with 20% Sand & 80% Bottomash	1	0.40	1.60	-	4.00
1:2.0:4.0 with 10% Sand & 90% Bottomash	1	0.20	1.80	-	4.00
1:2.0:4.0 with 0% Sand & 100% Bottomash	1	0.00	2.00	-	4.00

4.2.2.3.4 Design Mix for M-20 Grade of Concrete

Step 1 :

The characteristic compressive strength , $f_{ck} = 20 \text{ N/mm}^2$. (as explained under 4.2.2.2 Step 1).

Step 2 :

Parameters of materials used –

- i) 10 mm down size stone aggregate, angular and to some extent flaky in nature.
- ii) Degree of Workability = Low , Slump 25-75 mm
- iii) Degree of Quality Control = Very Good
- iv) Type of exposure = Moderate
- v) Cement used - type and grade = Portland Pozzolana Cement (PPC)
- vi) Specific gravity of cement to be used = 3.04
- vii) Specific gravity of coarse (stone) aggregate = 2.949
- viii) Specific gravity of fine (sand) aggregate = 2.667

- ix) Water absorption by coarse aggregate = 3%
- x) Water absorption by fine aggregate = 2%
- xi) Free (surface) moisture of coarse aggregate = Nil
- xii) Free (surface) moisture of fine aggregate = 2%
- xiii) Sieve analysis result of fine aggregate and determination of zone = As indicated against Cl.3.2.3, Zone II
- xiv) Sieve analysis result of coarse aggregate = As indicated against Cl.3.2.4
- xv) Entrapped air content corresponding to nominal maximum size of Aggregate = 3% [Table 3, BIS 10262].

Step 3 :

$$\begin{aligned} \text{Target Mean strength, } f_t &= f_{ck} + 1.65 \times S \\ &= 20 + 1.65 \times 3.5 [S=3.5 \text{ Table 1, IS 10262}] \\ &= 25.775 \text{ N/mm}^2 . \end{aligned}$$

Step 4 :

As suggested under Cl.4.2.2.2 Step 4, the free water-cement ratio (w/c) against the target compressive strength of concrete (f_t) is found to be 0.51. With the alternate suggestion under the same clause, the w/c is found to be 0.53. From durability aspect, BIS 456 provision under Table 5 states that maximum free w/c permitted is 0.50.

Choosing lowest of all the above, the w/c may be considered 0.50.

Step 5 :

As suggested under Cl. 4.2.2.2 Step 5, the approximate Sand content as percent of total aggregate by absolute volume is 40.0 , and Water content per cubic meter of concrete is 208 kg. These values are considered against nominal maximum size of aggregate, which is 10 mm for this case. In this case, the Sand content is fixed at 39%, and therefore the Stone Aggregate content stands at 61%.

Step 6 :

Considering w/c = 0.50, and free water content as $204 \text{ kg} < 208 \text{ kg}$,

$$\text{Cement content} = \frac{204}{0.50} = 408 \text{ kg/m}^3.$$

Step 7 :

To determine fine aggregate and coarse aggregate contents, the various values related to the equation in Step 7 are taken from Step 2 above.

Therefore, for fine aggregate quantity determination, the Equation is

$$(1 - 0.03) = \left\{ 204 + \frac{408}{3.04} + \left(\frac{1}{0.39} \right) \times \left(\frac{f_a}{2.667} \right) \right\} \times \frac{1}{1000}$$

Solving this, = 657.14 kg/m³ .

Again, for coarse aggregate quantity determination, the Equation is

$$(1 - 0.03) = \left\{ 204 + \frac{408}{3.04} + \left(\frac{1}{0.61} \right) \times \left(\frac{C_a}{2.949} \right) \right\} \times \frac{1}{1000}$$

Solving this, = 1136.52 kg/m³.

The final quantity stands after adjusting free moisture present in the aggregates, as follows :

Cement = 408 kg/m³

Water = 204 kg/m³

Fine Aggregate = 660 kg/m³

Coarse Aggregate = 1135 kg/m³

Water-Cement Ratio = 0.50

Workability = 25 mm

The Mix proportion for M-20 Grade Design Mix : 1: 1. 62: 2. 78

4.2.2.3.4(a) Sand replacement by Bottomash in the Mix proportion :

With Bottomash as gradual replacement of Sand, the proportions arrived at are tabulated below. As per the written down proportions, cubes had been cast and samples were made for various physical and thermal parameter testing.

Table 4.4 M-20 Design Mix composition with Sand replacement by Bottom ash

Mix proportion	Cement	Sand	Bottomash	Flyash	Coarse Aggregate
1:1.62:2.78 with 100% Sand	1	1.620	0.000	-	2.78
1:1.62:2.78 with 90% Sand & 10% Bottomash	1	1.458	0.162	-	2.78
1:1.62:2.78 with 80% Sand & 20% Bottomash	1	1.296	0.324	-	2.78
1:1.62:2.78 with 70% Sand & 30% Bottomash	1	1.134	0.486	-	2.78
1:1.62:2.78 with 60% Sand & 40% Bottomash	1	0.972	0.648	-	2.78
1:1.62:2.78 with 50% Sand & 50% Bottomash	1	0.810	0.810	-	2.78
1:1.62:2.78 with 40% Sand & 60% Bottomash	1	0.648	0.972	-	2.78
1:1.62:2.78 with 30% Sand & 70% Bottomash	1	0.486	1.134	-	2.78
1:1.62:2.78 with 20% Sand & 80% Bottomash	1	0.324	1.296	-	2.78
1:1.62:2.78 with 10% Sand & 90% Bottomash	1	0.162	1.458	-	2.78
1:1.62:2.78 with 0% Sand & 100% Bottomash	1	0.000	1.620	-	2.78

4.2.2.3.5 Alternate Design Mix I for M-20 Grade of Concrete :

Step 1 :

The characteristic compressive strength , $f_{ck} = 20 \text{ N/mm}^2$. (as explained under 4.2.2.2 Step 1).

Step 2 :

Parameters of materials used –

- i) 10 mm down size stone aggregate, angular and to some extent flaky in nature.
- ii) Degree of Workability = Low , Slump 25-75 mm
- iii) Degree of Quality Control = Very Good
- iv) Type of exposure = Moderate
- v) Cement used - type and grade = Portland Pozzolana Cement (PPC)
- vi) Specific gravity of cement to be used = 3.04
- vii) Specific gravity of coarse (stone) aggregate = 2.949
- viii) Specific gravity of fine (sand) aggregate = 2.667

- ix) Water absorption by coarse aggregate = 3%
- x) Water absorption by fine aggregate = 2%
- xi) Free (surface) moisture of coarse aggregate = Nil
- xii) Free (surface) moisture of fine aggregate = 2%
- xiii) Sieve analysis result of fine aggregate and determination of zone = As indicated against Cl.3.2.3, Zone II
- xiv) Sieve analysis result of coarse aggregate = As indicated against Cl.3.2.4
- xv) Entrapped air content corresponding to nominal maximum size of Aggregate = 3% [Table 3, BIS 10262].

Step 3 :

$$\begin{aligned}\text{Target Mean strength, } f_t &= f_{ck} + 1.65 \times S \\ &= 20 + 1.65 \times 3.5 \text{ [S=3.5, Table 1, IS 10262]} \\ &= 25.775 \text{ N/mm}^2 .\end{aligned}$$

Step 4 :

As suggested under Cl.4.2.2.2 Step 4, the free water-cement ratio (w/c) against the target compressive strength of concrete (f_t) is found to be 0.51. With the alternate suggestion under the same clause, the w/c is found to be 0.53. From durability aspect, IS 456 provision under Table 5 states that maximum free w/c permitted is 0.50.

Choosing lowest of all the above, the w/c may be considered 0.48.

Step 5 :

As suggested under Cl. 4.2.2.2 Step 5, the approximate Sand content as percent of total aggregate by absolute volume is 40.0 , and Water content per cubic meter of concrete is 208 kg. These values are considered against nominal maximum size of aggregate, which is 10 mm for this case. In this case, the Sand content is considered to be higher than all other previous mix, i.e. 42%, and the coarse aggregate content stands at 58%. This is done mainly to utilize maximum fine aggregate content, which is actually substituted by Coal ash in subsequent steps, and thus resulting reduction in costly coarse aggregate content.

Step 6 :

Considering $w/c = 0.48$, and free water content as 208 kg,

$$\text{Cement content} = \frac{208}{0.48} = 433.33 \text{ kg/m}^3.$$

Step 7 :

To determine fine aggregate and coarse aggregate contents, the various values related to the equation in Step 7 are taken from Step 2 above.

Therefore, for fine aggregate quantity determination, the Equation is

$$(1 - 0.03) = \left\{ 208 + \frac{433.33}{3.04} + \left(\frac{1}{0.42} \right) \times \left(\frac{f_a}{2.667} \right) \right\} \times \frac{1}{1000}$$

Solving this, $f_a = 693.88 \text{ kg/m}^3$.

Again, for coarse aggregate quantity determination, the Equation is

$$(1 - 0.03) = \left\{ 165 + \frac{433.33}{3.04} + \left(\frac{1}{0.58} \right) \times \left(\frac{C_a}{2.949} \right) \right\} \times \frac{1}{1000}$$

Solving this, = 1059.53 kg/m³ .

The final quantity stands after adjusting free moisture present in the aggregates, as follows :

$$\text{Cement} = 433.33 \text{ kg/m}^3$$

$$\text{Water} = 208 \text{ kg/m}^3$$

$$\text{Fine Aggregate} = 695 \text{ kg/m}^3$$

$$\text{Coarse Aggregate} = 1055 \text{ kg/m}^3$$

$$\text{Water-Cement Ratio} = 0.48$$

$$\text{Workability} = 25 \text{ mm}$$

The Mix proportion for M-20 Grade Design Mix :1: 1. 6: 2. 4

4.2.2.3.5(a) Sand replacement by Bottomash in the Mix proportion :

With Bottomash as gradual replacement of Sand, the proportions arrived at are tabulated below. As per the written down proportions, cubes had been cast and samples were made for various physical and thermal parameter testing.

Table 4.5 M-20 Alt. Design Mix composition with Sand replacement by Bottom ash

Mix proportion	Cement	Sand	Bottomash	Flyash	Coarse Aggregate
1:1.60:2.40 with 100% Sand	1	1.60	0.00	-	2.40
1:1.60:2.40 with 90% Sand & 10% Bottomash	1	1.44	0.16	-	2.40
1:1.60:2.40 with 80% Sand & 20% Bottomash	1	1.28	0.32	-	2.40
1:1.60:2.40 with 70% Sand & 30% Bottomash	1	1.12	0.48	-	2.40
1:1.60:2.40 with 60% Sand & 40% Bottomash	1	0.96	0.64	-	2.40
1:1.60:2.40 with 50% Sand & 50% Bottomash	1	0.80	0.80	-	2.40
1:1.60:2.40 with 40% Sand & 60% Bottomash	1	0.64	0.96	-	2.40
1:1.60:2.40 with 30% Sand & 70% Bottomash	1	0.48	1.12	-	2.40
1:1.60:2.40 with 20% Sand & 80% Bottomash	1	0.32	1.28	-	2.40
1:1.60:2.40 with 10% Sand & 90% Bottomash	1	0.16	1.44	-	2.40
1:1.60:2.40 with 0% Sand & 100% Bottomash	1	0.00	1.60	-	2.40

4.2.2.3.5(b) Sand replacement by Flyash in the Mix proportion :

With Fly ash as gradual replacement of Sand, the proportions arrived at are tabulated below. As per the written down proportions, cubes had been cast and samples were made for various physical and thermal parameter testing.

Table 4.6 M-20 Alt. Design Mix composition with Sand replacement by Fly ash

Mix proportion	Cement	Sand	Bottomash	Flyash	Coarse Aggregate
1:1.60:2.40 with 100% Sand	1	1.60	-	0.00	2.40
1:1.60:2.40 with 90% Sand & 10% Fly ash	1	1.44	-	0.16	2.40
1:1.60:2.40 with 80% Sand & 20% Fly ash	1	1.28	-	0.32	2.40
1:1.60:2.40 with 70% Sand & 30% Fly ash	1	1.12	-	0.48	2.40
1:1.60:2.40 with 60% Sand & 40% Fly ash	1	0.96	-	0.64	2.40
1:1.60:2.40 with 50% Sand & 50% Fly ash	1	0.80	-	0.80	2.40
1:1.60:2.40 with 40% Sand & 60% Fly ash	1	0.64	-	0.96	2.40
1:1.60:2.40 with 30% Sand & 70% Fly ash	1	0.48	-	1.12	2.40
1:1.60:2.40 with 20% Sand & 80% Fly ash	1	0.32	-	1.28	2.40
1:1.60:2.40 with 10% Sand & 90% Fly ash	1	0.16	-	1.44	2.40
1:1.60:2.40 with 0% Sand & 100% Fly ash	1	0.00	-	1.60	2.40

4.2.2.3.5(c) Total replacement of Sand by lime and bottomash / flyash for M-20 Grade

Table 4.7 M-20 Design Mix composition with Lime-Bottom ash/Lime- Fly ash

Mix proportion	Cement	Lime	Bottomash	Flyash	Coarse Aggregate
1:1.60:2.40 with No Sand, but 25% Lime & 75% Bottomash	1	0.40	1.20	0.00	2.40
1:1.60:2.40 with No Sand, but 33% Lime & 67% Bottomash	1	0.53	1.07	0.00	2.40
1:1.60:2.40 with No Sand, but 50% Lime & 50% Bottomash	1	0.80	0.80	0.00	2.40
1:1.60:2.40 with No Sand, but 25% Lime & 75% Flyash	1	0.40	0.00	1.20	2.40
1:1.60:2.40 with No Sand, but 33% Lime & 67% Flyash	1	0.53	0.00	1.07	2.40
1:1.60:2.40 with No Sand, but 50% Lime & 50% Flyash	1	0.80	0.00	0.80	2.40

4.2.2.3.6 Alternate Design Mix II for M-20 Grade of Concrete

Step 1 :

The characteristic compressive strength , $f_{ck} = 20 \text{ N/mm}^2$. (as explained under 4.2.2.2 Step 1).

Step 2 :

Parameters of materials used –

- i) 10 mm down size stone aggregate, angular and to some extent flaky in nature.
- ii) Degree of Workability = Low , Slump 25-75 mm
- iii) Degree of Quality Control = Very Good
- iv) Type of exposure = Moderate
- v) Cement used - type and grade = Portland Pozzolana Cement (PPC)
- vi) Specific gravity of cement to be used = 3.04
- vii) Specific gravity of coarse (stone) aggregate = 2.949
- viii) Specific gravity of fine (sand) aggregate = 2.667
- ix) Water absorption by coarse aggregate = 3%
- x) Water absorption by fine aggregate = 2%
- xi) Free (surface) moisture of coarse aggregate = Nil
- xii) Free (surface) moisture of fine aggregate = 2%
- xiii) Sieve analysis result of fine aggregate and determination of zone = As indicated against Cl.3.2.3, Zone II
- xiv) Sieve analysis result of coarse aggregate = As indicated against Cl.3.2.4
- xv) Entrapped air content corresponding to nominal maximum size of Aggregate = 3% [Table 3, IS 10262].

Step 3 :

Target Mean strength, $f_t = f_{ck} + 1.65 \times s$

$$= 20 + 1.65 \times 3.5 \text{ [S=3.5 Table 1, IS 10262]}$$

$$= 25.775 \text{ N/mm}^2 .$$

Step 4 :

As suggested under Cl.4.2.2.2 Step 4, the free water-cement ratio (w/c) against the target compressive strength of concrete (f_t) is found to be 0.51. With the alternate

suggestion under the same clause, the w/c is found to be 0.53. From durability aspect, BIS 456 provision under Table 5 states that maximum free w/c permitted is 0.50.

Choosing lowest of all the above, the w/c may be considered 0.48.

Step 5 :

As suggested under Cl. 4.2.2.2 Step 5, the approximate Sand content as percent of total aggregate by absolute volume is 40.0 , and Water content per cubic meter of concrete is 208 kg. These values are considered against nominal maximum size of aggregate, which is 10 mm for this case. In this case, the Sand content is considered to be higher than all other previous mix, i.e. 40.5%, and the coarse aggregate content stands at 59.5%. This is done mainly to utilize maximum fine aggregate content, which is actually substituted by Coal ash in subsequent steps, and thus resulting reduction in costly coarse aggregate content.

Step 6 :

Considering w/c = 0.48, and free water content as $206 \text{ kg} < 208 \text{ kg}$,

$$\text{Cement content} = \frac{206}{0.48} = 429.17 \text{ kg/m}^3.$$

Step 7 :

To determine fine aggregate and coarse aggregate contents, the various values related to the equation in Step 7 are taken from Step 2 above.

Therefore, for fine aggregate quantity determination, the Equation is

$$(1 - 0.03) = \left\{ 206 + \frac{429.17}{3.04} + \left(\frac{1}{0.405} \right) \times \frac{f_a}{2.667} \right\} \times \frac{1}{1000}$$

Solving this, $f_a = 672.74 \text{ kg/m}^3$.

Again, for coarse aggregate quantity determination, the Equation is

$$(1 - 0.03) = \left\{ 206 + \frac{429.17}{3.04} + \left(\frac{1}{(1 - 0.405)} \right) \times \frac{C_a}{2.949} \right\} \times \frac{1}{1000}$$

Solving this, $C_a = 1092.85 \text{ kg/m}^3$.

The final quantity stands after adjusting free moisture present in the aggregates, as follows :

Cement = 430 kg/m³

Water = 206 kg/m³

Fine Aggregate = 670 kg/m³

Coarse Aggregate = 1090 kg/m³

Water-Cement Ratio = 0.48

Workability = 25 mm

The Mix proportion for M-20 Grade Alt. Design Mix II :1: 1. 5: 2. 5

Sand replacement by Bottomash in the Alt, Design Mix II proportion :

With Bottomash as gradual replacement of Sand, the proportions arrived at are tabulated below. As per the written down proportions, cubes had been cast and samples were made for various physical and thermal parameter testing.

Table 4.8 M-20 Alt.Design MixII composition with Sand replacement by Bottom ash

Mix proportion	Cement	Sand	Bottomash	Flyash	Coarse Aggregate
1:1.50:2.50 with 100% Sand	1	1.50	0.00	-	2.50
1:1.50:2.50 with 90% Sand & 10% Bottomash	1	1.35	0.15	-	2.50
1:1.50:2.50 with 80% Sand & 20% Bottomash	1	1.20	0.30	-	2.50
1:1.50:2.50 with 70% Sand & 30% Bottomash	1	1.05	0.45	-	2.50
1:1.50:2.50 with 60% Sand & 40% Bottomash	1	0.90	0.60	-	2.50
1:1.50:2.50 with 50% Sand & 50% Bottomash	1	0.75	0.75	-	2.50
1:1.50:2.50 with 40% Sand & 60% Bottomash	1	0.60	0.90	-	2.50
1:1.50:2.50 with 30% Sand & 70% Bottomash	1	0.45	1.05	-	2.50
1:1.50:2.50 with 20% Sand & 80% Bottomash	1	0.30	1.20	-	2.50
1:1.50:2.50 with 10% Sand & 90% Bottomash	1	0.15	1.35	-	2.50
1:1.50:2.50 with 0% Sand & 100% Bottomash	1	0.00	1.50	-	2.50

4.2.2.3.7 Nominal Mix for M-20 Grade of Concrete

Generally the Nominal Mix concept is practised since long, and till the introduction of IS 456 – 2000, it was mostly followed for all general construction purpose, particularly in Building industry. Guidelines are provided in IS 456-2000 Cl. 9.3 & 9.3.1 and summarized in Table 9 of the Code, which are as below :-

1. Against per 50 kg (by mass) of Cement, total quantity of Dry aggregate (sum of individual masses of fine and coarse aggregates) shall be 250 kg (max.).
2. Proportion of Fine aggregate to Coarse aggregate (by mass) generally considered as 1:2, subject to an upper limit of 1:1.5 and a lower limit of 1.2.5.
3. Quantity of Water per 50 kg of Cement (max.) is 30 kg.

As per the Guideline, Fine Aggregate is considered as 75 kg, Coarse aggregate is considered as 150 kg, Water as 25 kg. per 50 kg Cement.

Total quantity of Aggregate = (75+150)kg = 225 kg < 250 kg

Fine Aggregate : Coarse Aggregate :: 1:2

Water content = 25 kg < 30 kg

Nominal Mix proportion for M 20 stands at 1: 1.5 : 3.0 w/c = 0.50

4.2.2.3.7(a) Sand replacement by Bottomash in the Mix proportion :

With Bottomash as gradual replacement of Sand, the proportions arrived at are tabulated below. As per the written down proportions, cubes had been cast and samples were made for various physical and thermal parameter testing.

Table 4.9 M-20 Nominal Mix composition with Sand replacement by Bottom ash

Mix proportion	Cement	Sand	Bottomash	Flyash	Coarse Aggregate
1:1.50:3.00 with 100% Sand	1	1.50	0.00	-	3.00
1:1.50:3.00 with 90% Sand & 10% Bottomash	1	1.35	0.15	-	3.00
1:1.50:3.00 with 80% Sand & 20% Bottomash	1	1.20	0.30	-	3.00
1:1.50:3.00 with 70% Sand & 30% Bottomash	1	1.05	0.45	-	3.00
1:1.50:3.00 with 60% Sand & 40% Bottomash	1	0.90	0.60	-	3.00
1:1.50:3.00 with 50% Sand & 50% Bottomash	1	0.75	0.75	-	3.00
1:1.50:3.00 with 40% Sand & 60% Bottomash	1	0.60	0.90	-	3.00

1:1.50:3.00 with 30% Sand & 70% Bottomash	1	0.45	1.05	-	3.00
1:1.50:3.00 with 20% Sand & 80% Bottomash	1	0.30	1.20	-	3.00
1:1.50:3.00 with 10% Sand & 90% Bottomash	1	0.15	1.35	-	3.00
1:1.50:3.00 with 0% Sand & 100% Bottomash	1	0.00	1.50	-	3.00

4.2.2.3.8 Nominal Mix for M 25 Grade of Concrete

Generally the Nominal Mix concept is practised since long, and till the introduction of α IS 456 – 2000, it was mostly followed for all general construction purpose, particularly in Building industry. Guidelines are provided in IS 456-2000 Cl. 9.3 & 9.3.1 and summarized in Table 9 of the Code, which are as below :-

1. Against per 50 kg (by mass) of Cement, total quantity of Dry aggregate (sum of individual masses of fine and coarse aggregates) shall be 200 kg (max.).
2. Proportion of Fine aggregate to Coarse aggregate (by mass) generally considered as 1:2, subject to an upper limit of 1: 1.5 and a lower limit of 1: 2.5.
3. Quantity of Water per 50 kg of Cement (max.) is 28 kg.

As per the Guideline, Fine Aggregate is considered as 50 kg, Coarse aggregate is considered as 100 kg, Water as 25 kg. per 50 kg Cement.

Total quantity of Aggregate = (50+100)kg = 150 kg < 200 kg

Fine Aggregate : Coarse Aggregate :: 1:2

Water content = 25 kg < 30 kg

Nominal Mix proportion for M 25 stands at 1:1:2 and w/c=0.50

4.2.2.3.8(a) Sand replacement by Bottomash in the Nominal Mix M 25 proportion :

With Bottomash as gradual replacement of Sand, the proportions arrived at are tabulated below. As per the written down proportions, cubes had been cast and samples were made for various physical and thermal parameter testing.

Table 4.10 M-25 Nominal Mix composition with Sand replacement by Bottom ash

Mix proportion	Cement	Sand	Bottomash	Flyash	Coarse Aggregate
1:1.0:2.0 with 100% Sand	1	1.0	0.00	-	2.0
1:1.0:2.0 with 90% Sand & 10% Bottomash	1	0.90	0.10	-	2.0
1:1.0:2.0 with 80% Sand & 20% Bottomash	1	0.80	0.20	-	2.0
1:1.0:2.0 with 70% Sand & 30% Bottomash	1	0.70	0.30	-	2.0
1:1.0:2.0 with 60% Sand & 40% Bottomash	1	0.60	0.40	-	2.0
1:1.0:2.0 with 50% Sand & 50% Bottomash	1	0.50	0.50	-	2.0
1:1.0:2.0 with 40% Sand & 60% Bottomash	1	0.40	0.60	-	2.0
1:1.0:2.0 with 30% Sand & 70% Bottomash	1	0.30	0.70	-	2.0
1:1.0:2.0 with 20% Sand & 80% Bottomash	1	0.20	0.80	-	2.0
1:1.0:2.0 with 10% Sand & 90% Bottomash	1	0.10	0.90	-	2.0
1:1.0:2.0 with 0% Sand & 100% Bottomash	1	0.00	1.00	-	2.0

4.2.2.4 Mortar Mix

4.2.2.4.1 General overview

Masonry construction required for any structure involves laying of bricks or stones on beds of mortar. One of the most important operations is mixing of batches, which are correctly proportioned to produce mortar of adequate strength and durability. Mortar, besides jointing of bricks / stones in different layers and configurations, also used as outermost skin layer of any structure. This layer is commonly termed as plaster, which offer even surface to receive further finish, paint etc. as also acts as outermost barrier against damp penetration.

However, in the present work, role of such thin outermost layer of building has been tried to be investigated from *thermal transmittance point of view*, besides maintaining adequate physical strength in conformity with the Indian Standard Code of Practice.



Fig.4.1 Typical Sand-Cement Plaster work on masonry surface is under progress. IS 2250 : 1981 is the Indian Code of practice for preparation and use of masonry mortar. Choice of masonry mortar is guided by several factors such as type of masonry, situation of use, degree of exposure to weather, strength criteria etc. The composition of mortar also varies considerably, depending on availability, functional requirements etc. Cementitious ingredients may be cement or lime or combinations thereof. The aggregates may be sand, burnt-clay aggregate or other filler materials. These ingredients possess wide variation in characteristics. With the development of standards to govern the quality of cement, lime, sand and other pozzolanic materials, it is possible to select and use masonry mortars, as per tailor made requirements.

Masonry mortars are classified in Grades in terms of minimum compressive strength at 28 days. In the Code, there are altogether 38 different varieties of mortars mentioned under the following Grades –

- i) MM 0.5
- ii) MM0.7
- iii) MM1.5
- iv) MM2
- v) MM3
- vi) MM5
- vii) MM 7.5

In the above Grading nomenclature, MM stands for Mortar Mix and the value indicates 28 days compressive strength. The mix of 1:6 and 1:4 are most common in building construction, which fall under MM3 and MM5 Grades respectively.

Further, Mortar mixes with Bottom ash and fly ash by replacing Sand in 10% steps for the most common proportions i.e.1:6 and 1:4 were prepared and samples were tested for 28 days' Compressive Strength, Apparent Porosity, Bulk Density and Thermal Conductivity parameters respectively.

4.2.2.4.2 The Mix composition for **1:6** under MM3 category with 10% gradual replacement of Sand by **Bottomash** are tabulated below :-

Table **4.11** MM3 Grade Mortar mix with Sand substitution by Bottom ash

Grade of Mortar	Cement	Sand	Flyash	Bottomash
MM3	1	6	-	-
MM3	1	5.4	-	0.6
MM3	1	4.8	-	1.2
MM3	1	4.2	-	1.8
MM3	1	3.6	-	2.4
MM3	1	3.0	-	3.0
MM3	1	2.4	-	3.6
MM3	1	1.8	-	4.2
MM3	1	1.2	-	4.8
MM3	1	0.6	-	5.4
MM3	1	0.0	-	6.0

4.2.2.4.3 The Mix composition for **1:6** under MM3 category with 10% gradual replacement of Sand by **Flyash** are tabulated below :-

Table **4.12** MM3 Grade Mortar mix with Sand substitution by Fly ash

Grade of Mortar	Cement	Sand	Flyash	Bottomash
MM3	1	6	-	-
MM3	1	5.4	0.6	-
MM3	1	4.8	1.2	-
MM3	1	4.2	1.8	-
MM3	1	3.6	2.4	-
MM3	1	3.0	3.0	-
MM3	1	2.4	3.6	-
MM3	1	1.8	4.2	-
MM3	1	1.2	4.8	-
MM3	1	0.6	5.4	-
MM3	1	0.0	6.0	-

4.2.2.4.4 The Mix composition for **1:4** under MM5 category with 10% gradual replacement of Sand by **Bottomash** are tabulated below :-

Table **4.13** MM5 Grade Mortar mix with Sand substitution by Bottom ash

Grade of Mortar	Cement	Sand	Flyash	Bottomash
MM5	1	4	-	-
MM5	1	3.6	-	0.4
MM5	1	3.2	-	0.8
MM5	1	2.8	-	1.2
MM5	1	2.4	-	1.6
MM5	1	2.0	-	2.0
MM5	1	1.6	-	2.4
MM5	1	1.2	-	2.8
MM5	1	0.8	-	3.2
MM5	1	0.4	-	3.6
MM5	1	0.0	-	4.0

4.2.2.4.5 The Mix composition for **1:4** under MM5 category with 10% gradual replacement of Sand by **Flyash** are tabulated below :-

Table **4.14** MM5 Grade Mortar mix with Sand substitution by Fly ash

Grade of Mortar	Cement	Sand	Flyash	Bottomash
MM5	1	4	-	-
MM5	1	3.6	0.4	-
MM5	1	3.2	0.8	-
MM5	1	2.8	1.2	-
MM5	1	2.4	1.6	-
MM5	1	2.0	2.0	-
MM5	1	1.6	2.4	-
MM5	1	1.2	2.8	-
MM5	1	0.8	3.2	-
MM5	1	0.4	3.6	-
MM5	1	0.0	4.0	-

In this experimental investigation, besides these two most common grades, some indigenous mixes are also explored, by totally replacing the most common ingredient, i.e. sand. Sand has been replaced totally by flyash in both the common composition of MM3 & MM5 i.e. 1:6 and in 1:4. Again by lime and flyash 50:50 basis, by lime and bottomash 50:50 basis, by marbledust and flyash 50:50 basis and by marbledust and bottomash 50:50 basis respectively. Therefore Sand had been eliminated in all the above stated compositions, and the Compressive strength after 28 days maturity, Apparent Porosity, Bulk Density and thermal Conductivity parameters were measured for such samples.

4.2.2.4.6 The Mix composition without Sand are tabulated below :-

Table 4.15 Mortar Mix composition (Conventional & Non-conventional)

Sl.No.	Grade of Mortar	Cement	Sand	Lime	Marbledust	Flyash	Bottomash
1	MM3	1	6	-	-	-	-
2	ND*(MM3)	1	-	-	-	6	-
3	ND*(MM3)	1	-	-	-	-	6
4	ND*(MM3)	1	-	3	-	3	-
5	ND*(MM3)	1	-	3	-	-	3
6	ND*(MM3)	1	-	-	3	3	-
7	ND*(MM3)	1	-	-	3	-	3
8	MM5	1	4	-	-	-	-
9	ND*(MM5)	1	-	-	-	4	-
10	ND*(MM5)	1	-	-	-	-	4
11	ND*(MM5)	1	-	2	-	2	-
12	ND*(MM5)	1	-	2	-	-	2
13	ND*(MM5)	1	-	-	2	2	-
14	ND*(MM5)	1	-	-	2	-	2

ND*- Not defined in IS Code

4.3 Concrete and Mortar Sample preparation and Curing

4.3.1 Introduction

Representative sample of mix are prepared for testing of various physical parameters of concrete and mortar. The calculated design strength and other parameters, which are considered for durability and or thermal property of concrete and mortar can be ascertained from the sample test.

4.3.2 Test sample size

4.3.2.1 Destructive testing : overview (Including Testing Machine)

Steel cube moulds of size 50mmX50mmX50mm, which can be dismantled and re-assembled had been used for compressive strength tests of various concrete and mortar mixes. Three cubes each were utilized for 7 days maturity, and 28 days

maturity respectively for various concrete mix samples, and three nos. cubes for 28 days maturity for different mortar mix samples. According to the mix ratio of different component as per relevant IS Code, concrete/mortar mixes were prepared and poured inside the cube moulds in three equal layers. After placing each layer of mix in the mould, the same was tamped with iron rod of bullet point for uniform compaction without air void left inside. After pouring and compacting 3rd layer of mix, the top portion of mould is scooped with steel trowel to flush the finished surface with the outer dimension of the cube mould. All the prepared samples were kept on vibrating table for final mechanized compaction to minimize formation of internal voids. Any excess material, oozed out had been cleaned with the help of the trowel. The samples had been left as it was under the room temperature for 24 hours, and after expiry of 24 hours, the steel moulds were dismantled, casted cubes were taken out, and kept inside the clean water storage tank for curing at the room temperature till the date of testing, depending upon 7 or 28 days of maturity.

Testing machine

The testing machine used was VEB WERKSTOFFPROFMASCHINEN, LEIPZIG (Fabr. No.263/14, Frequency 3-50 Hz., Loading rate Max.250 KP/cm². As per IS 516-1959 (Methods of Tests for Strength of Concrete), the testing machine is equipped with two steel bearing platens with hardened faces. One of the platens (the one that normally bear on the upper surface of the specimen) is fitted with a ball seating in the form of a portion of a sphere, the centre of which coincides with the central point of the face of the platen. The other compression platen is of plain rigid bearing block. The bearing faces of both platens are as large as, and preferably larger than the nominal size of the specimen to which the load is applied. The movable portion of the spherically seated compression platen are held on the spherical seat, but the design is such that the bearing face can be rotated freely and tilted through small angles in any direction. Tests had been undertaken at the recognized age of the maturity of the samples, usually 7 and 28 days. In the instant case, 7 and 28 days age of testing were followed for concrete samples and 28 days age of testing for mortar samples, strictly as per IS Code provisions. Three samples from each batch were tested. The measured compressive strength of the samples were calculated by dividing the maximum axial load (under which failure took place) with the area of

sample surface (on which load was applied), and expressed in either kgf/cm^2 or N/mm^2 (MPa).



Fig. 4.2 Compressive strength testing of cube samples under progress

4.3.2.2 Non-destructive testing : overview

Steel cube moulds of size $50\text{mm} \times 50\text{mm} \times 50\text{mm}$, which can be dismantled and re-assembled had been used for apparent porosity and bulk density parameter tests of various concrete and mortar mixes. Steel cube moulds of size $50\text{mm} \times 50\text{mm} \times 12\text{mm}$ were used for thermal conductivity tests of concrete and mortar mix samples. According to the design / nominal mix as per relevant IS Code, concrete/mortar mixes were prepared and poured inside the above size moulds in three equal layers. After placing each layer of mix in the mould, the same was tamped with iron rod of bullet point for uniform compaction without air void left inside. After pouring and compacting 3rd layer of mix, the top portion of mould is scooped with steel trowel to flush the finished surface with the outer dimension of the cube mould. All the prepared samples were kept on vibrating table for final mechanized compaction to minimize formation of internal voids. Any excess material, oozed out had been cleaned with the help of the trowel. The samples had been left as it was under the

room temperature for 24 hours, preferably within 22 to 32°C and after expiry of 24 hours, the steel moulds were dismantled, casted cubes were taken out, and kept inside the clean water storage tank for curing at the nominal temperature of 24 to 30°C till the date of testing or 28 days of maturity, whichever is later.

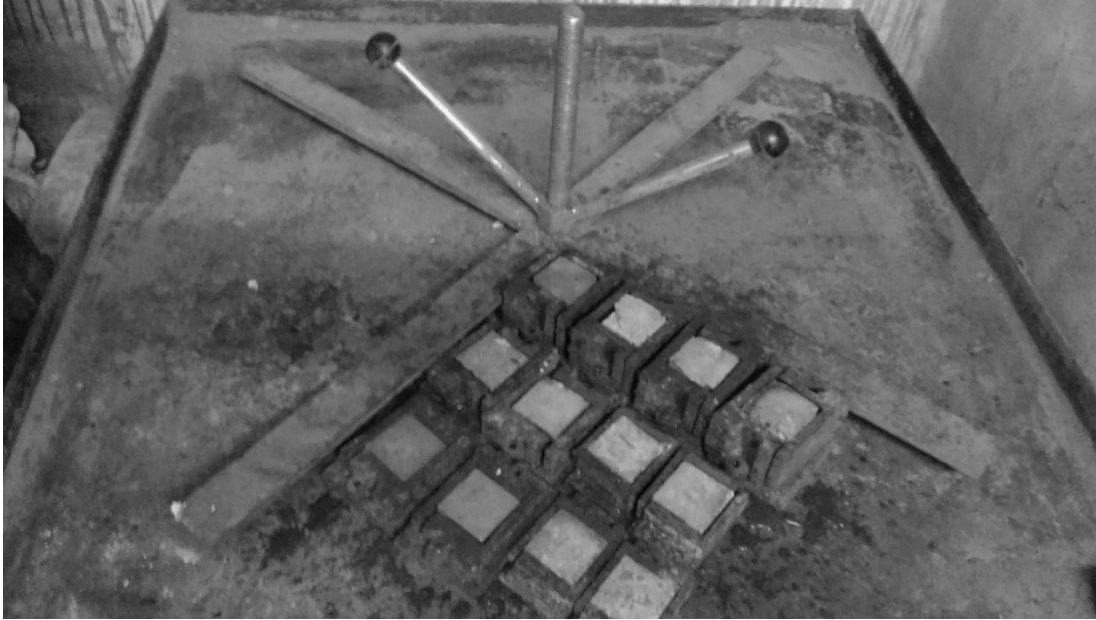


Fig. 4.3 Vibrating table set up



Fig.4.4 Curing of Samples

The flow sheet for the activity are as under :-

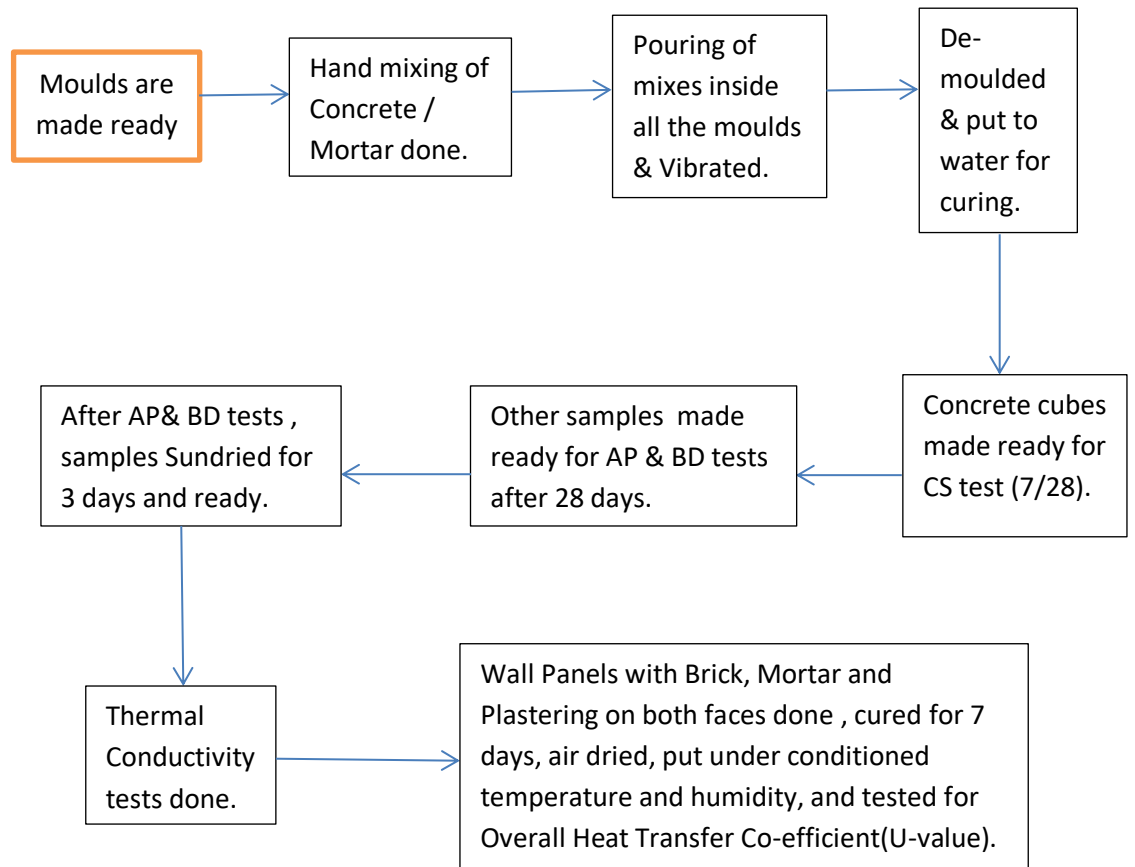


Fig. 4.5 Flow diagram of various test protocol for samples

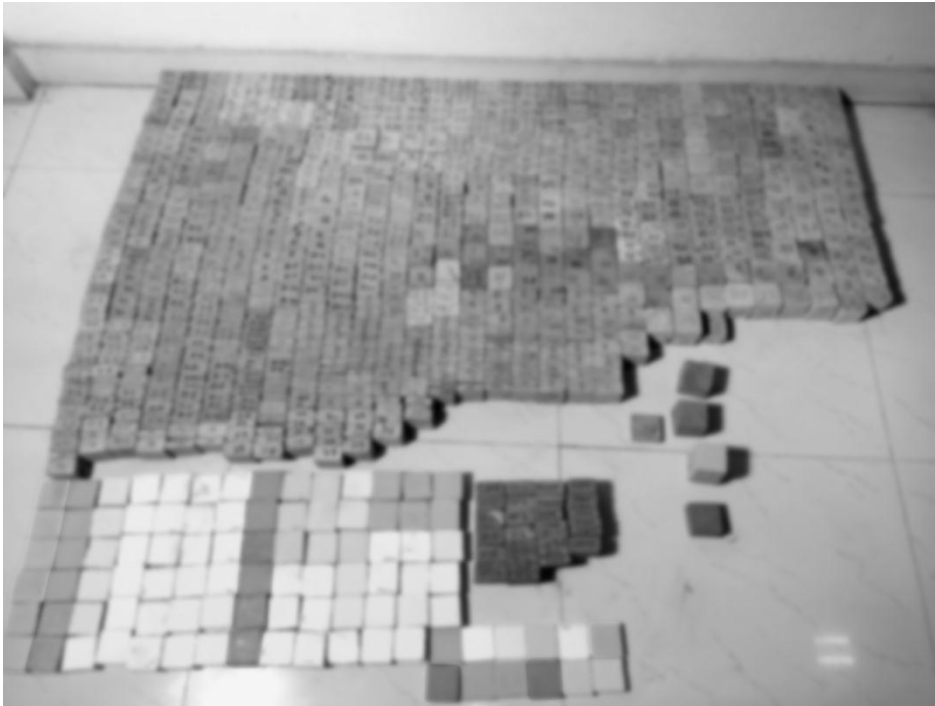


Fig.4.6 Display of cast samples

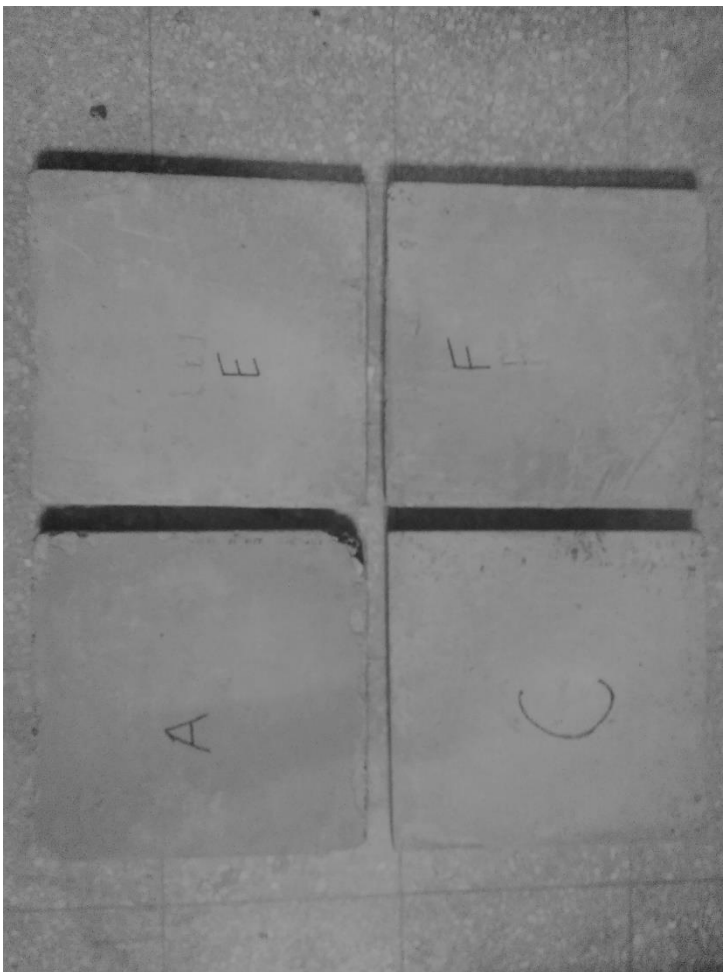


Fig.4.7 300mmX300mmX25mm Flyash Tiles (1:1.6:2.4 Concrete mix)

4.4(a) XRD Analysis of Concrete Samples

The X-Ray Diffractogram analysis were carried out for a few concrete samples with sand, with bottom ash in lieu of sand, with fly ash in lieu of sand at 7 days maturity and at 28 days maturity ages respectively to study the phases formed after chemical reaction took place. The XRD patterns are shown below :-

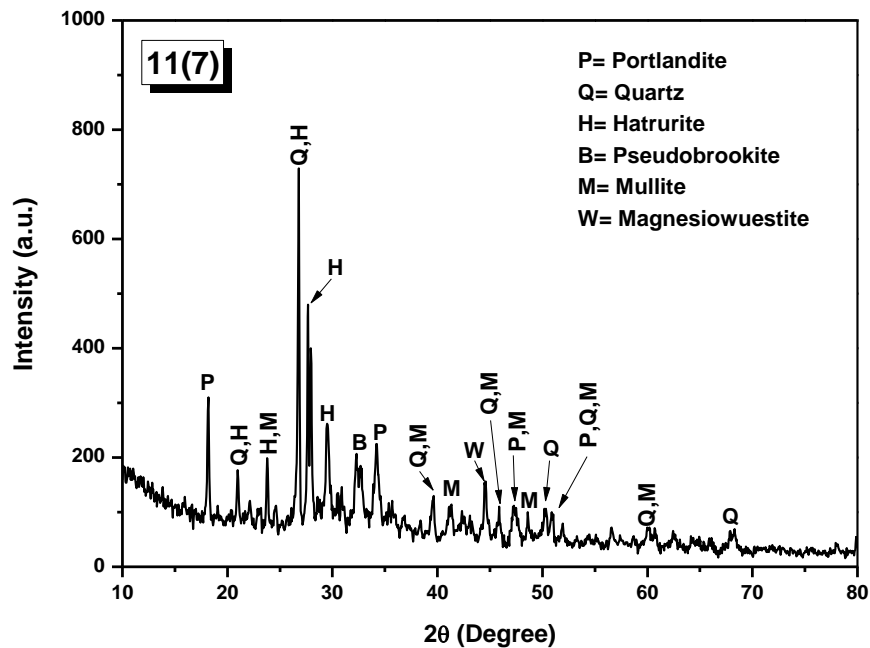


Fig.4.8 Phase Diagram of Concrete with 100% Sand (1:1.5:2.5) at 7 days [Sample id. 11(7)].

The constituent of concrete mix was 1 part of Cement, 1.5 parts of Sand and 2.5 parts of Stone Aggregate. The main phases formed are Quartz (SiO_2) and Hatrurite ($3\text{CaO}, \text{SiO}_2$), followed by Mullite ($3\text{Al}_2\text{O}_3, 2\text{SiO}_2$), Portlandite ($\text{Ca}(\text{OH})_2$), Magnesiowuestite ($\text{Mg}_{2.4}\text{Fe}_{1.6}\text{O}_4$), and Pseudobrookite ($\text{Fe}_2\text{O}_3, \text{TiO}_2$).

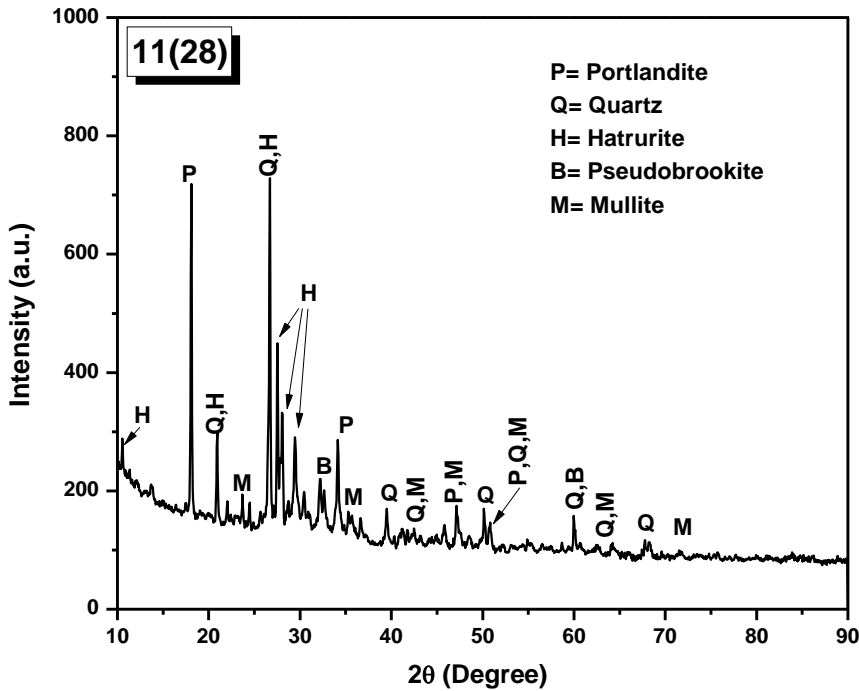


Fig.4.9 Phase Diagram of Concrete with 100% Sand (1:1.5:2.5) at 28 days [Sample id 11(28)].

The constituent of concrete mix was 1 part of Cement, 1.5 parts of Sand and 2.5 parts of Stone Aggregate. The main phases formed are Quartz (SiO_2) and Hatrurite ($3\text{CaO}, \text{SiO}_2$), followed by Mullite ($3\text{Al}_2\text{O}_3, 2\text{SiO}_2$), Portlandite ($\text{Ca}(\text{OH})_2$), and Pseudobrookite ($\text{Fe}_2\text{O}_3, \text{TiO}_2$).

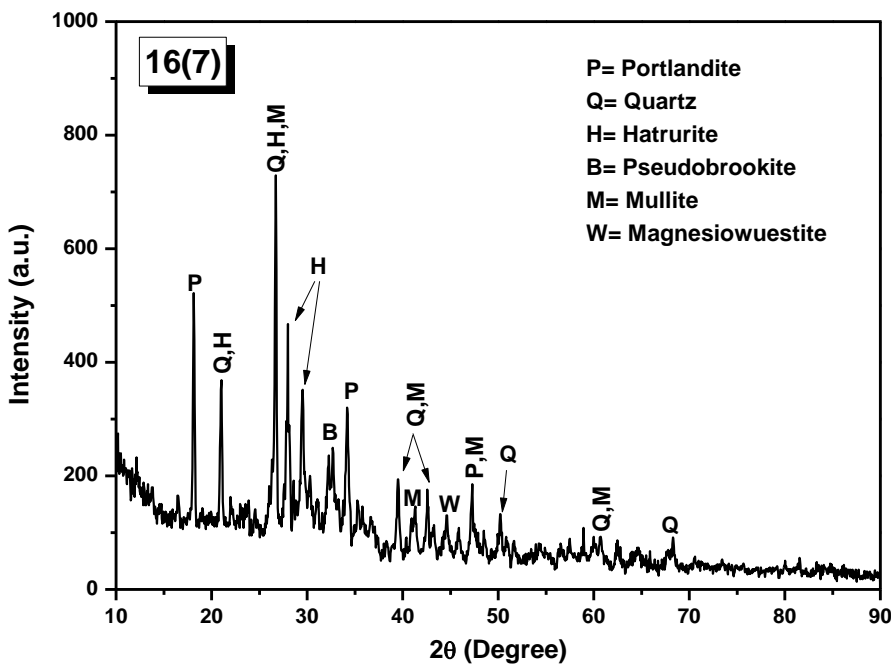


Fig.4.10 Phase Diagram of Concrete with 50% Sand and 50% Bottomash (1:0.75:0.75:2.5) at 7 days [Sample id. 16(7)].

The constituent of concrete mix was 1 part of Cement, 0.75 part of Bottomash, 0.75 part of Sand, and 2.5 parts of Stone Aggregate. The main phases formed are Quartz (SiO_2), Hatrurite ($3\text{CaO}, \text{SiO}_2$), and Mullite ($3\text{Al}_2\text{O}_3, 2\text{SiO}_2$), followed by Portlandite ($\text{Ca}(\text{OH})_2$), Pseudobrookite ($\text{Fe}_2\text{O}_3, \text{TiO}_2$) and Magnesiowuestite ($\text{Mg}_{2.4}\text{Fe}_{1.6}\text{O}_4$).

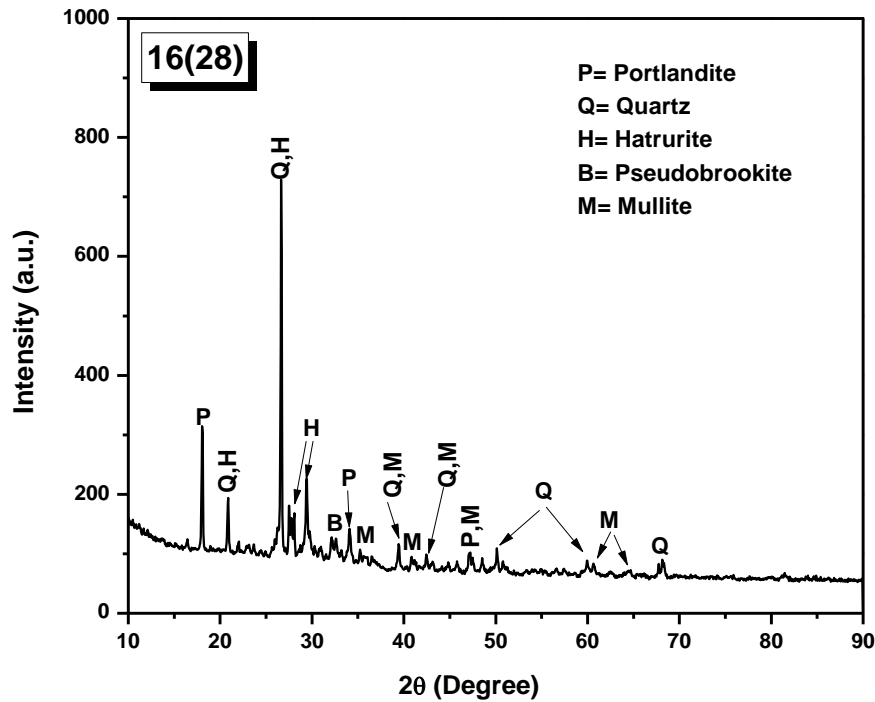


Fig.4.11 Phase Diagram of Concrete with 50% Sand and 50% Bottomash (1:0.75:0.75:2.5) at 28 days [Sample id.28(7)].

The constituent of concrete mix was 1 part of Cement, 0.75 part of Bottomash, 0.75 part of Sand, and 2.5 parts of Stone Aggregate. The main phases formed are Quartz (SiO_2), Hatrurite ($3\text{CaO}, \text{SiO}_2$), and Mullite ($3\text{Al}_2\text{O}_3, 2\text{SiO}_2$), followed by Portlandite ($\text{Ca}(\text{OH})_2$), Pseudobrookite ($\text{Fe}_2\text{O}_3, \text{TiO}_2$).

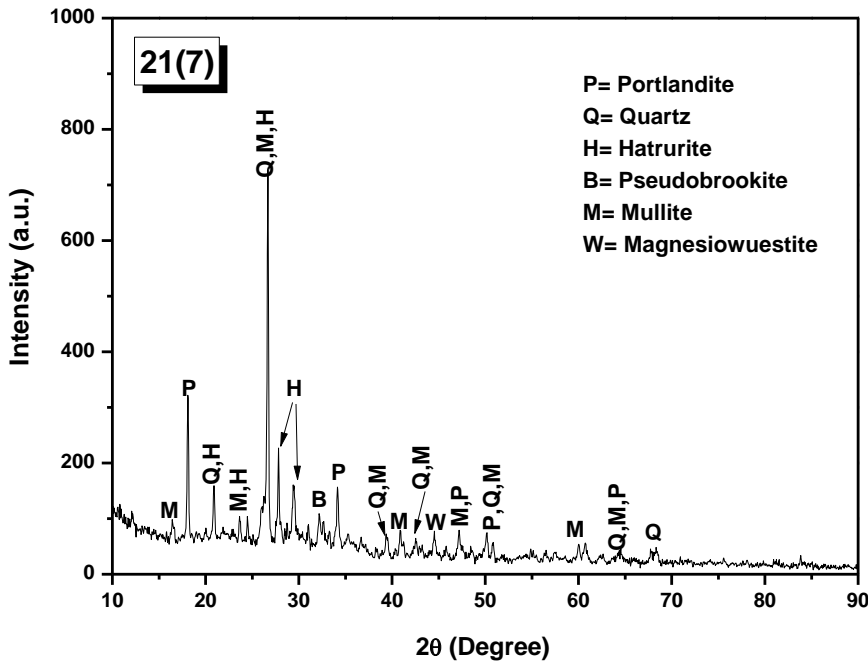


Fig.4.12 Phase Diagram of Concrete with 100% Bottomash (1:1.5:2.5) at 7 days [Sample id.21(7)]

The constituent of concrete mix was 1 part of Cement, 1.5 parts of Bottomash, and 2.5 parts of Stone Aggregate. The main phases formed are Quartz (SiO_2), Hatrurite ($3\text{CaO}, \text{SiO}_2$), and Mullite ($3\text{Al}_2\text{O}_3, 2\text{SiO}_2$), followed by Portlandite ($\text{Ca}(\text{OH})_2$), Pseudobrookite ($\text{Fe}_2\text{O}_3, \text{TiO}_2$) and Magnesiowuestite ($\text{Mg}_{2.4}\text{Fe}_{1.6}\text{O}_4$).

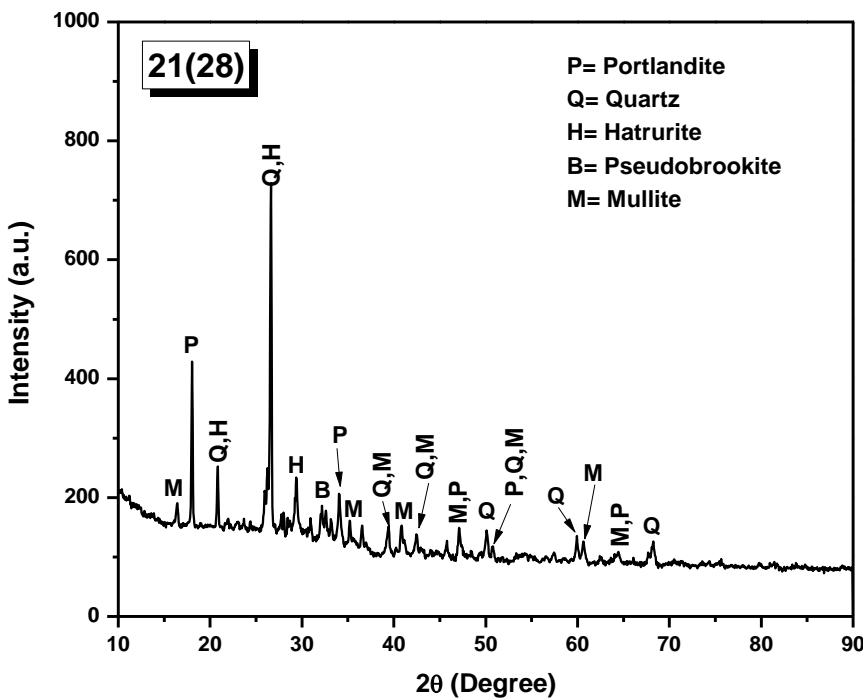


Fig.4.13 Phase Diagram of Concrete with 100% Bottomash (1:1.5:2.5) at 28 days [Sample id.21(28)]

The constituent of concrete mix was 1 part of Cement, 1.5 parts of Bottomash, and 2.5 parts of Stone Aggregate. The main phases formed are Quartz (SiO_2), Hatrurite (3CaO , SiO_2), and Mullite ($3\text{Al}_2\text{O}_3$, 2SiO_2), followed by Portlandite ($\text{Ca}(\text{OH})_2$), and Pseudobrookite (Fe_2O_3 , TiO_2).

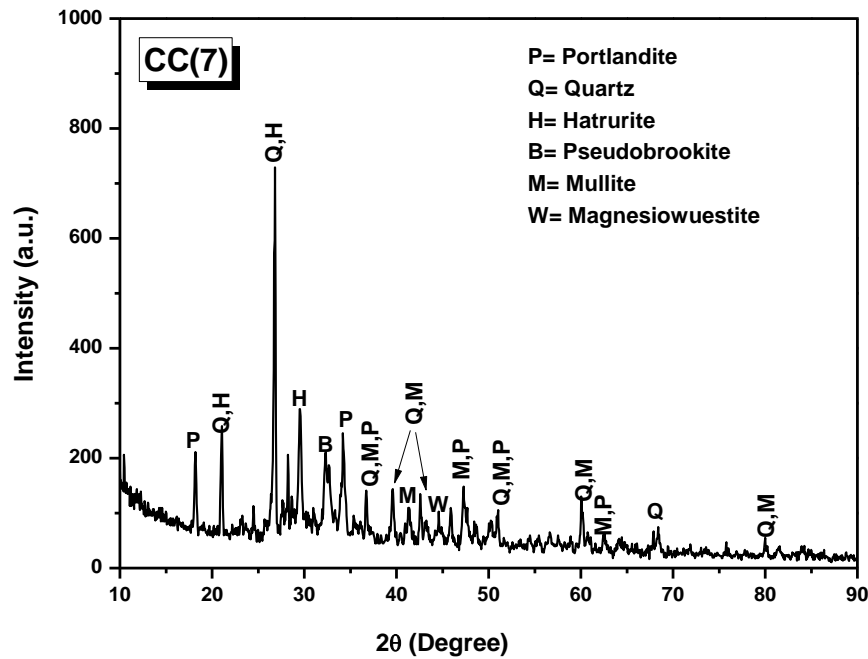


Fig.4.14 Phase Diagram of Concrete with 100% Sand (1:1.6:2.4) at 7 days [Sample id..CC(7)]

The constituent of concrete mix was 1 part of Cement, 1.6 parts of Flyash, and 2.4 parts of Stone Aggregate. The main phases formed are Quartz (SiO_2), Hatrurite (3CaO , SiO_2), and Mullite ($3\text{Al}_2\text{O}_3$, 2SiO_2), followed by Portlandite ($\text{Ca}(\text{OH})_2$), Pseudobrookite (Fe_2O_3 , TiO_2) and Magnesiowuestite ($\text{Mg}_{2.4}\text{Fe}_{1.6}\text{O}_4$).

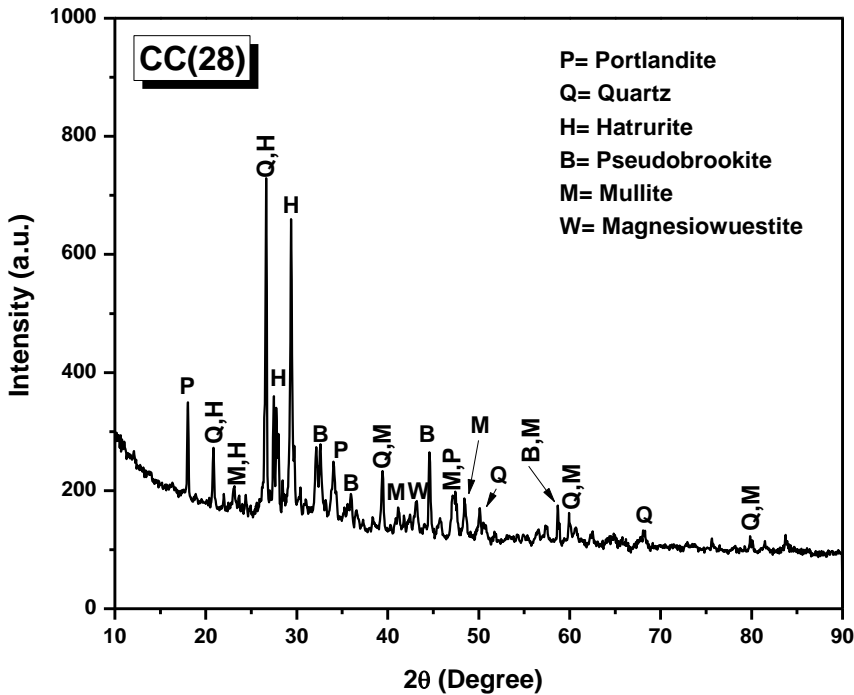


Fig.4.15 Phase Diagram of Concrete with 100% Sand (1:1.6:2.4) at 28 days [Sample id. CC(28)]

The constituent of concrete mix was 1 part of Cement, 1.6 parts of Flyash, and 2.4 parts of Stone Aggregate. The main phases formed are Quartz (SiO_2), Hatrurite ($3\text{CaO}, \text{SiO}_2$), and Mullite ($3\text{Al}_2\text{O}_3, 2\text{SiO}_2$), followed by Portlandite ($\text{Ca}(\text{OH})_2$), Pseudobrookite ($\text{Fe}_2\text{O}_3, \text{TiO}_2$) and Magnesiowuestite ($\text{Mg}_{2.4}\text{Fe}_{1.6}\text{O}_4$).

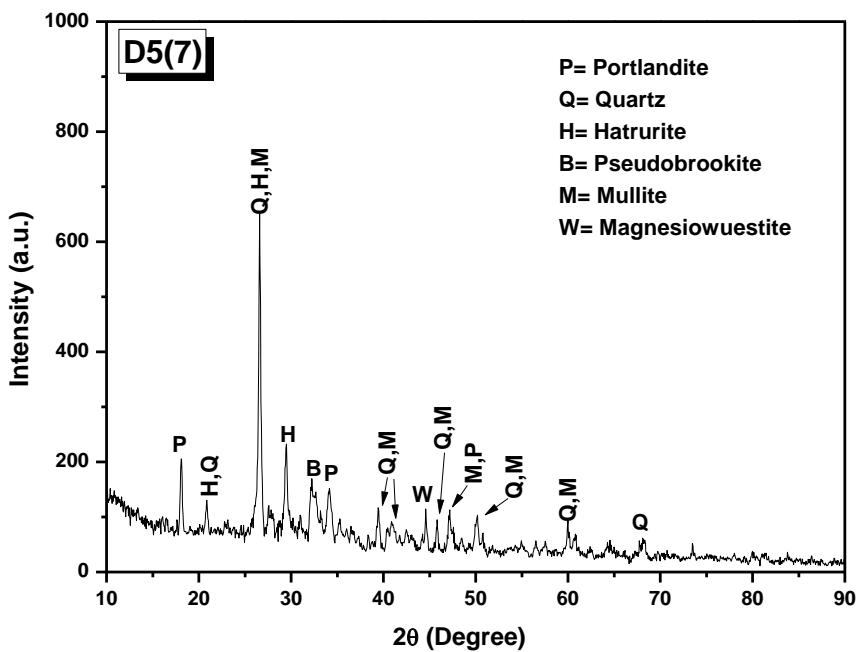


Fig. 4.16 Phase Diagram of Concrete with 50% Sand and 50% Flyash (1:1.6:2.4) at 7 days [Sample id. D 5(7)]

The constituent of concrete mix was 1 part of Cement, 0.8 part of Sand, 0.8 part of Flyash, and 2.4 parts of Stone Aggregate. The main phases formed are Quartz (SiO_2), Hatrurite ($3\text{CaO}, \text{SiO}_2$), and Mullite ($3\text{Al}_2\text{O}_3, 2\text{SiO}_2$), followed by Portlandite ($\text{Ca}(\text{OH})_2$), Pseudobrookite ($\text{Fe}_2\text{O}_3, \text{TiO}_2$) and Magnesiowuestite ($\text{Mg}_{2.4}\text{Fe}_{1.6}\text{O}_4$).

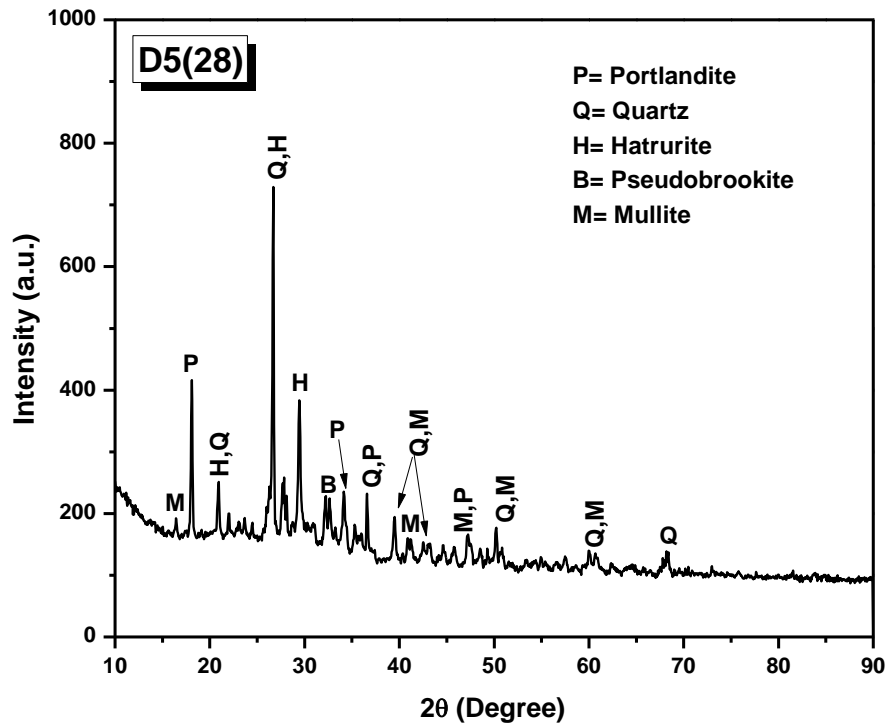


Fig.4.17 Phase Diagram of Concrete with 50% Sand and 50% Flyash (1:1.6:2.4) at 28 days [Sample id. D 5(28)]

The constituent of concrete mix was 1 part of Cement, 0.8 part of Sand, 0.8 part of Flyash, and 2.4 parts of Stone Aggregate. The main phases formed are Quartz (SiO_2), Hatrurite ($3\text{CaO}, \text{SiO}_2$), and Mullite ($3\text{Al}_2\text{O}_3, 2\text{SiO}_2$), followed by Portlandite ($\text{Ca}(\text{OH})_2$), Pseudobrookite ($\text{Fe}_2\text{O}_3, \text{TiO}_2$).

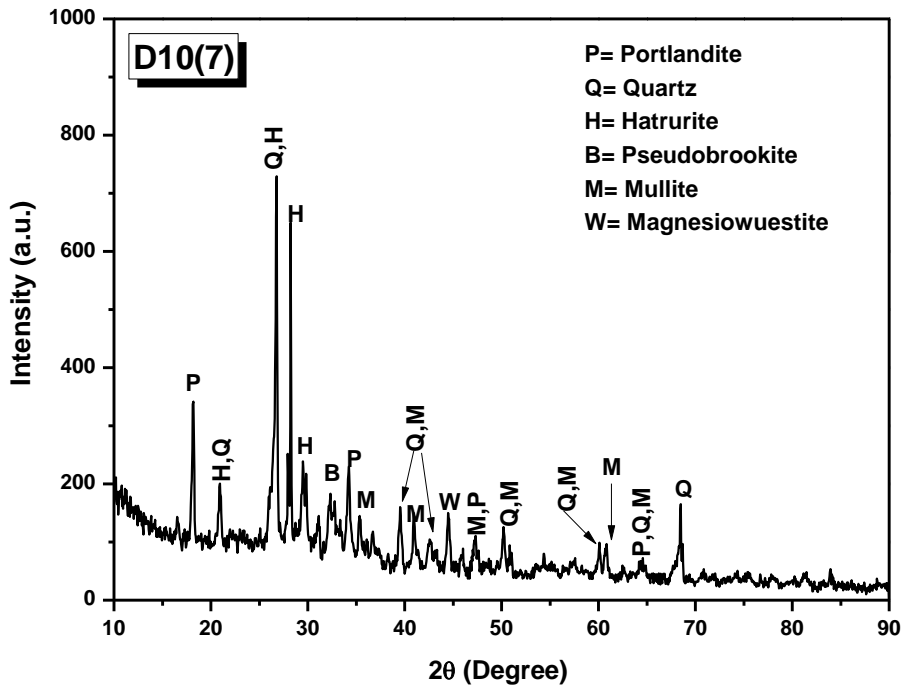


Fig.4.18 Phase Diagram of Concrete with 100% Flyash (1:1.6:2.4) at 7 days [Sample id. D10(7)].

The constituent of concrete mix was 1 part of Cement, 1.6 parts of Flyash, and 2.4 parts of Stone Aggregate. The main phases formed are Quartz (SiO_2), Hatrurite ($3\text{CaO}, \text{SiO}_2$), and Mullite ($3\text{Al}_2\text{O}_3, 2\text{SiO}_2$), followed by Portlandite ($\text{Ca}(\text{OH})_2$), Pseudobrookite ($\text{Fe}_2\text{O}_3, \text{TiO}_2$) and Magnesiowuestite ($\text{Mg}_{2.4}\text{Fe}_{1.6}\text{O}_4$).

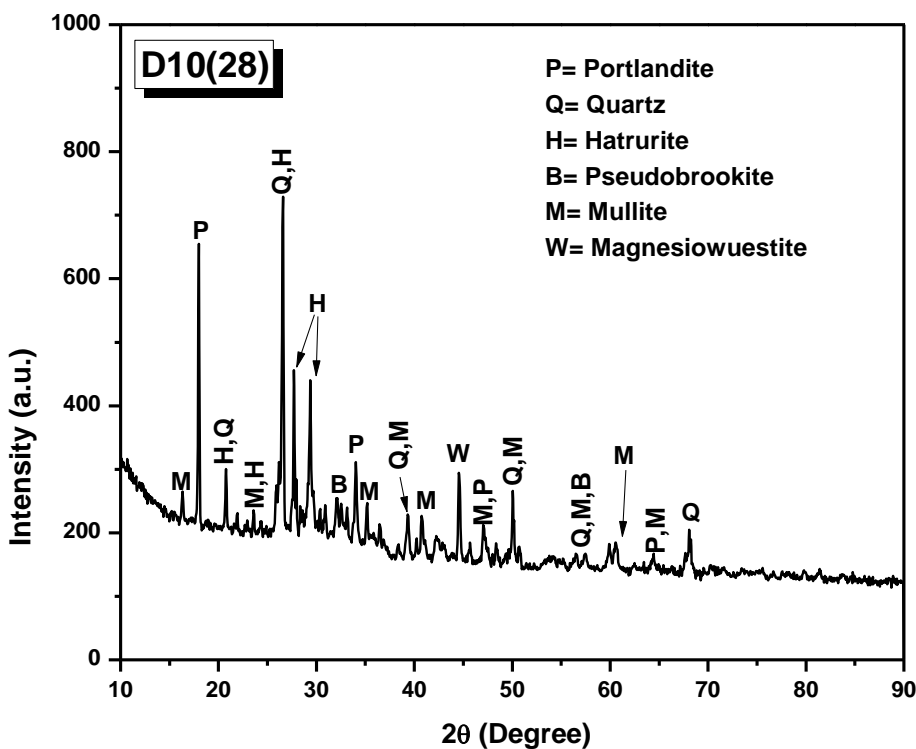


Fig. 4.19 Phase Diagram of Concrete with 100% Flyash (1:1.6:2.4) at 28 days [Sample id. D10(28)]

The constituent of concrete mix was 1 part of Cement, 1.6 parts of Flyash, and 2.4 parts of Stone Aggregate. The main phases formed are Quartz (SiO_2), Hatrurite (3CaO , SiO_2), and Mullite ($3\text{Al}_2\text{O}_3$, 2SiO_2), followed by Portlandite ($\text{Ca}(\text{OH})_2$), and Pseudobrookite (Fe_2O_3 , TiO_2).

4.4(b) XRD Analysis of Mortar Samples

The Phase Analysis by XRD of two most common mix compositions (MM3 = 1:6 and MM5 = 1:4) are as below :-

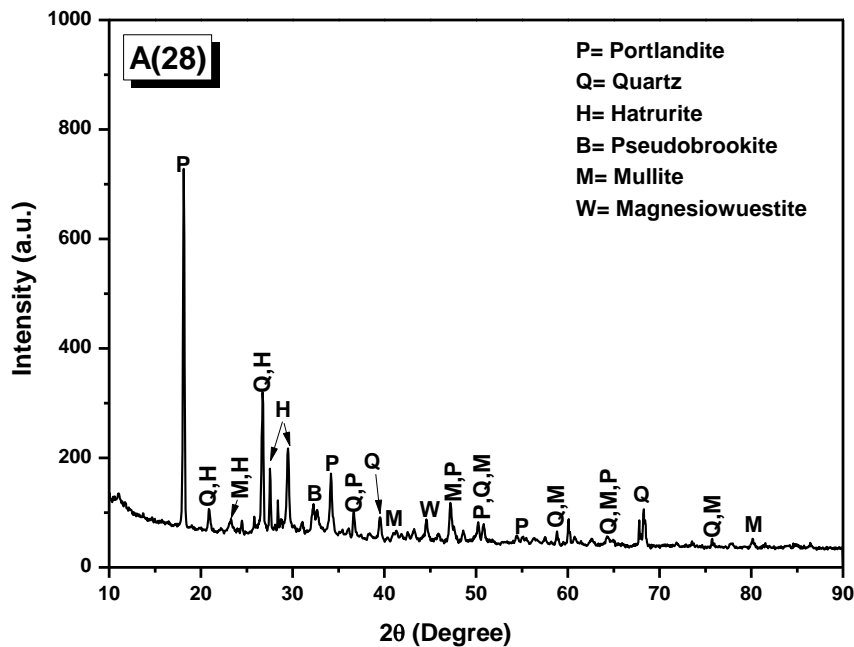


Fig.4.20 Phase Diagram of Mortar MM5 Grade with 100% sand (1:4) at 28 days [Sample id. A(28)]

The constituent of Mortar mix was 1 part of Cement and 4 parts of Sand. The most prominent phases were : 1.Portlandite ($\text{Ca}(\text{OH})_2$), 2.Quartz (SiO_2), 3.Hatrurite (3CaO , SiO_2), 4.Pseudobrookite (Fe_2O_3 , TiO_2), 5.Mullite ($3\text{Al}_2\text{O}_3$, 2SiO_2) and 6.Magnesiowuestite ($\text{Mg}_{2.4}\text{Fe}_{1.6}\text{O}_4$)

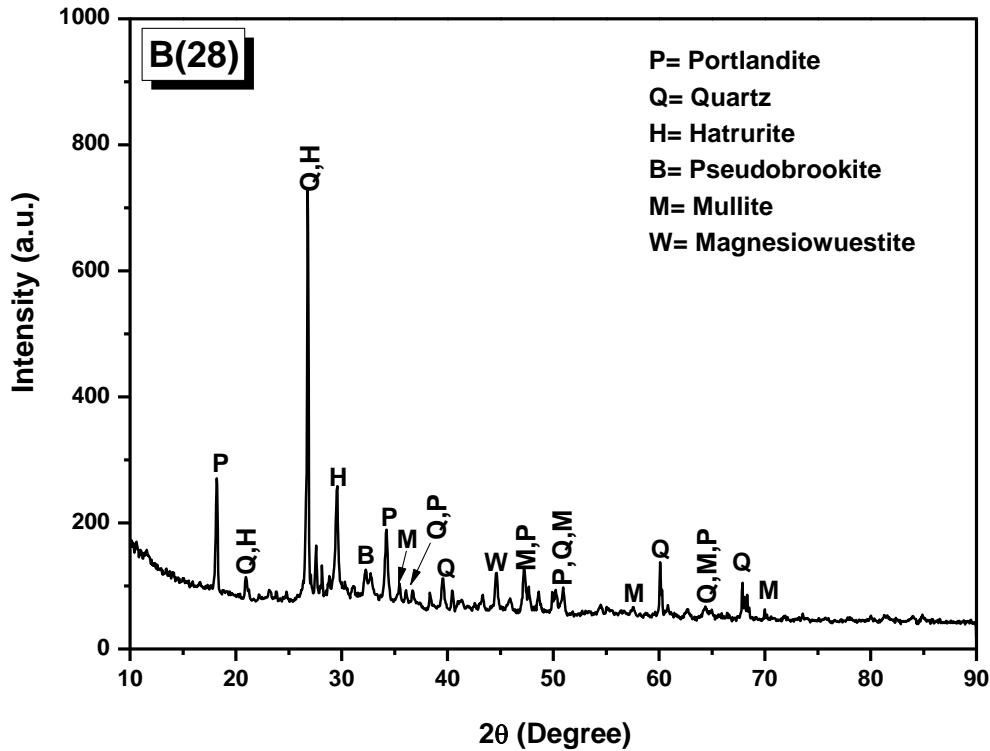


Fig.4.21 Phase Diagram of Mortar MM3 Grade with 100% Sand (1:6) at 28 days [Sample id. B(28)]

The constituent of Mortar mix was 1 part of Cement, and 6 parts of Sand. In this case, when Sand content is more in the mix, highest phase is shown by Quartz (SiO_2) and Hatrurite ($3\text{CaO}, \text{SiO}_2$), distantly followed by Mullite ($3\text{Al}_2\text{O}_3, 2\text{SiO}_2$), Magnesiowuestite ($\text{Mg}_{2.4}\text{Fe}_{1.6}\text{O}_4$), Pseudobrookite ($\text{Fe}_2\text{O}_3, \text{TiO}_2$) and Portlandite ($\text{Ca}(\text{OH})_2$).

4.4(c) XRD Analysis of Sand less Mortar samples

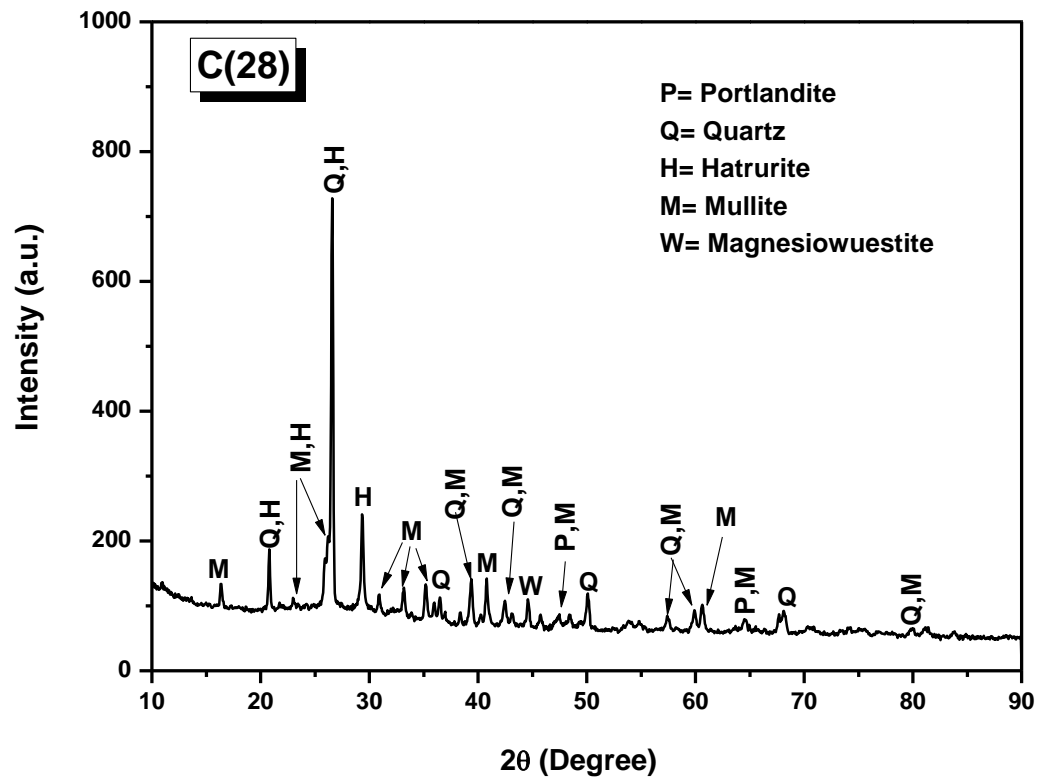


Fig.4.22 Phase Diagram of Mortar MM3 Grade with 100% Bottomash (1:6) at 28 days [Sample id. C(28)]

The constituent of Mortar mix was 1 part of Cement, and 6 parts of Bottomash. In this case, when Sand content is totally absent in the mix, and replaced entirely by bottom ash under **MM3** category, highest phase is occupied by Quartz (SiO_2) and Hatrurite ($3\text{CaO}, \text{SiO}_2$), distantly followed by Mullite ($3\text{Al}_2\text{O}_3, 2\text{SiO}_2$), Magnesiowuestite ($\text{Mg}_{2.4}\text{Fe}_{1.6}\text{O}_4$), and Portlandite ($\text{Ca}(\text{OH})_2$).

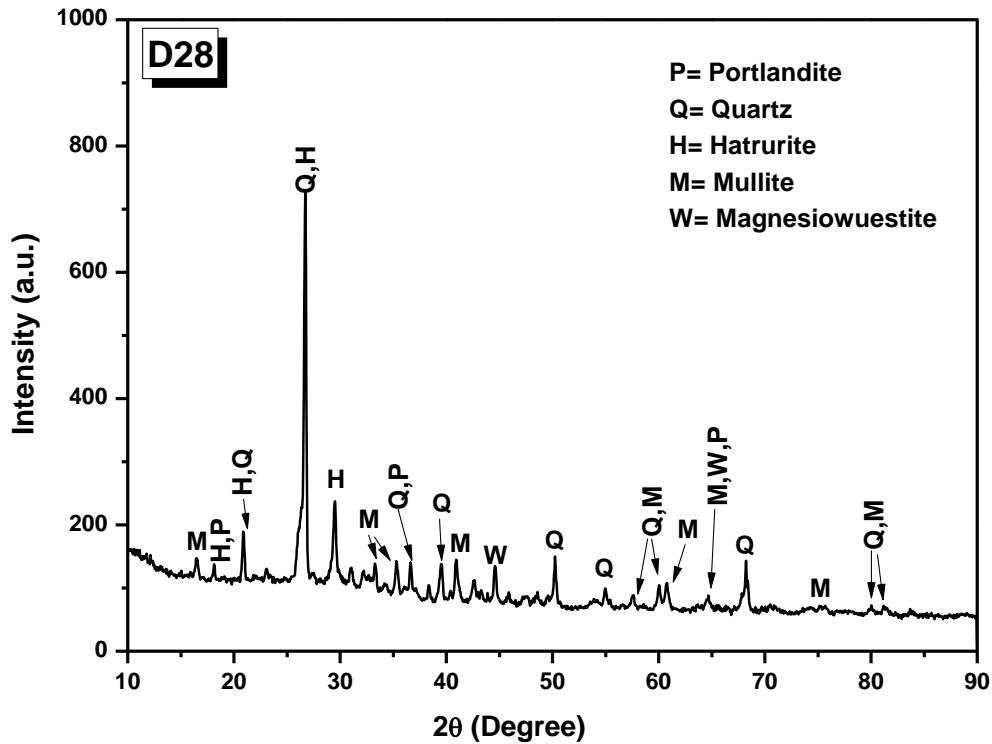


Fig.4.23 Phase Diagram of Mortar MM5 Grade with 100% Bottomash (1:4) at 28 days [Sample id. D(28)]

The constituent of Mortar mix was 1 part of Cement, and 4 parts of Bottomash. In this case also, when Sand content is totally absent in the mix under **MM5** category, and replaced entirely by bottom ash, highest phase is occupied by Quartz (SiO_2) and Hatrurite ($3\text{CaO}, \text{SiO}_2$), distantly followed by Mullite ($3\text{Al}_2\text{O}_3, 2\text{SiO}_2$), Magnesiowuestite ($\text{Mg}_{2.4}\text{Fe}_{1.6}\text{O}_4$), and Portlandite ($\text{Ca}(\text{OH})_2$).

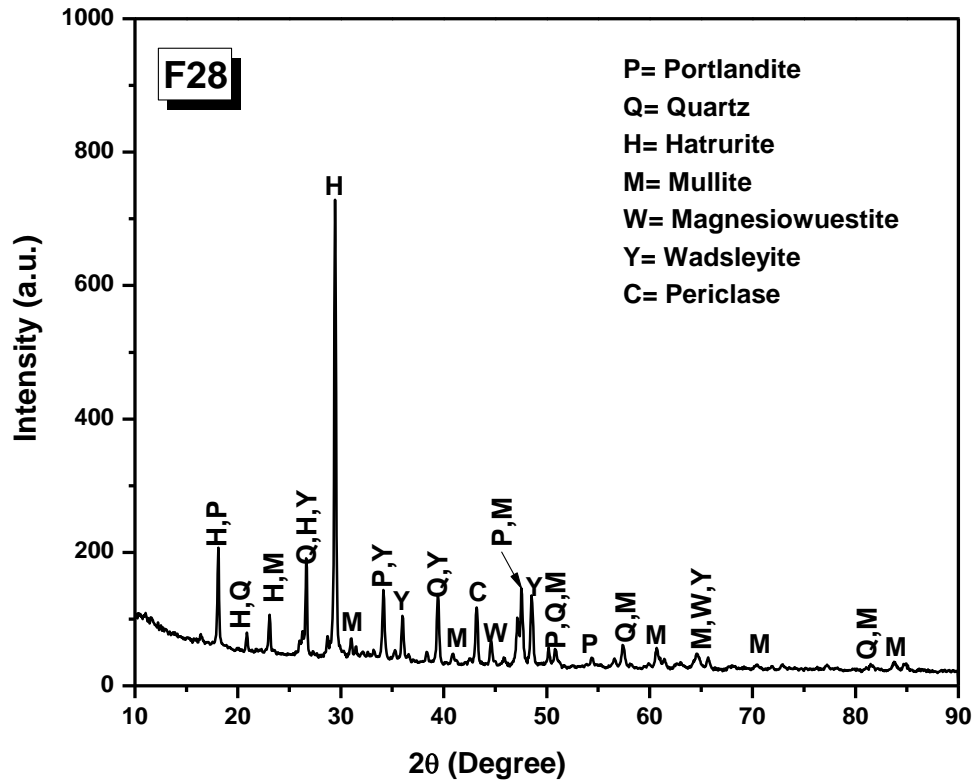


Fig.4.24 Phase Diagram of Mortar MM3 Grade with 50% Lime and 50% Bottomash (1:6) at 28 days [Sample id. F(28)]

The constituent of Mortar mix was 1 part of Cement, 3 parts of Lime and 3 parts of Bottomash. In this case, when Sand content is totally absent in the mix, and replaced by bottom ash and lime dust (50:50 basis) under **MM3** category, highest phase is occupied by Hatrurite ($3\text{CaO}, \text{SiO}_2$), followed by Quartz (SiO_2), Wadsleyite (Mg_2SiO_4), Portlandite ($\text{Ca}(\text{OH})_2$), Mullite ($3\text{Al}_2\text{O}_3, 2\text{SiO}_2$), Periclase (MgO), and Magnesiowuestite ($\text{Mg}_{2.4}\text{Fe}_{1.6}\text{O}_4$)

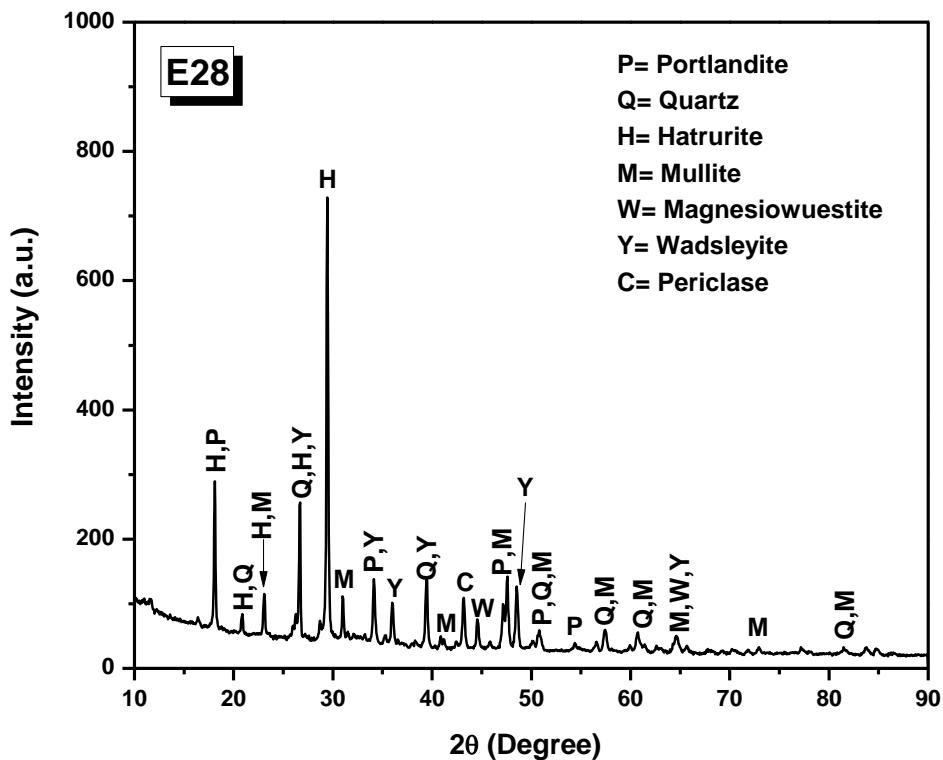


Fig.4.25 Phase Diagram of Mortar MM5 Grade with 50% Lime and 50% Bottomash (1:4) at 28 days [Sample id. E(28)]

The constituent of Mortar mix was 1 part of Cement, 2 parts of Lime, and 2 parts of Bottomash. In this case, when Sand content is totally absent in the mix, and replaced by bottom ash and lime dust (50:50 basis) under **MM5** category, highest phase is occupied by Hatrurite ($3\text{CaO}, \text{SiO}_2$), followed by Quartz (SiO_2), Wadsleyite (Mg_2SiO_4), Portlandite ($\text{Ca}(\text{OH})_2$), Mullite ($3\text{Al}_2\text{O}_3, 2\text{SiO}_2$), Periclase (MgO), and Magnesiowuestite ($\text{Mg}_{2.4}\text{Fe}_{1.6}\text{O}_4$).

4.5 Evaluation of Apparent Porosity and Bulk Density of cast samples

4.5.1 Introduction

Porosity is the percentage relationship between the volume of pore space and the total volume of the sample. Pore space are of two types, viz. open pore space and closed pore space. Apparent porosity considers the open pore space of the sample. The true porosity considers volume of closed pore spaces also. The usual difference between apparent and true porosity lies within 1-2% , provided the volume of sealed pores are not very much. Porosity of any manufactured material can be controlled by :

- i) By controlling the texture of the material, i.e. by controlling the particle size distribution.
- ii) By the methods of green manufacturing and composition, and
- iii) By controlling the firing temperature, time of curing etc.
- iv) Properly choosing the raw materials with grain size distribution etc.

Since apparent porosity is a measure of percentage ratio of the void space, it may be concluded that higher the porosity, lower will be the thermal energy transmission through such material, due to the offered resistance by the voids present within the material. There are two methods to determine apparent porosity parameter of refractory or solid materials. Boiling point method and Evacuation method

4.5.2 Test method

These tests were carried out on 50mmX50mmX25mm Or 50mmX50mmX12.5mm size samples. The samples were oven dried at 105⁰ C, and weighed in an electronic balance with accuracy level ± 0.05 gm after 12 hours. The measurements were recorded (w_1). The sample is then hung by wire through one attachment ring, which was affixed with the measuring steel platform of the balance. The sample was then kept immersed inside one glass jar with that hanging condition, and the weight recorded (w_2). The sample was then kept immersed fully inside one container filled with clean water for 24 hrs. After 24 hours, the sample was taken out, wiped and weighed in the same balance. The weightment was recorded (w_3). The volume of the sample was calculated by multiplying length, breadth and height in cm. The bulk density and apparent porosity of each sample was calculated by following the below formula.

$$\text{Bulk Density} = \frac{w_1}{w_3 - w_2} \text{ gm/cc} \quad (4.5)$$

$$\text{Apparent Porosity} = 100 \times \frac{w_3 - w_1}{w_3 - w_2} \% \quad (4.6)$$

4.6 Thermal Conductivity test of samples.

4.6.1 Introduction

Ever increasing energy costs and the growing realization about minimizing unwanted heat transfer is beneficial, clearly establishes commercial advantages for lower energy use construction methods and materials. The benefits of efficient thermal management by indoor electronics should also be coupled with thermally efficient building construction. The use of insulating (low thermal conductivity) materials may be desirable but nature did not provide true thermally insulating materials. One of the important parameters of thermal insulation material from the performance point of view is its thermal conductivity expressed as “k” value. Researching thermal properties for the common types of materials in building construction will result in data with significant variation, due to composition differences under varying test conditions.

4.6.2 Various test protocol

Numerous methods of determining the property have been used and very often, the results obtained by different methods are not same. The most common age old method is “Two-slab guarded hot plate method”, in which material to be tested can be laid flat between two parallel plates and can also be used for loose-fill materials, which can be filled between two plates. On the basis of ASTM C 177-1991 “Standard method of test for thermal conductivity of material by means of guarded hot plate”, the present revised IS Code 3346-1980 (Reaffirmed 2004) is available to test materials for determining the “k” value of material. This Standard prescribes the common procedures to find out thermal conductivity value of dry specimens, provided that :-

- a) The materials are homogenous and uniform with regard to its constituent aggregates and pores,

- b) The thermal conductance of such material does not exceed $60\text{W/m}^2\text{-K}$, and
- c) The two specimens used for testing are identical in thickness and density within 2% and also should comply with the thickness of specimen and dimensions of central and guard heater relation, as stipulated under Cl.5.1 Table 1 of the Code.



Fig.4.26 Guarded Hot Plate Test Apparatus

Two different types of Guarded Hot plate Apparatus have been stipulated in IS 3346. Those are similar in principle, but different in construction. The low temperature guarded hot plate is generally used for measurements at mean temperatures, such that the cold surface temperature may be as low as 77K and that of hot surface up to maximum 550K . The hot temperature guarded hot plate is generally used where hot side temperature is more than 550K but not crosses the limit of 1350K , which is the maximum for such apparatus. Another restriction with this method of testing is that the thermal conductivity value tested for any material, shall apply for that particular specimen tested only.

Alternative Technique to measure Thermal Conductivity of Materials

To introduce a quicker and accurate method by eliminating the influence of contact thermal resistance, present at the interface of probe and the specimen surfaces, a new

measurement technique has been evolved, which is described as Transient Plane Source (TPS). It offers a quick and precise method of studying thermal transport properties of materials simultaneously which are related to direct heat conduction namely, thermal conductivity, thermal diffusivity and specific heat capacity. TPS Technique is a device that can be used both in laboratory and in-situ measurements of all three related properties from cryogenic to high temperature (1000 K). It can measure thermal conductivities between 0.01 and 500 W/m-K.

The TPS method involves the use of a very thin double metal spiral, 10 μm thickness, sandwiched between two layers of Kapton (25 μm thickness), in close contact with the material to be investigated. The double metal spiral serves both as the heat source and as a resistance thermometer. When making measurements in solid bodies, the spiral is clamped between two surfaces of the same material, as shown in the Figure 1. The radius of the sensor can vary between 2 mm and 30 mm thus, the sample size can vary between 8 mm and 120 mm or larger.

TPS Applications are meant for the following :-

1. Standard – It measures thermal properties of solids (metal, ceramic, polymer), liquids, paste and powder.
2. Anisotropic – Thermal properties of an anisotropic material can be determined if the specific heat capacity is known beforehand.
3. Specific heat capacity - Determination of specific heat capacity of an anisotropic material is possible.
4. Slab – Determination of thermal conductivity of thin and high conductive material e.g. Aluminium. Thickness range of the samples should be within 1-3 mm.
5. Thin film – Textile, plastic foil, aluminium foil, paper etc. falls under thin film category. Thickness range of the sample varies from 25 μm to 500 μm .
6. Single sided – This is a special application of TPS Technique. The Sensor is attached to a material with known thermal conductivity and put on the sample (surface) under investigation. It is generally used for field measurements / verification purpose.

ISO 22007-2:2008(E) Part-2 describes the Transient Plane Heat Source (hot disc) Method. In general, this method is suitable having values thermal conductivity λ in the approximate range of $0.01 \text{ Wm}^{-1}\text{K}^{-1} < \lambda < 500 \text{ Wm}^{-1}\text{K}^{-1}$, and values of thermal diffusivity α in the range of $5 \times 10^{-8} \text{ m}^2 \text{ s}^{-1} \leq \alpha \leq 10^{-4} \text{ m}^2 \text{ s}^{-1}$, temperature being in the range of $50 \text{ K} < T < 1000 \text{ K}$. The specific heat capacity per unit volume, C can be obtained by dividing the thermal conductivity λ by thermal diffusivity α , i.e. $C = \lambda/\alpha$, and the approximate range lies between $0.2 \text{ MJm}^{-3}\text{K}^{-1} < C < 5 \text{ MJm}^{-3}\text{K}^{-1}$. It is sometimes referred as volumetric heat capacity.

Principle :

A pair of test specimen with hot-disc probe of negligible heat capacity attached on its surfaces is allowed to equilibrate at a given temperature. A heat wave in the form of a stepwise function is produced by an electrical current through the probe to generate a dynamic temperature field within the specimen, being tested. The increase in the temperature of the probe is measured against time function. The probe operates as a temperature sensor. The response of heating within the specimen is then analysed in accordance with the model developed for the specific probe and the assumed boundary conditions.

Main Component :

A typical hot-disc probe is shown in the figure . Convenient probes can be designed with diameters from 4 mm to 100 mm, depending on the specimen size and the thermal-transport properties of the material to be tested. The probe is constructed as a bifilar spiral etched out of a $(10 \pm 2) \mu\text{m}$ thick metal foil and covered on both sides by thin (from $7 \mu\text{m}$ to $100 \mu\text{m}$) insulating film. It is recommended that nickel or molybdenum be used as the heater/temperature-sensing metal foil due to their relatively high temperature coefficient of electrical resistivity and stability over a wide temperature range. It is recommended that polyimide, mica, aluminum nitride or aluminum oxide be used as the insulating film, depending on the ultimate temperature of use. The arms of the bifilar spiral forming an essentially circular probe shall have a width of $(0,20 \pm 0,03) \text{ mm}$ for probes with an overall diameter of 15 mm or less and a width of $(0,35 \pm 0,05) \text{ mm}$ for probes of larger diameter. The distance between the edges of the arms shall be the same as the width of the arms.

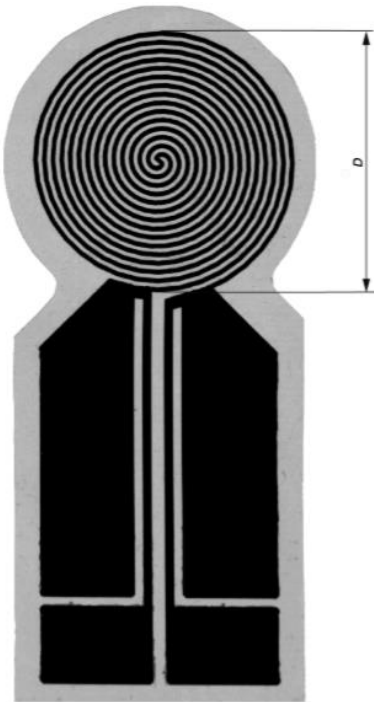


Fig. 4.27 Probe with bifilar spiral as sensing element (Sensor dia. between 4-100 mm)

An electrical bridge shall be used to record the transient increase in resistance of the probe. Through the bridge, which is initially balanced, the successive increases in resistance of the probe shall be followed by recording the imbalance of the bridge with a sensitive voltmeter (see Figure 3). With this arrangement, the probe is placed in series with a resistor which shall be designed in such a way that its resistance is kept strictly constant throughout the transient. These two components are combined with a precision potentiometer, the resistance of which shall be about 100 times larger than the sum of the resistances of the probe and the series resistor. The bridge shall be connected to a power supply which can supply 20 V and a current of up to 1 A. The digital voltmeter by which the difference voltages are recorded shall have a resolution corresponding to 6.5 digits at an integration time of 1 power line cycle. The resistance of the series resistor, R_S , shall be close to the initial resistance of the probe with its leads, $R_0 + R_L$, in order to keep the power output of the probe as constant as possible during the measurement.

Details about the Instrument used :

Hot Disk Thermal Constants Analyser (Hot Disk TPS2500 S), based on TPS technique had been used for all the experimental investigation purpose related to thermal properties of Concrete and Mortar of different grades and Mix. This instrument is capable of measuring thermal conductivity of materials ranging from 0.01 to 400 W/m.K by effectively utilizing highly sensitive components. The instrument consists of following items –

- i) Hot Disk TPS 2500 S with Software version 5.9
- ii) Hot Disk Sensor(s)
- iii) Room Temperature Sample Holder
- iv) Sample of Stainless Steel Disks as Reference material.

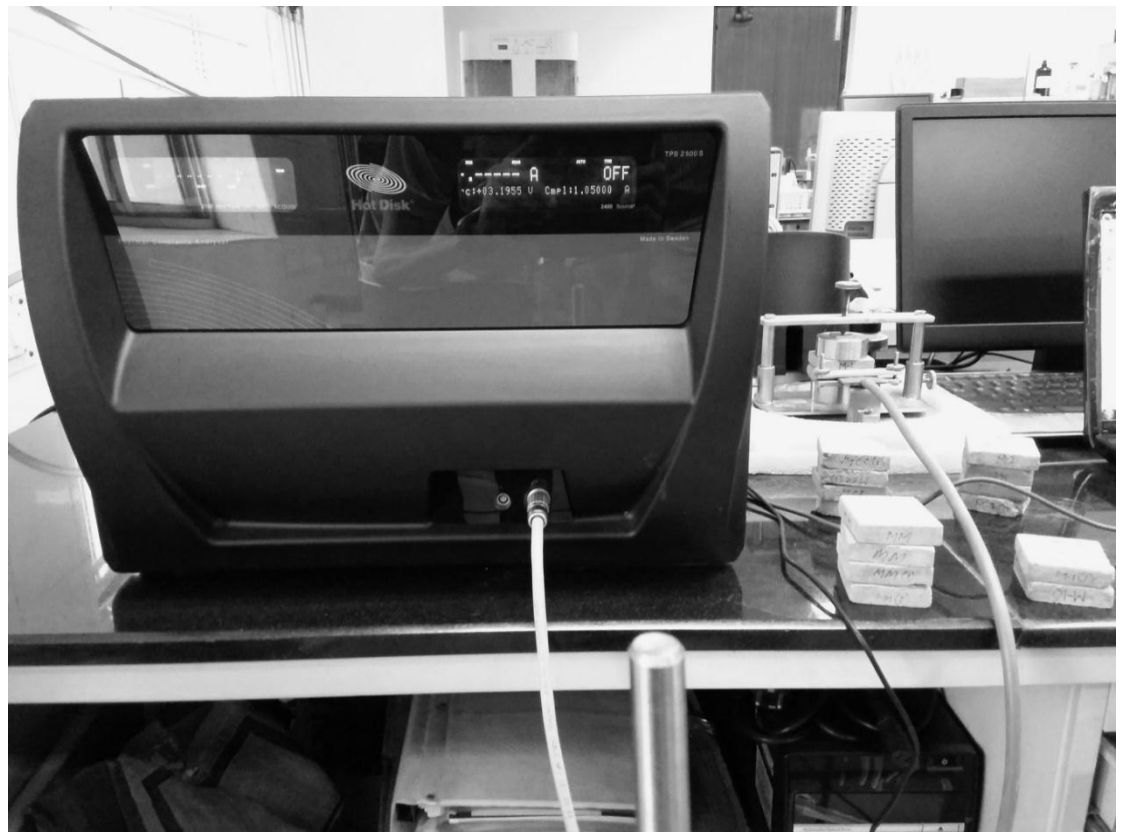


Fig.4.28 Hot Disk TPS 2500S Set up

Selection of Sensor : It depends upon the material to be tested, and the dimension of the sample. Different radii of Sensors are available as below :-

Table 4.16 Different Sensors used in Hot Disk Analyzer

Nomenclature	Radius (mm)	Sensor material	
		Kapton	Mica
7531	0.526	x	N.A.
7577	2.001	x	N.A.
5465	3.189	x	x
5501	6.403	X	N.A.
5082	6.631	N.A.	x
4921	9.719	x	x
8563	9.868	x	N.A.
4922	14.610	x	x
8562	14.725	x	N.A.
5599	29.52	x	x

The radius of the sensor must always be bigger than the porosity or the void structure of the sample, if the material is not dense or homogenous. For homogenous materials, where the structural variations are in atomic or molecular level, (e.g. ordinary metals) the hot disk sensor radii may be within the range of 3.2 -15 mm. For materials, where the structural voids are at the mm level, like in certain powders , glass wool, sponge etc. the largest sensor radius shall be more ideal.

Test Specimens : Bulk specimen

For bulk specimens, the requirement for specimen thickness depends on the thermal properties of the constituent material(s) from which the specimen is made. The expression for the probing depth contains the diffusivity, which remains un-known before the measurement. This means that the probing depth has to be calculated after an initial experiment has been completed.

The shape of the specimen can be cylindrical, square or rectangular. Machining to a certain shape is not necessary, as long as a flat surface of each of the two specimen halves faces the sensor.

The thickness of the specimen shall be at least 20 times the characteristic length of the components making up the material or of any inhomogeneity in the material, e.g. the average diameter of the particles if the specimen is a powder.

The specimen size shall be such that the distance from any part of the bifilar spiral of the hot-disc probe to any part of the outside boundary of the specimen remains larger than the overall mean radius of the bifilar spiral. An increase in this distance beyond the size of the diameter of the spiral does not influence the accuracy of the results obtained.

Specimen surfaces, which are in contact with the probe should be smooth enough to avoid any air-gap. It should also be taken into account that at the time of conducting the experiment, the heat load should not make any phase change of the specimen material.

In order to determine both the thermal conductivity and thermal diffusivity with good accuracy, the thickness of a flat surface should not be less than the radius of the hot disk sensor.

Probing depth :

In this method, to solve the thermal conductivity equation, the initial assumption made is that the sensor is located within an infinite material, which in turn means that the total time of the transient recording is limited by the presence of the finite boundaries of the sample size. Otherwise, it may be stated that the thermal wave or thermal penetration depth generated in this experiment must not reach the outside boundaries of the sample dimension during the recording of the transient test. The estimation of how far this thermal wave has proceeded in the sample during a recording, is the probing depth, given by the following formula :-

$$\Delta_p = 2\sqrt{\alpha \times t} \quad (4.7)$$

where α is the thermal diffusivity and t is the measuring time of the experiment and the constant 2 is determined so that the influence of external sample boundaries on the temperature of the sensor cannot be detected, when the probing depth Δ_p is limited to within the sample boundaries.

Steps involved in carrying out the test :

- 1.The probe is selected as per the specimen size and specification. The sensor is placed between the smooth faces of the samples. Clamping is done to secure the probe in the specified location.
- 2.The total system is assembled inside a constant temperature chamber. The room temperature and RH are recorded.
- 3.The test run is started with “New” under Bulk Specimen category. Probing depth, measuring time in second, heat pulse wattage and the selected sensor are mentioned in the test window.
- 4.After the test run, scattering of data points are visible on the computer screen. Then the selection of data points are to be mentioned in the Calculations window, with a possibility to allow for a time correction option. The time correction option takes care to compensate for a probable influence from the heat capacity of the sensor and other delays. In each experiment 200 data points are recorded irrespective of the selected total time of transient recording.
- 5.After selecting the data-point range, standard analysis button is hit in the window. The software calculates, and produces the results with 4 types of display viz. Drift, Transient, Calc and Residual with the tabulated parameters by the right side of the screen displayed. The experimental results window presents the following results out of the calculated transport properties as well as calculated indicators for the data analysis for a tested powder sample (Portland Pozzolana Cement) –

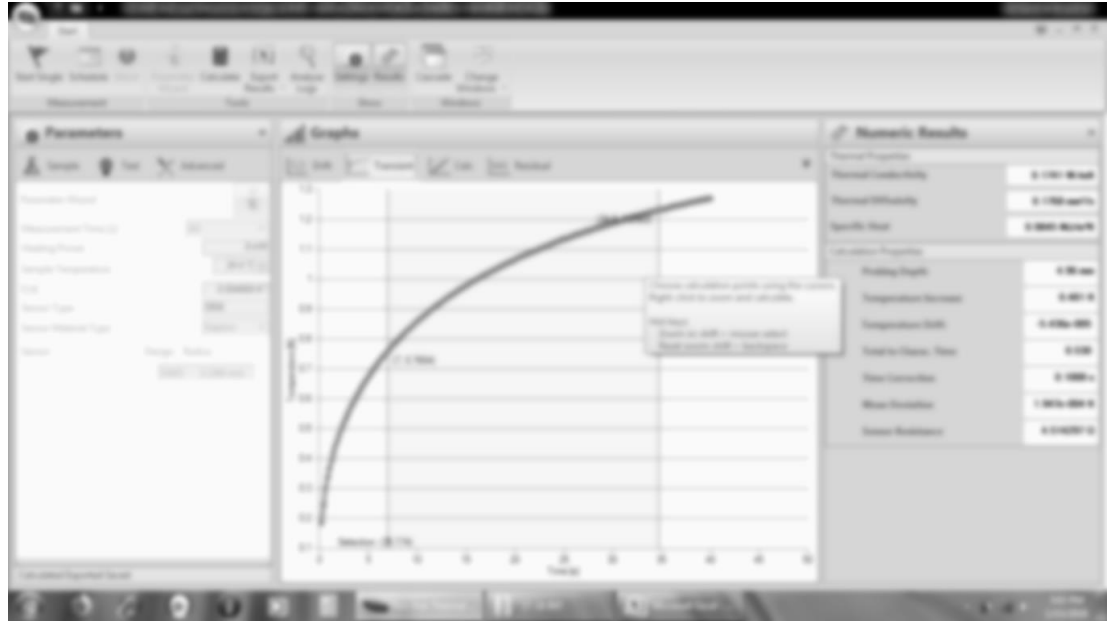


Fig.4.29 Typical test result vis Screenshot.

Left side data are the conditions, under which test performed, and the right side data are the desired test results of the specimen tested. The middle graph shows the transient nature of temperature variation versus time. The results are further explained as under :-

1. Thermal Conductivity
2. Thermal Diffusivity
3. Specific heat per unit volume
4. Probing depth is the distance from any part of the sensor to the nearest outside boundary of the sample should always be larger than the probing depth.
5. Temperature increase between the first and the last point used in the data analysis.
6. Total to Characteristic time gives the total time of the analysis divided by the characteristic time. This ratio should ideally be between 0.5 and 1.0.
7. Time correction.
8. Mean deviation of the points from the straight line fit from which the thermal conductivity is calculated.
9. Initial resistance of the Hot Disk sensor. This resistance is automatically measured prior to the transient recording.

4.6.3 Samples tested to determine Thermal Conductivity parameter

The following samples of dimension 50mmX50mmX12mm were prepared and tested for the thermal conductivity parameter under the above set steps, as fit for the instrument , and for the TPS method –

1. Concrete samples of various primary mix compositions (altogether 12 different mix compositions of various grades of concrete) with replacement of sand in stages by coal ash (bottom ash and fly ash separately) and also total sand free mix.
2. Mortar samples of various mix compositions (two primary mixes, which are most common in Indian building construction field) with replacement of sand in stages by coal ash (bottom ash and fly ash separately) and also total sand free mix.
3. Brick samples of various brands.
4. Basic materials like cement, sand, fly ash and bottom ash were also tested in powder form.

4.7 Burnt Clay Brick

4.7.1 Introduction

The common building bricks, which form the envelop portion of the building play a significant role in heat ingress and egress from building shell. The apparent porosity, bulk density are two major parameters, which are indirect fall-out of water absorption phenomena. IS 1077 provision on water absorption limits upto 20% by weight for Brick Class 12.5 or less and upto 15% for brick class above 12.5. Six numbers of random samples prepared from each brand variety clay brick, and altogether 6 different brands were chosen. All 36 samples of 50mmX50mmX25mm were soaked in water for 24 hours in cold water as per IS Code provisions, and water absorption were measured. Mostly water absorption values found to be just touching the permissible limit prescribed that of Class 12.5 or below . Thermal conductivity testing of all such samples were also carried out after drying the same.

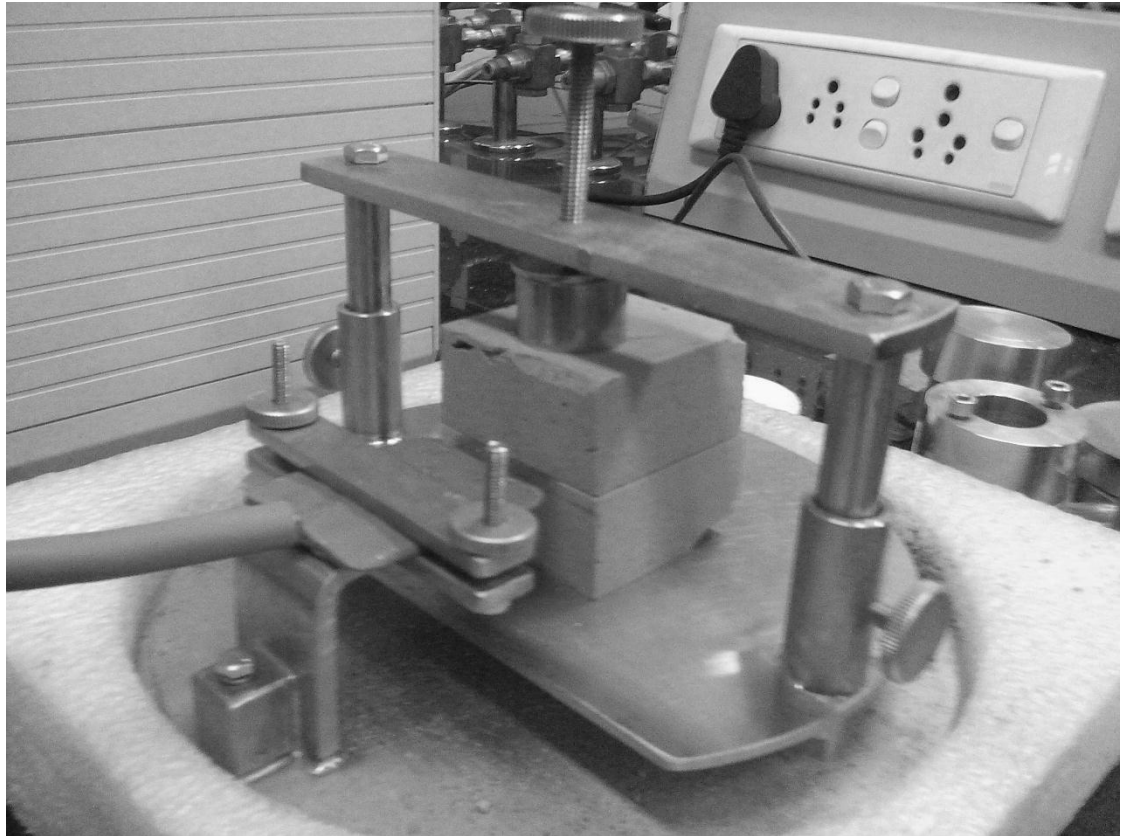


Fig.4.30 Burnt Clay Brick sample under thermal conductivity test

4.7.2 Burnt Clay Brick with Mortar on both faces

A few samples of burnt clay brick with 10 mm thick mortar on either face were prepared from the above brick variety. The sample sizes were 50 mmX50mmX35/40 mm (6 sets were of 35 mm thickness and 3 sets were of 40 mm thickness. Those were tested for water absorption and thermal conductivity values.

The flow sheet for the Physical & Thermal parametric testing activity are as under :-

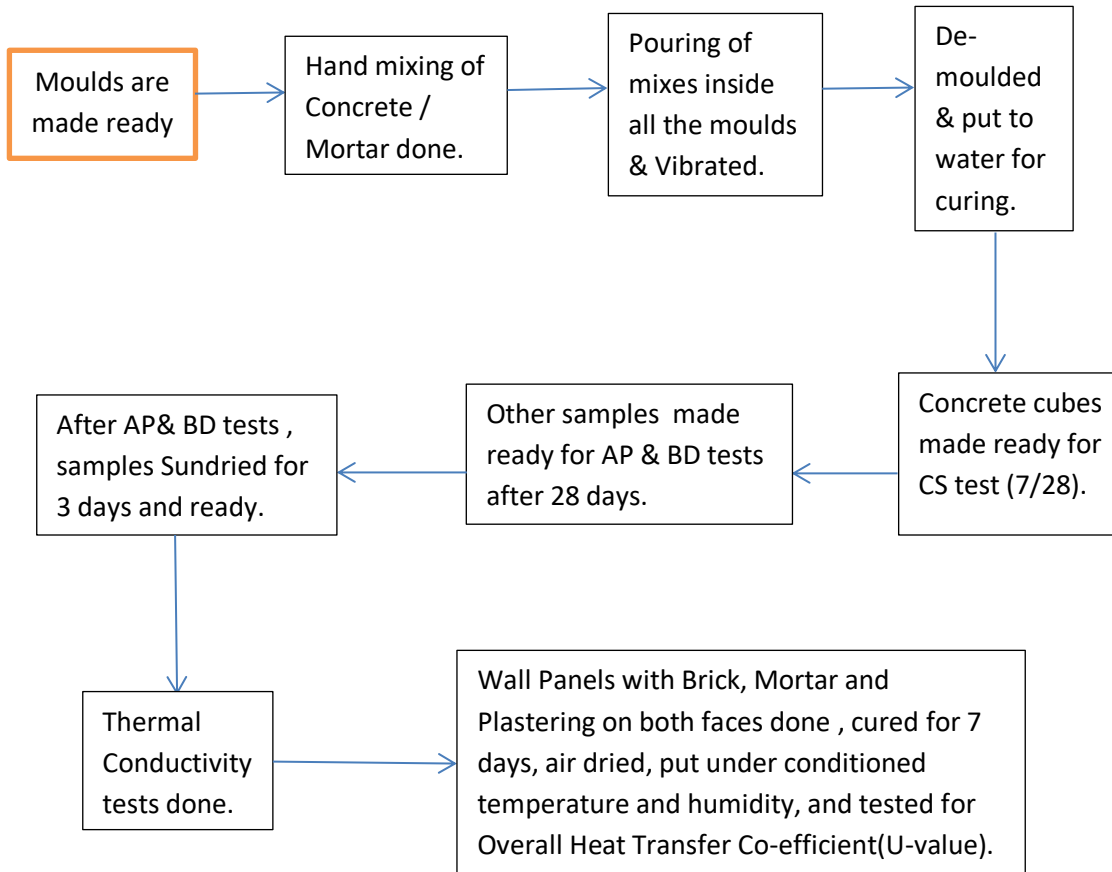


Fig. 4.31 Flow diagram of various test protocol for samples

4.8 Overall Heat Transfer Co-efficient (U-value) Test

4.8.1 Introduction

Heat transfer is thermal energy in transit due to a spatial temperature difference. Heat transfer through any material depends upon the temperature difference across the material and on the material properties. For building system, temperature difference across the building components is between the ambient temperature and the indoor air room temperature. When ambient temperature is higher compared to the indoor room temperature, heat flows into the building envelope. But, when the indoor temperature is higher compared to the ambient temperature, heat loss occurred through the components. So to control the heat flow through a building material, properties of the building material should be varied. For optimum design of energy efficient buildings, heat flow through the building envelope should be minimised.

4.8.2. Heat flow mechanisms

Heat can be transferred from one medium to another medium by three different processes. They are conduction, convection, and radiation. Exchange of thermal energy between bodies occurs through one of these modes or a combination of them. Conduction is the heat transfer process through solids or stationary fluids. Convection uses the movement of fluids to transfer heat. Radiation uses electromagnetic radiation emitted by an object for exchanging heat, it does not require a medium for heat transfer.

4.8.2.1 Conduction

Conduction is the mode of heat transfer that occurs from one part of a substance to another part of it within the substance itself in which energy exchange takes place from the region of high temperature to that of low temperature. Conduction occurs for fluids at rest by the kinetic motion or direct impact of molecules whereas in the case of metals, it happens by the drift of electrons. The heat transfer occurs here by the two mechanisms 1. By the transfer of free electrons. (Good conductors like metals have a plenty of free electrons to make conductive heat transfer). 2. The atoms and molecules having energy will pass that energy with their adjacent atoms or molecules by means of lattice vibrations. Higher temperatures are associated with higher molecular energies and when neighbouring molecules collide, as they are

constantly doing, a transfer of energy from the more energetic to the less energetic molecules must occur. In the presence of a temperature gradient, energy transfer by conduction occurs in the direction of decreasing temperature.

According to Fourier law, the rate of heat flow by conduction occurs in a direction that is proportional to the gradient of temperature in that direction and to the area normal to the direction of heat flow. The Fourier law is given as,

$$Q_x = -k \times A \times \frac{dT}{dx} \quad (4.8)$$

$$\text{Or } q_x = \frac{Q_x}{A} = -k \times \frac{dT}{dx} \quad (4.9)$$

where Q_x (W) and q_x (W/m^2) is the rate of heat flow through area A (m^2) and the heat flux in the positive x direction respectively. k is the proportionality constant. k [$\text{W}/(\text{m}^\circ\text{C})$] is defined as the thermal conductivity of the material which depends on the material properties and temperature. dT/dx is negative in positive x direction, as temperature decreases with the increase in x . k is a positive quantity. So, the negative sign converts Q_x and q_x to a positive quantity.

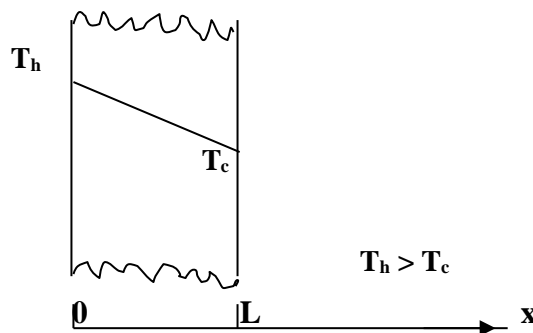


Fig.4.32. Conductive heat transfer through a sample

4.8.2.2 Convection

Convective heat transfer occurs when fluid flows over a solid body or within the fluid itself. Convection uses the motion of fluids to transfer heat. In a typical convective heat transfer, a hot surface heats the surrounding fluid, which is then carried away by fluid movement such as wind. The warm fluid is replaced by cooler fluid, which can draw more heat away from the surface. Since the heated fluid is constantly replaced by cooler fluid, the rate of heat transfer is enhanced. Convective heat transfer can be done in two ways:

1.If the fluid motion set up by the buoyancy effects resulting from the density difference caused by temperature difference in the fluid, then it is called natural convection. and,

2.Heat transfer is said to be forced convection when the fluid motion is artificially induced with a fan that forces the fluid flow over the surface. Convective heat flow from a hot wall surface to a cold fluid can be written as

$$q = h \times (T_w - T_f) \quad (4.10)$$

where, q (W/m^2) represents the heat flux from the hot fluid to cold wall,

T_w and T_f represent the wall and fluid temperature respectively,

' h ' is defined as the heat transfer coefficient.

The heat transfer coefficient depends upon several properties. They are:

- i. Type of flow, i.e. laminar or turbulent
- ii. Geometry of the body and flow passage area
- iii. Physical properties of the fluid
- iv. Average temperature and the position along the surface of the body
- v. Mechanism of heat transfer, i.e. natural convection or forced convection.

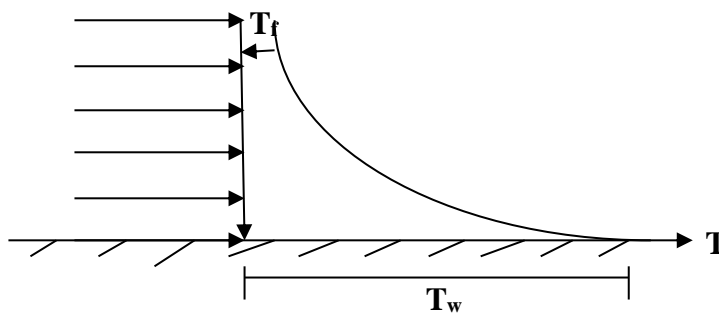


Fig.4.33. Convective heat transfer between a wall and fluid flow

When fluid flows over a body, temperature and velocity distribution at the vicinity of the surface highly influence the heat transfer by convection. Velocity and thermal boundary layer concept is used to explain the temperature and velocity profile of any fluid near the solid surface. When a fluid flows over a stationary surface, velocity of the fluid increases from the wall to a maximum in the main stream of the flow. We define the thickness of the velocity

boundary layer as the distance from the wall to the point where the velocity is 99% of the "free stream" velocity. The boundary layer grows from zero when a fluid starts to

flow over a solid surface. Similar to the velocity boundary layer, temperature boundary layer is also defined as the distance from the wall to the point where the flow temperature is equal to 99% of the "freestream" fluid temperature.

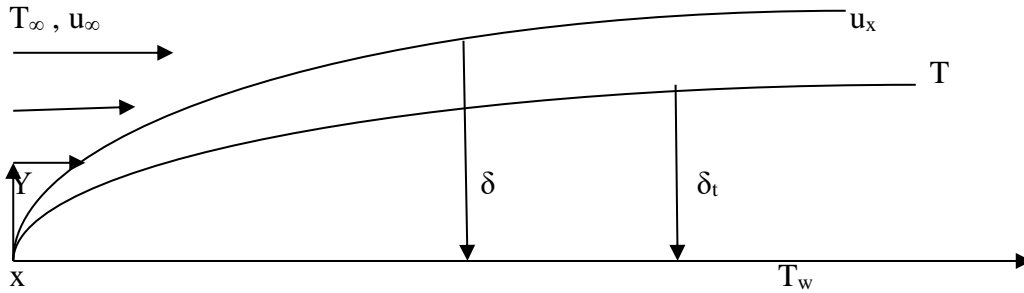


Fig.4.34. Velocity and thermal boundary layer

The relative thickness of the thermal boundary layer (δ_t) and velocity boundary layer (δ) depends on the Prandtl number of the fluid. Prandtl number is defined as the ratio of momentum diffusivity to thermal diffusivity, i.e.

$$Pr = \frac{\mu \times c_p}{\lambda} \quad (4.11)$$

where μ is the dynamic viscosity,

c_p is the specific heat and

λ is thermal conductivity.

When Prandtl number is equal to unity, thickness of the velocity and thermal boundary layers are equal. Prandtl number greater than one implies, thickness of thermal boundary layer is smaller than that of the velocity boundary layer.

4.8.2.3. Radiation

Thermal radiation is the energy emitted by matter that is at non-zero temperature. Radiative heat transfer does not require a medium to pass through. It is the only form of heat transfer that can occur in vacuum. It uses electromagnetic radiation (photons), which travels at the speed of light and is emitted by any matter with temperature above 0 Kelvin (-273 °C). Radiative heat transfer occurs when the emitted radiation strikes another body and is absorbed.

Radiative heat transfer occurs from all solids, liquids and gases. Regardless of the form of matter, emission may be attributed to changes in the electron configurations of the constituent atoms or molecules. The energy of the radiation field is transported by electromagnetic waves. The electromagnetic spectrum classifies radiation

according to wavelengths of the radiation. Main types of radiation are (from short to long wavelengths): gamma rays, x-rays, ultraviolet (UV), visible light, infrared (IR), microwaves, and radio waves. Radiations with shorter wavelengths are more energetic and contain more heat. Radiation that is emitted by the surface originates from the thermal energy of matter bounded by the surface, and the rate at which energy is released per unit area (W/m^2) is termed the surface emissive power. The amount of radiation emitted by an object is given by:

$$Q_{emitted} = \epsilon \times \sigma \times A \times T^4 \quad (4.12)$$

$$q_{emitted} = \frac{Q_{emitted}}{A} = \epsilon \times \sigma \times T^4 \quad (4.13)$$

where A is the surface area, T is the absolute temperature of the surface, σ is a constant called Stefan- Boltzmann constant, which is equal to $5.67 \times 10^{-8} \text{ W}/\text{m}^2\text{K}^4$, and ϵ is a material property called emissivity. The emissivity has a value between zero and 1, and is a measure of how efficiently a surface emits radiation. It is the ratio of the radiation emitted by a surface to the radiation emitted by a perfect emitter at the same temperature .i.e. 1 for a perfectly black body.

4.8.2.4 Combined heat transfer

Heat transfer through any material is a combination of all three mechanisms of heat transfer, i.e. conduction, convection and radiation. Total heat transfer through any component depends on the overall heat transfer coefficient of that material. U-value of any material can be calculated as

$$U = h_{conduction} + h_{convection} + h_{radiation} \quad (4.14)$$

$$h_{conduction} = \frac{L}{\lambda \times A} \quad (4.15)$$

$$h_{convection} = \frac{1}{h \times A} \quad (4.16)$$

Where, h_{cond} , h_{conv} and h_{rad} are conductive, convective and radiative heat transfer coefficient respectively. Total heat flow through any component can be evaluated as

$$Q = U \times A \times \Delta T \quad (4.17)$$

Q is the total heat transfer through that component,

U ($\text{W}/\text{m}^2\text{K}$) is the overall heat transfer co-efficient, A (m^2) is the surface area of the component, and ΔT is the temperature difference across the component surfaces.

4.8.3 Heat flow measurement methods

To measure the heat flow through any material, it is important to evaluate the overall heat transfer coefficient of the material. Guarded Hot Box is used to calculate the U-value of any material experimentally.

4.8.3.1. Guarded Hot Box method

Guarded hot box consists of mainly 3 parts; hot side, cold side and a surround panel. Hot side comprises of a metering box and a guard box.

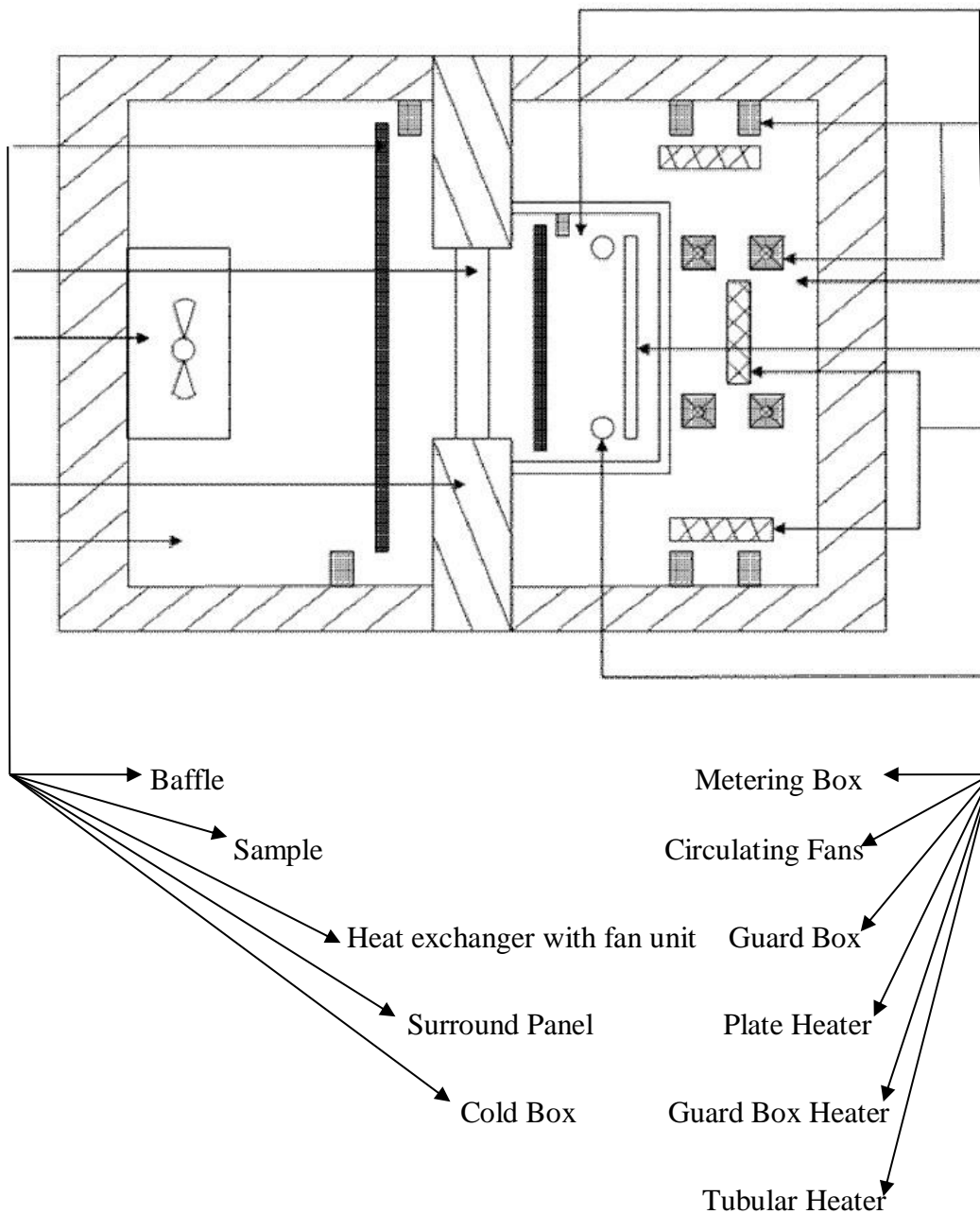


Fig.4.35 Schematic arrangement of Guarded Hot Box Test Set up

The specimen to be tested is placed in the surround panel, sandwiching between the hot side and the cold side. Constant temperature difference is maintained across the sample specimen. Heat supplied to the metering box passes through the sample to the cold box. To ensure one directional heat flow, heat flow through the metering box walls has to be prevented. Guard box is used to ensure one dimensional heat flow through metering box to the cold side of the system. According to standard BS EN ISO 8990 1996, U-value (W/m^2K) of the sample can be calculated using the equation

$$U = \frac{Q}{A(T_{ah} - T_{ac})} \text{ where} \quad (4.18)$$

Q is the heat flow rate through the test material, expressed in Watt, A is the area perpendicular to the direction of heat flow in m^2 , T_{ah} is the environmental temperature at the hot side in Kelvin and, T_{ac} is the environmental temperature at the cold side in Kelvin.

4.8.3.1(a) Metering Box

Metering box consists of five insulated walls namely ceiling wall, floor wall, right side wall, left side wall and back wall. One side of the metering box is open to allow the heat flow through the sample. Heaters are installed in the metering box for the power generation.

Circulating fans create forced circulation in the metering box to maintain constant uniform temperature throughout the metering box. A baffle plate with matt black surface is placed parallel to the test sample in the metering box. The reason behind the installation of the baffle plate is to achieve uniform level of radiative heat on the test sample. Baffle also acts as a shield to direct heat flow from any power input to the test sample. Baffle plate is coated with black to achieve higher value of emissivity.

4.8.3.1(b) Guard Box

Guard box surrounds the metering box. The main purpose of the guard box is to minimise the heat flow from the metering box walls by maintaining proper temperature inside it. According to the standard BS EN ISO 8990:1996, heat loss to the guard box through the metering box walls must be less than 10% of the total power input to the metering box. Guard box is highly insulated to reduce heat loss to

the surround environment. Heater and circulating fans are placed inside the guard box to ensure uniform temperature distribution.

4.8.3.1(c) Cold Box

A constant low temperature is maintained inside the cold box to ensure heat flow from the metering box. Heat exchanger and circulating fans are placed inside the cold box to remove heat from inside and to maintain uniform temperature distribution respectively. Similar to metering box, a baffle plate is placed in the cold box parallel to the sample to achieve uniform radiative heat transfer.

4.8.3.1(d) Test Procedure

In the Guarded hot box, there is a surround panel, which isolates the open faces of metering box, guard box and cold box completely. This surround panel which is placed between the hot and cold side forms an integrated test setup. Sample is placed in an aperture in the surround panel. Sufficient numbers of thermocouples are attached to the test element surface to measure the mean surface temperatures. Tie wires or Tie bars are used to attach the hot side, surround panel and the cold side as a single closed unit. Set point temperatures for hot and cold side depend on the climatic condition of the location where such products are intended to be utilised. According to the British standard BS EN ISO 8990:1996, minimum air temperature difference of 20 °C between hot and cold side needs to be maintained for U-value calculation of any material. Initially all the heating units in the hot side and cooling unit in the cold side along with all circulating fans are made to work simultaneously. This leads to gradual rise of temperature in the hot side and gradual drop in cold side. When air of both metering box and guard box temperature reaches the set point temperature, heaters are switched 'ON' and 'OFF' to maintain air set point temperature. Fans are in 'ON' state continuously throughout the time span of testing. After the system reaches steady state condition, power input and temperatures are measured and based on these values U-value calculation is done. At the steady state condition, rather than continuously increasing or decreasing, the input power and temperatures at different locations oscillate within a small range. According to the standard, when the temperature variations between two successive four hour span data sets are less than 1%, then the system is in steady state condition. The time required to reach the steady state condition depends on several factors like the thermal inertia of the system,

thermal capacity, resistance of the sample, surround panel material, surface conditions etc. System with higher thermal capacity takes longer time to reach steady state. Total heat input to the system not only depends on heater power, but also depends on the power generated by the circulating fans, as the motors of the fan are inside the test setup.

4.8.4 Guarded Hot Box test set-up

A Guarded Hot Box test setup was designed and developed in School of Energy Studies, Jadavpur University. The setup was constructed according to the standard BS EN ISO 8990:1996. This setup was constructed using high insulating material, extruded polystyrene, whose thermal conductivity is 0.027 W/m.K. This setup is capable to measure the U-value of any material whose thermal conductance is in the range of 0.1W/m².K to 15W/m².K.



Fig.4.36. Guarded Hot Box test setup with data logging and recording.

4.8.4 (a) Metering Box

External dimension of the metering box is 1840X1600X600. Metering box consists of 5 walls, and each wall is 50mm thick. According to the standard BS EN ISO

8990:1996, linear dimensions of the metering area should be at least 1000mm and it must not be less than three times of the maximum thickness of any test element. Surround panel thickness in this setup is 300mm. So, the maximum thickness of sample that can be tested in this setup is 300mm, whereas the metering area is 1740X1500. To reach the set point temperature and maintain that condition in the metering box, three heaters are used out of which two are DC tubular heaters of 60W each and one DC plate heater of 100W. Plate heater and tubular heaters operate at 12V and 48V respectively. Tubular heaters have Ni-chrome wire coil inside the ceramic body filled with sand to achieve higher thermal mass. For temperature control, different types of temperature controller have been developed on Agilent VEE software platform. To achieve uniform temperature distribution eleven DC circulating fans are installed in the metering box operating at a voltage of 24V DC. Total power consumption by the fans is 17W. To reduce the heat gain by fans, six fans were removed and the uniform temperature distribution is maintained using five DC circulating fans. Baffle plate installed in the metering box ensure the type of flow of air in the metering box. For natural convection, the distance between the baffle and the test element must not be less than 150mm. Forced convection occurs when the distance between the baffle and sample reduces.

4.8.4(b) Guard Box

External dimension of the guard box is 2760X2500X2100. Walls of the guard box are made of 250mm Extruded Polystyrene sheets. There are three tubular heaters out of which two are of 120W each and one is of 60W. Eight DC circulating fans are also present in the guard box. Heaters are operated at a voltage of 48V. Different types of temperature controller are also designed to control the desired temperature in guard box.

4.8.4(c) Cold Box

External dimension of the cold box is same as that of guard box, i.e. 2760X2500X2100. Walls of the guard box are 250mm thick. Cold box walls are well insulated by Extruded Polystyrene sheets to reduce the heat load on the cooling system and to prevent condensation on the outside of the chamber walls. Cold box

provides a controlled environment at constant low temperature. Main objective of cold box is to allow a constant one dimensional heat flux through the sample from metering box. Temperature control inside the cold box is achieved using a heat exchanger and a fan. A solution of 50% Calcium Chloride and 50% water is used as the working fluid of the medium. To maintain constant temperature in cold box, a PID controller is designed which controls the mass flow rate of the working fluid. Ten circulating fans are installed to maintain uniform temperature inside the cold box. A black baffle plate is placed inside the cold box parallel to the sample.

4.8.4(d) Surround Panel

Dimension of the surround panel is 2760X2500X300. Surround panel is made of Extruded Polystyrene sheets of 300 mm thickness. At the centre of the surround panel, there is an opening of 500X500 where the test sample can be placed.

4.8.4 (e) Temperature Measurement and Process Control Strategies

To calculate the U-value of any material, total power input to the system and temperatures at different suitable locations in all boxes i.e. metering box, guard box and cold box need to be measured. K type thermocouples with wire diameter of 0.2mm where Chromel is used as positive and Alumel as negative have been used for temperature measurement. K type thermocouples have a very wide temperature range of -270°C to 1260°C with a sensitivity of 41 μ V/°C. Temperatures are measured in the following locations:

- Temperatures at twelve suitable locations on the inner surface of the metering box walls.
- Temperatures at twelve suitable locations on the outer surface of the metering box walls.
- Air temperatures at three locations in the metering box in front of the baffle plate.
- Air temperatures at three locations in the guard box.
- Air temperatures at three locations in cold box in front of the baffle plate.

- Temperature of baffle surface facing the sample at nine different locations in the metering box.
- Temperature of baffle surface facing the sample at nine different locations in the cold box.
- Sample surface temperature at five different locations on both hot and cold side.
- Panel surface temperature at eight different locations on both hot and cold side.



Fig.4.37. Wall sample placed in position with Sensors

Air temperatures in the metering box and guard box have to be controlled very accurately and precisely for the calculation of U-value of any material. Thermo-emf signals obtained from the thermocouple junctions are logged and converted into equivalent temperatures with respect to time by the Agilent Data Acquisition System 34970A.

To control the cold box temperature, a PID controller is used. Air temperature at three different positions in front of the baffle in the cold box is measured and averaged out. Then difference between the set point temperature and the average air temperature is calculated and fed to the controller. Based on the deviation the controller activates a process relay which in turn controls mass flow rate of the working fluid in the pump. A by-pass path has been designed so that excess fluid can

return to the chilling plant. A flow-meter is installed in the input pipeline to measure the flow rate of the liquid.

4.8.4 (f) Sample preparation

Two wooden frames having dimension 500*500 were built in order to construct and hold the brick wall samples within them. This was done mainly in order to make it a modular system which would be portable enough so that after experimentation further developments of the samples like plastering, colouring etc are possible. Clay bricks, Portland Pozzolana Cement (PPC), sand and water were the raw materials used for the construction of the brick walls. Dimension of standard Indian bricks are 230 X 115 X 75. Two sets of brick walls were developed for the experimentation purpose, one with conventional plaster Grade MM5 with Cement-Sand ratio 1:4, another one with same grade of mortar and plaster but with 50% Sand and 50% flyash in place of 100% sand. Dimensions of the both brick walls were 480*480*115 and 480*480*115 with 12 mm plaster on either side.



Fig.4.38. Construction of the brick wall sample under progress

4.8.4.2 125mm brick wall sample testing

The testing of U-value of 125mm thick burnt clay brick wall was done in both the cold side open and closed condition. In closed condition metering box air temperature was fixed at 40°C, whereas cold box temperature was set at 25°C. In the open condition average temperature of the air conditioned room which acted as the heat removal unit was 24.079°C. Three thermocouples were attached to the brick surface and two thermocouples were attached to the joint mortar surface. In order to ensure the accuracy of the sample test, each sample was tested under similar conditions for a minimum of consecutive 3 days.

Chapter 5
Experimental Results
&
Observations

Chapter 5 : Experimental Results and Observations

5.1 Introduction:

As described in previous chapter, i.e. Chapter 4, all the design and nominal mix samples in respect of Concrete of various grades starting from M-15 to M-25 were put to test to determine various physical and thermal parameters. Similarly, Mortar mix samples of various proportions with respect to two most used grades MM3 and MM5 were put to tests. The tests performed on those samples were of destructive and non-destructive in nature. The tests are essential for durability and application worthiness of such concrete and mortar mixes.

5.2 Tests undertaken

The following tests were undertaken on the prepared samples –

- A. Compressive Strength Test (Destructive in nature) for 7 days maturity and 28 days maturity respectively for concrete samples and only 28 days maturity for mortar samples. To study strength development beyond 28 day's maturity, in some cases compressive strength of concrete samples at 90 day's maturity were also determined. As per IS Code 456-2000, and IS 2250-1981, the strength determination and acceptance limit for concrete and masonry mortar was fixed at 28 day's maturity
- B. Apparent Porosity Test (Non-destructive) after 28 days of maturity for all the samples as per IS 1528 (Pt.VIII), 1974.
- C. Bulk Density Test (Non-destructive) after 28 days of maturity for all the samples.
- D. X Ray Diffraction Analysis test after 28 days of maturity for few samples (Non-destructive in nature). Samples are basically powdery remains after compressive strength tests performed.
- E. Thermal Conductivity test after 28 days of maturity of all samples (Non-destructive in nature) by following Transient Plane Source method as per ISO 22007-2:2008.
- F. Thermal Transmittance (U-value) test of Masonry Wall Panel(Non-destructive test). Burnt Clay Brick wall panel of size 480 mmX480 mmX140 mm were prepared with bricks of size 230 mmX115 mmX75 mm and 12 mm thick Plaster on both the faces of wall panel, and left to cure. After curing was done for consecutive 7 days, the panel was made ready by applying putty for surface evenness and external quality paint, as actual condition.

Overall heat transfer co-efficient value evaluation was done by Guarded Hot Box Method as per BS EN ISO 8990-1996.

5.3 Design Concrete Mix Samples – Compressive Strength, Thermal Conductivity, Apparent Porosity and Bulk Density parameters Test Results

5.3.1 Design mix (1:1.6:2.4) (Set-1, Group-A) : Sand content replaced by **Flyash** in 10% stages from initial 100%, Cement used was Portland Pozzolana Cement (PPC), and Stone Aggregate used was 10 mm down .

Table 5.1 Compressive Strength test result for (Set-1, Group-A) 1:1.6:2.4 Concrete Mix with Flyash

Sample identity	Design Mix proportion – 1:1.6:2.4 (Grade M-20)					Compressive Strength (MPa)		
	Cement	Sand	Fly ash	Stone Aggregate	Water Cement ratio	7 days	28days	90days
CC	1.00	1.60	0.00	2.40	0.50	20.71	33.64	45.6
D1	1.00	1.44	0.16	2.40	0.50	15.02	33.2	45.56
D2	1.00	1.28	0.32	2.40	0.50	14.08	32.42	45.08
D3	1.00	1.12	0.48	2.40	0.50	9.95	24.28	26.29
D4	1.00	0.96	0.64	2.40	0.50	8.53	20.93	25.90
D5	1.00	0.80	0.80	2.40	0.50	7.10	19.80	21.77
D6	1.00	0.64	0.96	2.40	0.50	7.10	16.82	21.18
D7	1.00	0.48	1.12	2.40	0.50	6.20	13.43	14.85
D8	1.00	0.32	1.28	2.40	0.50	6.06	11.56	12.79
D9	1.00	0.16	1.44	2.40	0.50	6.07	10.01	11.88
D10	1.00	0.00	1.60	2.40	0.50	5.94	10.00	11.56

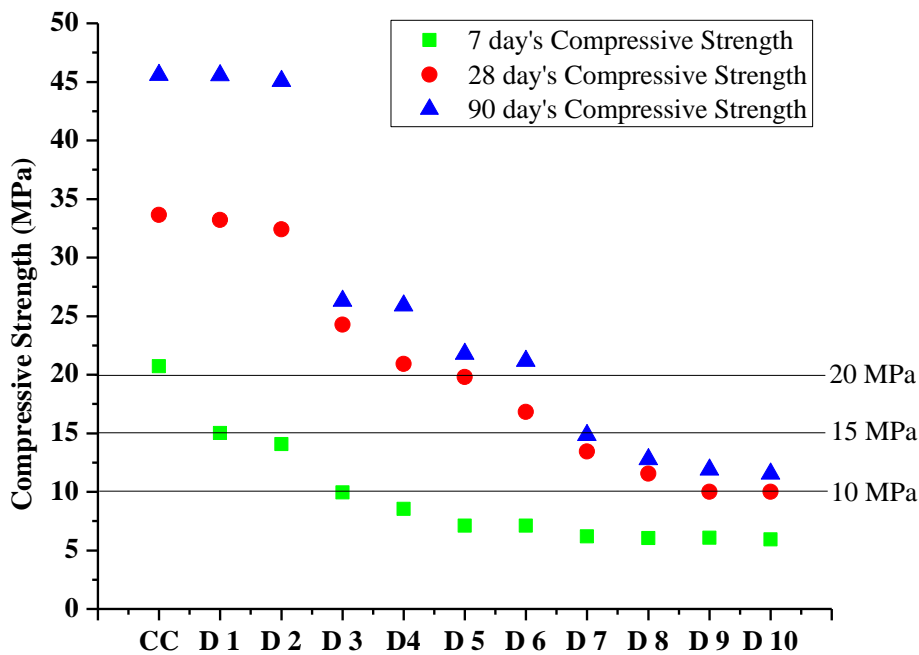


Fig.5.1 Variation in Compressive Strength for (Set-1, Group-A) Concrete Mix with Flyash (Refer Table 5.1)

Observation : From the above figure, it may be observed that the compressive strength of all the samples have reached at least 10 MPa strength at 28 day’s maturity. Samples with 50% replacement of sand by Flyash have attained at least 20 MPa strength at 28 day’s maturity, and samples with lesser replacement ratios i.e. 10% - 40% have attained >20 MPa strength at the same maturity level. At 90 day’s period of maturity, the strength increases further beyond that of 28 day’s for all category, but with varying degree.

Table 5.2 Thermal Conductivity test result for (Set-1, Group-A) 1:1.6:2.4 Concrete Mix with Flyash

Concrete mix identity	Thermal Conductivity (W/m.K)
CC	1.511
D1	1.407
D2	1.288
D3	1.006
D4	0.977
D5	0.973
D6	0.9601
D7	0.918
D8	0.848
D9	0.7907
D10	0.7389

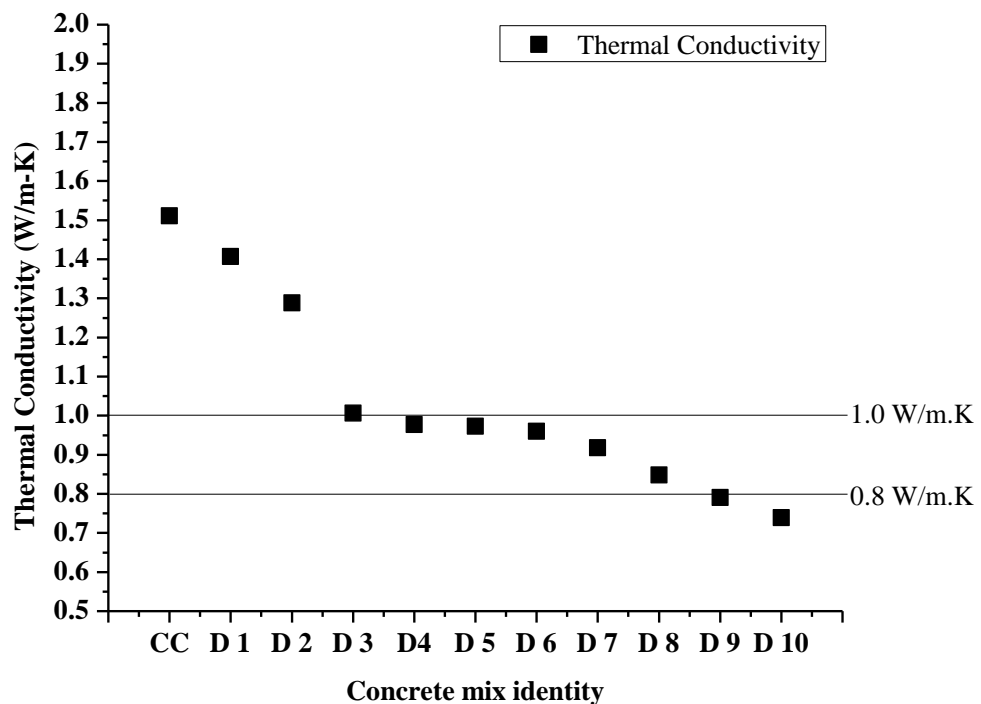


Fig. 5.2 Variation in Thermal Conductivity values for (Set-1, Group-A) Concrete Mix. (Refer Table 5.2)

Observation : From the above figure, it may be observed that thermal conductivity value started decreasing sharply till 30% sand substitution by Flyash (D3), and post that stage up to 60% substitution (D 6), the decrement rate is very less, and again thereafter the fall in rate increases. This trend is corroborated by the apparent porosity and bulk density value change at the same stages, as depicted in the later figure.

Table 5.3 Apparent Porosity and Bulk Density Test Results for (Set-1, Group-A) 1:1.6:2.4 Concrete Mix with Flyash

Concrete mix identity	Apparent Porosity (%)	Bulk Density (gm/cc)
CC	17.516	2.238
D1	20.843	2.104
D2	22.324	2.028
D3	25.663	1.963
D4	26.911	1.918
D5	28.159	1.901
D6	28.949	1.871
D7	30.432	1.832
D8	35.811	1.675
D9	35.869	1.669
D10	37.165	1.649

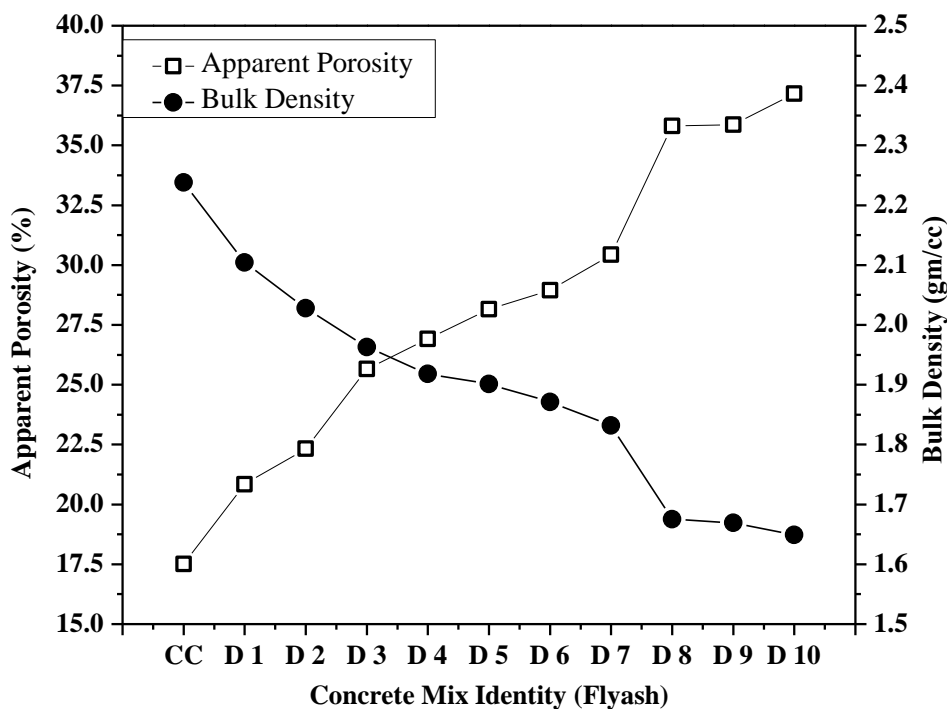


Fig.5.3 Variation in Apparent Porosity and Bulk Density for (Set-1, Group-A) Concrete Mix with Flyash (Refer Table 5.3)

Observation : From the above figure, it is evident that apparent porosity value increases and corresponding bulk density value decreases with each percentage step of sand substitution by Flyash, from 10% to 100% of such substitution by flash. More the Fly ash, more is apparent porosity percentage, and lesser is bulk density value.

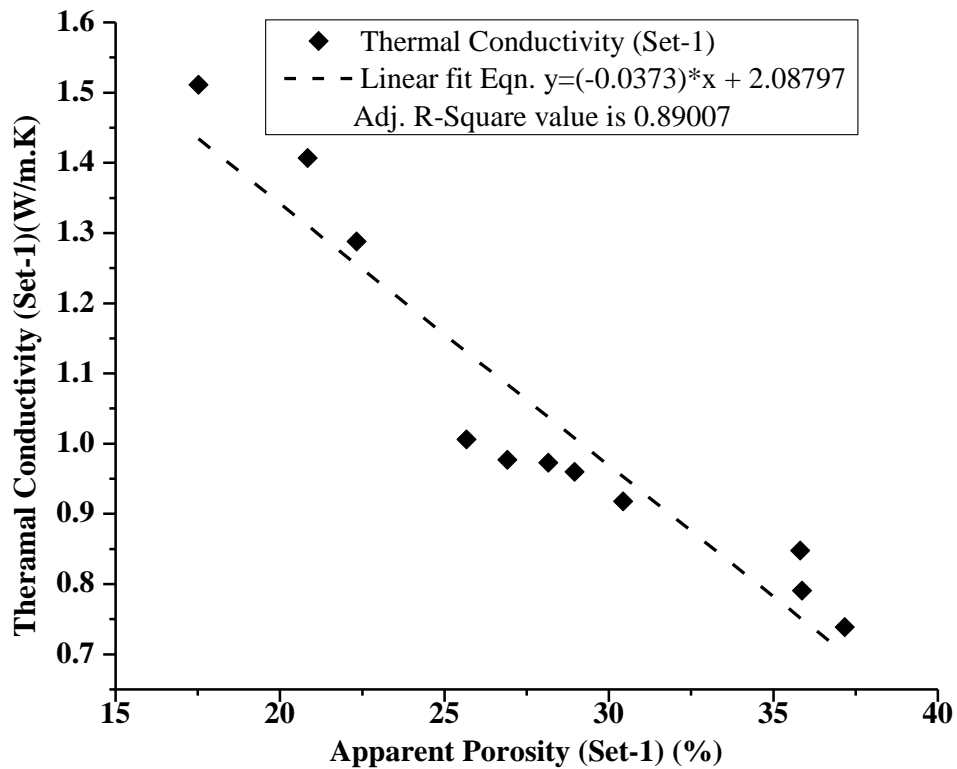


Fig. 5.4 Relationship between Apparent Porosity and Thermal Conductivity for the Concrete mix sample (Set 1, Group-A) (Refer Table 5.2 and 5.3)

Observations : Apparent Porosity is shown to have a close relationship with thermal conductivity of the concrete mix sample, and the adjusted R^2 value of 0.89, (assessed the goodness-of-fit for linear regression analysis by Origin 8) supports the same. The more is the apparent porosity, less is the thermal conductivity.

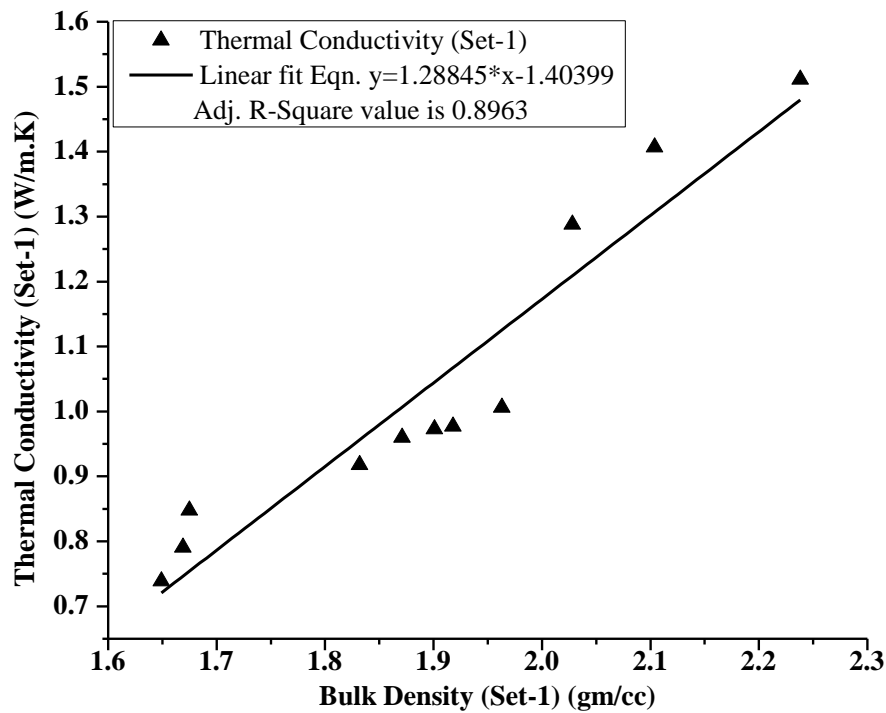


Fig. 5.5 Relationship between Bulk Density and Thermal Conductivity for the Concrete mix sample (Set 1, Group-A) (Refer Table 5.2 and 5.3).

Observations : Bulk Density is shown to have an almost linear fit relationship with thermal conductivity of the concrete mix sample, and the adjusted R^2 value of 0.8963, (assessed the goodness-of-fit for linear regression analysis by Origin 8) supports the same. The more is the bulk density, more is the thermal conductivity.

5.3.2 Design Concrete Mix 1:1.6:2.4 (Set-2, Group-A) - Sand content totally replaced by **Flyash & Lime** in varying proportions, Cement used was Portland Pozzolana Cement (PPC), and Stone Aggregate used was 10 mm down .

Table 5.4 Compressive Strength test result for (Set-2, Group-A) 1:1.6:2.4 Concrete mix with Flyash & Lime

Sample identity	Concrete mix proportion – 1:1.6:2.4 with total sand elimination					Compressive Strength (MPa)		
	Cement	Flyash	Lime	Stone Aggregate	Water-Cement ratio	7 day's	28 day's	90 day's
E (67:33)	1.00	1.07	0.53	2.40	0.50	13.73	16.93	30.80
F (25:75)	1.00	0.40	1.20	2.40	0.50	11.87	15.40	25.73
G (50:50)	1.00	0.80	0.80	2.40	0.50	12.80	15.93	26.20
H (75:25)	1.00	1.20	0.40	2.40	0.50	11.47	13.93	21.67
K (100:0)	1.00	1.60	0.00	2.40	0.50	6.40	11.80	12.33

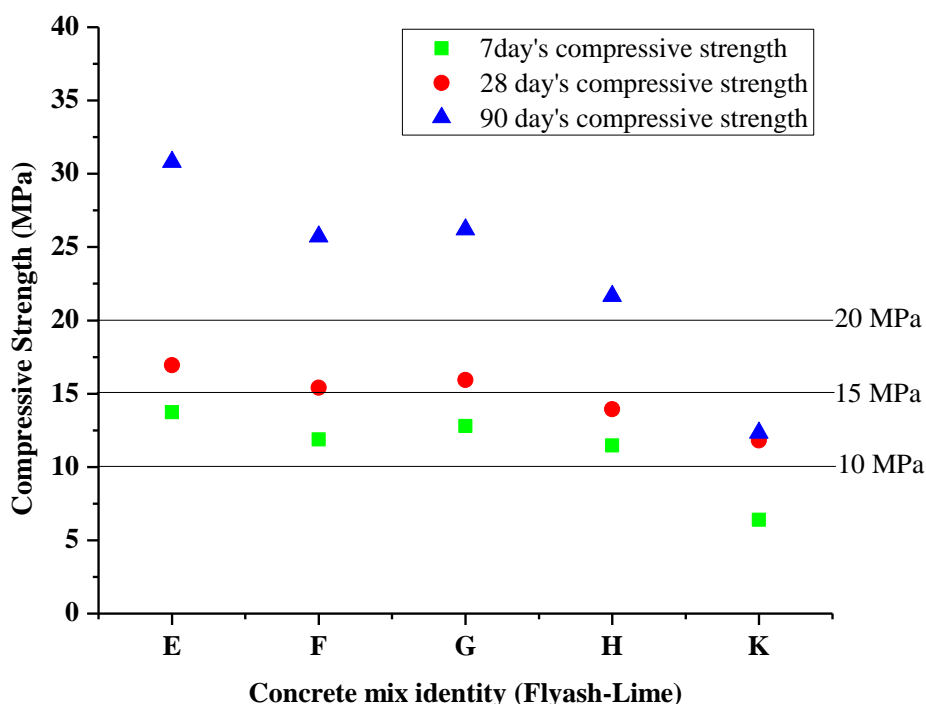


Fig. 5.6 Variation in Compressive Strength test results for (Set-2, Group-A) Concrete Mix with Flyash & Lime (Refer Table 5.4)

Observation : From the above figure, it is seen that compressive strength at 28 day's maturity is highest for E (67% Flyash+33% Lime) mix, and the other combinations like F (25% Flyash+75% Lime) and G (50% Flyash+50% Lime) are having strength >15 MPa value. At 90 day's maturity, the strength increased significantly in

comparison with 28 day’s strength for E,F,G and H samples, except for sample K (100% Flyash), where the increment is very marginal.

Table 5.5 Thermal Conductivity test results for (Set-2, Group-A) Concrete Mix with Flyash & Lime

Sample identity	Concrete mix proportion – 1:1.6:2.4 with total sand elimination					Thermal Conductivity (W/m.K)
	Cement	Flyash	Lime	Stone Aggregate	Water-Cement ratio	
E (67:33)	1.00	1.07	0.53	2.40	0.50	0.9214
F (25:75)	1.00	0.40	1.20	2.40	0.50	0.9863
G (50:50)	1.00	0.80	0.80	2.40	0.50	0.9787
H (75:25)	1.00	1.20	0.40	2.40	0.50	1.3040
K (100:0)	1.00	1.60	0.00	2.40	0.50	0.9045

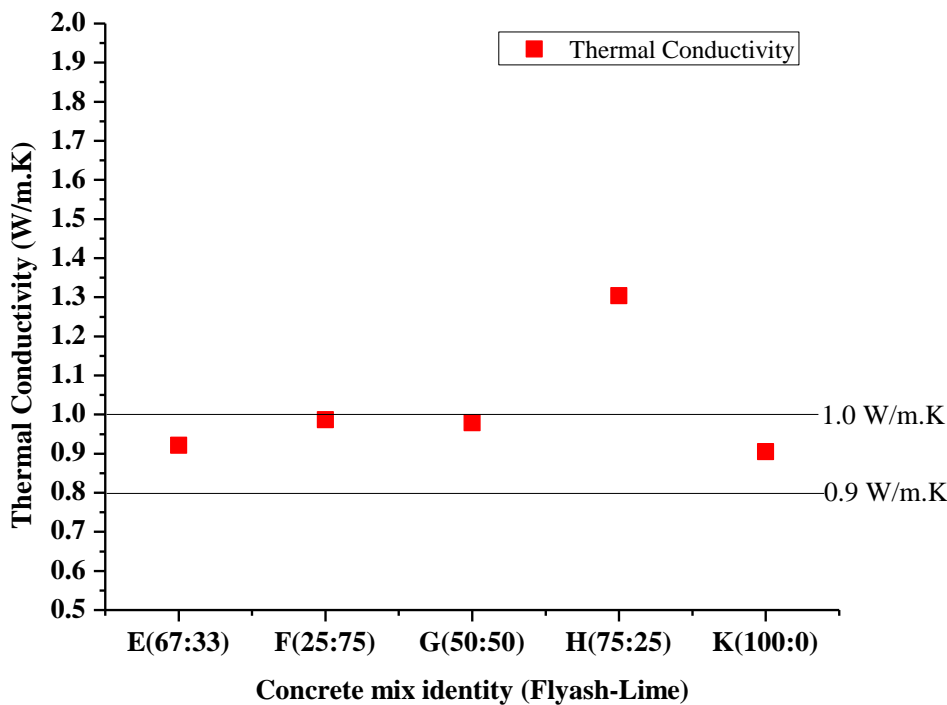


Fig. 5.7 Variation in Thermal Conductivity test results for (Set-2, Group-A) Concrete Mix with Flyash & Lime (Refer Table 5.5)

Observations : Thermal conductivity value is found to be lowest in the mix with 100% Flyash [K variety], and next one is with 67% Flyash +33% Lime combination mix (E variety). The highest value of conductivity is for H designated mix (75% Flyash + 25% Lime).

Table 5.6 Apparent Porosity and Bulk Density Test Results for (Set-2, Group-A) 1:1.6:2.4 Concrete Mix with Flyash and Lime

Concrete mix identity	Apparent Porosity (%)	Bulk Density (gm/cc)
E (67 Fa : 33 Lime)	30.875	1.930
F (75 Fa : 25 Lime)	32.675	1.840
G (50 Fa : 50 Lime)	32.520	1.855
H (25 Fa : 75 Lime)	38.200	1.635
K (100 Fa : 0 Lime)	38.800	1.595

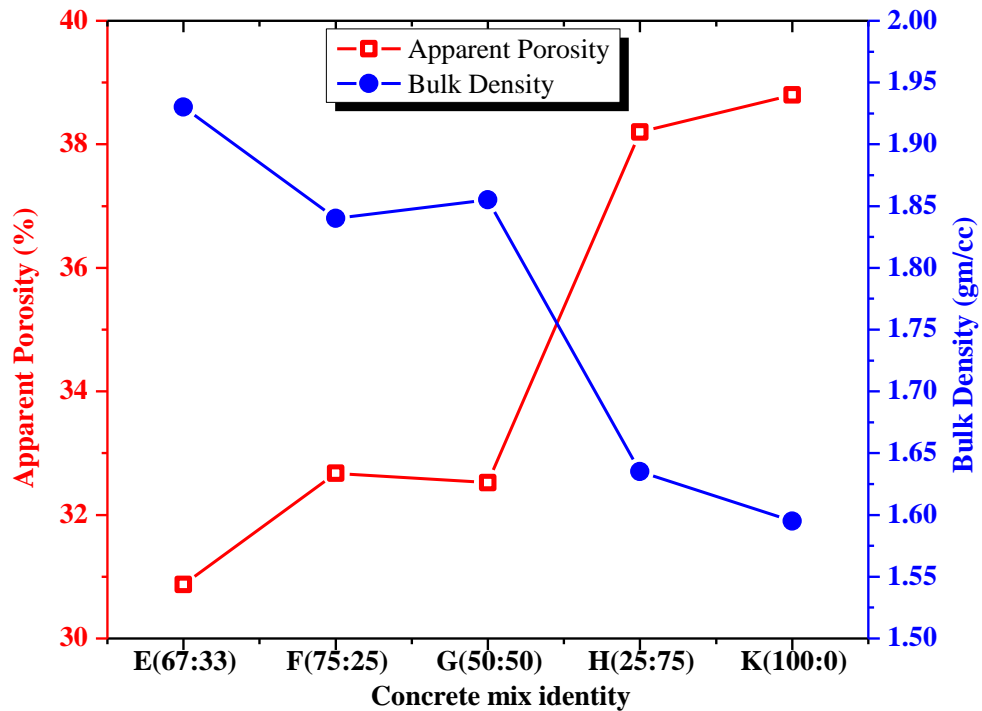


Fig. 5.8 Variation in Apparent Porosity and Bulk Density Test Results for (Set-2, Group-A) Concrete Mix with Flyash and Lime (Refer Table 5.6)

Observations : From the above curves of apparent porosity and bulk density of sand free samples, it may be seen that those parameters are inter-dependent, and these parameters are having direct bearing on strength parameters of the respective samples. The more is the strength, lower is the apparent porosity value.

5.3.3 Design Concrete Mix 1:1.6:2.4 (Set-3, Group-A) - Sand content totally replaced by (**Bottomash + Lime**) and (**Flyash+ Lime**) combinations in varying proportions, Cement used was Portland Pozzolana Cement (PPC), and Stone Aggregate used was 10 mm down .

Table 5.7 Compressive Strength values of (Set-3, Group-A) 1:1.6:2.4 Concrete mix

Sample identity	Mix proportion : 1:1.6:2.4 <u>Totally Sand less Concrete</u>						Compressive Strength (MPa)	
	Cement	Flyash	Bottomash	Lime	Stone Aggr.	Water Cement ratio	7 day's	28 day's
42(75:25)	1.00	-	1.20	0.40	2.40	0.50	11.76	19.03
41(67:33)	1.00	-	1.07	0.53	2.40	0.50	13.32	19.84
40(50:50)	1.00	-	0.80	0.80	2.40	0.50	11.82	17.19
39(75:25)	1.00	1.20	-	0.40	2.40	0.50	11.48	18.62
38(67:33)	1.00	1.07	-	0.53	2.40	0.50	11.62	18.89
37(50:50)	1.00	0.80	-	0.80	2.40	0.50	9.85	18.21

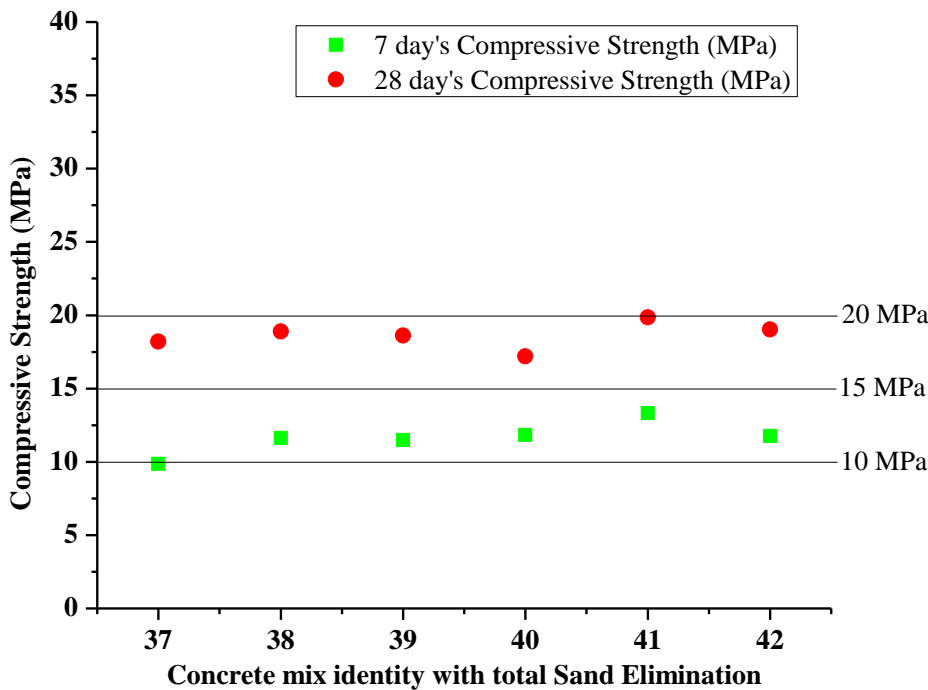


Fig.5.9 Variations in Compressive Strength values of (Set-3, Group-A) Concrete mix (Refer Table 5.7)

Observations : 28 day's compressive strength in respect of all the above concrete mix varieties more or less lies within 15 – 20 MPa region, with the highest value close to 20 MPa by mix variety 41(67% Bottomash + 33% Lime, in lieu of Sand), and the next highest value by mix variety 38 (67% Flyash + 33% Lime, in lieu of

Sand). The lowest values are by mix varieties 40 (100% Bottomash in place of Sand) and 37 (100% Flyash in place of Sand) respectively in the Concrete mix.

Table 5.8 Thermal Conductivity values of (Set-3, Group-A) 1:1.6:2.4 Concrete mix

Sample identity	Mix proportion : 1:1.6:2.4 Totally Sand less Concrete						Thermal Conductivity (W/m.K)
	Cement	Flyash	Bottomash	Lime	Stone Aggr.	Water Cement ratio	
42(75:25)	1.00	-	1.20	0.40	2.40	0.50	0.8948
41(67:33)	1.00	-	1.07	0.53	2.40	0.50	0.7317
40(50:50)	1.00	-	0.80	0.80	2.40	0.50	1.005
39(75:25)	1.00	1.20	-	0.40	2.40	0.50	0.9554
38(67:33)	1.00	1.07	-	0.53	2.40	0.50	0.8493
37(50:50)	1.00	0.80	-	0.80	2.40	0.50	0.9688

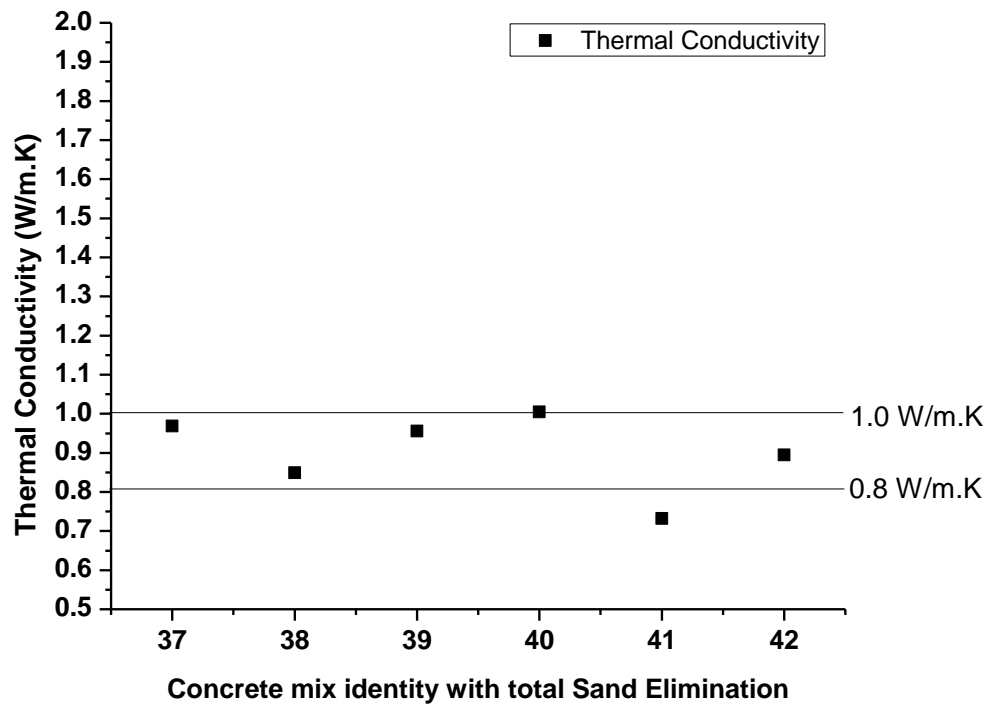


Fig.5.10 Variations in Thermal Conductivity values of (Set-3, Group-A) Concrete mix (Refer Table 5.8)

Observations : Minimum thermal conductivity value is found in respect of mix variety 41, and the same is followed by mix variety 38. On the other hand, the highest two values are occupied by mix varieties 40 and 39 respectively. The Bottomash- Lime and Flyash-Lime combination in lieu of sand in the proportions of 67:33 have produced results with lesser conductivity values respectively.

Table 5.9 Apparent Porosity and Bulk Density Test Results of (Set-3, Group-A) 1:1.6:2.4 Concrete mix

Concrete mix identity	Apparent Porosity (%)	Bulk Density (gm/cc)
42 (75 Ba : 25 Lime)	25.875	2.130
41 (67 Ba : 33 Lime)	25.105	2.195
40 (50 Ba : 50 Lime)	28.520	1.955
39 (75 Fa : 25 Lime)	26.500	2.035
38 (67 Fa : 33 Lime)	25.575	2.100
37 (50 Fa : 50 Lime)	26.100	1.985

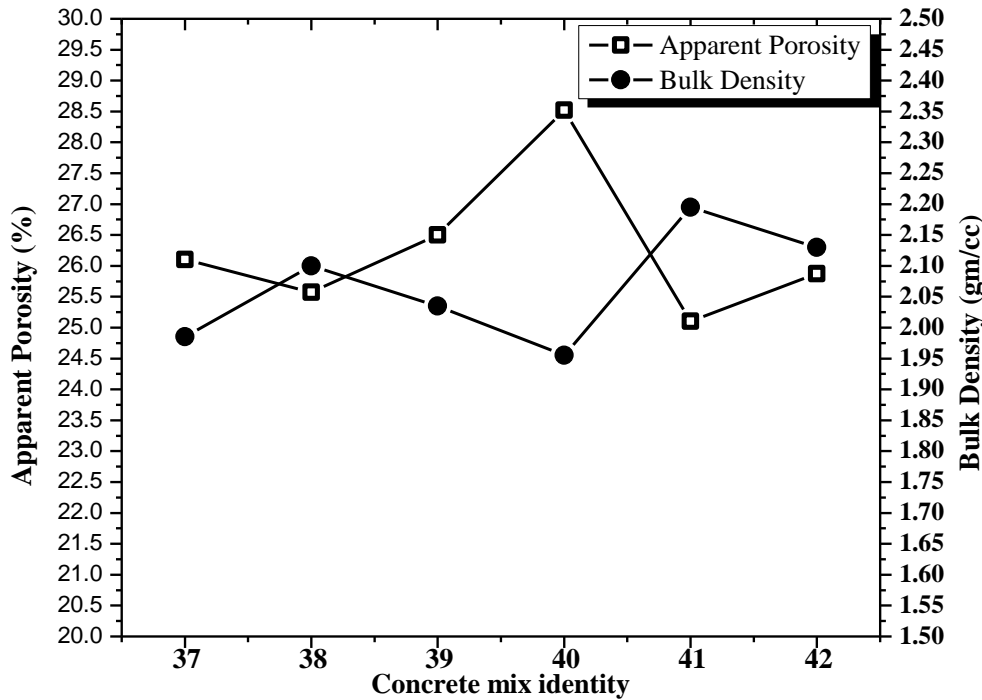


Fig. 5.11 Variations in Apparent Porosity and Bulk Density values of (Set-3, Group-A) 1:1.6:2.4 Concrete mix (Refer Table 5.9)

Observations : It may be observed that apparent porosity (AP) value against mix 42 is higher than that of mix 41. At the same time, bulk density (BD) value against mix 42 is lesser than that of mix 41. Again, AP value of mix 40 is higher than that of mix 39, and BD value of mix 40 is lower than that of mix 39. This trend is true for all the balance samples.

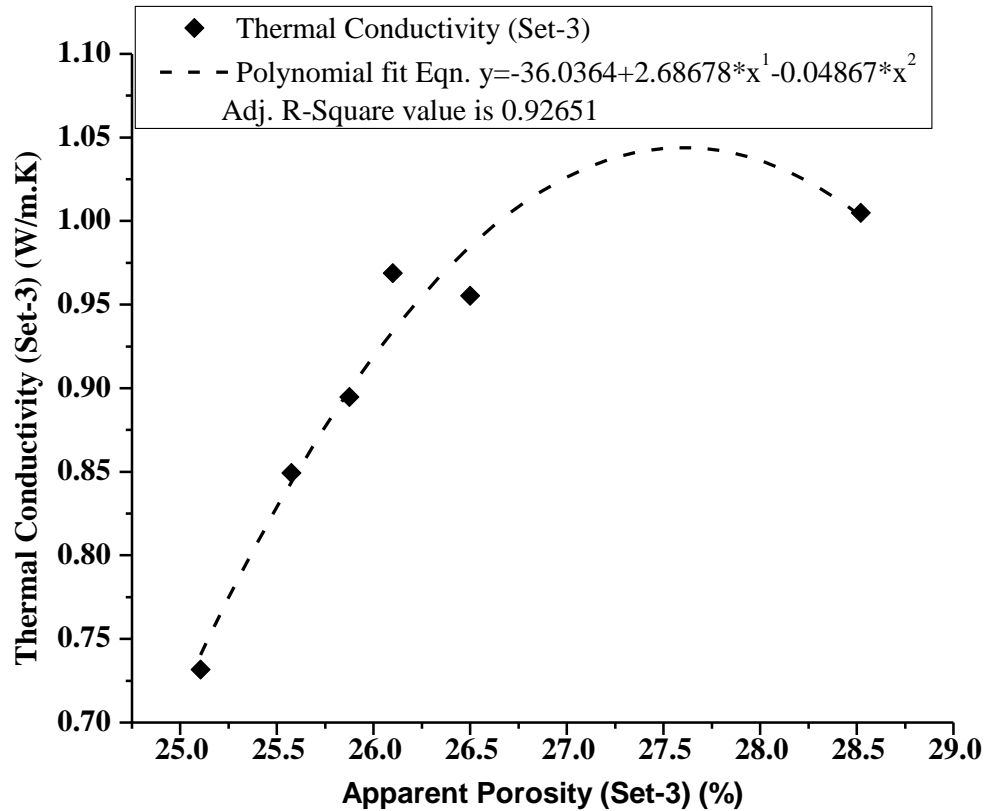


Fig. 5.12 Relationship between Apparent Porosity and Thermal Conductivity for the Concrete mix sample (Refer Table 5.8 and 5.9)

Observations : Apparent Porosity (AP) is shown to have a close relationship with thermal conductivity of the concrete mix sample, and the adjusted R^2 value of 0.93, (assessed the goodness-of-fit for regression analysis by Origin 8) supports the changes in both the parameters with respect to the mix proportions.

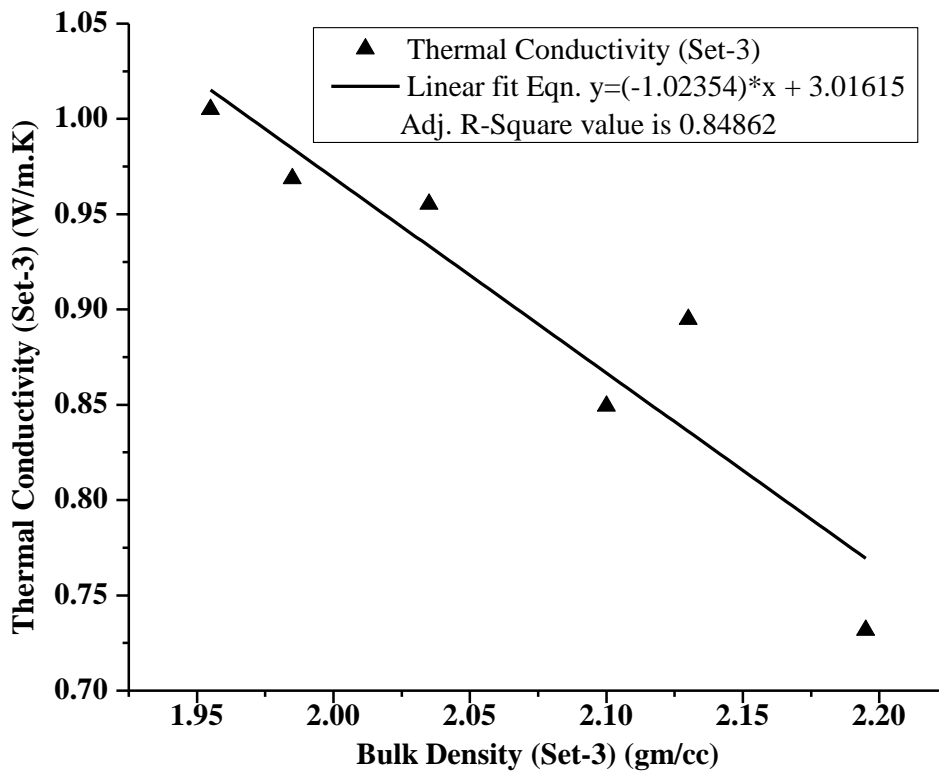


Fig. 5.13 Relationship between Bulk Density and Thermal Conductivity for the Concrete mix sample (Refer Table 5.8 and 5.9).

Observations : Bulk Density is shown to have an almost linear fit relationship with thermal conductivity of the concrete mix sample, and the adjusted R^2 value of 0.85, (assessed the goodness-of-fit for linear regression analysis by Origin 8) supports the same. The more is the bulk density, more is the thermal conductivity.

5.3.4 Design mix (1:1.6:2.4) (Set-4, Group-A) : Sand content replaced by **Bottomash** in 10% stages, Cement used was Portland Pozzolana Cement (PPC), and Stone Aggregate used was 10 mm down .

Table 5.10 Compressive Strength test result for (Set- 4, Group-A) 1:1.6:2.4 Concrete Mix with Bottomash

Concrete Identity	Mix	Concrete mix proportion – 1:1.6:2.4 Sand substitution by Bottomash				Compressive Strength (MPa)			
		Cement	Sand	Bottomash	Stone Aggregate	Water-Cement ratio	7 day's	28 day's	90 day's
SCC (100% Sand)		1.0	1.60	0.00	2.40	0.50	22.6	31.7	35.53
BCC-1 (90% Sand)		1.0	1.44	0.16	2.40	0.50	20.2	27.9	33.20
BCC-2 (80% Sand)		1.0	1.28	0.32	2.40	0.50	19.4	26.1	27.13
BCC-3 (70% Sand)		1.0	1.12	0.48	2.40	0.50	18.2	25.3	26.07
BCC-4 (60% Sand)		1.0	0.96	0.64	2.40	0.50	18.0	25.2	26.00
BCC-5 (50% Sand)		1.0	0.80	0.80	2.40	0.50	17.9	22.8	23.60
BCC-6 (40% Sand)		1.0	0.64	0.96	2.40	0.50	17.2	21.1	22.40
BCC-7 (30% Sand)		1.0	0.48	1.12	2.40	0.50	15.1	18.8	21.06
BCC-8 (20% Sand)		1.0	0.32	1.28	2.40	0.50	12.5	18.3	19.33
BCC-9 (10% Sand)		1.0	0.16	1.44	2.40	0.50	11.8	16.7	18.26
BCC-10 (0% Sand)		1.0	0.00	1.60	2.40	0.50	10.9	14.3	15.86

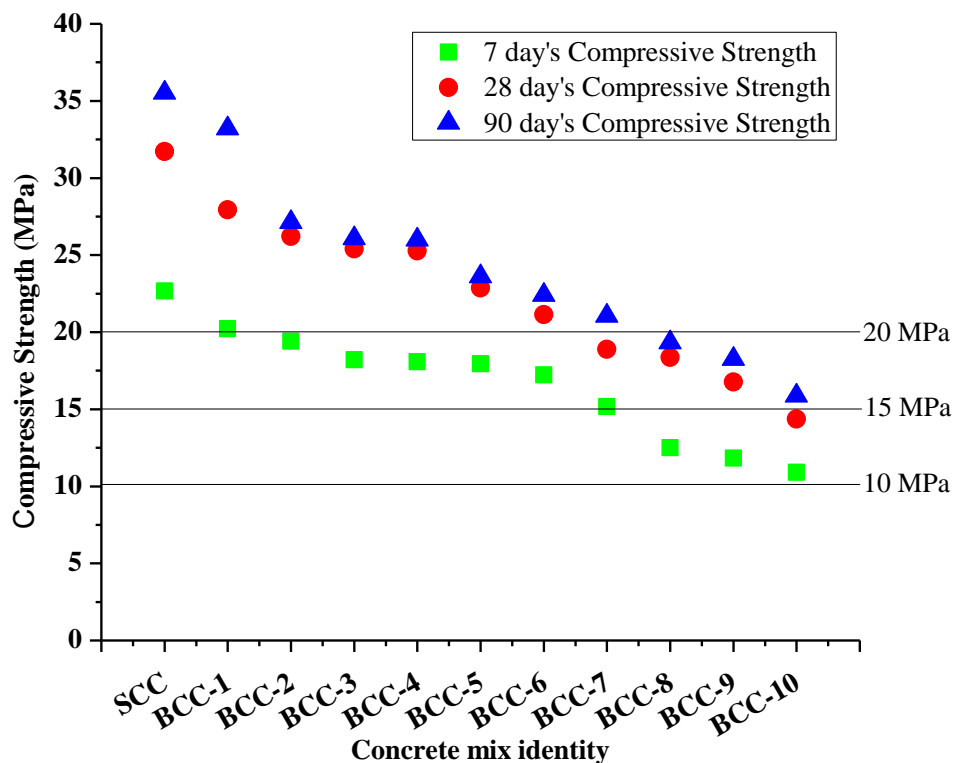


Fig. 5.14 Variations in Compressive Strength Test values of (Set-4, Group-A) Concrete mix (Refer Table 5.10)

Observations : It is observed that up to 50% sand replacement by Bottomash (mix H5) remain above 20 MPa range in 28 day’s maturity. From 60% to 90% replacement range, the strength falls within 20-15 MPa range. 90 day’s maturity follows closely the same trend by 28 day’s strength pattern by all the mixes, except on the higher side.

Table 5.11 Thermal Conductivity test results for (Set-4, Group-A) 1:1.6:2.4 Concrete mix with Bottomash

Sample identity	Thermal Conductivity (W/m.K)
SCC (100% Sand)	1.637
BCC-1 (90% Sand)	1.413
BCC-2 (80% Sand)	1.339
BCC-3 (70% Sand)	1.249
BCC-4 (60% Sand)	1.217
BCC-5 (50% Sand)	1.152
BCC-6 (40% Sand)	1.144
BCC-7 (30% Sand)	1.011
BCC-8 (20% Sand)	0.9837
BCC-9 (10% Sand)	0.8676
BCC-10 (0% Sand)	0.8169

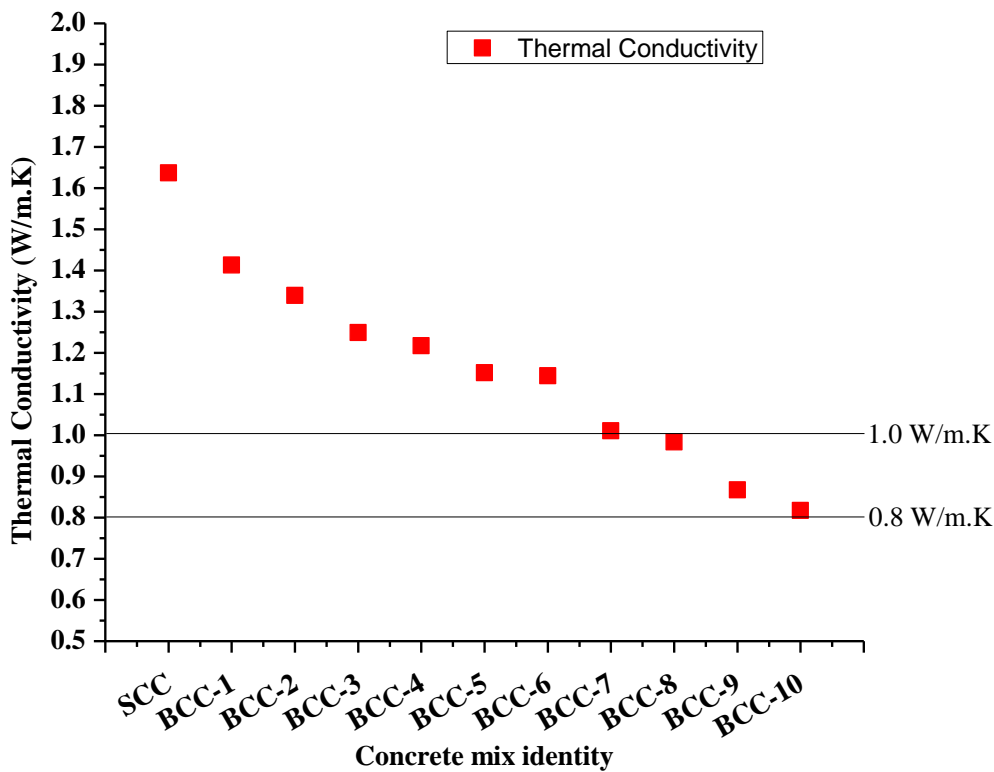


Fig. 5.15 Variation in Thermal Conductivity values for (Set-4, Group-A) Concrete mix with Bottomash (Refer Table 5.11).

Observations : It may be observed that there is a steady reduction in thermal conductivity value with the reduction in sand and replacement by Bottomash till 80% (up to mix H-8) with respect to the concrete mix with sand (mix HCC). Further reductions are observed in other two mixes.

Table 5.12 Apparent Porosity and Bulk Density test results for (Set-4, Group-A) 1:1.6:2.4 Concrete mix with Bottomash

Sample identity	Apparent Porosity (%)	Bulk Density (gm/cc)
SCC (100% Sand)	15.876	2.445
BCC-1 (90% Sand)	18.286	2.386
BCC-2 (80% Sand)	19.522	2.315
BCC-3 (70% Sand)	19.89	2.208
BCC-4 (60% Sand)	19.997	2.2
BCC-5 (50% Sand)	20.124	2.188
BCC-6 (40% Sand)	21.566	2.044
BCC-7 (30% Sand)	24.568	1.978
BCC-8 (20% Sand)	25.877	1.932
BCC-9 (10% Sand)	37.155	1.68
BCC-10 (0% Sand)	37.675	1.655

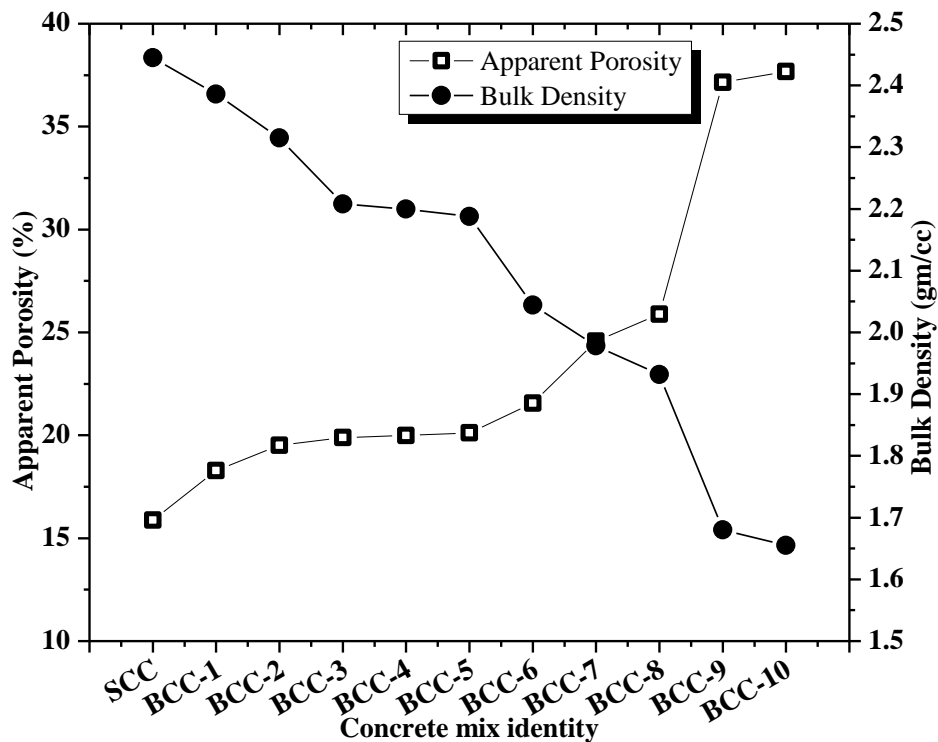


Fig. 5.16 Variations in Apparent Porosity and Bulk Density test results for (Set-4, Group-A) Concrete mix with Bottomash (Refer Table 5.12).

Observations : The trend of increasing apparent porosity and decreasing bulk density values with respect to sand substitution by Bottomash is established in clear

terms. Moreover, the higher thermal conductivity value and compressive strength values correspond to higher bulk density and lower apparent porosity values respectively.

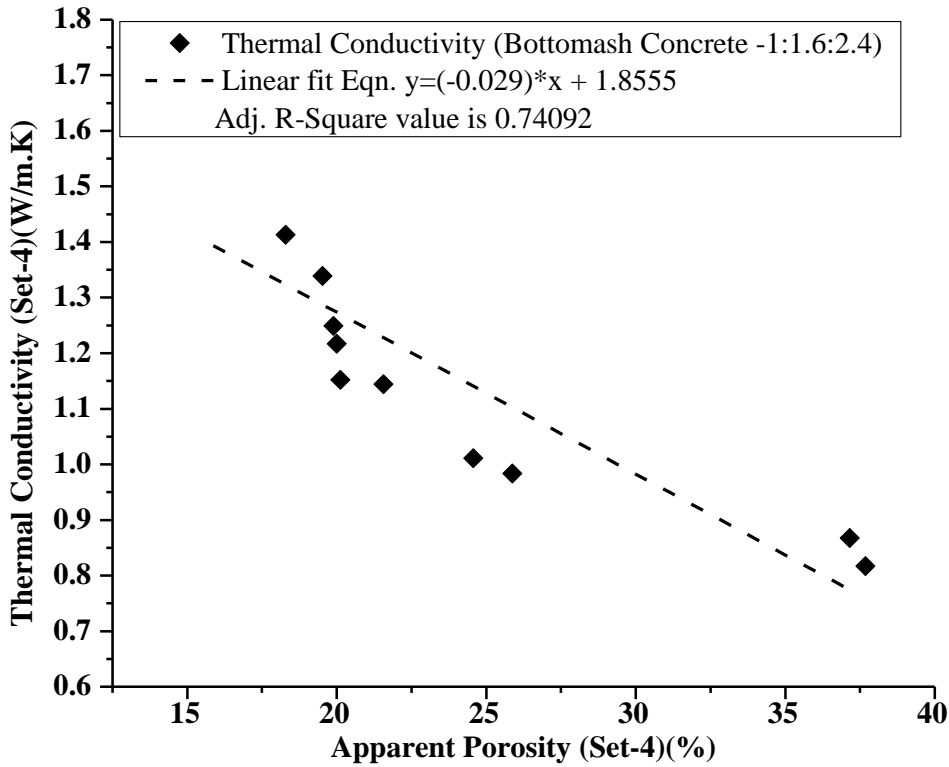


Fig. 5.17 Relationship between Apparent Porosity and Thermal Conductivity for the Concrete mix sample (Refer Table 5.11 and 5.12)

Observations : Apparent Porosity (AP) is shown to have a close relationship with thermal conductivity of the concrete mix sample, and the adjusted R^2 value of 0.74, (assessed the goodness-of-fit for regression analysis by Origin 8) supports the changes in both the parameters with respect to the mix proportions.

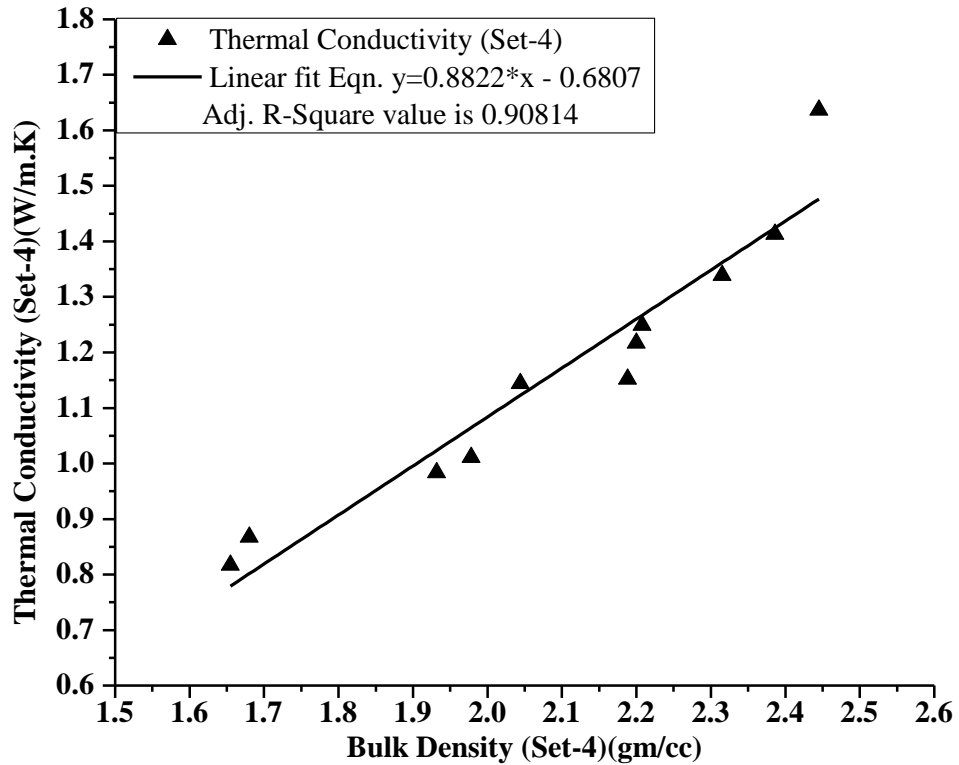


Fig. 5.18 Relationship between Bulk Density and Thermal Conductivity for the Concrete mix sample (Refer Table 5.11 and 5.12).

Observations : Bulk Density is shown to have an almost linear fit relationship with thermal conductivity of the concrete mix sample, and the adjusted R^2 value of 0.91, (assessed the goodness-of-fit for linear regression analysis by Origin 8) supports the same. The more is the bulk density, more is the thermal conductivity.

5.3.5 Design mix (1:1.6:2.4) (Set-5, Group-A) :

Comparison while Sand content replaced by Bottomash and Flyash in 10% stages from initial 100%, Cement used was Portland Pozzolana Cement (PPC), and Stone Aggregate used was 10 mm down

In this case, the same concrete mix proportion was followed for Bottomash and Flyash induced substitution of sand, and to compare side by side the strength gain/loss effects. In the nomenclature, mix 63 is the conventional concrete mmix with sand, mix 62 is the mix with Bottomash to the tune of 10%, replacing sand, and mix 52 side by side is the mix with Flyash of identical feature like Bottomash induced mix. Similarly mix 61 with 20% Bottomash and mix 51 is with 20% Flyash, and so on.

Table 5.13 Concrete mix identity and composition with Sand/Flyash/Bottomash (Set-5, Group-A)

Mix identity	Cement	Sand	Flyash	Bottomash	Stone Aggregate	Water-Cement
CC	1	1.60	-	-	2.40	0.50
BC-1	1	1.44	-	0.16	2.40	0.50
BC-2	1	1.28	-	0.32	2.40	0.50
BC-3	1	1.12	-	0.48	2.40	0.50
BC-4	1	0.96	-	0.64	2.40	0.50
BC-5	1	0.80	-	0.80	2.40	0.50
BC-6	1	0.64	-	0.96	2.40	0.50
BC-7	1	0.48	-	1.12	2.40	0.50
BC-8	1	0.32	-	1.28	2.40	0.50
BC-9	1	0.16	-	1.44	2.40	0.50
BC-10	1	0.00	-	1.60	2.40	0.50
FC-1	1	1.44	0.16	-	2.40	0.50
FC-2	1	1.28	0.32	-	2.40	0.50
FC-3	1	1.12	0.48	-	2.40	0.50
FC-4	1	0.96	0.64	-	2.40	0.50
FC-5	1	0.80	0.80	-	2.40	0.50
FC-6	1	0.64	0.96	-	2.40	0.50
FC-7	1	0.48	1.12	-	2.40	0.50
FC-8	1	0.32	1.28	-	2.40	0.50
FC-9	1	0.16	1.44	-	2.40	0.50
FC-10	1	0.00	1.60	-	2.40	0.50

Table 5.13(a) Compressive Strength test results for (Set-5, Group-A) Concrete mix with Sand / Bottomash / Flyash

Concrete Mix identity	Compressive Strength (MPa)					
	Conventional Concrete		Bottomash Concrete		Flyash Concrete	
	7 day's	28 day's	7 day's	28 day's	7 day's	28 day's
CC	27.18	35.88	-	-	-	-
BC-1/FC-1	-	-	25.76	30.85	26.03	33.98
BC-2/FC-2	-	-	22.22	29.9	20.05	30.31
BC-3/FC-3	-	-	19.71	27.05	18.62	29.22
BC-4/FC-4	-	-	19.03	26.57	16.17	23.11
BC-5/FC-5	-	-	18.42	23.85	14.88	22.29
BC-6/FC-6	-	-	18.28	23.17	12.71	20.12
BC-7/FC-7	-	-	17.87	23.105	12.1	17.67
BC-8/FC-8	-	-	16.85	21.54	10.125	17.67
BC-9/FC-9	-	-	15.15	17.47	7.82	17.19
BC-10/FC-10	-	-	13.18	15.7	7.95	15.77

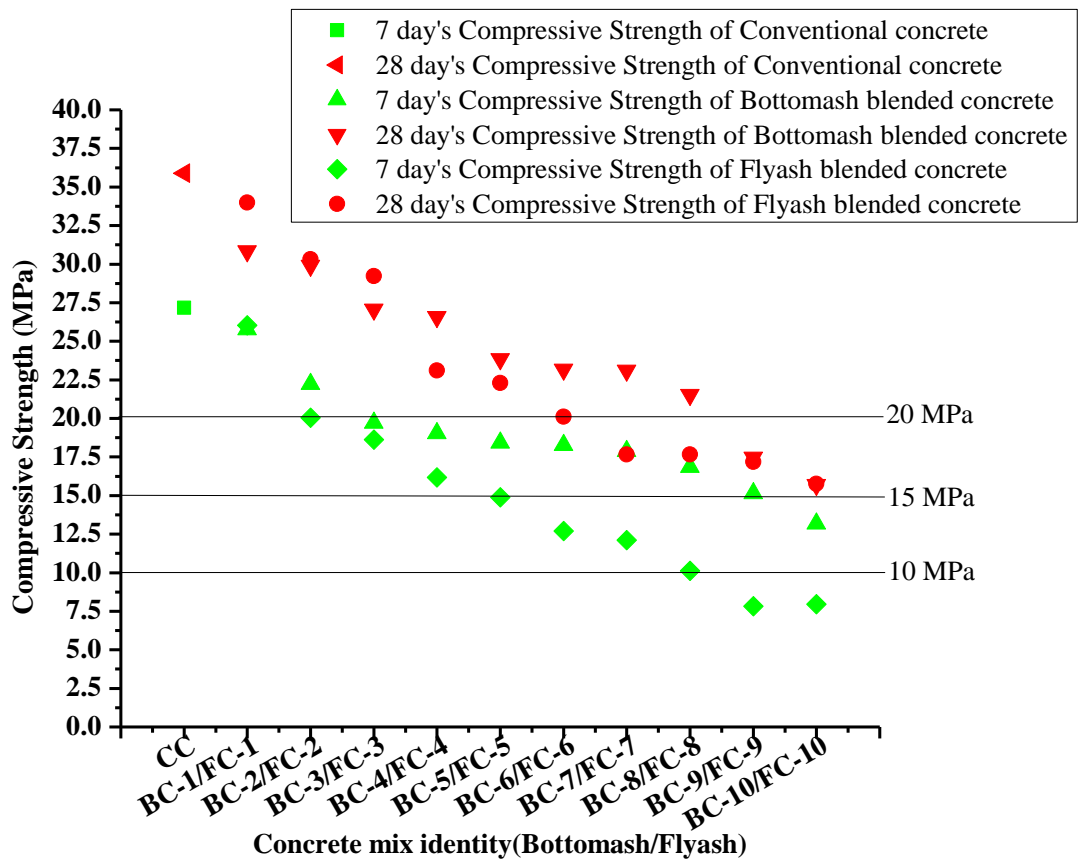


Fig. 5.19 Variations in Compressive Strength of (Set-5, Group-A) Concrete mix (Refer Table 5.13(a))

Observations : By observing the 28 day's compressive strength pattern of Bottomash blended concrete and Flyash blended concrete, it may be concluded that up to 30% replacement of sand by Flyash (mixes FC-1 to 3), the results are the

higher ones than the corresponding mixes by Bottomash (mixes BC-1 to 3). Beyond 30%, and up to 80% replacement of sand by Flyash (mixes FC-4 to 8), the results are **lower** than the corresponding mixes by Bottomash (mixes BC-4 to 8). For 90% and 100% replacement by both Flyash and Bottomash, the 28 day's strength values are almost identical.

Table 5.14 Thermal Conductivity test results for (Set-5, Group-A) Concrete mix with Sand / Bottomash / Flyash

Concrete mix identity	Thermal Conductivity (W/m.K)		
	For Conventional mix with Sand	For mix with Bottomash	For mix with Flyash
CC	1.637	-	-
BC-1/FC-1	-	1.2750	1.4070
BC-2/FC-2	-	1.1610	1.2880
BC-3/FC-3	-	1.0440	1.0060
BC-4/FC-4	-	0.9470	0.9770
BC-5/FC-5	-	0.9372	0.9730
BC-6/FC-6	-	0.9186	0.9601
BC-7/FC-7	-	0.8312	0.9180
BC-8/FC-8	-	0.8272	0.8480
BC-9/FC-9	-	0.7731	0.7907
BC-10/FC-10	-	0.6669	0.7389

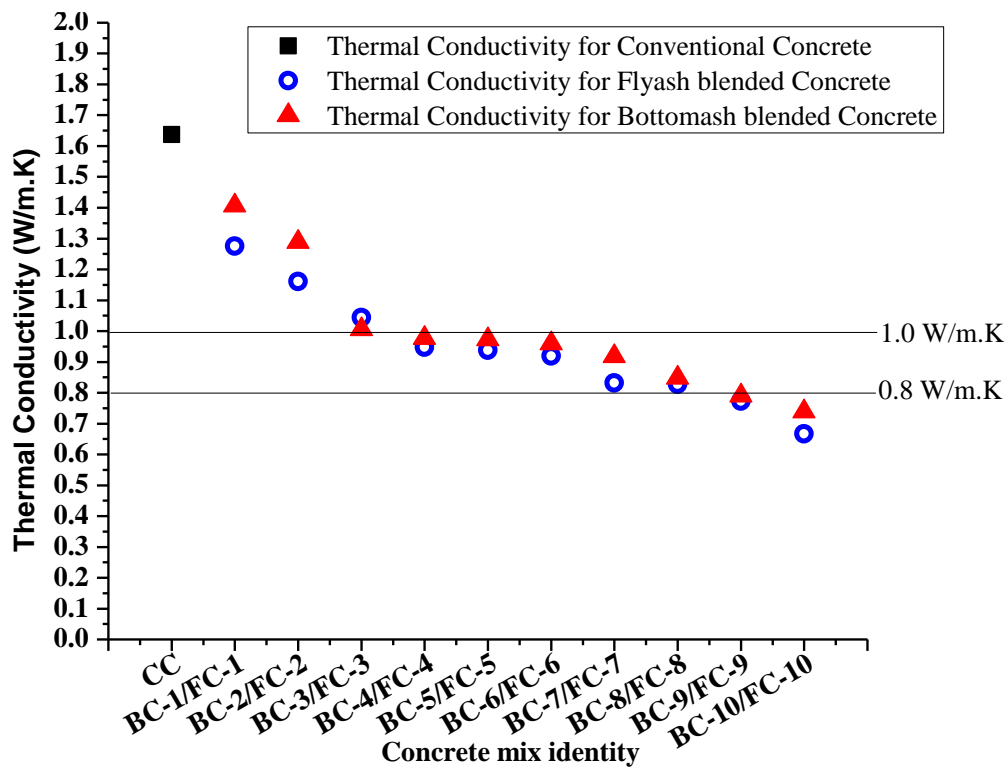


Fig. 5.20 Variations in Thermal Conductivity values for (Set-5, Group-A) Concrete mix with Bottomash and Flyash (Refer Table 5.14)

Observations : It may be observed that Bottomash blended concrete showed lesser thermal conductivity value than that by Flyash blended concrete. At 30% replacement ratio, both the blended mix conductivity values are almost identical.

Table 5.15 Apparent Porosity and Bulk Density Test Results of (Set-5, Group-A) 1:1.6:2.4 Concrete mix

Concrete mix identity	Conventional Concrete		Bottomash Concrete		Flyash Concrete	
	Apparent Porosity (%)	Bulk Density (gm/cc)	Apparent Porosity (%)	Bulk Density (gm/cc)	Apparent Porosity (%)	Bulk Density (gm/cc)
CC	10.656	2.443				
BC-1/FC-			17.522	2.23	18.286	2.386
BC-2/FC-			17.214	2.124	19.522	2.315
BC-3/FC-			19.080	1.989	19.89	2.208
BC-4/FC-			23.425	1.921	19.997	2.200
BC-5/FC-			23.867	1.917	20.124	2.188
BC-6/FC-			32.633	1.847	21.566	2.044
BC-7/FC-			37.575	1.656	24.568	1.978
BC-8/FC-			37.555	1.660	25.877	1.932
BC-9/FC-			38.012	1.648	37.155	1.68
BC10/FC1			40.002	1.580	37.675	1.655

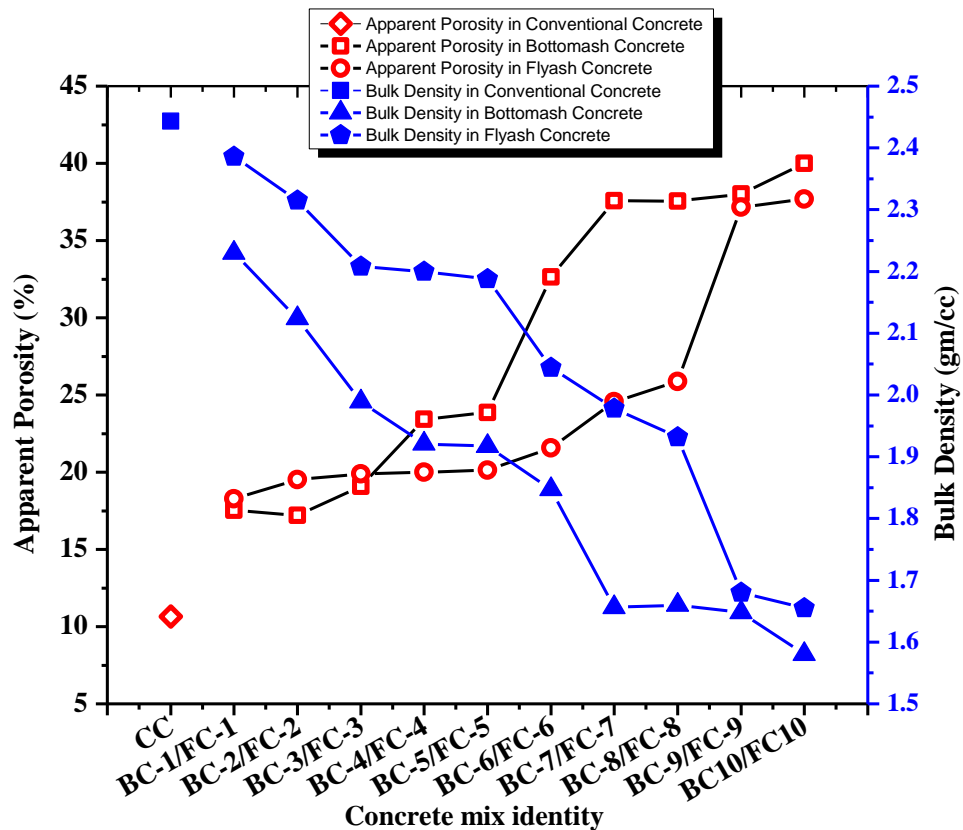


Fig.5.21 Variations in Apparent Porosity and Bulk Density values of (Set-5, Group-A) Concrete mix (Refer Table 5.15)

Observations : With the increasing replacement percentage of sand by Bottomash and Flyash in two sets of concrete mix, increasing trend in apparent porosity percentages and decreasing trend in bulk density values of such mix samples against sand substitution by respective ashes are observed from the plotted curves. Though the rate of change varies, but the trend is identical in both the Bottomash and Flyash related cases.

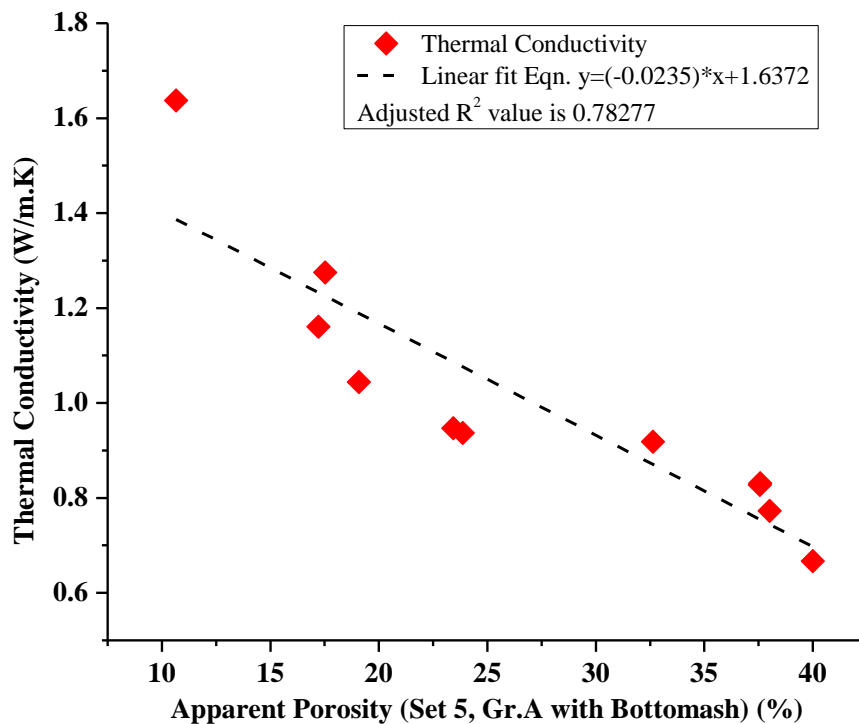


Fig. 5.22 Relationship between Apparent Porosity and Thermal Conductivity for the Concrete mix sample with BA (Refer Table 5.14 and 5.15)

Observations : Apparent Porosity (AP) is shown to have a close relationship with thermal conductivity of the concrete mix sample, and the adjusted R^2 value of 0.78, (assessed the goodness-of-fit for regression analysis by Origin 8) supports the changes in both the parameters with respect to the mix proportions.

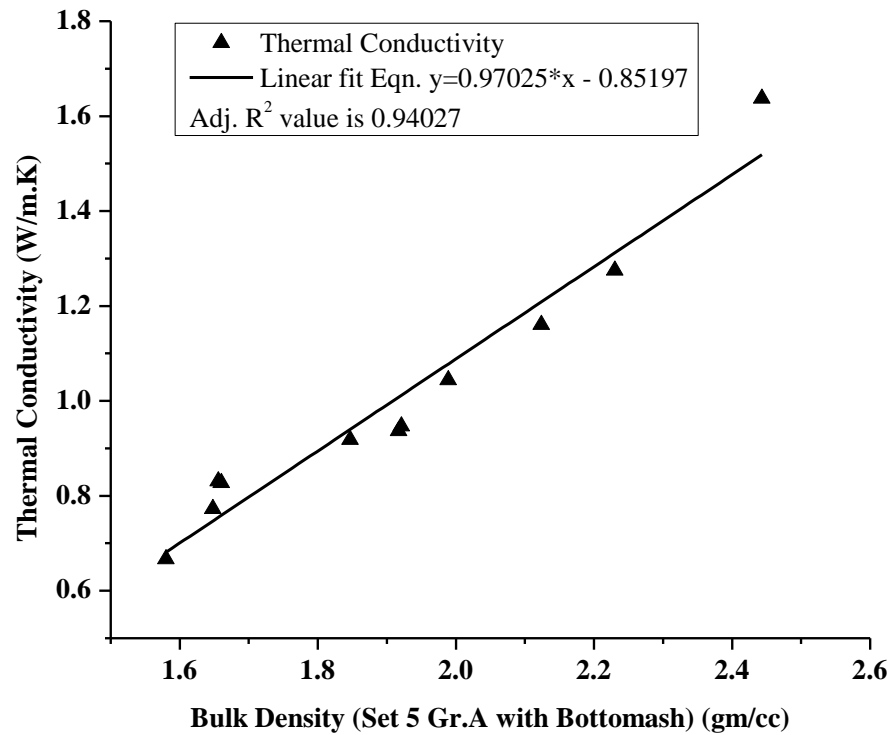


Fig. 5.23 Relationship between Bulk Density and Thermal Conductivity for the Concrete mix sample with BA (Refer Table 5.14 and 5.15).

Observations : Bulk Density is shown to have an almost linear fit relationship with thermal conductivity of the concrete mix sample, and the adjusted R² value of 0.94, (assessed the excellence-of-fit for linear regression analysis by Origin 8) supports the same. The more is the bulk density, more is the thermal conductivity.

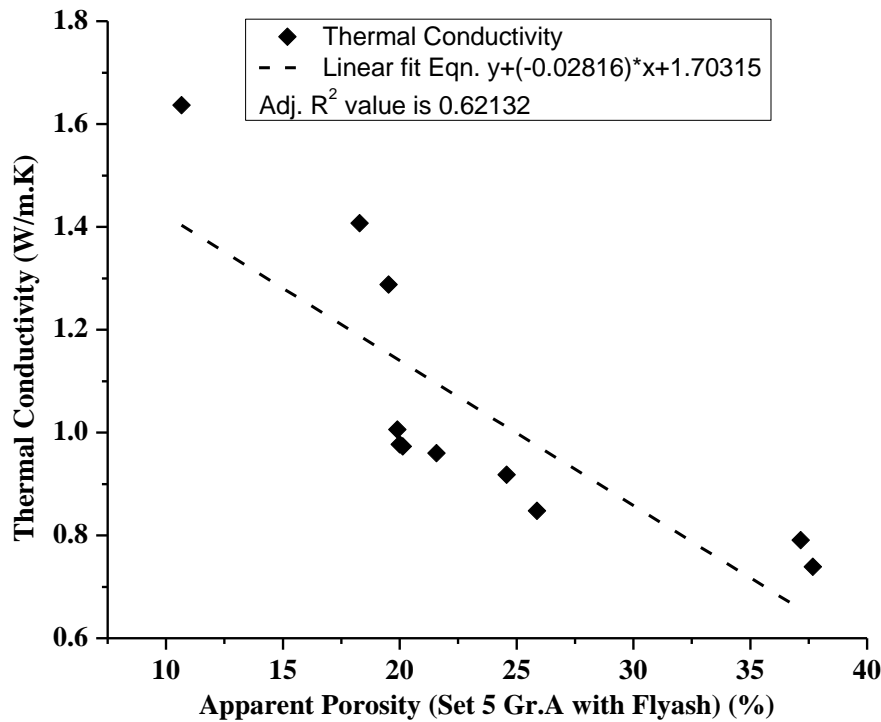


Fig. 5.24 Relationship between Apparent Porosity and Thermal Conductivity for the Concrete mix sample with FA(Refer Table 5.14 and 5.15)

Observations : Apparent Porosity (AP) is shown to have a close relationship with thermal conductivity of the concrete mix sample, and the adjusted R² value of 0.62, (assessed the fairness-of-fit for regression analysis by Origin 8) supports the changes in both the parameters with respect to the mix proportions.

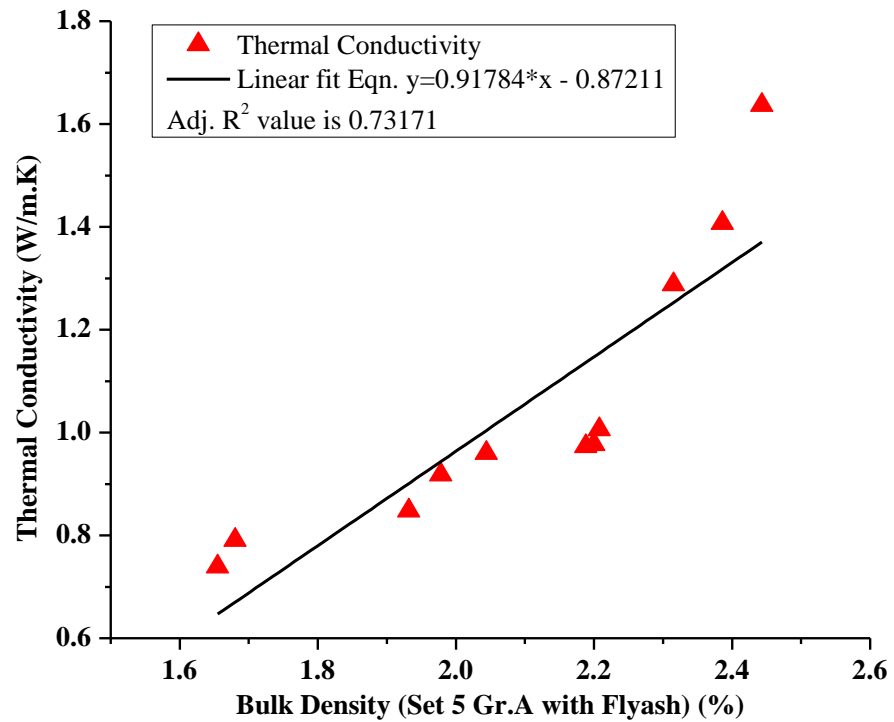


Fig. 5.25 Relationship between Bulk Density and Thermal Conductivity for the Concrete mix sample with FA (Refer Table 5.14 and 5.15).

Observations : Bulk Density is shown to have an almost linear fit relationship with thermal conductivity of the concrete mix sample, and the adjusted R^2 value of 0.73, (assessed the goodness-of-fit for linear regression analysis by Origin 8) supports the same. The more is the bulk density, more is the thermal conductivity.

5.3.6 Design mix (1:1.5:2.5) (Set-A, Group-B) : Sand content replaced by Bottomash in 10% stages, Cement used was PPC, and 10 mm down stone aggregate was used

Table 5.16 Compressive Strength test results for (Set-A, Group-B) 1:1.5:2.5 Concrete mix with Bottomash

Concrete Identity	Mix	Concrete mix proportion – 1:1.5:2.5 with Sand substitution in 10% stages					Compressive Strength (MPa)	
		Cement	Sand	Bottom ash	Stone Aggregate	Water-Cement ratio	7 day's	28 day's
MCC (100% Sand)		1.00	1.50	0.00	2.50	0.50	19.23	22.97
MM (67% Bottom ash & 33%lime)		1.00	0.00	1.00 + 0.50 L	2.50	0.50	19.16	25.01
M-1 (90% Sand)		1.00	1.35	0.15	2.50	0.50	19.1	22.49
M-2 (80% Sand)		1.00	1.20	0.30	2.50	0.50	17.26	21.88
M-3 (70% Sand)		1.00	1.05	0.45	2.50	0.50	15.56	19.98
M-4 (60% Sand)		1.00	0.90	0.60	2.50	0.50	14.54	18.62
M-5 (50% Sand)		1.00	0.75	0.75	2.50	0.50	10.19	18.14
M-6 (40% Sand)		1.00	0.60	0.90	2.50	0.50	9.65	16.04
M-7 (30% Sand)		1.00	0.45	1.05	2.50	0.50	8.7	15.15
M-8 (20% Sand)		1.00	0.30	1.20	2.50	0.50	10.06	13.32
M-9 (10% Sand)		1.00	0.15	1.35	2.50	0.50	8.22	11.62
M-10 (0% Sand)		1.00	0.00	1.50	2.50	0.50	7.2	9.65

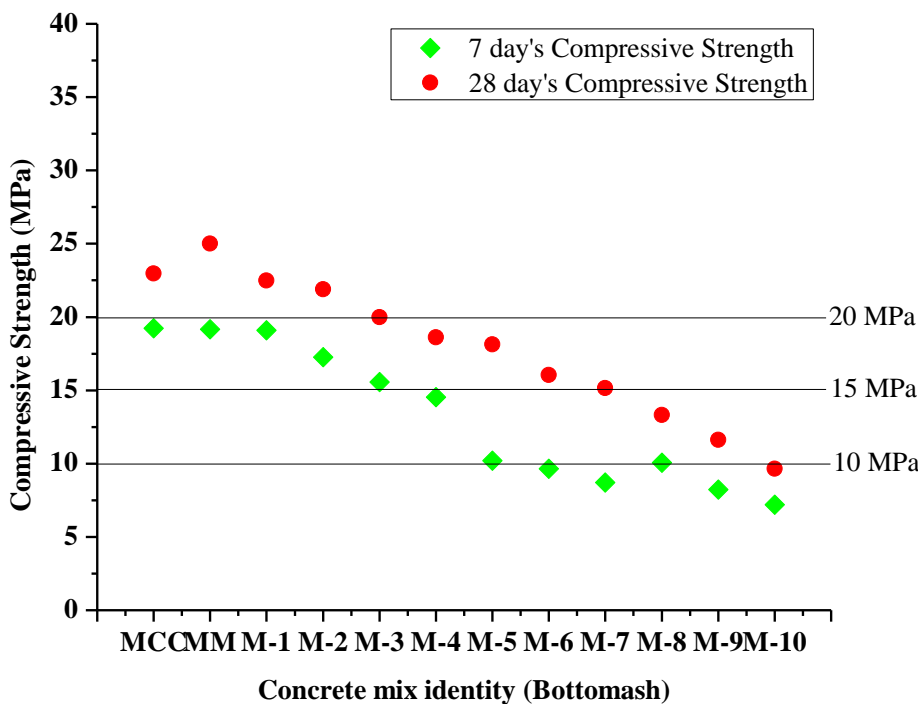


Fig.5.26 Variation in Compressive Strength for (Set-A, Group-B) Concrete mix with Bottomash (Refer Table 5.16)

Observations : Interestingly, it may be observed that Sand free mix (MM) shows higher 28 day’s compressive strength than the conventional mix with sand. Afterwards gradual declining trend is followed in all the mixes with sand replacement by Bottomash in 10% stages (mix MM1 to MM10).

Table 5.17 Thermal Conductivity test results for (Set-A, Group-B) 1:1.5:2.5 Concrete mix with Bottomash

Concrete Mix proportion with identity	Thermal Conductivity (W/m.K)
MCC (100% Sand)	1.446
MM (67% Bottom ash & 33%lime)	1.540
M-1 (90% Sand)	1.405
M-2 (80% Sand)	1.331
M-3 (70% Sand)	1.217
M-4 (60% Sand)	1.189
M-5 (50% Sand)	1.163
M-6 (40% Sand)	1.073
M-7 (30% Sand)	0.986
M-8 (20% Sand)	0.975
M-9 (10% Sand)	0.897
M-10 (0% Sand)	0.772

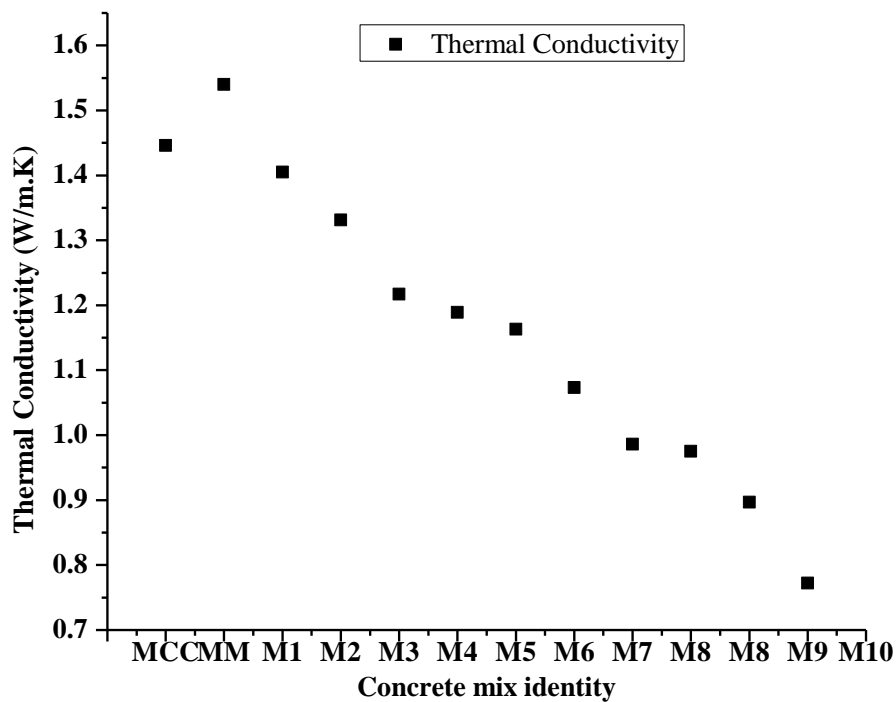


Fig.5.27 Variation in Thermal Conductivity values for (Set-A, Group-B) Concrete mix with Bottomash (Refer Table 5.17).

Observations : It may be observed that the highest conductivity value has been obtained for conventional mix with sand, and the mixes with gradual replacement of sand by bottomash found to be following declining trend. Even the mix with 67% bottomash and 33% Lime in lieu of sand is also found to possess lower conductivity value than that of conventional concrete mix value.

Table 5.18 Apparent Porosity and Bulk Density Test Results for (Set-A, Group-B) 1:1.5:2.5 Concrete mix

Sample identity	Apparent Porosity (%)	Bulk Density (gm/cc)
MCC (100% Sand)	20.100	2.285
MM (67% Bottomash+ 33% Lime)	16.250	2.365
M-1 (90% Sand)	20.300	2.240
M-2 (80% Sand)	22.500	2.150
M-3 (70% Sand)	24.650	2.105
M-4 (60% Sand)	25.100	2.100
M-5 (50% Sand)	29.350	1.988
M-6 (40% Sand)	29.950	1.850
M-7 (30% Sand)	30.125	1.805
M-8 (20% Sand)	32.045	1.755
M-9 (10% Sand)	34.125	1.640
M-10 (0% Sand)	35.2	1.595

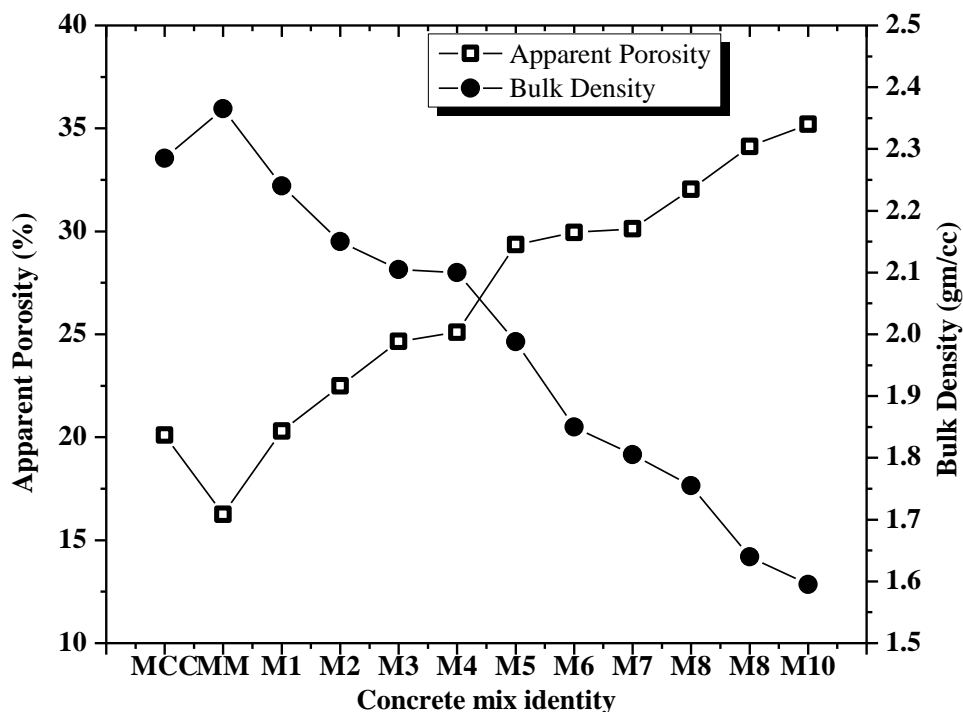


Fig. 5.28 Variations in Apparent Porosity and Bulk Density values of (Set-A, Group-B) Concrete mix (Refer Table 5.18).

Observations : For the concrete samples with identity MCC, M-1,...,M-10 are with decreasing sand content with matching substituted Bottomash content, except the sample identity MM, wherein total sand content is substituted by 67% Bottomash and 33% Lime. The apparent porosity had increased sharply, and then dropped further. Thereafter, it followed the continuous increasing trend. The bulk density values also followed the matching trend. Those are further corroborated by the compressive strength and thermal conductivity values respectively.

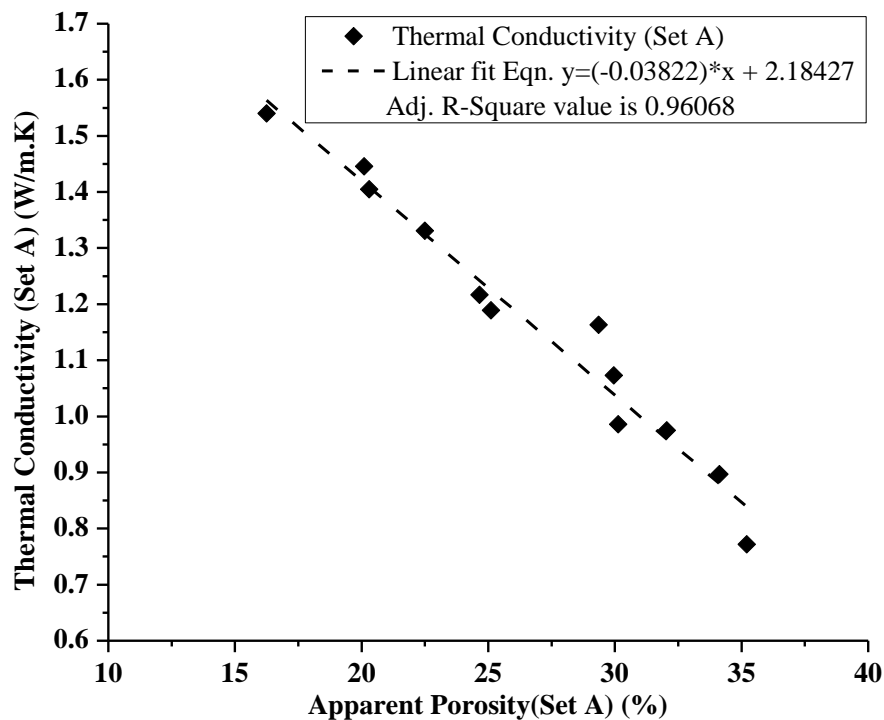


Fig. 5.29 Relationship between Apparent Porosity and Thermal Conductivity for the Concrete mix sample (Refer Table 5.17 and 5.18)

Observations : Apparent Porosity (AP) is shown to have a close relationship with thermal conductivity of the concrete mix sample, and the adjusted R^2 value of 0.96, (assessed the goodness-of-fit for regression analysis by Origin 8) supports the changes in both the parameters with respect to the mix proportions. The more is apparent porosity, less is the thermal conductivity.

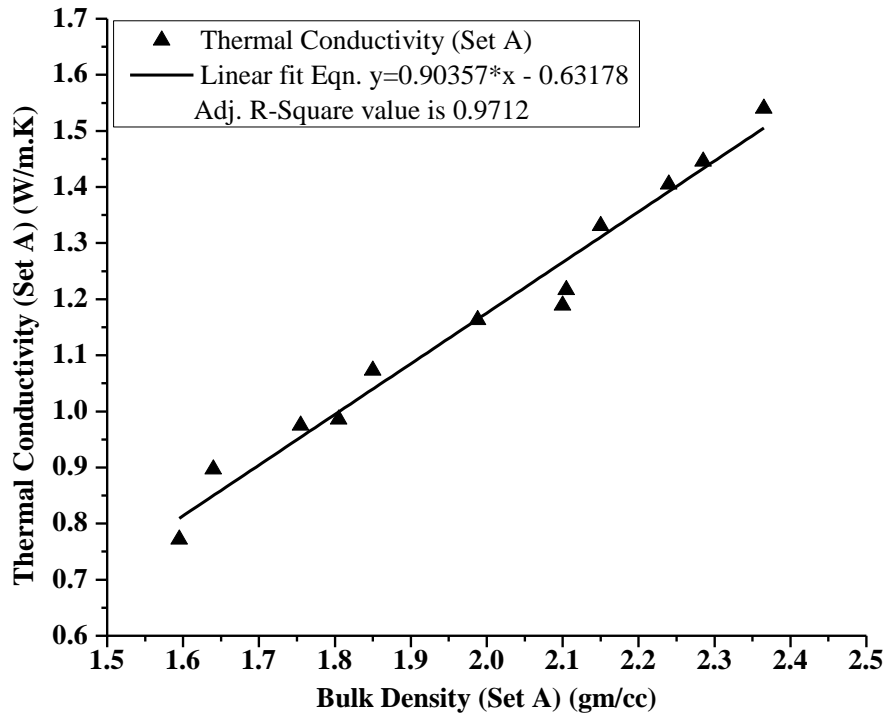


Fig. 5.30 Relationship between Bulk Density and Thermal Conductivity for the Concrete mix sample (Refer Table 5.17 and 5.18)

Observations : Bulk Density is shown to have an almost linear fit relationship with thermal conductivity of the concrete mix sample, and the adjusted R^2 value of 0.97, (assessed the goodness-of-fit for linear regression analysis by Origin 8) supports the same. The more is the bulk density, more is the thermal conductivity.

5.3.7 Design mix (1:1.62:2.78) (Set-B, Group-B): Sand content replaced by Bottom ash in 10% stages, Cement used was PPC and 10 mm down stone aggregate was used

Table 5.19 Compressive Strength test results of (Set-B, Group-B) 1:1.62:2.78 Concrete mix with Bottomash

Sample identity	Mix proportion (1:1.62:2.78)					Compressive Strength	
	Cement	Sand	Bottom ash	Stone Aggregate	Water-Cement ratio	7 day's (MPa)	28 day's (MPa)
B	1	1.620	0.000	2.78	0.5	20.66	34.11
B1	1	1.458	0.162	2.78	0.5	19.78	33.03
B2	1	1.296	0.324	2.78	0.5	18.42	31.4
B3	1	1.134	0.486	2.78	0.5	18.35	26.57
B4	1	0.972	0.648	2.78	0.5	18.08	25.01
B5	1	0.810	0.810	2.78	0.5	16.58	23.65
B6	1	0.648	0.972	2.78	0.5	14.54	21.47
B7	1	0.486	1.134	2.78	0.5	10.87	18.21
B8	1	0.324	1.296	2.78	0.5	10.6	18.21
B9	1	0.162	1.458	2.78	0.5	9.92	17.26
B10	1	0.000	1.620	2.78	0.5	9.31	16.44

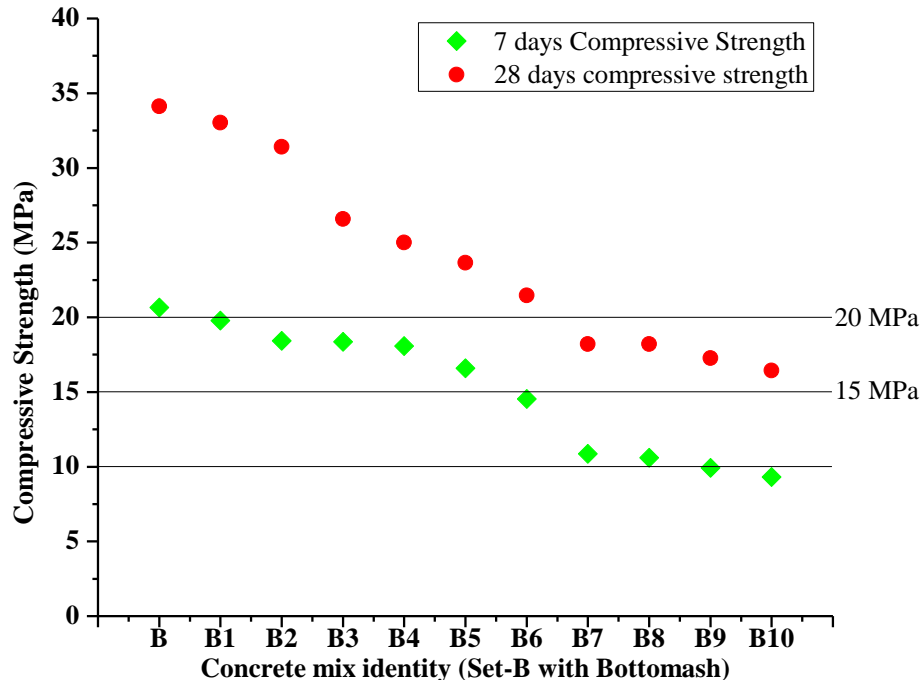


Fig.5.31 Variations in Compressive Strength values for (Set-B, Group-B) Concrete mix with Bottomash (Refer Table 5.19).

Observations : Up to 60% Sand replacement by Bottomash, the compressive strength attained more than 20 MPa at 28 day’s maturity, and from 70% - 100% replacement, the strength remains more than 15 MPa at the same maturity age.

Table 5.20 Thermal Conductivity test results for(Set-B, Group-B) 1:1.62:2.78 Concrete mix with Bottomash

Sample identity	Thermal Conductivity (W/m.K)
B	1.529
B1	1.519
B2	1.362
B3	1.327
B4	1.229
B5	1.108
B6	1.080
B7	0.970
B8	0.897
B9	0.827
B10	0.771

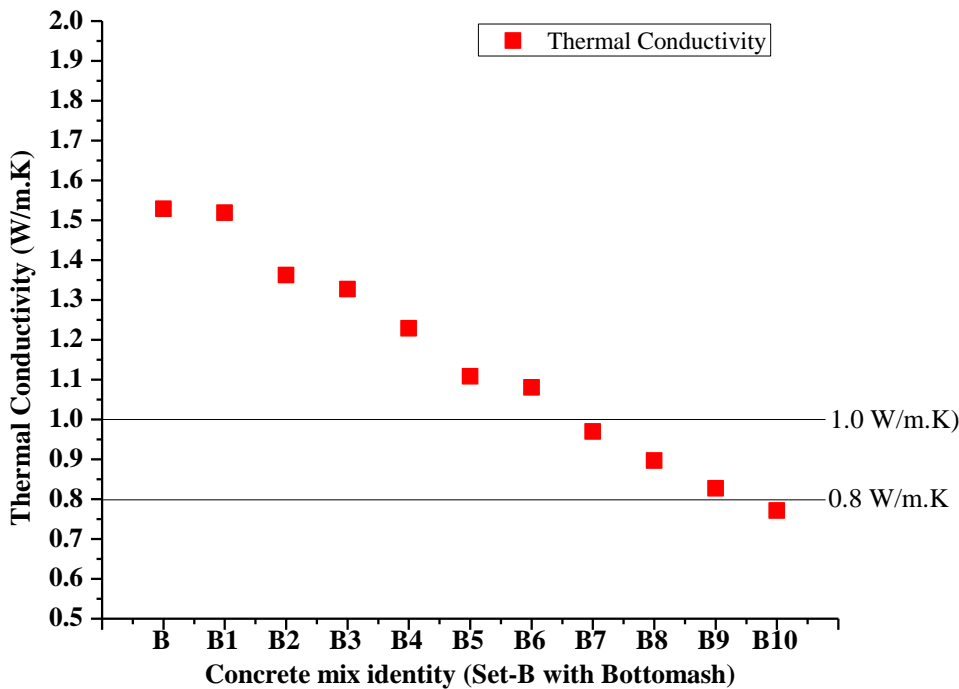


Fig. 5.32 Variations in Thermal Conductivity values for (Set-B, Group-B) Concrete mix with Bottomash (Refer Table 5.20)

Observations : Thermal conductivity values for all the substitution ratios declined steadily in comparison with conventional mix concrete.

Table 5.21 Apparent Porosity and Bulk Density test results for (Set-B, Group-B) 1:1.62:2.78 Concrete mix with Bottomash

Sample identity	Apparent Porosity(%)	Bulk Density (gm/cc)
B	10.400.	2.416
B1	13.043	2.409
B2	14.530	2.393
B3	16.379	2.388
B4	17.355	2.322
B5	17.699	2.319
B6	17.797	2.220
B7	18.421	2.210
B8	18.349	2.211
B9	21.698	2.123
B10	24.348	1.983

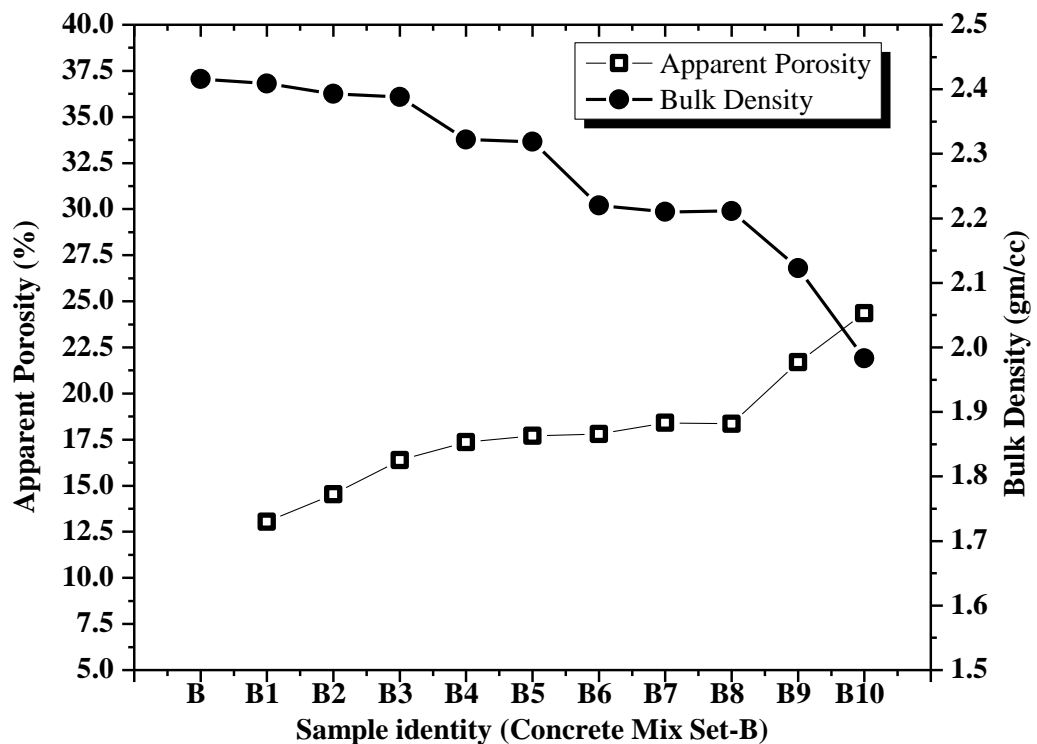


Fig. 5.33 Variations in Apparent Porosity and Bulk Density values for (Set-B, Group-B) Concrete mix with Bottomash.(Refer Table 5.21)

Observations : The apparent porosity value increases and the corresponding bulk density value decreases in the concrete mix with gradual sand reduction, and corresponding substitution by equivalent amount of Bottomash.

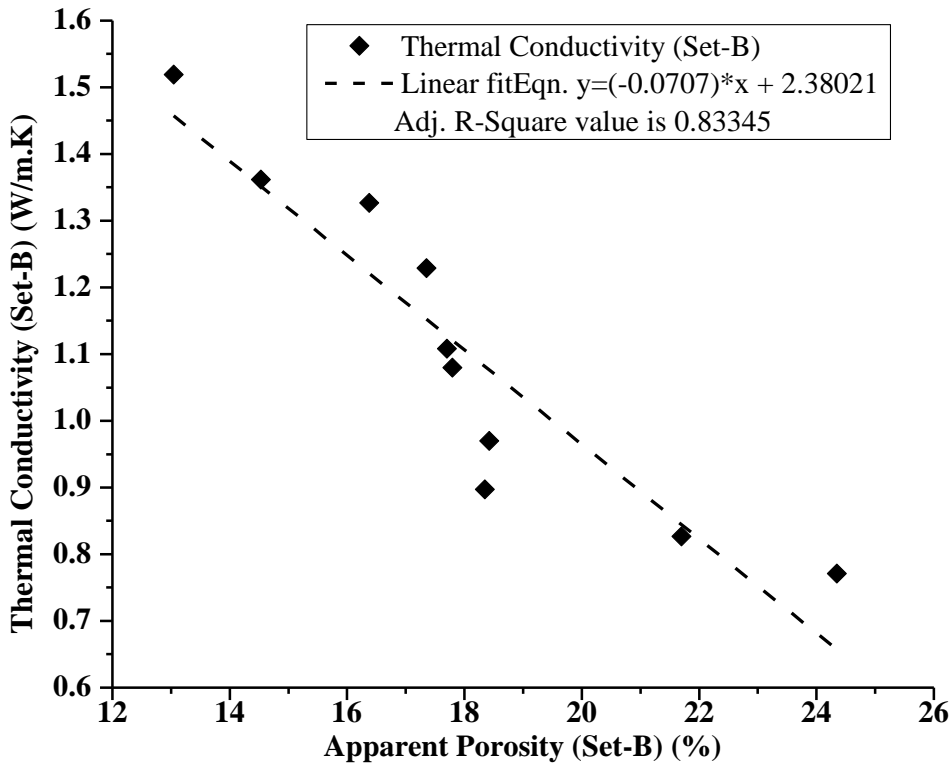


Fig. 5.34 Relationship between Apparent Porosity and Thermal Conductivity for the Concrete mix sample (Refer Table 5.20 and 5.21)

Observations : Apparent Porosity (AP) is shown to have a close relationship with thermal conductivity of the concrete mix sample, and the adjusted R^2 value of 0.83, (assessed the goodness-of-fit for regression analysis by Origin 8) supports the changes in both the parameters with respect to the mix proportions. The more is apparent porosity, less is the thermal conductivity.

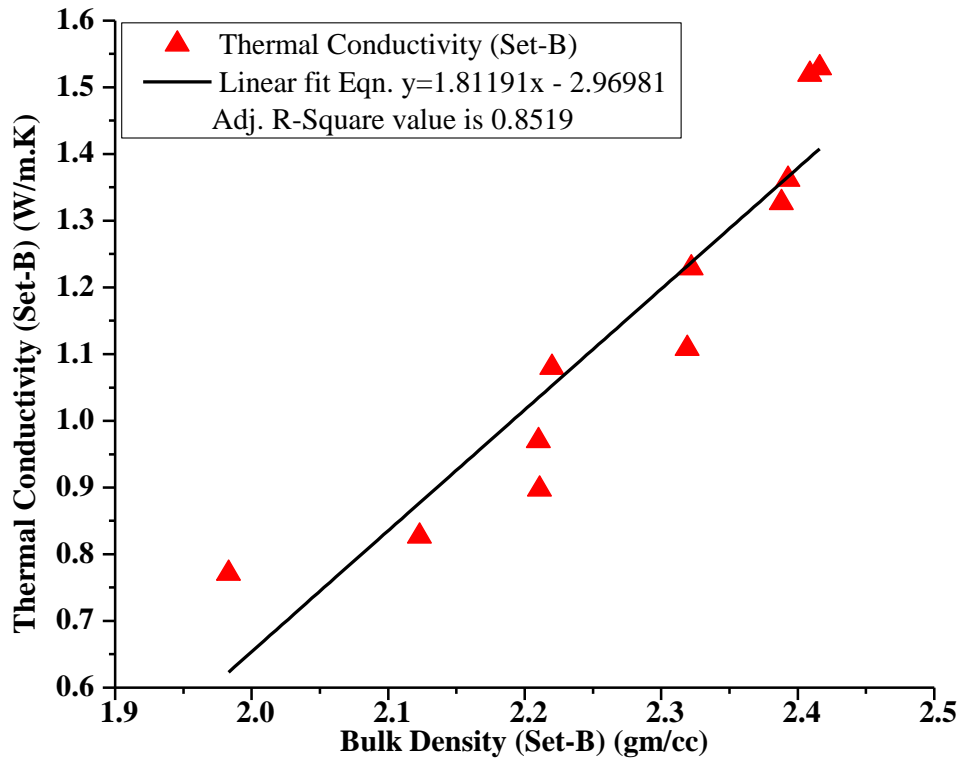


Fig. 5.35 Relationship between Bulk Density and Thermal Conductivity for the Concrete mix sample (Refer Table 5.20 and 5.21)

Observations : Bulk Density is shown to have a linear fit relationship with thermal conductivity of the concrete mix sample, and the adjusted R^2 value of 0.85, (assessed the goodness-of-fit for linear regression analysis by Origin 8) supports the same. The more is the bulk density, more is the thermal conductivity.

5.3.8 Design mix (1:2.4:3.6) (Set-C, Group-B) : Sand content replaced by Bottomash in 10% stages, Cement used was PPC and 10 mm down stone aggregate was used

Table 5.22 Compressive Strength test results for (Set-C, Group-B) 1:2.4:3.6 Concrete mix with Bottomash

Sample identity	Mix proportion (1 : 2.40 : 3.60)					Compressive Strength (MPa)	
	Cement	Sand	Bottom ash	Stone Aggregate	Water-Cement	7 day's	28 day's
C	1.0	2.400	0.000	3.60	0.50	18.42	33.03
C1	1.0	2.160	0.240	3.60	0.50	16.99	31.53
C2	1.0	1.920	0.480	3.60	0.50	16.72	30.31
C3	1.0	1.680	0.720	3.60	0.50	16.72	27.73
C4	1.0	1.440	0.960	3.60	0.50	16.58	25.28
C5	1.0	1.200	1.200	3.60	0.50	11.69	17.13
C6	1.0	0.960	1.440	3.60	0.50	10.06	16.65
C7	1.0	0.720	1.680	3.60	0.50	10.06	15.90
C8	1.0	0.480	1.920	3.60	0.50	9.04	14.34
C9	1.0	0.240	2.160	3.60	0.50	6.80	11.96
C10	1.0	0.000	2.400	3.60	0.50	5.50	9.24

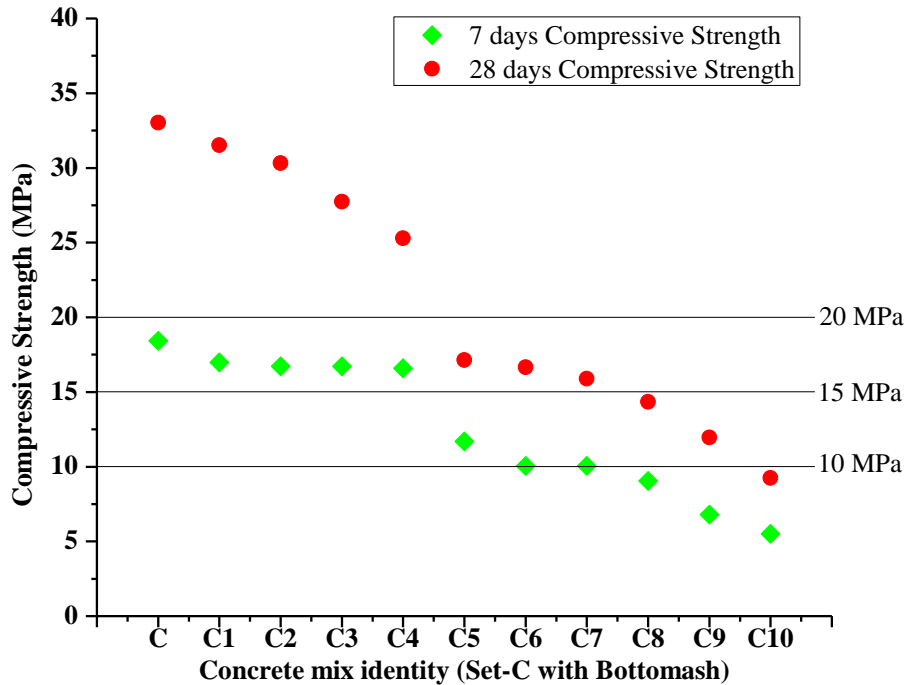


Fig. 5.36 Variations in Compressive Strength values (Set-C, Group-B)) Concrete mix with Bottomash (Refer Table 5.22)

Observations : It may be observed that up to 40% replacement of Sand by Bottomash, the strength at 28 day’s maturity remain above 20 MPa mark, and up to 70% replacement, the strength attained were above 15 MPa at the same maturity.

Table 5.23 Thermal Conductivity test results for (Set-C, Group-B) Concrete mix with Bottomash

Sample identity	Thermal Conductivity (W/m.K)
C	1.557
C1	1.300
C2	1.274
C3	1.071
C4	1.009
C5	1.034
C6	0.916
C7	0.863
C8	0.752
C9	0.678
C10	0.632

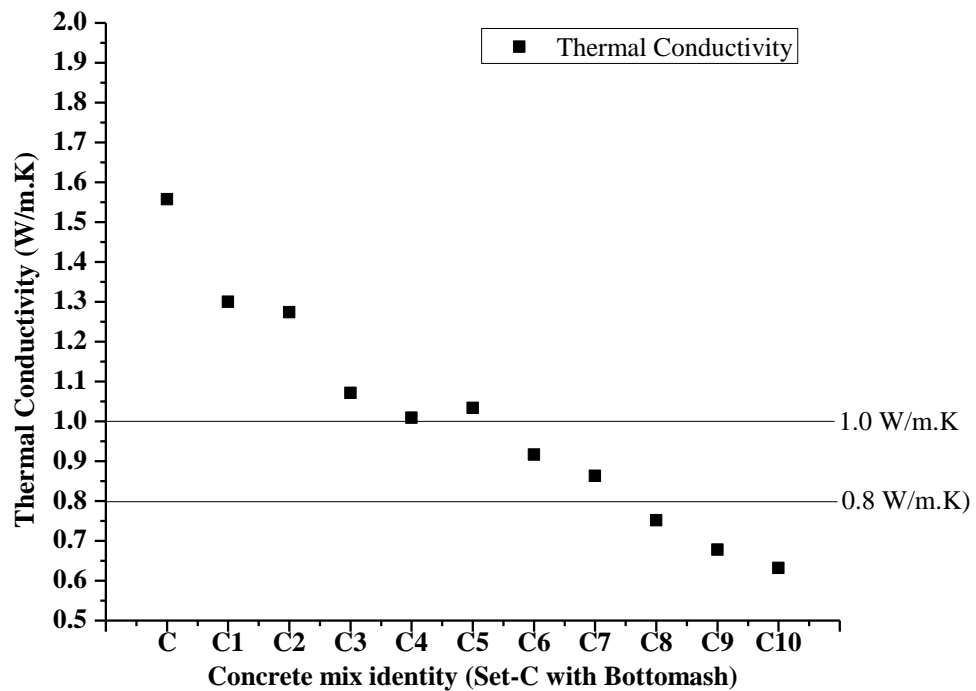


Fig. 5.37 Variations in Thermal Conductivity values for (Set-C, Group-B) Concrete mix with Bottomash (Refer Table 5.23)

Observations : With gradual reduction in thermal conductivity values w.r.t. sand replacement in stages by Bottomash, up to 70%, it remain within 0.8 W/m.K, and further reduction thereafter.

Table 5.24 Apparent Porosity and Bulk Density test results for (Set-C, Group-B) 1:2.4:3.6 Concrete mix with Bottomash

Sample identity	Apparent Porosity (%)	Bulk Density (gm/cc)
C	14.615	2.315
C1	16.000	2.304
C2	17.213	2.295
C3	20.472	2.165
C4	21.260	2.110
C5	23.770	2.098
C6	22.314	2.074
C7	28.571	2.017
C8	35.135	2.000
C9	37.273	1.973
C10	38.095	1.952

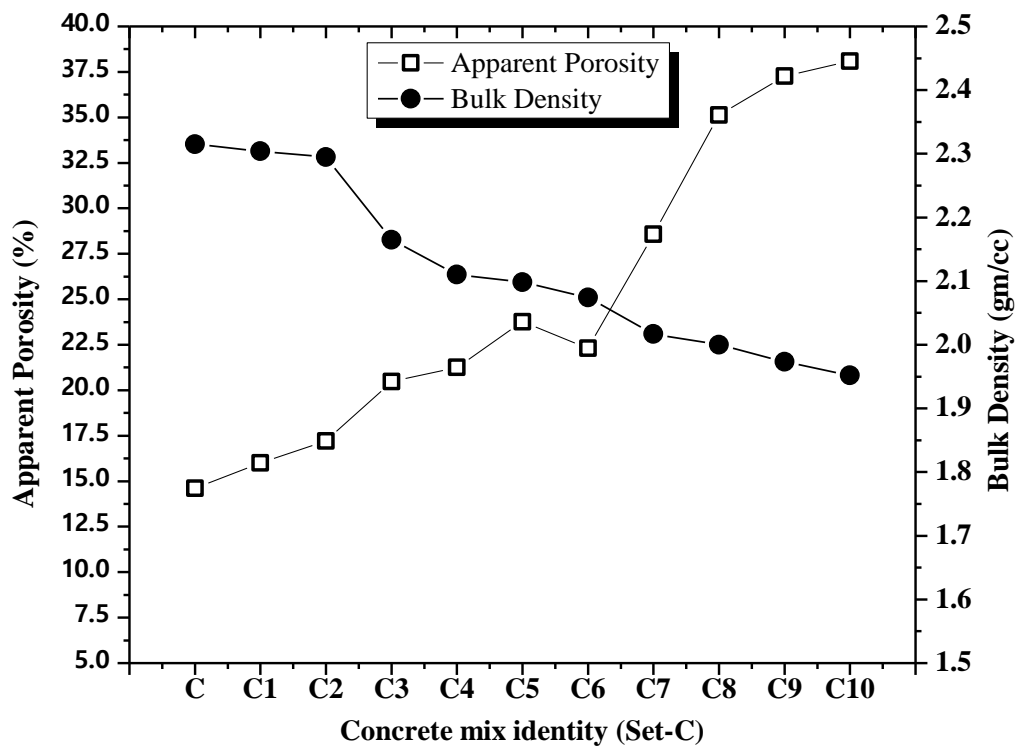


Fig. 5.38 Variations in Apparent Porosity and Bulk Density values for (Set-C, Group-B) Concrete mix with Bottomash. (Refer Table 5.24)

Observations : Apparent porosity value increases steadily up to 50% replacement ratio, and thereafter it declines and increases sharply from 60% to 70% range, while bulk density values also declined.

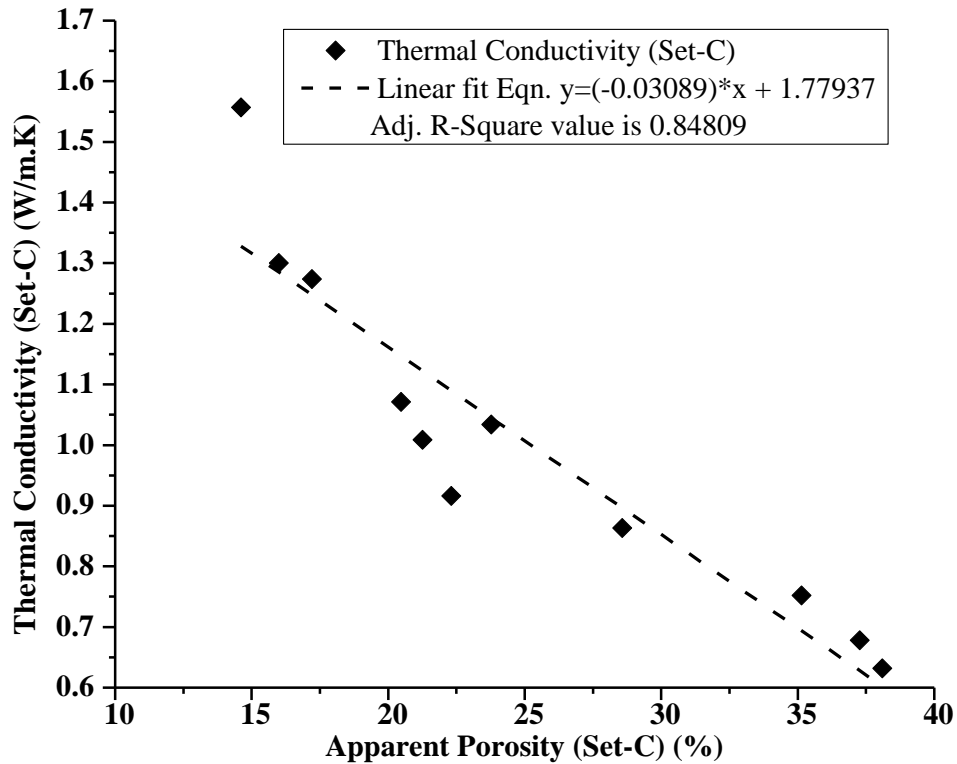


Fig. 5.39 Relationship between Apparent Porosity and Thermal Conductivity for the Concrete mix sample (Refer Table 5.23 and 5.24)

Observations : Apparent Porosity (AP) is shown to have a close relationship with thermal conductivity of the concrete mix sample, and the adjusted R^2 value of 0.85, (assessed the goodness-of-fit for regression analysis by Origin 8) supports the changes in both the parameters with respect to the mix proportions. The more is apparent porosity, less is the thermal conductivity.

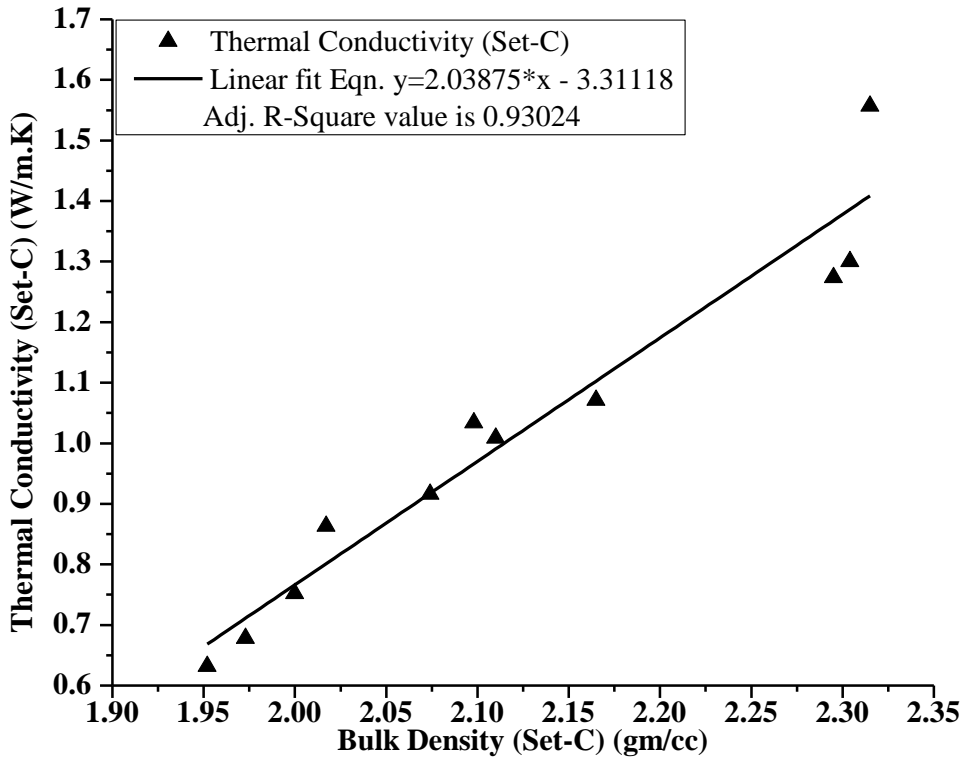


Fig. 5.40 Relationship between Bulk Density and Thermal Conductivity for the Concrete mix sample (Refer Table 5.23 and 5.24)

Observations : Bulk Density is shown to have a linear fit relationship with thermal conductivity of the concrete mix sample, and the adjusted R^2 value of 0.85, (assessed the goodness-of-fit for linear regression analysis by Origin 8) supports the same. The more is the bulk density, more is the thermal conductivity.

5.3.9 Design mix (1:2.0:3.0) (Set-D, Group-B) : Sand content replaced by Bottomash in 10% stages, Cement used was PPC and 10 mm down stone aggregate was use

Table 5.25 Compressive Strength test results for (Set-D, Group-B) Concrete mix with Bottomash

Sample identity	Mix proportion (1:2.00:3.00)					Compressive Strength (MPa)	
	Cement	Sand	Bottom ash	Stone Aggregate	Water-Cement	7 day's	28 day's
D	1.0	2.000	0.000	3.00	0.50	20.12	36.42
D1	1.0	1.800	0.200	3.00	0.50	19.03	35.27
D2	1.0	1.600	0.400	3.00	0.50	17.94	31.94
D3	1.0	1.400	0.600	3.00	0.50	17.47	28.68
D4	1.0	1.200	0.800	3.00	0.50	16.72	27.05
D5	1.0	1.000	1.000	3.00	0.50	15.36	22.43
D6	1.0	0.800	1.200	3.00	0.50	11.55	19.37
D7	1.0	0.600	1.400	3.00	0.50	10.87	19.16
D8	1.0	0.400	1.600	3.00	0.50	10.6	18.08
D9	1.0	0.200	1.800	3.00	0.50	9.17	17.53
D10	1.0	0.000	2.000	3.00	0.50	8.02	14.95

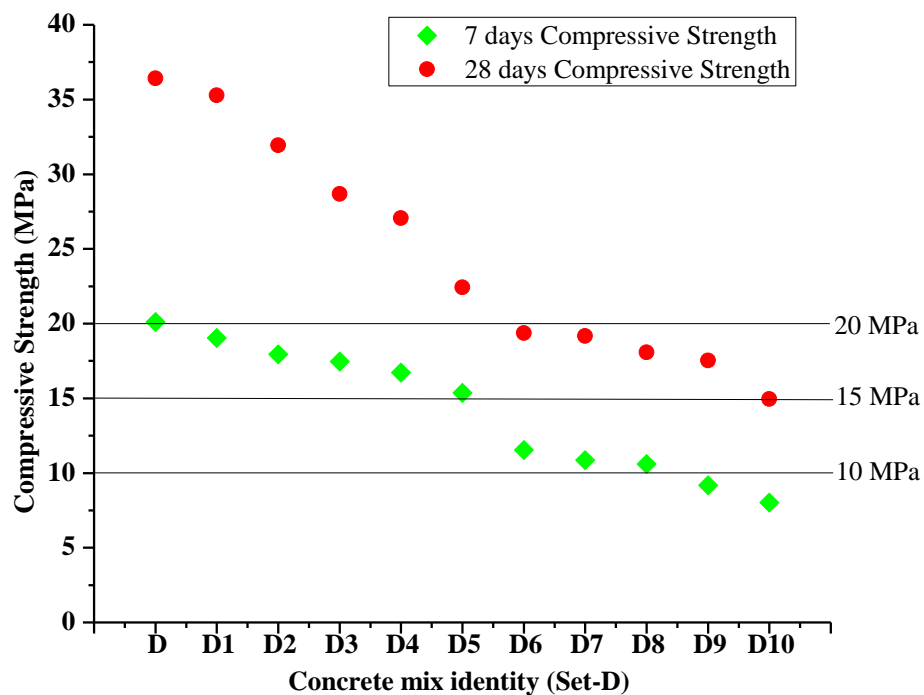


Fig. 5.41 Variations in Compressive Strength values for (Set-D, Group-B) Concrete mix with Bottomash (Refer Table 5.25)

Observations : Up to 50% replacement ratio, strength remains above 20 MPa, and beyond that up to 100% replacement, it attained 15 MPa strength at same age.

Table 5.26 Thermal Conductivity test results for (Set-D, Group-B) 1:2:3 Concrete mix with Bottomash

Sample identity	Thermal Conductivity (W/m.K)
D	1.693
D1	1.547
D2	1.383
D3	1.278
D4	1.107
D5	1.022
D6	0.897
D7	0.883
D8	0.855
D9	0.739
D10	0.722

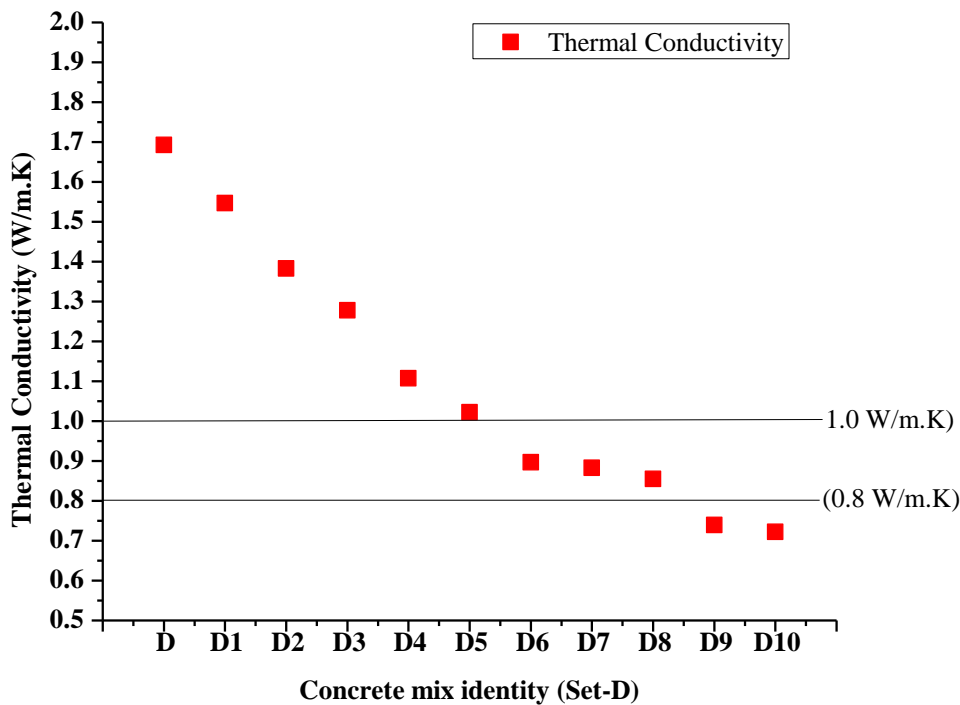


Fig. 5.42 Variations in Thermal Conductivity values for (Set-D, Group-B) Concrete mix with Bottomash (Refer Table 5.26)

Observations : Steady declining trend in thermal conductivity values are observed with respect to increasing substitution ratio of sand by Bottomash.

Table 5.27 Apparent Porosity and Bulk Density test results for (Set-D, Group-B) 1:2:3 Concrete mix with Bottomash

Sample identity	Apparent Porosity (%)	Bulk Density (gm/cc)
D	7.438	2.496
D1	9.735	2.407
D2	10.345	2.405
D3	10.909	2.390
D4	12.844	2.367
D5	13.592	2.359
D6	13.861	2.346
D7	14.019	2.224
D8	15.517	2.129
D9	19.091	2.082
D10	20.952	2.076

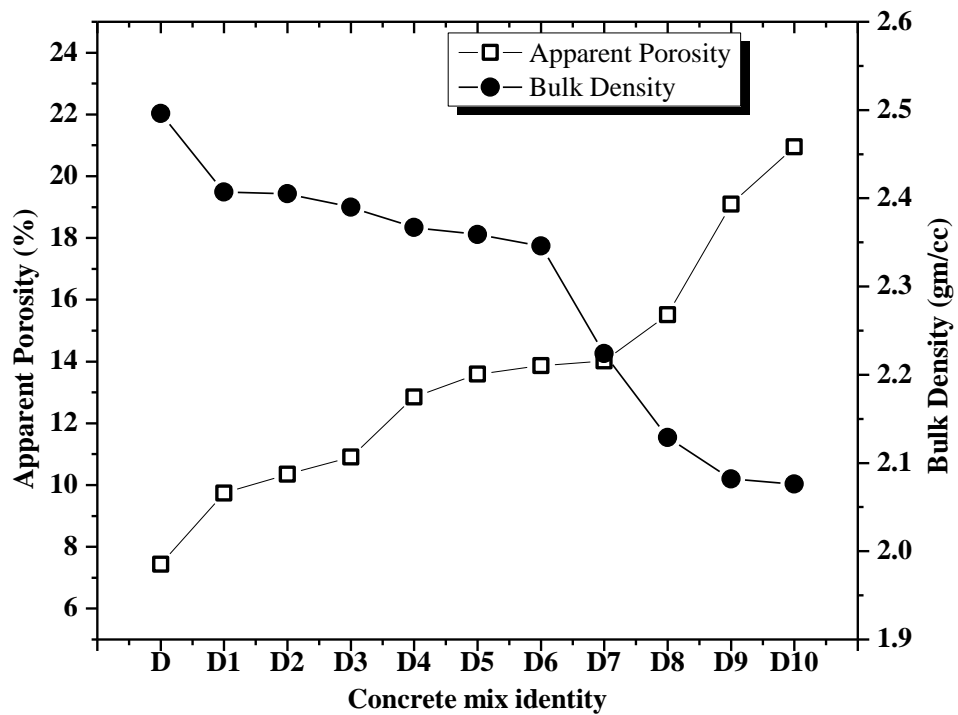


Fig. 5.43 Variations in Apparent Porosity and Bulk Density values for (Set-D, Group-B) Concrete mix with Bottomash (Refer Table 5.27)

Observations : It may be observed that apparent porosity increases with reduction in thermal conductivity , bulk density and compressive strength values, and vice-versa.

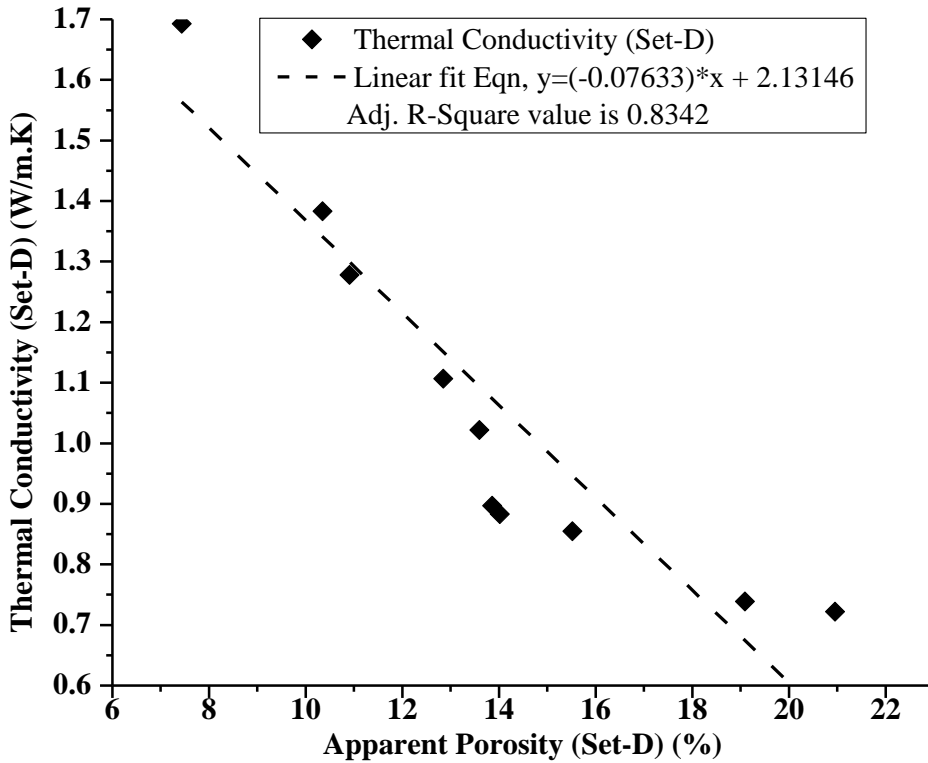


Fig. 5.44 Relationship between Apparent Porosity and Thermal Conductivity for the Concrete mix sample (Refer Table 5.26 and 5.27)

Observations : Apparent Porosity (AP) is shown to have a close relationship with thermal conductivity of the concrete mix sample, and the adjusted R^2 value of 0.83, (assessed the goodness-of-fit for regression analysis by Origin 8) supports the changes in both the parameters with respect to the mix proportions. The more is apparent porosity, less is the thermal conductivity.

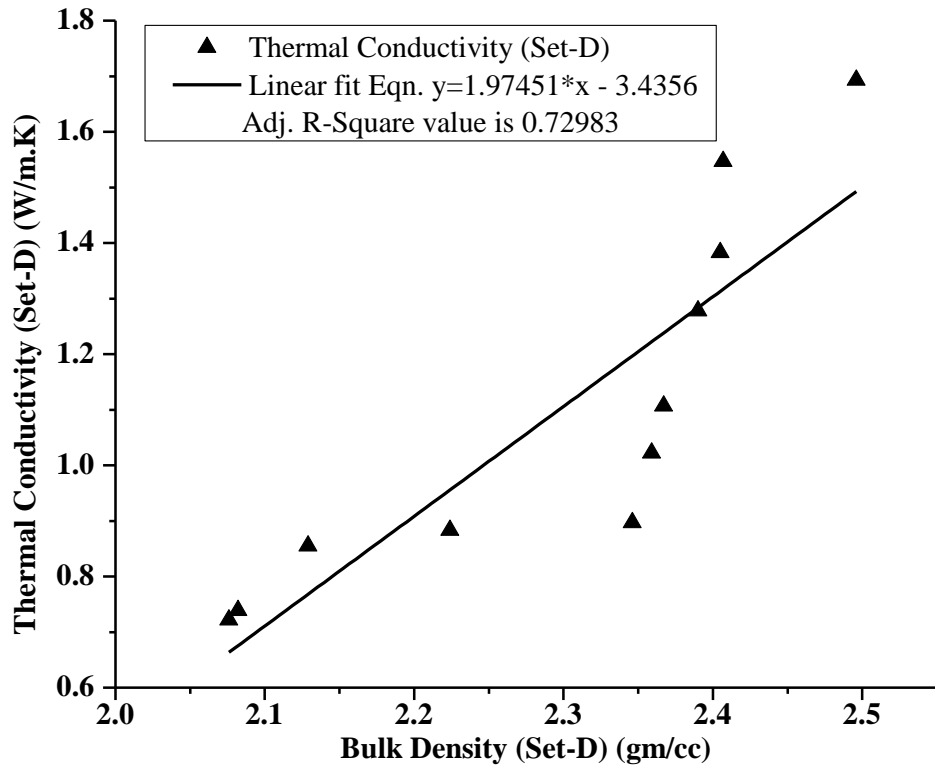


Fig. 5.45 Relationship between Bulk Density and Thermal Conductivity for the Concrete mix sample (Refer Table 5.26 and 5.27)

Observations : Bulk Density is shown to have a close to linear fit relationship with thermal conductivity of the concrete mix sample, and the adjusted R^2 value of 0.73, (assessed the average ness-of-fit for linear regression analysis by Origin 8) supports the same. The more is the bulk density, more is the thermal conductivity.

5.4 Nominal Mix Concrete by following IS 456-2000 stipulations for various Grades of Concrete.

5.4.1 Nominal mix (1:1.0:2.0) (Set-A, Group-C): Sand content replaced by Bottom ash in 10% stages, Cement used was PPC and 10 mm down stone aggregate was use

Table 5.28 Compressive Strength test results for (Set-A, Group-C) 1:1:2 Concrete mix with Bottomash

Sample identity	Mix proportion (1:1.0:2.0)					Compressive Strength (MPa)	
	Cement	Sand	Bottom ash	Stone Aggregate	Water-Cement	7 day's	28 day's
P	1	1.00	0.00	2.00	0.5	23.8	33.13
P-1	1	0.90	0.10	2.00	0.5	23.2	32.62
P-2	1	0.80	0.20	2.00	0.5	20.2	32.62
P-3	1	0.70	0.30	2.00	0.5	19.6	32.52
P-4	1	0.60	0.40	2.00	0.5	19.5	32.31
P-5	1	0.50	0.50	2.00	0.5	18.2	32.01
P-6	1	0.40	0.60	2.00	0.5	16.9	28.64
P-7	1	0.30	0.70	2.00	0.5	16.6	28.55
P-8	1	0.20	0.80	2.00	0.5	16.3	26.2
P-9	1	0.10	0.90	2.00	0.5	14.1	22.53
P-10	1	0.00	1.00	2.00	0.5	11.7	18.86

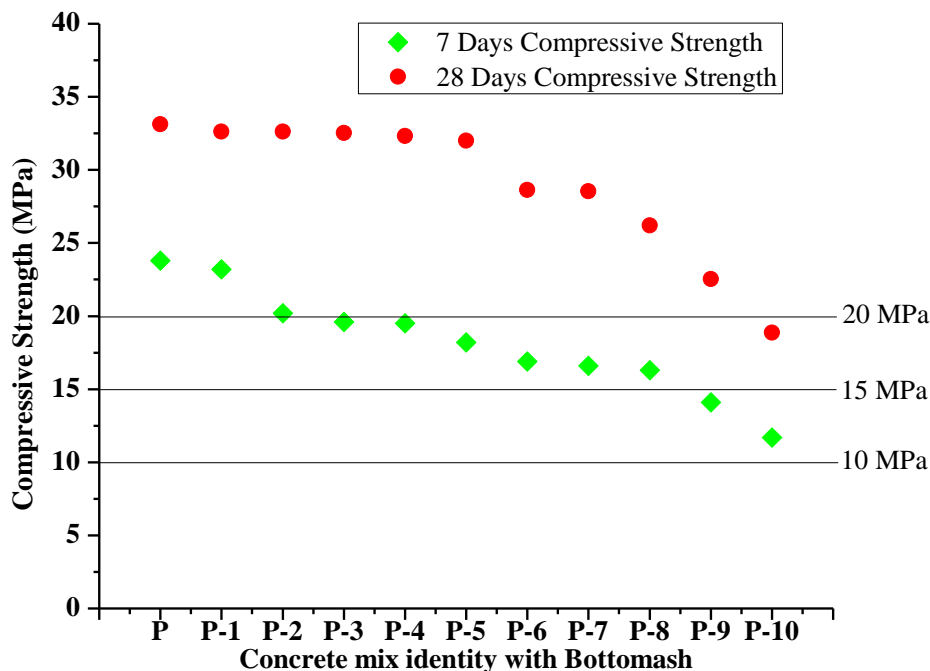


Fig. 5.46 Variations in Compressive Strength values for (Set-A, Group-C) Concrete mix with Bottomash. (Refer Table 5.28)

Observations : For all the sand substituted mixes with Bottomash (P-1 to P-9), 28day's compressive strength remain > 20 MPa, and the 100% substituted mix (P-10) remain nearer to 19 MPa.

Table 5.29 Thermal Conductivity test results for (Set-A, Group-C) 1:1:2 Concrete mix with Bottomash

Sample identity	Concrete Mix proportion (1 : 1.0 : 2.0)					Thermal Conductivity (W/m.K)
	Cement	Sand	Bottom ash	Stone Aggregate	Water - Cement	
P	1	1.00	0.00	2.00	0.5	1.613
P-1	1	0.90	0.10	2.00	0.5	1.51
P-2	1	0.80	0.20	2.00	0.5	1.446
P-3	1	0.70	0.30	2.00	0.5	1.377
P-4	1	0.60	0.40	2.00	0.5	1.286
P-5	1	0.50	0.50	2.00	0.5	1.227
P-6	1	0.40	0.60	2.00	0.5	1.12
P-7	1	0.30	0.70	2.00	0.5	1.078
P-8	1	0.20	0.80	2.00	0.5	1.044
P-9	1	0.10	0.90	2.00	0.5	0.9724
P-10	1	0.00	1.00	2.00	0.5	0.9118

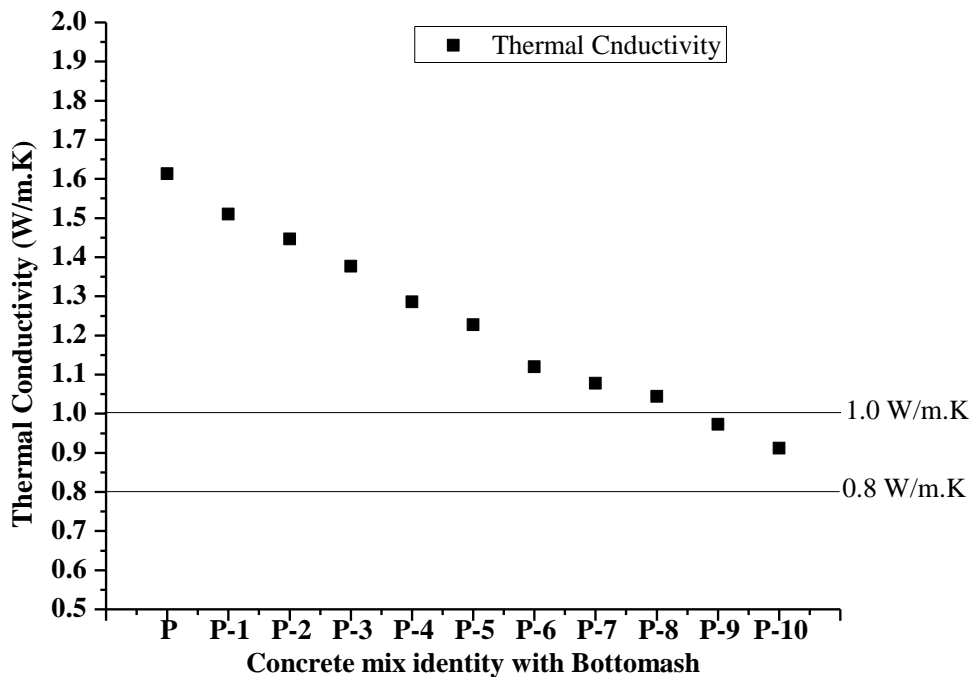


Fig. 5.47 Variations in Thermal Conductivity values for (Set-A, Group-C) Concrete mix with Bottomash. (Refer Table 5.29)

Observations : It is evident from the above plot that the thermal conductivity parameter followed a definite reduction trend, and only 90% and 100% replacement rated mixes (P-9 and P-10) conductivity values fall below 1.0 W/m.K.

Table 5.30 Apparent Porosity and Bulk Density test results for (Set-A, Group-C) 1:1:2 Concrete mix with Bottomash

Sample identity	Mix proportion (1:1.0:2.0)					Apparent Porosity (%)	Bulk Density gm/cc
	Cement	Sand	Bottom ash	Stone Aggregate	Water-Cement		
P	1	1.00	0.00	2.00	0.5	8.943	2.472
P-1	1	0.90	0.10	2.00	0.5	10.744	2.405
P-2	1	0.80	0.20	2.00	0.5	11.475	2.393
P-3	1	0.70	0.30	2.00	0.5	11.57	2.372
P-4	1	0.60	0.40	2.00	0.5	12.295	2.32
P-5	1	0.50	0.50	2.00	0.5	13.008	2.317
P-6	1	0.40	0.60	2.00	0.5	13.333	2.283
P-7	1	0.30	0.70	2.00	0.5	14.286	2.269
P-8	1	0.20	0.80	2.00	0.5	15.254	2.254
P-9	1	0.10	0.90	2.00	0.5	16.239	2.239
P-10	1	0.00	1.00	2.00	0.5	17.241	2.198

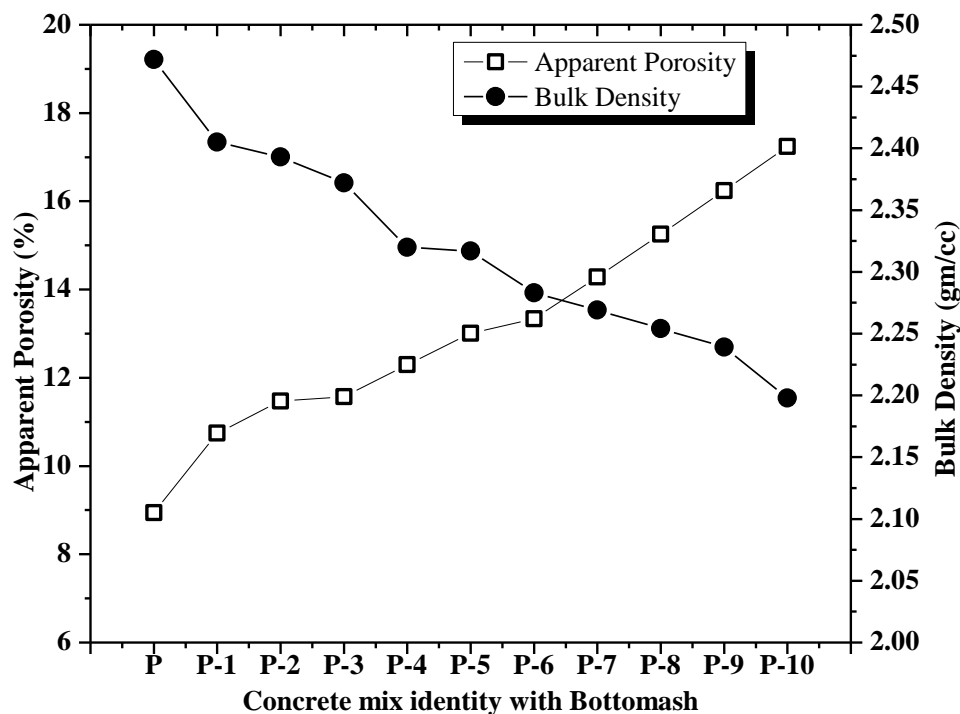


Fig. 5.48 Variations in Apparent Porosity and Bulk Density values for (Set-A, Group-C) Concrete mix with Bottomash (Refer Table 5.30)

Observations : Apparent porosity and bulk density values of all the concrete mixes follow the incremental and decremental rate respectively.

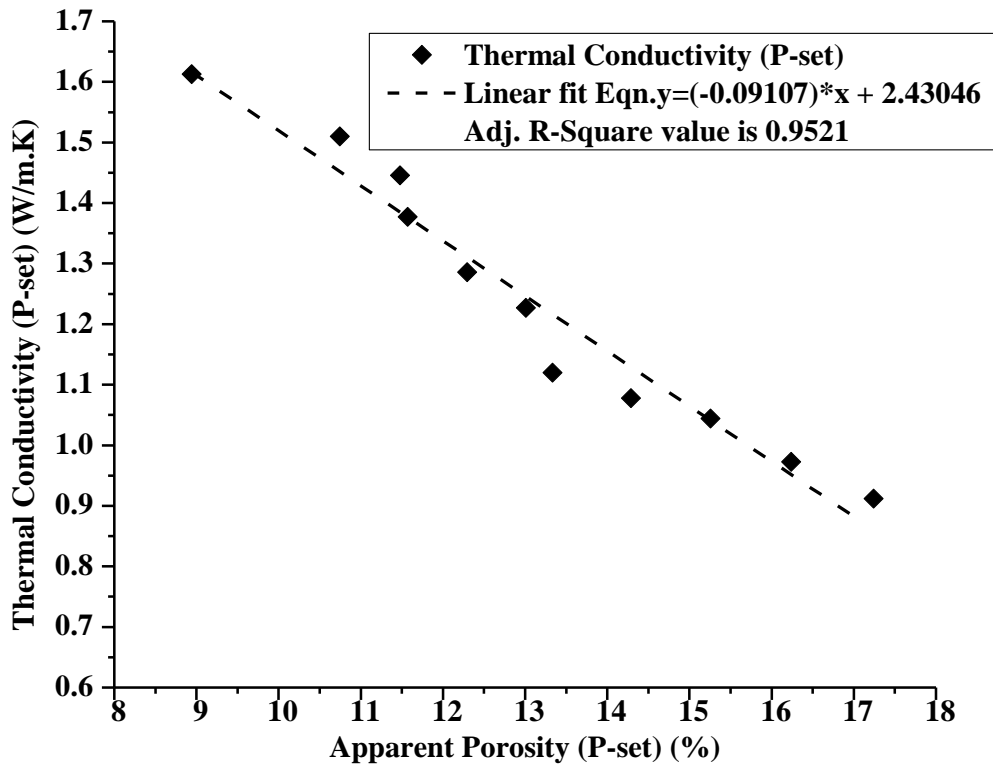


Fig. 5.49 Relationship between Apparent Porosity and Thermal Conductivity for the Concrete mix sample (Refer Table 5.29 and 5.30)

Observations : Apparent Porosity (AP) is shown to have a close relationship with thermal conductivity of the concrete mix sample, and the adjusted R^2 value of 0.95, (assessed the goodness-of-fit for regression analysis by Origin 8) supports the changes in both the parameters with respect to the mix proportions. The more is apparent porosity, less is the thermal conductivity.

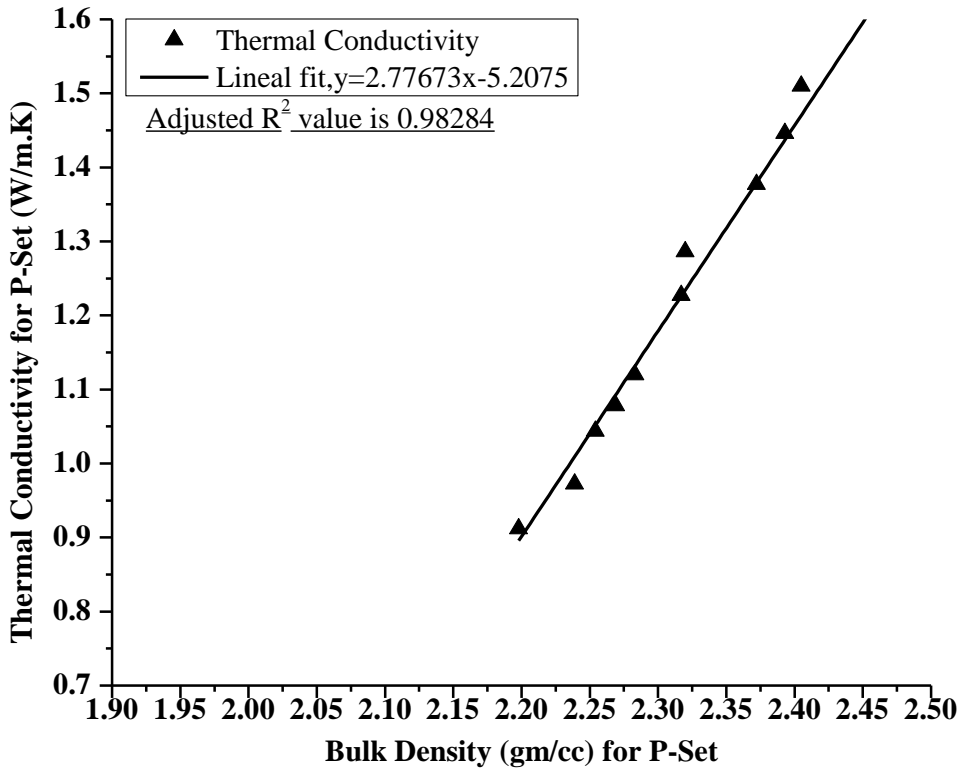


Fig. 5.50 Relationship between Bulk Density and Thermal Conductivity for the Concrete mix sample (Refer Table 5.29 and 5.30)

Observations : Bulk Density is shown to have an excellent linear fit relationship with thermal conductivity of the concrete mix sample, and the adjusted R^2 value of 0.98, (assessed the very goodness-of-fit for linear regression analysis by Origin 8) supports the same. The more is the bulk density, more is the thermal conductivity.

5.4.2 Nominal mix (1:1.5:3.0) (Set-B, Group-C) : Sand content replaced by Bottom ash in 10% stages, Cement used was PPC and 10 mm down stone aggregate was use

Table 5.31 Compressive Strength test results for (Set-B, Group-C) 1:1.5:3 Concrete mix with Bottomash

Sample identity	Mix proportion (1:1.5:3.0)					Compressive Strength (MPa)	
	Cement	Sand	Bottom ash	Stone Aggregate	Water-Cement	7 day's	28 day's
Q	1.0	1.50	0.00	3.00	0.50	22.9	32.3
Q-1	1.0	1.35	0.15	3.00	0.50	22.5	31.3
Q-2	1.0	1.20	0.30	3.00	0.50	20.1	31.2
Q-3	1.0	1.05	0.45	3.00	0.50	15.7	30.8
Q-4	1.0	0.90	0.60	3.00	0.50	14.0	26.6
Q-5	1.0	0.75	0.75	3.00	0.50	12.4	21.9
Q-6	1.0	0.60	0.90	3.00	0.50	11.2	21.6
Q-7	1.0	0.45	1.05	3.00	0.50	10.3	17.1
Q-8	1.0	0.30	1.20	3.00	0.50	10.0	15.8
Q-9	1.0	0.15	1.35	3.00	0.50	9.6	15.3
Q-10	1.0	0.00	1.50	3.00	0.50	8.7	14.5

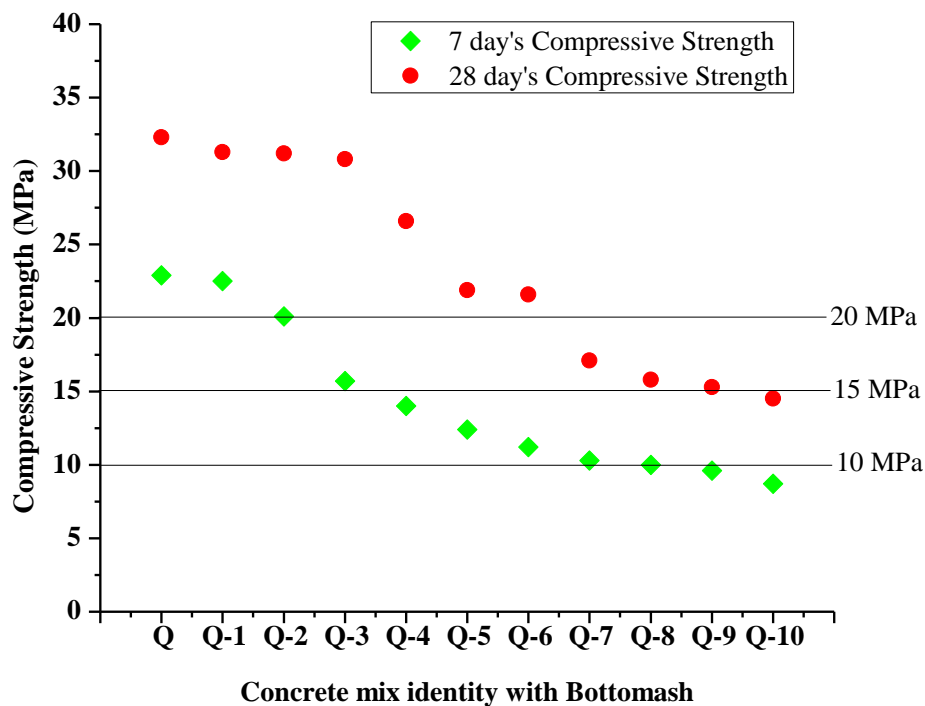


Fig. 5.51 Variations in Compressive Strength values for (Set-B, Group-C) Concrete mix with Bottomash. (Refer Table 5.31)

Observations : Up to 60% replacement rate of sand by bottomash (Q-1 to Q-6) attained more than 20 MPa strength, and rest remained within and around 15 MPa .

Table 5.32 Thermal Conductivity test results for (Set-B, Group-C) 1:1.5:3 Concrete mix with Bottomash

Sample identity	Concrete Mix proportion (1 : 1.5 : 3.0)					Thermal Conductivity (W/m.K)
	Cement	Sand	Bottom ash	Stone Aggregate	Water - Cement	
Q	1	1.50	0.00	3.00	0.5	1.579
Q-1	1	1.35	0.15	3.00	0.5	1.4
Q-2	1	1.20	0.30	3.00	0.5	1.421
Q-3	1	1.05	0.45	3.00	0.5	1.302
Q-4	1	0.90	0.60	3.00	0.5	1.238
Q-5	1	0.75	0.75	3.00	0.5	1.151
Q-6	1	0.60	0.90	3.00	0.5	1.017
Q-7	1	0.45	1.05	3.00	0.5	0.9639
Q-8	1	0.30	1.20	3.00	0.5	0.9417
Q-9	1	0.15	1.35	3.00	0.5	0.9393
Q-10	1	0.00	1.50	3.00	0.5	0.9002

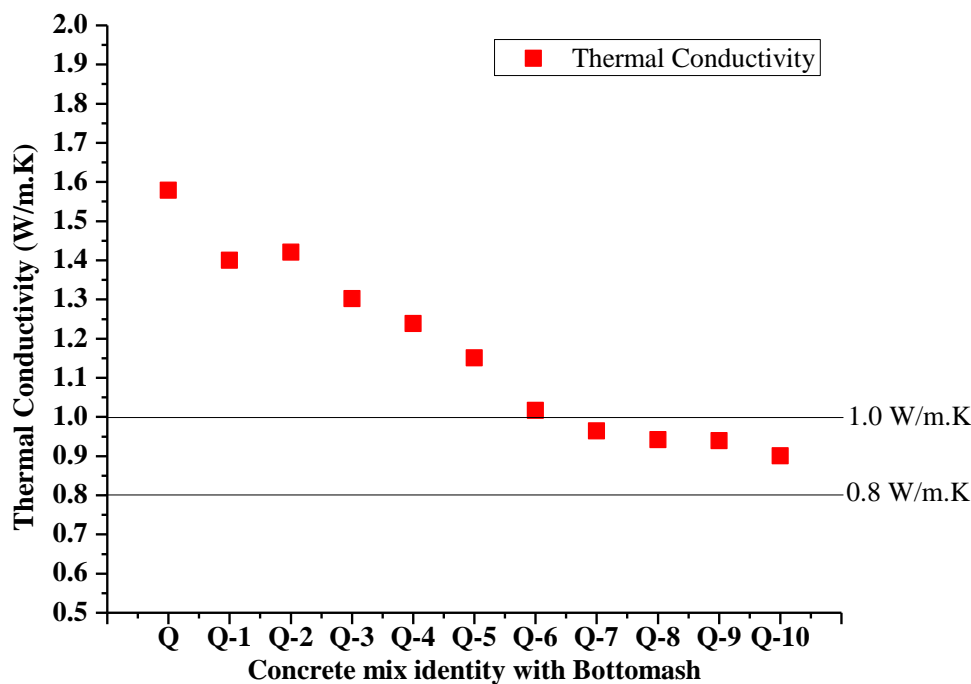


Fig. 5.52 Variations in Thermal Conductivity values for (Set-B, Group-C) Concrete mix with Bottomash. (Refer Table 5.32)

Observations : The thermal conductivity values in respect of all sand substituted concrete mixes (Q-1 to Q-10) follow the decremental rate with respect to the conventional concrete mix with sand (Q). Up to 60% replacement, conductivity value remain > 1.0 W/m.K, and beyond that, it remains within 1.0 - 0.8 W/m.K range.

Table 5.33 Apparent Porosity and Bulk Density test results for (Set-B, Group-C) 1:1.5:3 Concrete mix with Bottomash

Sample identity	Mix proportion (1:1.5:3.0)					Apparent Porosity (%)	Bulk Density gm/cc
	Cement	(%)	gm/cc	Stone Aggregate	Water-Cement		
Q	1	23.8	33.13	3.00	0.5	9.231	2.423
Q-1	1	23.2	32.62	3.00	0.5	11.029	2.309
Q-2	1	20.2	32.62	3.00	0.5	11.719	2.352
Q-3	1	19.6	32.52	3.00	0.5	13.077	2.254
Q-4	1	19.5	32.31	3.00	0.5	17.054	2.178
Q-5	1	18.2	32.01	3.00	0.5	18.045	2.113
Q-6	1	16.9	28.64	3.00	0.5	20.455	2.091
Q-7	1	16.6	28.55	3.00	0.5	22.481	2.078
Q-8	1	16.3	26.2	3.00	0.5	23.438	2.063
Q-9	1	14.1	22.53	3.00	0.5	23.438	2.055
Q-10	1	11.7	18.86	3.00	0.5	24.194	2.04

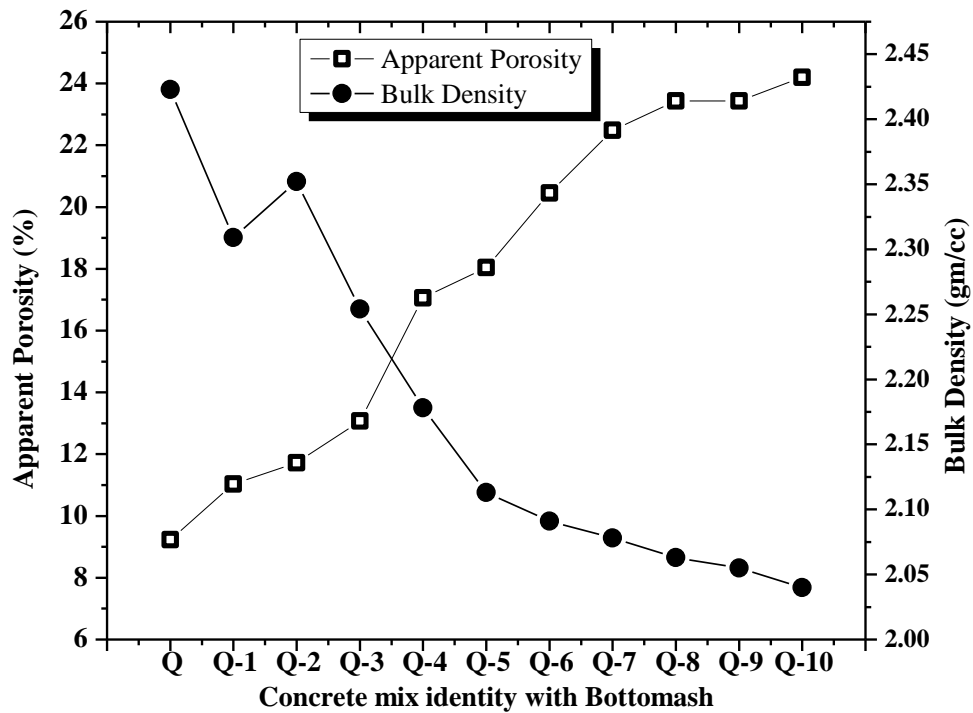


Fig. 5.53 Variations in Apparent Porosity and Bulk Density values for (Set-B, Group-C) Concrete mix with Bottomash. (Refer Table 5.33)

Observations : The apparent porosity value shows increasing trend, for all the sand substituted mixes . The bulk density values show the decreasing trend, mixes except in the case of mix Q-2, wherein the value is found more than that of mix Q-1. Afterwards, it follows the usual decreasing pattern. The abnormal kink might be due to some experimental error.

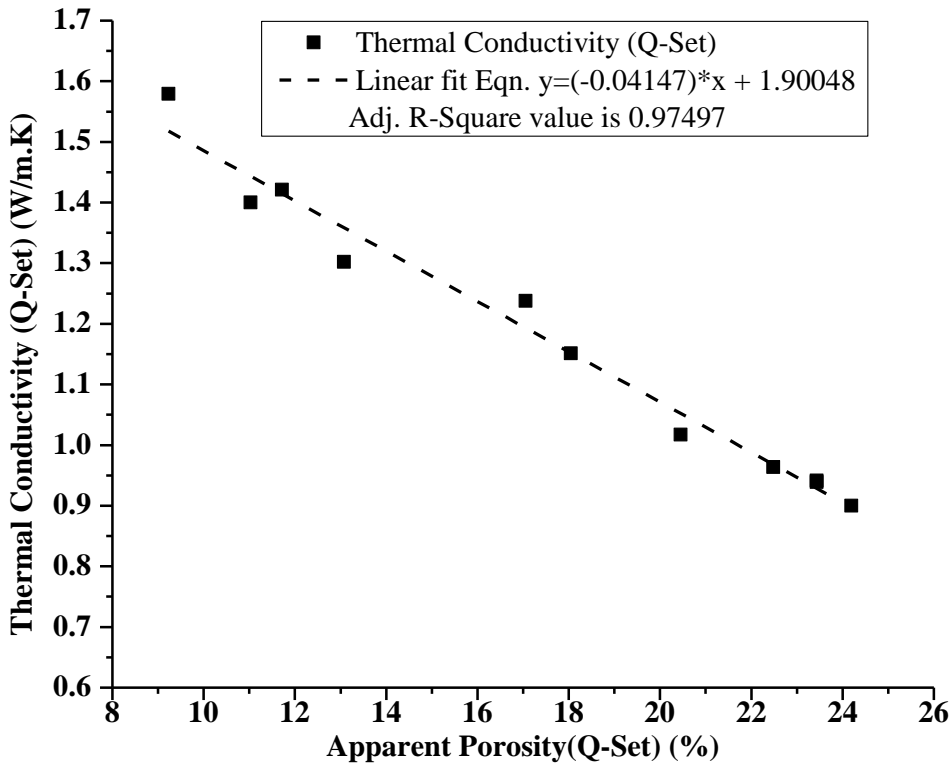


Fig. 5.54 Relationship between Apparent Porosity and Thermal Conductivity for the Concrete mix sample(Set B, Gr.C) (Refer Table 5.32 and 5.33)

Observations : Apparent Porosity (AP) is shown to have an excellent relationship with thermal conductivity of the concrete mix sample, and the adjusted R^2 value of 0.975, (assessed the very goodness-of-fit for regression analysis by Origin 8) supports the changes in both the parameters with respect to the mix proportions. The more is apparent porosity, less is the thermal conductivity.

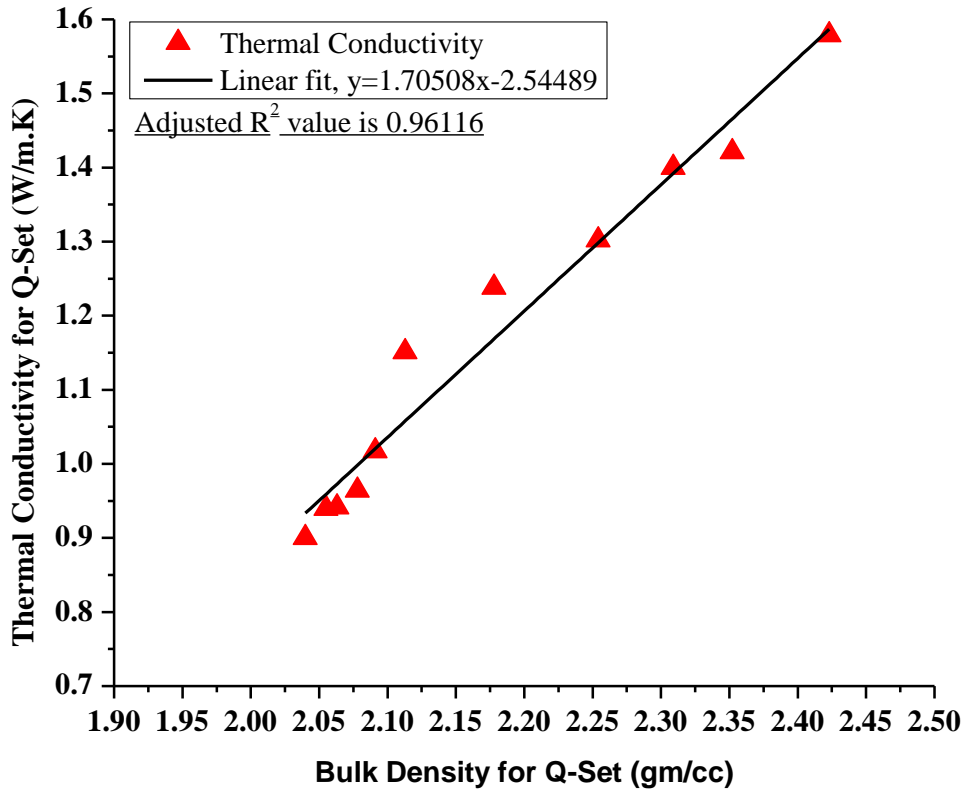


Fig. 5.55 Relationship between Bulk Density and Thermal Conductivity for the Concrete mix sample (Refer Table 5.32 and 5.33)

Observations : Bulk Density is shown to have an excellent linear fit relationship with thermal conductivity of the concrete mix sample, and the adjusted R^2 value of 0.96, (assessed the very goodness-of-fit for linear regression analysis by Origin 8) supports the same. The more is the bulk density, more is the thermal conductivity.

5.4.3 Nominal mix (1:2.0:4.0) (Set-C, Group-C) : Sand content replaced by Bottom ash in 10% stages, Cement used was PPC and 10 mm down stone aggregate was use

Table 5.34 Compressive Strength test results for (Set-C, Group-C) 1:2:4 Concrete mix with Bottomash

Sample identity	Mix proportion (1:2.0:4.0)					Compressive Strength (MPa)	
	Cement	Sand	Bottom ash	Stone Aggregate	Water-Cement	7 day's	28 day's
R	1	2.00	0.00	4.00	0.5	19.2	28
R-1	1	1.80	0.20	4.00	0.5	17.6	27.4
R-2	1	1.60	0.40	4.00	0.5	13.6	21.6
R-3	1	1.40	0.60	4.00	0.5	13.3	20.4
R-4	1	1.20	0.80	4.00	0.5	11.8	15.3
R-5	1	1.00	1.00	4.00	0.5	9.6	14.3
R-6	1	0.80	1.20	4.00	0.5	9	14
R-7	1	0.60	1.40	4.00	0.5	8.4	13
R-8	1	0.40	1.60	4.00	0.5	6.4	10.9
R-9	1	0.20	1.80	4.00	0.5	6.2	10.8
R-10	1	0.00	2.00	4.00	0.5	4.4	7.4

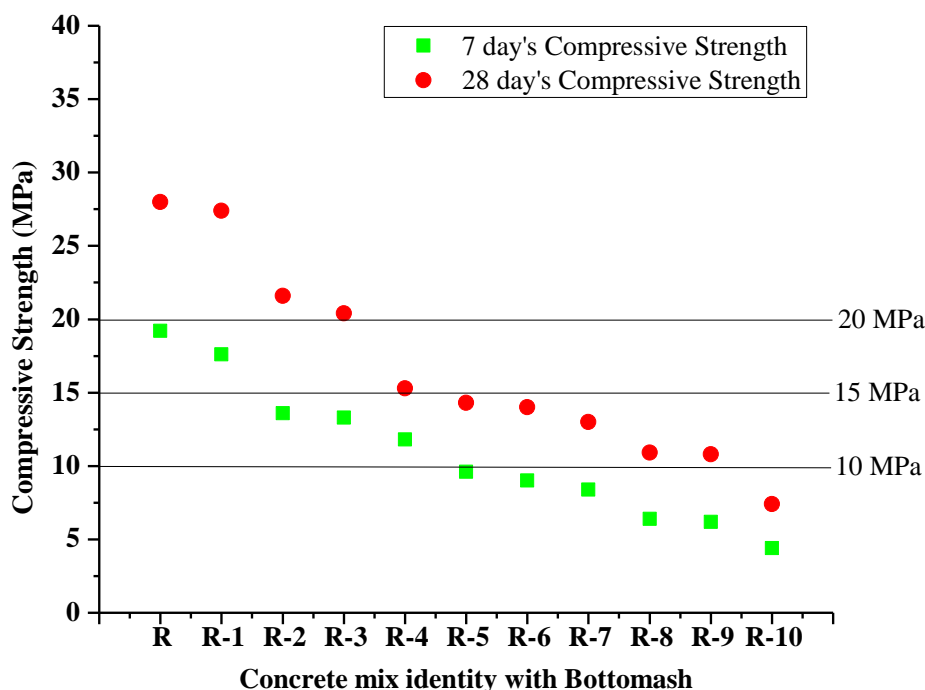


Fig. 5.56 Variations in Compressive Strength values for (Set-C, Group-C) Concrete mix with Bottomash. (Refer Table 5.34)

Observations : Up to 30% sand replacement by bottomash (Q-1 to Q-3), the strength remain above 20 MPa mark, Q-4 remain at 15 MPa, and up to 90% replacement (Q-5 to Q-9), the strengths remain within 15–10 MPa range. Q-10 possess < 10 MPa mark

Table 5.35 Thermal Conductivity test results for (Set-C, Group-C) 1:2:4 Concrete mix with Bottomash

Sample identity	Concrete Mix proportion (1 : 2.0 : 4.0)					Thermal Conductivity (W/m.K)
	Cement	Sand	Bottom ash	Stone Aggregate	Water - Cement	
R	1	2.00	0.00	4.00	0.5	1.52
R-1	1	1.80	0.20	4.00	0.5	1.445
R-2	1	1.60	0.40	4.00	0.5	1.299
R-3	1	1.40	0.60	4.00	0.5	1.183
R-4	1	1.20	0.80	4.00	0.5	1.056
R-5	1	1.00	1.00	4.00	0.5	1.051
R-6	1	0.80	1.20	4.00	0.5	0.934
R-7	1	0.60	1.40	4.00	0.5	0.8673
R-8	1	0.40	1.60	4.00	0.5	0.8287
R-9	1	0.20	1.80	4.00	0.5	0.826
R-10	1	0.00	2.00	4.00	0.5	0.7813

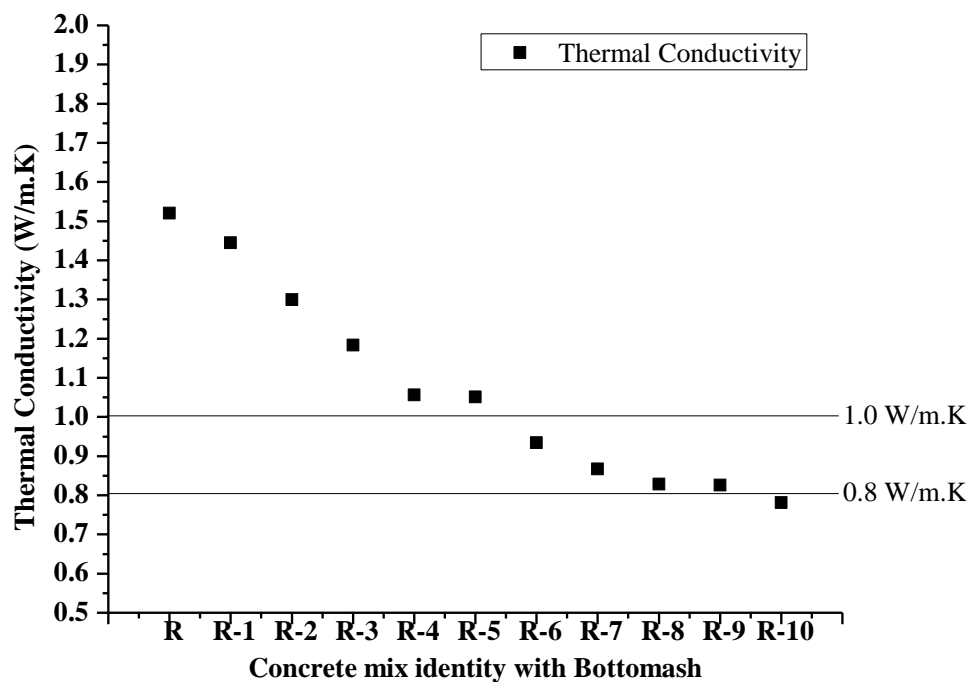


Fig. 5.57 Variations in Thermal Conductivity values for (Set-C, Group-C) Concrete mix with Bottomash. Refer Table 5.35)

Observation : Up to 50% replacement ratio, thermal conductivity value remain above 1.0 W/m.K, and up to 90% replacement range, it remain within 1.0 – 0.8 W/m.K value range. 100% sand replaced mix (Q-10) only remain < 0.8 W/m.K mark.

Table 5.36 Apparent Porosity and Bulk Density test results for (Set-C, Group-C) 1:2:4 Concrete mix with Bottomash

Sample identity	Mix proportion (1:2.0:4.0)					Apparent Porosity	Bulk Density
	Cement	(%)	gm/cc	Stone Aggregate	Water-Cement	(%)	gm/cc
R	1	2.00	0.00	4.00	0.5	7.937	2.397
R-1	1	1.80	0.20	4.00	0.5	8.594	2.352
R-2	1	1.60	0.40	4.00	0.5	11.278	2.256
R-3	1	1.40	0.60	4.00	0.5	11.450	2.252
R-4	1	1.20	0.80	4.00	0.5	14.286	2.093
R-5	1	1.00	1.00	4.00	0.5	17.518	2.088
R-6	1	0.80	1.20	4.00	0.5	19.118	2.051
R-7	1	0.60	1.40	4.00	0.5	20.930	2.039
R-8	1	0.40	1.60	4.00	0.5	21.481	1.993
R-9	1	0.20	1.80	4.00	0.5	22.222	1.978
R-10	1	0.00	2.00	4.00	0.5	25.373	1.925

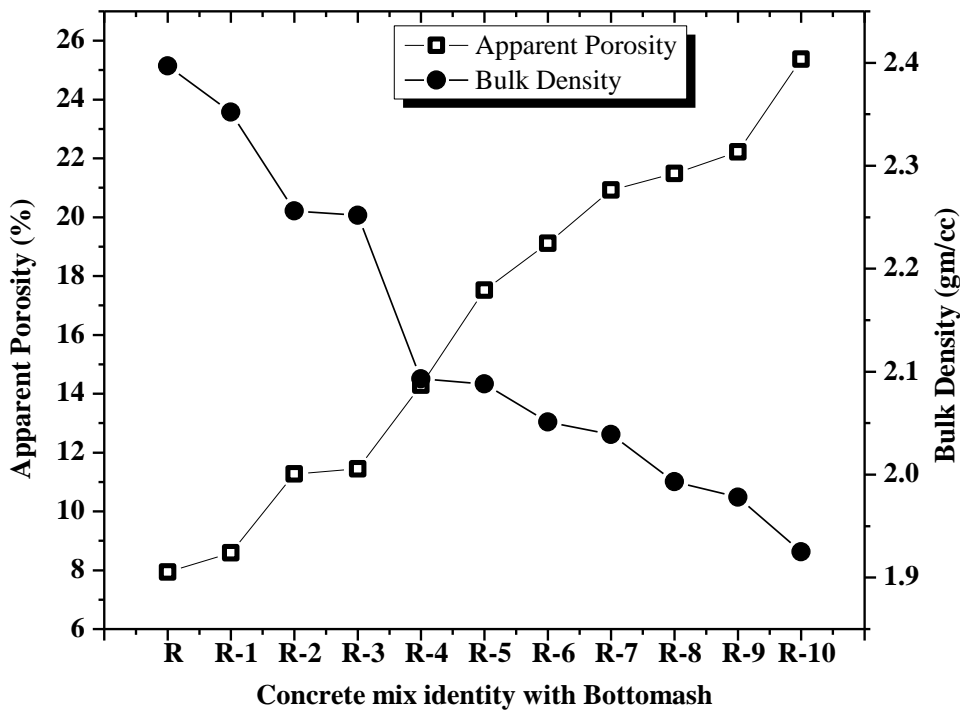


Fig. 5.58 Variations in Apparent Porosity and Bulk Density values for (Set-C, Group-C-) Concrete mix with Bottomash. (Refer Table 5.36)

Observations : Apparent porosity values of all the sand substituted mixes (R-1 to R-10) follow increasing trend w.r.t conventional mix with 100% sand (R). Bulk density values (of R-1 to R-10) also follow decreasing trend, while compared with mix R.

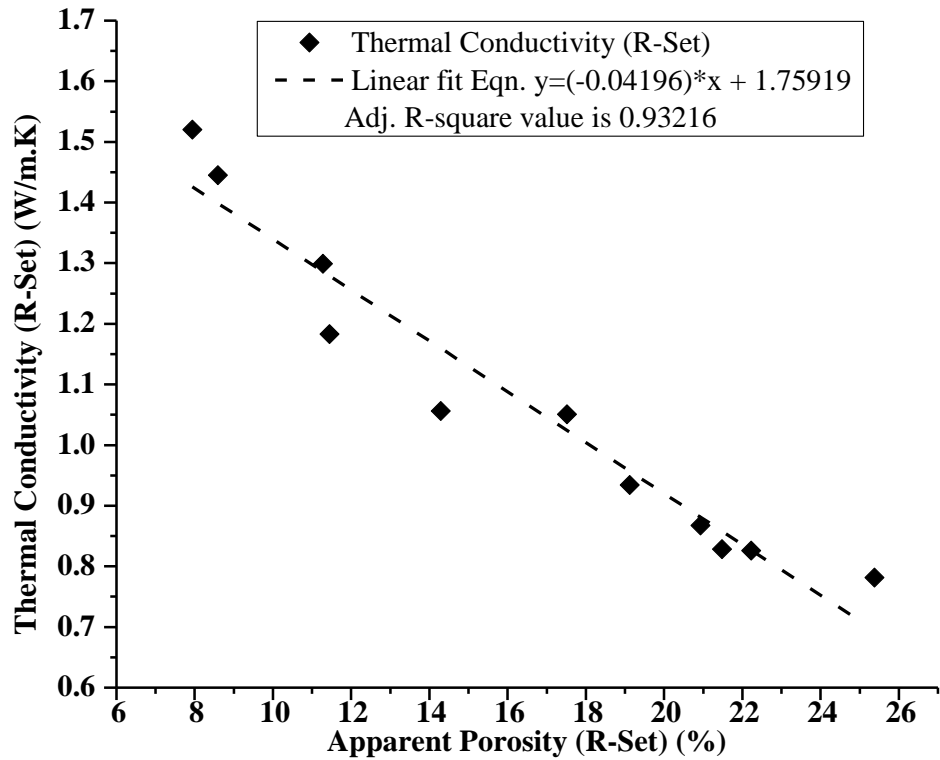


Fig. 5.59 Relationship between Apparent Porosity and Thermal Conductivity for the Concrete mix sample (Refer Table 5.35 and 5.36)

Observations : Apparent Porosity (AP) is shown to have an excellent relationship with thermal conductivity of the concrete mix sample, and the adjusted R^2 value of 0.93, (assessed the very goodness-of-fit for regression analysis by Origin 8) supports the changes in both the parameters with respect to the mix proportions. The more is apparent porosity, less is the thermal conductivity.

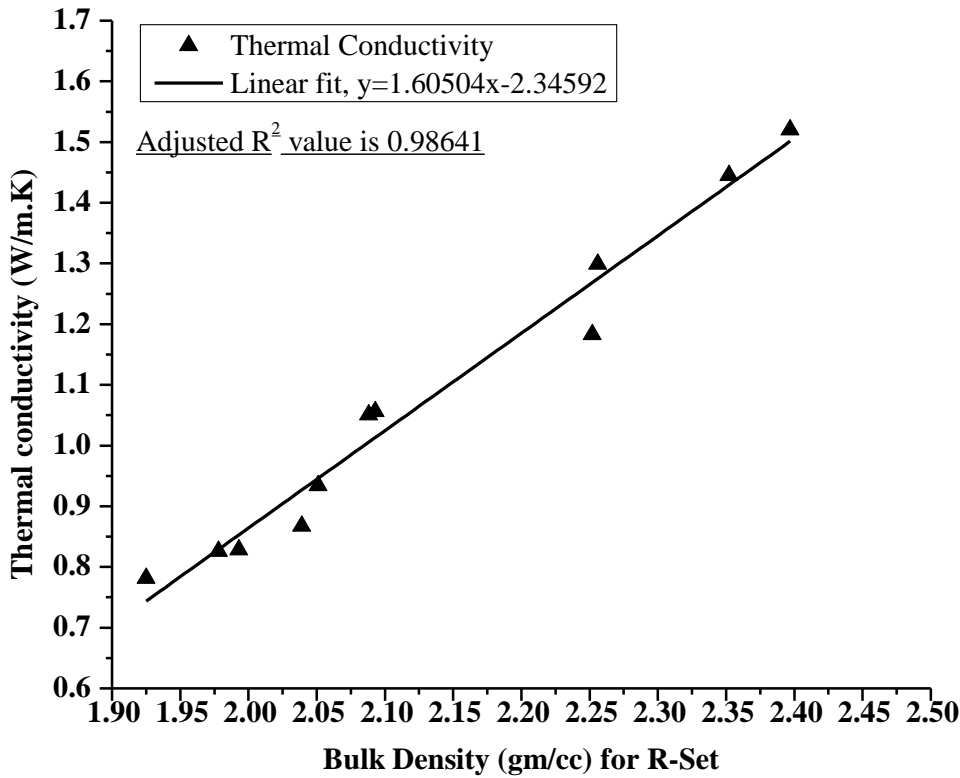


Fig. 5.60 Relationship between Bulk Density and Thermal Conductivity for the concrete mix sample (Refer Table 5.35 and 5.36)

Observations : Bulk Density is shown to have an excellent linear fit relationship with thermal conductivity of the concrete mix sample, and the adjusted R^2 value of 0.986, (assessed the very goodness-of-fit for linear regression analysis by Origin 8) supports the same. The more is the bulk density, more is the thermal conductivity.

5.5 MASONRY MORTAR

5.5.1 Introduction :

Masonry Mortars (MM) are generally specified by the grade in terms of their minimum compressive strength, as contained in IS 2250-1981. Most commonly used grades of MMs in building construction are MM3 and MM5, which contain 1 part of Cement and 6 parts of Fine Aggregate, and 1 part of Cement and 4 parts of Fine aggregate respectively. Sand is conventionally used all across the country for building construction as an integral part of Concrete and Masonry Mortar (including plaster) and termed as fine aggregate. In this work, these two grades i.e. MM3 and MM5 have been used extensively by replacing sand with flyash and bottomash separately, as well as with flyash-lime, bottomash-lime, flyash-marbledust, and bottomash-marbledust combinations in various proportions to see the changes in physical and thermal properties of the respective MMs in comparison with conventional MMs with sand.

5.5.2 Masonry Mortar of Cement – Fine aggregate combination of grade **MM3 (1:6)** Table 5.37 Gradual replacement of Sand by Fly ash and Bottom ash in MM3 Grade Mortar

Mortar mix identity	Mortar Mix (MM3 Grade)	Cement Wt. ratio	Sand Wt. ratio	Flyash Wt. ratio	Bottom ash Wt. ratio
Control	1Cement : 6 Sand	1.00	6.00	-	-
A-1	1Cement:(5.4Sand+0.6 Flyash)	1.00	5.40	0.60	-
A-2	1Cement:(4.8Sand+1.2 Flyash)	1.00	4.80	1.20	-
A-3	1Cement:(4.2Sand+1.8 Flyash)	1.00	4.20	1.80	-
A-4	1Cement:(3.6Sand+2.4 Flyash)	1.00	3.60	2.40	-
A-5	1Cement:(3.0Sand+3.0 Flyash)	1.00	3.00	3.00	-
A-6	1Cement:(2.4Sand+3.6 Flyash)	1.00	2.40	3.60	-
A-7	1Cement:(1.8Sand+4.2 Flyash)	1.00	1.80	4.20	-
A-8	1Cement:(1.2Sand+4.8 Flyash)	1.00	1.20	4.80	-
A-9	1Cement:(0.6Sand+5.4 Flyash)	1.00	0.60	5.40	-
A-10	1Cement : 6 Flyash	1.00	0.00	6.00	-
B-1	1Cement:(5.4Sand+0.6 Bottomash)	1.00	5.40	-	0.60
B-2	1Cement:(4.8Sand+1.2 Bottomash)	1.00	4.80	-	1.20
B-3	1Cement:(4.2Sand+1.8 Bottomash)	1.00	4.20	-	1.80
B-4	1Cement:(3.6Sand+2.4 Bottomash)	1.00	3.60	-	2.40
B-5	1Cement:(3.0Sand+3.0 Bottomash)	1.00	3.00	-	3.00
B-6	1Cement:(2.4Sand+3.6 Bottomash)	1.00	2.40	-	3.60
B-7	1Cement:(1.8Sand+4.2 Bottomash)	1.00	1.80	-	4.20
B-8	1Cement:(1.2Sand+4.8 Bottomash)	1.00	1.20	-	4.80
B-9	1Cement:(0.6Sand+5.4 Bottom ash)	1.00	0.60	-	5.40
B-10	1Cement : 6 Bottomash	1.00	0.00	-	6.00

Table 5.37(a) Test results of physical and thermal parameters of MM3 Grade Mortar (Gradual replacement of Sand by Flyash and Bottomash)

Mortar mix identity (MM3 Grade)	28 Days Compressive Strength (MPa)	Thermal Conductivity (W/m-K)	Apparent Porosity (%)	Bulk Density (gm/cc)	Equivalent Mortar Grade
Control	3.922	1.5890	23.333	1.933	MM3
A-1	5.91	0.9017	26.666	1.967	MM5
A-2	5.84	0.8574	22.580	1.935	MM5
A-3	5.3	0.6977	25.806	1.645	MM5
A-4	4.35	0.6505	28.125	1.594	MM4
A-5	3.26	0.5254	32.258	1.548	MM3
A-6	3.05	0.4861	35.483	1.452	MM3
A-7	2.31	0.3786	36.363	1.182	MM2
A-8	1.69	0.3484	37.142	1.171	MM1.5
A-9	1.16	0.2944	37.500	1.125	MM0.7
A-10	0.68	0.2908	38.235	1.088	MM0.7
B-1	3.19	0.8917	25.806	1.871	MM3
B-2	2.92	0.7272	26.470	1.588	MM3
B-3	2.45	0.5602	29.411	1.471	MM2
B-4	2.17	0.5681	30.555	1.389	MM2
B-5	1.7	0.5092	31.250	1.313	MM1.5
B-6	1.22	0.4341	31.250	1.281	MM0.7
B-7	1.22	0.4058	31.428	1.143	MM0.7
B-8	1.02	0.3247	32.432	1.027	MM0.7
B-9	0.95	0.2919	31.428	1.029	MM0.7
B-10	0.75	0.2876	31.428	1.000	MM0.7

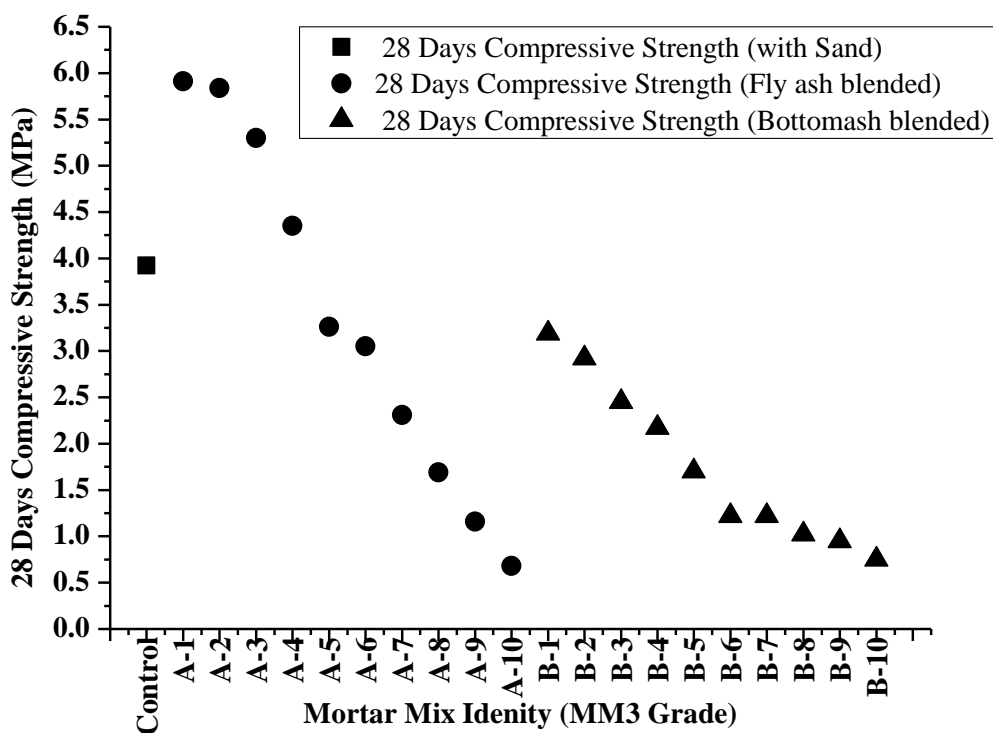


Fig. 5.61 Compressive Strength test values of MM3 Grade Mortar (Gradual replacement of Sand by Flyash in Series A and that by Bottomash in Series B) (Refer Table 5.37(a)).

Observations : Compressive strength at 28 day’s maturity for control, Flyash and Bottomash blended mortar samples are shown above. It may be seen that up to 60% and 10% sand replacement by Flyash (A-1 to A-6), and Bottomash (B-1) respectively satisfy the MM3 Grade criteria of attaining minimum 3.0 MPa value. Beyond that replacement level, the strength is reduced for both Flyash and Bottomash substituted mortar samples. From durability criteria, IS 2250 Code has specified minimum grade as MM0.7, which is satisfied by both the Flyash and Bottomash substituted mortar samples, even up to 100% sand replacement (A-10 and B-10).

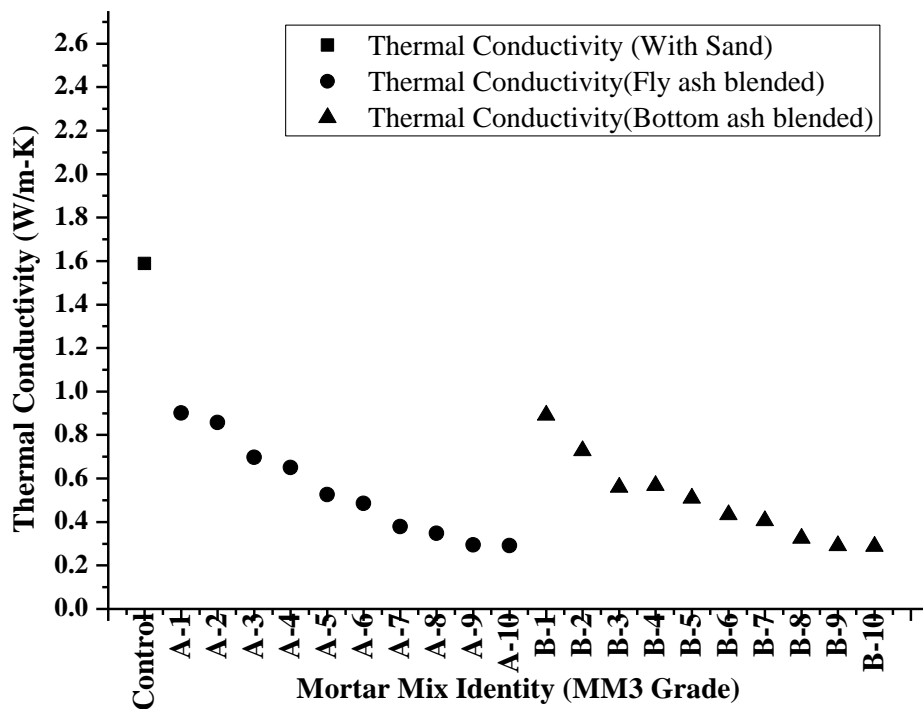


Fig. 5.62 Thermal Conductivity test values of MM3 Grade Mortar (Gradual replacement of Sand by Flyash in Series A and that by Bottomash in Series B) (Refer Table 5.37a))

Observations : It may be seen that both the Flyash and Bottomash substituted mortar mixes exhibit lesser thermal conductivity values than by control sample value. The level of reduction attained at 30% sand substitution by Flyash is 56%, at 10% sand substitution by Bottomash is 44%, and at 100% substitution rate for both Flyash and Bottomash mortar groups are 81.7% and 81.9% respectively. This reduction percentages are calculated with respect to that of control sample value.

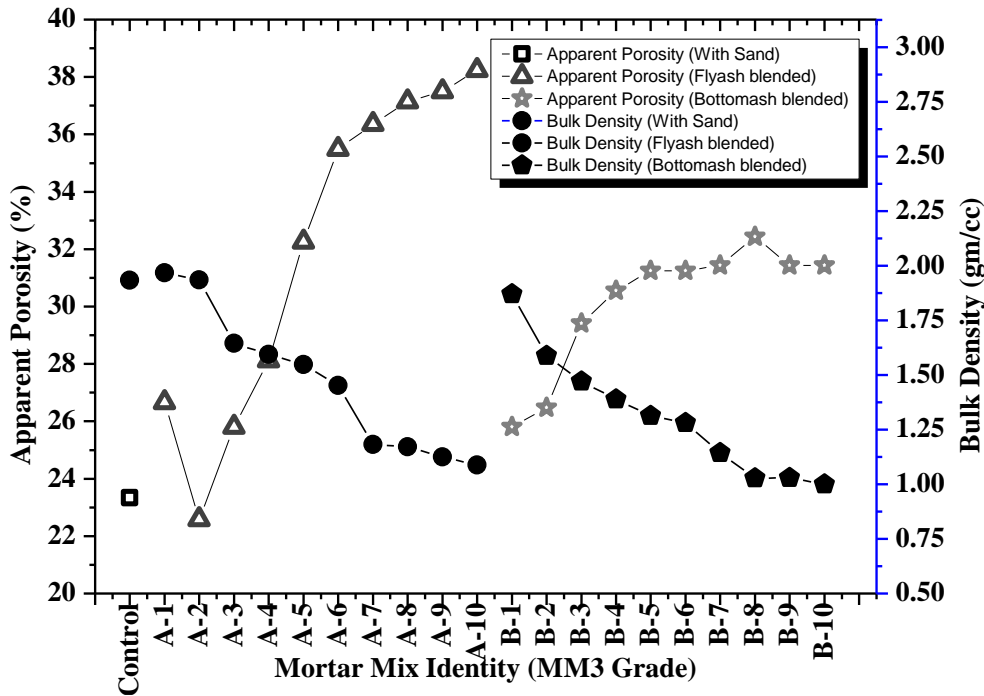


Fig. 5.63 : Apparent Porosity and Bulk Density test values of MM3 Grade Mortar (Gradual replacement of Sand by Flyash in Series A and that by Bottomash in Series B) (Refer Table 5.37a)

Observations : It may be seen that in both the cases of Flyash and Bottomash substituted mixes, initial apparent porosity values (A-1 and B-1) are higher than the control value. Bulk density values in both the cases are almost nearer to the control value. Subsequently, apparent porosity values are following increasing trend, and bulk density values are showing decreasing trend in both Flyash and Bottomash substituted mortars, in comparison with control value.

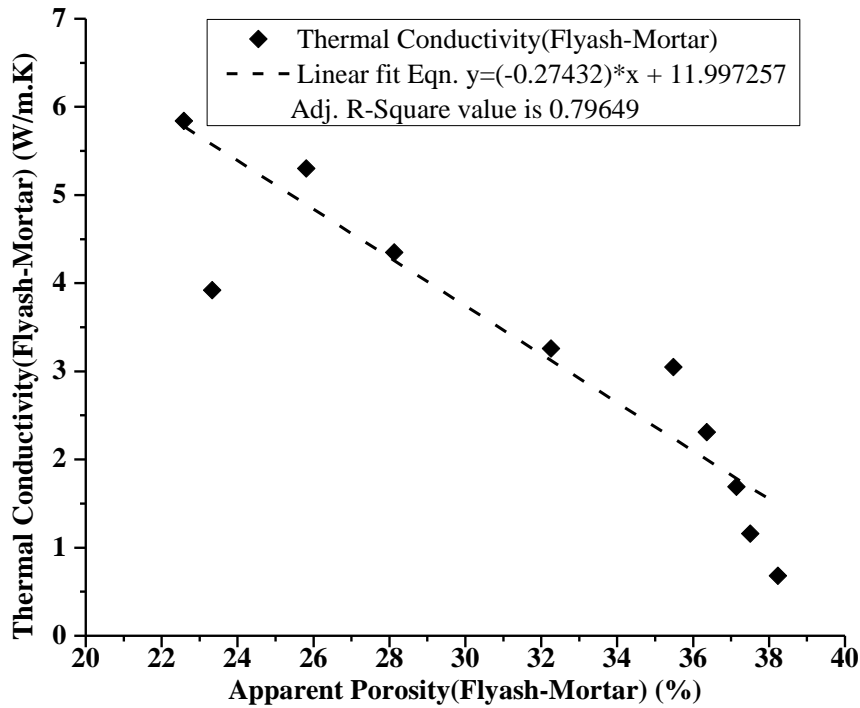


Fig. 5.64 Relationship between Apparent Porosity and Thermal Conductivity for the MM3 Grade Flyash Mortar mix sample (Refer Table 5.37a)).

Observations : Apparent Porosity (AP) is shown to have a good relationship with thermal conductivity of the concrete mix sample, and the adjusted R^2 value of 0.80, (assessed the goodness-of-fit for regression analysis by Origin 8) supports the changes in both the parameters with respect to the mix proportions. The more is apparent porosity, less is the thermal conductivity.

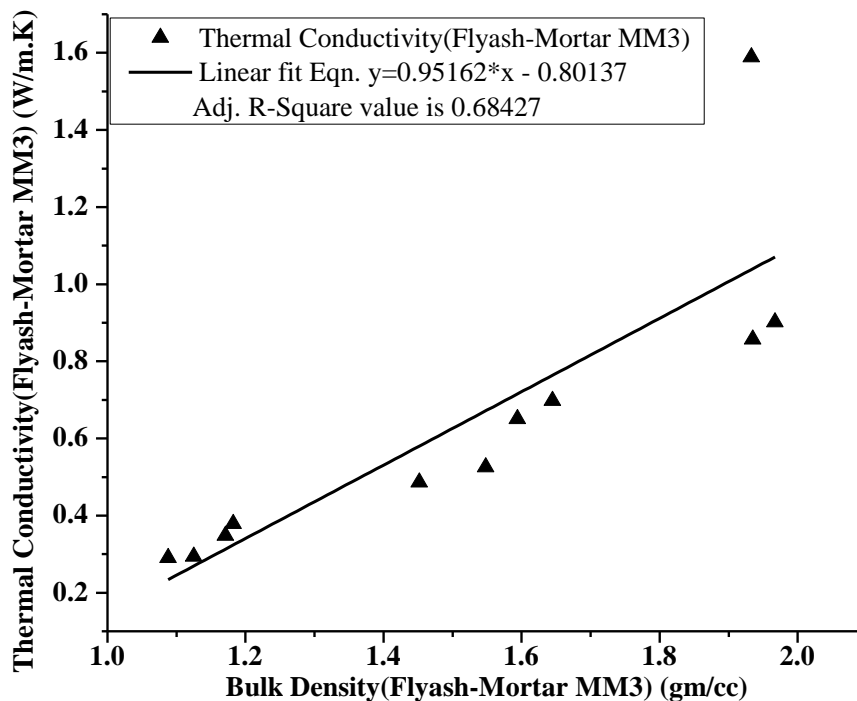


Fig. 5.65 Relationship between Bulk Density and Thermal Conductivity for the MM3 Grade Flyash Mortar mix sample (Refer Table 5.37a)).

Observations : Bulk Density is shown to have an average relationship with thermal conductivity of the concrete mix sample, and the adjusted R^2 value of 0.68, (assessed the goodness-of-fit for regression analysis by Origin 8) supports the changes in both the parameters with respect to the mix proportions. The more is apparent porosity, less is the thermal conductivity.

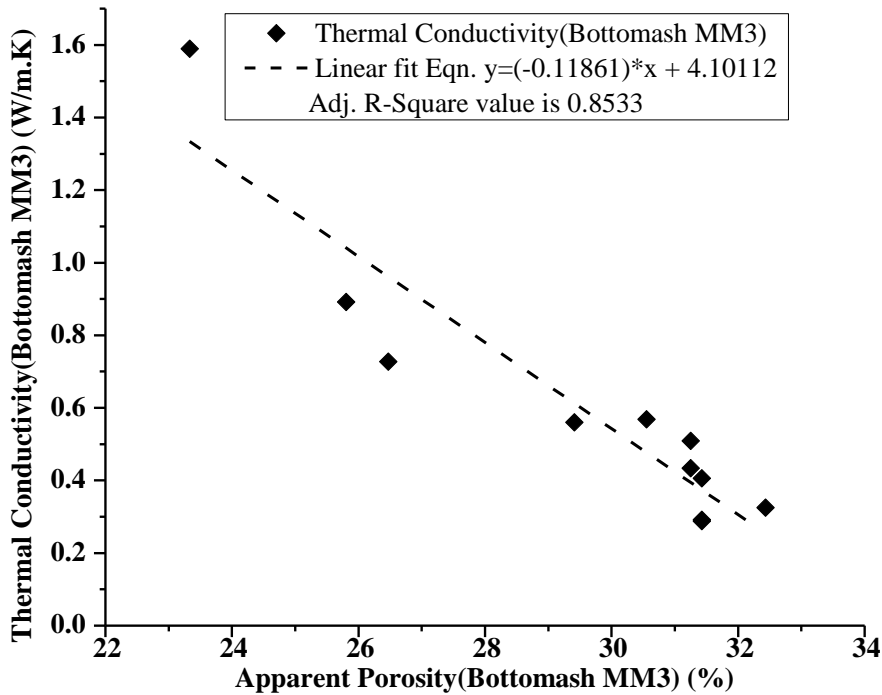


Fig. 5.66 Relationship between Apparent Porosity and Thermal Conductivity for the MM3 Grade Bottomash Mortar mix sample (Refer Table 5.37a)).

Observations : Apparent Porosity (AP) is shown to have a good relationship with thermal conductivity of the concrete mix sample, and the adjusted R^2 value of 0.85, (assessed the goodness-of-fit for regression analysis by Origin 8) supports the changes in both the parameters with respect to the mix proportions. The more is apparent porosity, less is the thermal conductivity.

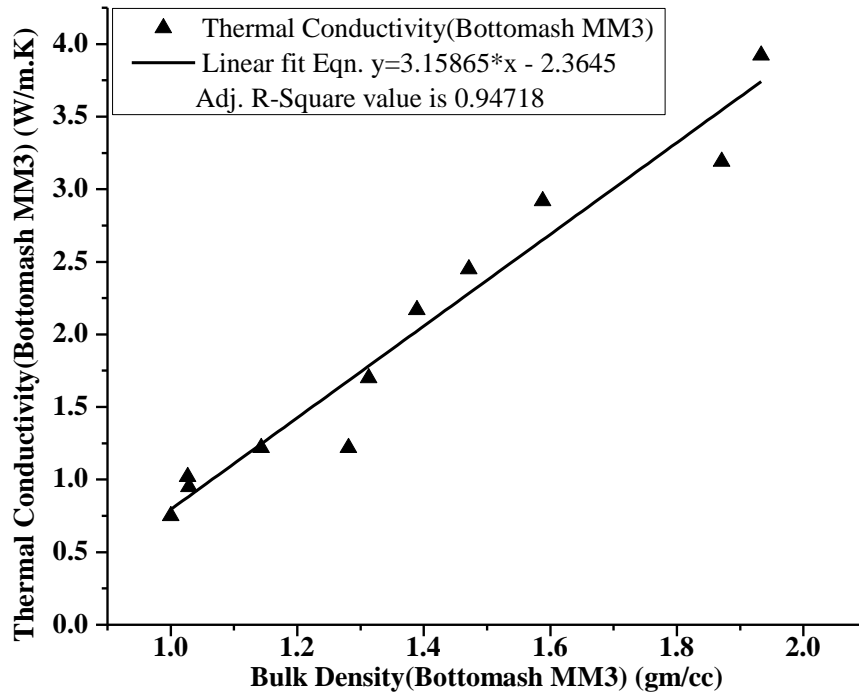


Fig. 5.67 Relationship between Bulk Density and Thermal Conductivity for the MM3 Grade Bottomash Mortar mix sample (Refer Table 5.37a)).

Observations : Bulk Density is shown to have an excellent relationship with thermal conductivity of the concrete mix sample, and the adjusted R^2 value of 0.95, (assessed the very goodness-of-fit for regression analysis by Origin 8) supports the changes in both the parameters with respect to the mix proportions. The more is bulk density, more is the thermal conductivity.

5.5.3 Masonry Mortar of Cement– Fine aggregate combination of Grade **MM5 (1:4)**

Table 5.38: Gradual replacement of Sand by Flyash & Bottomash in MM5 Grade Mortar

Mortar mix identity	Mortar Mix (MM5 Grade)	Cement Wt. ratio	Sand Wt. ratio	Fly ash Wt. ratio	Bottomash Wt. ratio
Control	1Cement : 4 Sand	1.00	4.00	-	-
C-1	1Cement: 4(3.6Sand+0.4 Flyash)	1.00	3.60	0.40	-
C-2	1Cement: 4(3.2Sand+0.8 Flyash)	1.00	3.20	0.80	-
C-3	1Cement: 4(2.8Sand+1.2 Flyash)	1.00	2.80	1.20	-
C-4	1Cement: 4(2.4Sand+1.6 Flyash)	1.00	2.40	1.60	-
C-5	1Cement: 4(2.0Sand+2.0 Flyash)	1.00	2.00	2.00	-
C-6	1Cement: 4(1.6Sand+2.4 Flyash)	1.00	1.60	2.40	-
C-7	1Cement: 4(1.2Sand+2.8 Flyash)	1.00	1.20	2.80	-
C-8	1Cement: 4(0.8Sand+3.2 Flyash)	1.00	0.80	3.20	-
C-9	1Cement: 4(0.4Sand+3.6 Flyash)	1.00	0.40	3.60	-
C-10	1Cement : 4 Flyash	1.00	0.00	4.00	-
D-1	1Cement: 4(3.6Sand+0.4 Bottomash)	1.00	3.60	-	0.40
D-2	1Cement: 4(3.2Sand+0.8 Bottomash)	1.00	3.20	-	0.80
D-3	1Cement: 4(2.8Sand+1.2 Bottomash)	1.00	2.80	-	1.20
D-4	1Cement: 4(2.4Sand+1.6 Bottomash)	1.00	2.40	-	1.60
D-5	1Cement: 4(2.0Sand+2.0 Bottomash)	1.00	2.00	-	2.00
D-6	1Cement:4(1.6Sand+2.4 Bottomash)	1.00	1.60	-	2.40
D-7	1Cement: 4(1.2Sand+2.8 Bottomash)	1.00	1.20	-	2.80
D-8	1Cement: 4(0.8Sand+3.2 Bottomash)	1.00	0.80	-	3.20
D-9	1Cement: 4(0.4Sand+3.6 Bottomash)	1.00	0.40	-	3.60
D-10	1Cement : 4 Bottomash	1.00	0.00	-	4.00

Table 5.38(a): Test results of physical and thermal parameters of MM5 Grade Mortar

Mortar Mix Identity	28 Days Compressive Strength (MPa)	Thermal Conductivity (W/m-K)	Apparent Porosity (%)	Bulk Density (gm/cc)	Equivalent Grade of Mortar
Control	10.06	1.198	24.242	1.970	MM10
C-1	11.96	1.103	25.000	1.650	MM10
C-2	9.45	0.9014	26.470	1.676	MM9
C-3	8.56	0.8008	27.777	1.667	MM8.5
C-4	6.8	0.6509	30.303	1.606	MM6
C-5	5.71	0.6073	33.333	1.606	MM5
C-6	3.81	0.5517	33.333	1.533	MM3
C-7	2.31	0.3874	38.709	1.484	MM2
C-8	1.09	0.3746	40.625	1.250	MM0.7
C-9	0.95	0.3509	41.935	1.258	MM0.7
C-10	0.88	0.3222	43.750	1.188	MM0.7
D-1	7.2	1.107	26.666	1.833	MM7
D-2	6.52	0.8861	29.032	1.742	MM5
D-3	5.91	0.6936	33.333	1.667	MM5

D-4	5.84	0.6171	33.333	1.600	MM5
D-5	5.16	0.5673	34.482	1.448	MM5
D-6	4.62	0.4802	35.294	1.324	MM3
D-7	3.94	0.4285	39.393	1.212	MM3
D-8	3.33	0.3644	39.393	1.152	MM3
D-9	2.85	0.3295	40.000	1.086	MM2
D-10	2.72	0.2812	42.424	1.091	MM2

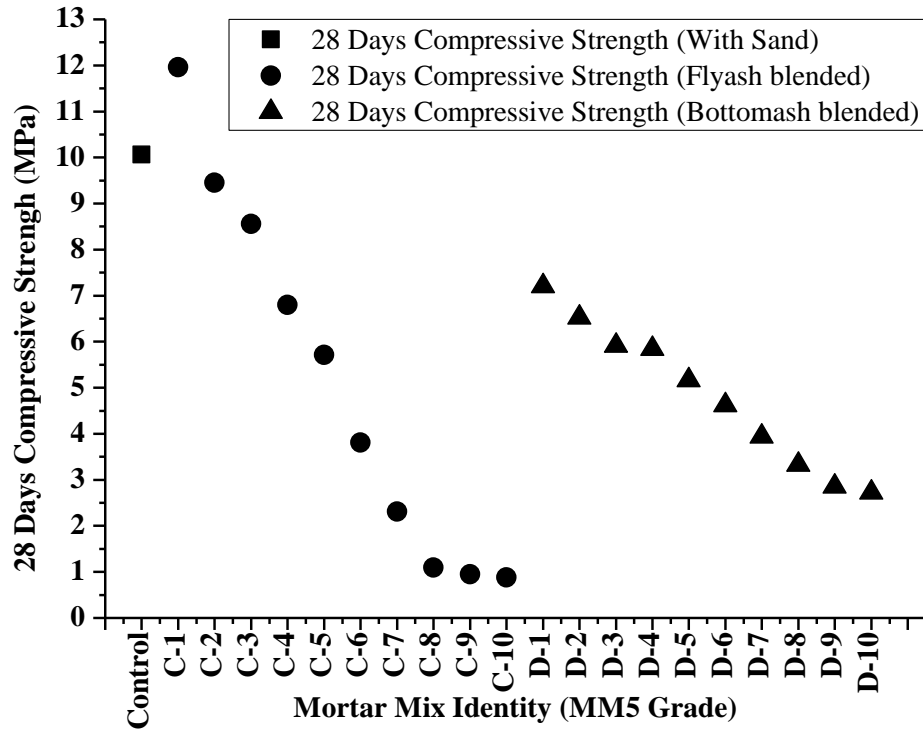


Fig. 5.68 Compressive Strength test values of MM5 Grade Mortar (Gradual replacement of Sand by Flyash in Series C and by Bottomash in Series D) (Refer Table 5.38a))

Observations : Up to 50% substitution of sand by Flyash and Bottomash mortar mixes (C-5 and D-5), the strength criteria of MM5 grade mortar as per IS 2250 are satisfied, and beyond that point up to 100% substitution, both the groups of mortars satisfy the minimum MM0.7 grade criteria, as specified in the Code. Even 100% Bottomash substituted mix exhibited strength value nearer to MM3 grade equivalent.

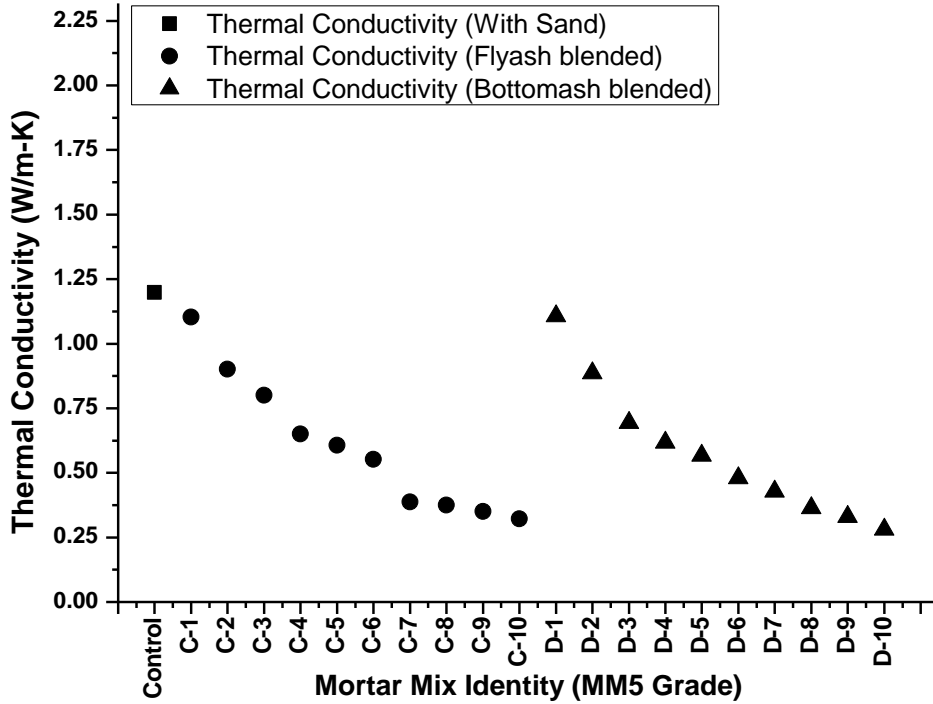


Fig. 5.69 Thermal Conductivity test values of MM5 Grade Mortar (Gradual replacement of Sand by Flyash in Series C and by Bottomash in Series D) (Refer Table 5.38a)

Observation : It may be seen that both the Flyash and Bottomash substituted mortar mixes exhibit lesser thermal conductivity values than by control sample value. The level of reductions attained at 50% sand substitution by Flyash and Bottomash are 49%, and 53% respectively. At 100% substitution rate for both Flyash and Bottomash mortar groups are 73% and 76.5% respectively.

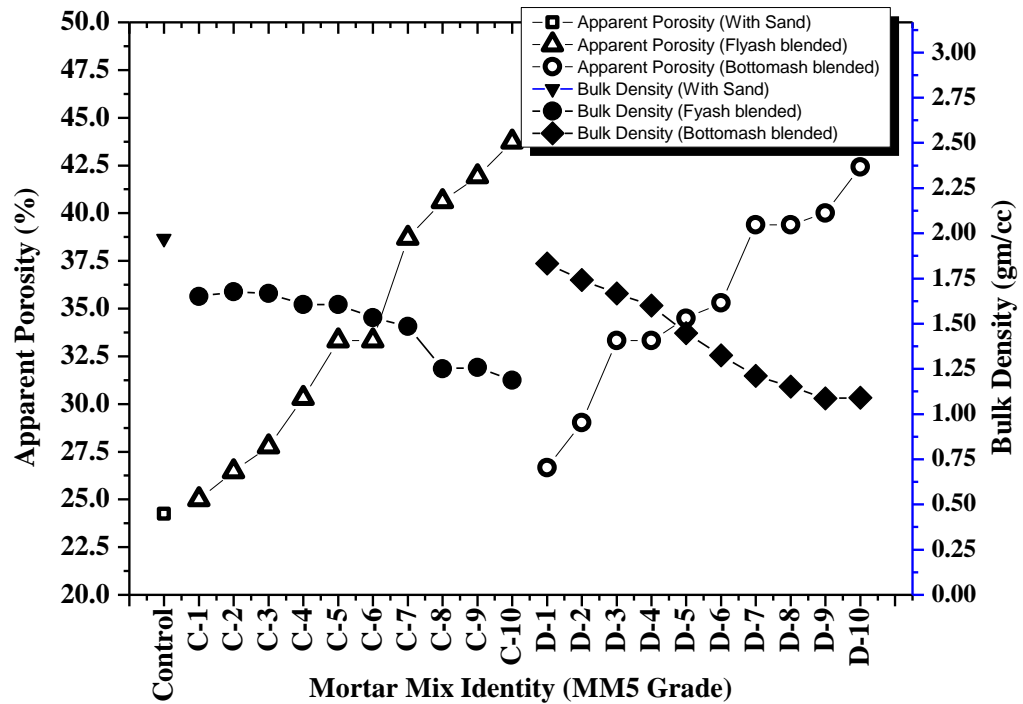


Fig.5.70 Apparent Porosity and Bulk Density test values of MM5 Grade Mortar (Gradual replacement of Sand by Flyash in Series C and by Bottomash in Series D) (Refer Table 5.38a))

Observations : It may be seen that in both the cases of Flyash and Bottomash substituted mixes, initial apparent porosity values (A-1 and B-1) are higher than the control value. Bulk density values in both the cases are lower than the control value. Subsequently, apparent porosity values are following increasing trend, and bulk density values are showing decreasing trend in both Flyash and Bottomash substituted mortars, in comparison with control mortar.

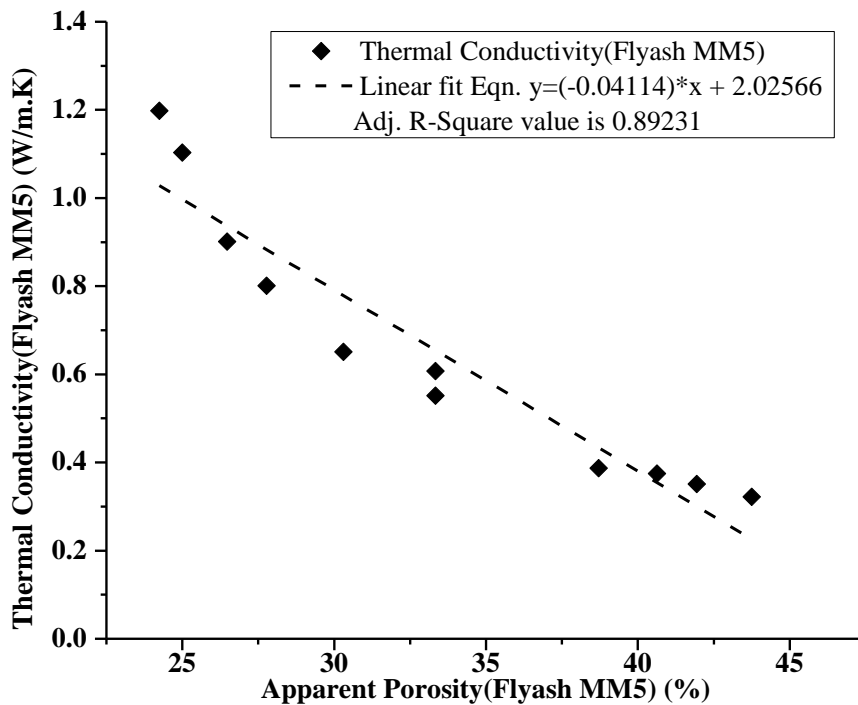


Fig. 5.71 Relationship between Apparent Porosity and Thermal Conductivity for the MM5 Grade Flyash Mortar mix sample (Refer Table 5.38a)).

Observations : Apparent Porosity (AP) is shown to have a good relationship with thermal conductivity of the concrete mix sample, and the adjusted R^2 value of 0.89, (assessed the goodness-of-fit for regression analysis by Origin 8) supports the changes in both the parameters with respect to the mix proportions. The more is apparent porosity, less is the thermal conductivity.

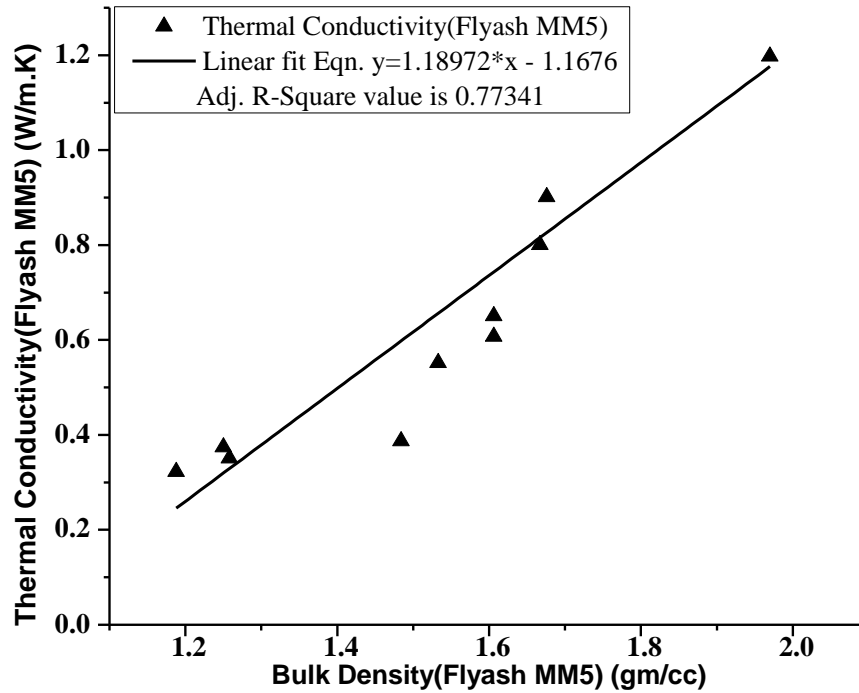


Fig. 5.72 Relationship between Bulk Density and Thermal Conductivity for the MM5 Grade Flyash Mortar mix sample (Refer Table 5.38a)).

Observations : Bulk Density is shown to have a good relationship with thermal conductivity of the concrete mix sample, and the adjusted R^2 value of 0.77, (assessed the goodness-of-fit for regression analysis by Origin 8) supports the changes in both the parameters with respect to the mix proportions. The more is bulk density, less is the thermal conductivity.

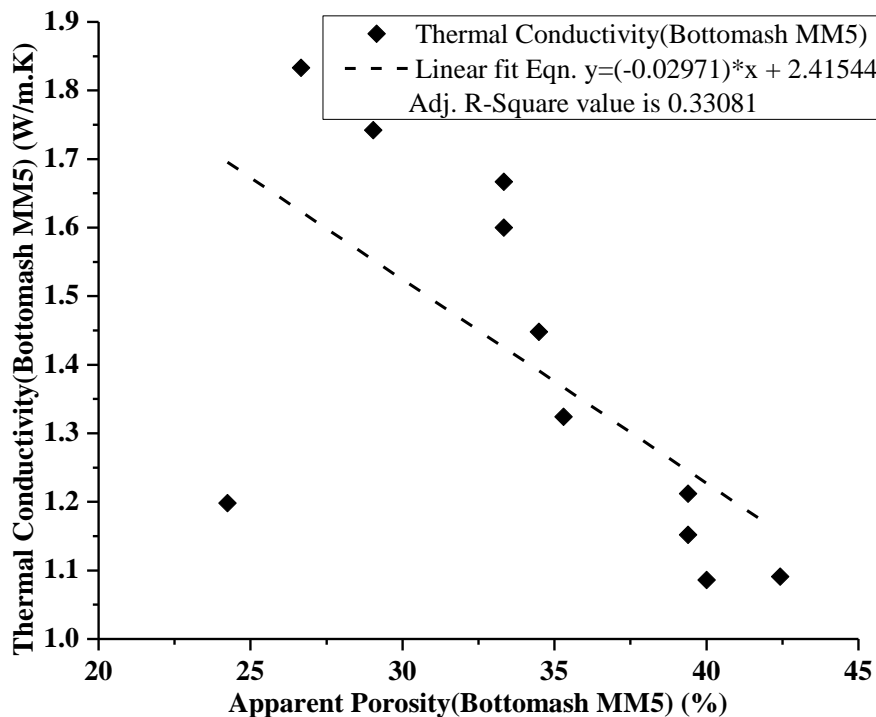


Fig. 5.73 Relationship between Apparent Porosity and Thermal Conductivity for the MM5 Grade Bottomash Mortar mix sample (Refer Table 5.38a)).

Observations : In this case, Apparent Porosity (AP) is shown to have not so good relationship with thermal conductivity of the concrete mix sample, and the adjusted R^2 value of 0.33, (assessed the goodness-of-fit for regression analysis by Origin 8) do not support well, the changes in both the parameters with respect to the mix proportions. The more is apparent porosity, less is the thermal conductivity is not clearly established, may be due to some experimental error in data recording and assimilation.

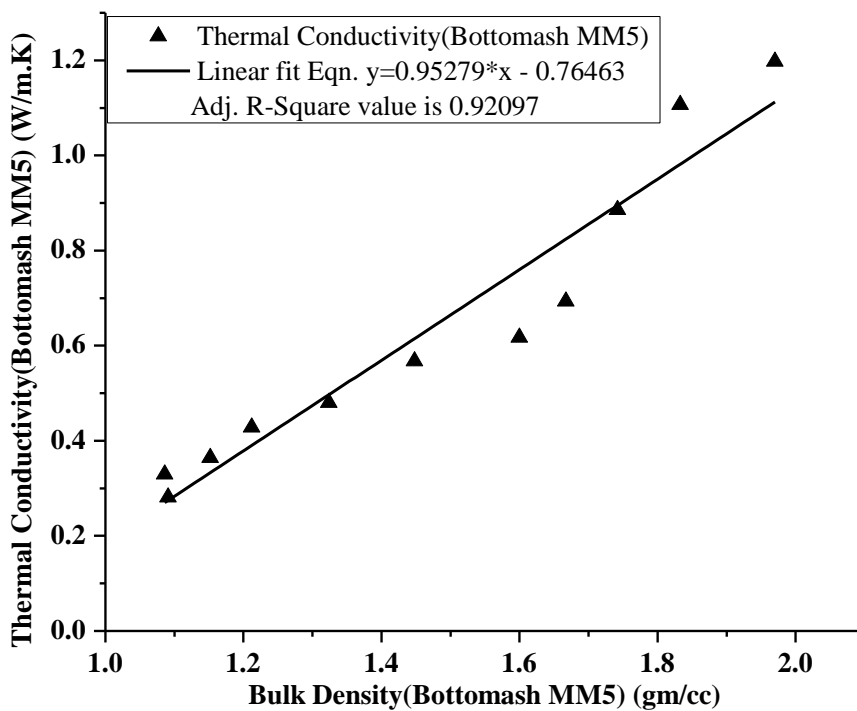


Fig. 5.74 Relationship between Bulk Density and Thermal Conductivity for the MM5 Grade Bottomash Mortar mix sample (Refer Table 5.38a)).

Observations : Bulk Density is shown to have a very good relationship with thermal conductivity of the concrete mix sample, and the adjusted R^2 value of 0.92, (assessed the goodness-of-fit for regression analysis by Origin 8) supports the changes in both the parameters with respect to the mix proportions. The more is bulk density, more is the thermal conductivity.

5.5.4 Masonry Mortar of Cement – Fine aggregate combination of grade **MM3 (1:6)** **Totally Sand less** by incorporating Limedust, Marbledust with Flyash and Bottomash in different proportion combinations.

Table 5.39 Total replacement of Sand by Flyash and Bottomash in MM3 Grade Mortar

Mortar Mix identit	Mortar Mix (MM3 Grade)	Cement	Sand	Fly ash	Bottom ash	Lime dust	Marble dust
1	1Cement : 6 Sand	1.00	6.00	-	-	-	-
2	1Cement: 6(3.0 Limedust+3.0 Flyash)	1.00	-	3.00	-	3.00	-
3	1Cement: 6(3.0 Marbledust+3.0 Flyash)	1.00	-	3.00	-	-	3.00
4	1Cement: 6Flyash	1.00	-	6.00	-	-	-
5	1Cement: 6(3.0Limedust+ 3.0 Bottomash)	1.00	-	-	3.00	3.00	-
6	1Cement: 6(3.0Marbledust + 3.0 Bottomash)	1.00	-	-	3.00	-	3.00
7	1Cement : 6 Bottomash)	1.00	-	-	6.00	-	-

Table 5.39(a) Test results of physical and thermal parameters of MM3 Grade Mortar (Total replacement of Sand by Fly ash and Bottom ash)

Mortar Mix Identity (MM3 Grade) Without Sand	28 Days Compressive Strength (MPa)	Thermal Conductivity (W/m-K)	Apparent Porosity (%)	Bulk Density (gm/cc)	Equivalent Grade of Mortar
1	3.922	1.589	23.333	1.933	MM3
2	3.591	0.686	22.222	1.667	MM3
3	2.310	0.480	31.578	1.132	MM2
4	0.930	0.346	30.769	1.059	MM0.7
5	3.490	0.676	23.529	1.735	MM3
6	2.650	0.578	34.482	1.448	MM2
7	0.900	0.325	31.250	1.037	MM0.7

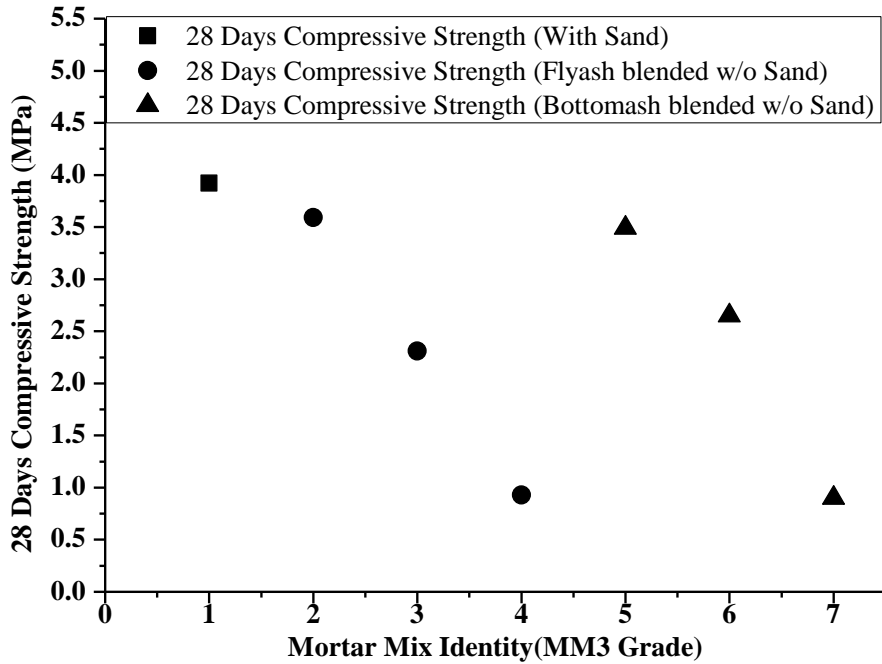


Fig. 5.75 Compressive Strength test values of MM3 Grade Mortar (Total replacement of Sand by Flyash and Bottomash) (Refer Table 5.39a)

Observations : It may be observed that Flyash-Lime and Bottomash-Lime combination mortar mixes (2 and 5), the strength criteria of MM3 grade mortar as per IS 2250 are well satisfied, and beyond that point up to 100% substitution, both the groups of mortars satisfy the minimum MM0.7 grade criteria, as specified in the Code.

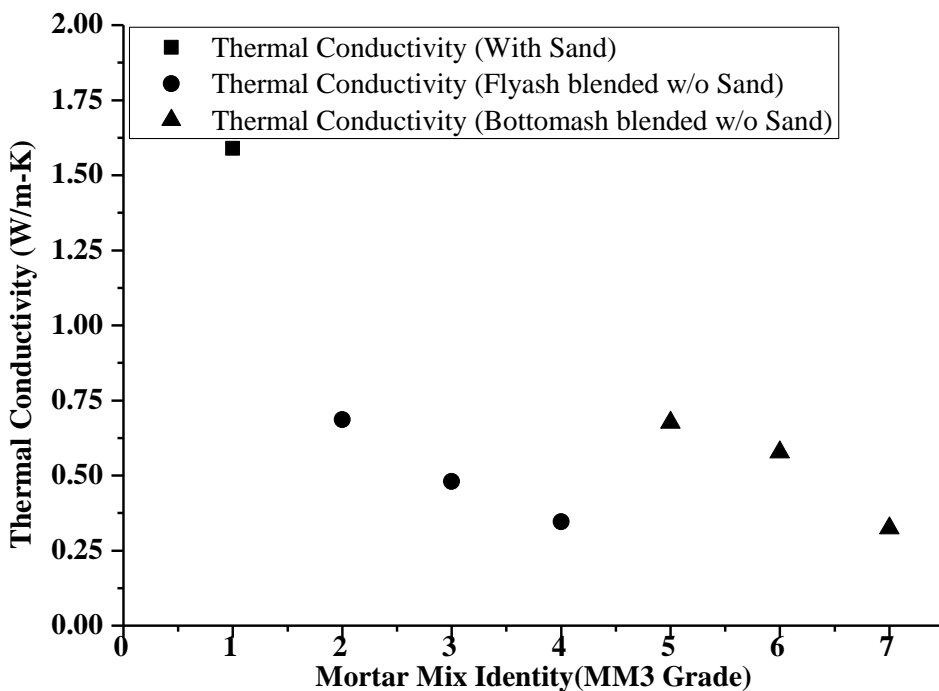


Fig. 5.76 Thermal Conductivity test values of MM3 Grade Mortar (Total replacement of Sand) (Refer Rable 5.39a))

Observations : It may be seen that both the Flyash and Bottomash substituted mortar mixes exhibit quite lesser thermal conductivity values than control sample value. The level of reductions attained by Flyash-Lime (2) and Bottomash-Lime (5) combinations in lieu of sand totally are 57%, and 57.5% respectively. At 100% Flyash and Bottomash substitutions (4 and 7), the reduction rate for both the mortar groups are 78% and 79.5% respectively.

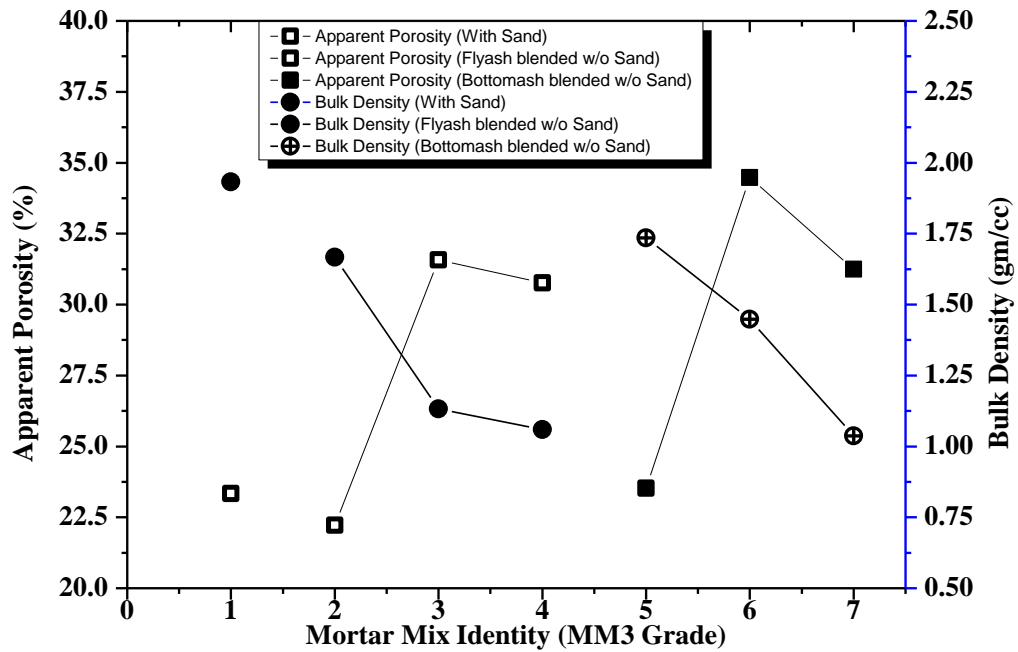


Fig.5.77 Apparent Porosity and Bulk Density test values of MM3 Grade Mortar (Total replacement of Sand by Flyash and Bottomash) (Refer Table 5.39a))

Observations : It may be seen that in Flyash-Lime combination mix (2) apparent porosity value is lower than control sample value (1) and Bottomash-Lime combination mix (5), that value is almost identical with control value. Bulk density values in both the cases are lower than the control value. Subsequently, apparent porosity values are following increasing trend, and bulk density values are showing decreasing trend in Flyash-Lime, Flyash-Marbledust, Flyash only, Bottomash-Lime Bottomash-Marbledust, and Bottomash only combination mortars (2,3,4,5,6 and 7), in comparison with control value (1).

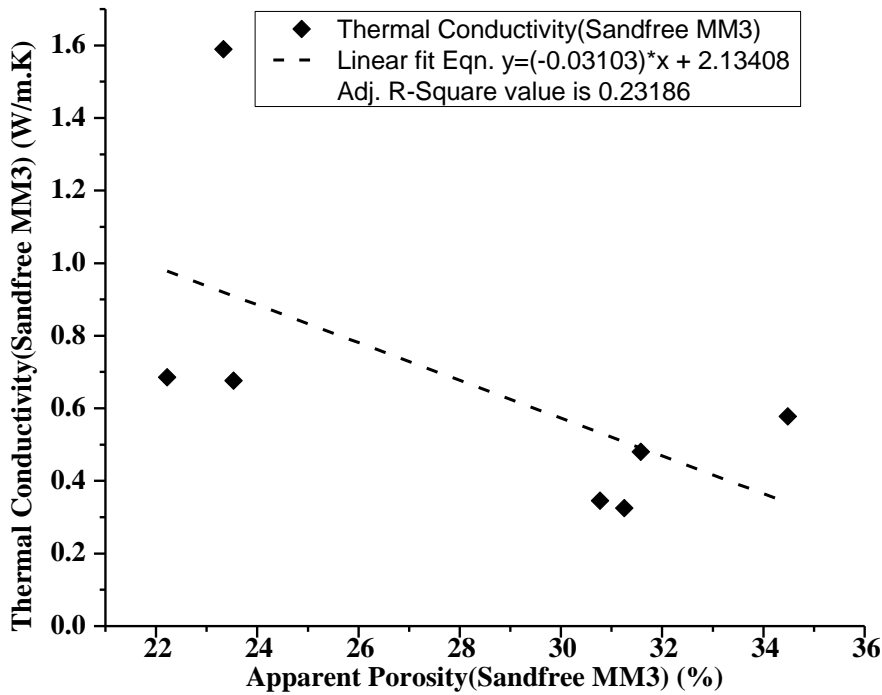


Fig. 5.78 Relationship between Apparent Porosity and Thermal Conductivity for the MM3 Grade Sand free Mortar mix sample (Refer Table 5.39a).

Observations : In this case, Apparent Porosity (AP) is shown to have not so good relationship with thermal conductivity of the concrete mix sample, and the adjusted R^2 value of 0.23, (assessed the goodness-of-fit for regression analysis by Origin 8) do not support well, the changes in both the parameters with respect to the mix proportions. The more is apparent porosity, less is the thermal conductivity is not clearly established, may be due to some experimental error in data recording and assimilation.

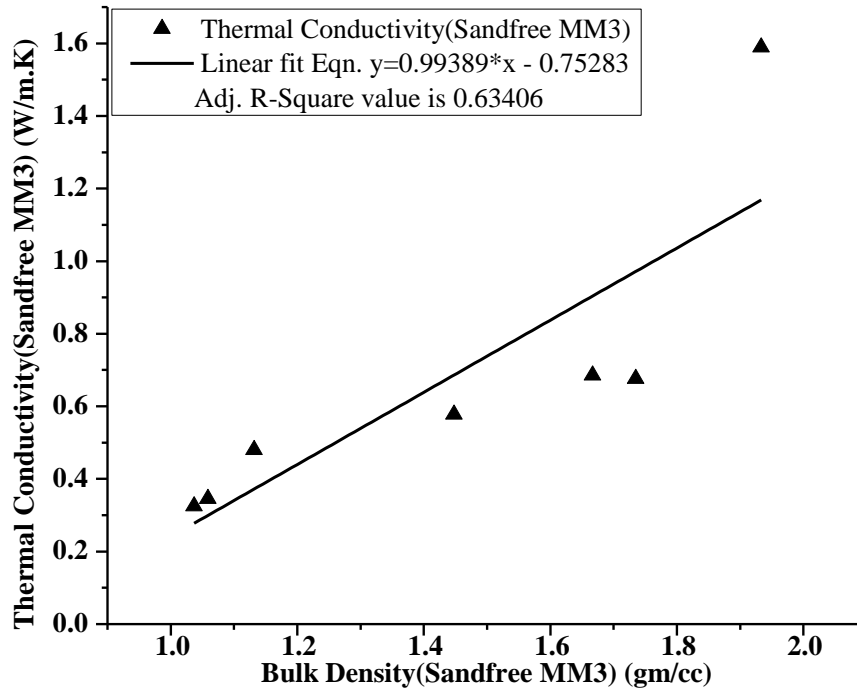


Fig. 5.79 Relationship between Bulk Density and Thermal Conductivity for the MM3 Grade Sand free Mortar mix sample (Refer Table 5.38a)).

Observations : Bulk Density is shown to have a fair relationship with thermal conductivity of the concrete mix sample, and the adjusted R^2 value of 0.63, (assessed the goodness-of-fit for regression analysis by Origin 8) supports the changes in both the parameters with respect to the mix proportions. The more is bulk density, more is the thermal conductivity.

5.5.5 Masonry Mortar of Cement – Fine aggregate combination of grade MM5 (1:4) Totally Sand less by incorporating Limedust, Marbledust with Flyash and Bottomash in different proportion combinations.

Table 5.40 Total replacement of Sand by Flyash and Bottomash in MM5 Grade Mortar

Mortar mix id.	Mortar Mix (MM5 Grade)	Cement	Sand	Flyash	Bottom ash	Lime dust	Marble dust
8	1Cement : 4 Sand	1.00	4.00	-	-	-	-
9	1Cement: 4(2.0 Limedust+2.0 Flyash)	1.00	-	2.00	-	2.00	-
10	1Cement: 4(2.0 Marbledust +2.0 Flyash)	1.00	-	2.00	-	-	2.00
11	1Cement : 4 Flyash	1.00	-	4.00	-	-	-
12	1Cement: 4(2.0 Limedust+2.0 Bottomash)	1.00	-	-	2.00	2.00	-
13	1Cement: 4(2.0 Marble dust +2.0 Bottomash)	1.00	-	-	2.00	-	2.00
14	1Cement : 4 Bottomash)	1.00	-	-	4.00	-	-

Table 5.40(a) Test results of physical and thermal parameters of MM5 Grade Mortar (Total replacement of Sand by Flyash and Bottomash)

Mortar Mix Identity	28 Days Compressive Strength (MPa)	Thermal Conductivity (W/m-K)	Apparent Porosity (%)	Bulk Density (gm/cc)	Equivalent Grade of Mortar
8	19.031	2.308	21.428	2.271	MM19
9	5.670	0.485	32.444	1.605	MM5
10	3.220	0.542	31.868	1.564	MM3
11	0.900	0.427	34.769	1.480	MM0.7
12	6.760	0.485	32.45	1.615	MM5
13	3.740	0.486	33.8	1.595	MM3
14	0.900	0.401	35.65	1.495	MM0.7

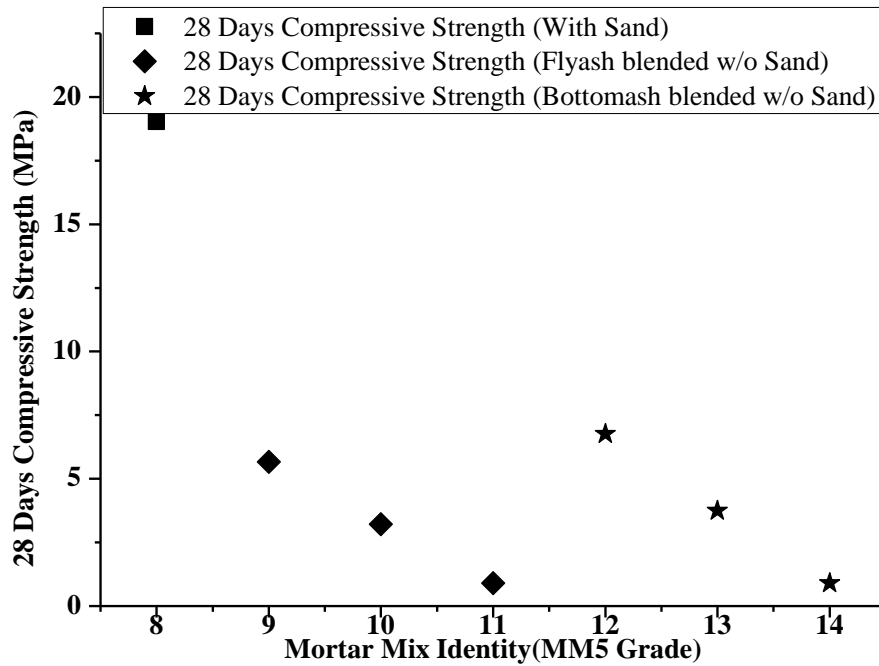


Fig.5.80 Compressive Strength test values of MM5 Grade Mortar (Total replacement of Sand by Flyash and Bottomash) (Refer Table 5.40a)

Observations : It may be observed that Flyash-Lime and Bottomash-Lime combination mortar mixes (9 and 12), the strength criteria of MM5 grade mortar as per IS 2250 are well satisfied, and beyond that point up to 100% substitution (11 and 14), both the groups of mortars satisfy the minimum MM0.7 grade criteria, as specified in the Code. Even Flyash-Marbledust and Bottomash-Marbledust combination mortar mixes (10 and 13) reach at least MM3 grade equivalent strength.

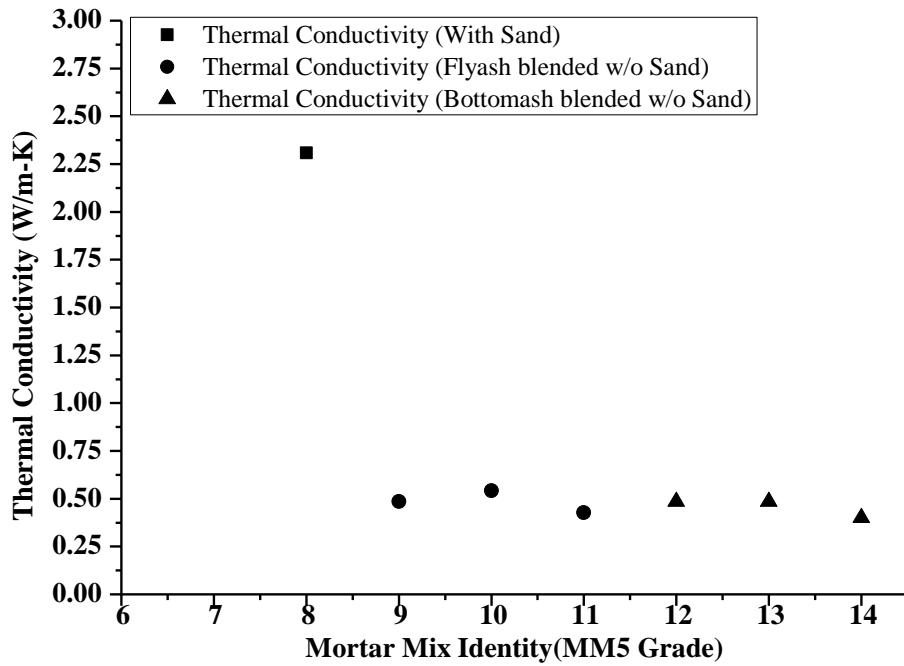


Fig.5.81 Thermal Conductivity test values of MM5 Grade Mortar (Total replacement of Sand by Flyash and Bottomash) (Refer Table 5.40a)

Observations : It may be seen that both the Flyash and Bottomash substituted mortar mixes exhibit quite lesser thermal conductivity values than control sample value. The level of reductions attained by Flyash-Lime (9), Flyash-Marbledust (10), Bottomash-lime (12), and Bottomash-Marbledust (13) combinations in lieu of sand are 79%, 76.5%, 79%, and 79% respectively. At 100% Flyash and Bottomash substitutions (11 and 14), the reduction rate for both the mortar groups are 81.5% and 82.6% respectively.

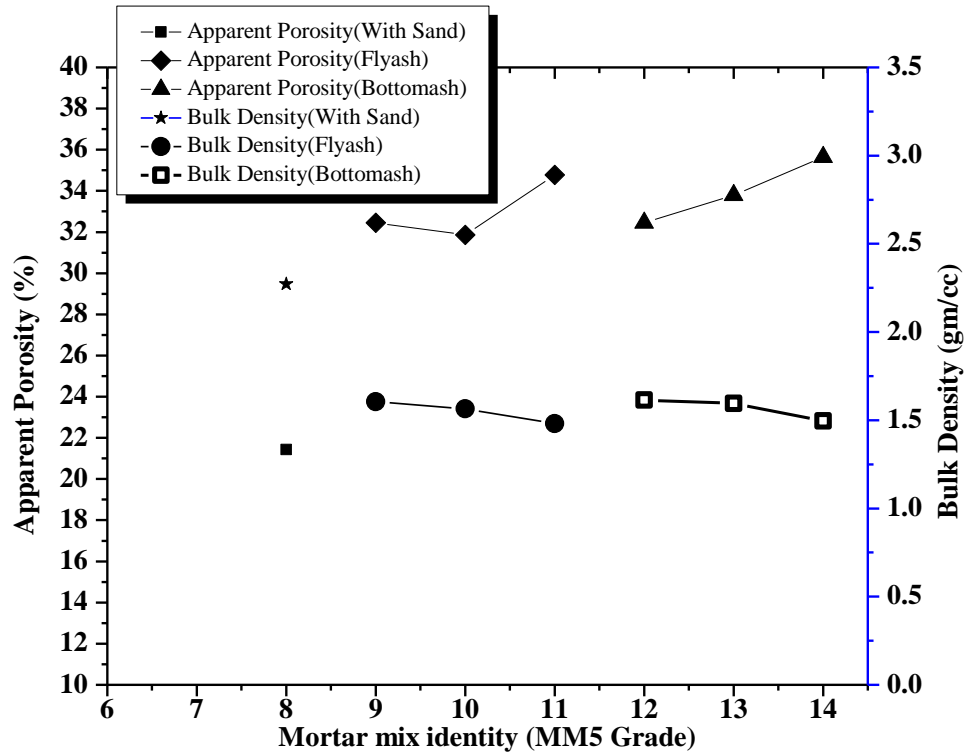


Fig. 5.82 Apparent Porosity and Bulk Density test values of MM5 Grade Mortar (Total replacement of Sand by Flyash and Bottomash) (Refer Table 5.40a)

Observations : It may be seen that in Flyash-Lime combination mix (9) apparent porosity value is higher than control sample value (8) and Bottomash-Lime combination mix (12), is also higher than the control value. Bulk density values in both the cases are lower than the control value. Subsequently, apparent porosity values are following increasing trend, and bulk density values are showing decreasing trend in Flyash-Lime, Flyash-Marbledust, Flyash only, Bottomash-Lime Bottomash-Marbledust, and Bottomash only combination mortars (9 to 14), in comparison with control value (8).

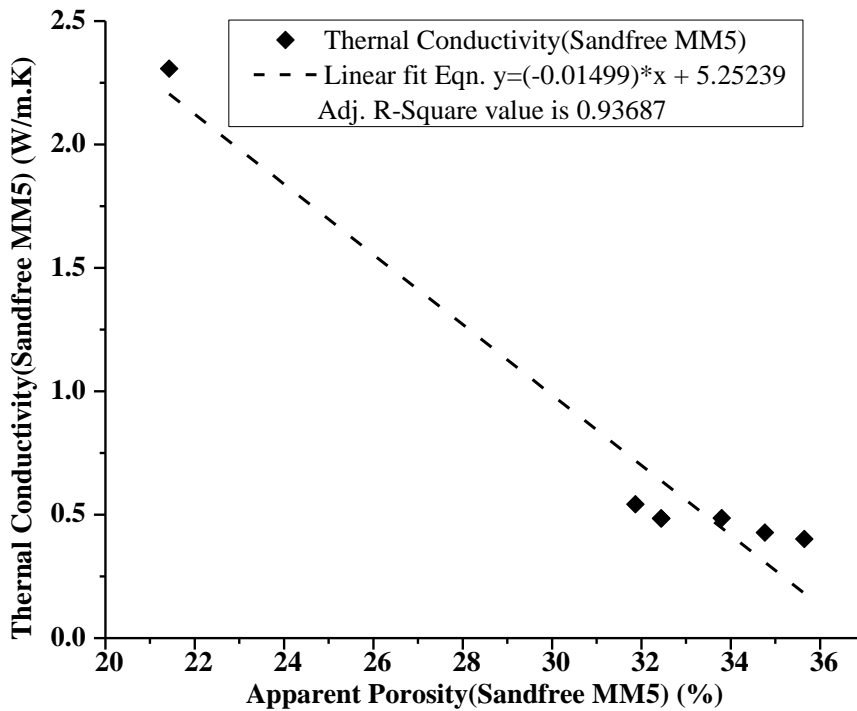


Fig. 5.83 Relationship between Apparent Porosity and Thermal Conductivity for the MM5 Grade Sand-free Mortar mix sample (Refer Table 5.40a)).

Observations : Apparent Porosity in this case is shown to have an excellent relationship with thermal conductivity of the concrete mix sample, and the adjusted R^2 value of 0.94, (assessed the very goodness-of-fit for regression analysis by Origin 8) supports the changes in both the parameters with respect to the mix proportions. The more is apparent porosity, lesser is the thermal conductivity, which has been established clearly in this sand-free mortar mix combinations.

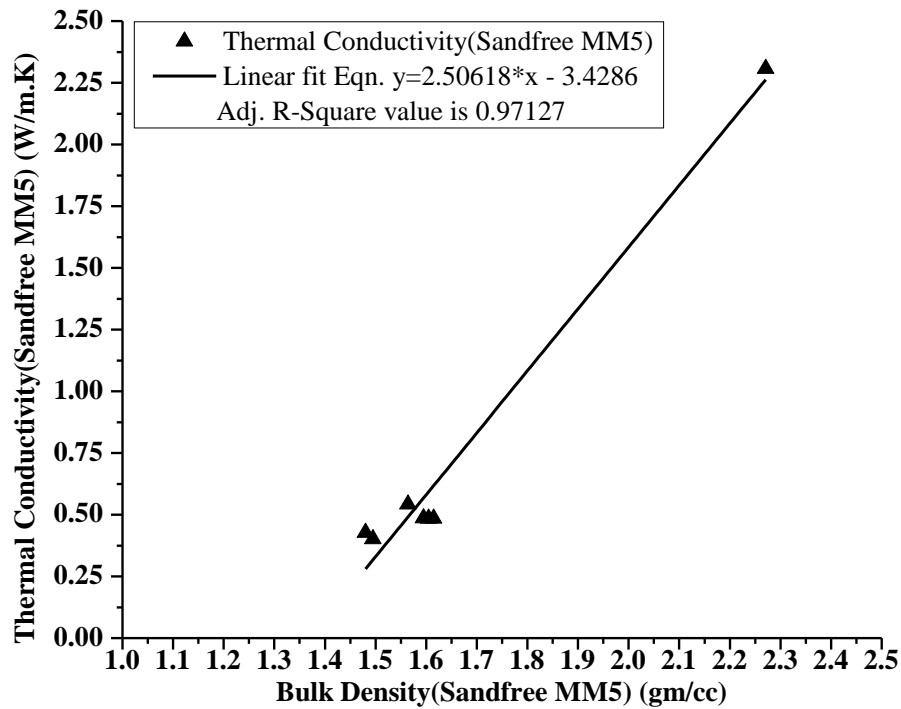


Fig. 5.84 Relationship between Bulk Density and Thermal Conductivity for the MM5 Grade Sand-free Mortar mix sample (Refer Table 5.40a)).

Observations : Bulk Density is shown to have an excellent relationship with thermal conductivity of the concrete mix sample, and the adjusted R^2 value of 0.97, (assessed the very goodness-of-fit for regression analysis by Origin 8) supports the changes in both the parameters with respect to the mix proportions. The more is bulk density, more is the thermal conductivity, which has been established excellently in this sand-free mortar mix combinations.

5.6 Thermal Transmittance Or Overall Heat Transfer Co-efficient (U-value)

5.6.1 Introduction

Steady-state thermal transmission properties of an actual Masonry Wall panel through Guarded Hot Box was determined by following methods described in BS EN ISO 8990-1996. Data on the thermal transmission properties of various building components like wall, roof, fenestration (overall) etc. are needed for various purposes including judging compliance with energy conservation regulations and energy efficiency specifications, models. Often heat transfer through such component is a complex combination of conduction, convection and radiation. Guarded Hot Box method measures the total amount of heat transferred from one side of the specimen to the other for a given temperature difference, irrespective of the individual modes of heat transfer, and the test results can therefore be applied to situations as at actuals. The thermal transmission properties often depend on the specimen properties and on the boundary conditions, specimen dimensions, direction of heat transfer, temperature differences, air velocities, and relative humidity. Thermal transmittance and thermal resistance properties can be measured by this method, and suitable for vertical specimens such as walls and for horizontal specimens such as roof/ceiling and floor. The method is formulated for laboratory measurements of large, inhomogeneous specimens, although homogeneous specimens can be tested for calibration and validation.

Measurements are made at steady-state of air and surface temperatures and of the power input to the hot side chamber. From these measurements, the thermal transfer properties of the specimen are calculated. Heat exchange at the surfaces of the test specimen involves both convective and radiative components. The former depends upon air temperature and air velocity, and the latter depends upon the temperatures and the total hemispherical emittances of specimen surfaces and of surfaces “seen” by the test specimen surface. The effects of the heat transfer by convection and radiation are combined in the method.

5.6.2 Test samples and other parameters :

Thermal performance of two Masonry test Wall panels of size 480mmX480mmX125mm were prepared, Locally available burnt clay brick, Portland pozzolana cement, local river sand, Flyash from nearby thermal power plant, and lime powder were used. In one panel, conventional MM5 grade (1:4) Cement-Sand mix mortar was used for wall construction and 12 mm plaster of same grade was used on both sides. After finishing and curing for 7 day's, rendering work with putty and external paint of two coats were applied on both the faces of the wall. Similarly for another panel, mortar mix grade was same, but the composition was made different. Flyash-Lime composition was adopted in lieu of sand. Hot side temperature was kept at 40°C and cold side temperature was kept at 25°C respectively. The various temperature profile inside the Metering box, Guard box, Cold box and on the hot and cold side sample surface temperatures were recorded for consecutive three days for both the cases separately.

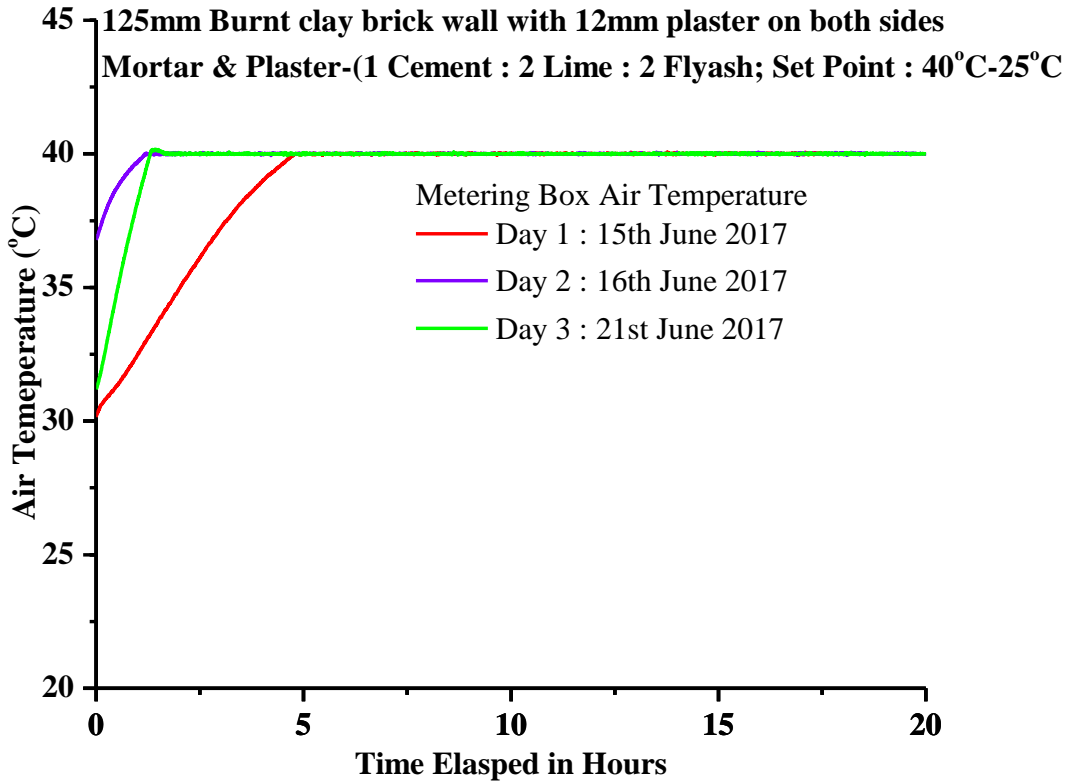


Fig. 5.85 Air temperature profile inside Metering Box for Consecutive 3 days (U-value Test)

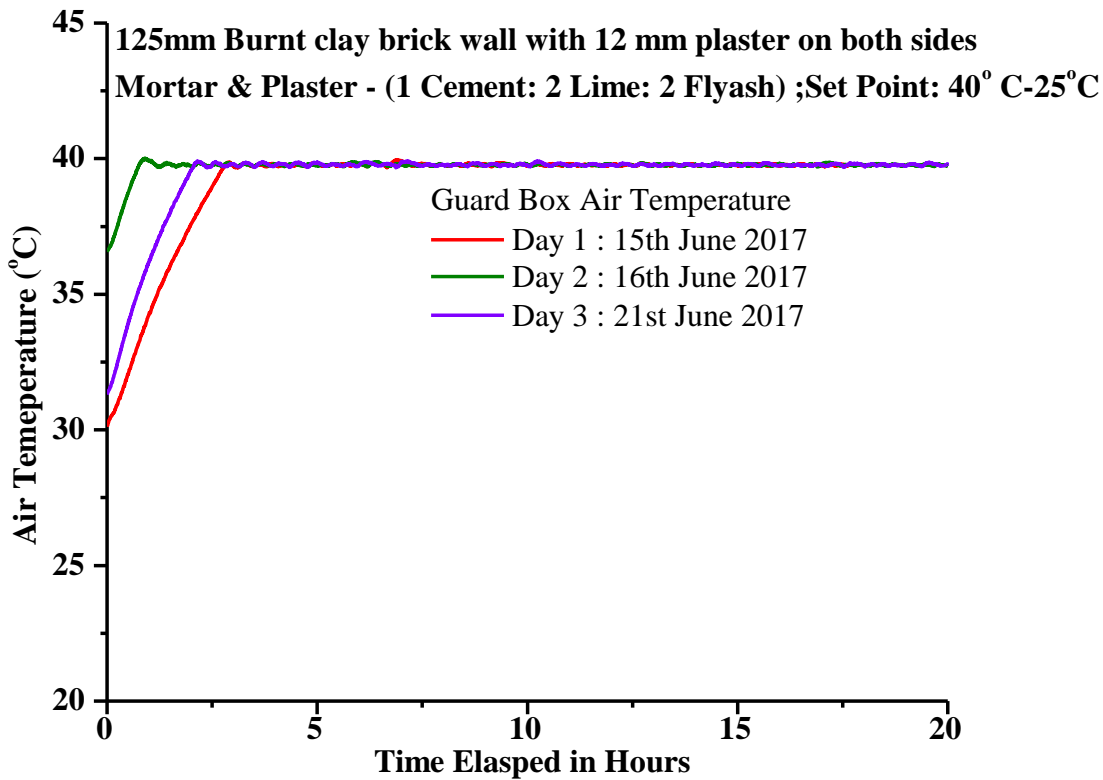


Fig. 5.86 Air temperature profile inside Guard Box for Consecutive 3 days (U-value Test)

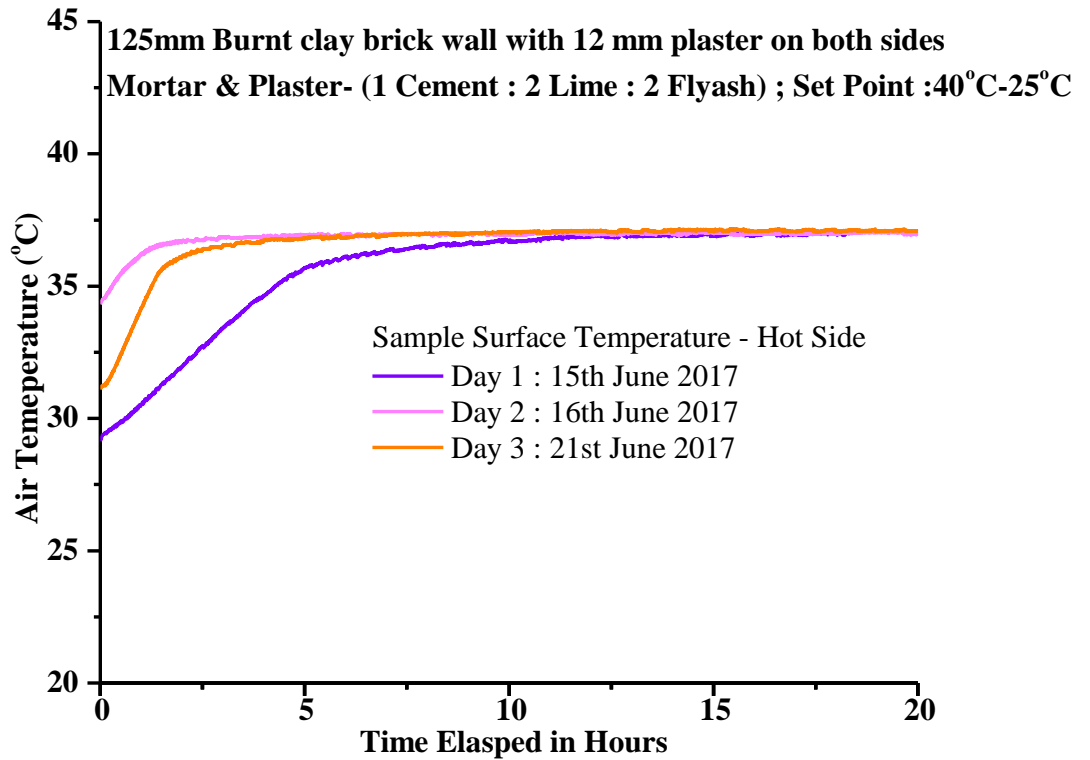


Fig. 5.87 Hot side sample surface temperature profile for consecutive 3 days (U-value Test)

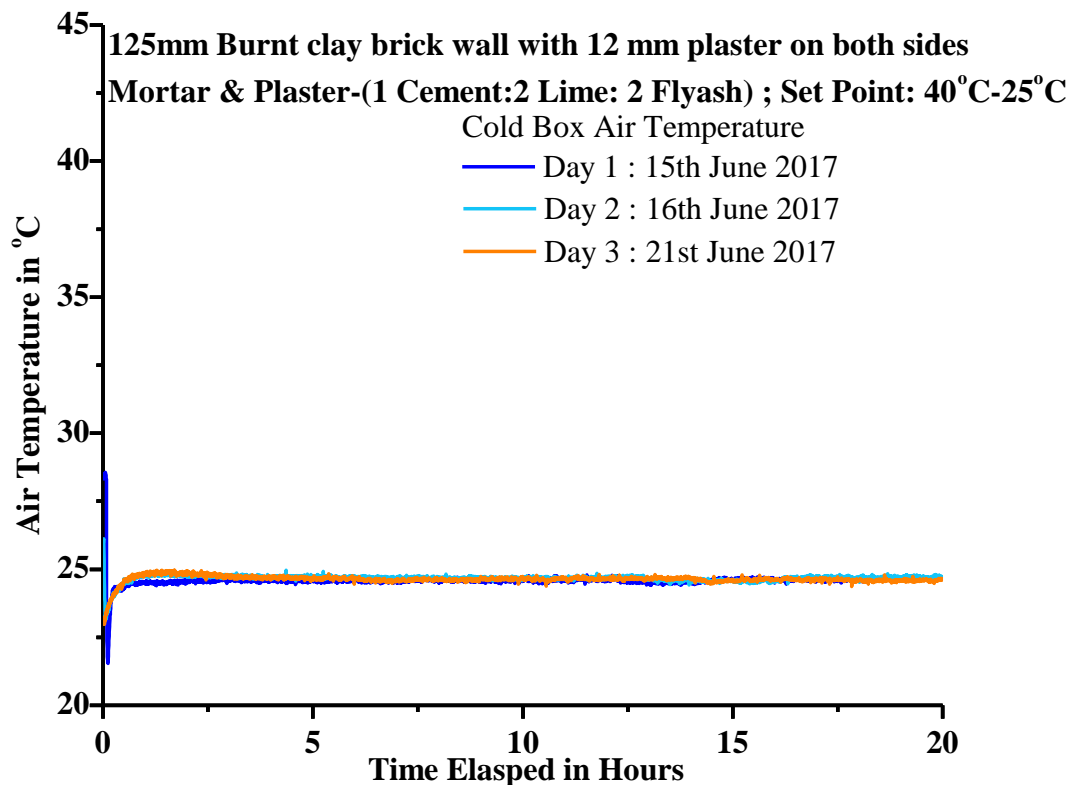


Fig. 5.88 Air temperature profile inside Cold Box for Consecutive 3 days (U-value Test)

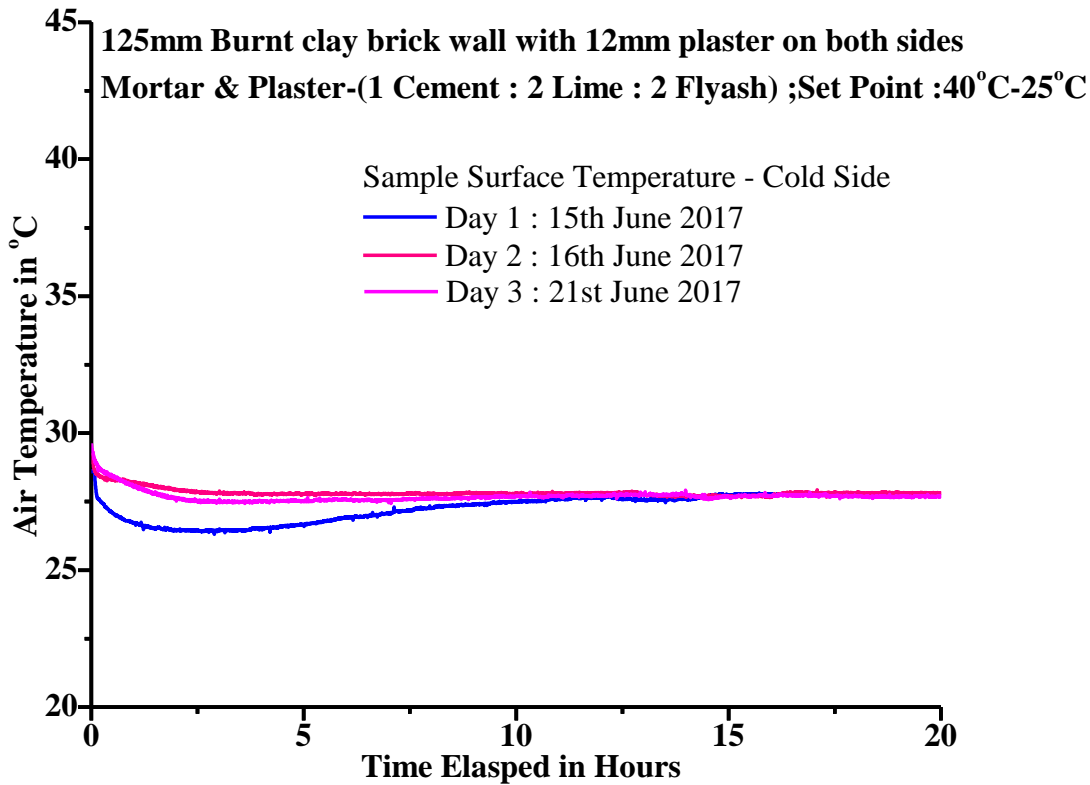


Fig.5.89 Cold side sample surface temperature profile for consecutive 3 days (U-value Test)

Thermal characterisation of the 125mm burnt clay brick wall sample with cement-flyash-lime plaster was carried out for 3 consecutive days. Metering box air temperature was fixed at around 40.01°C and cold box air temperature was set at around 25°C. Maximum fluctuation for metering box air was 0.060°C. Maximum fluctuation in cold box air temperature for 3 days was 0.167°C (Refer to Table 5.41). Sample hot side and cold side surface temperature difference on 1st day, 2nd day and 3rd day found to be 9.24°C, 9.22°C and 9.38°C respectively.

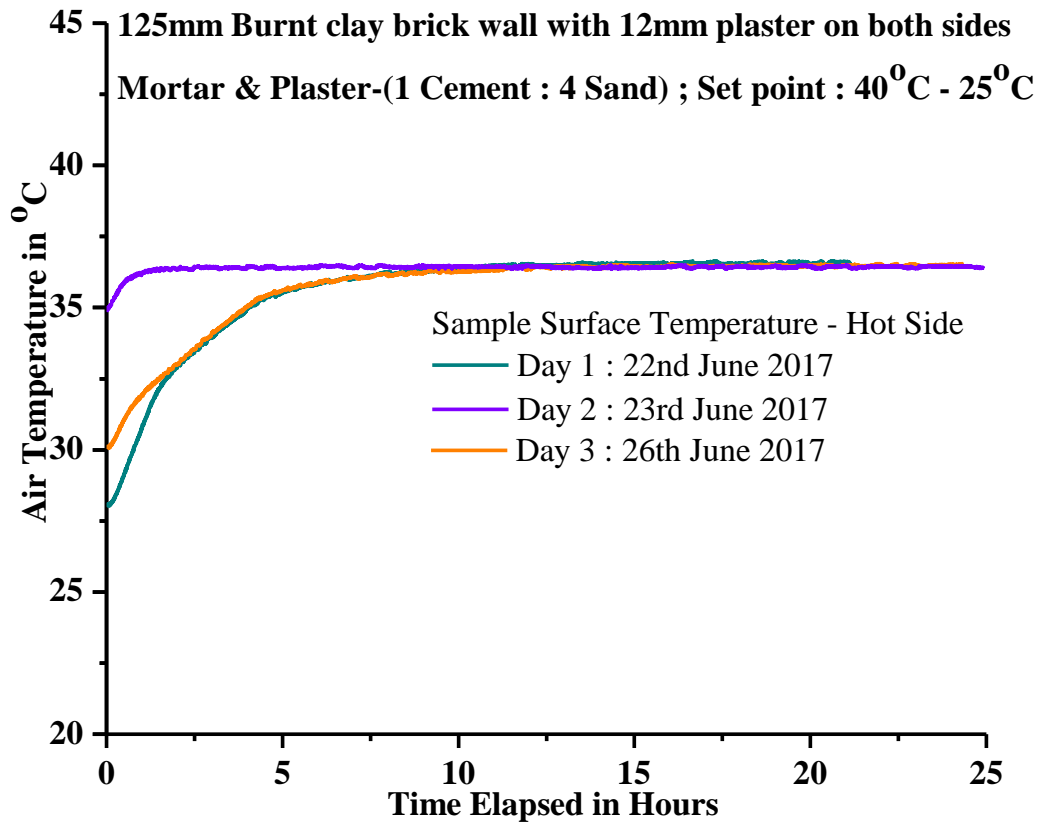


Fig. 5.90 Hot side sample surface temperature profile for consecutive 3 days (U-value Test)

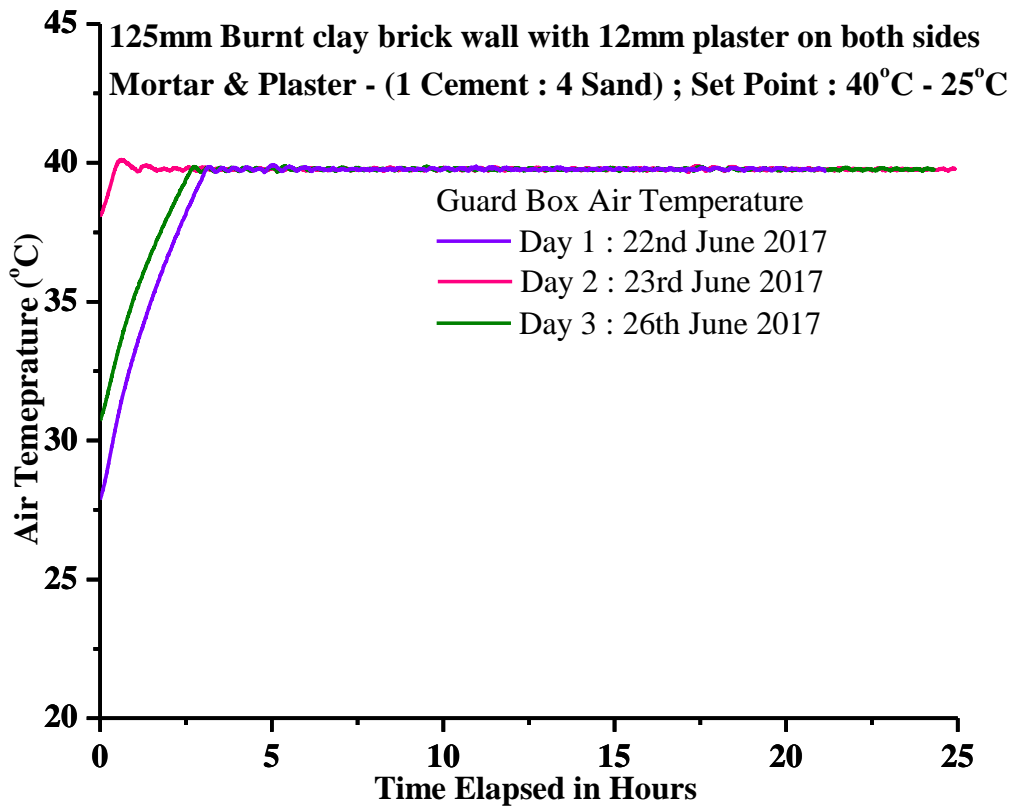


Fig. 5.91 Air temperature profile inside Guard Box for consecutive 3 days(U-value Test)

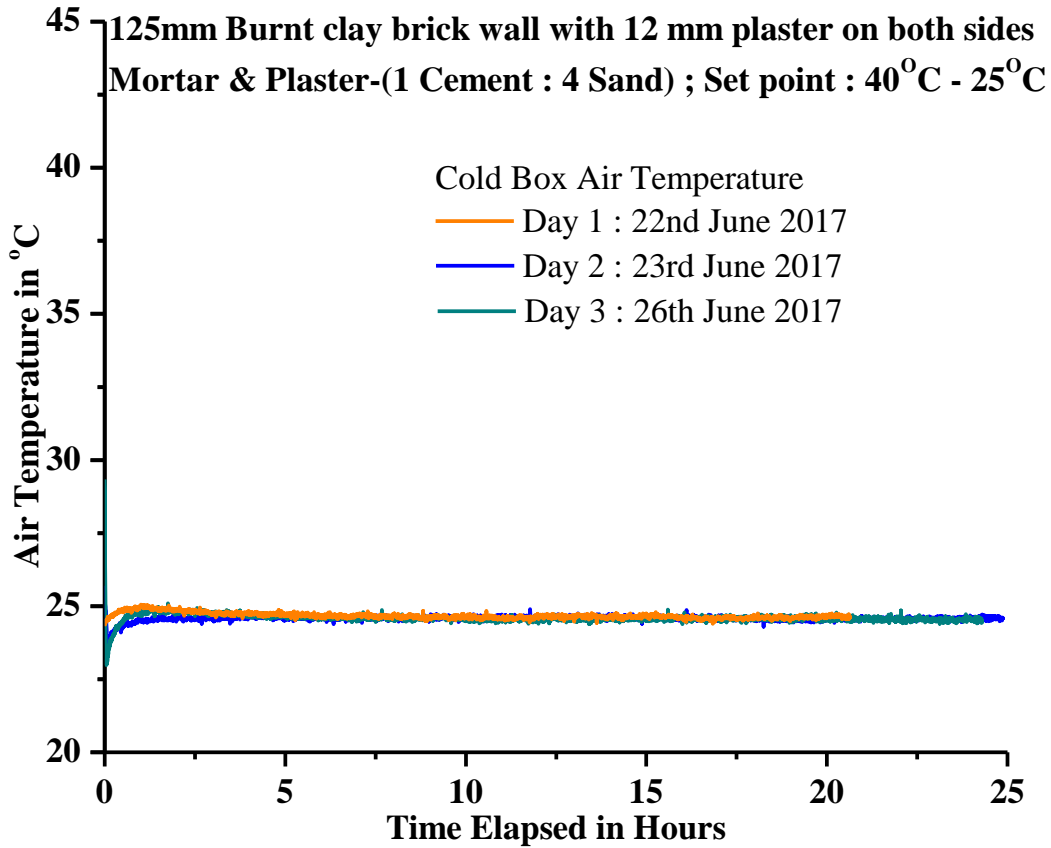


Fig.5.92 Air temperature profile inside Cold Box for consecutive 3 days (U-value Test)

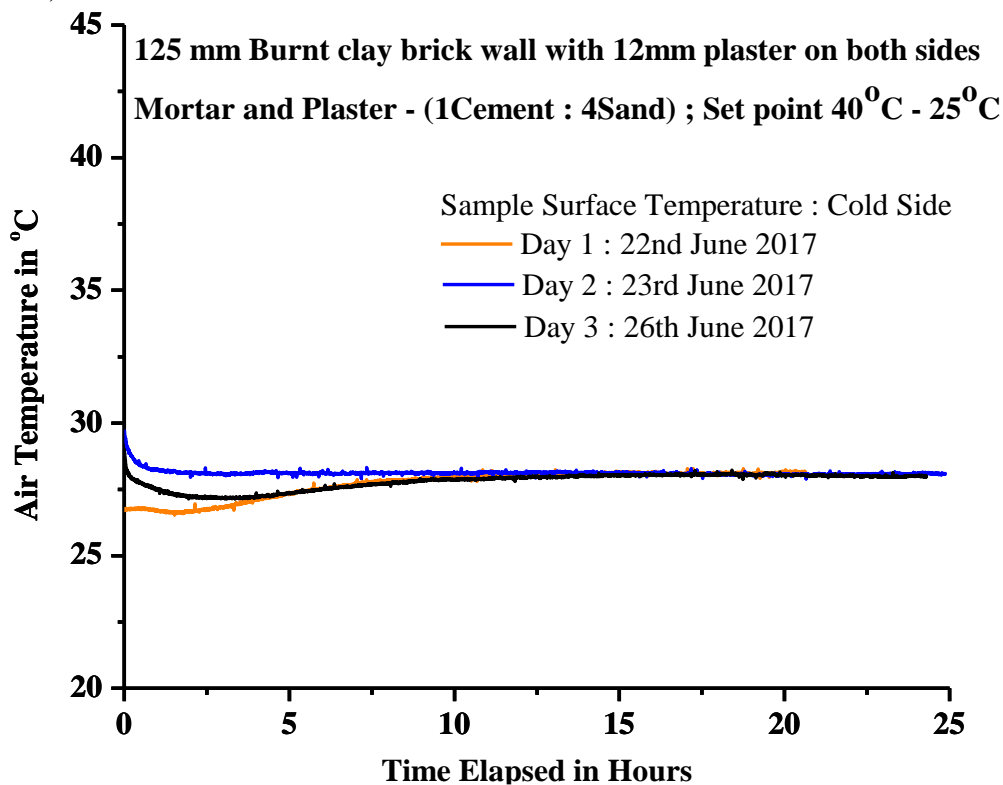


Fig.5.93 Cold side sample surface temperature profile for consecutive 3days (U-value Test)

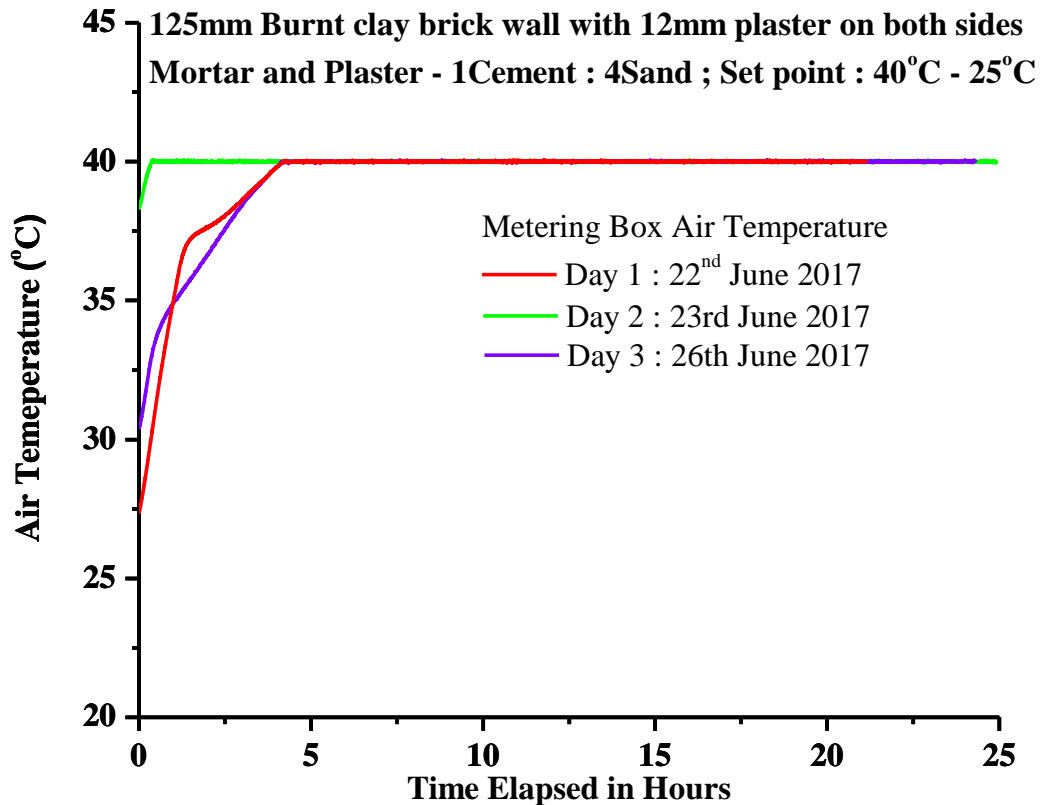


Fig. 5.94 Air temperature profile inside Metering Box for consecutive 3 days (U-value Test)

Thermal characterisation of the 125mm burnt clay brick wall sample with cement-sand plaster was carried out for 3 consecutive days. Metering box air temperature was fixed at around 40.01°C and cold box air temperature was set at around 25°C. Maximum fluctuation for metering box air was 0.060°C. Maximum fluctuation in cold box air temperature for 3 days was 0.231°C (Table 5.41). Sample hot side and cold side surface temperature difference on 1st day, 2nd day and 3rd day found to be 8.45°C, 8.31°C and 8.45°C respectively.

5.6.3 Test conditions

Table 5.41 Actual test parameters

Test Day	Metering Box Air Temperature			Cold Box Air Temperature		
	Air Temperature	Standard Deviation	Fluctuation	Air Temperature	Standard Deviation	Fluctuation
Sample : - 125mm Burnt Clay Brick Wall with 12mm Fly Ash based Plaster & Mortar, finished with putty & colour on both walls.						
Day 1	40.01° C	0.013° C	+ 0.054° C - 0.059° C	24.59° C	0.059° C	+0.145° C -0.167° C
Day 2	40.01° C	0.014° C	+0.053° C -0.060° C	24.66° C	0.075° C	+ 0.150° C - 0.155° C
Day 3	40.01° C	0.013° C	+ 0.048° C - 0.054° C	24.62° C	0.049° C	+ 0.129° C - 0.155° C
Sample : - 125mm Burnt Clay Brick Wall with 12mm Conventional Sand based Plaster & Mortar, finished with putty & colour on both walls.						
Day 1	40.00° C	0.012° C	+ 0.049° C - 0.051° C	24.61° C	0.049° C	+ 0.187° C - 0.231° C
Day 2	40.00° C	0.012° C	+ 0.053° C -0.053° C	24.60° C	0.045° C	+ 0.165° C - 0.108° C
Day 3	40.01° C	0.013° C	+ 0.060° C - 0.056° C	24.56° C	0.051° C	+ 0.196° C - 0.177° C

Maximum deviation in metering box air temperature of both days of testing is 0.098 °C whereas for guard box it is 0.166 °C (Refer to Table 5.2). Average brick surface and joint mortar temperature in hot side were 27.73 °C and 26.3 °C respectively. In cold side, brick surface temperature was 6.6 °C and joint mortar temperature was 7.7 °C. Therefore, it can be considered that the brick surface temperature is higher in hot side and lower in cold side compared to the joint mortar surface. In steady state condition, average standard deviation in brick surface temperature of both days of testing was 0.056°C on both the hot and cold side. Maximum standard deviation in surface temperature of the two days of joint mortar in hot side was 0.0673°C whereas in cold side, it was 0.0896°C.

5.6.4 U-value Calculations and Test Results :

SAMPLE 1 – 125 mm Burnt Clay Brick Wall panel with 12mm Cement-Flyash-Lime (1:2:2) based Plaster & Mortar, finished with putty & colour on both sides.

Test Day 1 – 15th June 2017

Metering Box (MB) Air Temperature = 40.01°C

Cold Box (CB) Air Temperature = 24.59°C

Air Temperature Difference between MB & CB = 15.42°C

Surround Panel Surface Temperature Difference = 15.15°C

Sample Surface Temperature (Hot Side) = 36.93°C

Sample Surface Temperature (Cold Side) = 27.69°C

Sample Surface Temperature Difference = 9.24°C

Total Heat Input into MB (A) = 19.08W

MB Wall Loss (B) = 1.549W

Heat Flow from MB to CB (C) = (A) – (B) = 17.53W

Flanking Loss (D) = 0.26W

Unaccounted Heat Flow (E) = 2.46W

Surround Panel Heat Flow (F) = 3.96W

Sample Heat Flow (G) = (C) – (D) – (E) – (F) = 10.84W

U-value = 3.051 W/m² °C

Test Day 2 – 16th June 2017

Metering Box (MB) Air Temperature = 40.01°C

Cold Box (CB) Air Temperature = 24.66°C

Air Temperature Difference between MB & CB = 15.35°C

Surround Panel Surface Temperature Difference = 15.12°C

Sample Surface Temperature (Hot Side) = 37.00°C

Sample Surface Temperature (Cold Side) = 27.77°C

Sample Surface Temperature Difference = 9.22°C

Total Heat Input into MB (A) = 18.55W

MB Wall Loss (B) = 1.432W

Heat Flow from MB to CB (C) = (A) – (B) = 17.11W

Flanking Loss (D) = 0.26W

Unaccounted Heat Flow (E) = 2.45W

Surround Panel Heat Flow (F) = 3.96W

Sample Heat Flow (G) = (C) – (D) – (E) – (F) = 10.45W

U-value = 2.954 W/m² °C

Test Day 3 – 21st June 2017

Metering Box (MB) Air Temperature = 40.01°C
Cold Box (CB) Air Temperature = 24.62°C
Air Temperature Difference between MB & CB = 15.38°C
Surround Panel Surface Temperature Difference = 15.17°C
Sample Surface Temperature (Hot Side) = 37.10°C
Sample Surface Temperature (Cold Side) = 27.72°C
Sample Surface Temperature Difference = 9.38°C
Total Heat Input into MB (A) = 18.96W
MB Wall Loss (B) = 1.465W
Heat Flow from MB to CB (C) = (A) – (B) = 17.50W
Flanking Loss (D) = 0.26W
Unaccounted Heat Flow (E) = 2.46W
Surround Panel Heat Flow (F) = 3.97W
Sample Heat Flow (G) = (C) – (D) – (E) – (F) = 10.81W

U-value = 3.050 W/m² °C

SAMPLE 2 – 125 mm Burnt Clay Brick Wall panel with 12mm Cement-Sand (1:4) based Plaster and Mortar, finished with putty & colour on both sides.

Test Day 1 – 22nd June 2017

Metering Box (MB) Air Temperature = 40.00°C
Cold Box (CB) Air Temperature = 24.60°C
Air Temperature Difference between MB & CB = 15.40°C
Surround Panel Surface Temperature Difference = 15.17°C
Sample Surface Temperature (Hot Side) = 36.56°C
Sample Surface Temperature (Cold Side) = 28.11°C
Sample Surface Temperature Difference = 8.45°C
Total Heat Input into MB (A) = 21.29 W
MB Wall Loss (B) = 1.631 W
Heat Flow from MB to CB (C) = (A) – (B) = 19.66 W
Flanking Loss (D) = 0.26 W
Unaccounted Heat Flow (E) = 2.46 W
Surround Panel Heat Flow (F) = 3.97 W
Sample Heat Flow (G) = (C) – (D) – (E) – (F) = 12.97 W

U-value = 3.655 W/m² °C

Test Day 2 – 23rd June 2017

MB Air Temperature = 40.00°C
CB Air Temperature = 24.60°C
Air Temperature Difference between MB & CB = 15.40°C
Surround Panel Surface Temperature Difference = 15.13°C
Sample Surface Temperature (Hot Side) = 36.43°C
Sample Surface Temperature (Cold Side) = 28.11°C
Sample Surface Temperature Difference = 8.31°C
Total Heat Input into MB (A) = 20.35W
MB Wall Loss (B) = 1.123W
Heat Flow from MB to CB (C) = (A) – (B) = 19.22W
Flanking Loss (D) = 0.26W
Unaccounted Heat Flow (E) = 2.46W
Surround Panel Heat Flow (F) = 3.96W
Sample Heat Flow (G) = (C) – (D) – (E) – (F) = 12.54W

U-value = 3.534 W/m² °C

Test Day 3 – 26th June 2017

Metering Box (MB) Air Temperature = 40.01°C
Cold Box (CB) Air Temperature = 24.56°C
Air Temperature Difference between MB & CB = 15.45°C
Surround Panel Surface Temperature Difference = 15.16°C
Sample Surface Temperature (Hot Side) = 36.47°C
Sample Surface Temperature (Cold Side) = 28.02°C
Sample Surface Temperature Difference = 8.45°C
Total Heat Input into MB (A) = 20.44W
MB Wall Loss (B) = 1.162W
Heat Flow from MB to CB (C) = (A) – (B) = 19.28W
Flanking Loss (D) = 0.26W
Unaccounted Heat Flow (E) = 2.47W
Surround Panel Heat Flow (F) = 3.97W
Sample Heat Flow (G) = (C) – (D) – (E) – (F) = 12.58W

U-value = 3.536 W/m² °C

Table 5.42 Summary Result of U-value test performed on two brick panels

Item description	SET – 1 : Burnt clay brick wall panel of size:480mmX480mmX125mm with 12 mm thick Mortar and Plaster of MM5 Grade, made of 1 part of Portland Pozzolana Cement, 2 parts of Flyash +2 parts of Lime combination (1:4)			SET – 2 : Burnt clay brick wall panel of size:480mmX480mm X125mm with 12 mm thick Mortar and Plaster of MM5 Grade, made of 1 part of Portland Pozzolana Cement and 4 parts of Sand combination (1:4)		
	Day 1	Day 2	Day 3	Day 1	Day 2	Day 3
Test Days	Day 1	Day 2	Day 3	Day 1	Day 2	Day 3
Surface Area, (m ²)	0.23	0.23	0.23	0.23	0.23	0.23
Metering Box (MB) Air temperature (°C)	40.01	40.01	40.00	40.00	40.00	40.01
Cold Box (CB) Air temperature (°C)	24.59	24.66	24.62	24.60	24.60	24.56
Air temperature difference between MB & CB, ΔT (°C)	15.42	15.35	15.38	15.40	15.40	15.45
Surround Panel Surface temperature difference (°C)	15.15	15.12	15.17	15.17	15.13	15.16
Sample surface temp. difference (°C)	9.24	9.22	9.38	8.45	8.31	8.45
Total heat input into MB (A) (Watt)	19.08	18.55	18.96	21.29	20.35	20.44
MB Wall loss (B) (Watt)	1.549	1.432	1.465	1.631	1.123	1.162
Heat flow from MB to CB(C)=(A)-(B) (Watt)	17.53	17.12	17.50	19.66	19.23	19.28
Flanking loss(D) Watt	0.26	0.26	0.26	0.26	0.26	0.26
Extraneous heat transfer (E) (Watt)	2.46	2.45	2.46	2.46	2.46	2.47
Surround Panel heat flow (F) Watt (Watt)	3.96	3.96	3.97	3.97	3.96	3.97
Sample heat flow(G)=(C)-(D)-(E)-(F) Watt	10.85	10.45	10.81	12.97	12.54	12.58
U value = (G)/A* ΔT (W/m ² °C)	3.051	2.954	3.050	3.655	3.534	3.536
Avg. U value in each Set (W/m ² °C)	3.018			3.575		
Difference in U value (%)	15.58					

Observations: Brick Wall panel with identity Set-1 (1 Cement : 2 Flyash : 2 Lime) mortar and plaster combination is found to exhibit thermal transmittance value lesser by 15.58% than identical panel with identity Set-2 (1 Cement : 4 Sand) mortar and plaster combination respectively.

Chapter 6
Discussions, Conclusions
&
Recommendations

Chapter 6 Discussions , Conclusions & Recommendations

6.1 Introduction :

After presenting the research work on effective utilization of Coal Combustion Residues (CCR) from thermal power plants in India in the previous Chapters from 1 – 5, the concluding findings are summarized in this chapter.

The utilization of CCR in building construction industry has been the focus area mainly on three counts simultaneously, which are –

1. Enhancement in utilization of CCR to create zero accumulation or gradually emptying the overflowing ash dykes, so that land utilization would be better, and environmental hazards through air and soil contamination would be totally avoided.
2. CCR has been tried to be utilized as an effective alternative to sand, which is facing another serious environmental degradation threat, due to mindless sand mining from river bed, the rate of which is much more than its replenishment.
3. Utilizing CCR in building construction activity, as a constituent material in concrete and mortar – plaster combinations, energy conservation by reduced cooling / heating demand could be established.

6.2 Summary Analysis of Results :

After obtaining all the test results of constituent materials and that of concrete mixes, those were critically evaluated. Sand with fineness modulus value of 2.884 is conforming to Zone-II limit (Fig. 3.9 a), which is ideal for concrete with coarser grain size, and angular shape which is corroborated by SEM image (Fig. 3.11 a-c). The quartz is of crystalline nature. Fineness modulus of bottom ash was found to be 1.446, conforming to Zone IV (Fig. 3.6 c) with finer irregular shaped particles of lower specific gravity (around 14% lower than that of sand).

Going by the phase structures of sand, Flyash and Bottomash, similarity in quartz silica phase was observed (Figs.3.10, 3.3 and 3.4) , though the crystalline phase of silica is more conductive than amorphous phase of silica (*Demirboga 2007*). Further, dissimilarities in grain shape and sizes between Sand, Flyash and Bottomash are evident from SEM analysis (Figs. 3.11, 3.7 and 3.8). The specific gravity value of bottomash was found lower than that of sand. The fine aggregate content in the concrete occupied around 25% of total volume, and since other two constituents remained constant, the physical properties of fine aggregate influenced considerably the overall property like bulk density and apparent porosity of concrete. Analyzing altogether twelve sets of concrete mixes, it was observed that as the bottom ash percentages increased and corresponding sand percentages decreased, the concrete mixes exhibited reduction in compressive strength. Due to change in fine aggregate component ratio (i.e. sand component decreased, and Flyash / Bottomash component increased in the mix), gradual reduction in thermal conductivity values also observed, and Apparent Porosity values increased and Bulk Density values decreased.

In most of the cases, apparent porosity versus thermal conductivity plot exhibited good co-relation with R^2 value varied from lowest 0.62 (Set 5 Gr.A with Bottomash, Fig. 5.24) to highest 0.97 (Set B Gr.B with Bottomash, Fig.5.54). Further, bulk density versus thermal conductivity plot also showed good co-relation with R^2 value varied from lowest 0.73 (Set 5 Gr.A with Bottomash, Fig. 5.25) to highest 0.986 (Set C Gr.C with Bottomash, Fig.5.60).

It was also observed that the grade of concrete or equivalent compressive strength values decreased gradually due to above stated reasons. For easy demarcation of strength values with respect to sand substitution, three arbitrary lines have been drawn,

at 20 MPa, 15 MPa and 10 MPa levels. Even after reduction in compressive strength values, M 20 grade strength was achieved at 28 days maturity in respect of Flyash blended concrete (Set 1, Gr.A, Fig. 5.1) and Bottomash blended concrete (Set 4, Gr. A, Fig. 5.14) up to 50% and 60% replacement of Sand by Flyash and Bottomash respectively. With 100% replacement of sand, Bottomash blended concrete attained M 15 grade strength, and Flyash blended concrete attained M10 grade strength respectively. Though, earlier researchers observed that due to pozzolanic effect, further strength gain in blended concrete took place beyond 28 days maturity period, the same was corroborated in both the above cases. However, we restricted our study up to 28 days limit only, since as per IS 456 stipulations, to determine characteristic compressive strength of any grade of concrete, 28 days compressive strength value shall be the decisive one. Reduction in thermal conductivity value to the tune of 36%, and 30% for Flyash blended and Bottomash blended concrete mixes respectively were observed up to 60% sand replacement level, while compared with conventional concrete with sand respectively (Fig.5.2 and Fig.5.15). For visual demarcation, two arbitrary lines at 1.0 W/m.K level and another one at 0.8 W/m.K level have been drawn, so that the sand substitution effect on thermal conductivity reduction could be assessed easily.

From this study, it is clearly established that by replacing Sand with Flyash and Bottom ash, thermal resistance against heat flow of concrete improved. The degree of improvement depends upon the replacement percentage of sand by bottom ash at desired strength level of concrete. Even embodied energy content of such blended concrete reduces, since embodied energy of river sand remains higher than that of bottom ash obtained from thermal power plants, mainly on two counts. The dredging of river sand involves diesel operated machines and the distance from loading site to construction site generally exceeds 100 km. distance, for which embodied energy considered as 175 MJ/m^3 (Reddy et al. 2003) plus dredging energy. The coal combustion residues remain available free of cost including transportation cost reimbursement by power plant authority to the consumer. Hence, for utilizing coal bottom ash from thermal power plants, there is a distinct economic advantage. Blended concrete could be produced with lesser carbon footprint, eliminate cumulative accumulation as landfill, and at the same time could effectively arrest rapid depletion of river sand due to mindless sand mining. Therefore, it is recommended to use bottom ash as fine aggregate in concrete mix for building construction work.

This research work also investigated the possibility of substituting sand with Flyash and Bottomash in mortar and plaster mix as low thermally conducting materials. Besides, finding the strength adequacy in compliance with relevant IS Code, thermal conductivity parameter also explored. To understand the change in thermal conductivity values with the change in substitution ratios of sand by Flyash and Bottom ash (separately), apparent porosity and bulk density values of such mortar mixes were also evaluated. From the study of inherent material properties of sand, Flyash and Bottomash like particle size, grading, shape, specific gravity etc., it could be established that fly ash and bottom ash produced mortar mix with lesser bulk density and more apparent porosity, than those compared with conventional mortar mix with sand. The lower density value of mortar mix is advantageous for reduced dead load of the whole envelop assembly. From the durability point of view as per Code provision, even the mix with 100% sand substitution complied with minimum grade of mortar MM0.7. Further, from the test result it is also revealed that up to 60% substitution by fly ash, MM3 and MM5 grades of mortar could be produced (Tables 5.37a and 5.38a). The reduction in thermal conductivity values for 100% substitution by Flyash alone for MM3 and MM5 grade mortars are found to be around 82% and 73% respectively with respect to the controlled mortar mix with sand (Tables 5.37a and 5.38a). For 100% bottom ash substitution, those reduction values are 68% and 75% respectively (Tables 5.37a and 5.38a). The overall heat transfer co-efficient U-value of brick wall panel with 50% Fly ash substituted mortar mix was found to be lesser by 15.58%, while compared with identical panel with conventional mix with sand (Table 5.42).

6.3 Conclusive Remarks :

From the study pertaining to this work, the following can be concluded –

1. Bottom ash, the 100% utilization of which is still not possible in India, can now be effectively put to use in concrete to act as replacement for sand for structural application in roof concrete and screed concrete layer as plain concrete with lesser strength and for other area application with higher thermal resistance property. The embodied energy content of coal bottom ash is lesser than river sand on extraction and transportation counts respectively.
2. Energy conservation and cost economy in building shall be resulted by such modified concrete blended with bottom ash, mainly on two counts. On account of cooling load reduction due to enhanced thermal resistance offered by such coal bottom ash blended concrete and on another count of overall cost reduction due to free availability of coal combustion residues from thermal power plants including free transportation up to 100 km.
3. Without any special technique or deploying specialized energy consuming equipment, only by conventional method of concreting (mixing, placing, compacting, curing) with the available work force, such green concrete production with bottom ash blending is possible.
4. The environmental hazards related to cumulative accumulation of coal combustion residues can be addressed with such application in building industry.
5. Rapid depletion of natural soft mineral, which is a serious concern across the globe, can be arrested by replacing sand with coal combustion residue in building concrete.
6. This work intends to throw open further research scope for life cycle assessment of such blended concrete application in buildings and energy saving aspect with the help of dynamic simulation.

Therefore, building envelop cladding made with such ash blended mix can be considered as energy efficient, since due to lesser heat transmission inside, cooling/heating demand by the building will be reduced. The important outcome from this work has been a way of effective utilization of thermal power plant ash towards energy efficient building envelop construction without any specialized technique or addition of chemical etc. Simultaneously, the ecological disturbances caused due to fast depletion of river sand, shall be minimized with such coal ash substitution.

6.4 Recommendations (for Future Scope of work) :

This work was restricted within M-25 to M-10 Grade of concrete, and further research work may be carried out for higher grades of concrete with additional blending of other waste. There remains future scope for this work to be extended with incorporation of some additional waste material(s) in addition to the coal ash varieties, to further enhance the insulating effect of the mix under lower embodied energy condition.

References

Chapter 1

Aeee (Alliance for Energy Efficient Economy), and LBNL (Lawrence Barkley National Laboratory) (2015), Energy Efficiency in Buildings for National Energy Policy, September 24, pp 1-8.

BEE. (2018), 1.0 – Energy Scenario Updates, Guide Book – Refresher Course for Certified Energy Managers and Auditors, Bureau of Energy Efficiency, New Delhi.

CEA, Central Electricity Authority. (2013), Growth of Electricity sector in India from 1947-2013, Ministry of Power, New Delhi.

CEA.(2013), All India electricity statistics, general review 2012, Government of India, Ministry of Power, Central Electricity Authority, Delhi.

Census of India Report. (2006), Population Projection for India and States 2001-2026, December 2006, and all projections are effective 1 March of each year.

Chaturvedi, V., Eom, J., Clarke, L.E., and Shukla, P.R. (2014), Long term building energy demand for India: Disaggregating end use energy services in an integrated assessment modelling framework. Energy Policy, 64, 226-242.

Down to Earth. (2018), Made of Sand, June 16-30, pp 35-45.

Global Buildings Performance Network (GBPN). (2013), Executive Summary, Mitigation Potential from India's Buildings, February, pp 1-8.

Global Buildings Performance Network (GBPN). (2014), Residential Buildings in India : Energy use projections and Savings potential, CEPT University, Ahmedabad, September, pp 1-50.

IEA. (2018), Coal 2018 - Executive Summary, Analysis and Forecasts to 2023, Market Report Series,

IESS. (2015), India Energy Security Scenario (IESS) 2047 Version 2.0, Part I Energy Demand Sectors, Part II Conventional Energy Supply Sectors, Niti Aayog, Government of India.

IPCC. 2014, Climate Change 2014: Synthesis Report. Geneva, Switzerland, 151 pp.

IS 2250, 1981 (Reaffirmed 2000), Indian Standard Code of Practice for preparation and use of Masonry Mortars, Bureau of Indian Standard, New Delhi.

Kumar.S.R. (2011), USAID ECO - III Project, Energy Use in commercial buildings - Key findings from the national benchmarking study. USAID - INDIA.

Mathur, Ajay.(2018), Public costs and private benefits : the governance of energy efficiency in India, *Building Research & Information*, 47:1, 123-126, <https://doi.org/10.1080/09613218.2018.1514743>

Mittal, L.M., Sharma, C., Singh, R.(2012), Estimates of Emissions from Coal fired Thermal Power Plants in India, 20th Emission inventory Conference, August 13-16, Tampa, Florida, 1-22.

Niti Aayog (2015), A Report on Energy Efficiency and Energy Mix in the Indian Energy System (2030), Using India Energy Security Scenario 2047, Government of India, April, pp 1-25.

Rawal, R., Vaidya, P., Ghatt, V., & Ward, A. (2012). Energy Code Enforcement for Beginners: A tiered approach to energy code in India. Alliance for an Energy Efficient Economy, Summer Study, 366.

Statistical Year Book, (2017)., Chapter : Area and Population, Ministry of Statistics and Programme implementation, Government of India.

TERI (The Energy Resources Institute), (2015)., Green growth and building sector in India, New Delhi, pp 39.

UN Environment and International Energy Agency (2017).,Towards a zero emission, efficient and resilient building and construction sector, Global Status Report 2017,p 48.

UNDP and GEF. (2011). *Energy efficiency improvements in Commercial Buildings*. Retrieved from http://www.undp.org/content/dam/india/docs/energy_efficiency_improvements_in_commercial_buildings_project_document.pdf

UNEP, 2014., Sand, rarer than one thinks, UNEP Global Environmental Alert Services, March, pp 1-15.

USAID and BEE. (2014). HVAC market assessment and transformation approach for India, PACE-D technical assistance programme. Retrieved from <https://www.climatelinks.org/resources/hvac-market-Assessment-and-Transformation-Approach-India>

Vaidya, C. (2009). Urban Issues, Reforms And Way Forward In India, Working Paper, Ministry of Finance, Government of India.

Chapter 2

Abubaker, A, U., Baharudin, K,S. (2012), Properties of concrete using Tanjung Bin power plant coal bottomash and flyash, International journal of sustainable construction engineering and technology, Vol.3, Issue 2.

Abubaker, A, U., Baharudin, K,S. (2013), Compressive strength of high volume coal bottom ash utilization as fine aggregate in flyash-cement blended concrete, International journal of engineering and technological sciences, 1(4) : 226-239.

Aggarwal, P., Aggarwal, Y., Gupta, S, M. (2007), Effect of bottomash as replacement of fine aggregates in concrete, Asian journal of civil engineering (building and housing), Vol.8, No.1, pages 49-62.

Aggarwal, Paratibha., Siddique, Rafat., Aggarwal, Yogesh. (2012), Influence of water / powder ratio on strength properties of self-compacting concrete containing coal flyash and bottomash, Construction and Building Materials, 29, 73-81.

Aggarwal, Yogesh., Siddique, Rafat. (2014), Microstructure and properties of concrete using bottomash and waste foundry sand as partial replacement of fine aggregates, Constructions and Building Materials, 54, 210-223.

Ajay, Mathur.(2018), Public costs and private benefits : the governance of energy efficiency in India, Building Research and Information, Vol.47, No.1, 123-126.
<https://doi.org/10.1080/09613218.2018.1514743>

Akbari, Hamid., Biney, Mensah, Robert., Simms, Jonathan. (2015), Production of geo-polymer binder from coal fly ash to make cement less concrete, 2015 world of Coal ash Conference, Nashville, TN, May 5-7.

Arumugam, K., Ilangovan, R., James, Manohar, D. (2011), A study on characterization and use of Pond ash as fine aggregate in concrete, International journal of civil and structural engineering, Vol.2, No.2.

Arumugam, Rathish., Garg, Vishal., Mathur, Jyothirmoy., et al.(2014), Experimental determination of comfort benefits from cool-roof application to an un-conditioned building in India, Advances in Building Energy Research, Vol.8, Issue 1

Aruna, Kanthi, E., Kavitha, M.(2014), Studies on partial replacement of sand with Flyash in concrete, European journal of advances in engineering and technology, 1(2) : 89-92.

- Asdrubali, Fransesco., D'Alessando, Fransesco., Schiavoni, Samuele.(2015), A review of unconventional sustainable building insulation material, *Sustainable Materials and Technologies*, 4, 1-17.
- Asokan, P., Saxena, Mohini., Asolekar, R, Shyam.(2005), Coal combustion residues – environmental implications and recycling potential, *Resources Conservation & Recycling*, 43, 239-262.
- Aydin, Ertug.(2016), Novel coal bottomash waste composites for sustainable construction, *Construction and Building Materials*, 124, 582-588.
- Aydin, Ertug., Arel, S, Hasan. (2017), Characterization of high-volume fly-ash cement pastes for sustainable construction applications, *Construction and Building Materials* 157 , 96–107.
- Bahoria, B, V., Parbat, D, K., Naganaik, P, B.(2013), Replacement of natural sand in concrete by waste products : A state of Art, *Journal of Environmental Research and Development*, Vol.7, No. 4A, April-June.
- Balasubramanium, T., Thirugnanam, G, S. (2015), An experimental investigation on the mechanical properties of bottomash concrete, *Indian journal of science and technology*, Vo.8(10), 992-997, May.
- Bhadoriya,, Gautam., Kumar, Lokesh.(2015), The result of partial replacement of cement by using waste Flyash and natural sand by using waste marble dust and stone dust on mechanical properties of concrete, *International journal of science technology and engineering*, Volume 2, Issue 6, December, pp 31-35.
- Bharathi, Ganesh., H, Sharada, Bai., R, Nagendra., Shivram, Bagade.(2011), Pond ash : an alternative material as fine aggregate in concrete for sustainable construction, *Advanced materials Research*, Vols. 306-307, pp 1071-1075, doi:10.4028/www.scientific.net/ AMR.306-307.1071
- Brake, A, Nicholas., Oruji, Soheil., Nalluri, Likhith., Guduru, K, Ramesh. (2017), Strength activity and microstructure of blended ultra-fine coal bottom, *Construction and Building Materials* 153 ,317–326.
- Bribain, I. Z., Capila, A. V., & Uson, A. A. (2011). Life cycle assessment of building materials: Comparative analysis of energy and environmental impacts and evaluation of the eco efficiency improvement potential. *Building and Environment*, 46, 1133–1140.

- Bruce, Edwards.(2015), The insatiable demand for sand, Finance and Development, December.
- Buddhi, D., Kumar, Ashok, Chauhan, D.S., 2012. Indexing of building material with embodied, operational energy and environmental sustainability with reference to green buildings. J. Pure Appl. Sci. Technol. 2 (1), 11e22, January.
- Butera, M, Federico.(2010), Climate change and the built environment, Advances in Building Energy Research, Vol.4, Issue 1.
- Cadersa, A, S., Auckburally, I. (2014), Use of unprocessed coal bottomash as partial fine aggregate replacement in concrete, University of Mauritius Research Journal , Vol. 20.
- Chahal, Navneet., Siddique, Rafat., Rajor, Anita. (2012), Influence of bacteria on the compressive strength, water absorption and rapid chloride permeability of flyash concrete, Construction and Building Materials, 12, 351-356.
- Chousidis, N., Ioannou, I., Rakanta, E., Koutsodontis, C., Batis, G. (2016), Effect of flyash chemical composition on the reinforcement corrosion, thermal diffusion and strength of blended cement concretes, Construction and Building Materials, 126, 86-97.
- Chousidis, N., Rakanta, E., Ioannou, I., Batis, G. (2015), Mechanical properties and durability performance of reinforced concrete containing flyash, Construction and Building Materials, 105, 810-817.
- Costanzo, Vincenzo., Evola, Gianpiero., Marletta, Luigi. (2013), Cool roofs for passive cooling: performance in different climates and for different insulation levels in Italy, Advances in Building Energy Research, Vol.7, Issue 2.
- Das, Sukhen., Sultana, Parveen., Bagchi, Bishwajoy., Bhattacharya, Alakananda., Basu, Ruma., and Nandy, Papiya.(2011), Effect of size of Flyash particle on enhancement of mullite content and glass formation, Bull. Mater. Sc. Vol.34, No.7, December, pp 1663-1670.
- de Brito, Jorge., Silvestre, D Jose., Kurda, Rawaz. (2018), Toxicity and environmental and economic performance of fly ash and recycled concrete aggregate use in concrete : a review. Heliyon 4 (4), e00611.
- de Brito., Jorge, Silvestre., D Jose, Kurda, Rawaz. (2017), Combined influence of recycled concrete aggregates and high contents of fly ash on concrete properties, Construction and Building Materials, 157, 554-572.

- Demirboga, R., Turkmen, I., Karakoc, B M. (2007), Thermo-mechanical properties of concrete containing high volume mineral admixtures, *Building and Environment* 42, 349-354.
- Demirboga, Ramaza. (2003), Thermo-mechanical properties of sand and high volume mineral admixtures, *Energy and Buildings*, 35, 435-439.
- Deo, S,V., Pofale, A,D.(2010), Comparative long term study of Concrete Mix Design Procedure for Fine Aggregate Replacement with Fly ash by Minimum Voids method and Maximum Density method, *KSCE Journal of Civil Engineering*, 14(5), 759-764. DOI:10.1007/s12205-010-0911-0.
- Deo, S., Pofale, A D. (2015), Parametric study for replacement of sand by fly ash for better packing and internal curing, *Open Journal of Civil Engineering*, 5, 118-130.
- Dilip, Kumar., Ashish, Gupta., SriRam. (2014), Uses of bottomash in the replacement of fine aggregate for making concrete, *International journal of current engineering and technology*, Vol.4, No.6, December.
- Dinakar, P., Nadesan, S, Manu.(2017), Mix design and properties of Flyash waste lightweight aggregates in structural lightweight concrete, *Case studies in construction materials*, 7, 336-347.
- Dinesh Kumar, G., Mohiuddin, Md.Younus., Haleem M,A. (2016), An experimental study on partial replacement of fine aggregate with coal bottomash in concrete, *International journal of research sciences and advanced engineering*, Vol.2, Issue 15, pp 39-49, August.
- Dixit, K, Manish. (2017), Embodied energy and cost of building materials : correlation analysis, *Building Research & Information*, Vol.45, Issue 5.
- Futane, S, Nityanand., Harle, M, Shrikant.(2016), Partial replacement of fine aggregate with various waste materials, *Journal of research in engineering and applied sciences*, Vol.1, Issue 4, October.
- Gamage, Nirdosha., Setunge, Sujeeva., Liyanage, Kasuni. (2013), An investigation of usability of brown coal flyash for building materials, *Applied Mechanics and MATERIALS*, Vols. 438-439, pp 30-35.
- Gardner, Diane., Pilegis, Martins., Lark, Robert.(2016), An investigation in to the use of manufactured sand as a 100% replacement for fine aggregate in concrete, *Materials*, 9, 440, doi:10.3390/ma9060440
- Gavriletea, Dan, Marius.(2017), Environmental impacts of sand exploitation. Analysis of sand market, *Sustainability*, 9, 1118, doi: 10.3390/su9071118

- Gencil, Osman., Bilir, Turhan., Topku, Bekir, Ilker. (2015), Properties of mortars with fly ash as fine aggregate, *Construction and Building Materials* 93 ,782–789.
- Haque, Md. Emamul. (2013), Indian flyash : production and consumption scenario, *International journal of waste resources*, Vol.3(1), 22-25.
- Harvey, Danny, L.D.(2007), Net Climatic impact of solid foam insulation produced with halocarbon and non-halocarbon blowing agents, *Building and Environment*, 42, 2860-2879.
- Hemalatha, A,C., Chandrakanth, M,G., Nagaraj, N.(2005), Effect of Sand mining on Groundwater depletion in Karnataka, *International R&D Conference of the Central Board of Irrigation and Power*, 15-18 February, Bangalore.
- Herrera, Duran, A., Dimas-Campos, J, K., Tamez-Valdez, P, L., Bentz, P, Dale.(2016), Effect of a micro co-polymer addition on the thermal conductivity of flyash mortars, *Journal of Building Physics*,Vol.40(1), 3-16, DOI: 10.1177/1744259115611650
- Higgins, D.(2006), Sustainable Concrete : How can additions contribute, *The Institute of Concrete Technology, U.K. , Annual Technical Symposium*, March 28.
- Hwang, Kwangryul., Noguchi, Takafumi., Tomosawa, Fuminiro. (2004), Prediction model of compressive strength development of flyash concrete, *Cement and Concrete Research*, 34, 2269-2276.
- Kadam, M, P., Patil, Y, D. (2014), The effect of sieved coal bottomash as a sand substitute on the properties of concrete with percentage variation in cement, *American journal of civil engineering and architecture*, Vol.2, No.5, 160-166.
- Kandpal, T,C., Bhattacharjee, Ujjwal.(2002), Potential of Flyash utilization in India, *Energy*, 27, 151-166.
- Kannan, Kai., Vijaya Kumar, R. (2017), An experimental study on effective utilization of bottomash (ennore) as fine aggregate in concrete under flexure, *International journal of research – Granthaalayah*, Vol.5, Issue 6, June. DOI : <https://doi.org/10.5281/zenodo.818491>
- Karim, M R., Zain, M F M., Jamil, M., Lai, F C., Islam, M N. (2011), Strength development of mortar and concrete containing fly ash, a review , *International Journal of the Physical Sciences*, Vol 6(17) pp 4137-4153, 2 September.
- Kasemchaisiri, R., Tangtermsirikul, S. (2008), Properties of self-compacting concrete incorporating bottomash as a partial replacement of fine aggregate, *Science Asia*, 34, 087-095.

- Kim, Ki, Hyeong. (2015), Utilization of sieved and ground coal bottom ash powders as a coarse binder in high-strength mortar to improve workability, *Construction and Building Materials* 91, 57–64.
- Konstantin, Kovler. (2012), Does the utilization of coal flyash in concrete construction present a radiation hazard ? *Construction and Building Materials*, 29, 158-166.
- Kumar, Satish., Singh, Mani, Kanwar., Mohapatra, S.K.(2015), Comprehensive characterization of Indian Bottomash : Assessment of its potential utilization, *Energy Sources, Part A : Recovery, Utilization and Environmental effects*, 38:18, 2704-2710, DOI:10.1080/15567036.2015.1110644
- Kwon, Jun, Seung., Jung, Hwa, Sang. (2013), Engineering properties of cement mortar with pond ash in South Korea as construction materials: from waste to concrete, *Cent. Eur. J. Eng.* 3(3), 522-533.
- Lacouture-Castro, D., Sefair, A. J., Florez, L., & Medaglia, I. A. (2009). Optimization model for the selection of material using a LEED based green building rating system in Colombia. *Building and Environment*, 44, 1162–1170.
- Lawrence, Mike.(2015), Reducing the Environmental Impact of Construction by using Renewable Materials, *Journal of Renewable Materials*, pp 1-12, Scrivener Publishing.
- Lee, H, K., Kim, H, K. (2011), Use of power plant bottomash as fine and coarse aggregates in high-strength concrete, *Construction and Building Materials*, 25, 1115 – 1122.
- Liew, K,M., Sojobi, A,O., Zhang, L, W.(2017), Green Concrete : Prospects and Challenges, *Construction and Building Materials*, 156, 1063-1095.
- Loya, M,I,M., Rawani, M,A.(2014), Flyash utilization forecast for its key applications, *International Journal of Applications or Innovation in Engineering and Management*, Vol. 3, Issue 5, May, pp 470-477.
- Madhswaran, C, K., Ambily, P,S., Dattatreya, J,K., Rajamane, N,P.(2014), Studies on use of copper slag as replacement material for river sand in building constructions, *Journal of Institution of Engineers(A)*, July-September, 95(3),169-177 DOI 10.1007/s40030-014-0084-9
- Mahapara, Abbas., Kumar, Ravi., Kumar, Dinesh. (2016), Study the effect of coal bottomash and limestone dust as partial replacement of sand and cement, *International journal of scientific research and education*, Vol.4, Issue 5, May, 5363 – 5372. DOI : [http:// dx.doi.org/10.18535/ij sre/v4i05.11](http://dx.doi.org/10.18535/ij sre/v4i05.11)

- Maliki, A, F, I, A., Sahidan, S., Ali, N., Hannan, R, R, I, N., Mohd. Zuki, S, S., Ibrahim, M, H, W., Md.Azmi, M, A., Rahim, M, A. (2017), Compressive and tensile strength for concrete containing coal bottomash, IOP Conf. Series : Materials Science and Engineering, 271, 012055, doi : 10.1088/1757-899X/271/1/012055
- Mani, Monto., Reddy, B,V,V,V., Praseeda, K,I.(2017), Embodied and operational energy of rural dwellings in India, International Journal of Sustainable Energy,
- Mishra, Sumit., Sharma, Neeraj, Kumar., Mitra, Soumik., Sehgal, Vinit.(2012), An assessment of physical properties of coal combustion residues w.r.t. their utilization aspects, International journal of environmental protection, Vol.2, No.2, February, pp 31-38.
- Monahan, J., & Powell, J. C. (2011). An embodied carbon and energy analysis of modern methods of construction in housing: A case study using a lifecycle assessment framework. *Energy and Buildings*, 43, 179–188.
- More, Ashok., Deshmukh, Rohit.(2014), Low energy green materials by embodied energy analysis, International Journal of Civil and Structural Engineering Research, Vo.2, Issue 1, pp 58-65, April-September.
- More, G, Tushar.(2015), a study on concrete properties by partial replacement of sand by pond ash, International Research Journal of Engineering & Technology, Vol.2, Issue 8, November.
- Pajchrowski, Grzegorz., Noskowiak, Andrzej., Lewandowska, Anna., Strykowski, Wladyslaw.(2014), Material composition or energy characteristic- What is more important in environmental life cycle of buildings ? *Building and Environment*, 72, 15-27.
- Pala, P, Kishan., Dhandha, J, Krunal., Nomodiya, N, Paresh.(2015), Use of marble powder and Flyash in self-compacting concrete, International journal for innovative research in science and technology, Vol.1, Issue 12, May, pp 475-479.
- Parvati, V, K., Prakash, B, K.(2013), Feasibility study of Flyash as a replacement for fine aggregate in concrete and its behaviour under sustained elevated temperature, International journal of scientific and engineering research, Vol.4, Issue 5, May.
- Patel, K, Gaurav., Pitroda, Jayeshkumar.(2013), Assessment of natural sand and pond ash in Indian context, International journal of engineering trends and technology, Vol.4, Issue 10, October, PP 4287-4292.
- Pennacchio, R., Savio, L., Bosia, D, et al.(2017), Fitness : Sheep-wool and hemp sustainable insulation panels, *Energy Procedia*, 111, 287-297.

- Pitchaiah, Shankara, Podila.(2017), Impacts of sand mining on environment – A review, SSRG International journal of Geo informatics and Geological science, Vol.4, Issue 1, Jan to April.
- Pramila, Kumari., Dhadse, Sharda., Bhagia, L.J.(2008), Fly ash characterization , utilization and Government initiatives – a Review, Journal of Scientific and Industrial Research, Vol.67, January, pp 11-18.
- Rafat, Siddique. (2014), Utilization of industrial by-products in concrete, Procedia Engineering, 95, 335-347.
- Rafieizonooz, Mahdi., Mirza, Jahangir., Salim, Razman, Mohd., Hussin, Warid, Mohd., Khankhaje, Elnaz. (2016), Investigation of coal bottom ash and fly ash in concrete as replacement of sand and cement, Construction and Building Materials, 116, 15-24.
- Rafieizonooz, Mahdi.,Salim, Razman Mohd. Et al.(2017), Toxicity characteristics and durability of concrete containing coal ash as substitute for cement and river sand, Construction and Building Materials 143, 234-246.
- Rai, Baboo., Kumar, Sanjay., Kumar, Satish. (2014), Effect of flyash on mortar mixes with quarry dust as fine aggregate, Advances in Materials Science and Engineering, <http://dx.doi.org/10.1155/2014/626425>.
- Rajamane N P., Ambily P S. (2013), Fly ash as a sand replacement material in concrete – a study, Indian Concrete Journal, July.
- Rajamane, N, P., Peter, J, Annie., Ambily, P. S.(2007), Prediction of compressive strength of concrete with Flyash as sand replacement material, Cement & Concrete Composites, 29, 218-223.
- Ramadoss, P., Sundararajan, T. (2014), Utilization of Lignite-Based Bottom Ash as Partial Replacement of Fine Aggregate in Masonry Mortar, Arab J.Sci Eng.,39, 737-745, DOI 10.1007/s13369-013-0703-1.
- Ramamurthy, K., Geetha, S. (2010), Re-use potential of low calcium bottomash as aggregate through pelletization, Waste Management, 30, 1528-1535.
- Ramamurthy, K., Nambiar, K,K,E. (2007), Sorption characteristics of foam concrete, Cement and Concrete Research, Vol.37, Issue 9.
- Ramesh, T, S., G, Rajan., Nidheesh, V, Puthiya., Rajakumar, S., Pratapkumar, S.(2013), Use of furnace slag and welding slag as replacement for sand in concrete, International journal of Energy and Environmental Engineering, 4, 3, pp 1-6.

- Rashad, M, Alaa. (2015), Review Article : A brief on high-volume Class F fly ash as cement replacement – A guide for Civil Engineer, *International Journal of Sustainable Built Environment*, 4, 278-306.
- Rattanasak, Ubolluk., Chindaprasirt, Prinya., Jaturapitakkul, Chai., Chalee, Wichian.(2009), Comparative study on the characteristics of flyash and bottomash geopolymer, *Waste Management*, 29, 539-543.
- Ravina, D. (1997), Properties of fresh concrete incorporating a high volume of fly ash as partial fine sand replacement, *Materials and Structures/Materiaux et Constructions*, Vol. 30, October, pp 473-479.
- Rocha, J, C., Andrade, L, B., Cheriaf, M. (2009), Influence of coal bottomash as fine aggregate on fresh properties of concrete, *Construction and Building Materials*, 23, 609-614.
- Sadon, S, N., Beddu, S., Naganathan, S., Kamal, Md., N, L., Hassan, H. (2017), Coal bottomash as sustainable material in concrete – A Review, *Indian journal of science and technology*, Vo.10(36), September, DOI : 10.17485/ijst/2017/v10i36/114595
- Sahmaran, Mustafa., Christi, Anto, Ari, Heru., Yaman, Ozgur, Ismail. (2006), The effect of chemical admixtures and mineral additives on the properties of self-compacting mortars, *Cement and Concrete Composites* 28,432-440.
- Sangoju, Bhaskar., Ramesh, G., Bharatkumar, B, H., Ramanjaneyulu, k.(2017), Evaluation of durability parameters of concrete with manufactured sand and river sand, *Journal of Institution of Engineers(A)*, September, 98(3), 267-275.
- Sani, H, S, Bin, Mohd., Muftah, F., Muda, Zulkifli. (2010), The properties of special concrete using washed bottom ash as partial sand replacement, *International journal of sustainable construction engineering and technology*, Vol.1, No.2, December.
- Sankh, C, Akshay., Biradar, M, Praveen., Naghathan, S,J., Ishwargol,B, Manjunath. (2014), Recent trends in replacement of natural sand with different alternatives, *IOSR Journal of Mechanical and Civil Engineering*, pp 59-66.
- Sata, Vanchai., Zaetang, Yuwadee., Wongs, Ampol., Chindaprasirt, Prinya. (2015), Use of coal ash as geopolymer binder and coarse aggregate in pervious concrete, *Construction and Building Materials*, 96, 289-295.
- Saxena, V,K., Kant, U., Sarkar, A., Varma, Atul, K., Mishra, K, K.(2012), Characterization of coal ash from a captive power plant for potential end uses,

Proceedings of the EUROCOALASH Conference, Thessaloniki, Greece, September 25-27.

Shahidan, Shahiron., Ramzi, R, I, N., Maarof, Z, M., Ali, N. (2016), Physical and chemical properties of coal bottom ash from Tanjung Bin Power Plant, IOP Conference Series, Materials Science and Engineering, 160, 012056, doi:10.1088/1757-899X/160/1/012056

Shah, A., Samad, S. (2017), Role of binary cement including Supplementary Cementing Materials (SCM) in production of environmentally sustainable concrete : A critical review, International journal of sustainable built environment, 6, 663 – 674.

Siddique, Rafat. (2003), Compressive strength, water absorption, sorptivity, abrasion resistance and permeability of self-compacting concrete containing coal bottomash, Construction and Building Materials, 47, 1444-1450.

Siddique, Rafat.(2003), Effect of fine aggregate replacement with Class F Flyash on the mechanical properties of concrete, Cement and Concrete Research, 33, 539-547.

Singh, Gurpit., Kumar, Satish., Mohapatra, S.K., Kumar, Kaushal.(2017), Comprehensive characterization of grounded bottom ash from Indian thermal power plants, Journal of Residual Science & Technology, Vol.14, No.1, January.

Singh, Malkit., Siddique, Rafat. (2014), Strength properties and micro-structural properties of concrete containing coal bottomash as partial replacement of fine aggregate, Construction and Building Materials, 50, 246-256.

Singh, Malkit., Siddique, Rafat. (2015), Properties of concrete containing high volumes of coal bottomash as fine aggregate, Journal of Cleaner Production, 91, 269-278.

Singh, Malkit., Siddique, Rafat. (2016), Effect of coal bottomash as partial replacement of sand on workability and strength properties of concrete, Journal of Cleaner Production, 112, 620-630.

Soman, K., Sasi, Divya., Abubaker, K, A. (2014), Strength properties of concrete with partial replacement of sand by bottomash, International journal of innovative research in advanced engineering, Vol.1, Issue 7, August.

Sukesh, C., Krishna, B, K., Sai Teja, S, L, P., Rao, S, K.(2013), Partial replacement of sand by quarry dust in concrete, International journal of innovative technology and exploring engineering, Vol.2, Issue 6, May.

Surabhi (2017), Flyash in India : Generation vis-à-vis utilization and global perspective, International Journal of Applied Chemistry, Volume 13, No.1, pp 29-52.

- Suresh S., Mishra, Animesh et al.2013, Green cement for sustainable concrete using marble dust, *International Journal of Chem Tech Research*, Vol.5, No.2, April-June, 2015, pp 616-622.
- Tae, Sungho., Kim, Taehyoung., Chae, U, Chang. (2016), Analysis of Environmental impact for Concrete using LCA by varying the Recycling components, the Compressive strength, and the Admixture material mixing, *Sustainability*, 8, 389, doi : 10.3390/su8040389
- Thaarrini, Janardhanan., Ramasamy, Venkatasubramani. (2015), Feasibility Studies on Compressive Strength of Ground Coal Ash Geopolymer Mortar, *Periodica Polytechnica Civil Engineering*, 59(3), pp. 373–379.
- Thormark, C. (2002). A low energy building in a life cycle – its embodied energy, energy need for operation and recycling potential. *Building and Environment*, 37, 429–435.
- UNEP (2014), Sand, rarer than one thinks, UNEP-Global Environmental Alert Service, March
- Vijayalakshmi, M.M., Natarajan, E., Shanmugasundaram, V. (2006), Thermal behaviour of building wall elements. *J. Appl. Sci.* 6 (15), 3128e3133.
- Yu, Jing., Lu, Cong., Leung, K,Y,C., Li, Gengying. (2017), Mechanical properties of green structural concrete with ultra high volume fly ash, *Construction and Building Materials*, 147, 510-518.
- Yukse, I. (2015). The evaluation of building materials in terms of energy efficiency. *Periodica Polytechnica Civil Engineering*, 59(1), 45–58. doi:10.3311/PPci.7050

Chapter 3

- ASTM C 618-12a (Dec.15, 2012) Standard Specification for Coal Fly ash and raw or calcined natural pozzolan for use in Concrete, DOI:10.1520/C0618–12a.
- Das, Sukhen., Sultana, Parveen., Bagchi, Biswajoy et al. (2011), Effect of size of fly ash particle on enhancement of mullite content and glass formation, *Bull. of Mater. Sc.*, Vol. 34, No.7, December, pp 1663-1670.
- Dasgupta, S., Roy, S, K.(1985), *Chemical Analysis of Ceramic and Allied Materials*, published by Indian Institute of Ceramics, Calcutta.

India Brand Equity Foundation (IBEF, 2018), Indian Cement Industry Analysis, October

IS 10262 –2009, Indian Standard Concrete Mix Proportioning – Guidelines, Bureau of Indian Standards, Manak Bhavan, New Delhi – 110002.

IS 1077-1992 (Reaffirmed 2002), Indian Standard Common Burnt Clay Building Bricks – Specification, Bureau of Indian Standards, Manak Bhavan, New Delhi – 110002.

IS 1489, Part-1(1991, Reaffirmed 2005), Indian Standard Portland Pozzolana Cement Specification, Part 1 fly ash based (Third revision), Bureau of Indian Standards, Manak Bhavan, New Delhi – 110002.

IS 2250-1981 (Reaffirmed 2000), Indian Standard Code of Practice for Preparation and use of Masonry Mortars, Bureau of Indian Standards, Manak Bhavan, New Delhi – 110002.

IS 2541-1991 (Reaffirmed 2000), Indian Standard Preparation and Use of Lime Concrete – Code of Practice, Bureau of Indian Standards, Manak Bhavan, New Delhi – 110002.

IS 3812-1981 (Reaffirmed 1999), Indian Standard Specification for Fly ash for use as pozzolan and admixture, Bureau of Indian Standards, Manak Bhavan, New Delhi – 110002.

IS 383 (1970, Reaffirmed 2002), Indian Standard Specification for Coarse and Fine Aggregates from Natural sources for Concrete, Bureau of Indian Standards, Manak Bhavan, New Delhi – 110002.

IS 456 – 2000 (Amended on May 4, 2013), Indian Standard Plain and Reinforced Concrete – Code of Practice, Bureau of Indian Standards, Manak Bhavan, New Delhi – 110002.

IS 516 – 1959 (Reaffirmed 2004), Indian Standard methods of tests for strength of concrete, Bureau of Indian Standards, Manak Bhavan, New Delhi – 110002.

IS 3495 (Pt. 1 to 4) – 1992 (Reaffirmed 2002), Indian Standard Methods of Tests of Burnt Clay Building Bricks, Bureau of Indian Standards, Manak Bhavan, New Delhi 2
Ohira, H *et al.*, 1991, *J. Mater. Sci., Lett.* **10**, 847

Schneider, H., Okada, K., and Pask, J., 1994, *Mullite and mullite ceramics*

SP 23 – 1982, Handbook on Concrete Mixes (based on Indian Standards), Bureau of Indian Standards, Manak Bhavan, New Delhi – 110002.

SP 41(S&T) – 1987, Handbook on Functional requirements of Buildings (Other than Industrial Buildings), Bureau of Indian Standards, Manak Bhavan, New Delhi – 110002

Chapter 4

Book: Inventors and Inventions, Volume 4, Marshall Cavendish Reference, New York.

IS 10262 (2009), Indian Standard Concrete Mix Proportioning – Guidelines, Bureau of Indian Standards, Manak Bhavan, New Delhi – 110002.

IS 456 (2000) (Amended on May 4, 2013), Indian Standard Plain and Reinforced Concrete – Code of Practice, Bureau of Indian Standards, Manak Bhavan, New Delhi – 110002.

Steiger, W, Richard. (1995), The history of concrete, Part 2, Publication # J950644.

Published Papers
&
Abstract Acceptance
Communications

[IC2UHI2019] Review Results of Abstract

Boxbe Waiting List x



IC2UHI2019 Organizers
<info@heatilandcountermeasures.org>

Wed, 2 Jan, 13:35 (9 days ago)

to me

boxbe IC2UHI2019 Organizers (info@heatilandcountermeasures.org) is not on [your Guest List](#) | [Approve sender](#) | [Approve domain](#)

Dear AVIJIT GHOSH,

We are pleased to inform you that the following abstract submitted to IC2UHI2019 has been Accepted.

CONTRIBUTION DETAILS

Paper ID: 269

Title: Coal Ash as Cool Material for Energy Efficient Building Envelop Construction

OpenConf Peer Review & Conference Management System

[OpenConf Home](#) | [Privacy Policy](#) | [Email Chair](#)

The first International Conference on Countermeasures to Urban Heat Islands (IC2UHI) was held in 2006 at Tokyo and since then it's been conducted at various locations such as Berkeley(California), [Venice](#), and [Singapore](#).

The Fifth International Conference on Countermeasure to Urban Heat Islands (5th IC2UHI), will be hosted at Hyderabad, India and will be devoted to the science, engineering, and public policies to help relieve the excess heat and air pollution of Summers in hot cities. It has long been recognized that the excessive heat and smog in many cities in the summer, the "Urban Heat Island", is partly due to the choices of building materials, vegetation, and urban design.

Scientist, engineers, builders, architects, and government officials, especially, but not limited to Asia Pacific countries, concerned with improving the urban environment are urged to participate in 5th IC2UHI which promises to advance the field.

Selected Conference papers will be published in Energy and Buildings Journal, Proposed Special Issue: Countering urban Heat Island (UHI) and Climate Change Through Mitigation and Adaptation.

Authors:

- [Edit Submission](#)
- [Check Status](#)

Review and Program Committees:

- [Sign In](#)

International Conference on Innovative Applied Energy

14-15 March 2019.

St Cross College, University of Oxford, United Kingdom



ACCEPTANCE LETTER

Dear respected professor **Avijit Ghosh**,

We are pleased to inform you that the Program Committee has recommended **acceptance** of your keynote talk proposal, entitled "**Coal Combustion Residues as Sand Substitute for Energy Efficient Building Envelop Construction**", for presentation at the International Conference on Innovative Applied Energy (IAPE'19). We cordially invite you to attend the IAPE'19 conference.

The conference will be held during March 14-15, 2019 in the St Cross College, University of Oxford, United Kingdom. Further information on the event can be accessed on the web at: <http://iape-conference.org/>.

Feel free to contact the conference management Chair for any questions through e-mail at contact@iape-conference.org.

We look forward to welcoming you in the conference.

Sincerely yours,

Fauzi Hidoussi,

IAPE'19 Management chair,

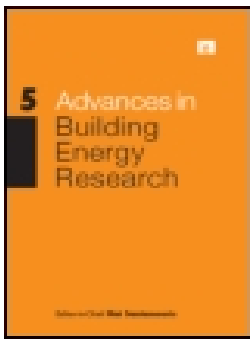
Director of Corgascience Limited, UK

Email: contact@iape-conference.org iape.oxford@gmail.com

Tel: +443301331367

Date: May 15, 2018





Evaluation of physical and thermal properties of coal combustion residue blended concrete for energy efficient building application in India

Avijit Ghosh, Arup Ghosh & Subhasis Neogi

To cite this article: Avijit Ghosh, Arup Ghosh & Subhasis Neogi (2018): Evaluation of physical and thermal properties of coal combustion residue blended concrete for energy efficient building application in India, *Advances in Building Energy Research*

To link to this article: <https://doi.org/10.1080/17512549.2018.1557076>



Published online: 20 Dec 2018.



Submit your article to this journal [↗](#)



View Crossmark data [↗](#)



Evaluation of physical and thermal properties of coal combustion residue blended concrete for energy efficient building application in India

Avijit Ghosh ^a, Arup Ghosh^a and Subhasis Neogi^b

^aCSIR-Central Glass & Ceramic Research Institute, Kolkata-32, West Bengal, India; ^bSchool of Energy Studies, Jadavpur University, Kolkata-32, West Bengal, India

ABSTRACT

At the backdrop of energy conservation efforts in building sector, this research paper presents a passive approach by producing less heat conducting concrete with the inclusion of coal combustion residue (bottom ash) as a substitute to conventional sand and using low embodied energy cement in the mix. The constituent phases and other physical and chemical parameters of both sand and bottom ash were evaluated. Three different sets of concrete mixes were prepared by following IS 456 code provisions, and the compressive strength, apparent porosity, bulk density and the thermal conductivity parameters of each mix set were evaluated. The reducing trend was observed in thermal conductivity and compressive strength parameters of concrete mixes against the increasing percentage of sand replacement by coal bottom ash. Reduction to the tune of around 25% in the thermal transmittance value (U -value) was observed while comparison was made between conventional concrete roof and bottom ash blended concrete roof with identical features. Coal combustion residue blended concrete could be applied for sustainable and energy efficient building construction for lowering cooling demand without any additional capital investment and also saving sand from faster depletion than its renewal rate.

ARTICLE HISTORY

Received 5 April 2018
Accepted 5 December 2018



KEYWORDS

Concrete; bottom ash;
thermal conductivity; energy;
building

1. Introduction

As per recent estimates, nearly 590 Million people will be living in Indian cities by 2030 (MoUD, 2016), and around 70% of the building stock that will be there in the year 2030 is yet to come up in the country (Kumar, 2010). An increase in 400% in the aggregate floor area of buildings and 20 billion m² of new building floor area is expected by 2030 (Satish, 2011).

On the other hand, urbanization, increased heat waves and gradual temperature rise are directing towards higher cooling demand. Heat gain by building envelop warrants the mechanical cooling requirement to maintain interior comfort condition. The increasing demand for conditioned thermal comfort is projected to continue its exponential growth with increasing numbers of building stock (both residential and commercial), and becoming one of the prime contributors to Greenhouse gas emission. Concrete is an integral material in building construction with considerable carbon footprint. Roof, floor and other structural components like

CONTACT Avijit Ghosh  avijitenergy@gmail.com; renewableenergyavijit@gmail.com  CSIR-Central Glass & Ceramic Research Institute, 196, Raja S. C. Mallick Road, Kolkata-32, West Bengal, India

© 2018 Informa UK Limited, trading as Taylor & Francis Group

beams, columns etc. are the important part of a modern concrete framed building. Since the roof portion of a reinforced concrete framed building is subjected to direct solar radiation, the thermal property of concrete is considered to be directly responsible for radiation induced heat entry inside the building. Through this work, it was tried to assess the changes in the physical and thermal properties of blended concrete with coal combustion residue in lieu of sand, while compared with conventional concrete with sand, and its suitability for energy efficient building application. It was found that Ordinary Portland Cement (OPC) contains the highest Global Warming Potential (GWP), Photochemical Ozone Creation Potential (POCP) and Abiotic Depletion Potential (ADP) (Tae, Kim, & Chae, 2016). To exhibit higher thermal resistance in building envelop, different insulation materials and cool roof paints are randomly considered by the energy efficient building designers, but the embodied energy content and global warming potential of popularly used insulation materials made of polystyrene, polyurethane, mineral wool, fibre glass, etc. are quite high (Harvey, 2007). High Albedo roof with white coating for Cool Roof feature contain embodied energy to the tune of 23 MJ/m² of roof surface (Gupta, Sharma, & Sharma, 2013). Since, the major carbon intensive component in concrete is cement, sustainable concrete mixes (three different mix proportions with gradual replacement of sand by bottom ash) had been adopted for this work with the inclusion of Portland Pozzolana Cement (PPC) (30% fly ash blended), stone aggregate, water and without additive of any kind. The extent of thermal resistance offered by such concrete mixes had been explored herein.

The earlier works related to utilization of coal bottom ash in concrete, by other researchers like Kumar, Gupta, and Ram (2014), Kadam and Patil (2013, 2014), Cadessa and Auckburally (2014), Aggarwal, Aggarwal, and Gupta (2007), Kumar, Dinesh, Younus, and Haleem (2016), Abbas, Kumar, and Kumar (2016) had been studied. All of them used OPC, sand, bottom ash and stone aggregate as the concrete mix constituents. The outcome more or less revealed that 10–30% replacement of sand by bottom ash did not adversely affect the strength gain in the concrete, except some losses in workability and flexural strength parameters. Ganesh, Bai, Nagendra, and Bagade (2011) adjudged the properties like shape, gradation, texture, physical, chemical and morphological limits of pond ash and found the same as partially suitable against sand in concrete. Physical and thermal properties of concrete with mineral admixtures like fly ash and blast furnace slag as partial replacement of OPC was investigated by Demirboga, Turkmen, and Karakoc (2007), and observed reduction in both thermal conductivity value, and strength value at 28 days maturity period. Rafeizonooz, Mirza, Salim, Hussin, and Khankhaje (2016, 2017) investigated about the effect of bottom ash and fly ash in concrete, which were used as replacement against sand and OPC respectively in different percentages. During 28 days maturity period, no significant changes in various strength parameters could be observed, though workability was compromised. At 91 and 180 days of curing, all the strength parameters were found to increase considerably. Toxicity parameters and durability aspects like leaching procedure, sulphate and acid attack and elevated temperature effects on concrete blended with coal ash as replacement of cement and sand were studied, and the test results revealed satisfactory results without any adverse effect, and recommended to be used as clean construction material. With the aim of developing guidelines for eco-design of buildings, Bribain, Capila, and Uson (2011) had undertaken life-cycle assessment of building materials. The assessment of building materials included energy requirement at production stage as also during utilization stage, based on which selection of appropriate material could be made for obtaining true energy efficiency. Monahan and Powell (2011) had undertaken embodied and carbon analysis for

modern construction methods, adopted in housing. It was found that concrete was having 51% more embodied carbon than offsite panelized timber framed house. Some suggestions were made to save embodied carbon like the selection of sustainable materials by cement substitute, thermal storage consideration, waste minimization at on-site location, etc. Thormark (2002) investigated about the total energy use in low energy building including embodied energy of materials, operational energy during effective usage period and recycling at the end of life. It was found in one of the most energy efficient building that embodied energy content was 40% of total energy and recycling potential was 15% of total energy, so it was advisable to address such potentialities adequately. Lacouture-Castro, Sefair, Florez, and Medaglia (2009) explored about the selection methodology for appropriate building materials on the basis of LEED-based Green building rating system in Columbia. The system in Columbia is highly dependent on the use of material with low VOC content, and a high content of recycling potential, influenced by cost aspect. Pajchrowski, Noskowiak, Lewandowska, and Strykowski (2014) had compared four types of constructions with different material compositions from Life-Cycle Analysis point of view and concluded that the building with lesser electrical energy demand was more environmentally beneficial, even though the building may not be passively oriented or designed. Lawrence (2015) had made a study with renewable bio based materials to reduce embodied and operational energy in the buildings. Straw-bale/straw-clay/hemp-lime constructions, sheep wool as insulation material, etc. were explored as materials with above two advantages. Asdrubali, D'Alessandro, and Schiavoni (2015) had tried to find out an alternative insulation material other than petroleum based polystyrene or glass/rock wool which were actually high process energy based materials. It was explored that organic plant-based by-products and residues and recycled materials could be the viable alternative against the conventional commercially available highly energy intensive EPS/XPS insulation materials. Yuksek (2015) explored the selection of energy efficient materials in designing energy efficient buildings. The embodied energy content and embodied CO₂ equivalent of commercial insulating materials also analysed before selection. Natural materials like wood, gypsum mud bricks, pumice, perlite, cellular concrete, etc. were assessed on parameters like local availability, recycle content, renewable source, consuming low energy at site, low thermal conductivity, etc. and found to be more advantageous from energy efficiency as also from the environmental sustainability point of views. Pennacchio et al. (2017) experimented with hemp and sheep-wool semi-rigid panel, which were tested as thermal insulation as well as acoustic purposes respectively. The test results for both the parameters were found more than satisfactory and fit to use. More and Deshmukh (2014) had tried to analyse the embodied energy of various building materials, and calculated that of various concrete mixes. To arrive at a strong correlation between embodied energy and cost of the material, Dixit (2017) had worked with 21 common building materials and found an improved input-output based hybrid model for accurate result. Mani, Reddy, and Praseeda (2017) had examined the embodied energy, operational energy and life-cycle energy of 27 dwelling units, spread across 4 different Climatic zones of India. With the accessibility of modern transportations, energy intensive construction materials are available in rural areas also, and the life-cycle energy values remain within the range of 0.77–4.05 GJ/m². Arumugam et al. (2014) had studied the effect of cool roof for an un-conditioned institutional building under Composite Climatic condition in India. Monitoring the effect of cool roof condition on a concrete surface for six months, it was observed that seasonal average air temperature was reduced by 1.07°C, and average heat flux reduction was around 14.4 W/m². Around 8% increase in adaptive comfort hours effected in comparison with dark roof. Role of cool material in arresting heat transmission

through roof was explored by Costanzo, Evola, and Marletta (2013) in an existing office building at Southern Italy. Simulation study was carried out to see the effect of cool paint on roof area from energy saving and thermal comfort points of views. Akbari and Touchaei (2013) had studied the effect of increasing the albedo of roofs of Greater Montreal area on air and skin temperature distribution patterns. Performing simulation study during Summer period, considerable reduction in air and skin temperature were predicted in comparison with cool roof effect. Butera (2010) had studied that to mitigate the global warming impact, a balancing pathway with low-carbon energy solutions must be in place, applicable equally for poor and rich cities with variations in standards of living. The analysis found the availability of technological solutions to reach the target of such convergence to mitigate global warming phenomena. In the light of the above literature survey, it may be summarized that coal bottom ash may be utilized as fine aggregate substitute in concrete mix, at different ratios.

The novelty in the present work was to use such ingredients in concrete, which are either with less embodied energy content or industrial waste, whose proper disposal or utilization remain difficult. In almost all the above referred works, OPC was used, as a major constituent of concrete. According to Higgins (2006), 17% less CO₂ emission to the atmosphere, 14% less primary energy requirement and 4% less mineral extraction effected for production of 1 t of concrete by PPC with 30% flyash in comparison with OPC. No additional energy or chemical input in preparing the concrete mix was adopted for this work. The coal combustion residue does not contain any embodied energy. The proposed blended concrete possesses lower level of operational energy requirement during the functional period due to its higher thermal resistance value than that of conventional concrete, and can act passively for energy conservation in buildings.

2. Materials and methods

Commercially available PPC, natural river Sand, Coarse aggregate of 10 mm down size, potable water for mixing and curing, and Bottom ash obtained from nearby Budge Budge Thermal Power Plant, (located at South 24 Paraganas in the State of West Bengal, India and at a road distance of 25 kms from the experimental set-up location) were utilized throughout the experiment. For all the mixes, those materials were used by following relevant Indian Standard (IS) Codes of Practices.

Quantitative Chemical Analysis of powder samples like sand and bottom ash were done by Wet Chemical method, which is the collective analysis through solution chemistry route for individual elements in their oxide form (CaO, MgO, Na₂O etc.), acid based titration route for silica analysis (for SiO₂) and gravimetric route for loss on ignition component. Sieve analysis for sand, bottom ash and coarse aggregate were done by using IS sieve set (IS 383 1970). Apparent porosity and bulk density tests were carried out with the help of electronic weighing machine, glass container and some hanging arrangement for immersing the samples within water inside the glass container. Specific gravity was determined as per IS 2386 Part III (1963). Compressive strength test of concrete samples was carried out under Concrete Compression Machine (CCM) as per IS 516 (1959). X-Ray Diffraction (XRD) analysis for sand and bottom ash were done with a PANalytical X'Pert's Pro powder diffractometer with X'Celerator detector and variable divergence- and receiving slits with Fe filtered Cu-K α radiation in a diffraction angle (2θ) range of 15°–70°. The phases of the materials were identified using X'Pert Highscore plus software. Field

Emission Scanning Electron Microscopy (FESEM SUPRA 35VP) was used for high resolution micro structural analysis for bottom ash and sand samples. Thermal conductivity of concrete samples was determined with the help of Hot Disk TPS 2500S Analyzer.

Three sets of different concrete mix were prepared by following IS 456 (2000) stipulations under Cl.9.3 for Nominal Mix Concrete. All the three sets consist of 1 part of PPC (fly ash based), 1/1.5/2 parts of Sand and Sand-bottom ash combinations, and 2/3/4 parts of Stone Aggregate, respectively. The mix proportions for A-set was 1:1:2, for B-set was 1:1.5:3 and for C-set was 1:2:4, respectively. The above mentioned proportions had been arrived at by the IS 456 stipulation which states that the proportion of fine aggregate to coarse aggregate (by mass) should be generally 1:2. In all the series, the mix with A, B and C nomenclatures were of controlled concrete with usual ingredients. Subsequent to A, B and C, sand was replaced by bottom ash in 10% steps and marked as A-1, B-1,C-1, A-2, B-2,C-2, ... etc. up to 100% replacement at A-10, B-10 and C-10. The proportions of these three sets are tabulated under Table 5.

Six numbers of 50 mm by 50 mm by 50 mm cubes were filled with above mixes for each identity and one pair each of 50 mm by 50 mm by 12.5 mm moulds were also filled with same concrete from the same batch of casting. Each of the moulds was filled in three layers, tamped with bullet pointed tamping rod of 10 mm diameter, and finally vibrated with the help of electrically operated vibrating table with regulated speed. Other samples were kept for thermal conductivity, apparent porosity and bulk density testing respectively. The samples, as cast were de-moulded after 24 h, and immediately kept immersed in to normal water storage bucket at room temperature for curing till the respective test age was attained. Three cubes each were tested with the help of CCM to determine 7 days' compressive strength, and 28 days' compressive strength respectively. Transient Plane Source (TPS) technique is a device that can be used both in laboratory and in-situ measurements of all three related properties from cryogenic to high temperature (1000 K). It can measure thermal conductivities between 0.01 and 500 W/m-K. The TPS method involves the use of a very thin double metal spiral, 10 μm thickness, sandwiched between two layers of Kapton (25 μm thickness), in close contact with the material to be investigated. The double metal spiral serves both as the heat source and as a resistance thermometer. When making measurements in solid bodies, the spiral is clamped between two surfaces of the same material (Johansson, Zarrabi-Adal, & Hagentoft, 2012), as shown in the Figure 10. The radius of the sensor can vary between 2 and 30 mm thus, the sample size can vary between 8 and 120 mm or larger. The testing of solid samples was done by this method following ISO-22007 Part-2 (2008).

3. Results

This section gathers results pertaining to all the tests carried out on raw materials used in this work about their physical, chemical and radiological parameters and the subsequent physical and thermal tests conducted on the concrete samples of described mix proportions, made out of the above ingredients.

3.1. Material test result

PPC with 30% fly ash content had been considered as the main constituent of blended concrete with lower embedded energy, and with adequate compressive strength. As

per stipulations made under IS 1489 (Part-1) (1991), fly ash-based PPC was used with the physical and chemical properties, listed under Tables 1 and 2, respectively, which showed that the code provisions had been complied with.

The specific gravity test and sieve analysis for sand used in this study were carried out as per IS 2386 (Part-III) (1963) and IS 383 (1970), respectively. The grading curve is shown under Figure 1, and other physical parameters are shown under Table 4. The grading curve of the sand used for this work fitted within the limit specified for Zone-II sand in the code. XRD Phase diagram and Scanning electron microscopic (SEM) image of sand are shown under Figures 2 and 3, respectively. The phase analysis by XRD showed main phases as (a) quartz (SiO_2), (b) Protoenstatite (MgSiO_3), (c) Hydromolysite ($\text{FeCl}_3, 6\text{SiO}_2$) and (d) Titanium Oxide (TiO). Angular and irregular shaped sand grains were observed through SEM image.

Alike sand, specific gravity test and sieve analysis of bottom ash were performed. XRD phase analysis and SEM image are shown under Figures 4 and 5 respectively, and the

Table 1. Physical properties of Portland Pozzolana Cement (fly ash based).

Properties	Limits prescribed in BIS 1489	Results as per test certificate
Fineness-specific surface	300 (m^2/kg), Minimum	440 (m^2/kg)
Initial setting time	30 min, Minimum	150 min
Final setting time	600 min, Maximum	600 min
3 Days' compressive strength	16 MPa, Minimum	24.5 MPa
7 Days' compressive strength	22 MPa, Minimum	33.5 MPa
28 Days' compressive strength	33 MPa, Minimum	49.5 MPa
Soundness by Le Chatelier	10 mm, Maximum	1.0 mm
Soundness by autoclave	0.8%, Maximum	0.6%
Drying shrinkage	0.15%, Maximum	0.06%

Table 2. Chemical properties of Portland Pozzolana Cement (Fly ash based).

Properties	Limits prescribed in BIS 1489	Results as per test certificate (%)
Loss on ignition, percent by mass.	5%, Maximum	1.5
Magnesia (MgO), percent by mass.	6%, Maximum	2.41
Sulphuric anhydride (SO_3), percent by mass.	3%, Maximum	2.15
Insoluble material, percent by mass	37.6 (%), Maximum	32.8
Percentage of fly ash	15-35% Maximum	30

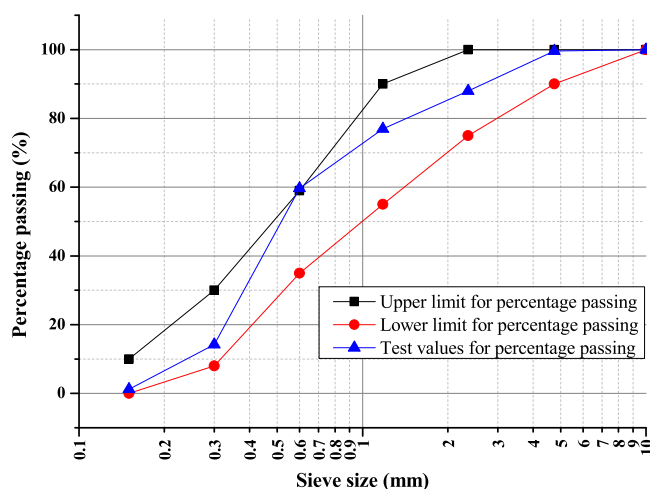


Figure 1. Sand grading curve showing compliance with Zone-II as per IS 383.

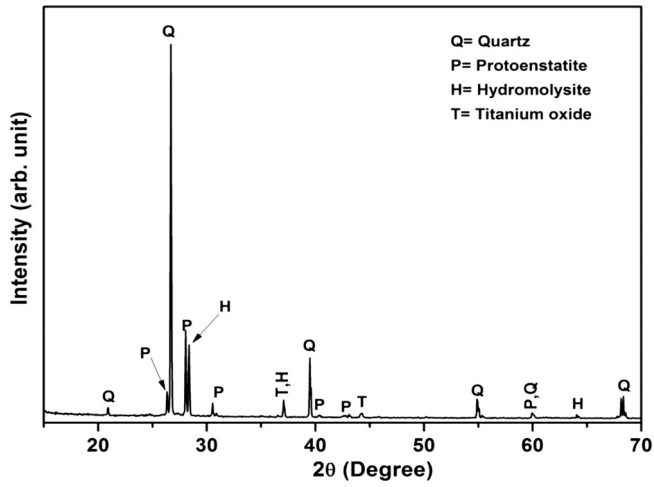


Figure 2. XRD pattern of sand, showing dominant phase of quartz and other minor phase compounds.

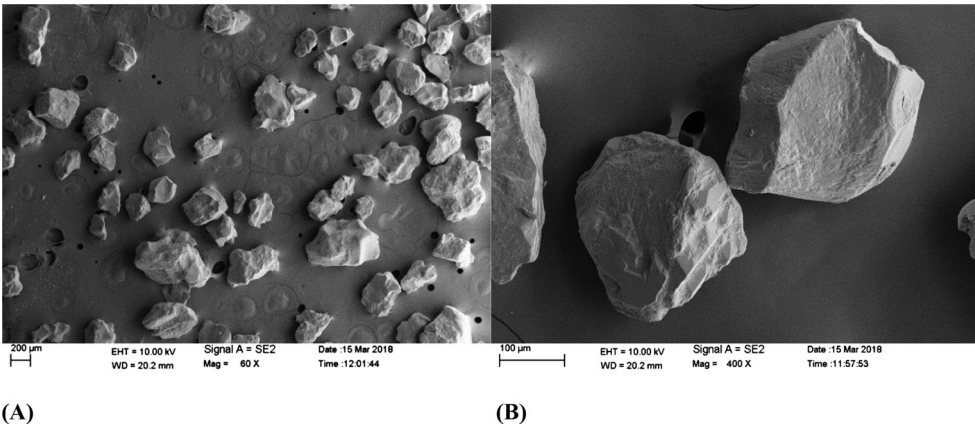


Figure 3. SEM images of sand, showing structural shape and size of particles.

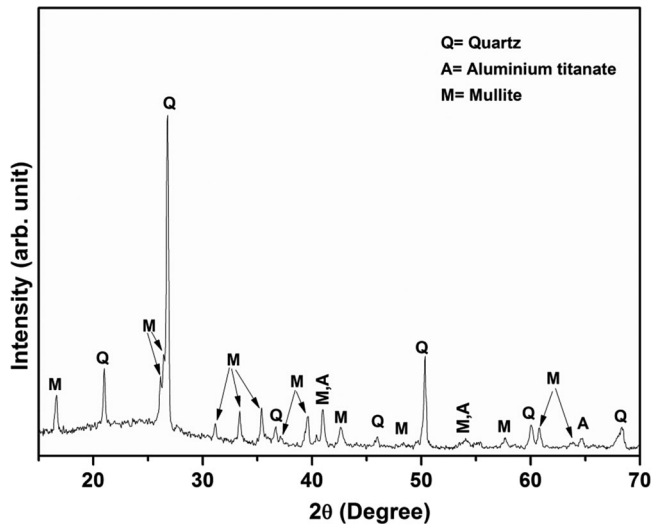


Figure 4. XRD pattern of bottom ash, showing dominant phase of quartz and other minor phase compounds.

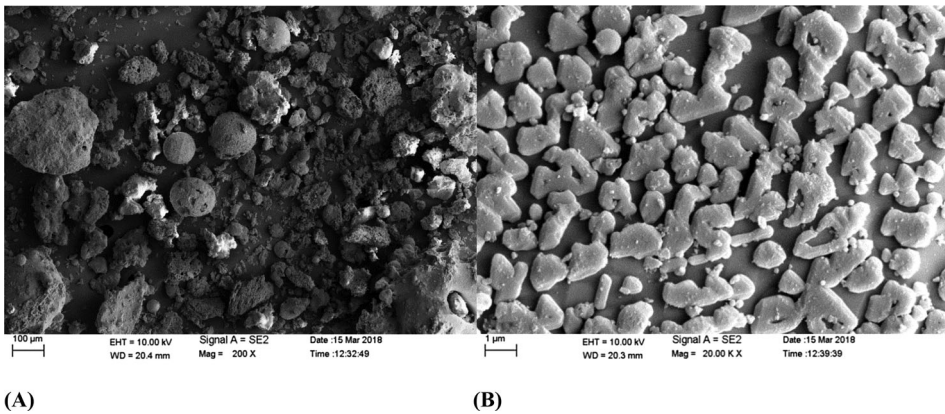


Figure 5. SEM images of bottom ash, showing its structural shape and size at higher magnification.

grading curve is shown under Figure 6. The grading of bottom ash fits within Zone-III limit, as specified in the code, and the specific gravity value established its lightness in comparison with sand particle. XRD phase analysis showed the quartz, aluminium titanate and mullite as main phases, and the SEM image showed irregular shaped hollow particles. Chemical properties and other physical parameters of bottom ash are listed under Tables 3 and 4, respectively. Chemical properties clearly indicated that the ash complied with IS 3812 (1981) stipulations for incorporations in cement mortar and in concrete, respectively.

The sieve analysis for 10 mm down size stone aggregate was carried out as per IS 383 (1970) stipulations and the grading curve for stone aggregate is shown under Figure 7, and the physical properties are listed under Table 4. The grading fitted well within the limit, as specified in the code, and shown in Figure 7.

3.2. Compressive strength test results

The concrete cube samples were tested as per IS 516 (1959). The compressive strength values of A-set, B-set and C-set concrete mixes at 7 and 28 days maturity are listed

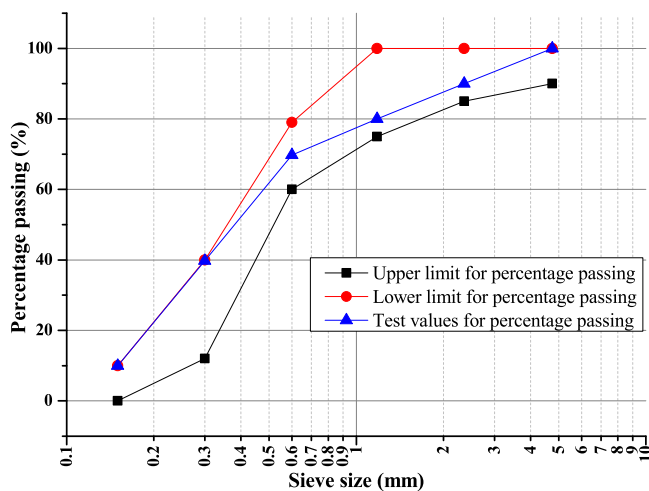


Figure 6. Bottom ash grading curve showing compliance with Zone-III limits as per IS 383.

Table 3. Chemical properties of bottom ash (BA).

Characteristics	Requirement as per IS-3812	Test data of bottom ash used (%)
Silicon di-oxide (SiO ₂)+Aluminium oxide (Al ₂ O ₃)+Iron oxide (Fe ₂ O ₃) (%) by mass	70% Minimum	93.38
Silicon di-oxide (SiO ₂)(%) by mass	35% Minimum	60.71
Magnesium oxide (MgO)(%) by mass	5% Maximum	0.63
Total sulphur as sulphur tri-oxide (SiO ₃) (%) by mass	2.75% Maximum	0.15
Available Alkalis as Sodium oxide (Na ₂ O) % by mass	1.5% Maximum	0.38
Loss on ignition, % by mass	12% Maximum	0.92

Table 4. Physical properties of aggregate.

Description of parameters	Sand	Bottom ash	Stone aggregate
Fineness modulus	2.288	1.924	2.793
Specific gravity	2.668	2.3	2.96
Surface area (m ² /g)	0.198	1.620	-

under Table 6 and the graphs are shown under Figure 8(a) and (b), respectively. From the test data, it is evident that with the gradual reduction of designed quantity of sand (keeping cement and stone aggregate proportions and also the water-cement ratio unchanged for all identity), reduction in compressive strength occurred. For A-set concrete mix, the controlled concrete with identity 'A' was found to have attained M-30 Grade equivalent strength. The subsequent values observed to be following reducing trend, and with 100% bottom ash, the strength stood at M-15 Grade equivalent strength. For B-set concrete mix, which is a leaner variety than the previous A-set mix, the grade of control concrete with identity 'B' is found to be equivalent to M-30, and subsequent values also showed similar downward trend, finished with marginally less than M-15 grade equivalent. For C-set concrete mix, which is further leaner mix, controlled concrete with identity 'C' is found to be equivalent to M-25, finished with less than M-10 grade equivalent.

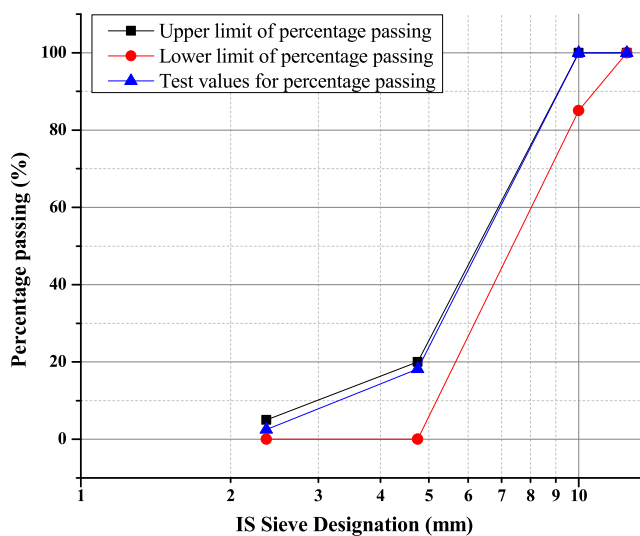
**Figure 7.** Stone aggregate grading curve showing compliance with 10 mm size limits as per IS 383.

Table 5. Concrete mix proportioning for A-set (1:1:2); B-set (1:1.5:3) and C-set (1:2:4).

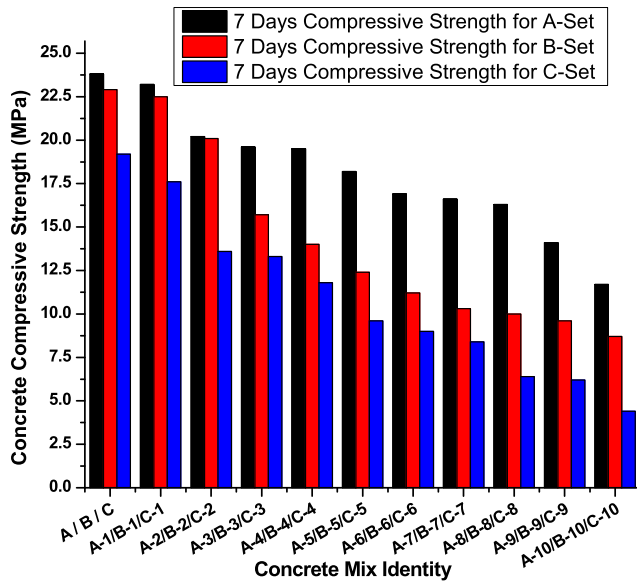
Concrete mix proportion	Cement (C)	Sand (S)	Bottom ash (BA)	Stone aggregate (A)	Water-cement ratio
A(1C:1.0S:0.0BA:2A)	1	1.0	0.0	2.0	0.5
A-1(1C:0.9S:0.1BA:2A)	1	0.9	0.1	2.0	0.5
A-2(1C:0.8S:0.2BA:2A)	1	0.8	0.2	2.0	0.5
A-3(1C:0.7S:0.3BA:2A)	1	0.7	0.3	2.0	0.5
A-4(1C:0.6S:0.4BA:2A)	1	0.6	0.4	2.0	0.5
A-5(1C:0.5S:0.5BA:2A)	1	0.5	0.5	2.0	0.5
A-6(1C:0.4S:0.6BA:2A)	1	0.4	0.6	2.0	0.5
A-7(1C:0.3S:0.7BA:2A)	1	0.3	0.7	2.0	0.5
A-8(1C:0.2S:0.8BA:2A)	1	0.2	0.8	2.0	0.5
A-9(1C:0.1S:0.9BA:2A)	1	0.1	0.9	2.0	0.5
A-10(1C:0.0S:1.0BA:2A)	1	0.0	1.0	2.0	0.5
B(1C:1.5S:0.0BA:3A)	1	1.5	0.0	3.0	0.5
B-1(1C:1.35S:0.15BA:3A)	1	1.35	0.15	3.0	0.5
B-2(1C:1.2S:0.3BA:3A)	1	1.2	0.3	3.0	0.5
B-3(1C:1.05S:0.45BA:3A)	1	1.05	0.45	3.0	0.5
B-4(1C:0.9S:0.6BA:3A)	1	0.9	0.6	3.0	0.5
B-5(1C:0.75S:0.75BA:3A)	1	0.75	0.75	3.0	0.5
B-6(1C:0.6S:0.9BA:3A)	1	0.6	0.9	3.0	0.5
B-7(1C:0.45S:1.05BA:3A)	1	0.45	1.05	3.0	0.5
B-8(1C:0.3S:1.2BA:3A)	1	0.3	1.2	3.0	0.5
B-9(1C:0.15S:1.35BA:3A)	1	0.15	1.35	3.0	0.5
B-10(1C:0.0S:1.5BA:3A)	1	0.0	1.5	3.0	0.5
C(1C:2.0S:0.0BA:4A)	1	2.0	0.0	4.0	0.5
C-1(1C:1.8S:0.2BA:4A)	1	1.8	0.2	4.0	0.5
C-2(1C:1.6S:0.4BA:4A)	1	1.6	0.4	4.0	0.5
C-3(1C:1.4S:0.6BA:4A)	1	1.4	0.6	4.0	0.5
C-4(1C:1.2S:0.8BA:4A)	1	1.2	0.8	4.0	0.5
C-5(1C:1.0S:1.0BA:4A)	1	1.0	1.0	4.0	0.5
C-6(1C:0.8S:1.2BA:4A)	1	0.8	1.2	4.0	0.5
C-7(1C:0.6S:1.4BA:4A)	1	0.6	1.4	4.0	0.5
C-8(1C:0.4S:1.6BA:4A)	1	0.4	1.6	4.0	0.5
C-9(1C:0.2S:1.8BA:4A)	1	0.2	1.8	4.0	0.5
C-10(1C:0.0S:2.0BA:4A)	1	0.0	2.0	4.0	0.5

3.3. Apparent porosity and bulk density test results

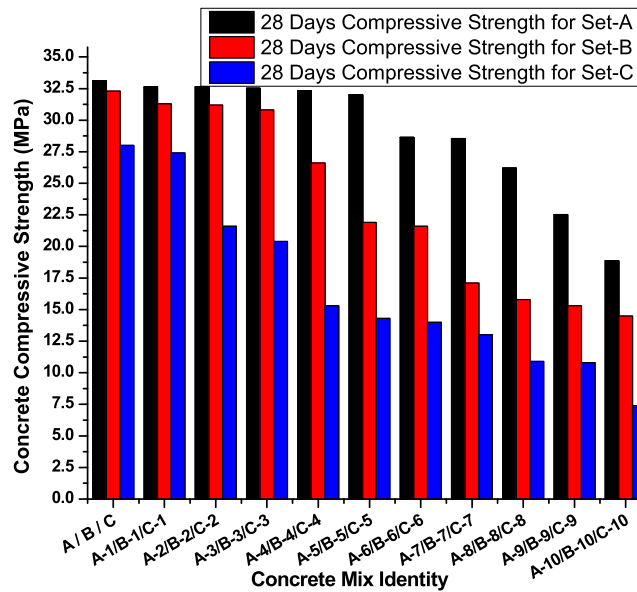
The test values are shown under Table 7 and graphs are shown under Figure 9(a) and (b), respectively. All the three sets of mix identities showed that the apparent porosity values increased with increasing content of bottom ash. For bulk density values, those show reverse trend, which means bulk density decreases with increasing content of bottom ash (Figure 9b).

Table 6. Compressive strengths at 7 and 28 days maturity: A-set, B-set and C-set concrete mixes.

Concrete mix identity	For A-set concrete compressive strength (MPa)		For B-set concrete compressive strength (MPa)		For C-set concrete compressive strength (MPa)	
	7 days	28 Days	7 days	28 Days	7 days	28 Days
A / B / C	23.8	33.13	22.9	32.3	19.2	28.0
A-1/B-1/C-1	23.2	32.62	22.5	31.3	17.6	27.4
A-2/B-2/C-2	20.2	32.62	20.1	31.2	13.6	21.6
A-3/B-3/C-3	19.6	32.52	15.7	30.8	13.3	20.4
A-4/B-4/C-4	19.5	32.31	14.0	26.6	11.8	15.3
A-5/B-5/C-5	18.2	32.01	12.4	21.9	9.6	14.3
A-6/B-6/C-6	16.9	28.64	11.2	21.6	9.0	14.0
A-7/B-7/C-7	16.6	28.55	10.3	17.1	8.4	13.0
A-8/B-8/C-8	16.3	26.2	10.0	15.8	6.4	10.9
A-9/B-9/C-9	14.1	22.53	9.6	15.3	6.2	10.8
A-10/B-10/C-10	11.7	18.86	8.7	14.5	4.4	7.4



(a)



(b)

Figure 8. (a) 7 days compressive strength test results of A, B and C-set concrete mixes . (b) 28 days compressive strength test results of A, B and C-set concrete mixes.

3.4. Thermal conductivity test results

The thermal conductivity test results along with reduction percentage with respect to conventional concrete, and corresponding grade of concrete are shown under Table 8 against A-set, B-set and C-set mixes, respectively. The thermal conductivity values shown graphically under Figure 11 for A-set, B-set and C-set mixes, respectively. All

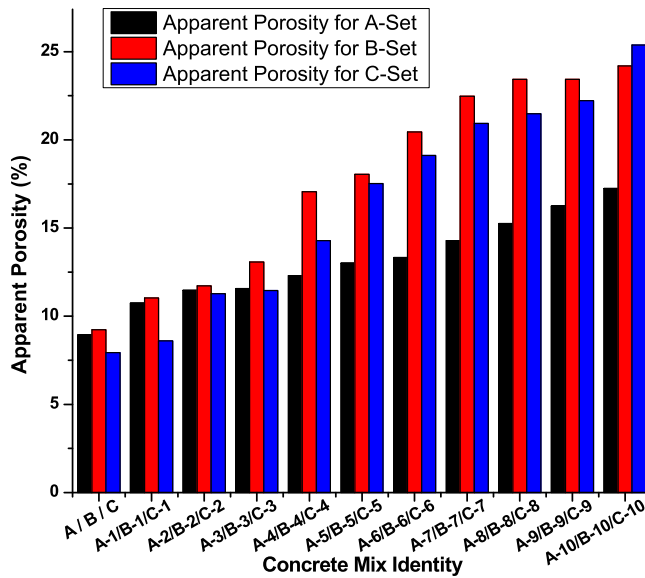
Table 7. Apparent porosity and bulk density of concrete mixes: A-set, B-set and C-set concrete mixes.

Concrete mix identity	For A-set concrete		For B-set concrete		For C-set concrete	
	Apparent porosity (%)	Bulk density (gm/cc)	Apparent porosity (%)	Bulk density (gm/cc)	Apparent porosity (%)	Bulk density (gm/cc)
A / B / C	8.943	2.472	9.231	2.423	7.937	2.397
A-1/B-1/C-1	10.744	2.405	11.029	2.309	8.594	2.352
A-2/B-2/C-2	11.475	2.393	11.719	2.352	11.278	2.256
A-3/B-3/C-3	11.570	2.372	13.077	2.254	11.450	2.252
A-4/B-4/C-4	12.295	2.320	17.054	2.178	14.286	2.093
A-5/B-5/C-5	13.008	2.317	18.045	2.113	17.518	2.088
A-6/B-6/C-6	13.333	2.283	20.455	2.091	19.118	2.051
A-7/B-7/C-7	14.286	2.269	22.481	2.078	20.930	2.039
A-8/B-8/C-8	15.254	2.254	23.438	2.063	21.481	1.993
A-9/B-9/C-9	16.239	2.239	23.438	2.055	22.222	1.978
A-10/B-10/C-10	17.241	2.198	24.194	2.040	25.373	1.925

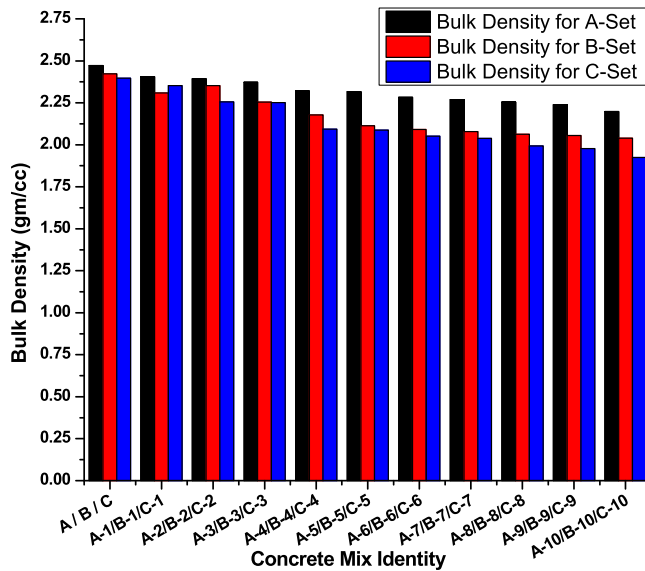
the mix identities from A to A-10 under Figure 11 showed a gradual decrease in thermal conductivity values with an increasing percentage of bottom ash and corresponding decreasing amount of sand. In Figure 11, variations in thermal conductivity found to be following decreasing trend, except in B-1 to B-2. The thermal conductivity value increased marginally from B-1 to B-2, which is supported by corresponding bulk density and apparent porosity changing trend, as shown under Figure 9(b) and (a) respectively. Similarly, for B-8 and B-9 mixes, thermal conductivity values remained almost constant, and corresponding bulk density and apparent porosity values also remained almost constant. The same reason is applicable for C-2, C-3, C-8 and C-9 designated mixes with almost constant bulk densities. Highest conductivity value shown again controlled concrete mix of each set, and the least conductivity value against the last mix of each set, which is with 100% bottom ash content. From start to end of each set, reduction trend is clear. Even with such reduction, the strength of M-30 grade equivalent was maintained up to 50% replacement rate, M-25 grade equivalent up to 80% replacement, M-20 grade equivalent up to 90% replacement and M-15 grade equivalent up to 100% replacement of sand by bottom ash in A-set mix. Thermal conductivity values against compressive strength values of each set of concrete mixes were plotted under Figure 12(a), (b) and (c), respectively, and the corresponding R^2 values obtained are of good order. Thermal conductivity values of each set were plotted against corresponding bulk density values, and the R^2 values of all the sets are in an excellent category, establishing the dependability of test data. These plots are shown under Figure 13(a), (b) and (c), respectively. The equivalent thermal resistance offered by each class of concrete mix for identical 125 mm thick concrete slab is graphically shown under Figure 14 and values, as calculated are shown under Table 9. The thermal transmittance value or U -value comparison has been made between conventional combinations (concrete slab + screed concrete overtopping + plaster on the soffit of slab) and various blended combinations, and shown under Table 10.

4. Discussions

The research work was undertaken with the aim to investigate the effect of sand replacement by bottom ash on thermal properties of concrete. After obtaining all the test results of constituent materials and that of concrete mixes, those were critically evaluated. Sand



(a)



(b)

Figure 9. (a) Apparent porosity test results of A, B and C-set concrete mixes . (b) Bulk density test results of A, B and C-set concrete mixes.

with fineness modulus value of 2.288, conforming Zone-II limit is ideal for concrete with coarser grain size, and angular shape which is corroborated by SEM image. The quartz is of crystalline nature. Fineness modulus of bottom ash was found to be 1.924 with finer irregular shaped particles of lower specific gravity (around 14% lower than that of sand).

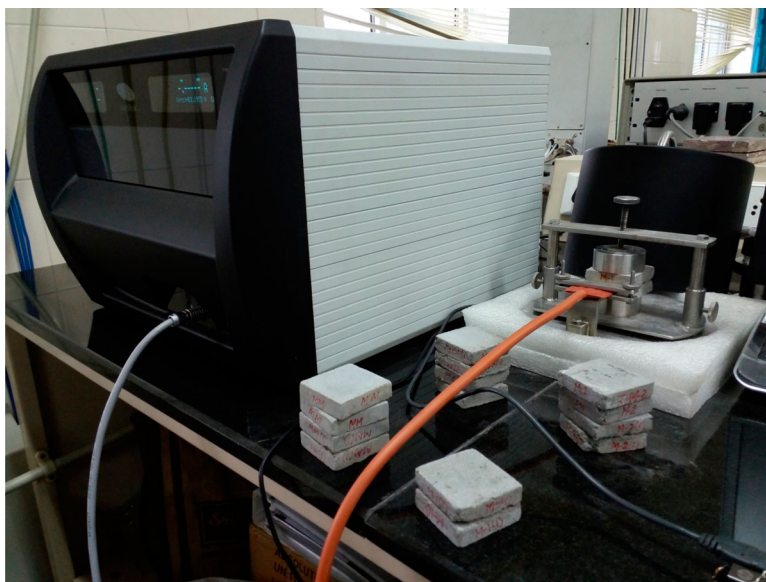


Figure 10. Thermal conductivity test set-up (Hot Disk TPS 2500S) showing test in progress.

Going by the phase structures of sand and bottom ash, similarity in quartz silica phase was observed, though the crystalline phase of silica is more conductive than the amorphous phase of silica (Demirboga, 2003). Further, dissimilarities in grain shape and sizes between sand and bottom ash were evident from SEM analysis. The specific gravity value of bottom ash was found lower than that of sand. The fine aggregate content in the concrete occupied around 25% of total volume, and since other two constituents remained constant, the physical properties of fine aggregate influenced considerably the overall property like bulk density and apparent porosity of concrete. It was observed that as the bottom ash percentages increased and corresponding sand percentages decreased, the mix exhibited lesser thermal conductivity value, primarily due to increasing porosity and lesser density. It was also observed that the grade of concrete or compressive strength value decreased gradually due to above stated reasons. Even after reduction in compressive strength values, A-set and B-set blended concrete mixes could achieve M-15 Grade equivalent strength with 100% bottom ash against the full replacement of sand. Though, earlier researchers observed that due to pozzolanic effect, further strength gain in blended concrete took place beyond 28 days maturity period, we restricted our study up to 28 days limit only, since as per IS 456 stipulations, to determine the characteristic compressive strength of any grade of concrete, 28 days compressive strength value shall be the decisive one. Reduction in thermal transmittance value to the tune of 18.6%, 23% and 24.9% for three different blending combinations were observed (Table 10).

From this study, it is clearly established that by replacing sand with bottom ash, thermal resistance against heat flow of concrete improved. The degree of improvement depends upon the replacement percentage of sand by bottom ash at the desired strength level of concrete. Even embodied energy content of such blended concrete reduces, since embodied energy of river sand remains higher than that of bottom ash obtained from thermal

Table 8. Thermal conductivity of concrete mixes and allied results: A-set, B-set and C-set concrete mixes.

Concrete mix identity	For A-set concrete			For B-set concrete			For C-set concrete		
	Thermal conductivity (W/m K)	Reduction in <i>k</i> value w.r.t A (%)	Equiv. grade of concrete (28 days strength basis)	Thermal conductivity (W/m K)	Reduction in <i>k</i> value w.r.t B (%)	Equiv. grade of concrete (28 days strength basis)	Thermal conductivity (W/m K)	Reduction in <i>k</i> value w.r.t C (%)	Equiv. grade of concrete (28 days strength basis)
A / B / C	1.613	0.00	M 30	1.579	0.00	M 25	1.520	0.00	M 25
A-1 / B-1 / C-1	1.510	6.39	M 30	1.400	11.34	M 25	1.445	4.93	M 25
A-2 / B-2 / C-2	1.446	10.35	M 30	1.421	10.01	M 25	1.299	14.54	M 20
A-3 / B-3 / C-3	1.377	14.63	M 30	1.302	17.54	M 25	1.183	22.17	M 20
A-4 / B-4 / C-4	1.286	20.27	M 30	1.238	21.60	M 25	1.056	30.53	M 15
A-5 / B-5 / C-5	1.227	23.93	M 30	1.151	27.11	M 20	1.051	30.86	M 14
A-6 / B-6 / C-6	1.120	30.56	M 25	1.017	35.59	M 20	0.934	38.55	M 14
A-7 / B-7 / C-7	1.078	33.17	M 25	0.964	38.96	M 15	0.867	42.94	M 10
A-8 / B-8 / C-8	1.044	35.28	M 25	0.942	40.36	M 15	0.829	45.48	M 10
A-9 / B-9 / C-9	0.972	39.71	M 20	0.939	40.51	M 15	0.826	45.66	M 10
A-10 / B-10 / C-10	0.912	43.47	M 15	0.900	42.99	M 14.5	0.781	48.60	M 7

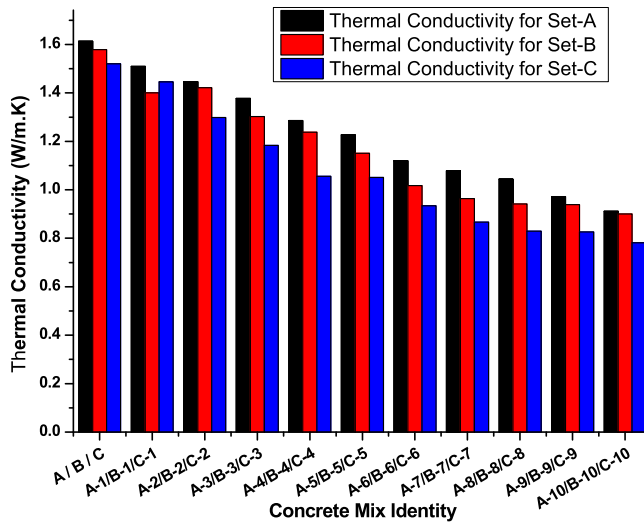


Figure 11. Thermal conductivity test results of A, B and C-set concrete mixes.

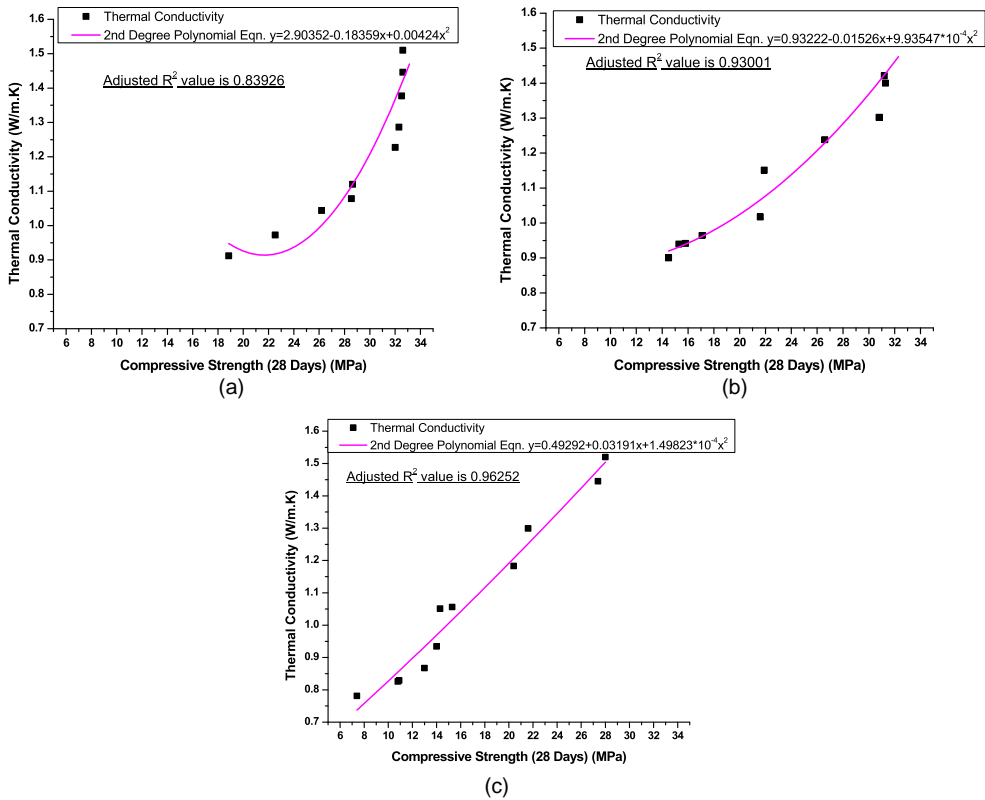


Figure 12. (a) Variation in thermal conductivity against compressive strength for A-set concrete mix. (b) Variation in thermal conductivity against compressive strength for B-set concrete mix. (c) Variation in thermal conductivity against compressive strength for C-set concrete mix.

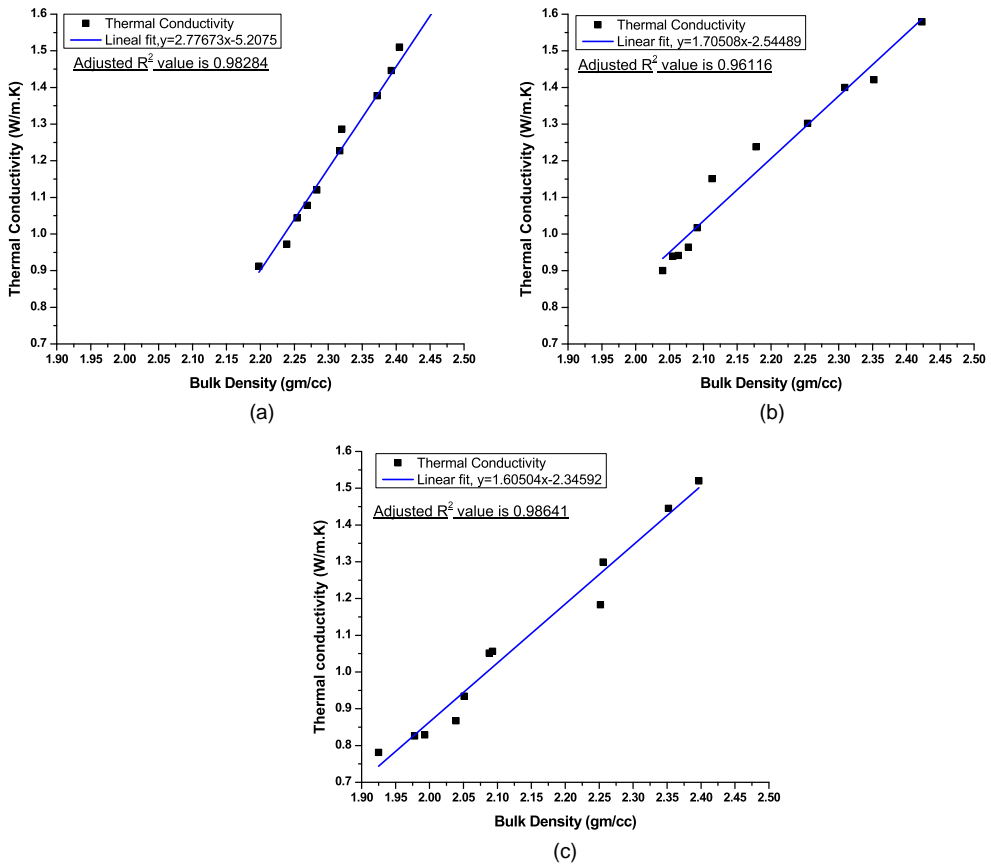


Figure 13. (a) Variation in thermal conductivity against bulk density for a-set concrete mix. (b) Variation in thermal conductivity against bulk density for B-set concrete mix. (c) Variation in thermal conductivity against bulk density for C-set concrete mix.

power plants, mainly on two counts. The dredging of river sand involves diesel operated machines and the distance from loading site to construction site generally exceeds 100 km. distance, for which embodied energy considered as 175 MJ/m^3 (Reddy & Jagadish, 2003) plus dredging energy. The coal combustion residues remain available free of cost including transportation cost reimbursement by power plant authority to the consumer (Gazette of India, 2016). Hence, for utilizing coal bottom ash from thermal power plants, there is a distinct economic advantage. Blended concrete could be produced with lesser carbon footprint, eliminate cumulative accumulation as landfill, and at the same time could effectively arrest rapid depletion of river sand due to mindless sand mining. Therefore, it is recommended use bottom ash as fine aggregate in concrete mix for building construction work.

5. Conclusions

From the study pertaining to this work, the following can be concluded –

1. Bottom ash, the 100% utilization of which is still not possible in India, can now be effectively put to use in concrete to act as replacement for sand for structural application in

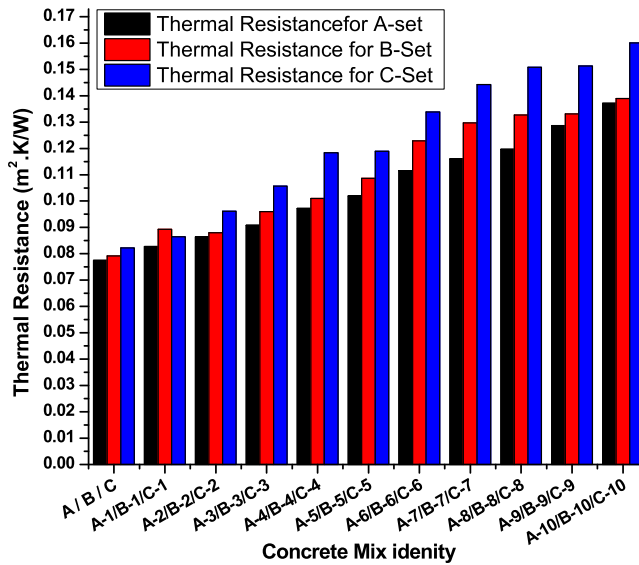


Figure 14. Thermal resistance offered by A, B and C-set concrete mixes.

Table 9. Thermal resistance values of concrete mix for 125 mm thick sample size (arbitrary).

A-set concrete mix		B-set concrete mix		C-set concrete mix	
Mix identity	thermal resistance ^a (m ² K/W)	Mix identity	thermal resistance ^a (m ² K/W)	Mix identity	thermal resistance ^a (m ² K/W)
A	0.0775	B	0.0792	C	0.0822
A-1	0.0828	B-1	0.0893	C-1	0.0865
A-2	0.0864	B-2	0.0880	C-2	0.0962
A-3	0.0908	B-3	0.0960	C-3	0.1057
A-4	0.0972	B-4	0.1010	C-4	0.1184
A-5	0.1019	B-5	0.1086	C-5	0.1189
A-6	0.1116	B-6	0.1229	C-6	0.1338
A-7	0.1160	B-7	0.1297	C-7	0.1442
A-8	0.1197	B-8	0.1327	C-8	0.1508
A-9	0.1286	B-9	0.1331	C-9	0.1513
A-10	0.1371	B-10	0.1389	C-10	0.1601

^aThermal resistance = Thickness of concrete(125 mm) / thermal conductivity of the concrete of particular mix.

roof concrete and screed concrete layer as plain concrete with lesser strength and for other area application with higher thermal resistance property. The embodied energy content of coal bottom ash is lesser than river sand on extraction and transportation counts, respectively.

2. Energy conservation and cost economy in building shall be resulted by such modified concrete blended with bottom ash, mainly on two counts. On account of cooling load reduction due to enhanced thermal resistance offered by such coal bottom ash blended concrete and on another count of overall cost reduction due to free availability of coal combustion residues from thermal power plants including free transportation up to 100 km.
3. Without any special technique or deploying specialized energy consuming equipment, only by the conventional method of concreting (mixing, placing, compacting, curing) with the available work force, such green concrete production with bottom ash blending is possible.

Table 10. Comparison of thermal transmittance parameter (U -value) between conventional concrete and plaster mix and blended concrete and plaster mix.

Screed concrete (m)	Roof slab (m)	Slab soffit plaster (m)	k_{screed} (W/m K)	k_{slab} (W/m K)	k_{plaster} (W/m K)	R_{screed} ($\text{m}^2 \text{ K}/\text{W}$)	R_{slab} ($\text{m}^2 \text{ K}/\text{W}$)	R_{plaster} ($\text{m}^2 \text{ K}/\text{W}$)	R_{se} ($\text{m}^2 \text{ K}/\text{W}$)	R_{si} ($\text{m}^2 \text{ K}/\text{W}$)	R_{total} ($\text{m}^2 \text{ K}/\text{W}$)	U -value (W/ $\text{m}^2 \text{ K}$)	Reduction (%)	Remarks
0.025	0.125	0.012	1.579	1.613	1.198	0.016	0.077	0.010	0.054	0.157	0.314	3.182	–	Base case scenario; R_{se} and R_{si} values are in compliance with BS (EN) ISO 6946: 2007 provisions for outside and inside surface resistance due to convective and radiative heat transfer
0.025	0.125	0.012	0.939	0.972	0.607	0.027	0.129	0.020	0.054	0.157	0.386	2.591	18.565	Reduction in U -value w.r.t base case
0.025	0.125	0.012	0.900	0.912	0.364	0.028	0.137	0.033	0.054	0.157	0.409	2.447	23.105	Reduction in U -value w.r.t base case
0.025	0.125	0.012	0.900	0.912	0.281	0.028	0.137	0.043	0.054	0.157	0.418	2.390	24.896	Reduction in U -value w.r.t base case

4. The environmental hazards related to the cumulative accumulation of coal combustion residues can be addressed with such application in building industry.
5. Rapid depletion of natural soft mineral, which is a serious concern across the globe, can be arrested by replacing sand with coal combustion residue in building concrete.
6. This work intends to throw open further research scope for life-cycle assessment of such blended concrete application in buildings and energy saving aspect with the help of dynamic simulation.

Acknowledgements

The corresponding author would like to express his sincerest gratitude to Dr.K. Muraleedharan, present Director of CSIR-CGCRI for his encouragement to complete the work and his kind permission to publish the paper and Prof. Indranil Manna, former Director of CSIR-CGCRI for his kind consent to pursue the research work on the above subject. Further, the continuous untiring support received from Mrs. M. Majumdar, Scientist, Mrs. M. Kanu, Mrs. S. Samanta, Mr. J. Mondal and Mr. S. Mondal of Material Characterization Division of CSIR-CGCRI, Mr. A. Mandal & Mr. N. Dey of EMD and Dr. J. Ghosh & Mrs. K. Chakraborty of XRD are sincerely acknowledged. Mr. Subrata Mistry needs special mentioning for extending his helping hands continuously to complete the study.

Disclosure statement

No potential conflict of interest was reported by the authors.

ORCID

Avijit Ghosh  <http://orcid.org/0000-0001-8300-8005>

References

- Abbas, M., Kumar, R., & Kumar, M. (2016). Study the effect of coal bottom ash and limestone dust as partial replacement of sand and cement. *International Journal of Scientific Research and Education*, 4(5), 5363–5372. doi:10.18535/ijrsre/v4i05.11
- Aggarwal, P., Aggarwal, Y., & Gupta, S. M. (2007). Effect of bottom ash as replacement of fine aggregates in concrete. *Asian Journal of Civil Engineering (Building and Housing)*, 8(1), 49–62.
- Akbari, H., & Touchaei, G. A. (2013). The climate effects of increasing the albedo of roofs in a cold region. *Advances in Building Energy Research*, 7(2), 186–191.
- Arumugam, R., Garg, V., & Mathur, J. (2014). Experimental determination of comfort benefits from cool-roof application to an un-conditioned building in India. *Advances in Building Energy Research*, 8(1), 14–27.
- Asdrubali, F., D'Alessandro, F., & Schiavoni, S. (2015). A review of unconventional sustainable building insulation material. *Sustainable Materials and Technologies*, 4, 1–17.
- Bribain, I. Z., Capila, A. V., & Uson, A. A. (2011). Life cycle assessment of building materials: Comparative analysis of energy and environmental impacts and evaluation of the eco-efficiency improvement potential. *Building and Environment*, 46, 1133–1140.
- Butera, M. F. (2010). Climate change and the built environment. *Advances in Building Energy Research*, 4(1), 45–75.
- Cadersa, A. S., & Auckburally, I. (2014). Use of unprocessed coal bottom ash as partial fine aggregate replacement in concrete. *University of Mauritius Research Journal*, 20, 62–84.

- Costanzo, V., Evola, G., & Marletta, L. (2013). Cool roofs for passive cooling: Performance in different climates and for different insulation levels in Italy. *Advances in Building Energy Research*, 7(2), 155–169.
- Demirboga, R. (2003). Influence of mineral admixtures on thermal conductivity and compressive strength of mortar. *Energy and Buildings*, 35, 189–192.
- Demirboga, R., Turkmen, I., & Karakoc, B. M. (2007). Thermo-mechanical properties of concrete containing high volume mineral admixtures. *Building and Environment*, 42, 349–354.
- Dixit, K. M. (2017). Embodied energy and cost of building materials: Correlation analysis. *Building Research & Information*, 45(5), 508–523.
- Ganesh, B., Bai, S. H., Nagendra, R., & Bagade, S. (2011). Pond Ash: An alternative material as fine aggregate in concrete for sustainable construction. *Advanced Materials Research*, 306-307, 1071–1075. doi:10.4028/www.scientific.net/AMR.306-307.1071
- Gazette of India. (2016). Part II, Section 3, Sub-section (ii), Ministry of Environment, Forests and Climate Change, Notification, New Delhi, 25TH January.
- Gupta, N. K., Sharma, A. K., & Sharma, A. (2013). Quantifying embodied energy using green building technologies under affordable housing construction. *Open Journal of Energy Efficiency*, 2, 171–175. doi:10.4236/ojee.2013.24022
- Harvey, D. L. D. (2007). Net climatic impact of solid foam insulation produced with halocarbon and non-halocarbon blowing agents. *Building and Environment*, 42, 2860–2879.
- Higgins, D. (2006). *Sustainable concrete: How can additions contribute*. The Institute of Concrete Technology, UK, Annual Technical Symposium, March 28.
- IS 1489 Part 1. (1991). (Reaffirmed 2005), Indian Standard Portland Pozzolana Cement – Specification, Part 1 Flyash based, Bureau of Indian Standards, New Delhi 110002.
- IS 2386 Part III. (1963). (Reaffirmed 2002), *Indian standard methods of test for aggregates for concrete, Part III, specific gravity, density, voids, absorption and bulking*, Bureau of Indian Standards, New Delhi 110002.
- IS 3812. (1981). (Reaffirmed in 1999), *Indian Standard Specification for flyash as pozzolana and admixture*, Bureau of Indian Standards, New Delhi 110002.
- IS 383. (1970). (Reaffirmed 2002), *Indian standard specification for coarse and fine aggregates from natural sources for concrete*, Bureau of Indian Standards, New Delhi 110002.
- IS 456. (2000). (Reaffirmed 2005), *Indian standard plain and reinforced concrete – code of practice*, Bureau of Indian Standards, New Delhi 110002.
- IS 516. (1959). (Reaffirmed 2004), *Indian standard methods of tests for strength of concrete*, Bureau of Indian Standards, New Delhi 110002.
- ISO 22007–2. (2008). *International standard plastics – determination of thermal conductivity and thermal diffusivity – Part 2: Transient plane heat source (hot disc) method*, ISO Copyright Office, Case Postale 56 CH-1211 Geneva 20.
- Johansson, P., Zarrabi-Adal, B., & Hagentoft, C.-E. (2012). Using transient plane source sensor for determination of thermal properties of vacuum insulation panels. *Frontiers of Architectural Research*, 1, 334–340.
- Kadam, M. P., & Patil, Y. D. (2013). Effect of coal bottom ash as sand replacement on the properties of concrete with different w/c ratio. *International Journal of Advanced Technology in Civil Engineering*, 2(1), 45–50.
- Kadam, M. P., & Patil, Y. D. (2014). *American Journal of Civil Engineering and Architecture*, 2(5), 160–166. doi:10.12691/ajcea-2-5-2.
- Kumar, S. R. (2010). *Developing an energy conservation building code implementation strategy in India*. Energy Conservation and Commercialization (ECO-III).
- Kumar, G., Dinesh, M., Younus, M., & Haleem, M. (2016, August). An experimental study on partial replacement of fine aggregate with coal bottom ash in concrete. *International Journal of Research Sciences and Advanced Engineering*, 2(15), 39–49.
- Kumar, D., Gupta, A., & Ram, S. (2014). Use of bottom ash in the replacement of fine aggregate for making concrete. *International Journal of Current Engineering and Technology*, 4(6), 3891–3895. December.

- Lacouture-Castro, D., Sefair, A. J., Florez, L., & Medaglia, I. A. (2009). Optimization model for the selection of material using a LEED based green building rating system in Colombia. *Building and Environment*, 44, 1162–1170.
- Lawrence, M. (2015). Reducing the environmental impact of construction by using renewable materials. *Journal of Renewable Materials*, 1–12. Scrivener Publishing LLC.
- Mani, M., Reddy, B. V., & Praseeda, K. I. (2017). Embodied and operational energy of rural dwellings in India. *International Journal of Sustainable Energy*. doi:10.1080/14786451.2017.1418742
- Ministry of Urban Development (MoUD). (2016). *Handbook of urban statistics*, Govt. of India.
- Monahan, J., & Powell, J. C. (2011). An embodied carbon and energy analysis of modern methods of construction in housing: A case study using a lifecycle assessment framework. *Energy and Buildings*, 43, 179–188.
- More, A., & Deshmukh, R. (2014, April–September). Low energy green materials by embodied energy analysis. *International Journal of Civil and Structural Engineering Research*, 2(1), 58–65.
- Pajchrowski, G., Noskowiak, A., Lewandowska, A., & Strykowski, W. (2014). Material composition or energy characteristic – What is more important in environmental life cycle of buildings? *Building and Environment*, 72, 15–27.
- Pennacchio, R., Savio, L., Bosia, D., Thiebat, F., Piccablotto, G., Patrucco, A., & Fantucci, S. (2017). Fitness: Sheep-wool and hemp sustainable insulation panels. *Energy Procedia*, 111, 287–297.
- Rafeizonooz, M., Mirza, J., Salim, M. R., Hussin, M. W., & Khankhaje, E. (2016). Investigation of coal bottom ash and fly ash in concrete as replacement for sand and cement. *Construction and Building Materials*, 116, 15–24.
- Rafeizonooz, M., Salim, R. M., Mirza, J., Hussin, M. W., Salmiati, K. R., & Khankhaje, E. (2017). Toxicity characteristics and durability of concrete containing coal ash as substitute for cement and river sand. *Construction and Building Materials*, 143, 234–246.
- Reddy, V. B. V., & Jagadish, K. S. (2003). Embodied energy of common and alternative building materials and technologies. *Energy and Buildings*, 35, 129–137.
- Satish, K. (2011). *USAID ECO – III project, energy use in commercial buildings – key findings from the National Benchmarking Study*, USAID – India.
- Tae, S., Kim, T., & Chae, U. C. (2016). Analysis of environmental impact for concrete using LCA by varying the recycling components, the compressive strength and the admixture material mixing. *Sustainability*, 8(389), 1–14. doi:10.3390/su8040389
- Thormark, C. (2002). A low energy building in a life cycle – its embodied energy, energy need for operation and recycling potential. *Building and Environment*, 37, 429–435.
- Yukseki, I. (2015). The evaluation of building materials in terms of energy efficiency. *Periodica Polytechnica Civil Engineering*, 59(1), 45–58. doi:10.3311/PPci.7050

Received:

18 July 2018

Revised:

27 September 2018

Accepted:

9 November 2018

Cite as: Avijit Ghosh,
Arup Ghosh,
Subhasis Neogi. Reuse of fly
ash and bottom ash in mortars
with improved thermal
conductivity performance for
buildings.

Heliyon 4 (2018) e00934.

doi: [10.1016/j.heliyon.2018.e00934](https://doi.org/10.1016/j.heliyon.2018.e00934)



Reuse of fly ash and bottom ash in mortars with improved thermal conductivity performance for buildings

Avijit Ghosh^{a,*}, Arup Ghosh^a, Subhasis Neogi^b

^a CSIR-Central Glass & Ceramic Research Institute, 196, Raja S.C. Mallick Road, Kolkata-32, West Bengal, India

^b School of Energy Studies, Jadavpur University, Kolkata-32, West Bengal, India

* Corresponding author.

E-mail address: avijitenergy@gmail.com (A. Ghosh).

Abstract

An approach towards effective utilization of fly ash and bottom ash in the construction of energy efficient buildings has been presented in this paper. Two masonry mortar grades MM3 and MM5 were considered for trial mix. Portland pozzolana cement with substitution of sand by fly ash and bottom ash separately in different substitution ratios (SR) were adopted for preparation of test samples. Fly ash and bottom ash with lime dust and marble dust combinations were also tested as sand free mortars. 28 days compressive strength, apparent porosity, bulk density and thermal conductivity parameters were evaluated for all such samples. By analysing the test results, it was observed that all the SR combinations satisfied the minimum masonry mortar grade MM0.7, as per IS 2250. Both the MM3 and MM5 grade mortars could be produced at 60% SR by fly ash, and corresponding reductions in thermal conductivity values were 69%, and 54% respectively, while compared with conventional mortar. Sand less mortar for both the grades resulted around 57% reductions in corresponding thermal conductivity values. Overall heat transfer co-efficient (U-value) for both side plastered and rendered brick masonry wall panel was found to be reduced by 15.58%, while comparison made between conventional mix of MM5 grade and corresponding 50% fly ash substituted mix. Thus such ash blended mortar

mix appears to be advantageous in building envelop application for lowering the overall cooling/heating demand of building, besides utilizing the coal ash up to largest extent and saving natural mineral sand from depletion.

Keywords: Civil engineering, Energy

1. Introduction

Considering the energy efficiency aspect of buildings to restrict the electrical energy demand, focus has been kept on the performance of building envelop. Building envelop performance directly influences operational energy and constituent materials directly impact embodied energy of the building. The design of the building envelop influences heat conduction through roof, opaque wall, and glazed windows and determine the quantum of sensible cooling/heating load. It also determines the amount of natural ventilation and day lighting. Due to rising frequency of hot and extreme weather events throughout the globe, the demand for space cooling is expected to triple between 2010 and 2050 (IEA, 2013). Thermal insulation and thermal mass have been used by building envelop designers for minimizing energy requirement. Since the commercially available insulations are manufactured from petroleum by-products, the cost and embodied energy content of those are very high. Choice of materials for energy efficient envelop construction should address issues of durability, ability of material to assist in passive design, local sourcing of materials to reduce transportation etc. For a conventional building, excluding fenestration area, balance opaque wall area is made up of brick-mortar-plaster combinations. The mortar and plaster compositions are normally made up of cement and sand of 1:6 (MM3 Grade) and 1:4 (MM5 Grade) proportions respectively.

Further, due to the growth in infrastructure sector, unprecedented sand mining from river bed is threatening the ecological balance seriously. On the other hand, 100% utilization of coal ash, which is generated from thermal power plants has not become possible till date. As a result of which, cumulative accumulation of the un-utilized ash each year in ash dykes are creating groundwater contamination, air pollution etc. The scenario of accumulated quantity of coal ash in India during last seven years period is shown under Table 1. In the present work, an effort has been made to replace sand by fly ash, bottom ash, fly ash- lime dust, bottom ash-lime dust, fly ash- marble dust and bottom ash- marble dust combinations in buildings' wall mortar and plaster mix application, and to study the resultant effects from structural as well as thermal adequacy points of views. Further, overall heat transfer co-efficient or U-value of a conventional fired clay brick wall panel, both side plastered with PPC and 50% sand and 50% fly ash combination mix was measured and also compared with another identical panel with conventional mix with PPC and 100% sand. The utilization of fly ash and bottom ash in building mortar and plaster mix could

Table 1. Year wise Ash production from Thermal Power Plants in India.

Year	Coal consumed (MMT)	Installed Capacity (GW)	Ash Produced (MMT)	Ash Utilized (MMT)	Ash Un-utilized (MMT)	Ash Utilized (%)	Avg. Ash content (%)
2016–17	509.46	157.377	169.25	107.10	62.15	63.28	33.22
2015–16	536.64	145.045	176.74	107.77	68.97	60.97	32.94
2014–15	549.72	138.916	184.14	102.54	81.60	55.69	33.50
2013–14	523.52	133.381	172.87	99.62	73.25	57.63	33.02
2012–13	482.97	120.312	163.56	100.37	63.19	61.37	33.87
2011–12	437.41	105.925	145.42	85.05	60.37	58.48	33.24
2010–11	407.61	80.458	131.09	73.13	57.96	55.79	32.16

Source: CEA Report (2010–11 to 2016–17).

revolutionize the building construction industry. Earlier works by other researchers on fly ash and bottom ash usage for cement/sand replacement in concrete and mortar mixes in building construction are reviewed and discussed herein.

Aydin and Arel, 2017 investigated about the effects of high volume of fly ash in cement mix for low strength applications. Supplementary cementitious material in the mix was optimized and physical and mechanical properties were evaluated and predictive model was developed. The model could be followed for low strength application of cement paste. Gencel et al. (2015) had performed various physical and mechanical tests of mortars with fly ash as constituent fine aggregate material, and up to 70% ratio of fly ash-sand mortar was found acceptable without significant property change. Brake et al. (2017) had explored the re-usability of coal bottom ash as cement replacement in mortar. The bottom ash was made pulverized and the effect on workability and setting time were studied. Improvement in micro-structure of cement mortar could effectively increase the strength parameter of such product with lower Ca/Si ratio, as observed. Kim (2015) had experimented with sieved and ground coal bottom ash in high strength cement mortar. The bottom ash powder was observed to increase the workability and compressive strength values than the equivalent mortar made of cement and fly ash. Tharrini and Ramasamy, 2015 proposed to utilize ground bottom ash in geo-polymer mortar. Influence of alkaline activator, Molar ratio and curing mode on compressive strength of such mortars were studied. With different molar ratio with different activator, improvement in compressive strength was observed under both ambient curing and steam curing atmospheres respectively. Demirboga (2003) had studied the effect of various mineral admixtures like fly ash, silica fume and blast furnace slag as cement replacement on thermal conductivity and compressive strength of mortar. In the experiment, it was observed that for 10, 20 and 30% replacement of cement by either of the admixtures, all mixes showed reduction in thermal conductivity but of varying degree. Silica fume showed highest reduction percentage, closely next was fly ash and blast furnace slag was

distant third. All mixes exhibited decreasing compressive strength during early ages, and marginal increase in strength beyond 120 days of maturity. [Herrera Duran A et al. \(2016\)](#) had studied the thermal conductivity effect by introducing a novel co-polymer on ordinary Portland cement – Class F fly ash combination mortar with water reducing super-plasticizer. Mortars were made with three different water-binder ratios to arrive at an optimized ratio to reach a target 3.4 MPa compressive strength. The reduction in thermal conductivity to the tune of 33% exhibited identical result by commercially available cellular concrete. [Shahidan et al. \(2016\)](#) had studied the physical and chemical properties of coal bottom ash, as a replacement material for sand. Specific gravity, particle size distribution, density, Scanning electron microscopy and X-ray fluorescence test results indicated that the angular porous structure and the rough texture of bottom ash affected its particle density and specific gravity on the lower magnitude than that of sand. However the gradation of particles in bottom ash and sand showed some similarity, and overall, bottom ash is recommended favourably as a replacement material to sand. [Abbas et al. \(2016\)](#) had studied the effect of partial replacement of cement and sand by limestone dust and bottom ash respectively. Sand replacement by bottom ash was done from 10% to 40%, 60% and 80%, and cement replacement by limestone dust was fixed at 5% flat for all categories of mixes. At constant water-cement ratio, up to 30% replacement of sand and 5% replacement of cement, strength increased (compressive, flexural, split tensile), but above the replacement ratio, strength values found decreased. [Sahmaran et al. \(2006\)](#) assessed the self-compacting properties of mortars with four mineral additives like fly ash, brick powder, limestone powder and kaolinite. Besides, three superplasticizers and two viscosity modifiers were also used. Workability, setting time and hardened properties of mortars were evaluated. It was observed that fly ash and limestone powder mixing increased workability and setting time was increased by fly ash influence alone, which could be adjusted by the ternary mix of fly ash and limestone powder. Brick powder and kaolinite adversely affected workability criteria. When part of cement was replaced by mineral additives, reduction in strength was resulted. [Rai et al. \(2014\)](#) carried out experimental investigations on mortars, modified with quarry dust and fly ash in different ratios as substitute of sand and cement respectively. The compressive and transverse strength results revealed better order due to micro-filling and pozzolanic activities by the two substitutes. [Ramadoss and Sundararajan, 2014](#) investigated about the suitability of lignite bottom ash as replacement of fine aggregate in masonry mortar. Among the various percentages tried, 20% replacement was found optimum from the point of view of mechanical strength adequacy including durability. [Hardjito and Fing, 2010](#) studied the replacement effect of sand by bottom ash in geo-polymer mortar. It was found that the increase in bottom ash content reduced the compressive strength of geo-polymer mortar. Effect of temperature and addition of alkaline solution also affected the strength development negatively beyond certain points. [Rafieizonooz et al. \(2016, 2017\)](#) had tried to explore the effect of bottom ash and

fly ash in concrete, as replacement of sand and cement respectively. Sand was replaced at 20, 50, 75 and 100% rate and cement was replaced at flat 20% rate for all four proportions of sand replacement. Though there was no change in strength up to 28 days of curing, except reduced workability, but the strength found increased at 91 and 180 days maturity period. Due to such slow strength gain, such blended concrete was found appropriate in foundation, pavement construction etc. works. While exploring the toxicity and durability characteristics of such concrete in application, no adverse effect through leaching, sulphate and acid attack etc. were noticed. Such blended concrete with cement and sand replacement by fly ash and bottom ash was recommended as suitable replacement of clean construction materials. Brito et al. (2018) had reviewed all earlier works done by the other researchers on the environmental impact and toxicity characteristics of recycled concrete aggregates (rca), fly ash (fa), cement production as well as their substitution aspect. The analysis with respect to abiotic depletion potential, ozone depletion potential, photochemical ozone creation, acidification potential, eutrophication potential, toxicity, leachability etc. were considered. It was revealed that environmental impact and cost of concrete reduced considerably with such incorporations, and also requirement of landfill space reduced drastically. While incorporated in concrete, the leaching metals which were otherwise present in fly ash were also found diminished. Gourav et al. (2017) had studied different envelop materials about their structural and thermal properties. Table moulded conventional clay brick and fly ash-lime-gypsum (fal-G) brick were compared in the study, and fal-G brick was found to be a better option for masonry construction under tropical climatic condition. Vijayalakshmi et al. (2006) investigated the thermo-physical behaviour of opaque wall materials under the influence of solar radiation. Finite difference mathematical model was developed and the result was compared with actual test results of different combination wall elements on U-value, Temperature Time Delay and Decrement Factor parameters respectively. Bergey (2010) had presented the comparative study of various commercially available insulating materials, among which XPS was found to be having highest embodied global warming potential (GWP). Buddhi et al. (2012), had made comparison between fire-clay brick made construction and ash brick made construction for calculating energy and environment indices. Ash block was found to be better option for heat load reduction and saving of natural resources and environment.

2. Materials and methods

2.1. Materials used

For the purpose of this experiment, we had used commercially available Portland Pozzolana Cement (PPC) conforming IS 1489 Part 1 (1991, Reaffirmed 2005), conventional river sand conforming IS 383 (1970, Reaffirmed 2002), siliceous pulverized fuel ash (fly ash and bottom ash) obtained from thermal power plant, located

at Kolkata conforming IS 3812 Part 2 (2003), lime dust from local market and marble residue from the marble slab cutting and polishing industry, and potable quality water. No admixtures or additives or electro-mechanical mixer were used in this study.

2.1.1. Evaluation of various parameters of raw materials

The physical properties and chemical composition of the materials used in this study are shown in Tables 2 and 3 respectively. The specific gravity parameter of cement, sand, fly ash and bottom ash were determined as per IS 1528 (Pt. IX). The specific surface area of Portland pozzolana cement sample was mentioned in the test report, as supplied by the manufacturer, and that of flyash was tested by BET Analysis method with the help of Quantachrome Nova instrument. Quantitative chemical analysis of cement, flyash, bottomash, lime dust and marble dust were done by Wet Chemical method (for SiO₂, Al₂O₃, and LOI) and by ICPAES method (for balance parameters) respectively. The type of flyash and bottomash, both are of Class F variety as per ASTM C 618-12a (ASTM International, 2012), since the CaO < 10%, and the sum of silica, aluminium and iron oxide percentages is > 70%. The bottom ash particles have a very low LOI value. Since the bottom ash particles have a higher residence time in the furnace than the fly ash particles, the bottom ash particles are likely to lose more carbon and this results in a lower LOI value for bottom ash.

The grading curves in respect of sand and bottom ash were done as per IS 383 (1970, Reaffirmed 2002). The particle size analysis for flyash was carried out by Microtrac 3500S (micron range) LASER Diffraction System. The grading curves in respect of sand and bottom ash and particle size distribution curve in respect of fly ash are shown against Figs. 1, 2, and 3 respectively.

The samples of cement, sand, flyash and bottomash were prepared for XRD analysis using a back loading preparation method. Those were analyzed with a PANalytical X'Pert's Pro powder diffractometer with X'Celerator detector and variable divergence- and receiving slits with Fe filtered Cu-K α radiation in a diffraction angle (2 θ) range of 15°–89°. The phases were identified using X'Pert Highscore plus software. The relative phase amounts (weights %) were estimated using the Rietveld method (Autoquan Program). X-Ray Diffraction analysis, showing the constituent phases of

Table 2. Physical properties of the material.

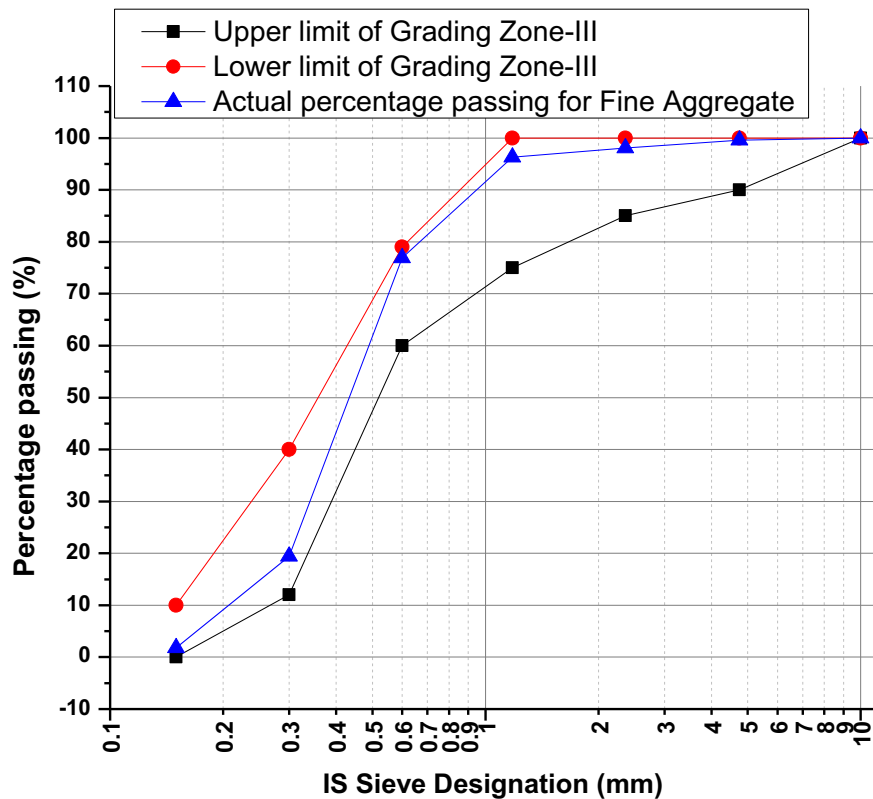
Description of material	Specific Gravity value	Sp. Surface area/Fineness Modulus
Portland Pozzolana Cement (PPC)	3.043	Sp. Surface area: 444 m ² /kg.
Fine Aggregate, Fly ash (FA)	2.434	Sp. Surface area: 552 m ² /kg.
Fine Aggregate, Bottom ash (BA)	2.246	Fineness Modulus: 1.446
Fine Aggregate, Sand	2.664	Fineness Modulus: 2.079

Table 3. Chemical composition of Cement, FlyAsh, BottomAsh, Lime dust and Marble dust.

Chemical parameter (%)	Portland Pozzolana Cement (PPC)	Fly ash (FA)	Bottom ash (BA)	Lime dust	Marble dust
SiO ₂	34.85	61.86	60.71	12.92	14.28
Al ₂ O ₃	10.65	27.85	25.86	0.94	1.20
TiO ₂	0.69	2.20	6.81	0.12	0.78
Fe ₂ O ₃	3.56	2.63	1.97	0.11	0.82
CaO	43.96	0.54	0.89	61.65	27.25
MgO	2.66	0.47	0.63	0.97	17.76
Na ₂ O	0.30	0.36	0.38	0.46	0.65
K ₂ O	1.10	1.27	1.28	0.09	0.42
L.O.I.	1.89	2.49	0.92	22.53	36.66

cement, flyash, bottomash and sand are shown against Figs. 4, 5, 6, and 7 respectively.

High Resolution Micro structural analysis by Field Emission Scanning Electron Microscopy (FESEM SUPRA 35VP) was carried out for fly ash, bottom ash and sand samples. Those are shown against Figs. 8, 9, and 10 respectively.

**Fig. 1.** Grading curve for Sand, used in the experiment (Fineness Modulus 2.079).

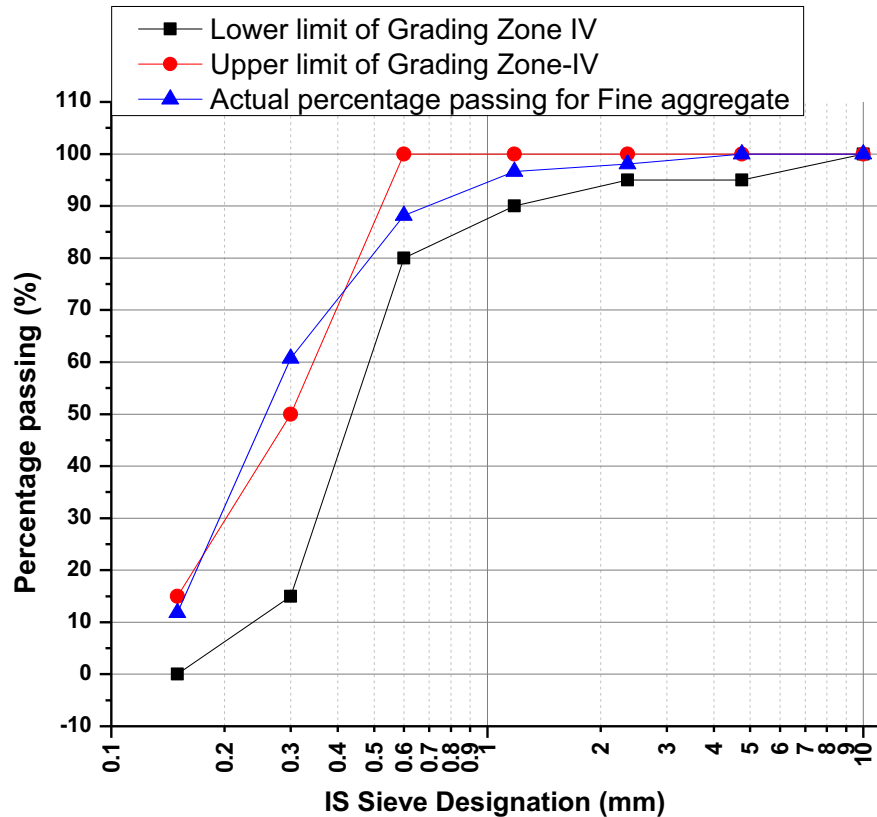


Fig. 2. Grading curve for Bottom ash, used in the experiment (Fineness Modulus 1.446).

2.1.2. Preparation of samples

Two grades of masonry mortar MM3 and MM5 (corresponding 28 days compressive strength values should be no less than 3 N/mm² and 5 N/mm²) as per IS 2250 (1981, Reaffirmed 2000) were selected for evaluation. These two grades are conventionally used throughout the country, with Cement-sand ratios of 1:6 and 1:4 respectively. In the experimental work, sand was gradually replaced by fly ash in one series of mix (A-Series, A,A-1,A-2,.....A-10), and by bottom ash in another (B-Series, B,B-1,B-2,....B-10), within the same grade of mortar MM3 (Table 4). Similarly for another grade MM5, such combinations were followed (Table 5). Sand less mortars with fly ash, bottom ash and marble dust combinations under MM3 and MM5 Grade are shown against Tables 6 and 7 respectively. There were fifty different combinations of mortar mixes, among which two were control mix, wherein sand was used as fine aggregate conventionally. For each combination of mix, three nos. 50 mm* 50 mm*50 mm mortar cube moulds, and pairs of 50 mm*50 mm *12 mm mortar square moulds were prepared. The samples were de-moulded after 24 hours of casting and kept immersed in potable water till 28 days at room temperature. After 28 days of water curing, samples were taken out of water, wiped clean and kept at room temperature before performing subsequent tests. Three cubes were tested to determine

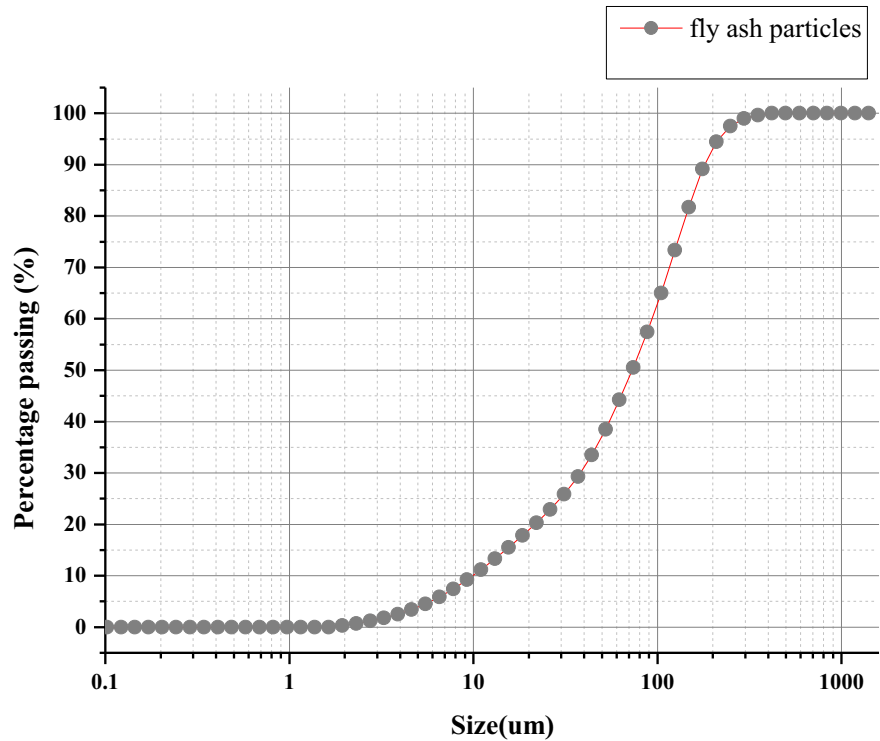


Fig. 3. Particle size distribution for fly ash, used in the experiment.

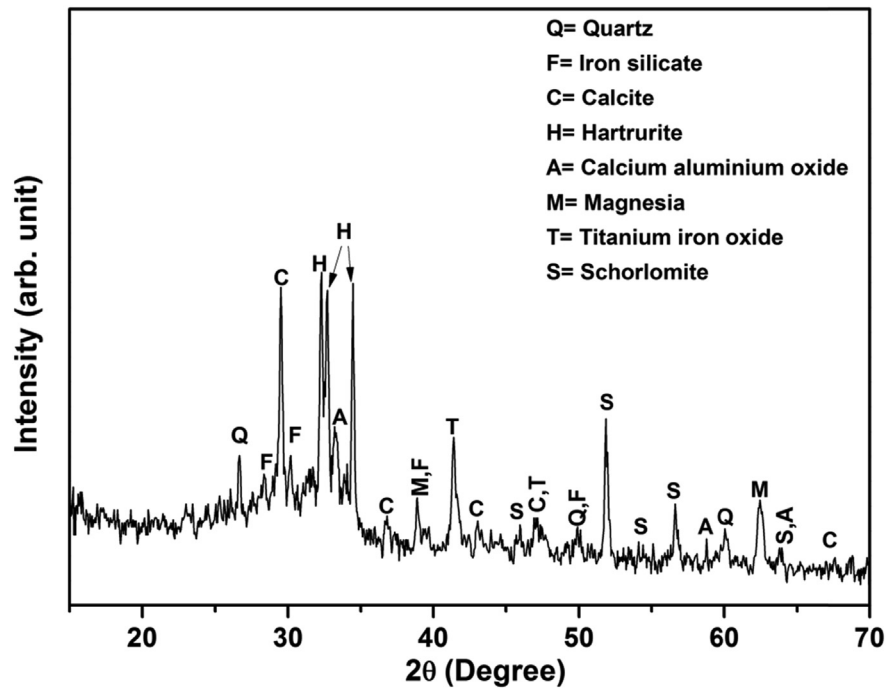


Fig. 4. XRD phase of PPC, used in the experiment.

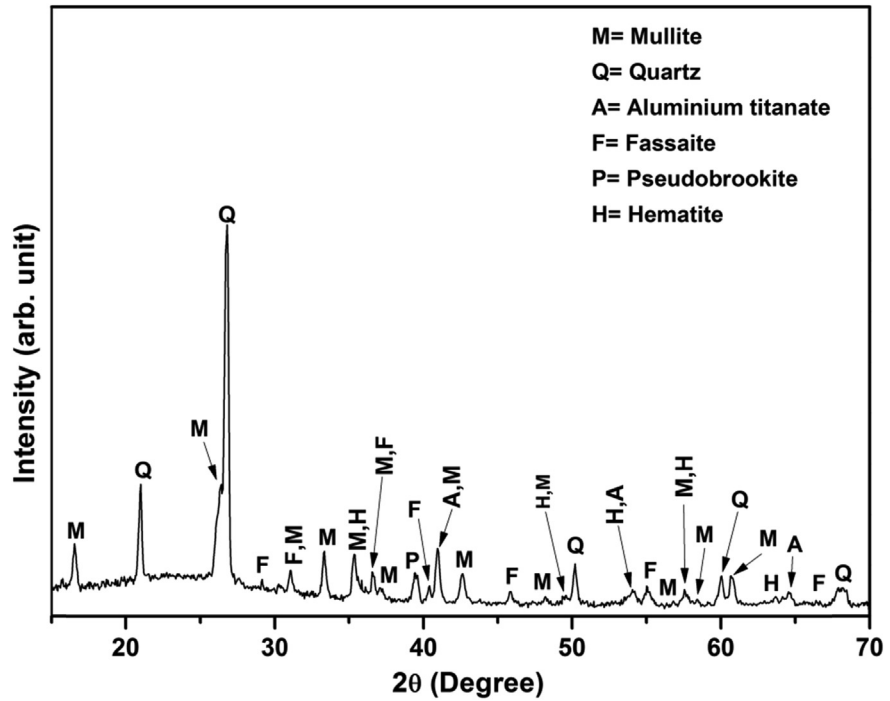


Fig. 5. XRD phase of fly ash, used in the experiment.

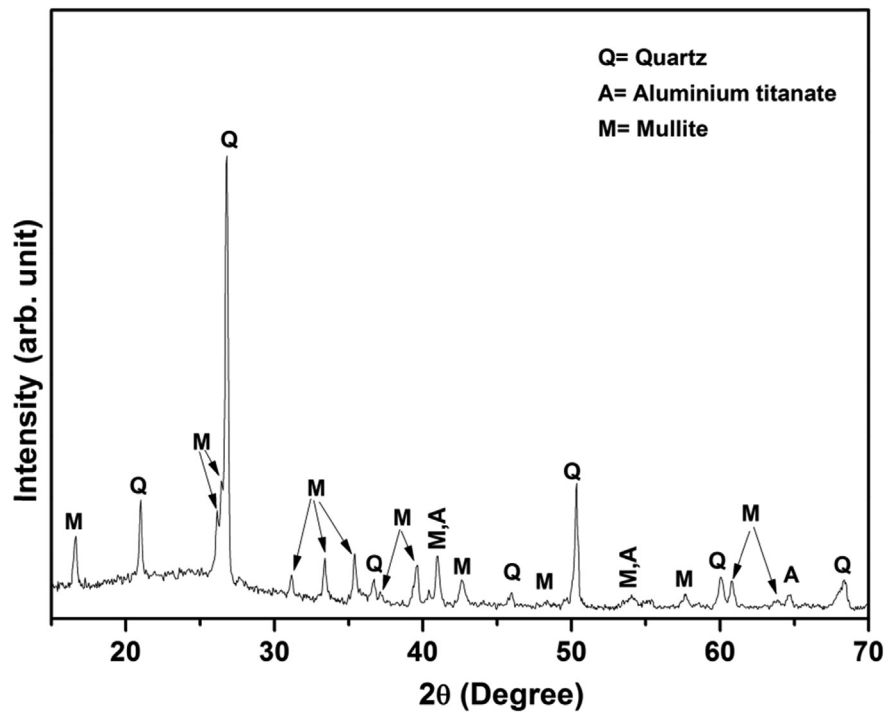


Fig. 6. XRD phase of bottom ash, used in the experiment.

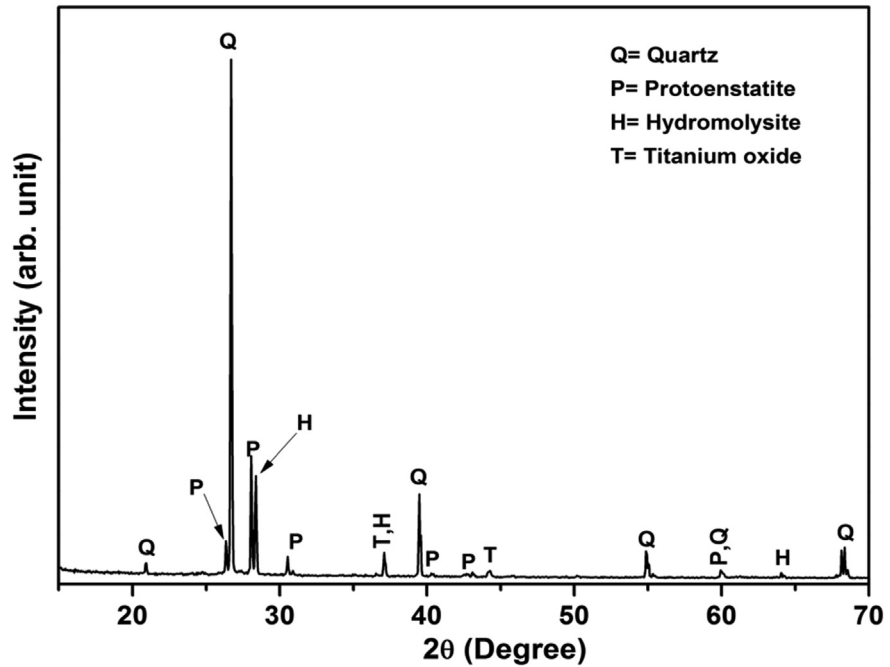


Fig. 7. XRD phase of sand, used in the experiment. Note: Q = Quartz, M = Mullite, A = Aluminium titanate, F = Fassaite ($\text{Ca}_{0.96}\text{Mg}_{0.57}\text{Fe}_{0.22}\text{Al}_{0.16}\text{Ti}_{0.059}(\text{Si}_{1.73}\text{Al}_{0.27})\text{O}_6$), P = Pseudobrookite ($\text{Fe}_2\text{O}_3 \cdot \text{TiO}_2$), Hematite (Fe_2O_3), Iron silicate (FeSiO_3), Calcite (CaCO_3), Hartrurite ($\text{Ca}_3(\text{SiO}_4)\text{O}$), Calcium aluminate oxide ($3\text{CaO} \cdot \text{Al}_2\text{O}_3$), Titanium iron oxide, Schorlomite ($\text{Ca}_3\text{Ti}_2(\text{Fe}_2 + 3\text{Si})\text{O}_{12}$), Protoenstatite (MgSiO_3), Hydromolysite ($\text{FeCl}_3 \cdot 6\text{H}_2\text{O}$).

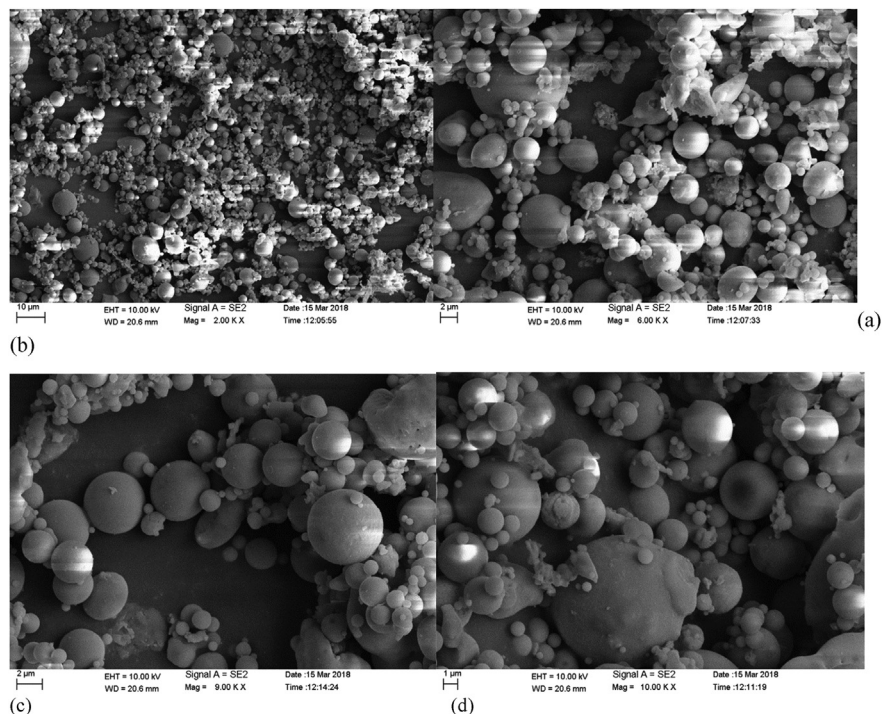


Fig. 8. (a),(b),(c),(d) SEM images of Flyash under different magnifications.

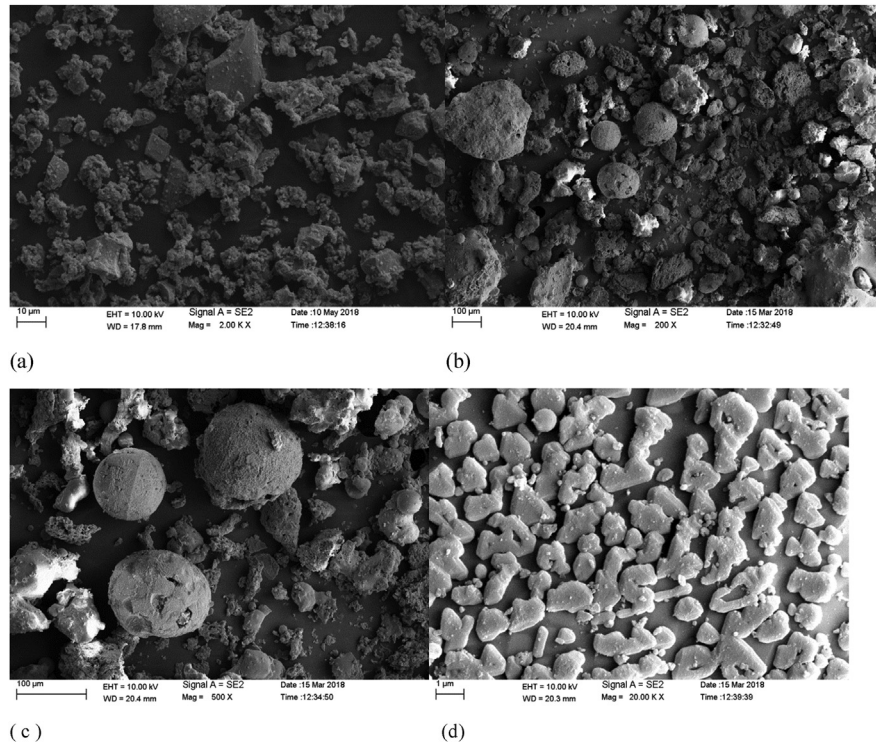


Fig. 9. (a),(b),(c),(d) SEM images of Bottom ash under different magnifications.

compressive strength of each sample, and pairs of sample of 12 mm thickness were tested for thermal conductivity parameter respectively. After compiling all the test results, the C-5 mix was identified under MM5 mortar grade category, being the lowest complied mix with 50% substitution of sand by flyash with thermal conductivity value reduction to the tune of 49.31%, in comparison with control mix with 100% sand for evaluating the overall heat transfer co-efficient (U-value) of masonry wall panel. The conventional burnt clay bricks were collected from the local market,

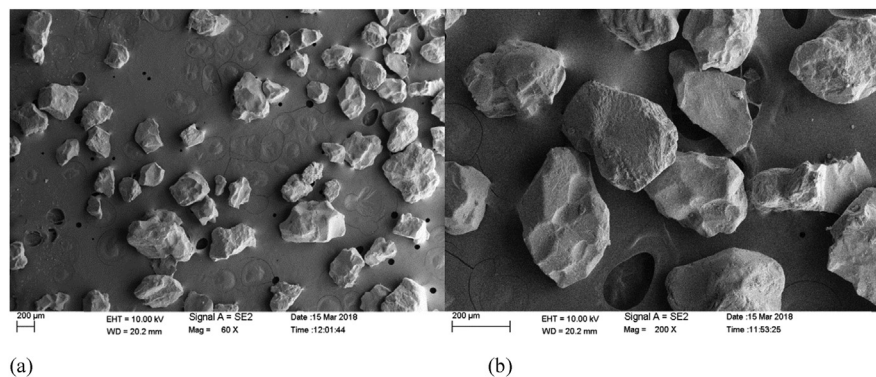


Fig. 10. (a),(b) SEM images of Sand under different magnifications.

Table 4. Gradual replacement proportion of Sand by Fly ash and Bottom ash (separately) for MM3 Grade Mortar mix.

Mortar Mix Identity	Mortar Mix (MM3 Grade)	Cement Wt. ratio	Sand Wt. ratio	Flyash Wt. ratio	Bottom ash Wt. ratio
Control	1Cement: 6 (100% Sand)	1.00	6.00	-	-
A-1	1Cement: 6 (90% Sand + 10% Fly ash)	1.00	5.40	0.60	-
A-2	1Cement: 6 (80% Sand + 20% Flyash)	1.00	4.80	1.20	-
A-3	1Cement: 6 (70% Sand + 30% Flyash)	1.00	4.20	1.80	-
A-4	1Cement: 6 (60% Sand + 40% Flyash)	1.00	3.60	2.40	-
A-5	1Cement: 6 (50% Sand + 50% Flyash)	1.00	3.00	3.00	-
A-6	1Cement: 6 (40% Sand + 60% Flyash)	1.00	2.40	3.60	-
A-7	1Cement: 6 (30% Sand + 70% Flyash)	1.00	1.80	4.20	-
A-8	1Cement: 6 (20% Sand + 80% Flyash)	1.00	1.20	4.80	-
A-9	1Cement: 6 (10% Sand + 90% Fly ash)	1.00	0.60	5.40	-
A-10	1Cement: 6 (100% Fly ash)	1.00	0.00	6.00	-
B-1	1Cement: 6 (90% Sand + 10% Bottom ash)	1.00	5.40	-	0.60
B-2	1Cement: 6 (80% Sand + 20% Bottom ash)	1.00	4.80	-	1.20
B-3	1Cement: 6 (70% Sand + 30% Bottom ash)	1.00	4.20	-	1.80
B-4	1Cement: 6 (60% Sand + 40% Bottom ash)	1.00	3.60	-	2.40
B-5	1Cement: 6 (50% Sand + 50% Bottom ash)	1.00	3.00	-	3.00
B-6	1Cement: 6 (40% Sand + 60% Bottom ash)	1.00	2.40	-	3.60
B-7	1Cement: 6 (30% Sand + 70% Bottom ash)	1.00	1.80	-	4.20
B-8	1Cement: 6 (20% Sand + 80% Bottom ash)	1.00	1.20	-	4.80
B-9	1Cement: 6 (10% Sand + 90% Bottom ash)	1.00	0.60	-	5.40
B-10	1Cement: 6 (100% Bottom ash)	1.00	0.00	-	6.00

and the brick wall panel of 125 mm thickness and of size 480 mm*480 mm was constructed with masonry mortar within wooden frame size of 500 mm*500 mm. Two sets of such panels with identical bricks, Portland pozzolana cement (PPC), sand, flyash etc. were constructed named as Set-1 and Set-2. In Set-1, mortar mix composition was PPC + 50% Sand and 50% Flyash combination mortar in 1:4 proportion (C-5 mix under Table 5 of MM5 Grade). The same mix was adopted for 12 mm thick plastering on both sides of wall panel, and after subsequent curing, 2 mm (approx.) white putty for evenness of the surface and two coats of acrylic paints were applied. Same steps were followed for construction of Set-2 panel with 100% sand combination (Control mix under Table 5 of MM5 Grade). The putty and two coats of acrylic paints had been applied to create an identical actual scenario of building wall surface, wherein the putty and paints both form some impervious blanket against moisture penetration by sealing the surface pores up to certain extent.

Table 5. Gradual replacement proportion of Sand by Fly ash and Bottom ash (separately) for MM5 Grade Mortar mix.

Mortar Mix Identity	Mortar Mix (MM5 Grade)	Cement Wt. ratio	Sand Wt. ratio	Fly ash Wt. ratio	Bottom ash Wt. ratio
Control	1Cement: 4 (100% Sand)	1.00	4.00	-	-
C-1	1Cement: 4 (90% Sand+ 10% Fly ash)	1.00	3.60	0.40	-
C-2	1Cement: 4 (80% Sand + 20% Fly ash)	1.00	3.20	0.80	-
C-3	1Cement: 4 (70% Sand + 30% Fly ash)	1.00	2.80	1.20	-
C-4	1Cement: 4 (60% Sand + 40% Fly ash)	1.00	2.40	1.60	-
C-5	1Cement: 4 (50% Sand + 50% Fly ash)	1.00	2.00	2.00	-
C-6	1Cement: 4 (40% Sand + 60% Fly ash)	1.00	1.60	2.40	-
C-7	1Cement: 4 (30% Sand + 70% Fly ash)	1.00	1.20	2.80	-
C-8	1Cement: 4 (20% Sand + 80% Fly ash)	1.00	0.80	3.20	-
C-9	1Cement: 4 (10% Sand + 90% Fly ash)	1.00	0.40	3.60	-
C-10	1Cement: 4 (100% Fly ash)	1.00	0.00	4.00	-
D-1	1Cement: 4 (90% Sand + 10% Bottom ash)	1.00	3.60	-	0.40
D-2	1Cement: 4 (80% Sand + 20% Bottom ash)	1.00	3.20	-	0.80
D-3	1Cement: 4 (70% Sand + 30% Bottom ash)	1.00	2.80	-	1.20
D-4	1Cement: 4 (60% Sand + 40% Bottom ash)	1.00	2.40	-	1.60
D-5	1Cement: 4 (50% Sand + 50% Bottom ash)	1.00	2.00	-	2.00
D-6	1Cement: 4 (40% Sand + 60% Bottom ash)	1.00	1.60	-	2.40
D-7	1Cement: 4 (30% Sand + 70% Bottom ash)	1.00	1.20	-	2.80
D-8	1Cement: 4 (20% Sand + 80% Bottom ash)	1.00	0.80	-	3.20
D-9	1Cement: 4 (10% Sand + 90% Bottom ash)	1.00	0.40	-	3.60
D-10	1Cement: 4 (100% Bottom ash)	1.00	0.00	-	4.00

2.1.3. Testing of samples

Compressive strength test was performed on 50 mm * 50 mm * 50 mm mortar cubes at 28 days age. Due to pozzolanic action, strength is generally found to be increasing for fly ash and bottom ash blended concrete and mortar beyond 28 days maturity period. Since the acceptable limit for strength was fixed at 28 days maturity as per IS 2250, the same was followed in this work.

Apparent porosity and bulk density samples were tested as per IS 1528 (Part-VIII) Specification. Thermal conductivity test was performed on 50 mm * 50 mm * 12 mm samples, and evaluated in accordance with ISO 22007-2 (2008). Table 8 shows the results of compressive strength at the age of 28 days, thermal conductivity, apparent porosity and bulk densities of MM3 grade mortar samples. The Hot Disc Transient Plane Source thermal conductivity test set up with samples are shown in Fig. 11.

Table 6. Total replacement proportions of Sand by Fly ash and Bottom ash (separately) in association with natural mineral (lime dust) and another industrial residue (marble dust) combination mix for MM3 Grade Mortar.

Mortar Mix Identity	Mortar Mix (MM3 Grade)	Cement Wt. ratio	Sand Wt. ratio	Flyash Wt. ratio	Bottomash Wt. ratio	Lime dust Wt. ratio	Marble dust Wt. ratio
1	1Cement: 6 (100% Sand)	1.00	6.00	-	-	-	-
2	1Cement: 6 (50% Lime dust +50% Fly ash)	1.00	-	3.00	-	3.00	-
3	1Cement: 6 (50% Marble dust + 50% Fly ash)	1.00	-	3.00	-	-	3.00
4	1Cement: 6 (100% Flyash)	1.00	-	6.00	-	-	-
5	1Cement: 6 (50% Lime dust + 50% Bottom ash)	1.00	-	-	3.00	3.00	-
6	1Cement: 6 (50% Marble dust + 50% Bottom ash)	1.00	-	-	3.00	-	3.00
7	1Cement: 6 (100% Bottom ash)	1.00	-	-	6.00	-	-

Table 7. Total replacement proportions of Sand by Fly ash and Bottom ash (separately) in association with natural mineral (lime dust) and another industrial residue (marble dust) combination mix for MM5 Grade Mortar.

Mortar Mix Identity	Mortar Mix (MM5 Grade)	Cement Wt. ratio	Sand Wt. ratio	Fly ash Wt. ratio	Bottom ash Wt. ratio	Lime dust Wt. ratio	Marble dust Wt. ratio
8	1Cement: 4 (100%Sand)	1.00	4.00	-	-	-	-
9	1Cement: 4 (50%Limedust +50% Fly ash)	1.00	-	2.00	-	2.00	-
10	1Cement:4 (50%Marbledust +50% Fly ash)	1.00	-	3.00	-	-	2.00
11	1Cement: 4 (100% Flyash)	1.00	-	4.00	-	-	-
12	1Cement: 4 (50%Limedust +50% Bottom ash)	1.00	-	-	2.00	2.00	-
13	1Cement:4 (50%Marble dust+50% Bottom ash)	1.00	-	-	2.00	-	2.00
14	1Cement:4 (100% Bottomash)	1.00	-	-	4.00	-	-

The U-value test was performed under Guarded Hot Box test facility conforming **BS EN ISO 8990 (1996)**. The U-value test specimen preparation, installing the same in the guarded hot box with sensors on test surface, and the overall test facility with data recording arrangements shown in Figs. 12 and 13 respectively.

3. Results and discussion

All the test results of fly ash and bottom ash substituted mortar mixes are presented in tabular form under Table Nos. 8, 9, 10 and 11. The compressive strength, thermal

Table 8. 28 days Compressive Strength, Thermal Conductivity, Apparent Porosity and Bulk Density values of test specimens for MM3 grade mortar mixes (gradual sand substitution by flyash and bottomash separately).

Mix Identity	Compressive Strength	Thermal Conductivity	Apparent Porosity	Bulk Density	Minimum Mortar GradeMM0.7 from Load bearing and Durability consideration	Compliance Status
Control	3.92	1.5890	23.333	1.933	>MM0.7	MM3 Complied
A-1	5.91	0.9017	26.666	1.967	..	MM3 Complied
A-2	5.84	0.8574	22.580	1.935	..	MM3 Complied
A-3	5.30	0.6977	25.806	1.645	,	MM3 Complied
A-4	4.35	0.6505	28.125	1.594	..	MM3 Complied
A-5	3.26	0.5254	32.258	1.548	..	MM3 Complied
A-6	3.05	0.4861	35.483	1.452	..	MM3 Complied
A-7	2.31	0.3786	36.363	1.182	..	MM2 Complied
A-8	1.69	0.3484	37.142	1.171	..	MM1.5Complied
A-9	1.16	0.2944	37.500	1.125	..	MM0.7Complied
A-10	0.68	0.2908	38.235	1.088	..	MM0.7Complied
B-1	3.19	0.8917	25.806	1.871	..	MM3 Complied
B-2	2.92	0.7272	26.470	1.588	..	MM2 Complied
B-3	2.45	0.5602	29.411	1.471	..	MM2 Complied
B-4	2.17	0.5681	30.555	1.389	..	MM2 Complied
B-5	1.70	0.5092	31.250	1.313	..	MM1.5Complied
B-6	1.22	0.4341	31.250	1.281	..	MM0.7Complied
B-7	1.22	0.4058	31.428	1.143	..	MM0.7Complied
B-8	1.02	0.3247	32.432	1.027	..	MM0.7Complied
B-9	0.95	0.2919	31.428	1.029	..	MM0.7Complied
B-10	0.75	0.2876	31.428	1.000	..	MM0.7Complied

conductivity, apparent porosity and bulk density values are reflected therein. The compliance to minimum grade of mortar as per IS Code has also been indicated.

3.1. Influence of mortar mix proportion on compressive strength

The 28 days compressive strength of control mix with conventional sand-cement combination under MM3 grade (1:6) have been compared with fly ash substituted mixes (A-1 to A-10) (Table 8 and Fig. 14). It may be observed that initially with 10% substitution ratio (SR) of fly ash to sand, the compressive strength increased beyond the control mix value, then started decreasing with increasing SR, i.e. 20%, 30%,... and so on. Up to 60% SR, the MM3 grade strength was maintained, and thereafter, the grades were gradually started reducing, and finally attained

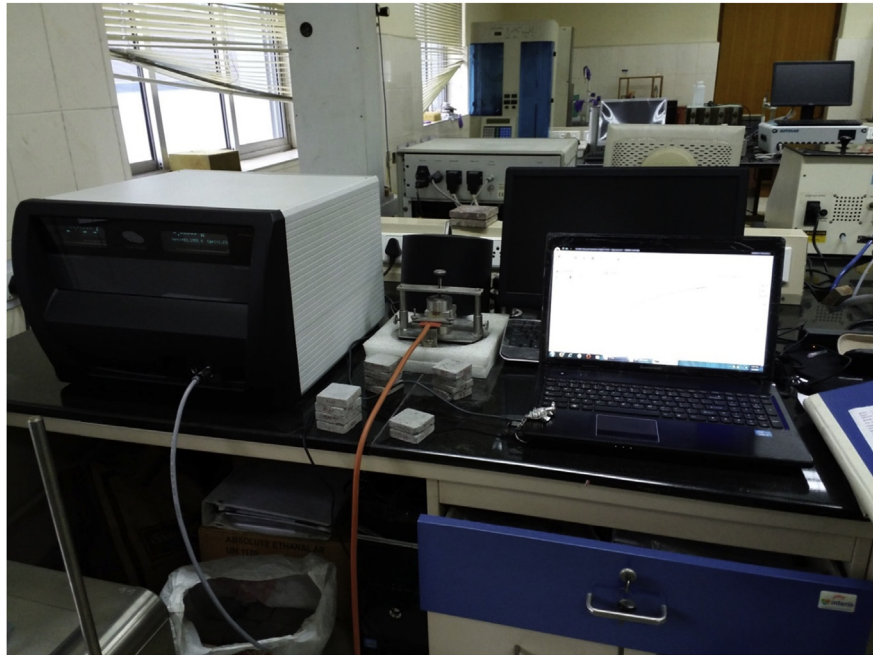


Fig. 11. Hot disc transient plane source measurement test set up, while plaster sample test was under preparation.

MM0.7 grade at 100% SR. The result complied IS 2250 (1981) provisions for maintaining durability and load bearing considerations for masonry mortar for external application. In case of bottom ash substituted mix (B-1 to B-10), the MM3 grade strength could be maintained at 10% SR only, and thereafter reduced gradually to MM0.7 at 100% SR (Table 8 and Fig. 14). For sand less mortar with fly ash and bottom ash (2–7) of MM3 grade, fly ash – Lime dust and bottom ash – lime dust combinations could achieve the grade strength, but combination with marble dust fell short of that grade (Table 9 and Fig. 15). Considering MM5 grade mortar (1:4), the 28 days compressive strength values for fly ash and bottom ash (C-1 to C-10 and D-1 to D-10) substituted mixes, the required grade strength could be maintained up to 50% SR, and thereafter reduced gradually (Table 10 and Fig. 16). Similarly for

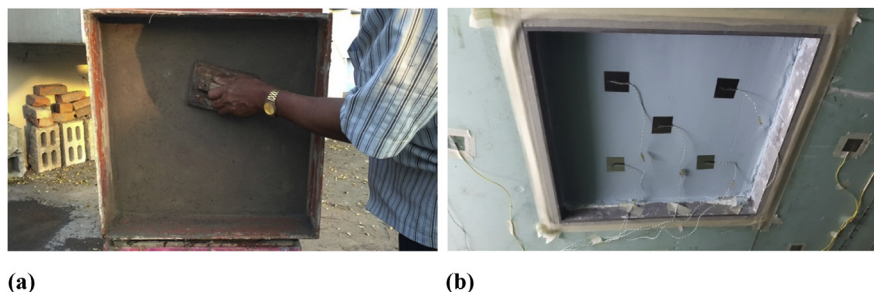


Fig. 12. 125 mm thick burnt clay brick wall panel with both side plaster (a) under preparation for U-value measurement test, and (b) subsequently installed within Guarded Hot Box test facility.



Fig. 13. Calibrated Guarded Hot Box Test facility with Instrumentation arrangement for U-value test.

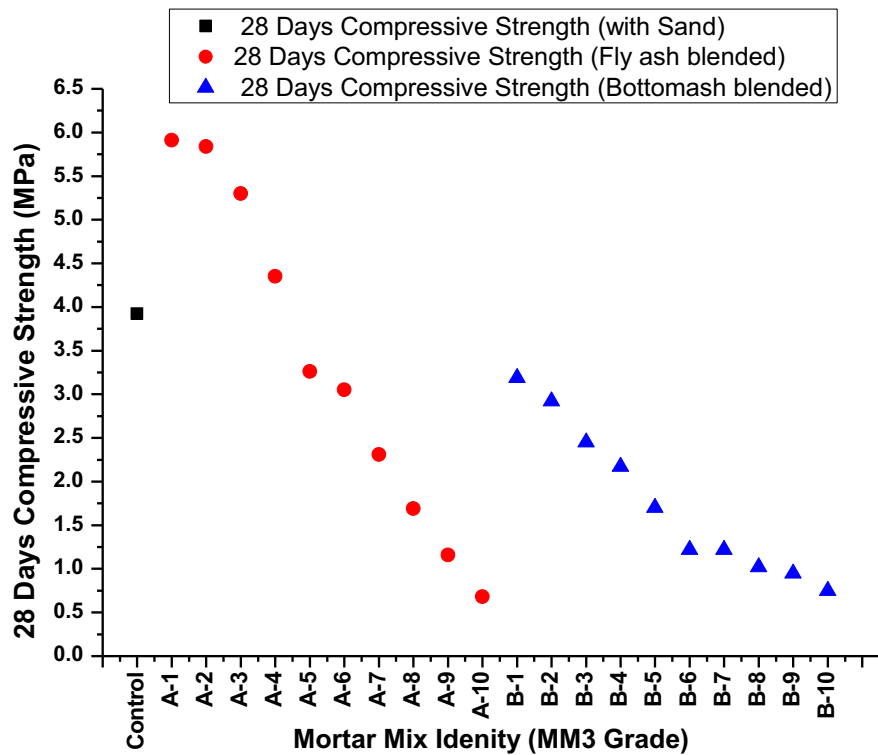


Fig. 14. Compressive Strength test values for MM3 Grade Mortar mixes (Gradual replacement of Sand by Fly ash in Series A and that by Bottom ash in Series B).

Table 9. 28 days Compressive Strength, Thermal Conductivity, Apparent Porosity and Bulk Density values of test specimens for MM3 grade mortar mixes for total sand substitution by flyash and bottomash (separately) in association with natural mineral (lime dust) and another industrial residue (marble dust) combination.

Mix Identity	Compressive Strength	Thermal Conductivity	Apparent Porosity	Bulk Density	Minimum Mortar GradeMM0.7 from Load bearing and Durability consideration	Compliance Status
1	3.92	1.5890	23.333	1.933	>MM0.7	MM3 Complied
2	3.59	0.6860	22.222	1.667	..	MM3 Complied
3	2.31	0.4800	31.578	1.132	..	MM2 Complied
4	0.93	0.3460	30.769	1.059	..	MM0.7Complied
5	3.49	0.6760	23.529	1.735	..	MM3 Complied
6	2.65	0.5780	34.482	1.448	..	MM2 Complied
7	0.90	0.3250	31.250	1.037	..	MM0.7Complied

sand less mortar with fly ash and bottom ash (9–14) of MM5 grade, fly ash-lime dust and bottom ash-lime dust combinations satisfied the grade strength criteria, but the same with marble dust combinations could reach MM3 equivalent strength only (Table 11 and Fig. 17). With respect to the MM3 grade of mortar test results, the

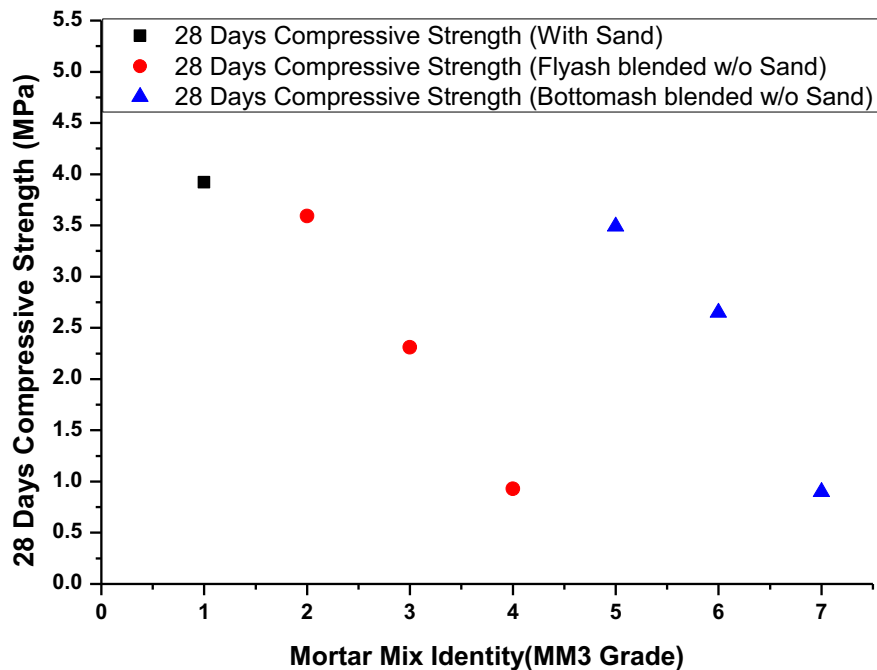


Fig. 15. Compressive Strength test values for MM3 Grade Mortar mixes (Total replacement of Sand by Fly ash and Bottom ash with Lime dust and Marble dust).

Table 10. 28 days Compressive Strength, Thermal Conductivity, Apparent Porosity and Bulk Density values of test specimens for MM5 grade mortar mixes (gradual sand substitution by flyash and bottomash separately).

Mix Identity	Compressive Strength	Thermal Conductivity	Apparent Porosity	Bulk Density	Minimum Mortar GradeMM0.7 from Load bearing and Durability consideration	Compliance Status
Control	10.06	1.1980	24.242	1.970	>MM0.7	MM5 Complied
C-1	11.96	1.1030	25.000	1.650	..	MM5 Complied
C-2	9.45	0.9014	26.470	1.676	..	MM5 Complied
C-3	8.56	0.8008	27.777	1.667	..	MM5 Complied
C-4	6.80	0.6509	30.303	1.606	..	MM5 Complied
C-5	5.71	0.6073	33.333	1.606	..	MM5 Complied
C-6	3.81	0.5517	33.333	1.533	..	MM3 Complied
C-7	2.31	0.3874	38.709	1.484	..	MM2 Complied
C-8	1.09	0.3746	40.625	1.250	..	MM0.7Complied
C-9	0.95	0.3509	41.935	1.258	..	MM0.7Complied
C-10	0.88	0.3222	43.750	1.188	..	MM0.7Complied
D-1	7.20	1.1070	26.666	1.833	..	MM5 Complied
D-2	6.52	0.8861	29.032	1.742	..	MM5 Complied
D-3	5.91	0.6936	33.333	1.667	..	MM5 Complied
D-4	5.84	0.6171	33.333	1.600	..	MM5 Complied
D-5	5.16	0.5673	34.482	1.448	..	MM5 Complied
D-6	4.62	0.4802	35.294	1.324	..	MM3 Complied
D-7	3.94	0.4285	39.393	1.212	..	MM3 Complied
D-8	3.33	0.3644	39.393	1.152	..	MM3 Complied
D-9	2.85	0.3295	40.000	1.086	..	MM2 Complied
D-10	2.72	0.2812	42.424	1.091	..	MM2 Complied

standard deviation (sd) was calculated. The sd observed to vary between 0.0417 (minimum) to 0.1445 (maximum), and the corresponding co-efficient of variation found to be 1.3072 and 12.4569 respectively. For MM5 grade mortar sd values varied between 0.0292 (minimum) to 0.8372 (maximum) and the corresponding co-efficient of variation found to be 3.3182 and 12.8405 respectively.

From the XRD phase analysis, SEM images, particle size distribution and sp. gravity value of fly ash, it may be observed that flyash particles are glassy spherical shaped, whereas sand particles are angular and fly ash is lighter by around 9% than sand. The mix becomes less closely packed, though the workability of the mix will increase due to glassy spherical shape. For bottom ash particles, though the sizes are bigger than fly ash, but much lighter (15.7%) than sand, and irregular shaped, creating more

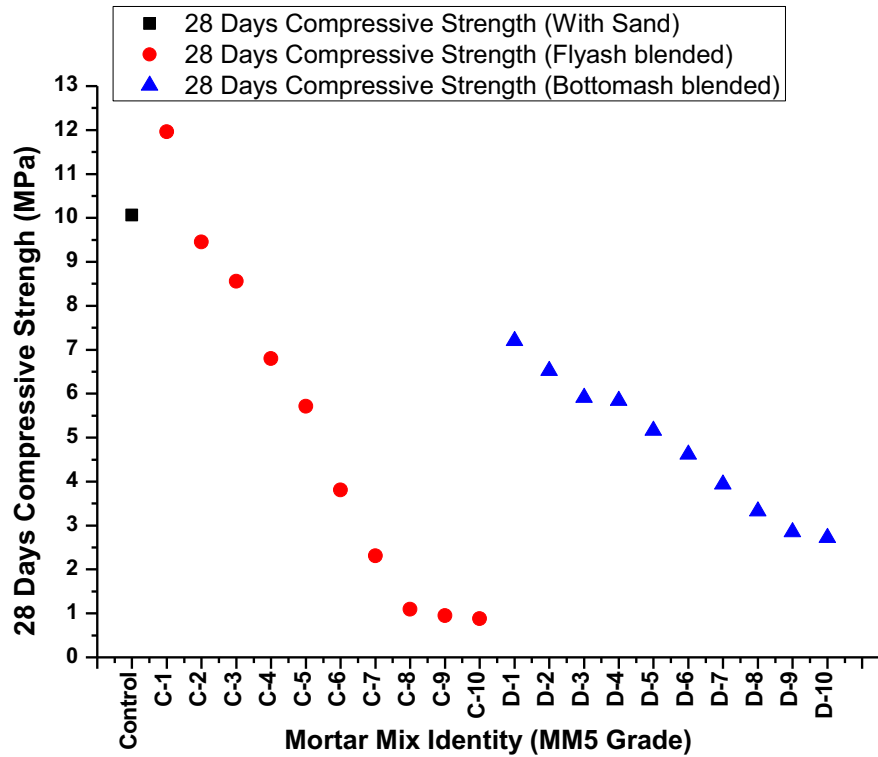


Fig. 16. Compressive Strength test values for MM5 Grade Mortar mixes (Gradual replacement of Sand by Fly ash in Series C and that by Bottom ash in Series D).

Table 11. 28 days Compressive Strength, Thermal Conductivity, Apparent Porosity and Bulk Density values of test specimens for MM5 grade mortar mixes for total sand substitution by flyash and bottomash (separately) in association with natural mineral (lime dust) and another industrial residue (marble dust) combination.

Mix Identity	Compressive Strength	Thermal Conductivity	Apparent Porosity	Bulk Density	Minimum Mortar Grade MM0.7 from Load bearing and Durability consideration	Compliance Status
8	10.06	1.1980	24.242	1.970	>MM0.7	MM5 Complied
9	5.670	0.485	19.444	1.805	„	MM5 Complied
10	3.220	0.542	15.868	1.324	„	MM3 Complied
11	0.900	0.427	30.769	1.410	„	MM0.7Complied
12	6.760	0.485	26.666	2.033	„	MM5 Complied
13	3.740	0.486	20.000	2.133	„	MM3 Complied
14	0.900	0.401	25.675	1.473	„	MM0.7Complied

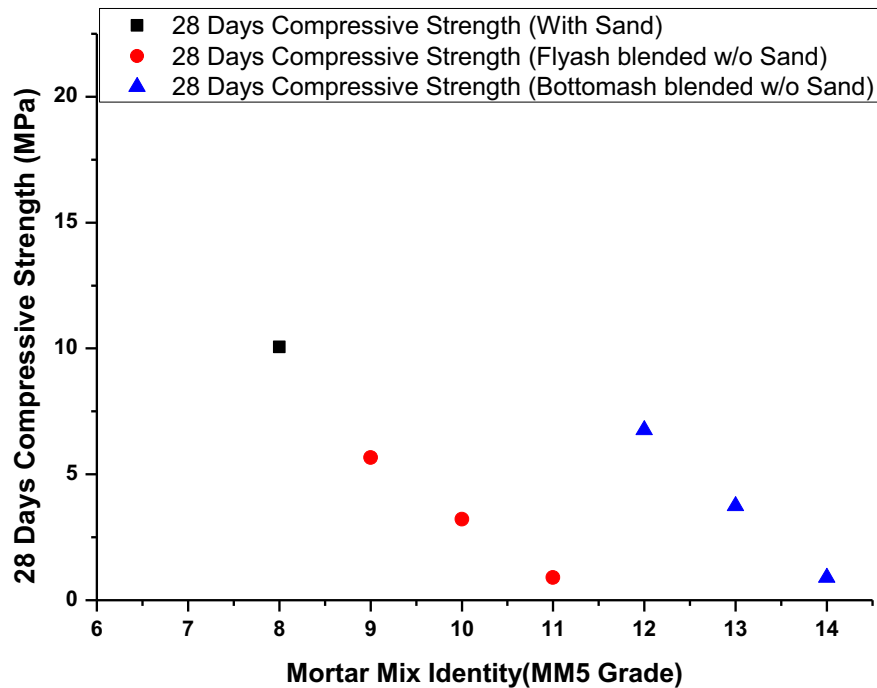


Fig. 17. Compressive Strength test values for MM5 Grade Mortar mixes (Total replacement of Sand by Fly ash and Bottom ash with lime dust and marble dust).

void. More the substitution ratio, more the void content, and less the density, which are evident from Figs. 18, 19, 20 and 21 for different mortar mix combinations, where apparent porosity and bulk density values are plotted. Therefore, it can be summarized that reasons for reduction in compressive strength with increasing substitution ratio are –i) increase in porosity, and ii) replacement of dense aggregate with lighter and porous aggregate.

3.2. Influence of mortar mix proportion on thermal conductivity

Under MM3 grade for fly ash substituted mix samples (A-1 to A-10), it was observed that the conductivity values gradually reduced, and at 60% SR (A-6, up to which MM3 grade was maintained) the reduction was 69.4%, and at 100% SR (A-10), the reduction was 81.7% (Table 8 and Fig. 22). Similarly for bottom ash substituted samples (B-1 to B-10), the conductivity value though reduced, but at 10% SR (since MM3 grade strength was maintained up to that level), the reduction was 43.9%, and thereafter it went on reducing till 100% SR (B-10), where the value was reduced by 81.9% (Table 8 and Fig. 22). For fly ash-lime dust (Mix identity 2) and fly ash-marble dust (Mix identity 3) combination mixes, the reductions were 56.8% and 69.8% respectively. For bottom ash-lime dust (Mix identity 5) and bottom ash-marble dust (Mix identity 6) combination mixes, the

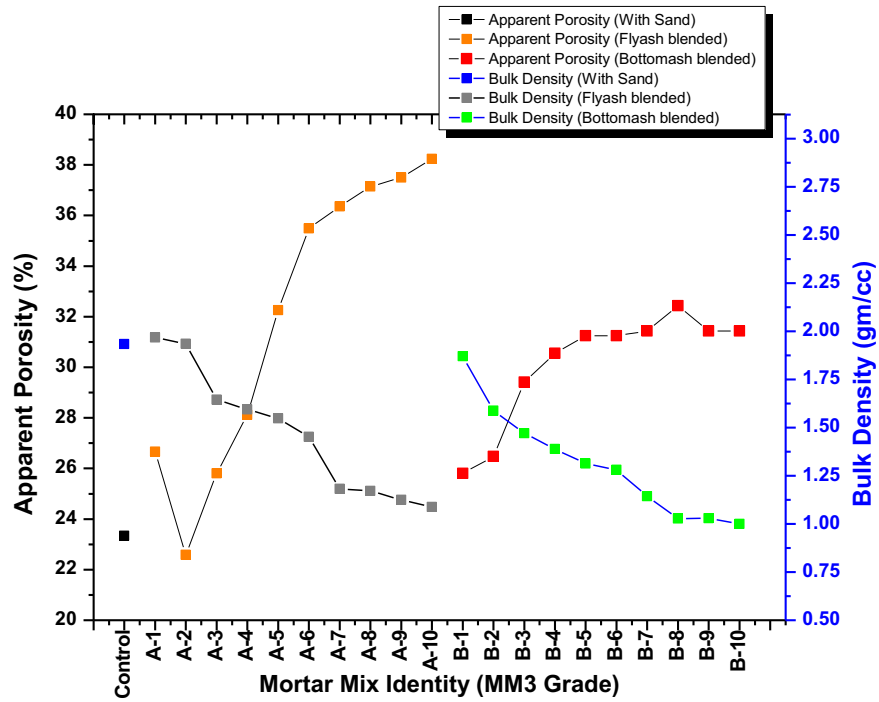


Fig. 18. Apparent Porosity and Bulk Density test values for MM3 Grade Mortar mixes (Gradual replacement of Sand by Fly ash in Series A and that by Bottom ash in Series B).

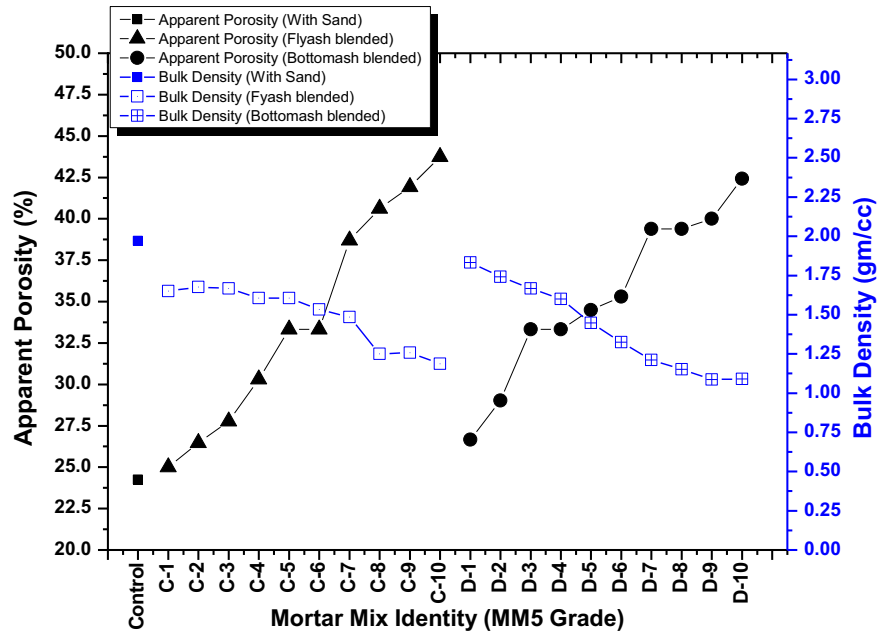


Fig. 19. Apparent Porosity and Bulk Density test values for MM5 Grade Mortar mixes (Gradual replacement of Sand by Fly ash in Series C and that by Bottom ash in Series D).

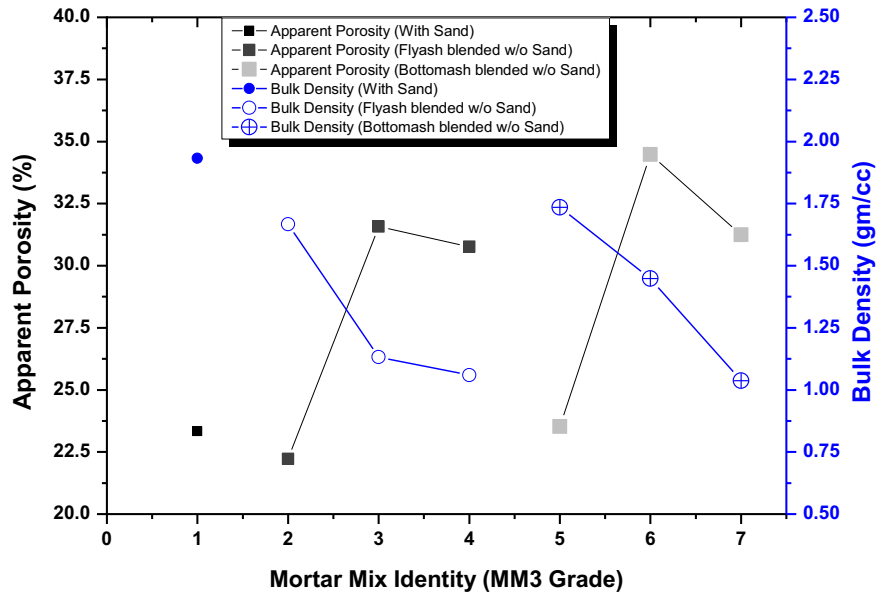


Fig. 20. Apparent Porosity and Bulk Density test values for MM3 Grade Mortar mixes (Total replacement of Sand by Fly ash and Bottom ash with lime dust and marble dust).

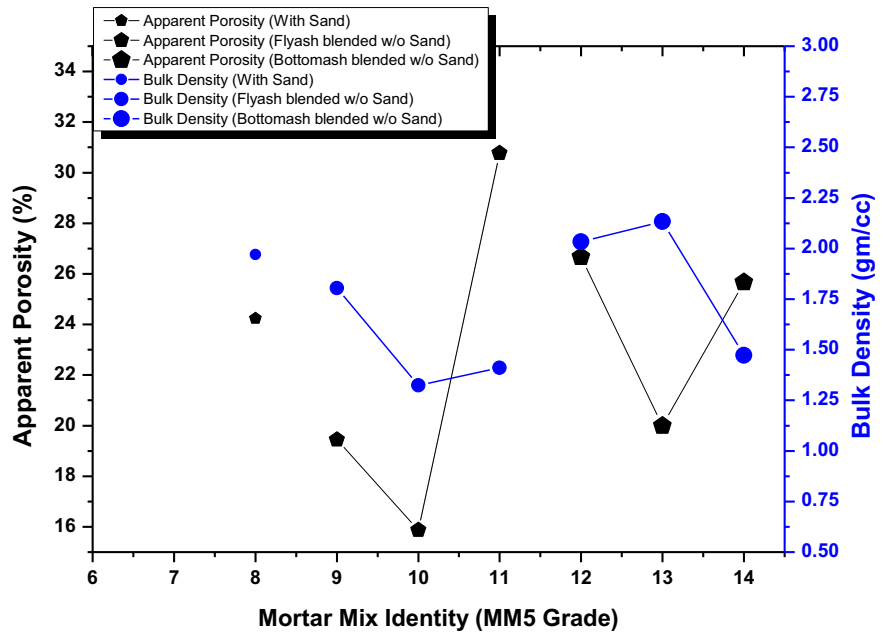


Fig. 21. Apparent Porosity and Bulk Density test values for MM5 Grade Mortar mixes (Total replacement of Sand by Fly ash and Bottom ash with Lime dust and marble dust).

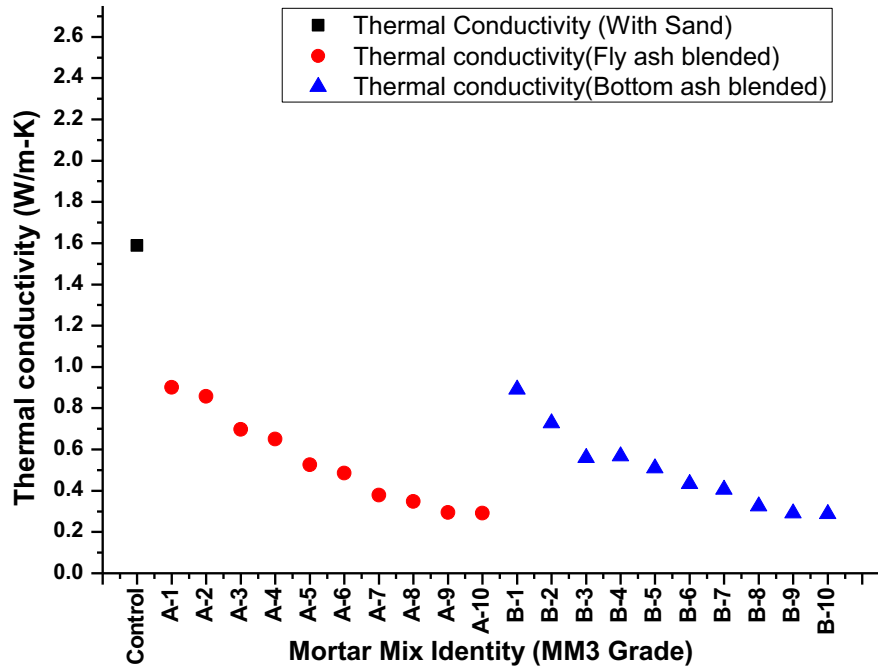


Fig. 22. Thermal Conductivity test values for MM3 Grade Mortar mixes (Gradual replacement of Sand by Fly ash in Series A and that by Bottom ash in Series B).

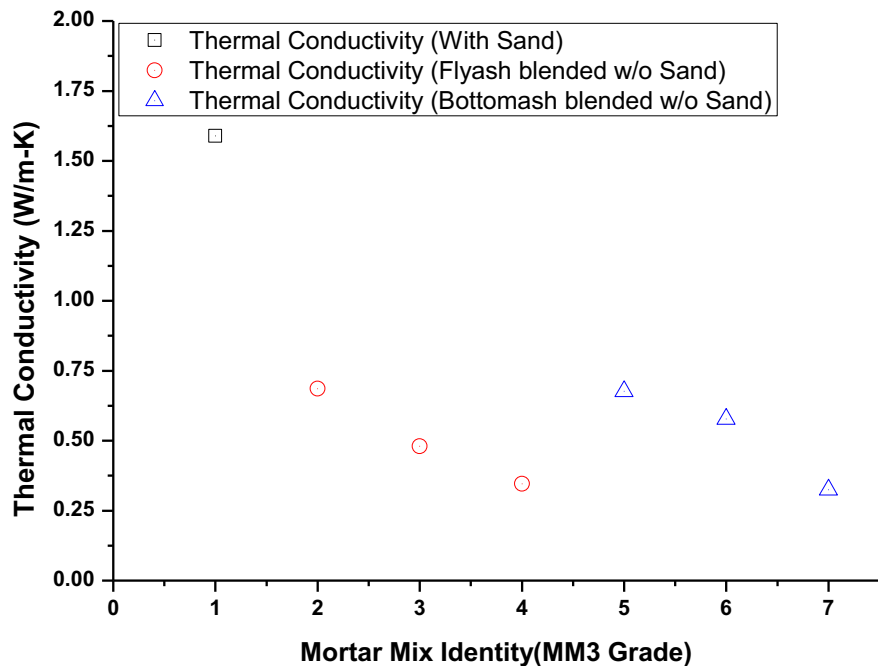


Fig. 23. Thermal Conductivity test values for MM3 Grade Mortar mixes (Total replacement of Sand by Fly ash and Bottom ash with Lime dust and Marble dust).

thermal conductivity value reductions were 57.4% and 63.6% respectively (Table 9 and Fig. 23).

Considering MM5 grade for fly ash (C-1 to C-10) and bottom ash (D-1 to D-10) substituted samples, at 50% SR (C-5 and D-5), the corresponding reductions in thermal conductivity values w.r.t. the control one were 54% and 52.6% respectively. At 100% SR for both the cases (C-10 and D-10), the corresponding reductions were 73.1% and 76.5% respectively (Table 10 and Fig. 24). For the sand less combinations (Mix identities 9,10,12 and 13) in this grade of mortar, the corresponding reductions were 59.5%, 54.7%, 59.5% and 59.4% respectively (Table 11 and Fig. 25). Presence of pore in the mortar contributes to increasing thermal conductivity, since air in pore offers the insulating effect. The absence of dense inner structure due to the shape of flyash and bottomash particles also add to lesser thermal conductance. Further the fused structure of fly ash and bottom ash with mullite and amorphous silica, hematite and anatase (TiO_2) offer lesser conductance than the quartz silica structure of river sand. The standard deviation for thermal conductivity test results for MM3 grade samples varied between 0.00205 (minimum) to 0.02523 (maximum), and the corresponding co-efficient of variation oscillated between 0.6988 and 2.7739 respectively. The same for MM5 grade was found as 7.07E-05 (minimum) to 0.02814 (maximum) and corresponding co-efficient of variation are 0.0189 and 5.6269 respectively.

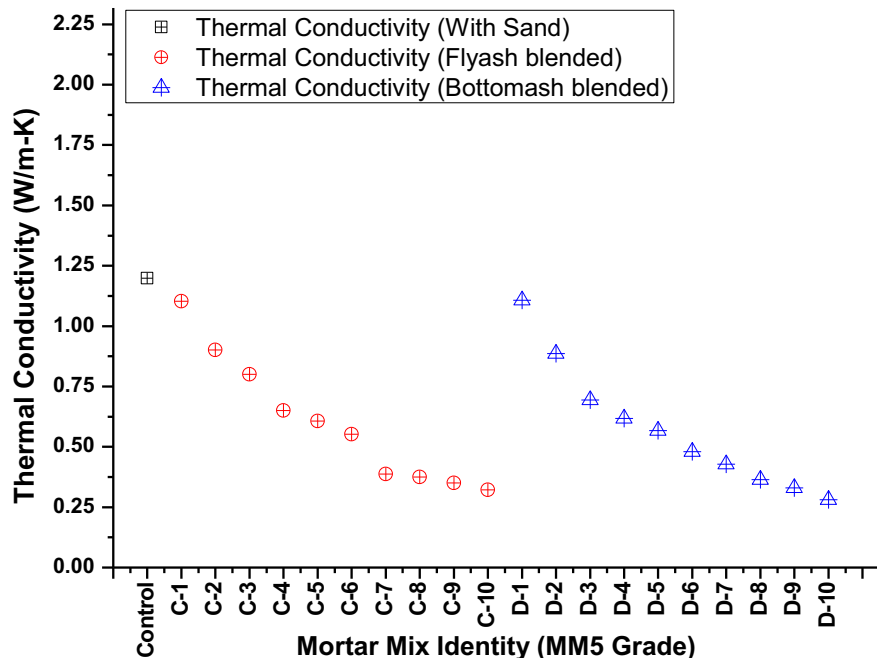


Fig. 24. Thermal Conductivity test values for MM5 Grade Mortar mixes (Gradual replacement of Sand by Fly ash in Series C and that by Bottom ash in Series D).

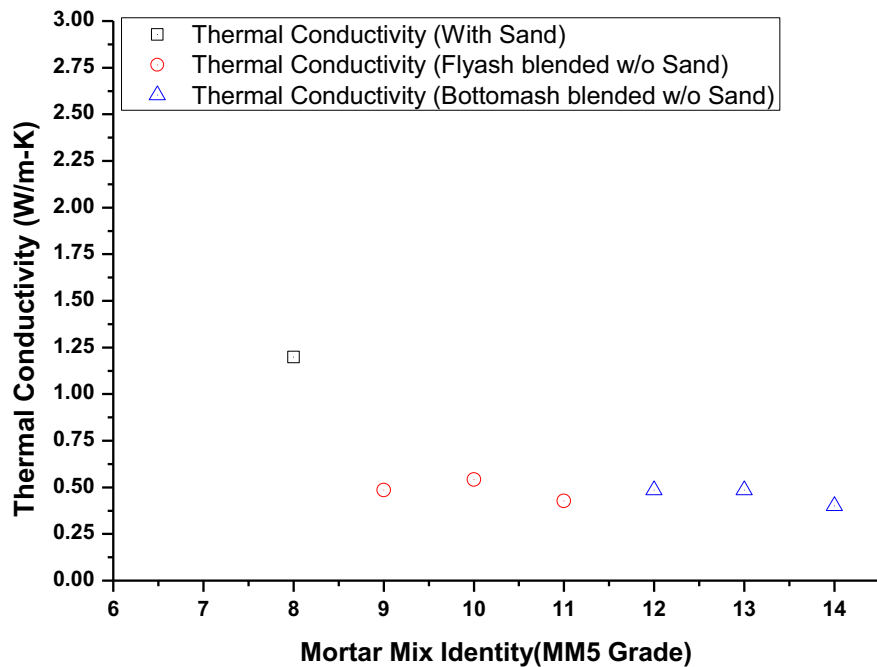


Fig. 25. Thermal Conductivity test values for MM5 Grade Mortar mixes (Total replacement of Sand by Fly ash and Bottom ash with Lime dust and Marble dust).

3.3. Influence of mortar mix proportion on apparent porosity and bulk density

The apparent porosity and bulk density test results of MM3 Grade, MM5 Grade and Sand-less MM3 Grade and Sand-less MM5 Grade Mortars are shown in Tables 8, 9, 10, and 11 and Figs. 18, 19, 20, and 21 respectively. It may be observed that with the increasing rate of SR for both fly ash and bottom ash substitutions, the corresponding porosity values increased and bulk density values decreased. The reason for such phenomena may purely be attributed to the fused alumina-silicate phase composition of fly ash and bottom ash, and particle shape and sizes of both.

3.4. Influence of mortar mix proportion on overall heat transfer co-efficient value or U-value

From the U-value test with one particular mortar mix of MM5 grade (C-5), it was observed that the reduction in U-value was 15.58% while compared with the conventional mortar mix of same grade (Table 12). Overall heat transfer coefficient of the total assembly is primarily dependent on individual constituent material's thermal conductivity value, and the corresponding resistance to one dimensional heat flow. The configuration or construction of the assembly also speed up or restrict the heat flow. Due to conductive nature of quartz silica, the mortar mix with ordinary sand has offered least resistance to the flow, whereas the mortar mix with fly ash,

Table 12. Test Results of U-value experiment.

Item description	Burnt clay brick wall panel of size 480 mm * 480 mm * 125 mm with Mortar Grade (MM5) & Plaster (12 mm thick) made of PPC and 50% Fly ash +50% Sand combination (1:4) SET - 1			Burnt clay brick wall panel of size 480 mm * 480 mm * 125 mm with Mortar Grade (MM5) & Plaster (12 mm thick) made of PPC and 100% Sand combination (1:4) SET - 2		
	Day 1, 16 th June 2017	Day 2, 17 th June 2017	Day 3, 21 st June 2017	Day 4, 22 nd June 2017	Day 5, 23 rd June 2017	Day 6, 26 th June 2017
Test Days with Date	Day 1, 16 th June 2017	Day 2, 17 th June 2017	Day 3, 21 st June 2017	Day 4, 22 nd June 2017	Day 5, 23 rd June 2017	Day 6, 26 th June 2017
Area of Surface, A (m ²)	0.23	0.23	0.23	0.23	0.23	0.23
Metering Box (MB) Air temperature (°C)	40.01	40.01	40.01	40.00	40.00	40.01
Cold Box (CB) Air temperature (°C)	24.59	24.66	24.62	24.61	24.60	24.56
Air temperature difference between MB & CB, ΔT (°C)	15.42	15.35	15.38	15.40	15.40	15.44
Surround Panel Surface temperature difference (°C)	15.15	15.12	15.17	15.17	15.13	15.16
Sample surface temperature difference (°C)	9.24	9.22	9.38	8.45	8.31	8.45
Total heat input into MB (A) (Watt)	19.08	18.55	18.96	21.29	20.35	20.44
MB Wall loss (B) (Watt)	1.549	1.432	1.465	1.631	1.123	1.162
Heat flow from MB to CB (C) = (A)-(B) (Watt)	17.53	17.11	17.50	19.66	19.22	19.28
Flanking loss (D) (Watt)	0.26	0.26	0.26	0.26	0.26	0.26
Extraneous heat transfer (E) (Watt)	2.46	2.45	2.46	2.46	2.46	2.47
Surround Panel heat flow (F) (Watt)	3.96	3.96	3.97	3.97	3.96	3.97
Sample heat flow(G)= (C)-(D)-(E)-(F) Watt	10.84	10.45	10.81	12.97	12.54	12.58
U value = (G)/A* ΔT (W/m ²⁰ C)	3.051	2.954	3.050	3.655	3.534	3.536
Avg. U value in each Set (W/m ²⁰ C)		3.018			3.575	
Difference in U value (%)			15.58			

which possess lesser conductivity value, due to its constituent phase, shape and structures offered higher resistance to the heat flow, and therefore the difference in U-value resulted.

4. Conclusions

Building sector is one of the major energy consumer and the spiralling incremental increase need to be curbed by way of energy efficient construction. Energy consumption due to cooling/heating requirement may be effectively controlled by efficient envelop design with low embodied constituent materials.

This paper investigates the possibility of substituting sand with fly ash and bottom ash in mortar and plaster mix as low thermally conducting materials. Besides, finding the strength adequacy in compliance with relevant IS Code, thermal conductivity parameter also explored. To understand the change in thermal conductivity values with the change in substitution ratios of sand by fly ash and bottom ash (separately), apparent porosity and bulk density values of such mortar mixes were also evaluated. From the study of inherent material properties of sand, fly ash and bottom ash like particle size, grading, shape, specific gravity etc., it could be established that fly ash and bottom ash produced mortar mix with lesser bulk density and more apparent porosity, than those compared with conventional mortar mix with sand. The lower density value of mortar mix is advantageous for reduced dead load of the whole envelop assembly. From the durability point of view as per Code provision, even the mix with 100% sand substitution complied with minimum grade of mortar MM0.7. Further, from the test result it is also revealed that up to 60% substitution by fly ash, MM3 and MM5 grades of mortar could be produced. The reduction in thermal conductivity values for 100% substitution by fly ash alone for MM3 and MM5 grade mortars are found to be around 82% and 73% respectively. For 100% bottom ash substitution, those values are 68% and 75% respectively. The overall heat transfer co-efficient U-value of brick wall panel with 50% fly ash substituted mortar mix was found to be lesser by 15.58%, while compared with identical panel with conventional mix with sand. Therefore, building envelop made with such ash blended mix can be considered as energy efficient, since due to lesser heat transmission inside, cooling/heating demand by the building will be reduced. The important outcome from this work has been a way of effective utilization of thermal power plant ash towards energy efficient building envelop construction without any specialized technique or addition of chemical etc.. Simultaneously, the ecological disturbances caused due to fast depletion of river sand, shall be minimized with such coal ash substitution.

There remains future scope for this work to be extended with incorporation of some additional waste material(s) in addition to the coal ash varieties, to further enhance the insulating effect of the mix under lower embodied energy scenario.

Declarations

Author contribution statement

Avijit Ghosh: Conceived and designed the experiments; Performed the experiments; Wrote the paper.

Arup Ghosh: Analyzed and interpreted the data; Contributed reagents, materials, analysis tools or data.

Subhasis Neogi: Performed the experiments; Analyzed and interpreted the data.

Funding statement

This research did not receive any specific grant from funding agencies in the public, commercial, or not-for-profit sectors.

Competing interest statement

The authors declare no conflict of interest.

Additional information

No additional information is available for this paper.

Acknowledgements

The authors would like to record their sincerest gratitude to Dr.K. Muraleedharan, present Director of CSIR-CGCRI for his encouragement to complete the work and Prof. Indranil Manna, former Director of CSIR-CGCRI for his kind consent initially to pursue the research work on the above subject. Further, the kind help and support received from Colleagues of MCD, XRD, Analytical Chemistry, FESEM Divisions, KRC of CGCRI, and fellow Research Scholar of Jadavpur University are sincerely acknowledged. Special gratitude expressed to Mr. Subrata Mistry for immensely helping in preparing the samples.

References

- Abbas, Mahapara, Kumar, Ravi, Kumar, Dinesh, 2016. Study the effect of coal bottom ash and limestone dust as partial replacement of sand and cement. *Int. J. Sci. Res. Educ.* 4 (5), 5363–5372. May.
- Aydin, Ertug, Arel, S. Hasan, 2017. Characterization of high-volume fly-ash cement pastes for sustainable construction applications. *Construct. Build. Mater.* 157, 96–107.
- Brake, Nicholas A., Oruji, Soheil, Nalluri, Likhith, Guduru, Ramesh K., 2017. Strength activity and microstructure of blended ultra-fine coal bottom. *Construct. Build. Mater.* 153, 317–326.

Bergey, Daniel, 2010. Net Global Warming Due to Insulating Foams, Northeast Sustainable Energy Association Conference, Building Science Corporation, March 10.

de Brito, Jorge, Silvestre, D Jose, Kurda, Rawaz, 2018. Toxicity and environmental and economic performance of fly ash and recycled concrete aggregate use in concrete : a review. *Heliyon* 4 (4), e00611.

Buddhi, D., Kumar, Ashok, Chauhan, D.S., 2012. Indexing of building materials with embodied, operational energy and environmental sustainability with reference to green buildings. *J. Pure Appl. Sci. Technol.* 2 (1), 11–22. January.

BS EN ISO 8990, 1996. Thermal Insulation — Determination of Steady-state thermal Transmission Properties — Calibrated and Guarded Hot Box.

Central Electricity Authority (CEA), 2010-11 to 2016-17. Report on Fly Ash Generation at Coal/Lignite Based Thermal Power Stations and its Utilization in the Country for the Year 2016–17, 2015–16, 2014–15, 2013–14, 2012–13, 2011–12 and 2010–11. Ministry of Power, Govt. of India.

Demirboga, Ramazan, 2003. Influence of mineral admixtures on thermal conductivity and compressive strength of mortar. *Energy Build.* 35, 189–192.

Gencil, Osman, Bilir, Turhan, Topku, Bekir Ilker, 2015. Properties of mortars with fly ash as fine aggregate. *Construct. Build. Mater.* 93, 782–789.

Gourav, K., Balaji, N.C., VenkataramaReddy, B.V.V., Mani, Monto., 2017. Studies in to structural and thermal properties of building envelop materials. *Energy Procedia* 122, 104–108.

Hardjito, Dwjantoro, Fing, Shen Shaw, 2010. Flyash based geo-polymer mortar incorporating bottom ash. *Mod. Appl. Sci.* 4 (1). January.

Herrera Duran, A., Dimas-Campos, J.K., Tamez-Valdez, P.L., Bentz, P. Dale., 2016. Effect of a micro co-polymer addition on the thermal conductivity of fly ash, mortars. *J. Build. Phys.* 40 (1), 3–16.

International Energy Agency (IEA), 2013. Transition to Sustainable Buildings — Strategies and Opportunities to 2050, Paris.

IS 1489, Part-1, 1991, Reaffirmed 2005. Indian Standard Portland-pozzolana Cement-specification , Part 1 Fly Ash Based (Third Revision), Bureau of Indian Standards, ManakBhavan, 9, Bahadur Shah ZafarMarg, New Delhi- 110002.

IS 2250, 1981, Reaffirmed 2000. Indian Standard Code of Practice for Preparation and Use of Masonry Mortars (First Revision), Bureau of Indian Standards, ManakBhavan, 9, Bahadur Shah ZafarMarg, New Delhi- 110002.

IS 3812 Part 2, 2003. Indian Standard Pulverized Fuel Ash – Specification Part 2 for Use as Admixture in Cement Mortar and Concrete (Second Revision), Bureau of Indian Standards, ManakBhavan, 9, Bahadur Shah ZafarMarg, New Delhi- 110002.

IS 383, 1970, Reaffirmed 2002. Indian Standard Specification for Coarse and Fine Aggregate from Natural Sources for concrete (Second Revision), Bureau of Indian Standards, ManakBhavan, 9, Bahadur Shah ZafarMarg, New Delhi- 110002.

ISO 22007-2, 2008. International Standard Plastics – Determination of thermal Conductivity and thermal Diffusivity – Part 2: Transient Plane Heat Source (Hot Disc) Method, ISO Copyright Office, Case Postale 56, CH-1211, Geneva 20.

Kim, Ki Hyeong, 2015. Utilization of sieved and ground coal bottom ash powders as a coarse binder in high-strength mortar to improve workability. *Construct. Build. Mater.* 91, 57–64.

Rafeizonooz, Mahdi., Mirza, Jahangir, et al., 2016. Investigation of coal bottom ash and fly ash in concrete as replacement for sand and cement. *Construct. Build. Mater.* 116, 15–24.

Rafeizonooz, Mahdi, Salim, Razman Mohd, et al., 2017. Toxicity characteristics and durability of concrete containing coal ash as substitute for cement and river sand. *Construct. Build. Mater.* 143, 234–236.

Rai, Baboo, Kumar, Sanjay, Kumar, Satish, 2014. Effect of fly ash on mortar mixes with quarry dust as fine aggregate. *Adv. Mater. Sci. Eng.*

Ramadoss, P., Sundararajan, T., 2014. Utilization of lignite-based bottom ash as partial replacement of fine aggregate in masonry mortar. *Arabian J. Sci. Eng.* 39, 737–745.

Sahmaran, Mustafa, Christi, antoAri Heru, Yaman, Ozgur Ismail, 2006. The effect of chemical admixtures and mineral additives on the properties of self-compacting mortars. *Cement Concr. Compos.* 28, 432–440.

Shahidan, Shahiron., Ramzi, Raihan Izzati Nurul, Maroof, Zulkhairi Mohamad, Ali, Noorwirdawati, 2016. Physical and chemical properties of Coal Bottom Ash (CBA) from Tanjung Bin Power Plant, International Engineering Research and Innovation Symposium (IRIS). *IOP Conf. Series Mater. Sci. Eng.* 160, 012056.

Thaarrini, Janardhanan., Ramasamy, Venkatasubramani, 2015. Feasibility Studies on compressive strength of ground coal ash Geopolymer Mortar. *Period. Polytech. Civ. Eng.* 59 (3), 373–379.

Vijayalakshmi, M.M., Natarajan, E., Shanmugasundaram, V., 2006. Thermal behavior of building wall elements. *J. Appl. Sci.* 6 (15), 3128–3133.



5th International Conference on Advances in Energy Research, ICAER 2015, 15-17 December 2015, Mumbai, India

Preservation of Sand and Building Energy Conservation

Avijit Ghosh^{1,*}, Surajit Gupta², Arup Ghosh², Subhasis Neogi³

¹Maintenance Division, CSIR-Central Glass and Ceramic Research Institute, Kolkata-700032, India.

²Refractory Division, CSIR-Central Glass and Ceramic Research Institute, Kolkata-700032, India.

³School of Energy Studies, Jadavpur University, Kolkata-700032, India.

Abstract

Due to developmental need of humankind, growing trend of energy generation and consumption results more and more Green House Gas emissions, which contribute significantly to the phenomena of Climate Change and Global Warming. The issue is further compounded by huge ash generation from thermal power plants. Judicious utilization of such waste in a greener way is another challenge. It is estimated that by 2030, 40.8% of Indian population shall be living under Urban environment, and huge no. of dwelling units would be required. Sand, being one of the conventional constituent of Concrete, and also the non-renewable soft mineral, is being mined mindlessly across the Globe. The energy consumed by building sector is around 40% of global energy use. HVAC load is the major contributor in overall energy profile in buildings situated under Hot & Humid climatic zones in tropical countries. Solar heat gain is resulted through building envelope, and the conventional concrete and plastered masonry surfaces contribute significantly to the same. An experimental work has been carried out to produce sustainable energy efficient concrete with Portland Pozzolana Cement, Sand, Coal Ash from Thermal Power Plant, Stone aggregate and water. Test samples are prepared with reducing quantities of Sand and increasing quantities of Coal Ash for a Design Mix Concrete. While characteristic strength of concrete could be achieved with replacement of Sand by Coal Ash, thermal conductivity value of concrete is reduced, while compared with normal concrete of same Mix.

© 2016 Published by Elsevier Ltd. This is an open access article under the CC BY-NC-ND license (<http://creativecommons.org/licenses/by-nc-nd/4.0/>).

Peer-review under responsibility of the organizing committee of ICAER 2015

Keywords: Sand, Energy; Fly ash; Bottom Ash; Thermal conductivity

*Corresponding Author. Tel. (+91) 33 24730615

Email : avijit@cgcri.res.in

1. Introduction

1.1 Climate change and effect of thermal energy generation

Human activities are influencing the climate and the trend in recent anthropogenic emissions of greenhouse gases is found to be the highest. Fossil fuel combustion and industrial processes together attributed around 78% of total Green House Gas (GHG) emission's increase during the period from 1970 to 2010. Considering the global scenario, population increase and economic growth are the two key contributors in CO₂ emission from fossil fuel combustion. [1] Coal based thermal power plants contribute around 65% of the total electricity generation in India, and the ash content in the coal used in Indian thermal power plants vary between 25-45% [2]. Considering various sectors (Transport, Industry, Cooking, Building, Telecom, Pumps and Tractors) from electricity demand point of view in India, Building Sector demand is projected to touch 2287 TWh in 2047 from a figure of 238 TWh in 2012 (around 49% of total electricity demand shall arise from Building sector alone). The projected total installed capacity of Coal based power stations shall stand at 333 GW, which will generate around 1963 TWh of electricity in 2047 [3].

1.2 Coal ash generation and its impact

In India, 130 Coal based power plants are producing around 165 M.T. of ash per year [4]. The pulverized coal when burnt, produces ash in the category of flay ash 80% and bottom ash (coarser variety) 20% [5]. The effective disposal of fly ash is a critical proposition. Fly ash is being used widely as constituent of Portland Pozzolana Cement, as Building Blocks / Bricks, Landfill and Embankment constructions, and to some limited extent for agriculture purpose. Disposal of ash in slurry state in low lying areas/dumping yards cause leaching and serious ground water pollution in adjoining areas. It also creates a state of suspended respiratory particulate matter under dry state in the air, which is extremely hazardous for human health.

1.3 Sand, a major constituent of concrete and masonry in construction industry

With the above projection in Building Sector, huge quantities of concrete would be required, and as a natural consequence, sand, one of the key ingredient would also be required in justified proportions. With the mindless sand mining from the river bed, ecological balances are disturbed in the form of depletion in ground water table, lesser availability of water for agricultural, industrial and drinking purposes, destruction of agricultural land, damage to roads and bridges etc.[6].

1.4 Other works and Energy conservation

P. Aggarwal et al. [7] had investigated about the effect of bottom ash in concrete, as partial replacement of fine aggregate component. Dan Ravina et al. [8] had studied the role of Class F fly ash in properties of concrete as partial replacement of fine sand. Kadam et al. [9] had made an experimental study to see the effects of coal bottom ash as fine aggregates in place of sand in varying proportions in concrete and various physical parameters viz. Compressive strength, tensile strength, flexural strength, modulus of elasticity, density, water permeability etc. were noted. Fine aggregate replacement by low Calcium ash in plain concrete, and the resultant effect on mechanical properties of concrete was studied by Siddique et al.[10] Deo et al. [11] had undertaken long term comparative study on concrete mix design procedure for fine aggregate replacement by fly ash with the help of Minimum Voids Method and Maximum Density Method. Rajamane et al. [12] had evolved formulation with respect to prediction of compressive strength of concrete when sand is replaced by fly ash. Demirboga et al. [13] had noted the influential effect of mineral admixtures on thermal conductivity and compressive strength of mortar. To address the issues listed at 1.1-1.3, reduction in sand content and replacing the same by coal bottom ash can be proved beneficial from energy conservation point of view.

2. Experimental Study

2.1 Considerations

In the present research work, a comparison has been made with normal concrete and sand replaced by coal bottom ash concrete from strength point of view and heat conductivity point of views respectively. In the experimental study, the mix has been designed as per IS Code, and the proportions of various ingredients have been arrived at accordingly.

A cement concrete design mix of arrived proportion was considered. Bottom ash concretes with bottom ash as sand replacement with varying proportions were undertaken. Samples were prepared for each proportion and were tested to find out the compressive strength at 7 Days, 28 Days and conductivity values respectively. Change in conductivity value with changed proportion of bottom ash as sand replacement were noted.

2.2 Materials for experiment

Cement used was Portland Pozzolana Cement (PPC) from commercially available brand, complying with IS 1489 (Part.1) : 1991 [14], Fly ash (FA) / Bottom ash (BA) conforming IS 3812 (Part 1) : 2003 [15], Sand, and 10 mm down aggregate conforming to IS 383 : 1970 (Reaffirmed 2002) [16] and potable water were used for this work.

Table 1 Chemical composition of PPC, FA & BA

Chemical constituent	Portland Pozzolana Cement	Fly ash	Bottom ash
SiO ₂	32.38	54.07	60.71
Al ₂ O ₃	10.21	26.73	25.86
Fe ₂ O ₃	3.97	6.87	6.81
CaO	41.67	0.97	0.89
MgO	1.49	0.7	0.63
Na ₂ O	0.32	0.39	0.38
K ₂ O	1.25	1.86	1.28
TiO ₂	0.71	2.56	1.97
SO ₃	3.73	0.71	0.15
LOI	3.21	3.74	0.92
Free Moisture	0.96	0.28	0.14

Table 2 Sp. Gravity values of PPC, FA, BA, Sand and Coarse aggregate

Description	Portland Pozzolana Cement	Fly ash	Bottom ash	Sand	Coarse aggregate
Sp. Gravity	3.15	2.43	2.46	2.65	2.70

Specific gravity test was performed following IS 1122-1974 (Reaffirmed 2003) [17]

2.3 Mix Calculations done as per IS 10262 : 2009[18], the steps are described broadly, as below -

$$\text{Target strength for Mix: } f'_{ck} = f_{ck} + 1.65s \quad (1)$$

where, f'_{ck} = target average compressive strength at 28 days,

f_{ck} = characteristic compressive strength at 28 days, and s = standard deviation.

Selection of Water-Cement Ratio – From Table 5 of IS 456: 2000 [19],

Selection of Water & Cement content –

From Table-2 of IS 10262, Maximum Water content for 10 mm aggregate is taken and Cement content is calculated accordingly.

Selection of Sand content – Corresponding to W/C & Workability (Applicable for Concrete grade up to M 35) ,according to IS 10262.

Adjustment of values in Sand content & Water content , as applicable –

Entrapped Air content is considered as per IS 10262 .

Determination of Coarse & Fine aggregate content was possible by solving Equations 2 and 3 below–

$$V = \left[W + \frac{C}{S_c} + \frac{1}{p} * \frac{f_a}{S_{fa}} \right] * \frac{1}{1000} \quad (2)$$

$$V = \left[W + \frac{C}{S_c} + \frac{1}{1-p} * \frac{C_a}{S_{ca}} \right] * \frac{1}{1000} \quad (3)$$

where, V = absolute volume of fresh concrete = gross volume (1 m^3) minus the volume of entrapped air,

S_c = specific gravity of Cement,

W = mass of water (kg) per m^3 of Concrete,

C = mass of Cement (kg) per m^3 of Concrete,

p = ratio of fine aggregate to total aggregate by absolute volume,

f_a , C_a = total masses of fine aggregate and coarse aggregate (kg) per m^3 of Concrete respectively,

S_{fa} , S_{ca} = specific gravities of saturated surface dry fine aggregate and coarse aggregate respectively.

Solving Equations (2) and (3), the Mix proportion becomes -

$$C : f_a : C_{sa} :: 1 : 1.5 : 2.5$$

By repeating the above steps, but without adjustment in Sand or Water Content, the Mix proportion worked out

$$C : f_a : C_{sa} :: 1 : 1.6 : 2.4$$

2.4 Preparation of Samples and Testing

Concrete samples with above proportion was prepared as Controlled one, and thereafter reducing the Sand content by 10% in each successive mix, and replacing the same by bottom ash of equal weight . Conductivity value (k) was measured for samples of above Mix by Hot Disk [20], based on Transient Plane Source Technique.

Two inches Concrete cubes were prepared for determination of compressive strength at 7 days and at 28 days respectively as per IS 516 – 1959 (Reaffirmed 2004) [21]. The Compressive strength of concrete cube samples were tested under compression loading in Universal Testing Machine.

Samples of size 50 mm by 50 mm and thickness 25 mm / 12 mm were used to determine thermal conductivity value by Transient Plane Source (TPS) method. This is one of the most precise and less time consuming techniques for studying thermal transport properties. The method uses transiently heated plane sensor, which consists of an electrically conducting pattern in double spiral shape, etched out of a thin Nickel foil. The spiral remains in between

two thin layers of insulating material - Kapton, Mica etc. The Hot Disk sensor is fitted between two identical sized samples, each one with a plane surface, touching the sensor. Electric current of pre-determined value is passed to increase the temperature of the sensor, and simultaneously recording the resistance increase as a function of time.



Fig.1 Thermal Conductivity Test Set up

Table 3 Details of Concrete Mixes

Sl.	Identification of Mix	Remarks
1.	CC	Controlled Concrete with Cement, Sand, Aggregate and Water for Mix 1:1.6:2.4.
2.	D-1	Having 10% of Sand quantity replacement by Ash, for same Mix.
3.	D-2	Having 20% of Sand quantity replacement by Ash, for same Mix
4.	D-3	Having 30% of Sand quantity replacement by Ash, for same Mix
5.	D-4	Having 40% of Sand quantity replacement by Ash, for same Mix
6.	D-5	Having 50% of Sand quantity replacement by Ash, for same Mix
7.	D-6	Having 60% of Sand quantity replacement by Ash, for same Mix
8.	D-7	Having 70% of Sand quantity replacement by Ash, for same Mix
9.	D-8	Having 80% of Sand quantity replacement by Ash, for same Mix
10.	D-9	Having 90% of Sand quantity replacement by Ash, for same Mix
11.	D-10	Having 100% of Sand quantity replacement by Ash, for same Mix

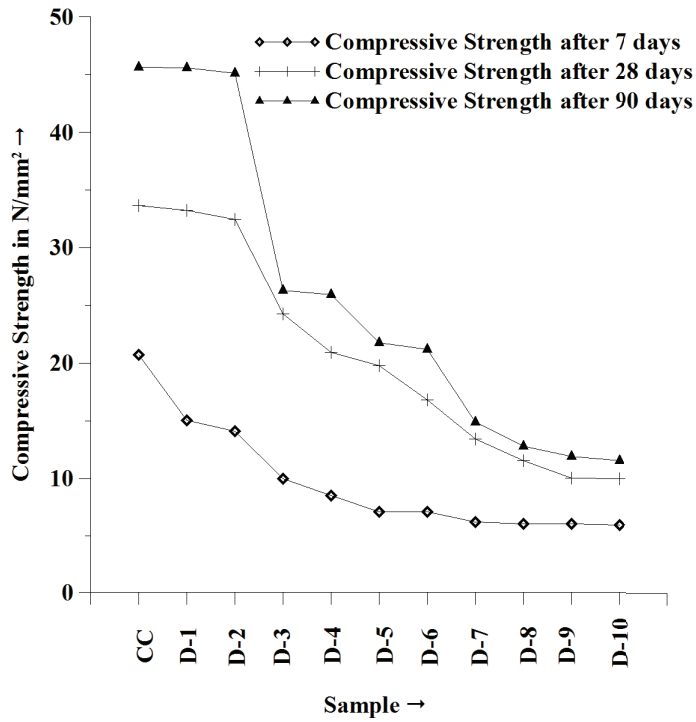


Fig.2 Graphical presentation about variations in Compressive Strength of different Concrete Mixes.

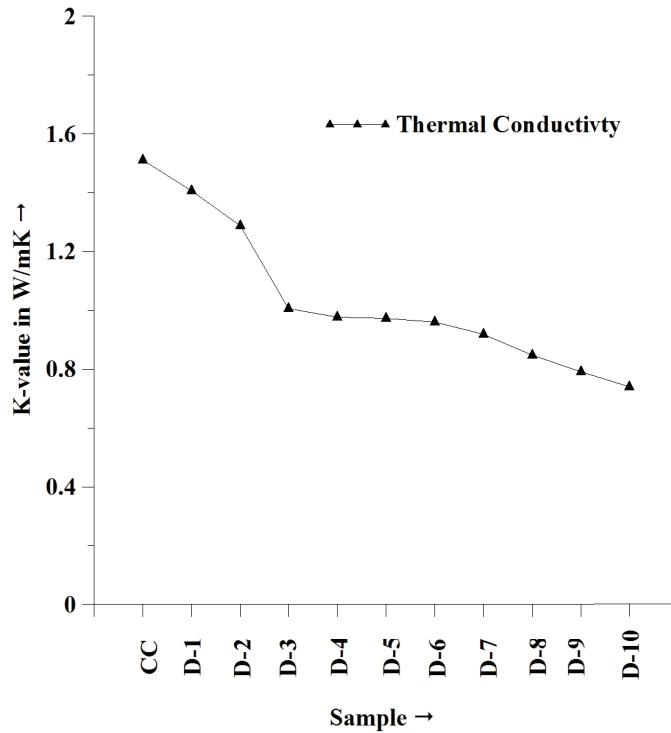


Fig.3 Graphical presentation about variations in Thermal Conductivity (k) values of different Concrete Mixes.

Similarly Cement- Sand and Cement – Fly ash / Cement – Fly ash – Lime Mortar Mix proportions were also studied, and “k” value reduction results were obtained.

Table 4 Details of Mortar Mixes

Sl.	Identification of Mix	Remarks
1.	A1	Cement : Sand is 1:6, Grade MM3
2.	A2	Cement : Sand is 1:4, Grade MM5
3.	A3	Cement : Fly ash is 1:6.
4.	A4	Cement : Fly ash is 1:4.
5.	A5	Cement : Fly ash : Lime = 1:3:3
6.	A6	Cement : Fly ash : Lime = 1:2:2

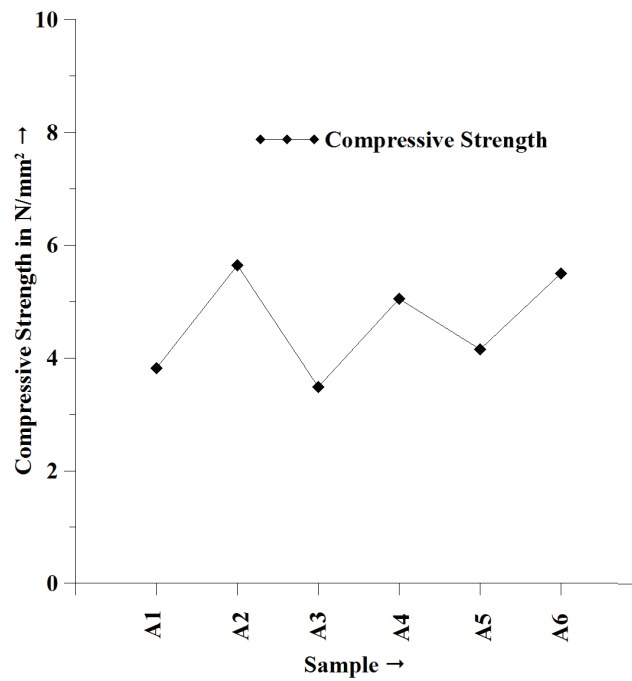


Fig.4 Graphical presentation about variations in Compressive Strength of different Mortar Mixes

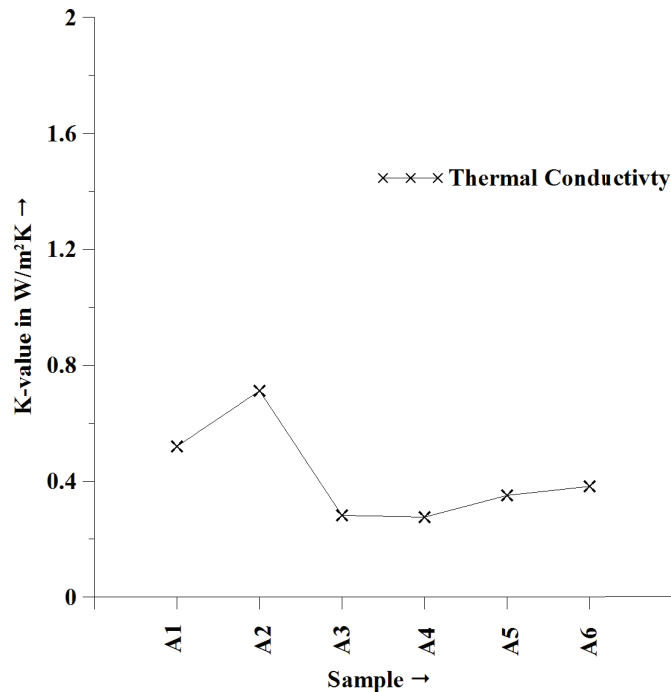


Fig.5 Graphical presentation about variations in Thermal Conductivity (k) values of different Mortar Mixes.

3. Results and discussions

From the graph in Fig.2, it may be observed that from compressive strength point of view, samples marked CC to D 3, have attained more than M-25 strength at 28 days curing condition and D 4 sample has attained M 20 strength at 28 days curing conditions respectively. D 5 and D 6 samples have attained more than M 15 strength at 28 days curing condition and M 20 strength at 90 days curing conditions respectively. D 7 to D 10 samples have attained more than M 10 strength at 28 days curing condition and M 12 strength at 90 days curing conditions respectively.

From the graph in Fig.3, it may be observed that, for 40% replacement case (D 4), thermal conductivity value has been reduced by around 35%, for 60% replacement case (D 6), thermal conductivity value has been reduced by 36.5%, and for 100% replacement case (D 10), thermal conductivity value has further been reduced by around 51%. All are compared with the base case sample (CC).

Similarly, from the graph in Fig.4, it is observed that samples marked A 3 and A 4, both attained compressive strength values at 28 days curing conditions around M 3 and M 5 respectively, which conforms to IS 2250 :1981 (Reaffirmed 2000) [22]. For mixes with marking A 5 and A 6, the compressive strength values at 28 days curing conditions are around M 4 and M 5.5 respectively. Compressive strengths for samples marked A 1 and A 2 for 28 days curing conditions are also shown.

From the graph in Fig.5, it is observed that for cement- sand mortar with 1:6 proportion (A 1) is compared with cement - fly ash with same proportion (Sample mark A 3), and found the same with 46% lesser conductivity than the base case sample (A 1). Cement - sand mortar with 1:4 composition (Sample mark A 2) is compared with cement - fly ash identical composition (Sample mark A 4). It is observed that the thermal conductivity value is reduced by 61% than the base case sample (A 2).

4. Energy impact out of this finding

Considering a room size of 3m by 4m in plan dimension, and outside room temperature as 40⁰ C (exposed to direct Solar radiation) and inside electro-mechanically controlled temperature as 25⁰ C, and thermal conductivity of screed concrete layer of 25 mm in the base case scenario (Cement : Sand : Stone aggregate :: 1:1.6:2.4) for sample

CC and for Ash concrete sample D 6, the conductive heat gain through the exposed roof are worked out as 10879 Watts and 6913 Watts respectively. For an 8 hour use room under controlled temperature condition and considering 26 working days in a month, the difference in energy quantity is worked out as 825 kWh. The corresponding monthly saving in monetary term is Rs.6930.00 (@ Rs.8.40/- per kWh) , and CO₂ emission avoided shall be in the tune of 660 kg monthly at the user end.

5. Conclusion

From the above experimental data, it may be concluded that by replacing sand with Coal ash, natural soft mineral can be preserved, and the water table balance can be ensured. Further, Energy Conservation in Building industry is possible up to a considerable extent, by reducing Solar heat ingress through Building envelope, and resultant reduction in mechanical cooling load.

Acknowledgement

Prof. Indranil Manna, former Director of CSIR-CGCRI (current Director of IIT-Kanpur) immensely encouraged and permitted initially to undertake such work for Ph.d. study. Dr. K. Muraleedharan, present Director of the Institute kindly permitted to submit the full paper for ICEAR-2015. The Colleagues in Material Characterization Division and Refractory Division of the Institute also helped , without which various experimental tests would not have been possible to carry out.

References

- [1] Climate Change 2014 Synthesis Report Summary for Policymakers, www.ipcc.ch.
- [2] Ujjwal Bhattacharjee, Tara Chandra Kandpal, Potential of fly ash utilization in India, Energy 27 (2002) 151-166
- [3] India Energy Security Scenarios 2047, www.niti.gov.in
- [4] Fly ash scenario in India by R.K.Joshi, Scientist D, Department of Science & Technology, Govt. Of India.
- [5] Indian fly ash : Production and consumption scenario, Internat .J. Waste Resources, Vol.3 (1) 2013:22-25, Md Emamul Haque ISSN 2252-5211. [http:// www.ijwr.co](http://www.ijwr.co)
- [6] M. Naveen Saviour, Environmental impact of soil and sand mining : a review, , International Journal of Science, Environment and Technology, Vol.1, No.3, 2012, 125-134.
- [7] P. Aggarawal, Y. Aggarwal, S. M.Gupta, Effect of bottom ash as replacement of fine aggregate in concrete, Asian journal of Civil engineering (Building and Housing) Vol.8, No.1 (2007) Pages 49-62.
- [8] Dan Ravina, Properties of fresh concrete incorporating a high volume of fly ash as partial fine sand replacement, Materials and Structures/Materiaux et Constructions, Vol. 30, October 1997, pp 473-479.
- [9] M.P.Kadam, Dr.D.Y.Patil, Effect of coal bottom ash as sand replacement on the properties of concrete with different w/c ratio, International Journal of Advanced Technology in Civil Engineering, ISSN : 2231-5721, Volume 2, Issue 1, 2013.
- [10] Effect of fine aggregate replacement with Class F fly ash on the mechanical properties of concrete, Rafat Siddique, Cement and Concrete Research 33 (2003) 539-547.
- [11] A.D.Pofale and S.V.Deo, Comparative long term study of concrete mix design procedure for fine aggregate replacement with fly ash by Minimum Voids Method and Maximum Density Method, KSCE Journal of Civil Engineering (2010) 14 (5) : 759-764.
- [12] N.P.Rajamane, J.Annie Peter, P.S.Ambily, Prediction of compressive strength of concrete with fly ash as sand replacement material, Cement and Concrete Composites 29 (2007) 218-223.
- [13] Ramazan Demirboga, Influence of mineral admixtures on thermal conductivity and compressive strength of mortar, Energy and Buildings, 35 (2003) 189-192.
- [14] IS 1489 Part 1 (1991) Indian Standard Portland Pozzolana Cement – Specifications Part-1, fly ash based (Third Revision)
- [15] IS 3812 (Part 1) 2003 Indian Standard Pulverised fuel ash –Specification Part-1 for use as Pozzolana in Cement, Cement mortar and Concrete (Second Revision)
- [16] IS 383 1970 (Reaffirmed 2002) Indian Standard Specification for Coarse and Fine Aggregates from Natural Sources for Concrete (Second Revision).
- [17] IS 1122 1974 (Reaffirmed 2003) Indian Standard Method of test for determination of true specific gravity of natural building stones (First Revision)
- [18] IS 10262 : 2009 Indian Standard Concrete Mix Proportioning – Guidelines (First Revision)
- [19] IS 456 : 2000 Indian Standard Plain and Reinforced Concrete – Code of Practice (Fourth Revision)
- [20] Hot Disk Thermal Constants Analyser (Hot Disk TPS2500)
- [21] IS 516 : 1959 (Reaffirmed 2004) Indian Standard Methods of tests for strength of concrete .
- [22] IS 2250 :1981 (Reaffirmed 2000) Indian Standard Code of practice for preparation and use of masonry mortars (First Revision).